Greg Corbett
Corbett Geological Services
29 Carr Street
North Sydney NSW 2060
Australia
Ph (61 2) 9959 3060
Fax (61 2) 9954 4834

Terry Leach
Terry Leach and Co
P.O. Box 150
Coromandel
New Zealand
Ph (64 7) 866 7642
E-mail leach@ihug.com.nz

SOUTHWEST PACIFIC RIM

GOLD-COPPER SYSTEMS:

Structure, Alteration,

and Mineralization.

SHORT COURSE MANUAL

DRAFT as at 24 May 1997

G J Corbett and
T M Leach

SUMMARY

This manual classifies and describes differing styles of southwest Pacific rim gold-copper systems, and analyses hydrothermal ore-forming processes. Investigations of these systems in terms of structure, alteration and styles of mineralization provide information which may help determine the direction of fluid flow within evolving hydrothermal systems.

Major structures localize magmatic hydrothermal systems in magmatic arc settings and create ore-hosting dilational environments within subsidiary structures, commonly at high angles to the controlling structures. Differing styles of convergence influence the style of major structures and ore-forming environments. Breccias occur in most gold-copper deposits and may be categorised as a guide to understanding the ore-forming environment as broad correlations are apparent between breccia and mineralization styles.

Temperature and fluid pH are considered to be the most important of many factors which control the types of hydrothermal alteration. Hydrothermal minerals are classified in terms of these two factors to create a meaningful interpretation of alteration data. Possible mechanisms of metal transport and transport, provide a framework to understand the distribution of metals in intrusion-related systems.

Porphyry copper-gold systems develop around intrusions which are localized within volcanoplutonic arcs by regional accretionary (arc parallel) or transfer (arc normal) structures. Cooling of intrusions emplaced at high crustal levels results in the conductive heat loss and initial formation of zoned alteration assemblages. This is followed by the exsolution of magmatic fluids and the formation of stockwork to sheeted quartz-dominated vein systems, generally along the margins and around the carapace of the intrusion. Subsequent mineralization occurs within an environment which is conducive to metal deposition, and it is interpreted that these conditions are created as a result of cooling, predominantly by dilute meteoric waters. Porphyry copper mineralization concentrates in zones of greatest paleo-permeability, commonly along the fault controlled margins of the host intrusion and refractured pre-existing stockwork veins. It is proposed that mineralization mainly results from mixing of meteoric waters with metal-bearing magmatic fluids, possibly derived from larger magma sources at depth. Skarn deposits exhibit similar prograde and retrograde alteration and mineralization in response to the emplacement of intrusions into calcareous rocks.

High sulfidation gold-copper systems are formed from hot, acidic, magmatic-derived fluids and extend from porphyry to epithermal regimes. High sulfidation alteration forms as shoulders and caps to porphyry intrusions, where zonations in alteration reflect progressive cooling and subsequent decrease in fluid pH in response to gradual dissociation of reactive magmatic gases. The high formation temperature of these systems, proximal to the source intrusion, is inferred to inhibit the formation of copper-gold mineralization which occurs in cooler, more distal environments. These systems are classified according to the predominance of either structural or lithological control to fluid flow as members of a continuum. All mineralized systems exhibit characteristic alteration zonation resulting from progressive cooling and neutralization of hot acidic magmatic-dominated fluids by reaction with host rocks and ground waters. Variations in the style of mineralization, metal content and alteration mineralogy, depend upon temperature and fluid composition. A two stage alteration and mineralization model is proposed which suggests that initial vapour-dominated fluids develop zoned, commonly pre-mineralization alteration, which is overprinted and typically brecciated during influxes of mineralized liquid-rich fluids. High sulfidation systems are copper-rich at depth and are gold-rich at higher crustal levels.

Varying styles of low sulfidation gold systems predominate in settings of oblique subduction, where magmatic fluids migrate away from intrusion source rocks into environments which contain meteoric waters of different compositions and temperatures. Metals grade from gold and possible copper-bearing at depth, through gold with base metals at intermediate levels, to gold-silver bearing at highest crustal levels.

Quartz sulfide gold + copper systems form proximal to magmatic source rocks, predominantly by the mixing of magmatic fluids with deep circulating cool and dilute meteoric waters. Carbonate-base metal gold systems form at higher levels, mainly by reaction of magmatic-dominated fluids with low pH, CO_2-rich waters. Epithermal quartz gold-silver systems form at the highest crustal levels and display the most distal relationship to the magmatic source. Bonanza gold grades develop in these systems by the mixing of more dilute, boiling, magmatic-derived fluids with oxidizing ground waters. This latter group of deposits is transitional to the classic adularia-sericite epithermal gold-silver vein systems. Telescoping may overprint the varying styles of low sulfidation gold mineralization upon each other or upon the source porphyry intrusion. Sediment hosted replacement gold deposits are herein classified as genetically related to low sulfidation quartz-sulfide systems, but develop in reactive carbonate rocks.

Adularia-sericite epithermal gold-silver deposits form at elevated crustal settings in the absence of an obvious intrusion source for the mineralization. These systems vary with increasing depth from: generally barren surficial sinter/hot spring deposits, to stockwork vein/breccias, and fissure veins. Brittle basement rocks fracture well and so represent competent hosts for fissure veins within dilational structural settings. Boiling models account for the deposition from meteoric waters of the characteristic gangue minerals comprising banded quartz, adularia and quartz pseudomorphing platy carbonate. However, precious and base metals are postulated to be magmatic-derived and are concentrated in thin sulfide-rich bands, commonly with low temperature clay minerals. Mineralization is therefore interpreted to have been deposited mainly by the mixing of upwelling, commonly boiling, mineralized fluids with cool, oxidizing ground water.

The ore deposit models defined herein are useful in all stages of mineral exploration, from the recognition of the style of deposit, to the delineation of fluid flow paths as a means of targeting high grade ores, or porphyry source rocks. The exploration geologist may be aided by the use of conceptual exploration models which are interpretative and so vary from the more rigorously defined deposit and exploration models. Conceptual models should not be applied rigidly but modified using an understanding of the processes described herein to develop models which are tailored to individual prospects.

CONTENTS

LIST OF FIGURES

LIST OF TABLES

1 CHARACTERISTICS OF GOLD-COPPER HYDROTHERMAL SYSTEMS

i) Introduction

This is the manual used for the short course of the same name presented at the SME/SEG Meeting in Phoenix in March 1996, with modifications in response to reviewers comments. The manual provides additional detailed information to the verbal presentation, and is designed so that the figures can be followed during the lectures, in which the slides of rocks, remote sensing images, etc, further support the concepts presented.

Terminology
We have tried where possible to use terms which are technically correct and in common use by short course attendees - predominantly field geologists working in mineral exploration. However, our terminology may not always be in strict agreement with some geological literature, to which the readers are referred, and terms utilized in research studies.

ii) Exploration Models

This workshop demonstrates and describes ore deposit styles as well as exploration and conceptual exploration models as aids to the exploration and evaluation of southwest Pacific rim magmatic arc mineral resources. However, careful consideration of the nature of these exploration models is necessary before any reliance can be placed upon them.

Exploration geologists compare, contrast and classify mineral occurrences in order to build up empirical patterns from data such as field observations. Deposit models are developed as empirical descriptions of individual deposits, or of more use to the exploration geologist, styles of deposits. Exploration models are derived from interpretations, focusing upon those characteristics of a deposit model which aid in the discovery of ore deposits of a particular style. Progressively lateral interpretations depart from rigorously reviewed science and so become conceptual exploration models. Such a conceptualization may give the explorationist a competitive advantage (Henley and Berger, 1993) in the increasingly difficult search for ore deposits. These models may also assist in ranking projects and aid in the abandonment of lower order targets.

Conceptual exploration models evolve through their application to exploration examples, and are refined by research, many being abandoned during this process. Although luck plays a part, the competitive nature of the model. The very innovative nature which makes a conceptual exploration model of use to the explorationist, precludes the lengthy process of rigorous evaluation of many of the concepts by exhaustive research studies.

It is important that models must not be applied rigidly, but should be modified to become project-specific. Great care must be taken to abandon or modify inappropriate models. It is intended in this manual to outline to explorationists, the processes involved in the derivation of conceptual exploration models, rather than in the rigid application of existing models. Structure and petrology are tools which the explorationist may use in the development of conceptual exploration models. This manual illustrates how the integration of these can lead to the development of conceptual exploration models. Major structures localize intrusions and minor structures provide ground preparation. The study of petrology delineates styles of alteration and mineralization, fluid characteristics and mechanisms of ore deposition. The synthesis of structure and petrology may define fluid flow paths in hydrothermal ore systems. search for ore bodies encourages explorationists to be the first to develop or utilise a conceptual exploration

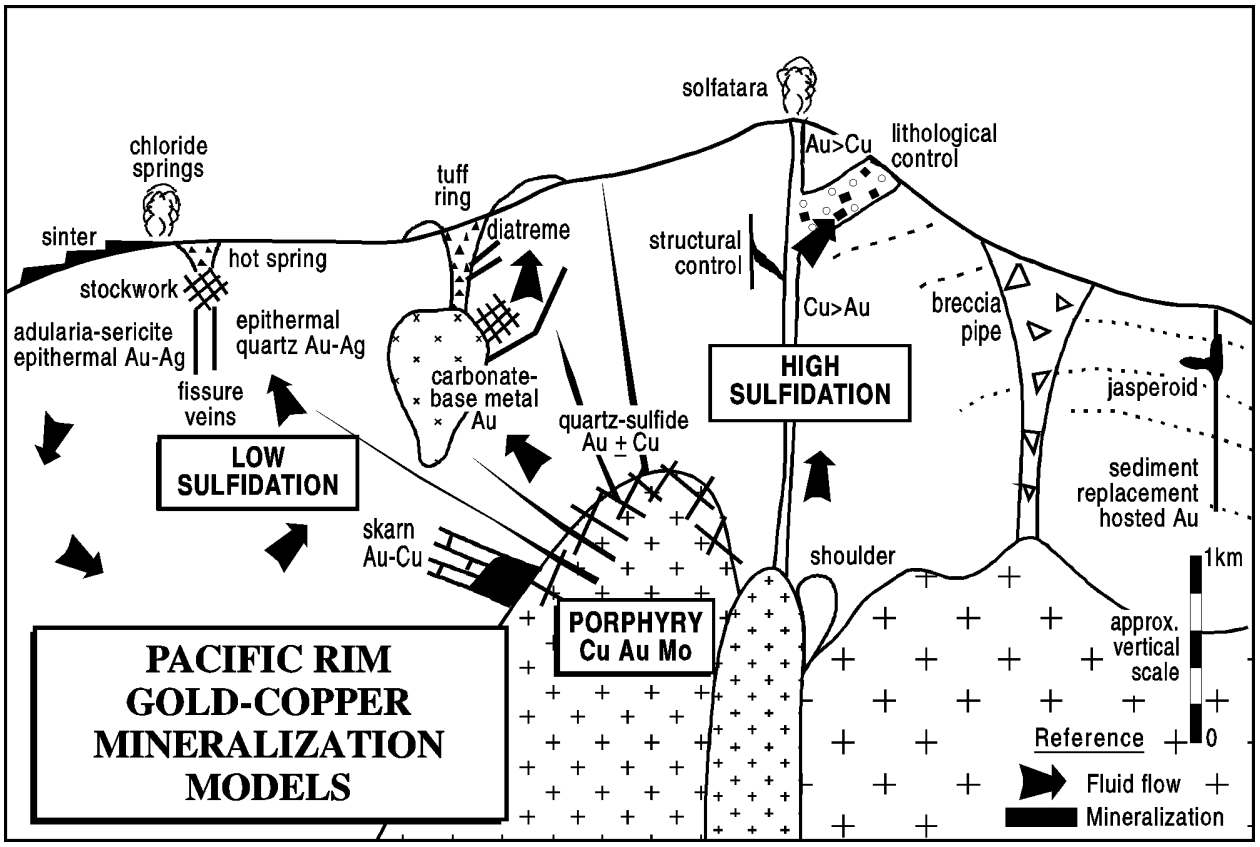

FIG. 1.1

iii) Classification

A simple classification is used to distinguish and evaluate differing styles of southwest Pacific rim gold-copper mineralization (Fig. 1.1, Table 1). Elements of this classification are:
* Crustal level which reflects the proximity to the magmatic source.
* Degree of sulfidation classified as high or low sulfidation refers to the chemical characteristics of the mineralizing fluids (below).

Varying crustal levels of formation provide the primary basis for the distinction of different styles as:
Porphyry systems are hosted within or subjacent to intrusions at depths of typically greater than 1 km. Cox and Singer (1988) provide a mean depth of 3.6 km for plutonic copper-molybdenum porphyry deposits, mainly of the eastern Pacific, and median depths of about 1 km for gold-copper porphyries typical of the southwest Pacific rim. Sillitoe (1993a) emphasises the vertical extent (1 km to >2 km) and cylindrical shape of the latter deposits. These deposits may contain the greatest metal contents of the different styles of southwest Pacific rim copper-gold systems, but grades are generally lower than other styles of mineralization (Fig. 1.3), and so these represent prime exploration targets for bulk tonnage, low grade mineralization.

The term porphyry is used in this manual to describe a high level intrusive rock commonly, but not always with a porphyritic texture, and should not be confused with a porphyry copper-gold body in the strict sense.

SOUTHWEST PACIFIC RIM PLATE MARGINS and GOLD-COPPER OCCURRENCES

Fig. 1.2

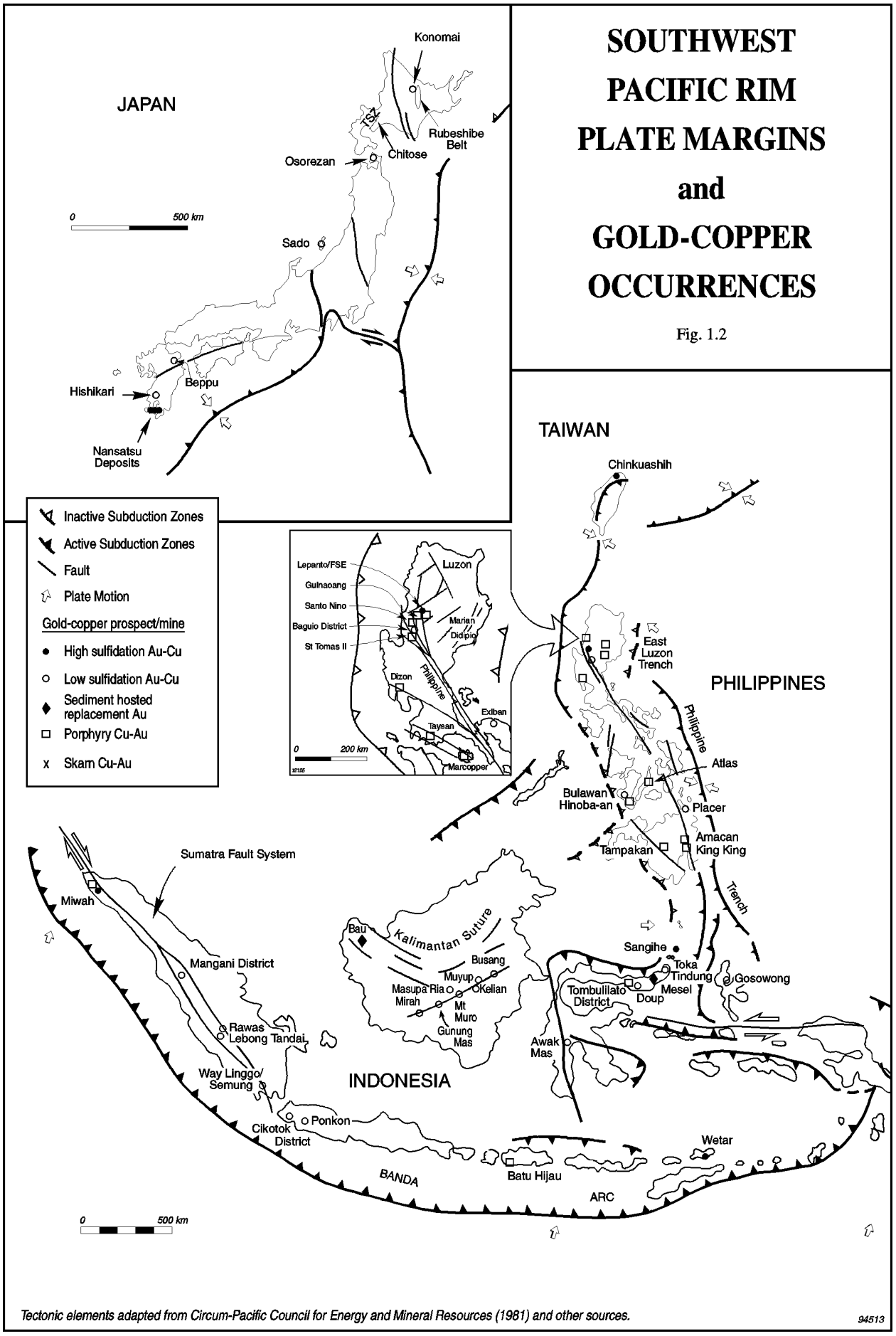

Tectonic elements adapted from Circum-Pacific Council for Energy and Mineral Resources (1981) and other sources.

94513

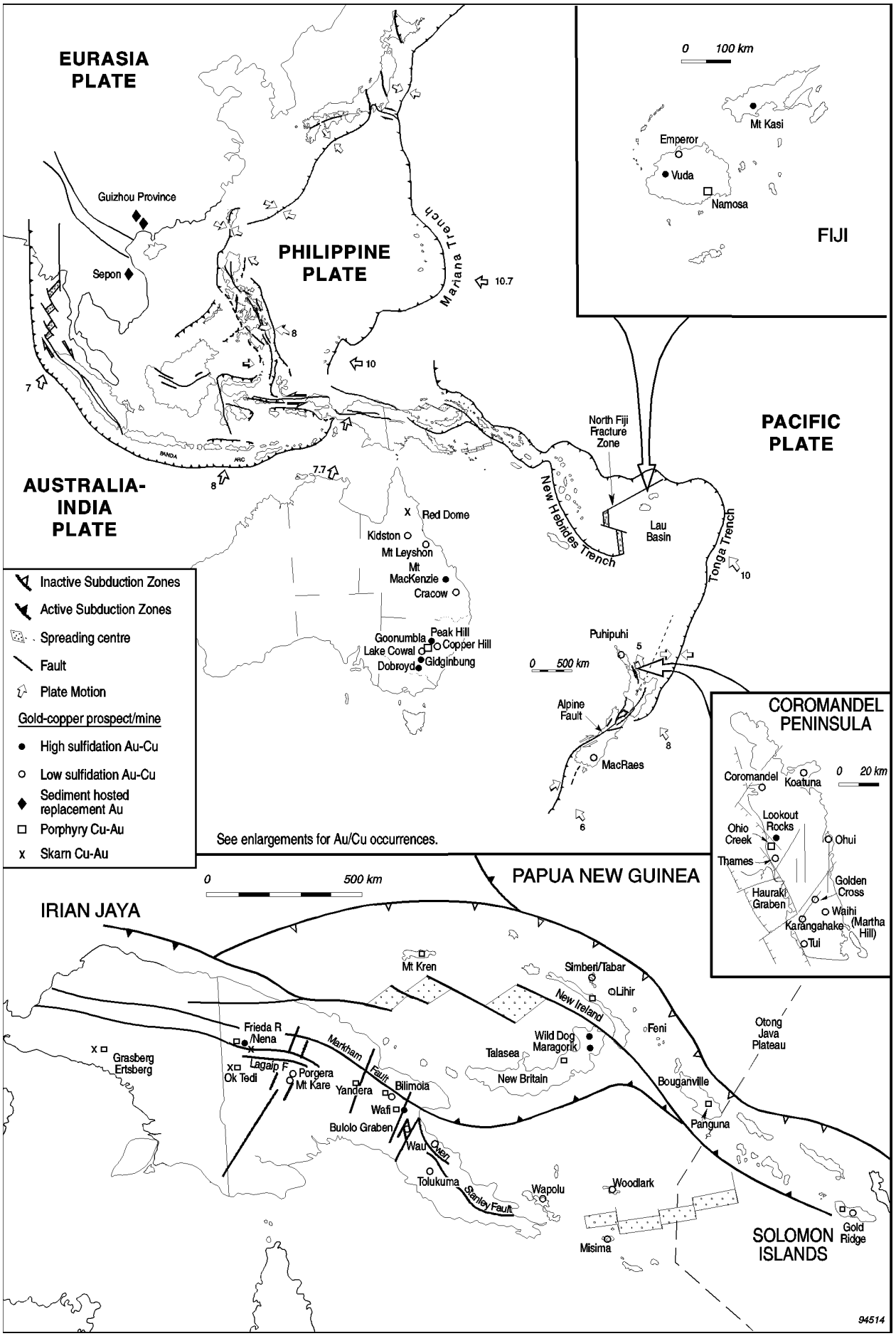
EURASIA PLATE
PHILIPPINE PLATE
AUSTRALIA-INDIA PLATE
PACIFIC PLATE
PAPUA NEW GUINEA
IRIAN JAYA
SOLOMON ISLANDS
FIJI
Guizhou Province
Sepon
Mariana Trench
10.7
8
10
7
7.7
8
BANDA ARC
North Fiji Fracture Zone
New Hebrides Trench
Lau Basin
Tonga Trench
10
Red Dome
Kidston
Mt Leyshon
Mt MacKenzie
Cracow
Goonumbla
Peak Hill
Lake Cowal
Copper Hill
Dobroyd
Gidginbung
Puhipuhi
5
0 500 km
Alpine Fault
8
MacRaes
6
0 100 km
Mt Kasi
Emperor
Vuda
Namosa
Inactive Subduction Zones
Active Subduction Zones
Spreading centre
Fault
Plate Motion
Gold-copper prospect/mine
High sulfidation Au-Cu
Low sulfidation Au-Cu
Sediment hosted replacement Au
Porphyry Cu-Au
Skarn Cu-Au
See enlargements for Au/Cu occurrences.
COROMANDEL PENINSULA
0 20 km
Coromandel
Koatuna
Lookout Rocks
Ohio Creek
Ohui
Thames
Golden Cross
Hauraki Graben
Waihi
Karangahake
(Martha Hill)
Tui
0 500 km
Mt Kren
Simberi/Tabar
Lihir
New Ireland
Feni
Otong Java Plateau
Frieda R /Nena
Grasberg Ertsberg
Ok Tedi
Lagaip F
Porgera
Mt Kare
Markham Fault
Yandera
Bilimoia
Wafi
Bulolo Graben
Wau
Owen
Tolukuma
Stanley Fault
Wild Dog Maragorik
Talasea
New Britain
Bougainville
Panguna
Wapolu
Woodlark
Misima
Gold Ridge
94514

Mesothermal deposits are described by Lindgren (1922) as "formed ... at intermediate temperature and pressure" and in this classification includes those which developed at temperatures higher than for epithermal deposits, that is >300°C (Hayba et al. 1985). Morrison (1988) also uses Lindgen's mesothermal term for veins of the Charters Towers district, eastern Australia, while Henley and Berger (1993) recognise the difficulties of continuing with the term epithermal for a range of deeper deposits such as Kelian, Indonesia (Section 7.iii.j). Southwest Pacific rim mesothermal deposits are described herein as quartz-sulfide gold ± copper (including Charters Towers) or carbonate-base metal gold (including Kelian), in order to avoid confusion with the use of the term mesothermal with Slate Belt and Mother Lode deposits (Hodgson, 1993), to which the quartz-sulfide deposits may be related (Morrison, 1988). The quartz-sulfide gold + copper and carbonate-base metal gold deposits may form resources of considerable size and moderate gold grades (Fig. 1.3).

Epithermal deposits form at shallow depths and temperatures less than 300°C (Hayba et al. 1985) and encompass a variety of low and high sulfidation deposits. Some, mainly low sulfidation, display elevated silver contents and others are characterized by bonanza metal grades exceeding 30 g/t Au (Fig. 1.3). Higher metal grades are amenable to underground mining of deposits, which commonly form fissure veins, particularly in environmentally sensitive settings (e.g., Hishikari, Japan).

The different styles of southwest Pacific rim gold-copper systems are therefore classified as:

* Porphyry-related which includes:
    # porphyry copper-gold
    # skarn copper-gold
    # breccia gold-copper
    # porphyry (and alkaline) gold

* High sulfidation gold-copper. Although commonly described as epithermal in the geological literature, high sulfidation systems extend to the mesothermal and porphyry regimes, and vary from:
    # barren porphyry shoulders,
    # structurally controlled gold-copper,
    # lithologically controlled gold-copper,
    # composite structurally-lithologically controlled gold-copper,
    # hybrid systems high-low sulfidation gold,
    # exhalative gold.

* Low sulfidation systems are grouped as:
    # porphyry-related deposits demonstrate the closest relationship to a magmatic source and form a continuum to progressively shallow crustal levels and away from the intrusion source as:
        # quartz-sulfide gold ± copper,
        # carbonate-base metal gold,
        # epithermal quartz gold-silver,
    # sediment-hosted replacement gold,
    # adularia-sericite epithermal gold-silver systems are subdivided with increasing depth as:
    # sinter and hydrothermal breccia gold-silver (hot spring deposits in Sillitoe, 1993b),
    # stockwork quartz vein gold-silver,
    # fissure vein gold-silver,

Many of these terms are defined below, and the characteristics of different deposit types and some examples are summarised in Table 1.1.

iv) Fluid Characteristics

The physico-chemical characteristics of the hydrothermal fluids control the:

* type and quantity of metals transported,
* processes which produce mineralization,
* location of the mineralization,

whereas the characteristics of the host rock control the mechanisms of fluid flow (Hedenquist, 1987). A conceptual model for the transportation of fluids from a degassing magma to porphyry, high sulfidation and low sulfidation systems is illustrated in Figure 1.4 and the characteristics of high and low sulfidation systems compared in Table 1.2.

Country rocks become more competent (brittle) as a result of contact metamorphism during the initial emplacement of high level porphyry intrusions. Fracturing is initiated at the cooled margins of the intrusion and extends into the host country rocks. Cooling of the porphyry intrusion and the parent melt is accompanied by the progressive exsolution of dissolved salts, magmatic volatiles (mainly H_2O, SO_2, CO_2, H_2S, HF and HCl), and metals, and their transfer into the fractured carapace (Henley and McNabb, 1978). Dispersion and mixing of these magmatic fluids with circulating meteoric-dominated fluids, results in the zoned alteration and mineralization which characterizes porphyry copper deposits (Henley and McNabb, 1978; e.g., Grasberg and Batu Hijau in Indonesia; Ok Tedi and Panguna in Papua New Guinea). Skarns form where mineralizing porphyry intrusions are emplaced into calcareous host rocks (e.g., Ertsberg, Indonesia; Frieda River Copper, Papua new Guinea; Red Dome, eastern Australia).

Volatiles may become overpressured where confined within the intrusion. Tectonic movements may fracture the carapace and facilitate venting which causes the formation of breccia bodies (e.g., Kidston, eastern Australia) and fracture systems which host later mineralized magmatic fluids.

<u>High sulfidation</u> gold-copper deposits form if magmatic volatiles (SO_2, CO_2, H_2S, HCl, HF) and brines are channelled from the source intrusion up deep seated fracture/fault zones and rise rapidly with minimal rock reaction or mixing with circulating meteoric fluids. The progressive disproportionation of magmatic SO_2 into H_2S and H_2SO_4 within the vapour plume, occurs at temperatures below approximately 400^oC, and as the temperature decreases, increasing amounts of H_2SO_4 and H_2S are produced (Rye et al., 1992). H_2SO_4 and HCl are inferred to start to dissociate at temperatures of around 300^oC (Hedenquist and Lowenstern, 1994), and progressively form hot acidic fluids as a result of the transition from SO_2 to H_2SO_4. Within dilational structures and/or permeable lithologies, these hot acidic fluids mix with circulating meteoric waters and react with country rock to form gold-copper deposits (Rye, 1993). Initially Hedenquist (1987) termed these systems 'high sulfidation' as sulfur is in a high oxidation state of +4, because of the dominance of magmatic SO_2. However, more recently (Hedenquist et al., 1994; White and Hedenquist, 1995), the term high sulfidation has been used to indicate the presence of the relatively high sulfidation state sulfide minerals such as enargite, luzonite and tennantite in these systems. The abundance of sulfur cannot be used solely as a criteria to distinguish between low and high sulfidation systems. Although sulfur species are commonly abundant in most southwest Pacific high sulfidation systems, some low sulfidation systems are sulfur-rich (e.g., Ladolam, Papua New Guinea). Examples of high sulfidation gold-copper deposits include: Lepanto, Philippines; Nena and Wafi, Papua New Guinea; Mt Kasi, Fiji; Gidginbung and Peak Hill, eastern Australia.

DEPOSIT TYPE	STYLES	EXAMPLES	GEOLOGICAL SETTING	STRUCTURE	ALTERATION	VEIN PARAGENESIS	MINERALIZATION
Adularia-sericite Epithermal Au-Ag	Sinter/breccia	Champagne Pool, Puhipuhi, Osorezan	Fluid upflow zones within dilational settings, controlled by regional structures varying from fissures at depth to shallow stockworks. Eruption breccias common Back-arc basins	Brecciated sinter	Shallow argillic/ advanced argillic to deep argillic/phyllic and marginal propylitic	Polyphasal sinters -> veins ->breccias	Electrum, cinnabar realgar, stibnite
	Stockwork/ fissure veins	Hishikari, Golden Cross, Waihi, Sado, Pajingo		Stockwork vein/breccia grades downwards to locally brecciated and banded fissure veins.		Colloform/crustiform veins: i) quartz-adularia -bladed calcite ii) fine-coarse quartz iii) quartz-clay-carbonate sulfates	Electrum, silver, Ag-sulfosalts/sulfides, chalcopyrite+Au-Ag-tellurides/selenides
Porphyry - Related Low Sulfidation	Quartz-sulfide gold ± copper	Ladolam, Kidston, Hamata, Bilimola, Arakompa, Exiban, Kerimenge	Peripheral to intrusions in pre-existing structures commonly with hydrothermal breccias.	Fissure or sheeted veins and fluidized breccias.	Phyllic overprinting propylitic/potassic	Veins: i) hematite-magnetite ii) quartz-pyrite -pyrrhotite-As-pyrites iii) chalcopyrite	Gold, pyrite, pyrrhotite arsenopyrite chalcopyrite hematite, magnetite, Pb-Bi-Cu-Te phases
	Carbonate-base metal gold	Kelian, Porgera, Mt Kare, Hidden Valley, Edie Ck, Misima, Maniape, Gold Ridge, Acupan, Woodlark, Karangahake	Locally with intrusion centres, commonly diatreme breccias	Dilational fractures, fissure veins commonly in association with diatreme or milled matrix fluidized breccias. Strongly dilated fissure or sheeted veins.	Phyllic overprinting propylitic	Veins and breccias: i) quartz-adularia/sericite ii) sulfides iii) carbonates	Gold, pyrite sphalerite, galena, chalcopyrite, tennantite/tetrahedrite
	Epithermal quartz gold-silver	Tolukuma, Porgera Zone VII, Emperor, Mt Kare, Cracow	Commonly with carbonate-base metal gold systems distal to intrusions.		Phyllic/argillic overprinting propylitic, late advanced argillic	Veins and breccias: i) quartz-sulfides ii) quartz-adularia/carb iii) quartz-chlorite-illite	Gold, pyrite sulfosalts, Au-Ag tellurides & selenides, Cu-Pb-Zn sulfides, hematite
	Sediment-hosted replacement gold	Bau, Mesel	Hosted in impure limestone, extensional structures important.	Structural control to fluid upflow and lithological control to fluid outflow.	Decalcification, dolomitization and silicification	Fluidized breccias: i) quartz-pyrite ii) quartz-As-pyrites	Pyrite, As-pyrite, arsenopyrite, stibnite, orpiment, realgar
High Sulfidation	Porphyry shoulder	Horse Ivaal, Lookout Rocks, Vuda, Cabang Kiri	Regional structures control intrusion emplacement, and dilational structures, host rock permeability and focus fluid from upflow into outflow zones	Alteration and mineralization zonations influenced by host rock permeability and dilational structures; ore commonly occurs as breccia matrix	Zoned potassic, phyllic, to advanced argillic	Replacement dominated	Barren to very low grade; covellite-pyrite +enargite
	Structurally Controlled	Nena, Lepanto, Mt Kasi			Core silicic, and advanced argillic, marginal argillic, to peripheral propylitic	Veins and fluidized breccias: i) quartz ii) alunite, barite iii) pyrite iv) Cu-sulfides	Vertically zoned: covellite, enargite, luzonite, tennantite, goldfieldite lateral zones: as above outward to tennantite, chalco., base metal sulfides
	Lithologically Controlled	Wafi, Nansatsu, Miwah					
	Composite Structural and Lithological	Sangihe, Peak Hill, Maragorik					
Porphyry	Porphyry Cu-Au	Panguna, Ok Tedi Grasberg, Batu Hijau Frieda River, Cadia, Goonumbla, Yandera, FSE, Dizon	Regional structure control to intrusion emplacement as splays in accretionary structures or along transfer structures, subsurface batholith topography influences breccia intrusion	Sheeted veins important and fracture mineralization at intrusive margins and breccia matrix infill	Early potassic to peripheral propylitic; late phyllic, then argillic overprints	Stockwork/sheeted: i) quartz ii) silicates iii) Fe-oxides -> sulfides iv) carbonates/sulfates	Vertical zones: chalco.-mag., to chalco.-bornite-Au-pyrite, to pyrite ± chalco.
	Skarn	Ertsberg, Ok Tedi			Zoned isothermal, overprinted by metasomatic, and late retrograde	Veins: i) garnet-pyroxene-etc. ii) magnetite iii) chlorite-sericite-quartz iv) carbonates	As porphyry Cu-Au
	Breccia Au	Kidston, Mt Leyshan			As quartz-sulfide gold		As quartz-sulfide-gold
	Alkaline/Porphyry Au-Cu	Porgera, Lihir, Emperor/ Dinkidi			Potassic, overprinted by successive phyllic, and argillic	Stockwork/sheeted: i) quartz-magnetite ii) Ca-, Na-, K-silicates iii) sulfides iv) carbonates, sulfates	As-porphyry Cu-Au

TABLE 1.1 Pacific rim gold-copper systems - Summary of characteristics and examples

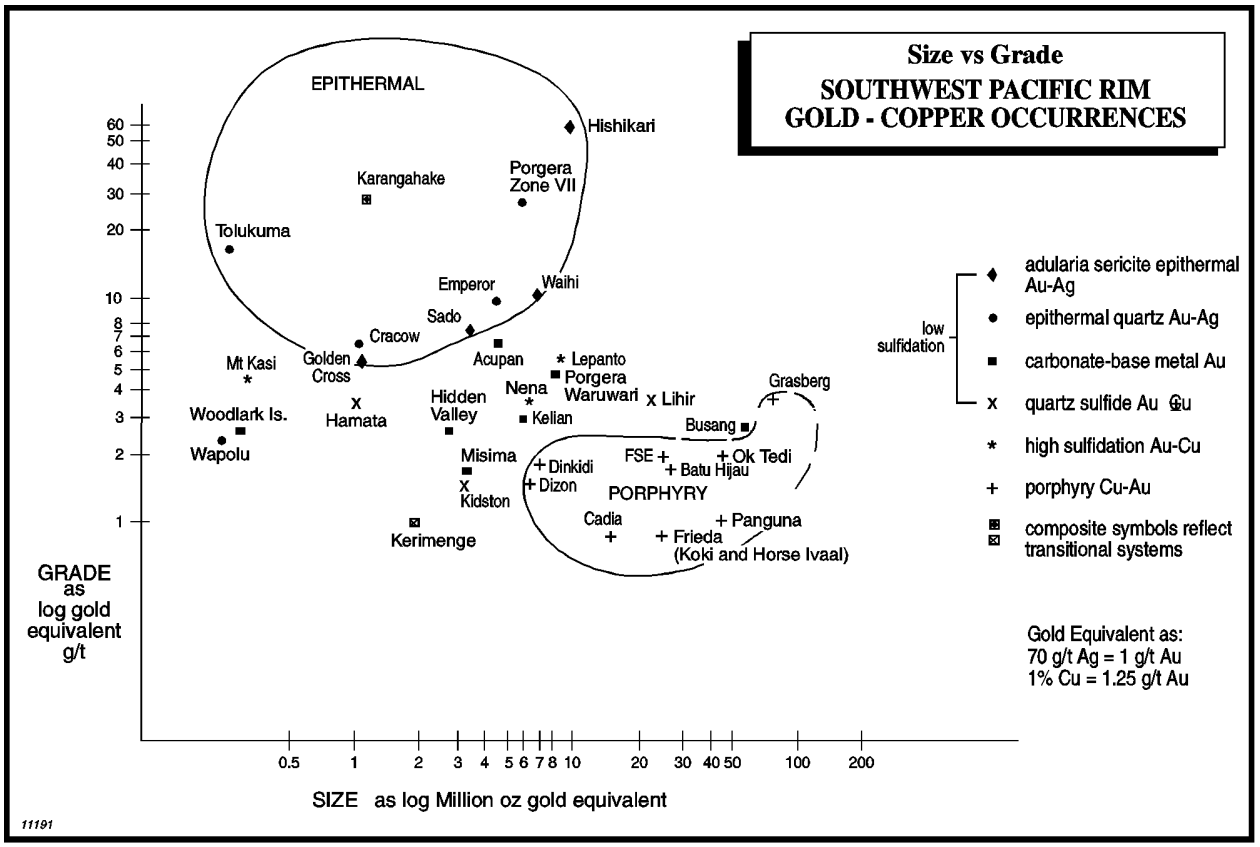
Size vs Grade
SOUTHWEST PACIFIC RIM
GOLD - COPPER OCCURRENCES
EPITHERMAL
Hishikari
Karangahake
Porgera Zone VII
Tolukuma
Emperor
Waihi
Sado
Cracow
Mt Kasi
Golden Cross
Acupan
Lepanto
Porgera
Nena
Waruwari
Lihir
Grasberg
Hamata
Hidden Valley
Kelian
Woodlark Is.
Wapolu
Busang
Misima
Dinkidi
FSE
Ok Tedi
Batu Hijau
Dizon
Kidston
PORPHYRY
Cadia
Panguna
Kerimenge
Frieda
(Koki and Horse Ivaal)
GRADE as log gold equivalent g/t
SIZE as log Million oz gold equivalent
low sulfidation
adularia sericite epithermal Au-Ag
epithermal quartz Au-Ag
carbonate-base metal Au
quartz sulfide Au Cu
high sulfidation Au-Cu
porphyry Cu-Au
composite symbols reflect transitional systems
Gold Equivalent as:
70 g/t Ag = 1 g/t Au
1% Cu = 1.25 g/t Au
11191

FIG. 1.3

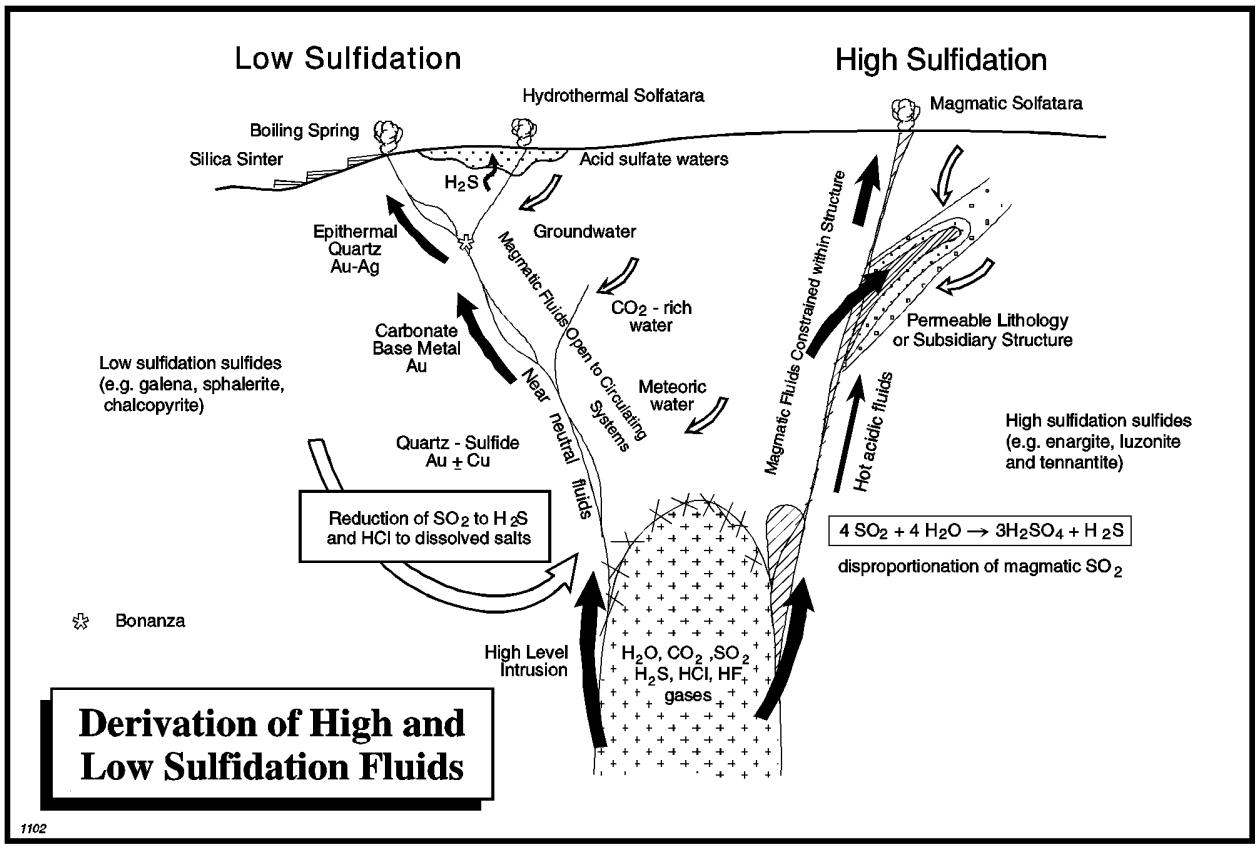
Low Sulfidation
High Sulfidation
Hydrothermal Solfatara
Magmatic Solfatara
Boiling Spring
Silica Sinter
Acid sulfate waters
H2S
Epithermal Quartz Au-Ag
Groundwater
Magmatic Fluids Open to Circulating Systems
CO2 - rich water
Carbonate Base Metal Au
Magmatic Fluids Constrained within Structure
Permeable Lithology or Subsidiary Structure
Low sulfidation sulfides (e.g. galena, sphalerite, chalcopyrite)
Meteoric water
Near neutral fluids
Hot acidic fluids
High sulfidation sulfides (e.g. enargite, luzonite and tennantite)
Quartz - Sulfide Au ± Cu
Reduction of SO2 to H2S and HCl to dissolved salts
4 SO2 + 4 H2O → 3H2SO4 + H2S
disproportionation of magmatic SO2
Bonanza
High Level Intrusion
H2O, CO2, SO2, H2S, HCl, HF gases
Derivation of High and Low Sulfidation Fluids
1102

FIG. 1.4

In low sulfidation systems, magmatic fluids which contain dissolved reactive gases, are reduced by rock reaction and dilution by circulating meteoric waters (Simmons, 1995). This reduction results in a fluid dominated by dissolved salts (mainly NaCl) and by H_2S as the main sulfur species, and is interpreted (Giggenbach, 1992) to occur at the roots of low sulfidation systems, where circulating meteoric waters acquire magmatic volatiles and probably metals. In this case the sulfur is present at an oxidation state of -2 (dominated by H_2S) and was therefore termed by Hedenquist (1987) as 'low sulfidation'. More recently (e.g., White and Hedenquist, 1995), the term 'low sulfidation' has been used to indicate the deposition of low sulfidation sulfide minerals (such as sphalerite, galena, chalcopyrite), from these reduced, near-neutral pH fluids. Under these reduced conditions, sulfides are the only secondary sulfur-bearing minerals, with pyrrhotite dominant above 300°C, and pyrite at lower temperatures (Giggenbach, 1987). Low sulfidation gold and gold-silver deposits include: Lihir and Porgera, Papua New Guinea; Kelian, Indonesia; Kidston, eastern Australia; Golden Cross and Waihi, New Zealand; Hishikari, Japan.

It is interpreted herein, that there is an evolution from porphyry to low sulfidation-style fluids through progressive mixing of the magmatic-derived fluid with circulating fluids and water-rock reaction. The mixing of low sulfidation, mineralized fluids with circulating fluids of different physico-chemical characteristics produces deposits which are zoned vertically and horizontally with relation to the source intrusion, from proximal high temperature to cooler distal settings as: quartz-sulfide gold $\pm$ copper, to carbonate-base metal gold, and epithermal quartz gold-silver. Adularia-sericite epithermal gold-silver systems are formed mainly from circulating boiling meteoric waters and are characterized by the presence of banded quartz, adularia and quartz pseudomorphing platy carbonate. However, a significant proportion of the gold mineralization in these systems is interpreted herein to have deposited as a result of the quenching of circulating fluids, which have incorporated the metals from deep magmatic sources.

DISTINCTION between HIGH and LOW SULFIDATION		
	Low Sulfidation	High Sulfidation
Fluid	Dilute H_2S-dominant	Saline, SO_2-dominant
Alteration	Generally neutral alteration adjacent to structures dominated by sericite/illitic clays → peripheral propylitic veins dominated by quartz ± carbonate	Characteristic zoned pervasive acid alteration from: residual (vughy) quartz → alunite → kaolin minerals → illite minerals → propylitic
Associated minerals	Low % pyrite galena, sphalerite, chalcopyrite	High % pyrite engarite - luzonite
Metals : Economic Accessory	Au ± Ag Pb, Zn, Cu As, Te, Hg, Sb at high levels	Au ± Cu As Te at high levels
Gold fineness	Variable fineness with depth high fineness (silver-poor) at depth low fineness (silver-rich) at high levels	High fineness (silver-poor)
Form of mineralization	Veins common with crystalline phases at depth, banded at shallow levels	Matrix to brecciated hosted in competent wall rock alteration
Structure	Pre-existing fractures at depth Subsidiary dilational structures at higher levels Magmatic, diatreme and eruption breccias	Dilational structural and permeable lithological control Diatreme breccias common
11153		

Table 1-2

2 GEOTHERMAL ENVIRONMENT FOR SOUTHWEST PACIFIC GOLD-COPPER

i) Settings of Active Hydrothermal-Geothermal Systems

Geothermal systems studied over the past two decades provide an increased understanding of the processes which take place during the formation of hydrothermal ore deposits. Geothermal systems are encountered in a wide range of geological settings and each one may be analogous to a distinct style of ore-forming system. These can be classified in terms of their crustal setting and probable heat source (e.g., Henley, 1985a; Fig. 2.1).

Magmatic-sourced oceanic geothermal systems occur in association with: oceanic crust along mid-ocean ridges, ocean island volcanoes formed in relation to hot spots, back-arc basins, and volcanic arcs along inter-oceanic subduction zones (de Ronde, 1995). Exhalative features associated with sea floor geothermal systems, such as sulfide-rich black smokers, are interpreted to be analogous to volcanogenic massive sulfide or Kuroko-style ore deposits (Binns et al., 1993, 1995).

Active hydrothermal systems which have a magmatic heat source may be associated with crustal rifting within a continental crust, either in back-arc rift zones (e.g., Taupo Volcanic Zone, New Zealand), or in continental rift zones (e.g., East African Rift). As will be shown later in this section, these types of geothermal systems have a geological setting and fluid chemistry comparable to the circulating meteoric waters associated with adularia-quartz vein systems which host epithermal gold-silver deposits (e.g., Waihi and Golden Cross, New Zealand).

Geothermal systems encountered in magmatic arcs associated with subducting oceanic crust (e.g., Philippines, Indonesia) are actively forming porphyry-related systems. These systems form porphyry and skarn copper-gold ($\pm$ molybdenum), high sulfidation gold-copper, and mesothermal to epithermal precious and base metal deposits.

Geothermal systems are also encountered in continental environments in the absence of any obvious magmatic heat source. Rapid uplift results in high geothermal gradients which may facilitate the leaching of metals from a thick sedimentary pile by circulating meteoric waters. Fluids migrate along major fault zones associated with plate collisions (e.g., along the Alpine fault, South Island, New Zealand), and deposit gangue minerals and metals in dilational structural settings as post-metamorphic gold veins (e.g., Macraes Flat, South Island, New Zealand). Overpressuring in response to rapid deposition in thick sedimentary basins (e.g., southeast USA) results in the establishment of circulating hydrothermal systems and these may be related to Mississippi Valley-style massive sulfide deposits (Henley, 1985a).

ii) Silicic Continental and Volcanic Arc Hydrothermal Systems

There are considerable differences in the geological setting and fluid characteristics between geothermal systems formed in silicic continental rift environments (e.g., New Zealand), and volcanic arc environments (e.g., Philippines; Henley and Ellis, 1983; Reyes, 1995). The geochemistry of representative wells and surface springs from selected Philippine and New Zealand geothermal systems is given in Table 2.1.

In geothermal systems typical of those encountered in silicic rift environments, the heat source is considered to be deeply buried (>5-6 km) batholiths (Hedenquist, 1986), of inferred granite/granodiorite composition, which formed from melted continental crust (Henley, 1985b; Fig. 2.2). Water recharge is derived from meteoric ground waters and the intrusion supplies heat, chloride, some gases, and possibly other elements. The resultant fluid is commonly termed chloride reservoir or chloride hydrothermal fluids in geothermal sciences. Boiling occurs at shallow levels in response to reduced pressure and forms near-surface two phase zones. The upwelling

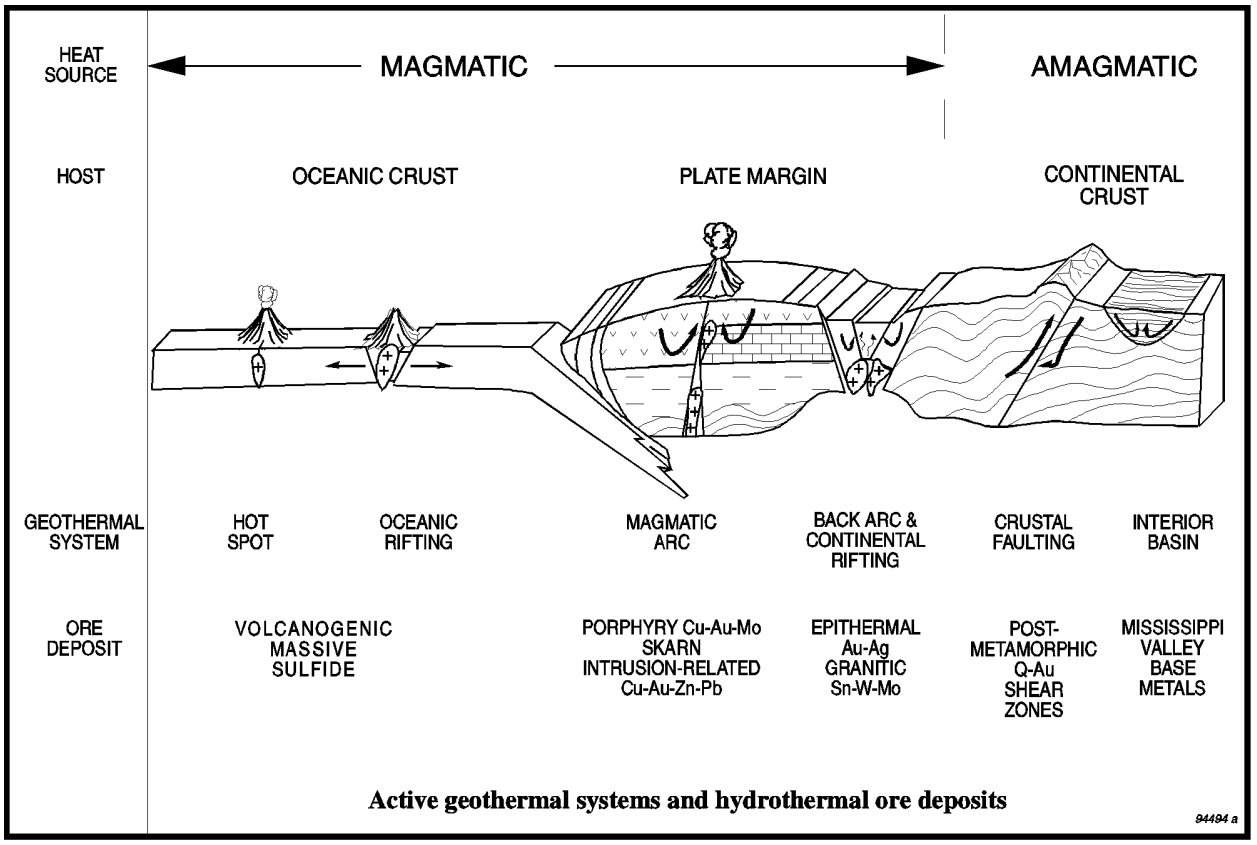
HEAT SOURCE
MAGMATIC
AMAGMATIC
HOST
OCEANIC CRUST
PLATE MARGIN
CONTINENTAL CRUST
GEOTHERMAL SYSTEM
HOT SPOT
OCEANIC RIFTING
MAGMATIC ARC
BACK ARC & CONTINENTAL RIFTING
CRUSTAL FAULTING
INTERIOR BASIN
ORE DEPOSIT
VOLCANOGENIC MASSIVE SULFIDE
PORPHYRY Cu-Au-Mo SKARN INTRUSION-RELATED Cu-Au-Zn-Pb
EPITHERMAL Au-Ag GRANITIC Sn-W-Mo
POST-METAMORPHIC Q-Au SHEAR ZONES
MISSISSIPPI VALLEY BASE METALS
Active geothermal systems and hydrothermal ore deposits
94494 a

FIG. 2.1

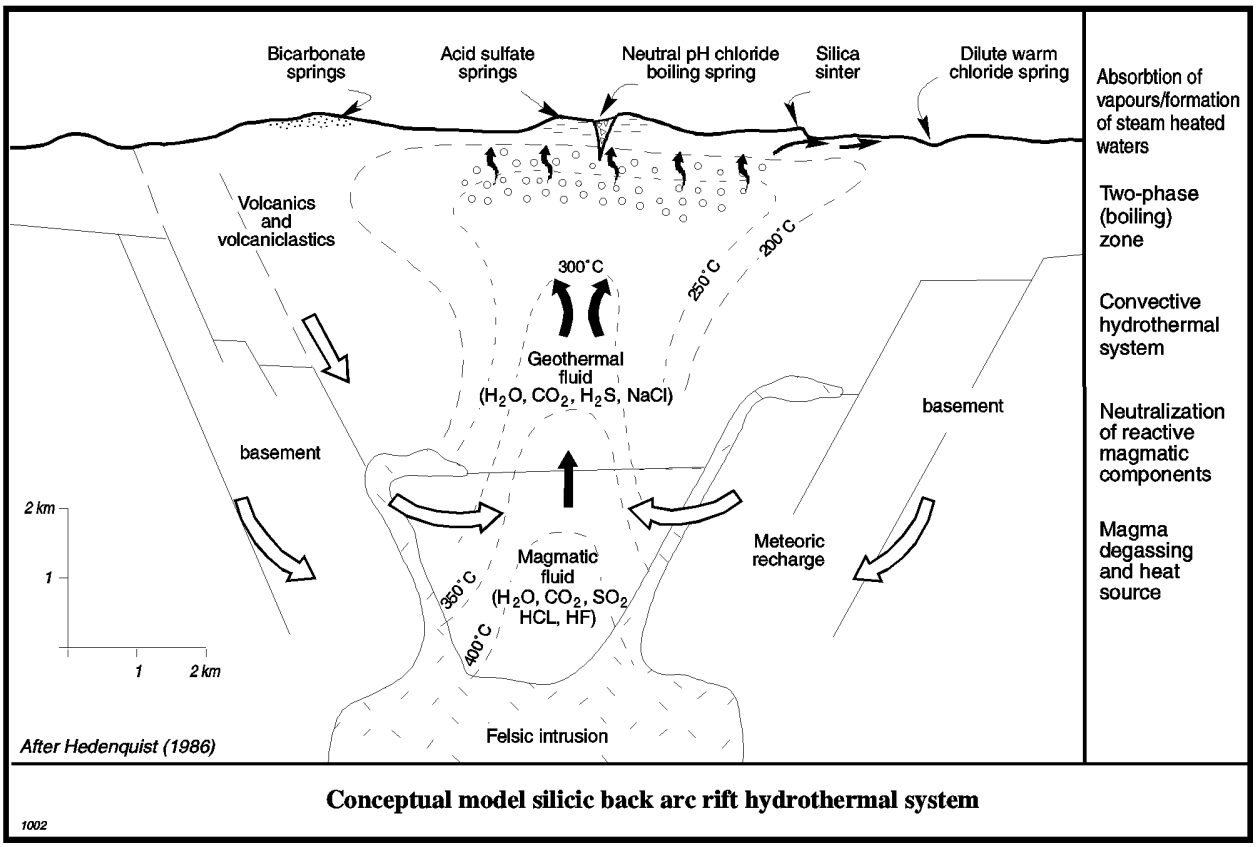
Bicarbonate springs
Acid sulfate springs
Neutral pH chloride boiling spring
Silica sinter
Dilute warm chloride spring
Absorbtion of vapours/formation of steam heated waters
Two-phase (boiling) zone
Convective hydrothermal system
Neutralization of reactive magmatic components
Magma degassing and heat source
Volcanics and volcaniclastics
300°C
250°C
200°C
Geothermal fluid (H_2O, CO_2, H_2S, NaCl)
basement
basement
2 km
1
1
2 km
Meteoric recharge
Magmatic fluid (H_2O, CO_2, SO_2 HCL, HF)
350°C
400°C
Felsic intrusion
After Hedenquist (1986)
Conceptual model silicic back arc rift hydrothermal system
1002

FIG. 2.2

chloride hydrothermal fluid, or chloride reservoir, generally reaches the surface as boiling springs, which deposit silica sinters either above the main upflow zone associated with hydrothermal eruption craters (e.g., Champagne Pool, Waiotapu, and Ohaaki Pool, Broadlands in New Zealand; Hedenquist, 1990: Table 2.1), or in outflow zones (e.g., Orakeikorako, New Zealand; Sheppard and Lyon, 1984; Simmons et al., 1992). Minor zones of acid sulfate fluids result from the oxidation of H_2S in surface ground waters (e.g., Rotokawa, New Zealand; Krupp and Seward, 1987: Waimangu, New Zealand; Simmons et al., 1992). CO_2-rich waters form at shallow levels where the gas is absorbed into cool hydrothermal fluids or ground water, and the recharge of these waters to depths of up to 1200 m has been recorded at the margins of the Broadlands geothermal field, New Zealand (Hedenquist, 1990).

Active hydrothermal systems associated with volcanic arc terrains display a number of characteristics which are significantly different from those in continental silicic environments (Henley and Ellis, 1983; Reyes, 1995; Figs. 2.2, 2.3). In these systems meteoric recharge is typically heated by multiple shallow (<2-3 km) porphyry intrusions, which contribute significant amounts of magmatic gases, solutes, and metals to the circulating hydrothermal system (Henley and McNabb, 1978). The upwelling neutral chloride fluids do not reach the surface above the upflow zones (Bogie and Lawless, 1987). This may be due to: sealing caused by silicification and carbonate/sulfate deposition at the interface between surficial and chloride fluids (see below), the presence of good horizontal permeability, or insufficient pressure in the chloride reservoir. Horizontal permeability can be provided by either regional or subsidiary structures, or porous pyroclastic units. The topography in volcanic terrains above the upflow zones is typically steep, and therefore the pressure (gas + hot hydrostatic) is insufficient to overcome this high hydrostatic head. Rather, the chloride reservoir fluids flow laterally for up to 5-10 km to lower elevations, commonly near sea level (Bogie et al., 1987; see Cambucal Spring chemistry, Table 2.1). In some cases drilling has not encountered circulating chloride hydrothermal waters until up to 500-1000 m below surface.

Fluid chemistry of the deep circulating hydrothermal fluid is also significantly different between silicic continental (New Zealand) and magmatic arc (Philippines) geothermal systems (Reyes, 1995; Table 2.1). Philippine geothermal systems locally contain up to 50 percent magmatic component, whereas New Zealand geothermal systems commonly contain <3-4 percent magmatic component (Reyes et al., 1993). The fluids in New Zealand systems are dilute ($\leq$ 1000-2000 ppm Cl), whereas the Philippine systems are almost an order of magnitude more saline (up to $\geq$ 10,000-15,000 ppm Cl). In addition, the Philippine systems generally exhibit a significantly higher dissolved gas content. The apparent salinity (actual salinity + dissolved gases) of Philippine active hydrothermal systems ranges from 2-6 wt percent NaCl, whereas the apparent salinity of New Zealand systems is generally <1 wt percent NaCl (Hedenquist and Henley, 1985b). These apparent salinities of Philippine geothermal systems are comparable to salinities which are derived from fluid inclusion analyses on veins in porphyry-related gold deposits (Section 7). On the other hand, the apparent salinity of fluids in New Zealand geothermal systems approximates the dilute fluid composition derived from fluid inclusion data on banded quartz-adularia veins which host epithermal gold-silver deposits (Hedenquist and Henley, 1985b).

The following section investigates the Philippine active porphyry systems in more detail as a guide to the understanding, exploration, and development of intrusion-related gold-copper ore systems.

iii) Characteristics of Active Philippine Intrusion-Related Hydrothermal systems

a) Physico-chemical zonations of Philippine geothermal systems

The following four distinct physical and chemical zones have been identified (Mitchell and Leach, 1991) in active Philippine hydrothermal systems (Fig. 2.3):

a) Well Analyses

	Location	Well No. (25˚C)	Water Concentrations (mg/kg)											Gas Chemistry (mmol/100 mol)	
			pH	Li	Na	K	Ca	Mg	Cl	SO_4	B	SiO_2	HCO_3	CO_2	H_2S
Philippines	Bacon-Manito	CN-1	7.7	7.57	4486	914	172	0.07	8668	22.5	36.8	797	2.29	43	1.06
		CN-1 (1400m)	3.1	b.d.	1130	104	4.5	17.2	833	1955	10.7	n.d.	n.d.	n.d.	n.d.
	Tongonan	407	6.8	34.0	8635	2666	184	0.28	16505	41	399	1148	b.d.	697	11.0
		402	4.0	10.0	4041	617	58	68	6500	2270	152	522	b.d.	3850	73
	Alto Peak	AP-1D	7.3	21.4	6335	1216	685	5.00	12515	36	190	633	137	928	16.6
	Biliran	BN-1	8.36	2.7	2947	101	2.7	0.14	3936	122	24	421	1085	1522	5.7
		BN-3	3.0	2.49	1409	332	2.7	45.8	2526	3176	323	1252	b.d.	1191	151
	Palinpinon	OK-7	7.62	18.2	3950	1000	117	0.09	7232	35.5	86.8	1122	43	434	10.5
	Amacan	AM-1	7.9	3.5	1374	289	24.0	1.2	2183	57	112	835	163	8290	134
	Daklan	DK-1	7.16	29.8	7278	1968	250	1.88	14110	54.7	156	629	18	1526	10.8
New Zealand	Broadlands	BR-13	8.60	12.9	990	200	2.8	0.11	1664	2.5	48.6	780	168	262.8	6.00
		BR-6 (850m)	7.08	1.3	500	40.9	7.3	56	25	19	b.d.	170	1786	n.d.	n.d.
	Wairakei	W24	8.3	n.d.	1250	219	12	0.04	2210	28	28.8	670	23	5.5	0.26

Water phase analyses for samples separated from steam at atmospheric pressure and local boiling temperatures.
Gas analyses expressed as concentrations of gas in total discharge composition (i.e. concentration in reservoir brines prior to boiling occurence).
Philippine well data from Mitchell and Leach (1991) with permission from PNOC; Broadlands well data from Hedenquist (1990).
Wairakei well data from Henley et al. (1984). Waireki gas data is field average.
n.d. not determined; b.d. below detection.

b) Spring Analyses

Location		pH	Li	Na	K	Ca	Mg	Cl	SO_4	B	SiO_2	HCO_3
Palinpinon	Cambacal (92.5˚C)	7.87	8.3	1887	167	175	5.5	3500	64	40.4	175	58
	Malaunay (49˚C)	7.87	0.02	41	4.5	390	23	2.1	778	0.04	75	216
	Ilijan (39.5˚C)	2.83	0.05	14.5	2.6	60	7.1	0.3	480	0.13	85	n.d.
Waiotapa	Champagne Pool (99˚C)	8.20	n.d.	1070	102	26	0.4	1770	26	21.9	294	76
Broadlands	Ohaaki Pool (95˚C)	7.1	n.d.	860	82	2.5	0.1	1060	100	32	338	679

Concentrations are in mg/kg; Palinpinon spring date from Ward (1980); Waiotapu and Broadlands spring data from Henley et al (1984).

TABLE 2.1 Fluid geochemistry of selected Philippine and New Zealand geothermal systems.

1449

1. A Conductive zone is encountered at depth in many systems, typically within impermeable intrusions or basement sediments. Heat transfer is predominantly by conduction due to lack of fracturing. Where high-level intrusions have been emplaced into volcanic rocks, impermeable contact metamorphic mineral assemblages comprise biotite-magnetite and clinopyroxene ± amphibole ± biotite. Local skarn mineral assemblages are encountered at contacts between intrusions and calcareous sediments (e.g., Alto Peak, Leyte; Fig. 2.7: Palinpinon, Southern Negros; Figs. 2.11, 2.12).

2. A Convective zone forms within the upwelling plume of all Philippine geothermal systems, within permeable deep-seated fault zones and shatter zones at the intrusion contacts. The reservoir fluid is commonly slightly less than neutral pH (<5-6, at 250°C) due to significant dissolved gas contents, and is saturated with respect to quartz (Henley et al., 1984). The alteration exhibits a zonation from: potassic (predominantly biotite with minor secondary feldspar) alteration at depth, to various propylitic alteration zones dominated by actinolite, epidote, or chlorite-zeolites at progressively shallower levels.

3. A Two-Phase zone is encountered at shallow levels and in outflow zones where the vapour pressure exceeds the confining pressure, and results in exsolution of water vapour and other gases (mainly CO_2, and lesser amounts of H_2S) from the hydrothermal fluid. This gas exsolution (or boiling) can be initiated at depths of 2 km or more in some systems (Bogie and Lawless, 1987). Absorption of these gases at shallower levels, into cool hydrothermal waters or ground waters, results in the formation of moderately low pH, CO_2-rich waters.

4. A Phreatic zone (zone of saturation) comprises a number of ground water aquifers which are perched above the chloride hydrothermal system (Fig. 2.3). CO_2 gases, which exsolved from the two phase zone at depth, are absorbed into these ground waters to produce CO_2-rich waters. The degassing of CO_2 at the surface produces neutral bicarbonate waters which commonly deposit travertine deposits (e.g., Amacan geothermal field, Mindanao; PNOC-EDC, 1985a).

The oxidation of H_2S gases, which are also derived from the two phase zone at depth, can only occur in the Vadose zone (i.e. the zone of aeration above the phreatic zone) where abundant free oxygen is available. The oxidation of H_2S upon contact with the atmosphere produces native sulfur in 'hydrothermal solfataras' by a series of reactions summarised as $H_2S + 1/2O_2 \rightarrow S^o + H_2O$ (Schoen et al., 1973). The oxidation of H_2S within aerated ground waters produces cool sulfuric acid, or 'acid sulfate waters', through a complicated series of reactions which can be summarised as $H_2S + 2O_2 \rightarrow H_2SO_4$ (Schoen et al., 1973; see Ilijan Spring chemistry, Table 2.1). Leaching of host rocks at the site of formation of the acid sulfate waters produces porous silica alteration which consists of amorphous silica, cristobalite and/or tridymite. Progressive neutralization in response to wall rock reaction and/or mixing with ground water forms zones of silica-alunite, silica-kaolinite and silica-smectite alteration (Schoen et al., 1973). Gypsum is commonly encountered with carbonates near surface in mixed bicarbonate/CO_2-rich and acid sulfate waters (Leach et al., 1986; see Malaunay spring analyses, Table 2.1).

Cool acid sulfate waters are also formed in a surficial supergene environments, where they are related to the oxidation of sulfides, and raised above the water table by tectonic uplift or exposed by erosion (Rye et al., 1992).

Steam-heated acid sulfate waters formed in the vadose zone and in supergene environments, are distinctly different from hot sulfuric acid in high sulfidation systems (Section 6). In these magmatic environments, SO_2 and HCl gases, which are exsolved from the crystallising melt, disproportionate and dissociate at shallower (i.e. cooler) levels to form hot acidic fluids (Rye, 1993; Hedenquist and Lowenstern, 1994). Where these magmatic fluids reach the surface directly 'magmatic solfataras' may develop. Geothermal drilling in the Philippines attempts to avoid intersection of these hot corrosive fluids, although as described below, exploration of Vulcan,

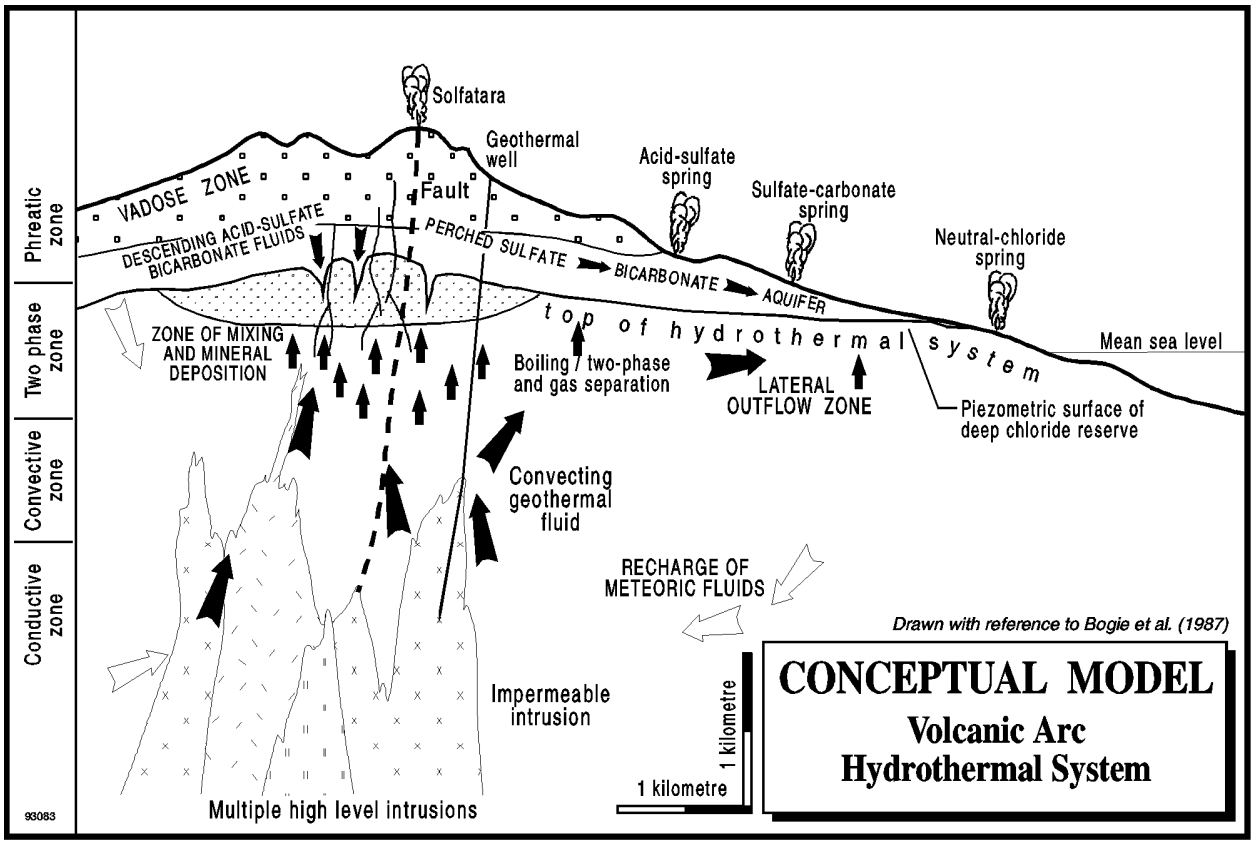
Phreatic zone
Two phase zone
Convective zone
Conductive zone
Solfatara
Geothermal well
Acid-sulfate spring
Sulfate-carbonate spring
Neutral-chloride spring
VADOSE ZONE
Fault
DESCENDING ACID-SULFATE BICARBONATE FLUIDS
PERCHED SULFATE
BICARBONATE
AQUIFER
top of hydrothermal system
Mean sea level
ZONE OF MIXING AND MINERAL DEPOSITION
Boiling / two-phase and gas separation
LATERAL OUTFLOW ZONE
Piezometric surface of deep chloride reserve
Convecting geothermal fluid
RECHARGE OF METEORIC FLUIDS
Drawn with reference to Bogie et al. (1987)
CONCEPTUAL MODEL
Volcanic Arc Hydrothermal System
Impermeable intrusion
1 kilometre
1 kilometre
Multiple high level intrusions
93083

FIG. 2.3

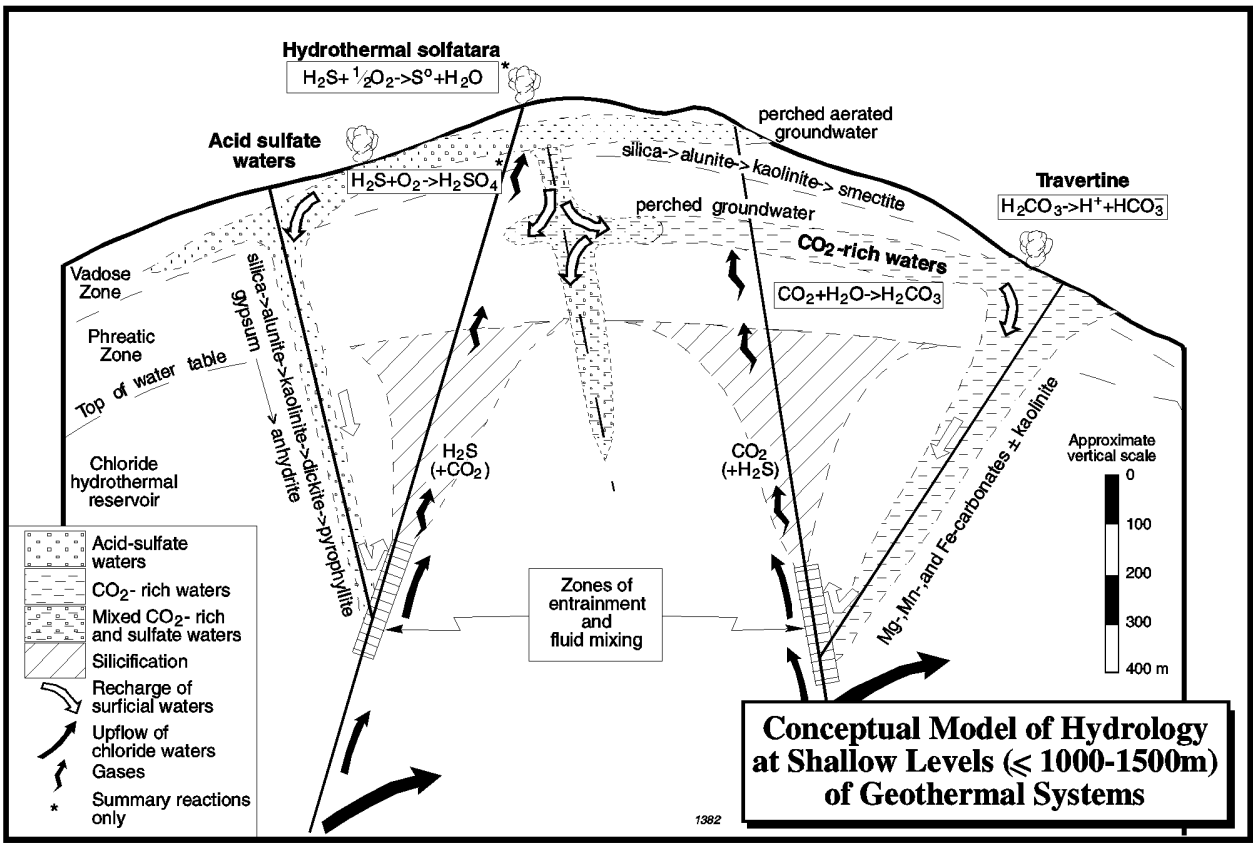
Hydrothermal solfatara
$H_2S+\frac{1}{2}O_2 \rightarrow S^o+H_2O$ *
Acid sulfate waters
$H_2S+O_2 \rightarrow H_2SO_4$ *
perched aerated groundwater
silica->alunite->kaolinite->smectite
perched groundwater
Travertine
$H_2CO_3 \rightarrow H^+ + HCO_3^-$
CO_2-rich waters
$CO_2+H_2O \rightarrow H_2CO_3$
Vadose Zone
Phreatic Zone
Top of water table
Chloride hydrothermal reservoir
silica->alunite->kaolinite->dickite->pyrophyllite
gypsum
anhydrite
H_2S (+CO_2)
CO_2 (+H_2S)
Mg-,Mn-,and Fe-carbonates ± kaolinite
Approximate vertical scale
0
100
200
300
400 m
Zones of entrainment and fluid mixing
Acid-sulfate waters
CO_2- rich waters
Mixed CO_2- rich and sulfate waters
Silicification
Recharge of surficial waters
Upflow of chloride waters
Gases
* Summary reactions only
Conceptual Model of Hydrology at Shallow Levels (≤ 1000-1500m) of Geothermal Systems
1382

FIG. 2.4

Biliran Island, has encountered magmatic-derived acidic fluids at around 1 km from the surface. Recent drilling at Alto Peak (Reyes et al., 1993) and Mt. Pinatubo (Ruaya et al., 1992) intersected zones which were dominated by magmatic acid fluids.

b) Waning stages of the active Philippine systems

As intrusions cool and hydrothermal systems wane, the decrease in temperature and reservoir pressure results in draw down of surficial waters deep into the hydrothermal system. Cool, low pH CO_2-rich and acid sulfate waters have been encountered at depths up to 2000 m in some Philippine geothermal fields (Reyes, 1990b). Down-hole pressure/temperature (Leach et al., 1986), geochemical (Lawless et al., 1983), and stable isotope analyses (Robinson et al., 1987) of these waters have confirmed that they are derived from perched aquifers in the phreatic and vadose zones.

Mixing of cool, descending, low pH sulfate and/or CO_2-rich surficial fluids with hot silica-saturated deep hydrothermal fluids (Fig. 2.4) results in deposition of carbonates and sulfates (in response to increasing temperatures) and silicification (in response to cooling; Leach et al., 1986). As the hydrothermal systems are invariably located in tectonically active areas, major fracture/fault systems may be continually reopened, permitting descent of surficial fluids to progressively deeper levels. The overall effect of this is to seal most permeable features and form impermeable caps in the upper levels of these hydrothermal systems (Bogie and Lawless, 1987).

Acid sulfate waters have been encountered at significant depths channelled down permeable structures (e.g., up to 1500 m below the surface in the Bacon Manito geothermal field; Reyes, 1990a). The waters maintain, to some extent, their acidity to these depths due to isolation from the deep neutral chloride fluids, possibly by brought about by wall rock alteration and mineral deposition within the structures. The vertical zonation within these structures, from shallow to deeper levels of: gypsum to anhydrite, and of alunite --> alunite + kaolinite --> dickite --> pyrophyllite + diaspore in these structures (Leach et al., 1986; Reyes, 1990a), is indicative of progressive heating and neutralization of descending acid sulfate waters.

Evidence for the incursion of CO_2-rich waters into the chloride hydrothermal system is provided by the occurrence of dolomite, siderite and ankerite at depth in some Philippine geothermal systems (Leach et al., 1983; Reyes, 1990b). In New Zealand, the identification of siderite + kaolinite at depths of up to 600-1200 m on the margins of the Broadlands geothermal field (Hedenquist, 1990) and of Mn-carbonates at shallow levels in the Rotokawa geothermal field (Krupp and Seward, 1987), are also indicative of the draw down of CO_2-rich waters into the chloride reservoir.

The near-neutral chloride hydrothermal fluid is depleted in magnesium (generally <1 ppm; Table 2.1) and iron (<0.3-0.4 ppm; P.R.L. Browne, pers. commun.; Gunnlaugsson and Arnorsson, 1982) relative to calcium (>100-200 ppm for Philippine systems; Table 2.1). Although data on the manganese levels in geothermal systems are generally not available, the authors infer these to also be low, comparable to iron and manganese. On the other hand magnesium (and probably iron and manganese) is enriched in the low pH CO_2-rich and acid sulfate waters (Malaunay springs, Table 2.1), and in some feeder zones in wells (e.g., down hole samples at 1400 m in CN-1, Bacon Manito, and at 850 m in BR-6, Broadlands). The presence of Fe-, Mg- and Mn-carbonates to deep levels in active geothermal systems is therefore related to the incursion of CO_2-rich surficial waters. As calcium is common in both surficial and deep fluids, calcite can be deposited from both types of fluids (Simmons and Christensen, 1994).

It is interpreted herein that the descending acid sulfate and CO_2-rich waters are locally entrained in fractures which contain upwelling chloride fluids. The mixing of these fluids of substantially different fluid physico-chemistry results in the deposition of sulfates, carbonates and quartz to form mineral deposits, in a

similar manner to the deposition of these phases within geothermal wells (Reyes, 1990b). It is proposed herein that this mixing is a significant mechanism in metal deposition in intrusion-related hydrothermal ore deposits.

c) Analogues to ore-forming systems

As outlined above, the fluid chemistry of geothermal systems in New Zealand are interpreted to be comparable to fluids associated with epithermal precious metal deposits (Hedenquist and Henley, 1985b). On the other hand, the geological setting, fluid chemistry, metal contents, and zonation of alteration and mineralization, indicate that Philippine geothermal systems are analogues to porphyry-related copper-gold deposits encountered throughout the Pacific rim.

In New Zealand, Brown (1986) described bonanza gold grades in scales from surface pipes in the Broadlands (up to 5.4% Au, 17.4% Ag and 13.2% Cu) and Kawerau (6.4% Au, 29.4% Ag) geothermal fields. He interpreted these deposits to have been caused by the flashing, at the surface, of deep chloride hydrothermal fluids (Section 4.vi.a).

A number of surface thermal features in New Zealand geothermal systems also actively precipitate metals. These mineralized precipitates are interpreted herein to form as a result of the mixing of neutral pH fluids, which are derived from the deep chloride reservoir, with surface acid sulfate waters. Mud precipitates from hot neutral chloride springs at Sinter Flat on the banks of the cool acid sulfate Lake Rotokawa (16.4^{o}C; pH 2.15) grade up to 20-25 ppm Au, 3,000 ppm As and 1500 ppm Sb (Krupp and Seward, 1987). These muds cover an area of 2 ha, are estimated to be 5 m thick, and comprise an inferred resource of 250,000 metric tons averaging about 1 g/t Au. Metal precipitates (up to 4.5% W, 8.8% As, 500 ppm Mo and 2 g/t Ag; Seward and Sheppard, 1986, in Simmons et al., 1992) in the Waimangu geothermal system occur where hot neutral pH waters percolate into the outflow stream from the cool acid sulfate Frying Pan Lake (pH $\leq$ 4). At Champagne pool, Waiotapu, orange precipitates interbedded with white silica sinter, are deposited from neutral chloride waters (Table 2.1) which discharge into an environment of acid sulfate waters (Section 8.vii). These precipitates grade up to 80 ppm Au, 175 ppm Ag, 2 percent As and 2 percent Sb (Weissberg, 1969).

Precious and base metal mineralization has not been encountered in economic quantities in drill core and cuttings from the New Zealand geothermal fields. However, significant base metal mineralization has been reported down to 1200 m along the margins of the Waiotapu geothermal field and has been interpreted to result from the mixing of descending low pH CO_2-rich waters and the neutral chloride hydrothermal waters (Hedenquist, 1990). Silver mineralization, in core and cuttings from shallow depths in the Rotokawa geothermal field, is associated with alunite and Mn-carbonates (Krupp and Seward, 1987), and is interpreted herein to be associated with the mixing of upwelling chloride hydrothermal fluids and surficial acid sulfate, and possibly CO_2-rich, waters.

Although drilling of active hydrothermal systems in the Philippines has not encountered economic porphyry copper-gold ore, grades of 0.1-0.2 percent copper were recorded (Mitchell and Leach, 1991) from core which contains chalcopyrite-chlorite veinlets which cut potassic alteration at Palinpinon. In the Tongonan geothermal field, common chalcopyrite is locally abundant at depth around the contacts of high level intrusions. On the other hand, sphalerite and galena are less abundant and are restricted to the margins and at shallower crustal levels (Arevalo, 1986).

Deposits of sphalerite, galena, chalcopyrite and native gold occur as scales within Palinpinon wells, and are intergrown with anhydrite and barite gangue minerals (A.G. Reyes, pers. commun.). These scales occur where there is an inflow of shallow acid sulfate waters, and are herein interpreted to result from entrainment and mixing of these low pH waters with deep saline chlorite fluids during discharge.

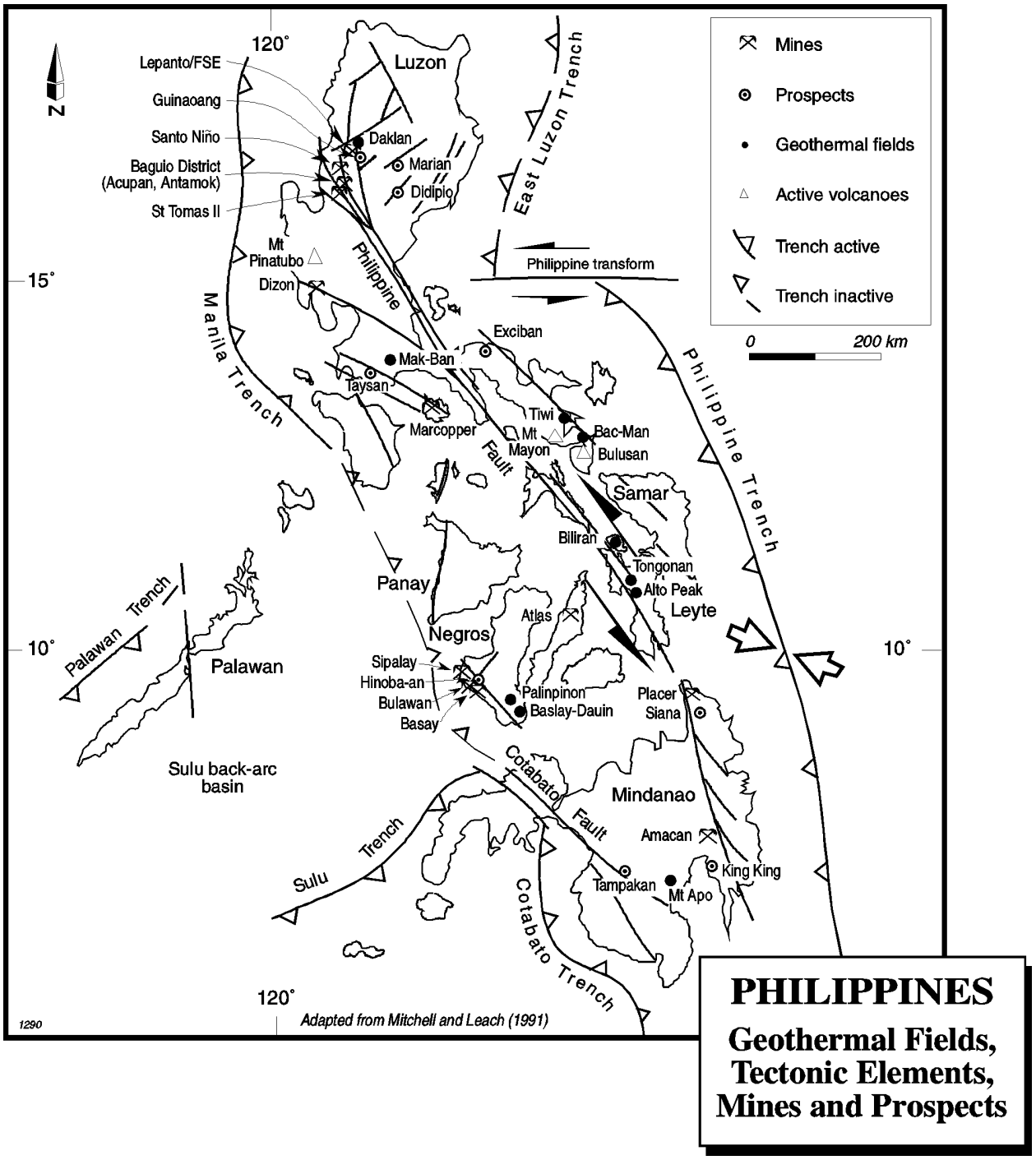

FIG. 2.5

Scales deposited from deep chloride reservoir fluids in back-pressure plates in surface pipework from the Tongonan geothermal field have graded up to tens of percent of copper (mainly as tennantite), percents of lead and zinc, thousands of ppm silver, and hundreds of ppm gold (R. Harper and T. Leach; unpubl. PNOC-EDC reports; Mitchell and Leach, 1991). Up to 1 percent Cu + Pb + Zn have been deposited downstream in drains and channels at Tongonan (Arevalo, 1986).

Drilling for geothermal energy in the Philippines has enabled the investigation of porphyry-style hydrothermal systems at depths of greater than 3.5 km below surface, over areas of up to 20-50 km^2, and at temperatures of

up to >300-350°C. These investigations have permitted the inspection of potential ore-forming systems during various stages of development. Detailed petrological work (e.g., Reyes, 1985, 1990a, 1990b; Leach and Bogie, 1982, Leach et al., 1983, 1986) has been carried out on these systems. This has allowed zonations in alteration and mineralization with fluid chemistry to be compared to pressure-temperature measurements at depths from which samples were recovered. The formation conditions of the various mineral phases have therefore been empirically determined (e.g., Leach et al., 1986; Reyes, 1990b).

d) Styles of Philippine active hydrothermal systems

The Philippines is a typical magmatic arc setting for porphyry-related hydrothermal systems (Fig. 2.5). Neogene magmatic arcs parallel the Philippine trench to the southeast and the Manila trench to the northwest, and minor arcs are associated with the Negros and Cotabato trenches in the southwest of the Philippines (Mitchell and Leach, 1991; Fig. 2.5). Circulating neutral chloride hydrothermal systems in the Philippines have not been encountered in association with large stratovolcanoes (Bogie and Lawless, 1986) such as Mt. Mayon and Mt. Pinatubo (Ruaya et al., 1992). Volcanic deposits derived from these stratovolcanoes are typically uniform in composition through time (e.g., basaltic andesite at Mt. Mayon), indicative of a deep (<4-5 km), large, predominantly undifferentiated magma chamber.

Active hydrothermal systems in the Philippines are, however, encountered in the following two main geological/tectonic settings (Reyes, 1990b; Mitchell and Leach, 1991):

1. Large hydrothermal systems are hosted in thick volcanic or volcaniclastic sequences. These systems occur within composite volcanic terrains either parallel to subduction zones (e.g., Alto Peak, Palinpinon, Bacon Manito), and are probably derived from differentiating magma chambers at shallow crustal levels; or occur within favourable structures, such as dilational jogs and splays related to major faults (e.g., Tongonan, Biliran). These large convective systems form extensive alteration haloes which are herein interpreted to be similar to porphyry-copper/skarn systems.

2. Hydrothermal systems, with restricted fluid flow paths, are hosted in dilational structural settings within competent and relatively impermeable basement metasediments and older intrusions, in Cordillera regions of Eastern Mindanao and Central Luzon (e.g., Amacan, Daklan and Acupan). This setting is interpreted to be a favourable environment for intrusion-related gold systems.

e) Evolution of active porphyry systems

Each geothermal system drilled in the Philippines is at a different stage in its evolution, and each one is a 'time slice' in the development of an intrusion-related hydrothermal system. Some very young geothermal systems are associated with the recent emplacement of intrusions at shallow crustal levels, whereas other systems that have been drilled are at late, waning stages. The following sequence of events is interpreted by the authors to characterize the development of Philippine geothermal systems:

1. <u>Contact metamorphism</u>
It is only when active hydrothermal systems evolve sufficiently to exhibit surface thermal manifestations that they become targets for geothermal energy exploration. All active porphyry systems drilled in the Philippines are interpreted herein to have already undergone the transfer of heat into the host country rock (see below for Alto Peak) which has resulted in the formation of hornfels at the intrusion-volcanic rock/sediment contacts (e.g., Tongonan, Palinpion, Alto Peak, Bacon-Manito), and zoned skarns in calcareous host rocks (e.g., Palinpinon, Alto Peak).

2. Magmatic volatile plume
On Biliran Island (Vulcan region) and at Alto Peak, plumes of magmatic volatiles are currently being emplaced into pre-existing zoned skarn and contact hydrothermal alteration assemblages (Reyes et al., 1993; Lawless and Gonzalez, 1982). Down hole measurements indicate that these magmatic vapours are possibly derived from a very hot (>300-400°C) fluid which is interpreted by the authors to have exsolved during early crystallization of a high level melt (below), and has locally vented directly to the surface as magmatic solfataras (e.g., Vulcan, Biliran Is.).

3. Convective hydrothermal alteration
Release of heat and fluids from the high level intrusions establishes deep circulating meteoric hydrothermal systems into which magmatic fluids are entrained (Henley and Ellis, 1983; Hedenquist, 1987). These circulating systems create zoned hydrothermal alteration which grades from an inner potassic zone dominated by biotite to peripheral propylitic alteration (Henley and McNabb, 1978; Gustafson and Hunt, 1975). The Tongonan geothermal system is interpreted herein to currently occur at this stage of development. The high fluid temperatures (>320°C; Reyes, 1990b) and salinities (>15,000 ppm Cl^{-}; Table 2.1) suggest that a significant input of magmatic brine from the cooling melt has been entrained into the convecting hydrothermal system. Although only minor base metal mineralization has been deposited from this hot, moderately saline system (Leach and Weigel, 1984; Arevalo, 1986), significant lead-zinc mineralization has been produced by flashing fluids from depths of >2.5 km to near ambient conditions within surface pipework (Mitchell and Leach, 1991). It has therefore been interpreted (Arevalo, 1986) that the circulating chloride brine at Tongonan is substantially undersaturated with respect to base and precious metals. However, the deposition of significant base and precious metal mineralization can be induced under extreme artificial conditions as outlined above.

4. Draw down of surficial waters
Cooling of the intrusive heat source is herein interpreted to induce a pressure draw down of cool dilute meteoric waters and shallow, moderately low pH acid sulfate and CO_2-rich waters to considerable depths within the chloride reservoir (e.g., Palinpinon, Bacon Manito). This draw down of shallow-derived waters is interpreted (e.g., Reyes, 1990b) to result in the formation of a zoned phyllic and later argillic overprints on pre-existing hydrothermal alteration. The draw down of these fluids can result in mineral deposition and subsequent progressive sealing of permeable channels at shallow levels, and the development of an impermeable cap on the system (Lawless et al., 1983). Although systems such as Palinpinon are dilute relative to Tongonan (Table 2.1) and interpreted herein to have been drilled at a late stage in its evolution, the most significant copper mineralization intersected to date in a Philippine geothermal system is from Palinpinon.

iv) Examples of Active Intrusion-Related Hydrothermal Systems in the Philippines

a) Large disseminated systems in permeable host rocks in composite volcanic terrains

1. Young Systems Dominated by Magmatic Vapours

i) Alto Peak Geothermal System
(summarised from Reyes et al., 1993)

The Alto Peak geothermal system, in northern Leyte, is hosted in a volcanic arc which extends along the eastern margin of the Philippine fault (Figs. 2.5, 2.6). Drilling within the Alto Peak geothermal system intersected a spatially restricted magmatic vapour plume sourced from a degassing high level intrusion at depth (Fig. 2.7).

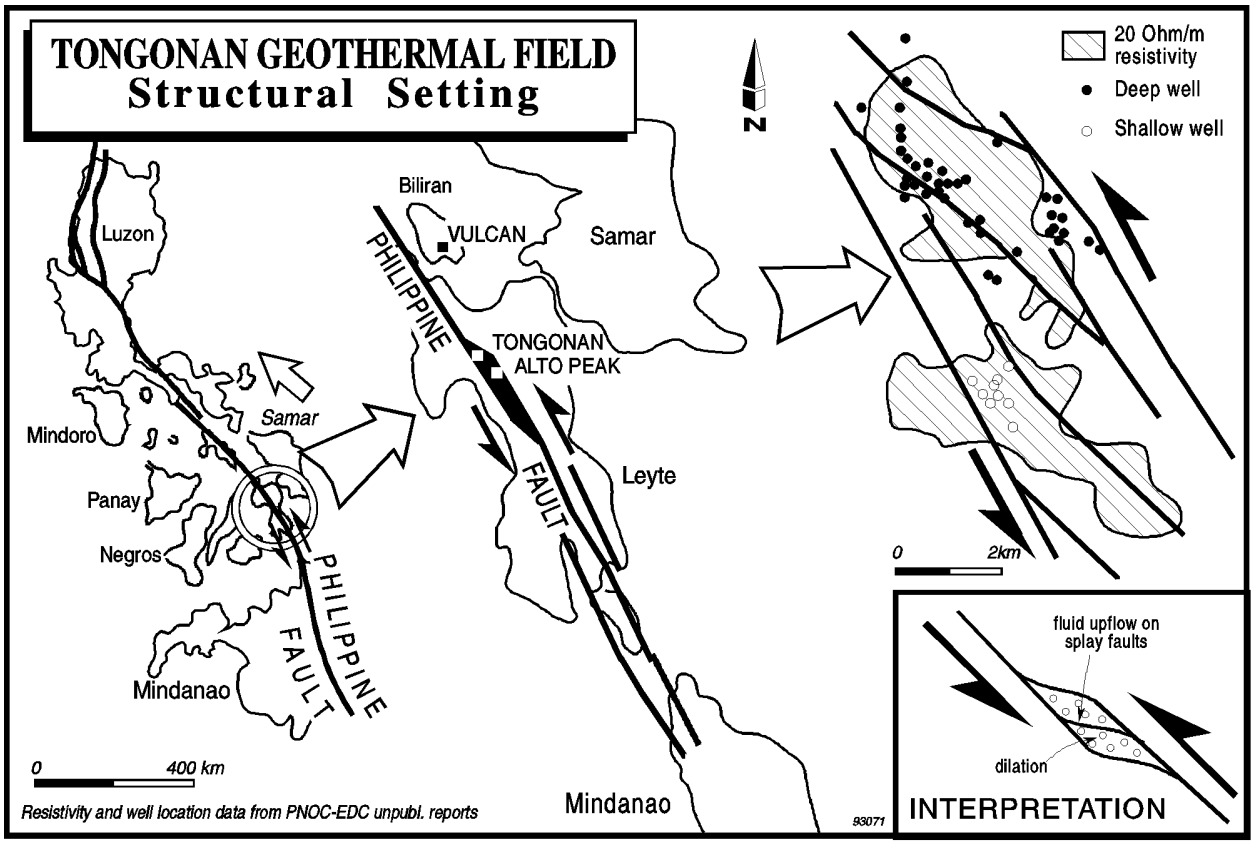
TONGONAN GEOTHERMAL FIELD
Structural Setting
N
20 Ohm/m resistivity
Deep well
Shallow well
Luzon
Biliran
VULCAN
Samar
PHILIPPINE
TONGONAN
ALTO PEAK
Mindoro
Samar
Leyte
FAULT
Panay
Negros
PHILIPPINE
FAULT
Mindanao
0
400 km
Resistivity and well location data from PNOC-EDC unpubl. reports
Mindanao
93071
0
2km
fluid upflow on splay faults
dilation
INTERPRETATION

FIG. 2.6

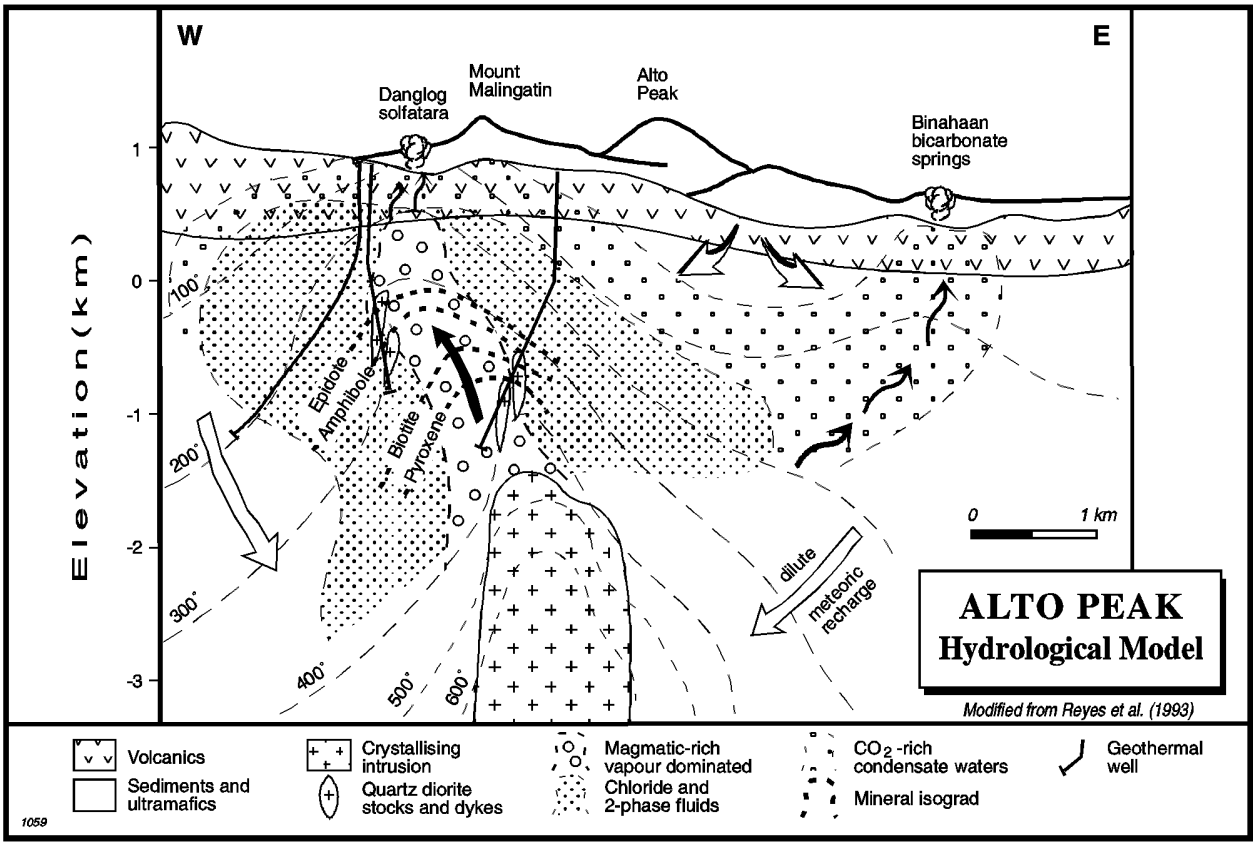
W
E
Danglog solfatara
Mount Malingatin
Alto Peak
Binahaan bicarbonate springs
Elevation (km)
1
0
-1
-2
-3
100°
200°
300°
400°
500°
600°
Epidote
Amphibole
Biotite
Pyroxene
dilute
meteoric recharge
0
1 km
ALTO PEAK
Hydrological Model
Modified from Reyes et al. (1993)
Volcanics
Sediments and ultramafics
Crystallising intrusion
Quartz diorite stocks and dykes
Magmatic-rich vapour dominated
Chloride and 2-phase fluids
CO2 -rich condensate waters
Mineral isograd
Geothermal well
1059

FIG. 2.7

This vapour plume penetrates into a weak, circulating, moderately saline (7500 ppm Cl^-) hydrothermal system, and at depth has caused a localized advanced argillic alteration assemblage to overprint on zoned potassic-propylitic alteration.

The active hydrothermal system at Alto Peak (Fig. 2.7) is hosted in Pliocene to Recent andesite-dacite volcanics and subvolcanic quartz diorite dikes, which pass down into a thick sequence (>2000 m) of Late Miocene to Pleistocene, locally calcareous, marine sedimentary breccias, siltstones, mudstones and hyaloclastites (Binahaan Formation). Basement rocks comprise Cretaceous harzburgite and pyroxenite.

Composite volcanic centres, domes and collapse calderas are developed within dilational NW trending segments (Alto and Cental faults) of the Philippine fault system. Additional permeability within the volcanic-sedimentary sequence is also provided by subsidiary EW, NS, and NE trending faults. Alteration mapping indicates that earlier low temperature clay alteration has been locally overprinted by vertically zoned epidote-amphibole-biotite-pyroxene mineralogy, indicative of a later influx of considerably hotter fluids. Locally, skarns which formed at the contacts of calcareous sediments and high level quartz diorite dikes, display the zonation: garnet-pyroxene --> wollastonite-vesuvianite --> biotite-pyroxene-amphibole --> quartz-biotite-anhydrite + epidote.

Two wells intersected a near vertical magmatic-derived vapour-rich 'chimney', 1 km wide and 2-3 km deep, which connects a deep vapour-dominated zone at depth to a shallow zone of steam heated ground water. Gas geochemistry, fluid isotope, and fluid inclusion data suggest that the vapour plume contains up to 40-50 percent magmatic component, and is derived from a very hot (>400°C), saline (>17,000 ppm Cl^-) fluid. It is interpreted herein that the source of this fluid and the quartz diorite dikes is a degassing recent intrusion at depth. Alteration at depth (1700-1800 m below surface) within this magmatic vapour-rich chimney is localized along fractures and consists of quartz-pyrophyllite-alunite + diaspore-anhydrite and minor apatite, zunyite and topaz.

The vapour 'chimney' is dominated by CO_2 as the main gas phase. Reyes et al. (1993) interpreted that the lack of Cl-SO_4 in the magmatic waters (despite the local occurrence of magmatic-derived advanced argillic alteration) indicates that either the conversion of acidic oxidizing magmatic to neutral pH fluids is now complete, or it is limited to regions of the geothermal field which have not yet been drilled. Recent drilling has in fact intersected permeable fracture zones which produce hot acidic, magmatic-derived acidic fluids (A.G. Reyes pers. commun., 1995).

ii) <u>Biliran</u>
(data from: Mitchell and Leach, 1991; Lawless and Gonzalez, 1982)

The Vulcan thermal area is aligned for 3-4 km along a NE trending suture zone (Vulcan fault) which transects the island of Biliran, north of Leyte as a possible arc normal structure formed perpendicular to the Philippine trench (Fig. 2.8). The presence of super-heated steam, SO_2 gases and HCl condensates in the Vulcan thermal area has been interpreted (Lawless and Gonzalez, 1982) to indicate that the Vulcan fault is directly venting hot magmatic volatiles to the surface. The Biliran system is therefore herein inferred to represent an active analogue of high sulfidation systems.

The geothermal system at Biliran is hosted in basement metamorphics which are overlain by 300 m of calcareous sediments and then by a 1.5-2 km thick sequence of andesitic volcanic and volcaniclastic rocks (Fig. 2.9). There are no recent volcanics at the surface which might represent the extrusive rock equivalents of an intrusive source for the heat and magmatic fluids within the currently active hydrothermal system.

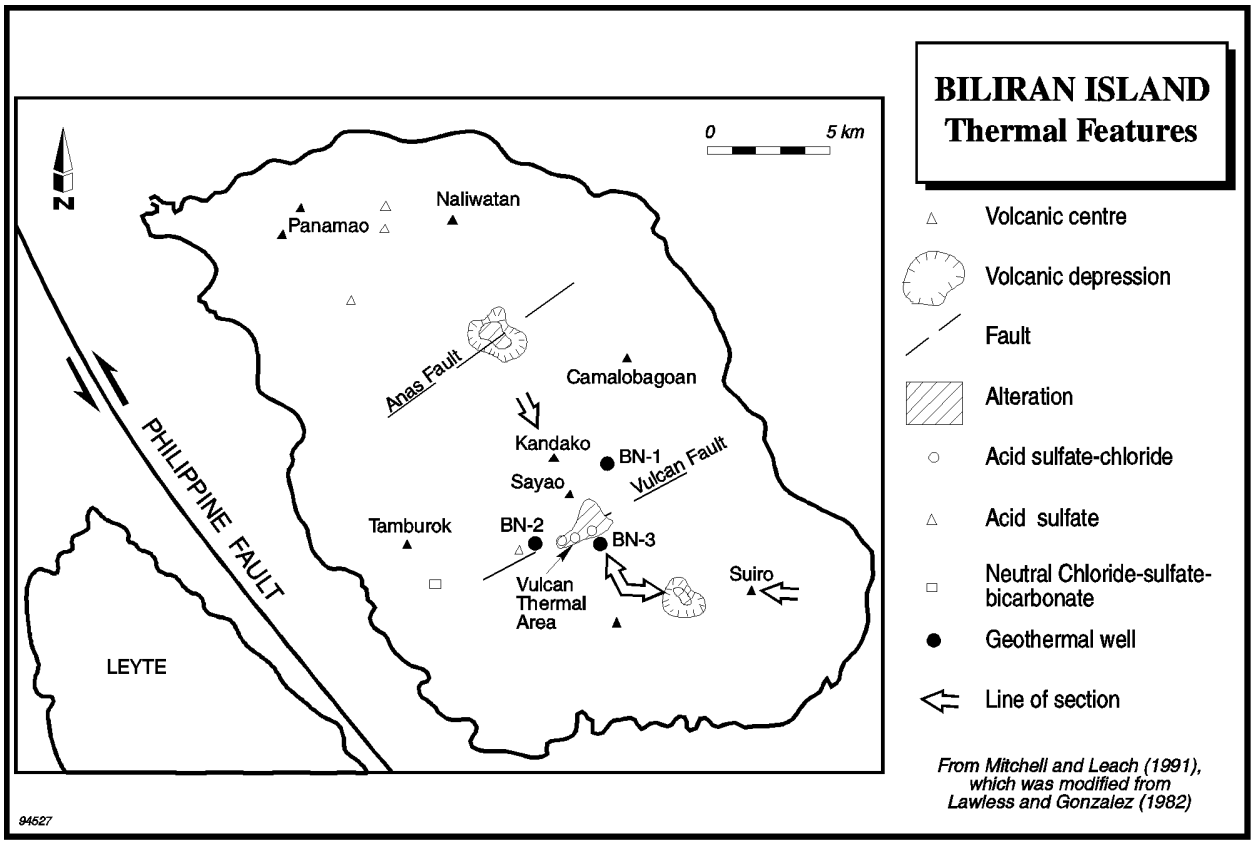
BILIRAN ISLAND
Thermal Features
0
5 km
N
Naliwatan
Panamao
Anas Fault
Camalobagoan
Kandako
BN-1
Vulcan Fault
Sayao
Tamburok
BN-2
BN-3
Vulcan Thermal Area
Suiro
PHILIPPINE FAULT
LEYTE
Volcanic centre
Volcanic depression
Fault
Alteration
Acid sulfate-chloride
Acid sulfate
Neutral Chloride-sulfate-bicarbonate
Geothermal well
Line of section
From Mitchell and Leach (1991), which was modified from Lawless and Gonzalez (1982)
94527

FIG. 2.8

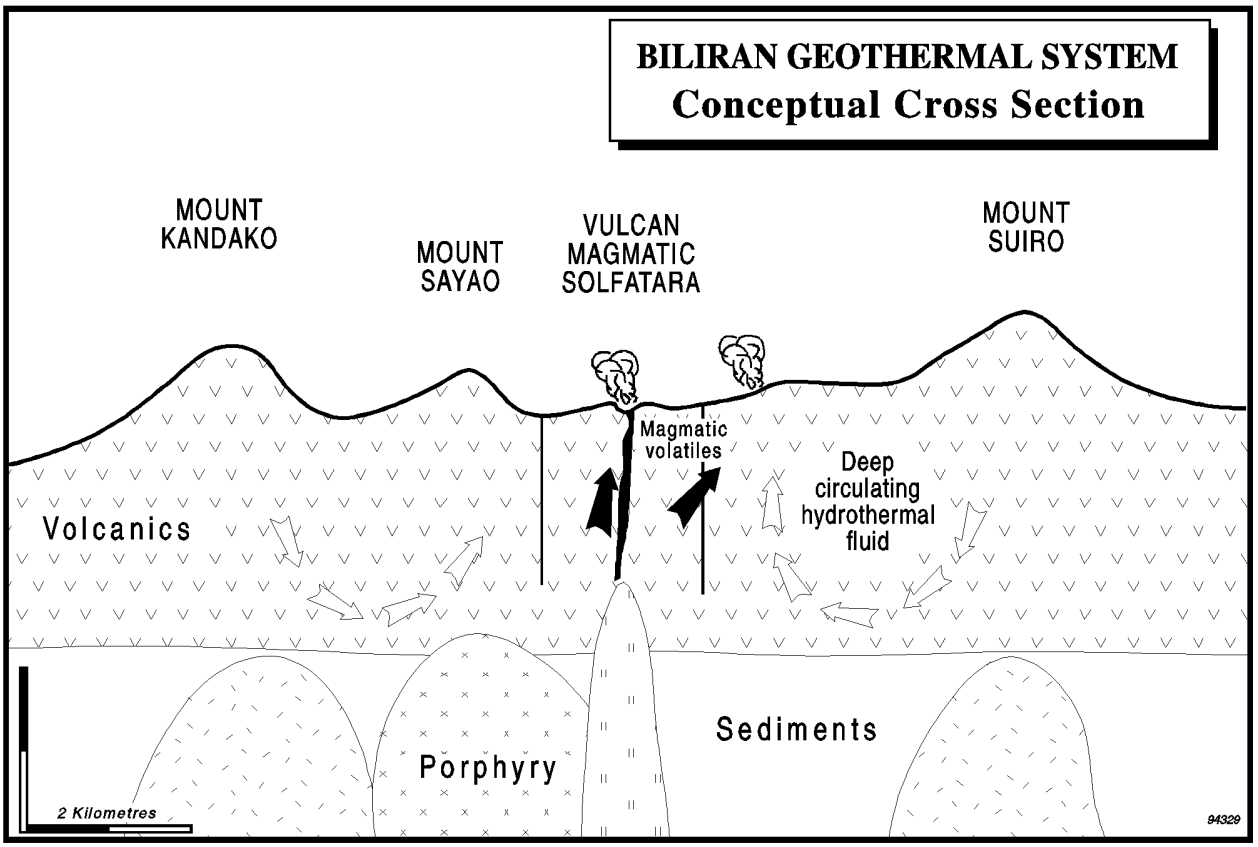
BILIRAN GEOTHERMAL SYSTEM
Conceptual Cross Section
MOUNT KANDAKO
MOUNT SAYAO
VULCAN MAGMATIC SOLFATARA
MOUNT SUIRO
Magmatic volatiles
Deep circulating hydrothermal fluid
Volcanics
Sediments
Porphyry
2 Kilometres
94329

FIG. 2.9

Drilling peripheral to the Vulcan fault encountered neutral fluids with a significant fluorine content (up to 35 ppm, compared to 1-3 ppm from other Philippine systems; Mitchell and Leach, 1991), which suggests that there is a significant input of magmatic fluids. Drill hole BN-3 intersected a permeable zone at around 1000 m, interpreted herein to be a splay off the Vulcan fault, and this produced very hot (310-320°C), acidic (pH <3) fluids (Table 2.1).

Down hole temperatures, estimated from alteration mineralogy, are lower than actual measured temperatures in Biliran wells (Lawless and Gonzalez, 1982), implying that the hydrothermal system is still heating up. Drilling at Biliran failed to encounter an extensive hydrothermal system for geothermal exploitation, possibly because of the youthful nature of the system.

The Biliran geothermal system illustrates strong structural control for the venting of magmatic volatiles from a degassing magma at depth. The inferred youthful nature of the high sulfidation system at Biliran, implies that the exsolution of volatiles from a degassing magma, and the formation of hot acidic fluids, could occur at an early stage in the evolution of a hydrothermal system.

2. Circulating Hydrothermal Systems

i) Tongonan
(data from: Leach et al., 1983; Arevalo, 1986; Reyes, 1990b; Mitchell and Leach, 1991)

The Tongonan geothermal field is situated in a 12 km long graben formed within a dilational jog in the Philippine fault, on the island of Leyte (Fig. 2.6). This jog has been active at least since the Miocene, and controlled the emplacement of a number of intrusions ranging from: a large quartz diorite to granodiorite (10-11 Ma.) pluton between the east and central Philippine faults, diorite porphyries (3 Ma.) along the margins of the older pluton, and recent felsic porphyries and associated high level dacite plugs and dikes emplaced along dilational splays cutting the diorite pluton (Figs. 2.6, 2.10). The heat source for the currently active system is interpreted to be a deep melt which has fed the felsic dikes. The suite of intrusions were emplaced into a thick sequence of Miocene to Pliocene volcanics, and there are no volcanics that could represent extrusive equivalents of the recent dacitic intrusions. Ten km to the southeast, the volcanic centres of Mt. Janagdan and Alto Peak are aligned parallel to the trend of subduction along the Philippine trench.

The high salinity of the circulating hydrothermal fluids (up to 16,000 ppm Cl; well 407, Table 2.1) suggests that there is a significant input of magmatic-derived fluids. Conditions interpreted from the alteration mineralogy in the Sambaloran and Mahiao regions (Fig. 2.10) are generally comparable to those derived from down hole temperature and chemical analyses (Leach et al., 1986; Reyes, 1990b). This agreement between data from the alteration assemblages and fluid conditions in this part of the field suggests that there is equilibrium between the fluids and wall rock, and is herein interpreted to suggest that the current system is at least stable, if not waxing. On the other hand, argillic to advanced argillic alteration, caused by descending cool low pH fluids (e.g., well 402, Table 2.1), overprints earlier potassic and inner propylitic assemblages associated with diorite intrusions along the branches of the Philippine fault. The neutral chloride fluids migrate laterally (outflow) along the central Philippine fault, and vent to the surface as neutral chloride springs at lower elevations in the Bao Valley, 5-6 km to the southwest.

The Tongonan geothermal field is an example of a system in which there is strong structural control to the setting of intrusion emplacement and associated overprinting porphyry-style hydrothermal systems. The large dilational fault jog which hosts the geothermal system has been reactivated several times and allowed the emplacement of different generations of intrusions. This strong structural control of multiple porphyry-style hydrothermal systems at Tongonan is analogous to the tectonic control described herein for the emplacement of intrusions associated with many circum Pacific porphyry copper deposits (e.g., Yandera, Papua New Guinea;

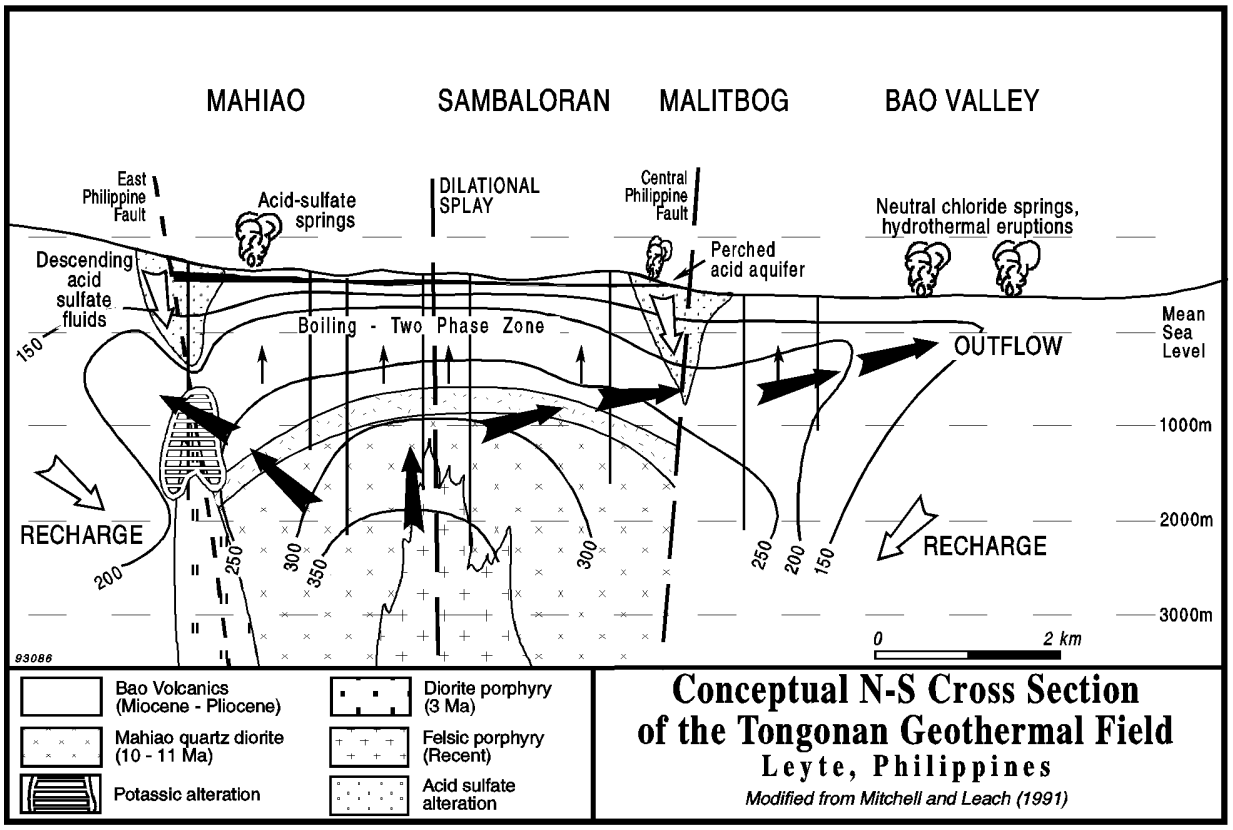

FIG. 2.10

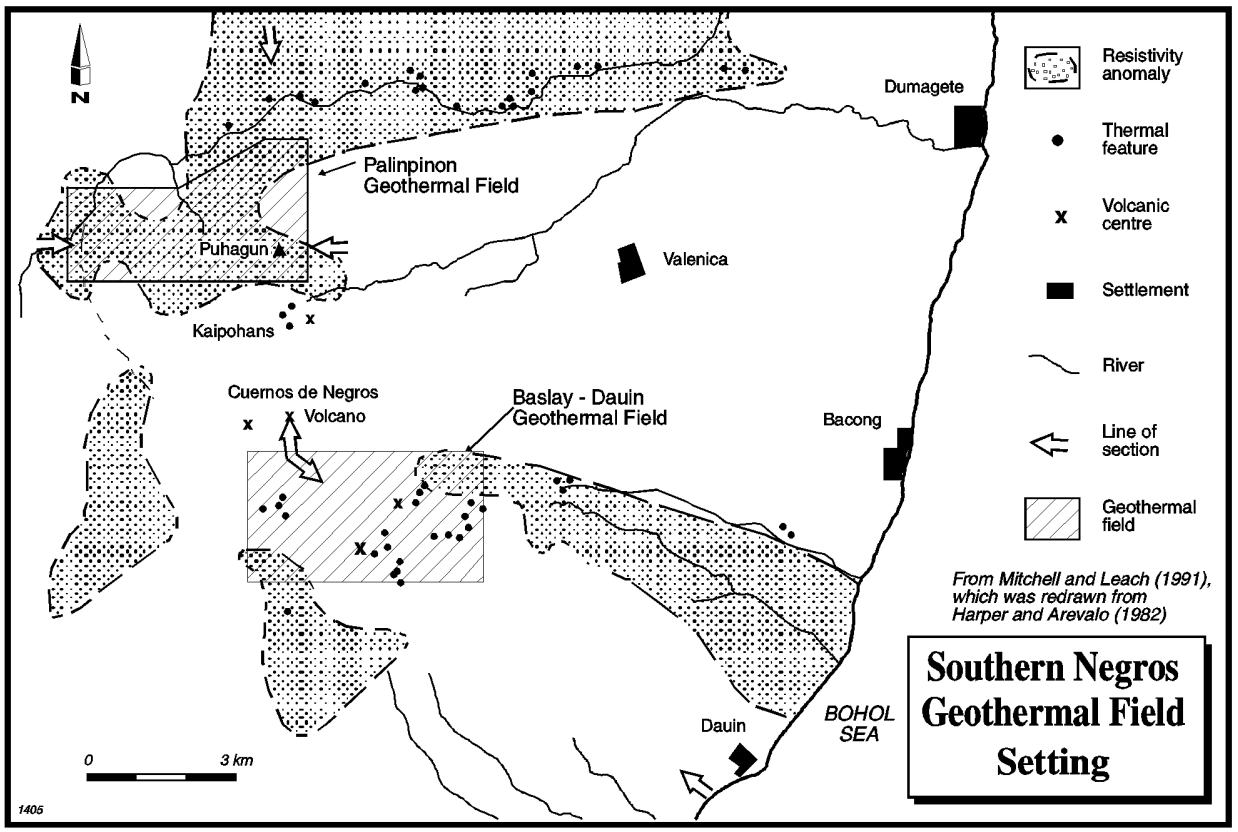

FIG. 2.11

Titley et al., 1978).

3. Collapsing Hydrothermal Systems

i) Southern Negros Geothermal Field
(data from: Seastress, 1982; Leach and Bogie, 1982; Zaide, 1984; Reyes, 1990b; Mitchell and Leach, 1991)

Two geothermal systems occur within the Cuernos de Negros volcanic centre. These are the northern Palinpinon and the southern Baslay-Dauin fields (Fig. 2.11). The volcanic centre comprises twin peaks, dacite domes, and parasitic cones to the south and east, and a pyroclastic plateau to the north. The most recent pyroclastic flows (14,000 years BP) are dacitic and were erupted from a vent 2 km north of the summit craters.

The Palinpinon geothermal system is hosted in a 1.5 km thick sequence of Miocene-Recent volcanics which overlie Eocene-Miocene calcareous sediments and early Eocene volcanics and volcaniclastics (Fig. 2.12). A large Miocene monzonite pluton was emplaced into the volcanic and sedimentary rocks in the western portion of the field. Recent porphyry stocks have been emplaced along the eastern margin of the monzonite, facilitated by movement along a parallel set of NS trending structures which also controlled the venting of the recent pyroclastic flows. The porphyry stocks, or more likely their deeper equivalents, are the heat source for the currently active hydrothermal system.

Two distinct phases of hydrothermal alteration are encountered (Leach and Bogie, 1982). A relict phase of potassic and advanced argillic alteration occurs in the west, with propylitic alteration to the east, and there is a current phase of phyllic alteration in the central regions of the system (Fig. 2.12). The potassic zone grades from an inner assemblage of clinopyroxene-biotite, outward to zones of biotite-quartz and actinolite-biotite. In places, zoned hornblende-pyroxene-biotite hornfels occur at intrusion-volcanic contacts. Elsewhere, zoned skarns are intersected within calcareous sediments adjacent to porphyry intrusions. Alteration grades vertically and laterally (west to east) as zones of: potassic, epidote-chlorite, and shallow chlorite-zeolite alteration assemblages.

Advanced argillic alteration was intersected from surface to 1300-1500 m depth in the western Sogongon region, and crops out as prominent 2-3 km long ridges aligned NS along regional structures (Fig. 2.12). The volcanic rocks have undergone alteration to intense silicification and zoned kaolinite, alunite, and pyrophyllite-diaspore + tourmaline mineral alteration assemblages. Trace hypogene covellite mineralization is associated with this advanced argillic alteration. These zones of intense silicification and advanced argillic alteration are comparable to high sulfidation alteration which occurs marginal to porphyry copper deposits (Section 6.II), and are interpreted herein to have formed from magmatic vapour plumes similar to those which are currently venting at Alto Peak and Vulcan, Biliran Is. Similar porphyry-related silicified ridges extend for 3-4 km along major structures in the Amlan River area 5-6 km north of the Palinpinon geothermal system, as well as in a belt extending north along the island of Negros and into Masbate Island (Mitchell and Leach, 1991).

Phyllic alteration (illite/muscovite-quartz-pyrite $\pm$ anhydrite $\pm$ carbonate) occurs at shallow levels within a two-phase zone dominated by mixed CO_2-rich and acid sulfate waters, and at depth overprinting earlier potassic and propylitic alteration (Leach and Bogie, 1982; Reyes, 1990b). It is speculated by the authors that the deep phyllic overprint has been caused by the draw down of shallow waters. Elsewhere, localized cool acid sulfate and dilute meteoric recharge fluids have been encountered at depths up to 2 km, where they have migrated down permeable structures and laterally along contacts with sills and dikes (Reyes, 1990b).

The hydrothermal system at Palinpinon exhibits all the major features encountered in southwest Pacific rim porphyry copper deposits, including early formed skarns, hornfels, and potassic alteration zones proximal to the source intrusions, and more distal propylitic alteration zones. Advanced argillic alteration and silicification also

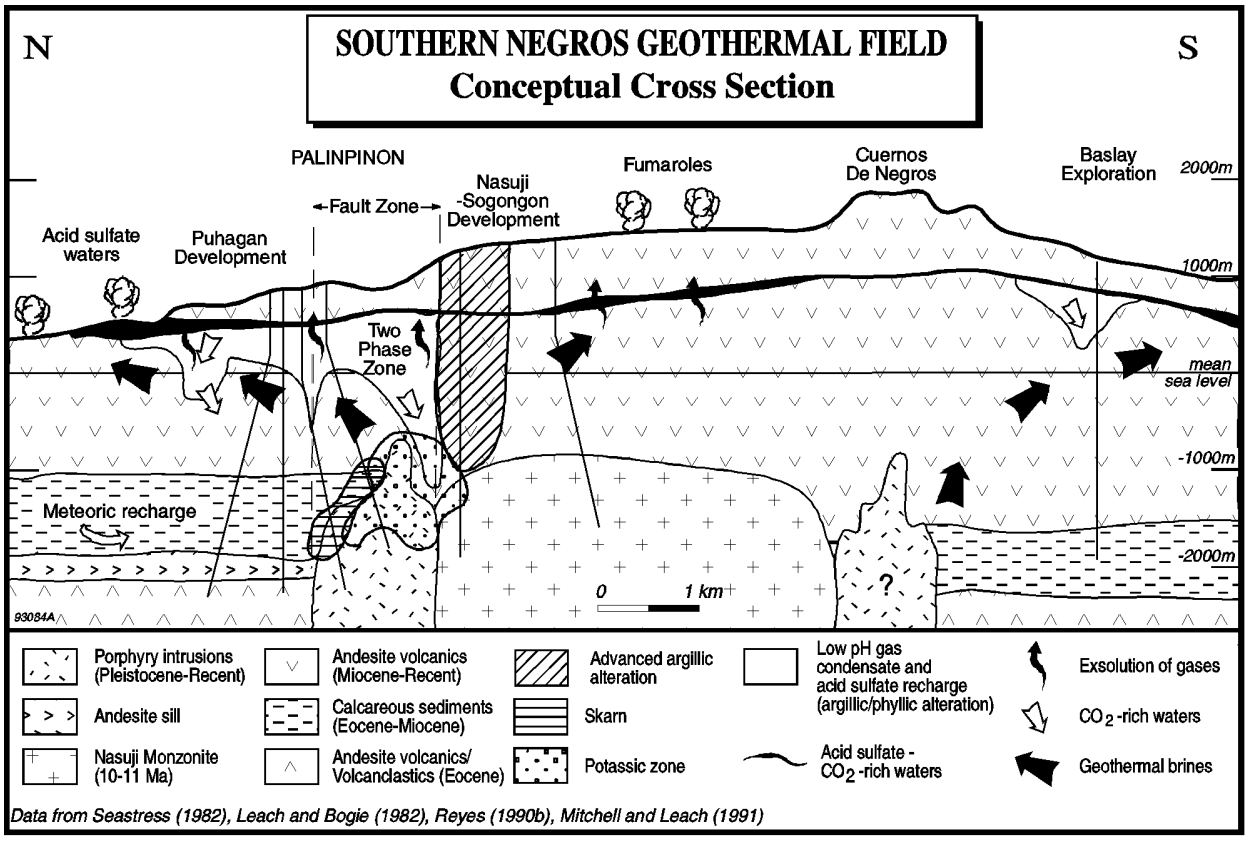

FIG. 2.12

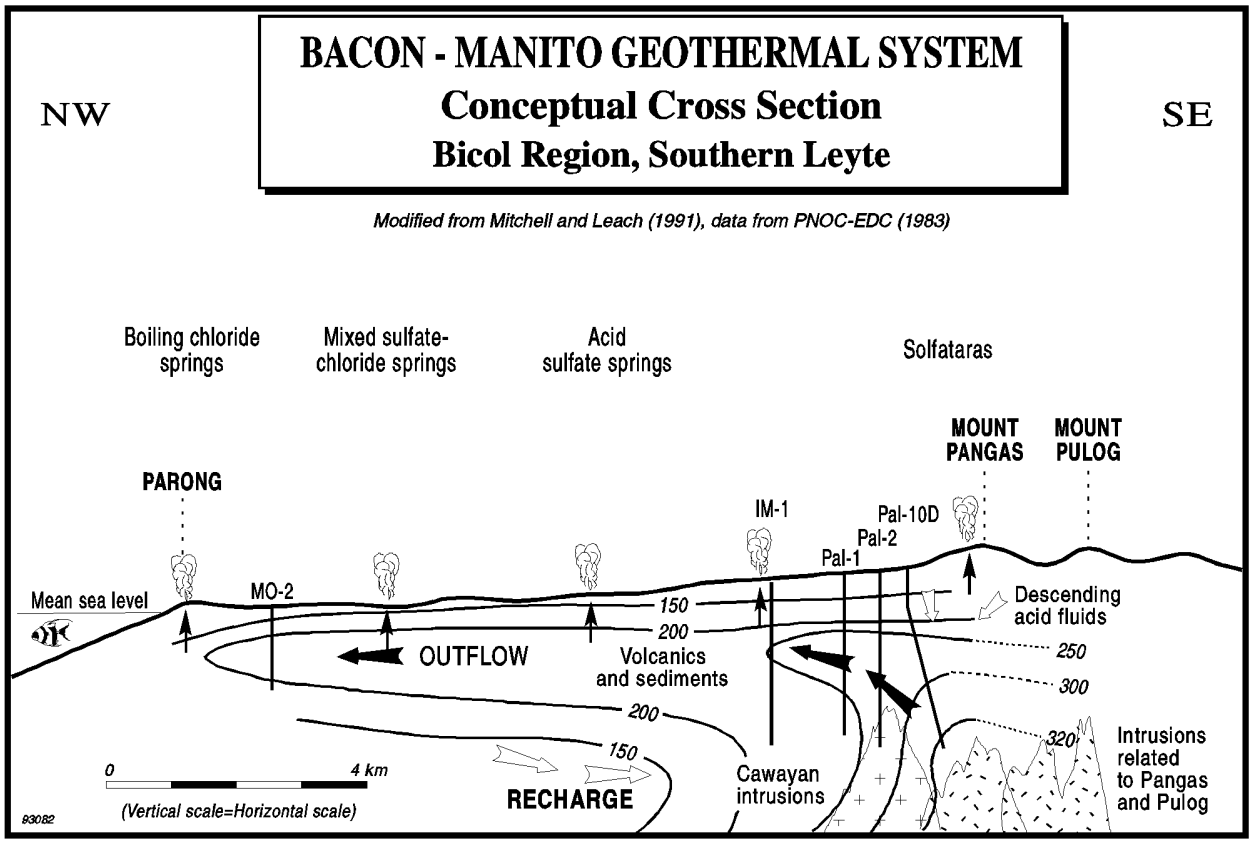

FIG. 2.13

formed early in the evolution of the Palinpinon system, and are strongly structurally controlled by faults which facilitated the emplacement of the multiple porphyry intrusions. At present, the Palinpinon active porphyry system is at an early stage of collapse, such that cool acid sulfate, CO_2-rich and meteoric waters are descending in response to pressure draw down. This draw down has created a phyllic alteration overprint on the existing zoned propylitic-potassic alteration. The relatively dilute (<7,000 ppm Cl) nature of these fluids suggests that there is only a minor magmatic input at this stage of evolution of the hydrothermal system.

The geological setting of Palinpinon has many similarities to the Panguna porphyry copper deposit, Bouganville, Papua New Guinea (Baldwin et al., 1978), where multiple mineralizing porphyry intrusions were emplaced at the margin of a large quartz diorite pluton. The geochemistry and down hole temperature/pressure data from the Baslay-Dauin geothermal field, 6 km to the south, is interpreted (Harper and Arevalo, 1982) to indicate that this system probably relates to a separate series of intrusions at depth, which are co-genetic with the Cuernos de Negros volcanics.

ii) Bacon-Manito Geothermal Field, Southern Luzon
(data from: Lawless et al., 1983; Reyes, 1985; Mitchell and Leach, 1991)

The Bacon-Manito geothermal field occurs in the Bicol volcanic arc in southern Luzon, midway between the active large stratovolcanoes of Mayon and Bulusan (Fig. 2.5). The Bacon-Manito hydrothermal system is hosted in a complex composite volcanic terrain of domes, plugs, and collapsed calderas ranging in composition from dacite to basaltic andesite. Up to 2800 m of volcanic rocks comprising mainly andesites, but ranging from dacite to basalt, overlie a succession of Miocene to Eocene sedimentary and volcanic rocks (Fig. 2.13). A number of small stocks and plugs intersected at depth by drilling in the Cawayan sector vary from pyroxene gabbro to hornblende quartz diorite (Fig. 2.14).

Thermal features occur over a 15-20 km outflow zone and exhibit a vertical zonation common to volcanic arc geothermal systems. Hydrothermal solfataras are present on the flanks of Mount Pangas in the region of the main upflow, whereas acid sulfate and mixed sulfate-chloride springs vent at intermediate elevations. Boiling chloride springs are encountered at Parong at about sea level 12 km from Mount Pangas (Fig. 2.13).

Although the current upflow zone at Bacon-Manito is interpreted to be related to intrusions associated with the domes of Mount Pangas and Mount Pulog, the presence of residual hot spots in the Cawayan region implies that previous hydrothermal activity was centred on the Cawayan intrusions. The draw down of acid sulfate and CO_2-rich waters down structures and caldera margins to depths of over 1500 m (Lawless et al., 1983; e.g., Table 2.1, 1400 m down hole sample, CN-1), caused progressive overprinting alteration events (Fig. 2.14). The descent of cool, low pH fluids into hotter environments has resulted in widespread deposition of carbonates, sulfates, and silica causing the upper 1000 m to become impermeable (Leach et al., 1986). These fluids have formed extensive phyllic and local argillic alteration which overprint potassic alteration within, and proximal to, the Cawayan intrusions. It is speculated herein that the draw down of acid sulfate and CO_2-rich waters was caused by the waning of the heat source for the hydrothermal system in the Cawayan region.

The multiple high level intrusions, and overprinted potassic-propylitic, phyllic and argillic alteration assemblages at Cawayan, are similar to features recorded in the El Salvador porphyry copper deposit, Chile (Gustafson and Hunt, 1975).

b) Cordillera-hosted intrusion-related active hydrothermal systems

The two main cordillera regions in the Philippines are in northern Luzon and eastern Mindanao. These ranges are composed of uplifted early Tertiary sedimentary and volcanic sequences, early arc intrusions (typically of

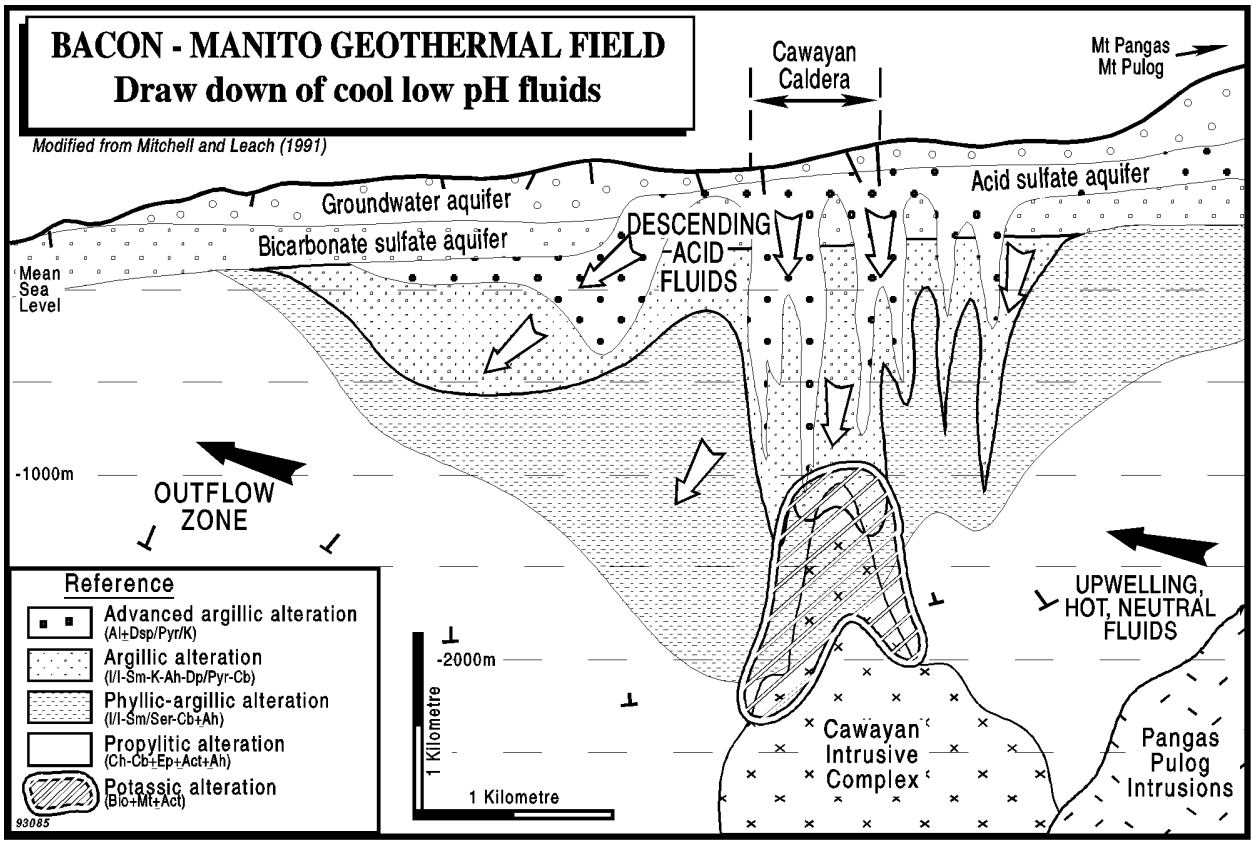

FIG. 2.14

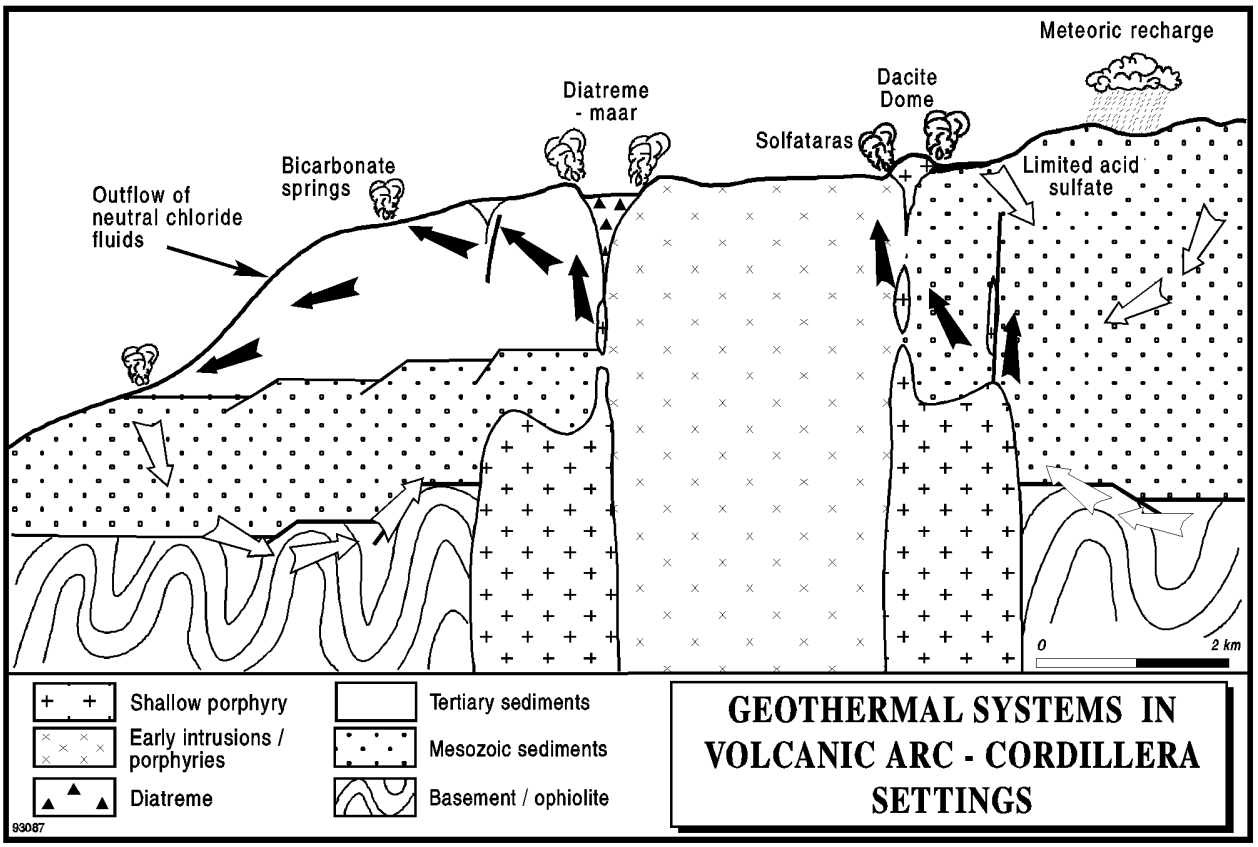

FIG. 2.15

Miocene age and locally containing outcropping porphyry copper deposits), and Mesozoic metamorphic basement complexes (Mitchell and Leach, 1991).

Recently emplaced shallow level plugs and stocks, commonly along contacts of pre-existing intrusions, are herein interpreted to represent the heat sources for hydrothermal systems. Dacite domes, diatreme breccias and associated pyroclastic rocks form extrusive phases of these plugs and stocks. Meteoric recharge originates at elevations higher than the active hydrothermal system. The restriction of vertical permeability to structures, and dome and diatreme contacts, causes the chloride fluids to approach the surface within confined upflow features, thereby facilitating the mixing of the upwelling fluids with surficial CO_2-rich and acid sulfate fluids. Distal outflows follow dilational structures and form dilute neutral chloride springs at lower elevations.

These active hydrothermal systems associated with volcanic arcs in cordillera settings are analogous to porphyry-related quartz-sulfide gold $\pm$ copper, carbonate-base metal gold, and epithermal quartz gold-silver deposits described herein (Section 7).

i) Amacan Geothermal Field
(data from: Barnett et al., 1985; PNOC-EDC, 1985a; Mitchell and Leach, 1991)

The Amacan geothermal field in North Davao, east Mindanao (Fig. 2.5) is hosted in Mesozoic metamorphic and Early Tertiary sedimentary rocks into which have been emplaced multiple Miocene intrusions ranging from early quartz diorite to later microdiorite porphyry (Fig. 2.16). The adjacent North Davao porphyry copper deposit, occurs within quartz diorite porphyry intruded into the metamorphic rocks. A number of Pliocene to Recent volcanic plugs and domes are aligned in a NS trend parallel to regional structures formed in relation to subduction along the Philippine trench, to the east. Lake Leonard caps a maar volcano/diatreme breccia complex rimmed by pyroclastic material dated at 1800 years BP (Barnett et al., 1985).

The heat source for the active hydrothermal system is interpreted to be felsic magmas which are the sources for the domes, plugs and maar volcano pyroclastic rocks. Thermal manifestations and deeper circulating hydrothermal fluids are restricted to the margins of domes and diatremes, with outflows extending 6-12 km northward, controlled by NS regional structures associated with the Philippine fault. Hydrothermal solfataras occur at the contact of the Ugos dome and around the margins of the Leonard diatreme. Neutral chloride springs occur 100 m below the Ugos steam vents. Abundant CO_2-rich/bicarbonate springs in the region deposit spectacular travertine deposits. The high gas content of the hydrothermal system (approx. 4 wt % CO_2; Table 3, AM-1) is indicative of either incursions to depth of the CO_2-rich surficial waters, or a significant input of magmatic volatiles into the circulating hydrothermal system.

ii) Daklan Geothermal Field
(data from: PNOC-EDC, 1982; Reyes, 1990b; Mitchell and Leach, 1991)

The Daklan geothermal field, 30 km north of Baguio in the central Cordillera of Luzon (Fig. 2.5), is hosted in Miocene andesite overlying a thick (<2 km) sequence of 'sub-intrusive andesite breccias' (Reyes, 1990b) which may represent a diatreme breccia (Fig. 2.17). A number of Recent dacite and andesite plugs and domes intrude the volcanic and sedimentary rocks, and are the site of fumarolic activity. The only permeability encountered during drilling occurs at the contacts with dacite dikes which are inferred to represent feeders for the Balukbok Dome. The deep fluids from well DK-1 are saline (14110 ppm Cl^-; Table 3) and relatively hot (260-270°C) fluid.

iii) Acupan
(data from: PNOC-EDC, 1985b; Mitchell and Leach, 1991)

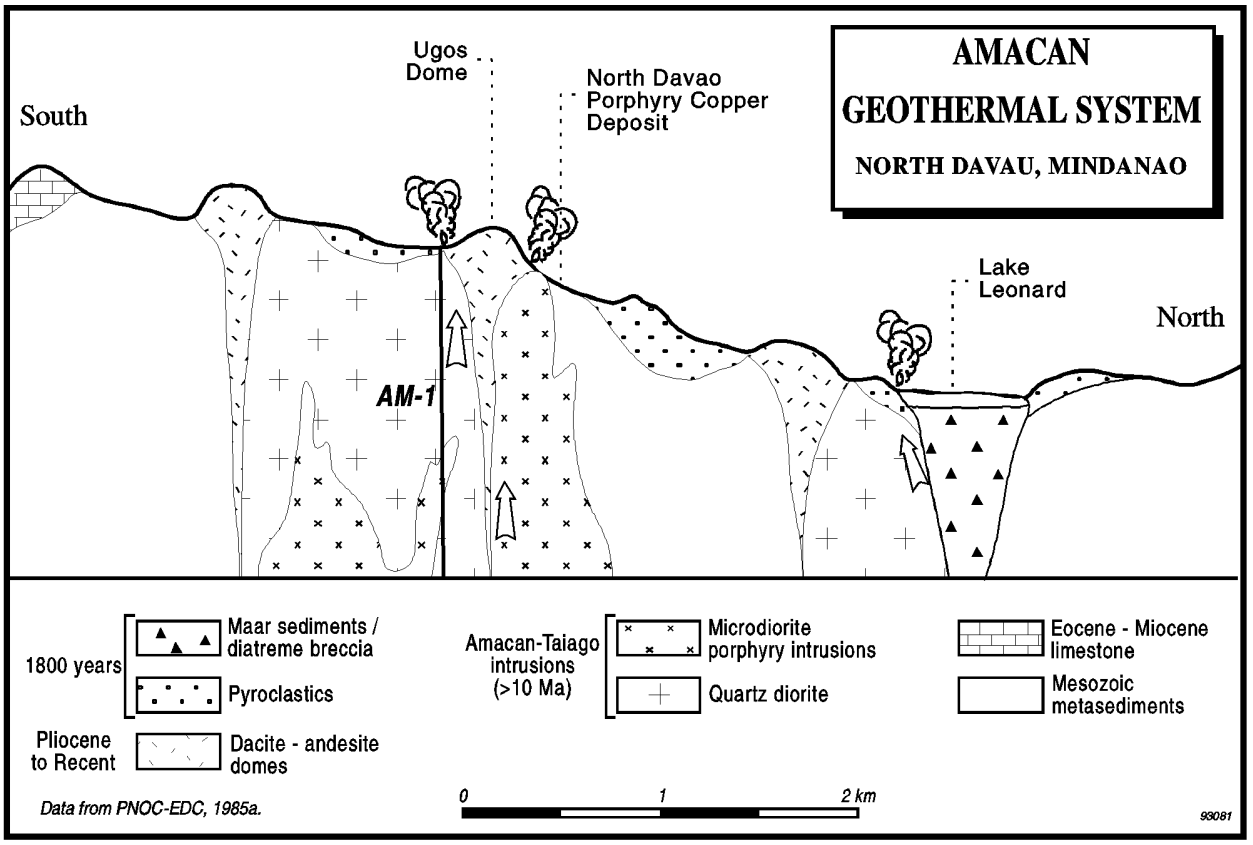

FIG. 2.16

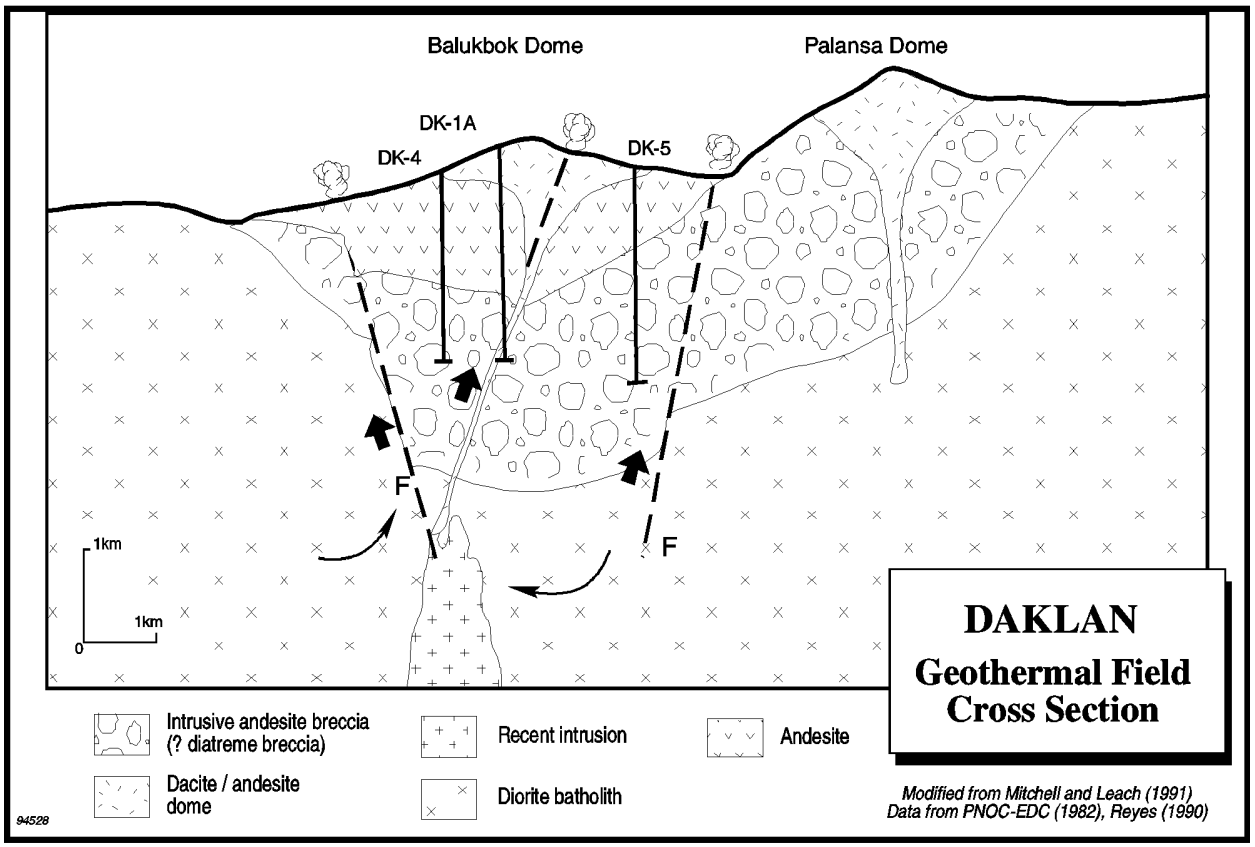

FIG. 2.17

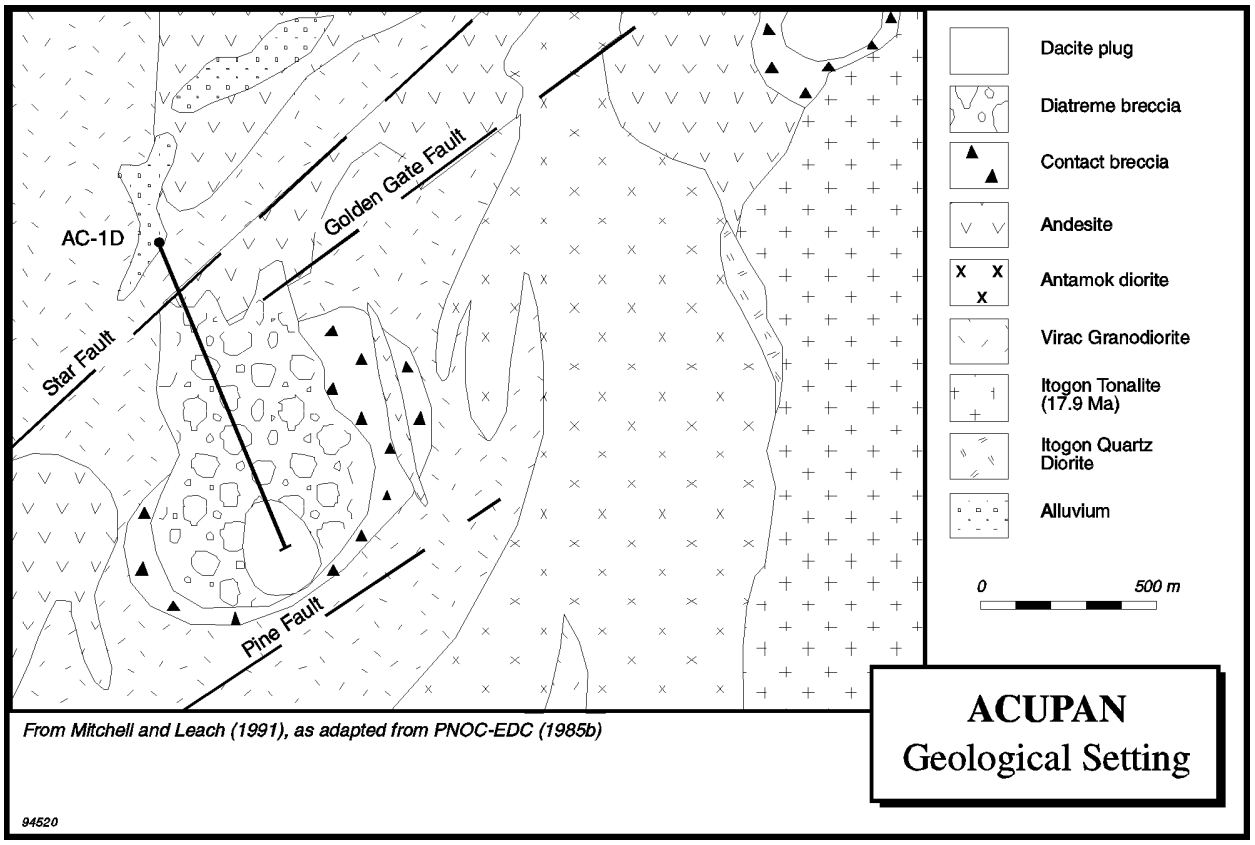

FIG. 2.18

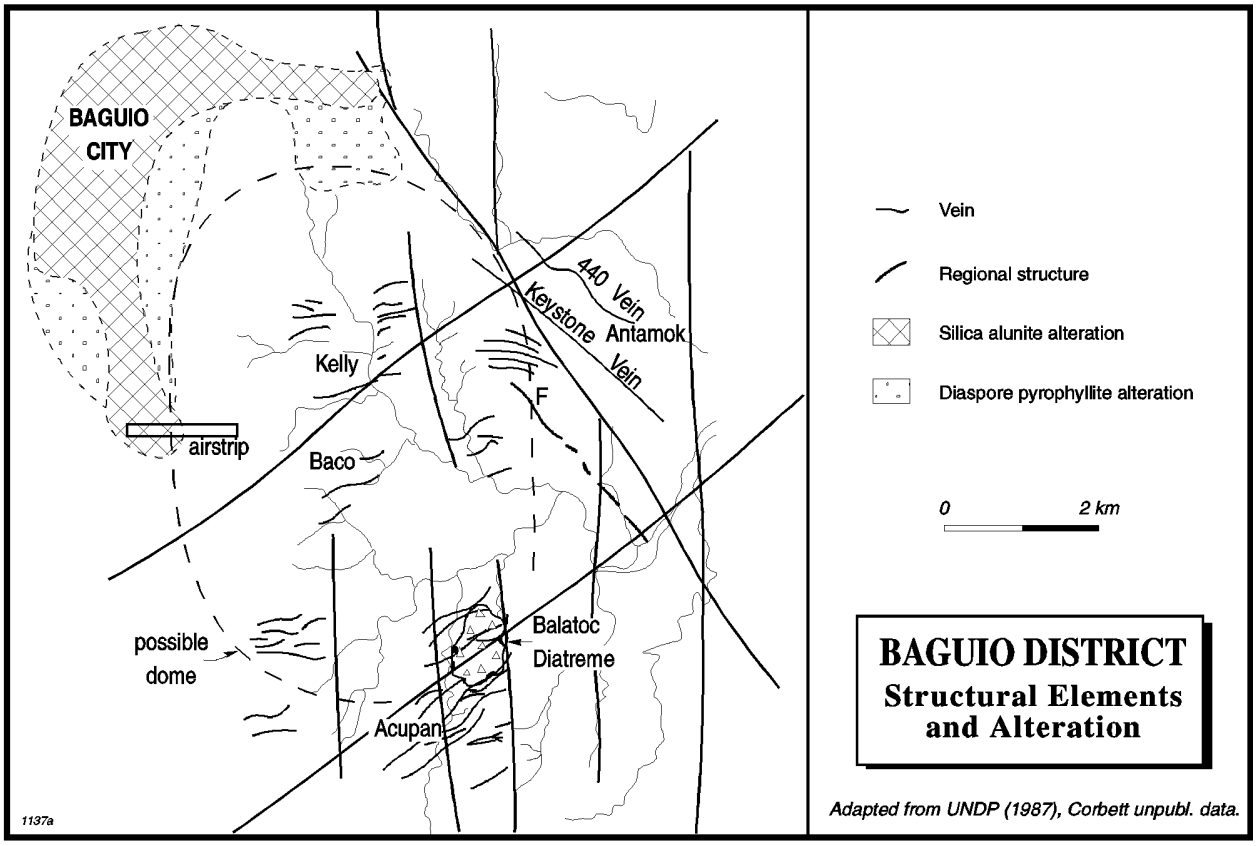

FIG. 2.19

The Acupan gold mine, 15 km southeast of Baguio (Figs. 2.5, 2.19) exploited gold mineralization hosted in NE trending structures which cut the 1 Ma Balatoc diatreme and associated dacite plug (Fig. 2.18). The diatreme and plug (an endogenous dome) were emplaced into a series of older Miocene to Pliocene intrusions and andesite volcanic rocks. Hot water seepages were common throughout the upper levels of the Acupan gold mine, and steam and boiling water discharges at deeper levels. Geothermal drilling encountered only minor permeability within the diatreme at around 1000-1200 m depth.

A comparison of down hole conditions (PNOC-EDC, 1985b) and fluid inclusion data (Sawkins et al., 1979; Cooke and Bloom, 1990) suggests that the water and steam encountered in the mine are manifestations of the dying phase of a once extensive hydrothermal system which deposited the gold mineralization (Cooke and Bloom, 1990). The styles of alteration and mineralization at the Acupan mine are described in more detail in Section 7.iii on carbonate-base metal gold deposits.

v) Conclusions

1. Types of Active Porphyry Systems

Active geothermal systems in the Philippines provide insights into the process of formation of porphyry copper and porphyry-related gold deposits. Drilling to depths of over 3.5 km, over more than 20-30 squ km, enables the development of comprehensive alteration, mineralization, and fluid flow models for these active porphyry systems.

Intrusion-related active hydrothermal systems in the Philippines are of two main types (Reyes 1990b), either:
i) large diffuse systems adjacent to, or flanked by, composite andesitic volcanic complexes (e.g., Tongonan, Palinpinon, Bacon-Manito), or
ii) smaller systems associated with dacite or silicic andesite plugs or domes hosted in cordillera settings (e.g., Amacan, Daklan, Acupan).

The large geothermal systems at Tongonan, Palinpinon, and Bacon-Manito, are associated with permeability provided by either regional structures, or composite volcanic environments. Shallow (<2-3 km) multiple intrusions and/or parent melts at depth represent the heat sources and possibly provide a significant component of magmatic fluids for the circulating hydrothermal system. In such settings, intrusions are emplaced into sequences of relatively permeable fractured volcanic rocks. This widespread lateral permeability causes fluids to permeate a significant rock volume, thereby producing large areas of alteration and mineralization zonations which are comparable to many porphyry copper-gold systems.

If intrusions are emplaced into basement sedimentary, metamorphic or intrusive rocks which occur within the cordillera regions of the Philippines, hydrothermal fluid flow will be restricted to permeable structures and intrusion contacts. Here, volcanism is limited to domes, diatreme/maar volcano complexes, and associated pyroclastic material. The confinement of fluids to narrow permeable zones permits the chloride hydrothermal fluids to reach very shallow crustal levels, where they are able to interact with ground water, CO_2-rich and acid sulfate waters. This type of active hydrothermal system is postulated to be analogous to the low sulfidation intrusion-related gold deposits encountered throughout the southwest Pacific rim (Section 7).

2. Evolution of Active Porphyry Systems

The geothermal systems in the Philippines provide a selection of 'time slices' during the evolution of intrusion-related hydrothermal systems. In each case, the initial emplacement of high level intrusions has resulted in the conductive transfer of heat during formation of contact metamorphic hornfels or skarns (e.g., Alto Peak, Palipinon).

Subsequent cooling of the intrusions has been accompanied by exsolution of fluids and the formation of magmatic vapour plumes (e.g., Alto Peak and Biliran). Fluid flow may be controlled by the same dilational structures which facilitated the emplacement of the intrusion. These vapours can vent to the surface as magmatic solfataras (e.g., Vulcan). The progressive disproportionation of magmatic SO_2, and the dissociation of HCl and H_2SO_4 are inferred to form acidic fluids which locally produce an advanced argillic overprint on the earlier high temperature contact alteration (e.g., Alto Peak).

Convective hydrothermal systems develop when the heat provided by an intrusion at depth, and possibly also by venting magmatic fluids, results in the formation of circulating meteoric-dominated hydrothermal systems at higher crustal levels. Early convective systems are generally poorly developed and have a high magmatic component (e.g., Alto Peak and Biliran), whereas later ones are better developed and more saline (e.g., Tongonan). The convective transfer of heat from the source intrusion causes zoned alteration composed of potassic (dominated by biotite) alteration at deeper, hotter levels, grading to propylitic alteration (actinolite, epidote, and zeolites) at shallower and cooler levels, and finally to near surface clay alteration (e.g.,Tongonan; Reyes, 1990b).

Cooling of the source intrusion creates pressure draw down and collapse in the hydrothermal system. This results in the descent of cool meteoric and relatively low pH, CO_2-rich and acid sulfate waters (e.g., Palinpinon, Tongonan, Bacon Manito) to depths up to 2 km below the surface, and causes overprinting phyllic and argillic alteration. The deposition of sulfates, carbonates and quartz from the descending waters seals zones of permeability.

3 STRUCTURE OF MAGMATIC ORE SYSTEMS

i) Introduction

Hydrothermal systems develop from the interplay of fluids and structures, as well as many other variables such as hot rock type, temperature, geochemistry etc. Fluids facilitate structural dynamics and the structures distribute fluids into the surrounding rocks. Brittle fracturing within competent host rocks in the upper portion of the crust provides permeability for the formation of magmatic-arc gold-copper alteration and mineralization. Very large quantities of fluid may be required to transport economic quantities of gold. At solubilities of 10 ppb (Fig. 4.6), 10^{6-7} litres of fluid (or about the equivalent of an olympic swimming pool) would be required to transport about 3 ounces of gold (Brown, 1986).

Major regional crustal structures act as conduits for rising porphyry intrusions which are the heat sources for hydrothermal systems. Fluids exsolve from porphyry intrusions, mix with ground waters and deposit minerals in peripheral settings and fill fractures as veins, or the open space within breccias. Movement on the major controlling structures commonly creates ore-hosting dilational environments in high angle subsidiary structures, particularly in settings of oblique convergence. Drilling grid orientations should take these angular relationships between the structural grain of a district and subsidiary mineralized structures into consideration.

Styles of mineralization and fracture patterns in outcrop scale may be governed by tectonic setting at continental scale. Existing fracture patterns will be activated during continuing deformation.

ii) Tectonic Setting

The southwest Pacific rim (Figs. 1.2, 3.1) encompasses the 'ring of fire', defined by the linear zone of volcanism and seismic activity at the boundary between the Pacific and adjacent Australia-(India), Philippine, and Eurasian plates. Although mostly convergent, variations in the style of tectonism in time and space are apparent along this plate boundary. Tertiary magmatic arcs along the 'ring of fire' host gold-copper mineralization and assist in the understanding of older arcs such as the Ordovician-Silurian Lachlan fold belt of eastern Australia. Sillitoe (1992) characterizes different styles of arcs as: simple, associated with transcurrent faulting, rifting, and back-arc extension, and describes associations with different magma suites in drawing attention to the dependency of mineralization style upon setting. The discussion focuses upon the influence of tectonic setting on structural framework, rather than on the style of magmatism, and seeks to demonstrate that some mineralization styles characteristically form in different tectonic settings (e.g., adularia-sericite epithermal veins in back-arc basins). Readers are referred to more specific texts for detailed analyses of tectonism (Kearey and Vine, 1996; Park, 1988) and related magmatism (Tatusumi and Eggins, 1995).

Porphyry intrusions and related mineralization are emplaced during arc-building magmatism. A typical scenario for a southwest Pacific rim magmatic arc might feature collision between continental and oceanic plates, in which the heavier basaltic oceanic plate is subducted along the Benioff zone, below the lighter sialic continental plate (Fig. 3.3). The subduction zone, marked by an oceanic trench or trough at the plate contact, is commonly concave in the direction of dip and movement, and dips under the magmatic island arc (e.g., Banda, Mariana arcs; Figs. 1.2, 3.1). During subduction, continental rocks and offshore sediments may become metamorphosed and deformed and develop into a mountainous accretionary prism (e.g., the Highlands of Papua New Guinea). Partial melting of subducted continental and oceanic material at depth will give rise to magmatic island arcs which constitute volcanic and volcaniclastic rocks at surface and pass downward to intrusion phases. Porphyry intrusions are emplaced at depths of 1-2 km, while differentiated felsic and volatile-rich intrusions may rise to

higher crustal levels, and large batholithic bodies occur at greatest depths. Under ideal conditions fluids may

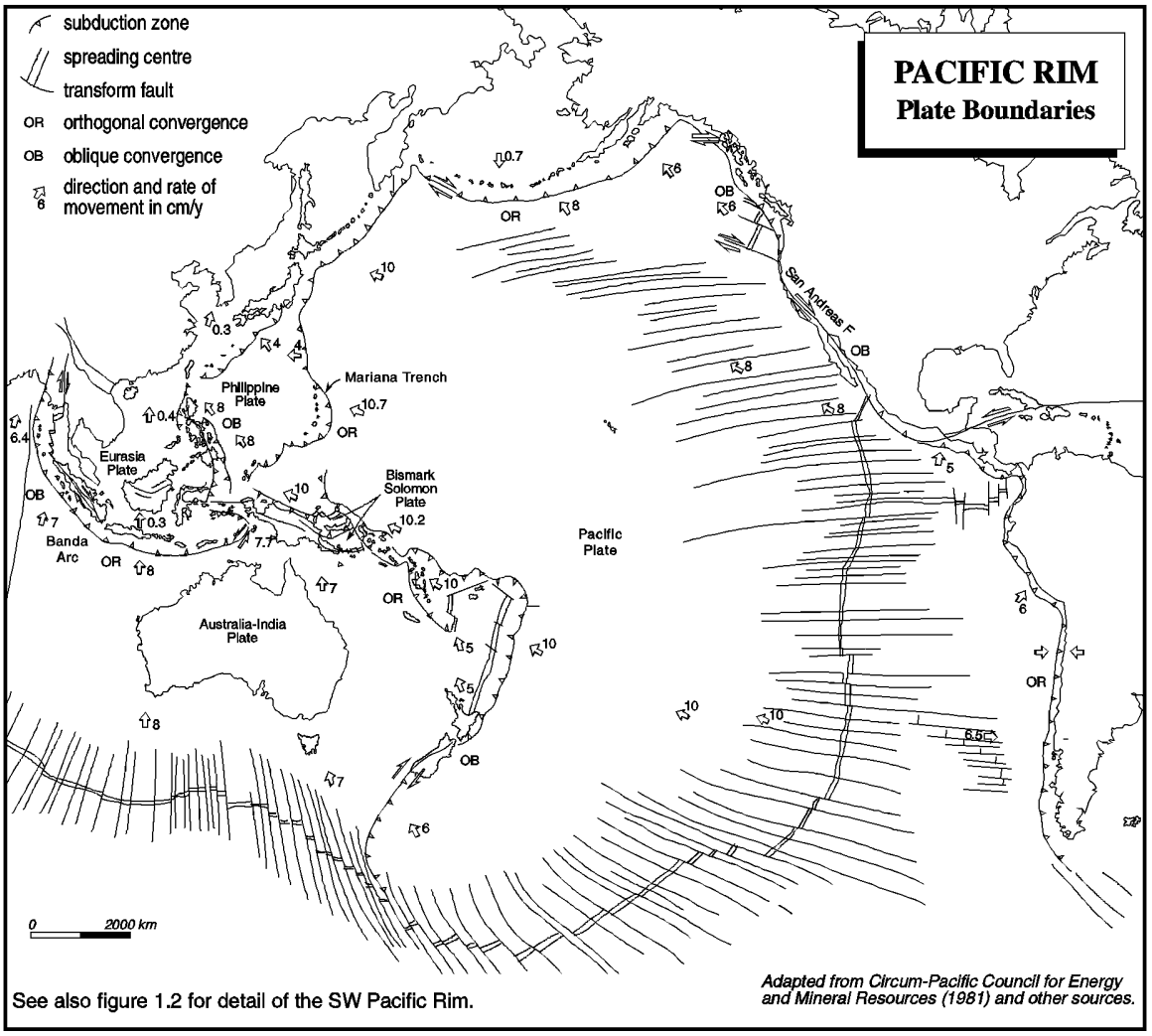

FIG. 3.1

evolve from the porphyry environment to form low and high sulfidation gold-copper mineralization outside the porphyry environment. The classification of Sillitoe (1992) has been modified to categorize four tectonic settings for southwest Pacific rim ore-related magmatism as:

a) <u>Orthogonal convergence</u>

In orthogonal convergence two plates collide at angles of roughly 90° to each other in a manner similar to the scenario described above. Examples of orthogonal convergence occur within younger active and older possibly dismembered arcs. These include the currently active Mariana and Banda arcs, magmatism in the Central Andes of Chile, which has been active over a protracted period of time, and some formerly active or now dismembered arcs in Papua New Guinea (Figs. 1.2, 3.1). In the Philippines, eastward subduction on a formerly more extensive Manila trench developed mid Miocene magmatic arcs and porphyry copper mineralization in Northern Luzon (Sillitoe, 1992), and possibly older porphyry systems in Negros (Burton, 1983). Oligocene-Miocene plutonism in northern Sulawesi formed in relation to a former subduction zone which has since been rotated to dip to the south (Fig. 5.8; Kavalieris et al., 1992). From the Eocene to Miocene, southwest subduction

of the Pacific plate facilitated the formation of the now dismembered island arcs extending from the islands of Manus to New Ireland, New Britain, and Bouganville in Papua New Guinea, and Guadalcanal the Solomon Islands, but ceased with the jamming of subduction by the Otong Java Plateau (Fig. 1.2; Davies, 1994 and references therein). While Miocene porphyry mineralization at New Britain (Titley, 1978) and Manus Island (Mason and McDonald, 1978) developed under conditions of orthogonal convergence, younger systems are described below.

Analyses of vein and fracture patterns formed in association with porphyries emplaced in orthogonal arcs suggest that many intrusions formed during extension regimes. Tectonic relaxation within an overall contractional environment provides one possible mechanism for localized extension in both time and place. Non-planar and high angle structures in orthogonal arcs may also facilitate localized extension. Relaxation may take the form of a reversal of orthogonal convergence, or change to oblique convergence. Molten volatile-rich magma which has been constrained at depth during orthogonal convergence, may be induced to rise rapidly to form porphyry intrusions under these changed conditions. Mineral deposition occurs at higher crustal levels under cooler conditions. Settings of orthogonal convergence are conducive to the formation of porphyry copper-gold deposits in which most mineralization occurs close to, or within, the intrusion.

b) Oblique convergence

In settings of oblique convergence (Figs. 3.1, 3.2), the plates slide past each other. Major transcurrent fault systems accommodate much of the displacement (e.g., Philippine fault, Philippines, Figs. 2.1, 2.5; Sumatran fault system, Indonesia, Fig. 1.2; Alpine fault, New Zealand, Fig. 7.47; Queen Charlotte fault, western Canada; San Andreas fault, western USA). Southwest Pacific arcs characterized by settings of oblique convergence include: the Pliocene to Recent in Northern Luzon and Mindanao in the Philippines, and the current western portion of the Banda arc in Indonesia; Plio-Pleistocene Taiwan (Sillitoe, 1992) and the Ordovician-Silurian of the Lachlan fold belt (below). Analyses of fracture systems suggest that mineralization develops in many orthogonal magmatic arcs during localized changes to oblique convergence.

Settings of oblique convergence are characterized by dilation formed in association with major strike-slip or transcurrent faults (Section 3.iv.b). This dilation facilitates not only the emplacement of intrusions into extensional settings, but also the evolution of mineralized fluids from the magmatic source to higher crustal levels, where mineral deposition occurs in cooler conditions. We suggest that settings of oblique convergence promote the formation of not only porphyry copper-gold systems, but also a wide range of low and high sulfidation porphyry-related gold-copper and gold-silver systems, which form outside, and in many instances distal to, the source intrusion. These vary from deeper porphyry copper-gold (e.g., Frieda, Papua New Guinea; Far South East [FSE], Tongonan geothermal system, Philippines), to wall rock- porphyry gold-copper (e.g., Cadia, eastern Australia), high sulfidation copper-gold (e.g., Nena adjacent to Frieda River; Lepanto adjacent to FSE), to low sulfidation quartz-sulfide and carbonate-base metal (e.g., Lake Cowal, eastern Australia; Kerimenge, Papua New Guinea), and epithermal systems at the highest crustal levels (e.g, Thames, New Zealand; Cracow, eastern Australia; McLaughlin, California).

The structural settings and mineralization styles vary in part according to the crustal level (Section 3.vii). At depth, regional structures in transpressional settings localize porphyry intrusions in splays or horsetails (e.g., FSE and others in the Philippines; Sillitoe and Gappe, 1984: Frieda River, Papua New Guinea; Corbett, 1994: Chuquicamata, Chile; Boric et al., 1990). At higher crustal levels, dilatant structures (e.g., Lepanto, Philippines; Nena, Papua New Guinea), fissure (e.g., Lake Cowal, Cracow; eastern Australia: Thames, New Zealand) and sheeted veins (e.g., Cadia, McLaughlin), localize magmatic-derived mineralization outside the porphyry environment.

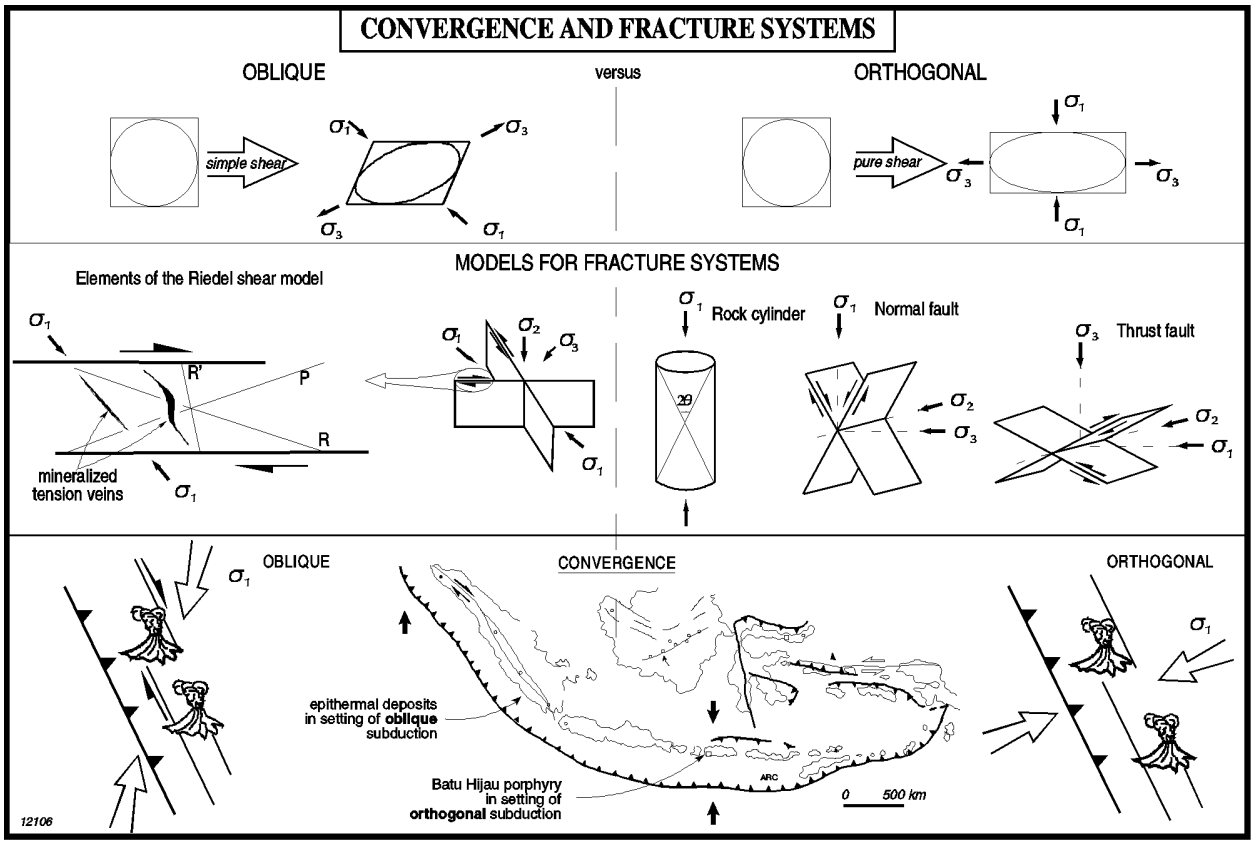
CONVERGENCE AND FRACTURE SYSTEMS
OBLIQUE
versus
ORTHOGONAL
simple shear
pure shear
MODELS FOR FRACTURE SYSTEMS
Elements of the Riedel shear model
R'
P
R
mineralized tension veins
Rock cylinder
Normal fault
Thrust fault
OBLIQUE
CONVERGENCE
ORTHOGONAL
epithermal deposits in setting of oblique subduction
Batu Hijau porphyry in setting of orthogonal subduction
ARC
0 500 km
12106

FIG. 3.2

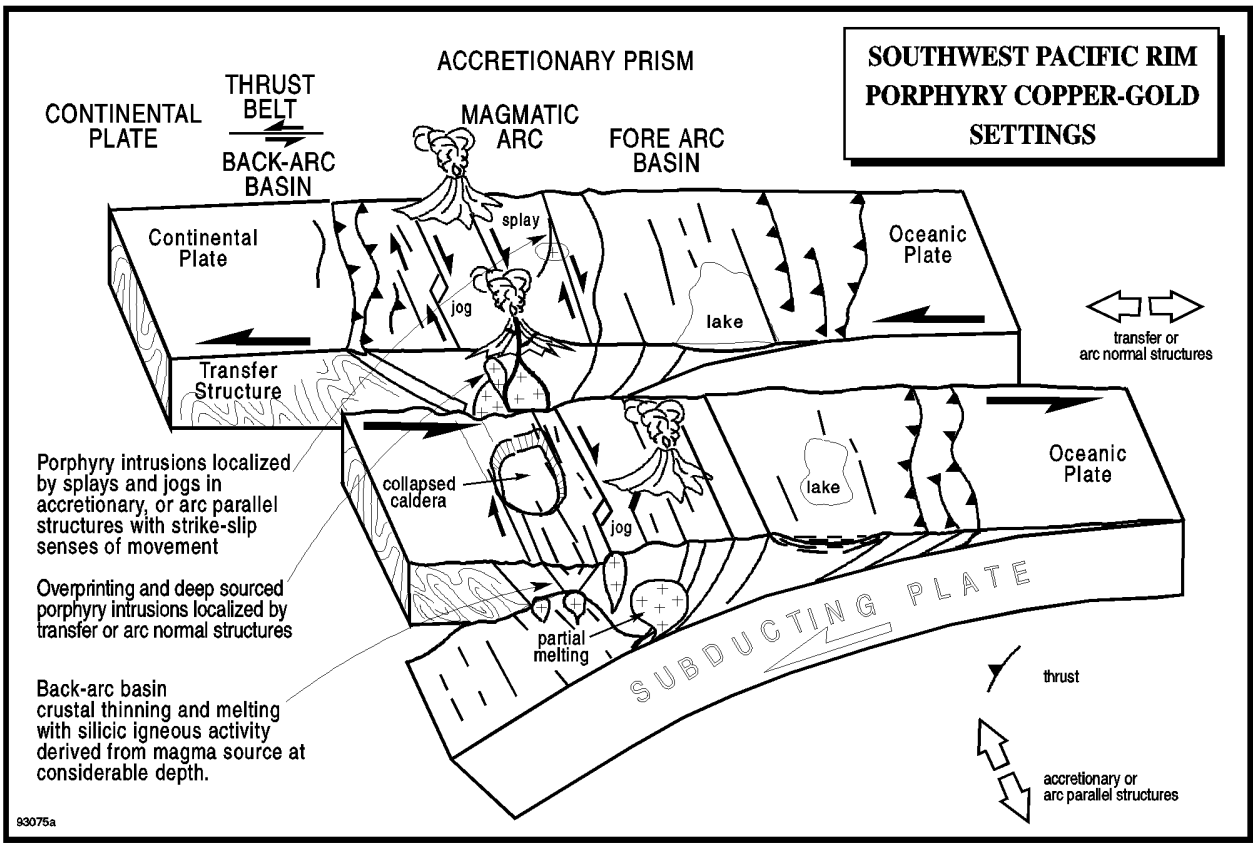
SOUTHWEST PACIFIC RIM PORPHYRY COPPER-GOLD SETTINGS
ACCRETIONARY PRISM
CONTINENTAL PLATE
THRUST BELT
BACK-ARC BASIN
MAGMATIC ARC
FORE ARC BASIN
Continental Plate
Oceanic Plate
splay
jog
lake
Transfer Structure
transfer or arc normal structures
Porphyry intrusions localized by splays and jogs in accretionary, or arc parallel structures with strike-slip senses of movement
Overprinting and deep sourced porphyry intrusions localized by transfer or arc normal structures
Back-arc basin crustal thinning and melting with silicic igneous activity derived from magma source at considerable depth.
collapsed caldera
partial melting
SUBDUCTING PLATE
thrust
accretionary or arc parallel structures
93075a

FIG. 3.3

c) Intra-arc rifts

Intra-arc rifts are distinguished from back-arc basins by the closer relationship with the magmatic arc and predominance of calc-alkaline arc-related magmatism. Although smaller than back-arc basins, intra-arc rifts initiate significant volcanoplutonism at sites of crustal thinning, and are significantly larger than pull-apart basins which host clastic sediments and may focus intrusion emplacement within magmatic arcs. Mineralization demonstrates a relationship with the intrusions emplaced into the rift and is typically localized by extension on the rift-bounding or intra-rift structures. Carbonate-base metal gold and epithermal quartz gold-silver mineralization predominate in many intra-arc rifts.

Displacement on transfer structures facilitated rifting and formation of the Bulolo graben, Papua New Guinea, into which are emplaced Edie porphyry intrusions and Bulolo 'agglomerate' extrusive equivalents (Section 7.iii.i; Dow, 1974; Lowenstein, 1982; Corbett, 1994). The Bulolo graben hosts the Morobe goldfield from which 3.7 million ounces of (mainly alluvial) gold has been produced, and published hard rock reserves of 5.5 million ounces remain. Mineralization is localized mostly by graben-bounding and intra-graben faults and occurs in adjacent extensional fractures formed by rifting (Section 7.iii.i). Similarly, the Tolukuma gold deposit is localized by an intra-arc rift bounding structure, but much of the ore occurs in subsidiary fractures (Corbett et al., 1994c; Section 7.iv.d.3). A jog in the Hauraki fault, which separates the Coromandel Peninsula from the intra-arc rift defined by the Hauraki graben, hosts the Ohio Creek porphyry and Thames epithermal goldfield (Figs. 7.47, 7.48). Many workers (Sillitoe, 1992; Mitchell and Garson, 1981) describe the Green Tuff Belt of Japan, which hosts Kuroko massive sulfide deposits, as also of this setting.

d) Back-arc extension

Back-arc basins (also termed marginal basins and back-arc rifts) form in settings further removed from the subduction zone than the magmatic arc, overlying the down-dip extensions of the subducting plate (Fig. 3.3). They represent sites of crustal thinning, commonly within continental rocks, and high heat flow, from which Sillitoe (1989, 1992) characterizes bimodal igneous rock suites. Adularia-sericite gold-silver deposits typically form within back-arc basins, in settings distal to the inferred magmatic metal sources.

In New Zealand, the back-arc environment of the Taupo Volcanic Zone (Fig. 8.2; Cole, 1984, 1990) provides a modern analogy for the setting of Miocene adularia-sericite epithermal gold-silver gold mineralization of the Coromandel Peninsula (Fig. 7.47; Henley, 1985b; Henley and Hoffman, 1987). The terms ensialic marginal basin (Cole, 1984) and intra-arc rift (Sillitoe, 1992) are also used to describe the Taupo Volcanic Zone. In Japan, adularia-sericite epithermal gold-silver vein systems, many of apparent Pliocene to younger ages, are localized by structures in competent basement metamorphic rocks which also facilitated the formation of Miocene Green Tuff Belts (e.g., Rubeshibe Belt, Hokkaido; G. Corbett, unpubl. reports 1987-92).

Deep crustal rifting during arc reversals (Section 3.v.c) may localize alkaline intrusions such as at Didipio and Marian, Philippines, and the Tabar-Lihir-Feni chain, Papua New Guinea, which some workers (Sillitoe, 1992) place in back-arc environments.

iii) Major Structures and Porphyry Systems

The spatial relationships between major structures and mineralization through geological time are well documented (O'Driscoll, 1986). In magmatic arcs, regional structures may localize intrusions and also create dilational structural environments which host ore. Other segments of the same structures may be compressional. Major structures may demonstrate protracted histories of activity as: pre-mineralization controls on basin sedimentation in host rocks, localization of pre-mineralization intrusion or breccias, through syn-mineralization formation of ore systems, and post-mineralization deformation of ore deposits. Pre-existing fracture systems are

common ore environments especially in the deposit styles most proximal to magmatic source rocks, whereas more distal deposit styles occur in dilational structures. Pre-existing structural grains will influence the formation of later mineralized fracture/vein systems, and waters hosted in strongly fractured rocks may promote mineral deposition.

Major structures in subduction-related Pacific rim settings (Figs. 3.1, 3.3) may be classified as:

a) Accretionary structures
b) Transfer structures
c) Conjugate transfer structures
d) Transform faults

a) Accretionary or arc parallel structures

These structures form parallel to the subducting plate margin and in part define the structural grain of the accretionary prism, particularly in arcs characterised by orthogonal convergence (Figs. 3.3, 3,5: e.g., Domeyko and Atacama faults, Chile: Lagaip, Fiak-Leonard Schultz fault, Papua New Guinea; Figs. 3.4, 6.18). In settings of oblique subduction, arc parallel structures may form as steeply dipping transcurrent faults which display predominantly strike-slip components of displacement and extend for hundreds of kilometres (e.g., Philippine fault, Philippines; Sumatran fault system, Indonesia; Alpine fault, New Zealand; San Andreas fault, California; Figs. 1.2, 3.1). While many accretionary structures may be identifiable as one or more discontinuities (e.g., Philippine, alpine, and Sumatran faults), others occur as structural corridors (e.g., 'Tokuryu structural zone' [TSZ], in southern Hokkaido which hosts Chitose, Kouryu, Tokuryu, and other gold deposits; G. Corbett, unpubl. data, 1987), and some as sutures which separate differing segments of accreted terrains within magmatic arcs (e.g., Gilmore suture, eastern Australia; Fig. 3.11: Kalimantan suture, Indonesia, Fig. 3.12: below).

Porphyry and porphyry-related mineralization are localized along accretionary structures at splays, jogs, and flexures by strike-slip movement. These dilatant environments provide fracture mechanisms for fluids to evolve considerable distances from porphyry source rocks to form epithermal gold deposits. These dilatant features display a configuration of extensional or negative flower structures (Lowell, 1985) in profile (Fig. 3.14). Splays or horsetails host porphyry systems at deepest levels, typically in arcs characterised by oblique convergence (e.g., in the Philippines; Lepanto, Fig. 6.24; Tongonan geothermal field, Fig. 2.6: in Papua New Guinea; Frieda Copper; Fig. 6.18), or temporary changes to oblique convergence (e.g. Chuquicamata, Chile; Boric et al., 1990). The Tongonan geothermal field occurs within a jog at surficial levels in the Philippine fault, and splays at depth delineate areas of highest heat flow (Fig. 2.6). Jogs (e.g., Misima, Papua New Guinea; Fig. 7.43: Cracow, eastern Australia; Fig. 7.54) and flexures (e.g, Cinola, British Columbia) typically host ore at intermediate levels. At higher crustal levels pull-apart basins form as jogs in strike-slip accretionary structures and host epithermal gold-silver mineralization (e.g., Sumatran fault, Indonesia at Mangani, Kavalieris et al., 1987; and Lampumg [Semung], G. Corbett, unpubl. report, 1993). Structures which facilitated basin formation and intra-basin faults may continue dilation after basin formation and act as hosts to mineralization (e.g., Gympie, eastern Australia; Fig. 3.15: Kelian, Indonesia; Figs. 7.18, 7.19).

b) Transfer or arc normal structures

These structures accommodate the along-strike or dip variations in linear detachment faults (Etheridge et al., 1988), and have been expanded using the classification of Lowell (1985) to include collision settings. Where at high angles to the accretionary prism, these structures may separate segments of a subducting slab and so accommodate variations in the dip or rate of subduction (Corbett, 1994; Fig. 3.3). They may act as deep crustal

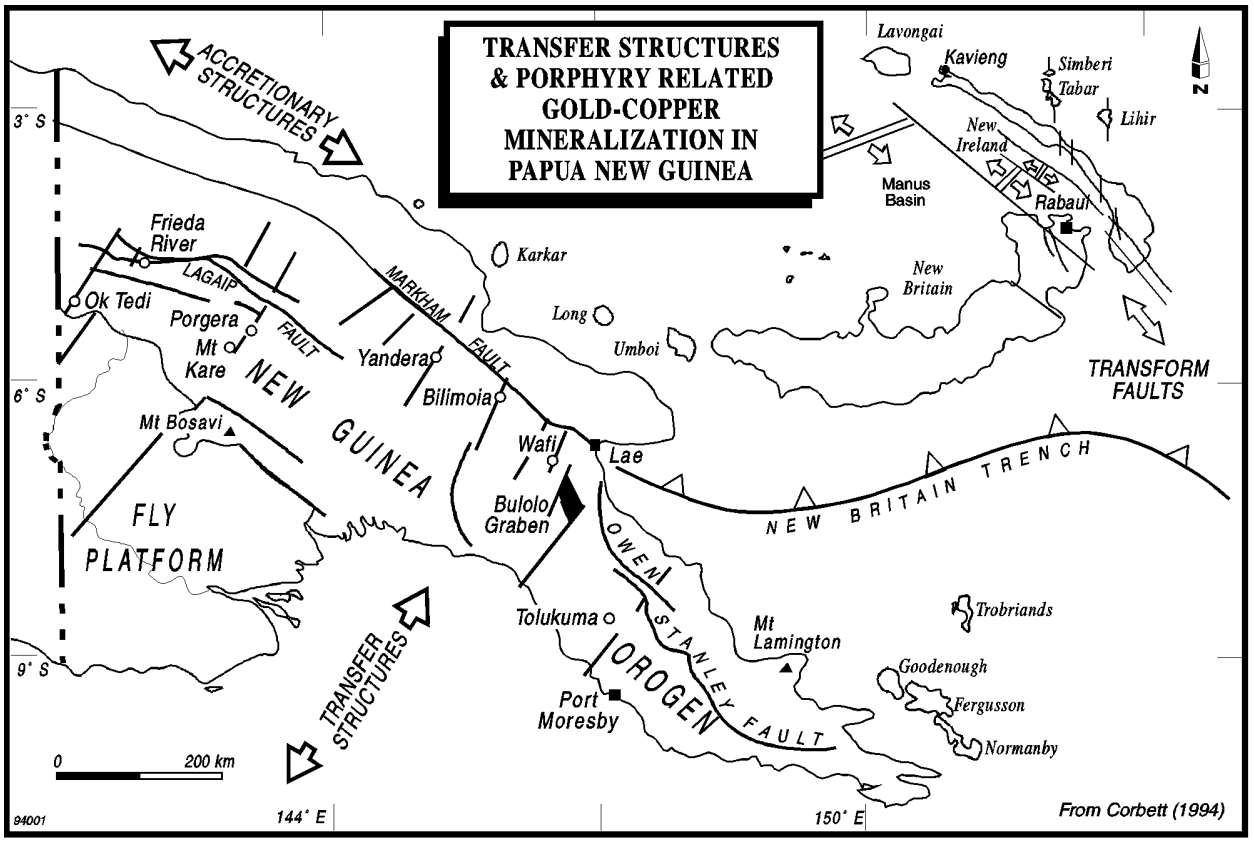
TRANSFER STRUCTURES & PORPHYRY RELATED GOLD-COPPER MINERALIZATION IN PAPUA NEW GUINEA
ACCRETIONARY STRUCTURES
3° S
6° S
9° S
Frieda River
Ok Tedi
Porgera
Mt Kare
LAGAIP FAULT
MARKHAM FAULT
Yandera
Bilimoia
Mt Bosavi
NEW GUINEA
FLY PLATFORM
Karkar
Long
Umboi
Wafi
Lae
Bulolo Graben
OWEN STANLEY FAULT
OROGEN
Tolukuma
Port Moresby
TRANSFER STRUCTURES
Lavongai
Kavieng
Simberi
Tabar
Lihir
New Ireland
Manus Basin
Rabaul
New Britain
TRANSFORM FAULTS
NEW BRITAIN TRENCH
Mt Lamington
Trobriands
Goodenough
Fergusson
Normanby
0
200 km
94001
144° E
150° E
From Corbett (1994)

FIG. 3.4

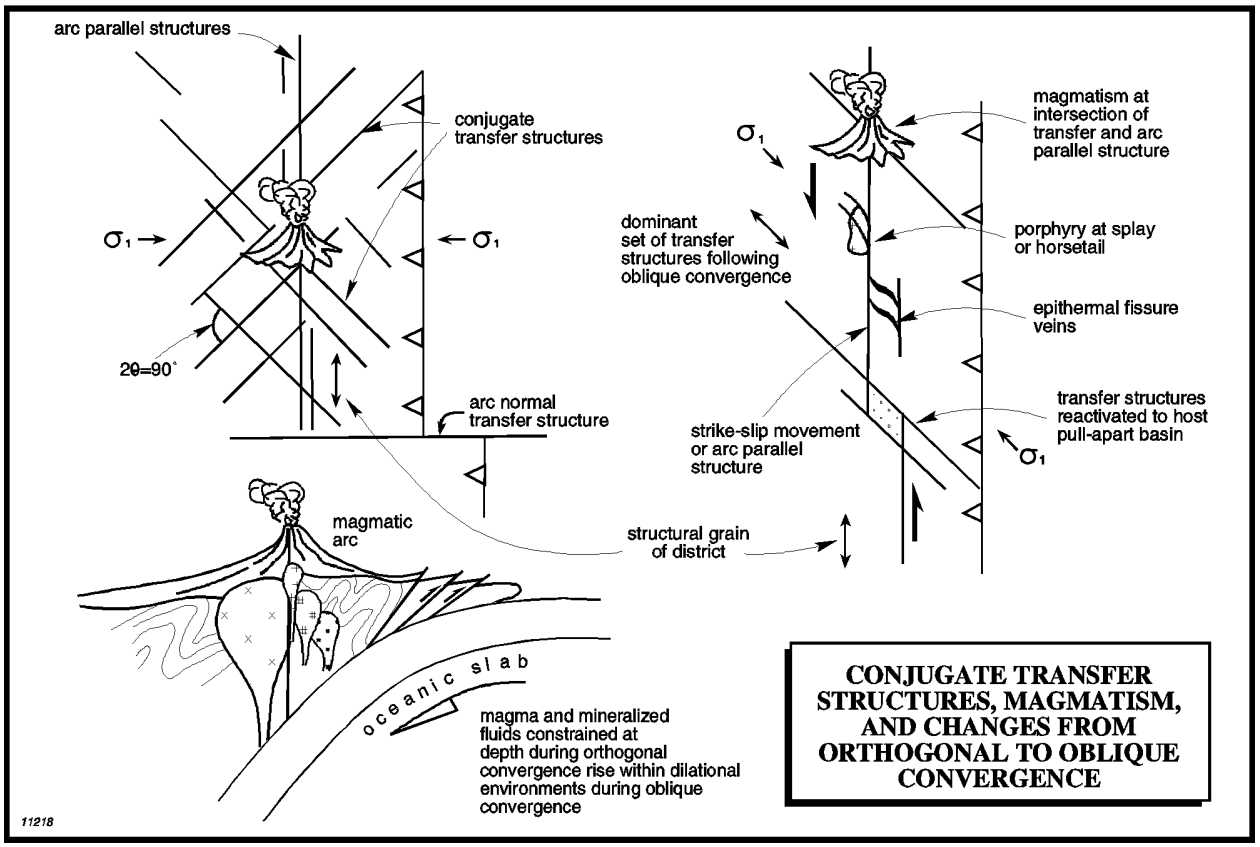
arc parallel structures
conjugate transfer structures
σ1
σ1
2θ=90°
arc normal transfer structure
magmatic arc
oceanic slab
magma and mineralized fluids constrained at depth during orthogonal convergence rise within dilational environments during oblique convergence
σ1
dominant set of transfer structures following oblique convergence
magmatism at intersection of transfer and arc parallel structure
porphyry at splay or horsetail
epithermal fissure veins
strike-slip movement or arc parallel structure
transfer structures reactivated to host pull-apart basin
σ1
structural grain of district
CONJUGATE TRANSFER STRUCTURES, MAGMATISM, AND CHANGES FROM ORTHOGONAL TO OBLIQUE CONVERGENCE
11218

FIG. 3.5

discontinuities to facilitate the emplacement of melts derived from considerable depths into settings at higher crustal levels (e.g., Porgera and Mt Kare are localized by the Porgera transfer structure, Papua New Guinea, Figs. 3.4, 7.22; Corbett, 1994; Corbett et al., 1995), or focus overprinting intrusions (e.g., Grasberg, Indonesia; Wafi, Papua New Guinea, Fig. 6.11), and by reactivation, facilitate the formation of intra-arc rifts (e.g., Bulolo graben, Fig. 7.28). Porphyry systems are commonly localized at the intersections of transfer and accretionary structures (e.g., Porgera, Corbett et al., 1995). As deep basement features, transfer structures may not occur as easy to map faults, especially if obscured by folded and thrusted cover rocks within accretionary prisms (e.g., the Highlands of Papua New Guinea). However, in rapidly uplifted and eroded terrains (e.g., the island of New Guinea) transfer structures may be identified as fractures which penetrate the cover rocks, most readily discernible on quality landsat imagery (Corbett, 1994), or aeromagnetic data. Individual fractures associated with transfer structures host vein systems at Porgera and mineralized milled matrix fluidized breccias at Mt Kare in Papua New Guinea (Section 7.iii.i).

c) Conjugate transfer structures

These structures are inferred to form in settings of orthogonal convergence and display angular relationships to the accretionary prism typical of conjugate fracture patterns (Fig. 3.5), and so contrast with arc normal transfer structures. Although two orientations generally develop at angles of typically 90° (below), one may become dominant, particularly as a result of changes to oblique subduction at some stage in the history of the arc (Section 3.v.c). For instance, in the northern Lachlan fold belt, Laing (1994) describes NE fractures localizing ore systems (e.g., Gilberton fault, Fig. 7.6) which dominate the NW set in a region of generally NS oriented magmatic arcs of different ages. NW transfer structures localize ore systems in the cental Lachlan Fold of New South Wales (below; Fig. 3.11). Conjugate transfer structures localize porphyry intrusions at the intersections with accretionary structures or develop as mineralized corridors. At prospect scale conjugate transfer structures commonly host vein mineralization formed peripheral to porphyry intrusions (e.g., Batu Hijau, Indonesia).

d) Transform faults

Transform faults are strike-slip faults which show variations in the form and direction of displacement and most commonly separate segments of spreading centres within oceanic ridges (Fig. 3.1; Wilson, 1965; Biddle and Christie-Blick, 1985), but may locally continue to onshore settings (Price and Cosgrove, 1990) and facilitate ore-formation (e.g., East New Britain, Papua New Guinea; Corbett and Hayward, 1994; Fig. 6.31). Many of the major strike-slip faults cited above (e.g., San Andreas fault system, Queen Charlotte fault, Sumatran fault system) terminate against spreading centres and so have been related to transform faults (San Andreas fault, Wilson, 1965). However, the more recent distinction which describes these as strike-slip faults (Price and Cosgrove, 1990) is preferred herein.

iv) Fracture Patterns in Magmatic Arcs

It is useful for the explorationist to consider the different styles of fracture patterns which develop in varying tectonic settings, and the influence these have upon mineralization styles. Readers are referred to more specific texts (Ramsay, 1967; Bles and Feuga, 1986; Price and Cosgrove, 1990; Price, 1966; Hancock, 1985) for detailed analyses of fracture patterns, outside to scope to this work. Fracture patterns are considered in the framework of differing tectonic elements described above, typically with the end members orthogonal or oblique, according to the angular relationship of convergence.

Fracture systems are described in very broad terms as pure shear which equates to settings of orthogonal convergence (and also localized extension), and simple shear which equates to settings of oblique convergence (Fig. 3.2; Ramsay, 1967; Bles and Feuga, 1986; Price and Cosgrove, 1990). Alternatively, Hancock (1983)

presents three classes of fracture systems based upon the relationship between dihedral angles (2O) and principle stress o_1, as extension fractures, hybrid shear failure, and shear failure. There is a link between differences in convergence as described above (Sections 3.ii.a, 3.ii.b) and the development of varying forms of fracture systems and associated styles of mineralization at different crustal levels. Note that it is common for pre-existing fractures to behave differently during reactivation under varying stress regimes.

a) Orthogonal convergence

In settings of orthogonal convergence (Section 3.i.a) magmatic arcs form in relation to subducting plates which collide at roughly 90° (Figs. 3.2, 3.3, 3.5). Fracture patterns formed in this setting include: arc normal or tension fractures, arc parallel or compressional fractures, and conjugate fractures (Figs. 3.5, 3.6). If porphyry intrusions are emplaced into conditions of oblique convergence, the strongly dilational conditions may facilitate the formation of extensive peripheral vein systems (e.g., Cadia, eastern Australia). By contrast, porphyries in orthogonal arcs typically display more restricted peripheral vein systems (e.g., Batu Hijau, Indonesia), and the inferred retention of magmatic fluids within the porphyry environment. Intrusion emplacement may be enhanced by relaxation of convergence to localized extension, or periodic changes to oblique convergence (below).

In the case of the conjugate fractures, biaxial pure shear in isotropic rocks form conjugate shear fractures each oriented at angles <45° to principle stress, as O = 45- //2 where o is the angle of internal friction (Figs. 3.2). Hancock (1985) describes conjugate fractures as hybrid shear failure. Angles in the order of 60° between conjugate fractures are common in brittle dry rock (Hobbs et al., 1976; McClay, 1987), and as a general rule are higher where o_3 is compressive (Bles and Feuga, 1986) under high pressure settings (at considerable depth, McClay, 1987), and lower in some experimental conditions (McKinstry, 1948). Thus, conjugate transfer structures commonly intersect at angles in the order of 90° (Fig. 3.5; G. Corbett, unpubl. data). Although conjugate fractures form normal, thrust and strike-slip fault patterns (Fig. 3.2), those developed in plan view by orthogonal convergence are of greatest interest here (Figs. 3.5, 3.6).

Movement on conjugate fractures during orthogonal compression may result in the formation of small scale dilatant tension gash veins in brittle host rocks (McClay, 1987; Fig. 3.6). However, in ore systems this is of most interest in extensional settings. If porphyry intrusions are emplaced in settings of orthogonal convergence, both tension and conjugate shears (fractures) may become activated and host styles of mineralization typical of near porphyry environments (e.g., quartz-sulfide gold $\pm$ copper veins; Section 7.ii). Porphyry intrusions may be emplaced during relaxations in compression which equate to localized extension. Conjugate fractures developed during compression, may become reactivated in the opposite sense to host vein mineralization during extension (Fig. 3.6). This movement may create dilational sigmoidal shaped thicker vein segments formed as flexures and tension gash veins, and which typically host higher metal grades (Fig. 3.6: e.g., quartz-sulfide gold veins peripheral to Batu Hijau, Indonesia; Meldrum et al., 1994).

Tension fracture/veins develop in the orientation of principle compression and may be related to arc normal transfer structures (Figs. 3.6). If porphyry intrusions are emplaced during compression then the tension fractures may host adjacent veins, (e.g., Arakompa, Papua New Guinea; Fig. 7.10).

Orthogonal fracture/veins form as subsidiary features to sheeted veins, in an orientation normal to a primary vein trend. These commonly develop in the tension fracture orientation, possibly by reactivation of existing tension fractures, during a relaxation of orthogonal convergence (Fig. 3.16).

Compression fracture/veins form normal to the principle compression and represent the structural grain of the magmatic arc, including folds and cleavage, which form at greater depths than of interest here, but may be

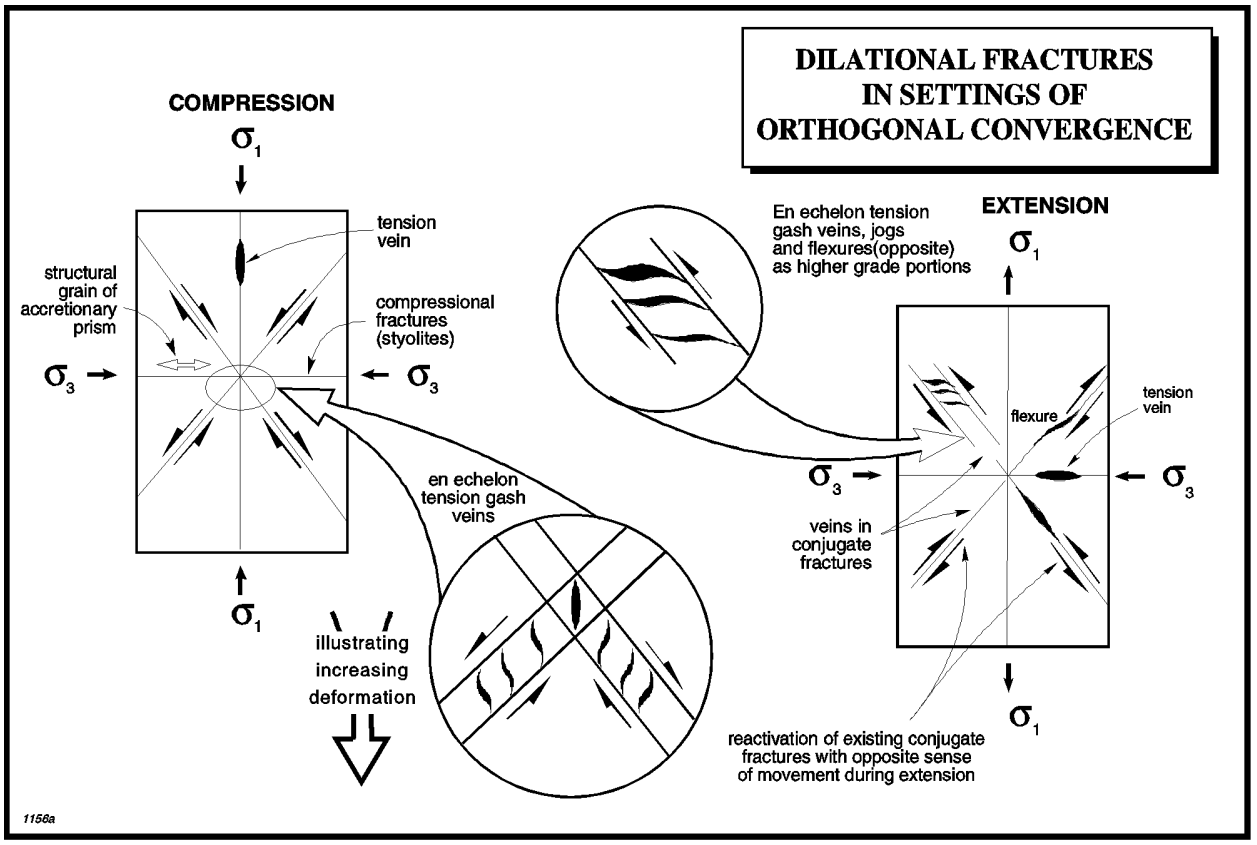
DILATIONAL FRACTURES
IN SETTINGS OF
ORTHOGONAL CONVERGENCE
COMPRESSION
σ1
tension vein
structural grain of accretionary prism
compressional fractures (styolites)
σ3
σ3
σ1
en echelon tension gash veins
illustrating increasing deformation
En echelon tension gash veins, jogs and flexures(opposite) as higher grade portions
EXTENSION
σ1
flexure
tension vein
σ3
σ3
veins in conjugate fractures
σ1
reactivation of existing conjugate fractures with opposite sense of movement during extension
1156a

FIG. 3.6

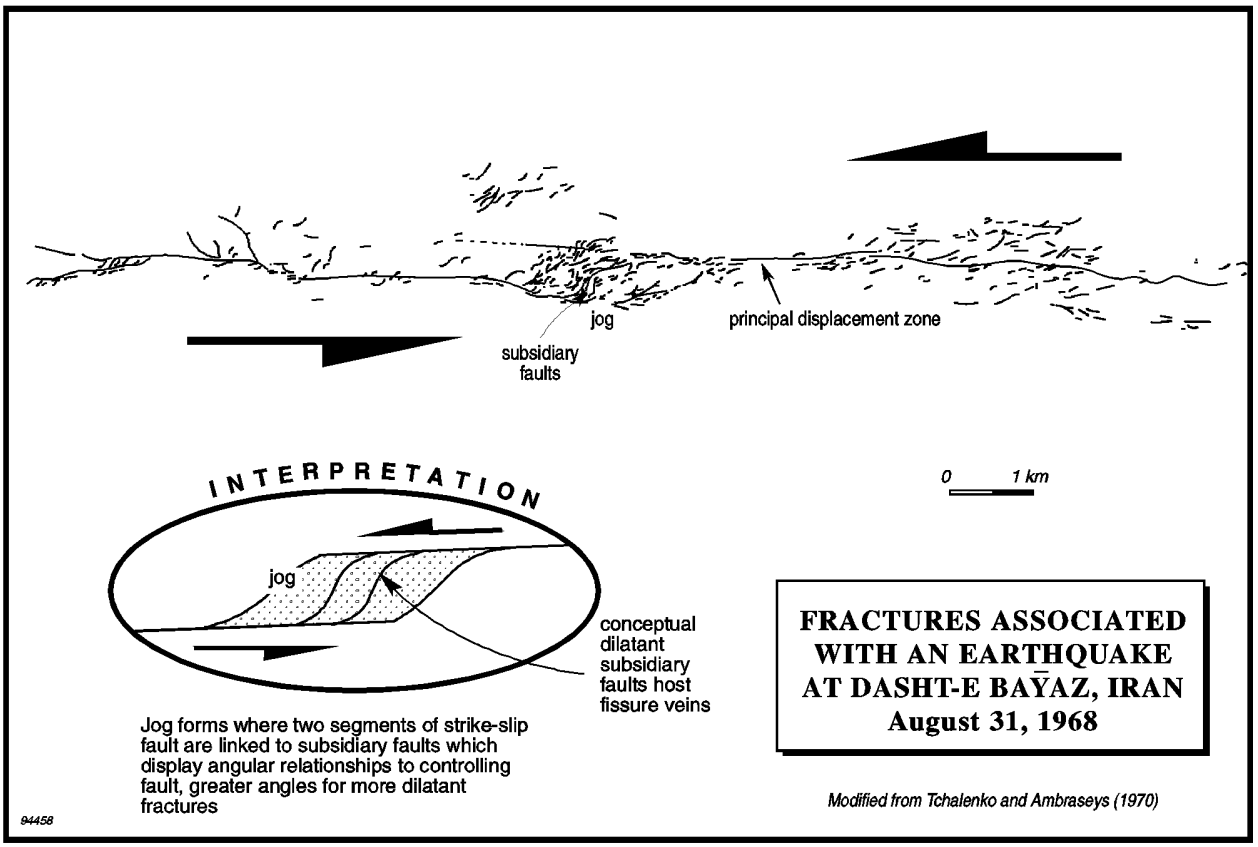
jog
principal displacement zone
subsidiary faults
INTERPRETATION
jog
conceptual dilatant subsidiary faults host fissure veins
Jog forms where two segments of strike-slip fault are linked to subsidiary faults which display angular relationships to controlling fault, greater angles for more dilatant fractures
0 1 km
FRACTURES ASSOCIATED
WITH AN EARTHQUAKE
AT DASHT-E BĀYAZ, IRAN
August 31, 1968
Modified from Tchalenko and Ambraseys (1970)
94458

FIG. 3.7

exhumed by erosion and mineralized (e.g. Bilimoia; Section 7.11.d). These fabrics are commonly termed styolites in much of the geological literature (cf Hancock, 1985). Although generally the strongest fractures in a region, arc parallel fractures are unlikely to be mineralized unless dilated by a change in the stress regime. The Grasberg porphyry copper-gold deposit is inferred to have been localized by the intersection of arc parallel SW-WSW trending faults and a major NE-ENE trending transfer structure which transects Iran Jaya. Stockwork quartz veins lie within these (060°-070°, transfer; 120°, arc parallel) and lesser NS fracture trends, while high grade ore is aligned in the 120° trend (Pennington and Kavalieris, 1996), parallel to the structural grain of the district. These workers stress that high grade mineralization is fracture controlled, post-dates porphyry intrusion, and is derived from a larger magma source at depth (similar to the model described in Section 4.c). Mineralization is assumed to take place during relaxation of compression, in a extensional regime.

b) Oblique convergence

Oblique convergence develops as plates slide past each other, generally facilitated by considerable strike-slip movements of major transcurrent faults with consistent senses of movement (Fig. 3.2; Section 3.ii.b: e.g., San Andreas fault, 260 km; Crowell, 1962: Philippine fault, 100 km; Mitchell and Leach, 1991: Alpine fault, 480 km; Carter and Norris, 1976), although variations are described for the Alpine fault (Cox and Craw, 1995). The Sumatran fault system (Fig. 1.2) is another major strike slip fault which localizes ore systems (e.g., Miwah; Williamson and Fleming, 1995: Mangani; Kavalieris et al., 1987; Rawas and Lampung; G. Corbett, unpubl. data). Transcurrent or strike-slip faults represent arc parallel faults formed as part of the accretionary prism of a magmatic arc.

Settings of oblique convergence including localized changes to oblique convergence in arcs generally categorized by orthogonal convergence, are ideal for the development of a range of porphyry-related mineralization styles in which (gold, copper, silver) mineralization occur outside the porphyry environments. Thus many of the porphyry copper-gold (e.g., Far Southeast, Philippines; Frieda River, Papua New Guinea), mesothermal gold-copper (e.g., West Wylong, Lake Cowal, Cadia, in eastern Australia), and epithermal gold-silver (e.g., Waihi, Golden Cross in the Coromandel Peninsula, New Zealand) deposits have formed under these conditions. Ore systems generally occur in association with major strike-slip structures, but within high angle subsidiary fracture systems described below.

1. A framework of active systems

Earthquake epicentre locations indicate that the same major transcurrent structures, such as the San Andreas fault, facilitate oblique convergence by reactivation during successive earthquakes (Sibson, 1989). Similarly, individual structures commonly show reactivation during the history of an ore system. Modern analogues of plate motions, which impart distinguishable and consistent strike-slip fault movements at the frequency of earthquake activity, contribute towards a model of ore formation. These provide mechanisms for the development of extensional fractures which transport fluids and host mineralization.

An earthquake at Dasht-e Bayaz, Iran in 1968 provides an excellent example of dilation in relation to a strike-slip structure (Fig. 3.7, Tchalenko and Ambraseys, 1970). These workers used aerial photographs taken following a 7.2 magnitude earthquake to plot the trace of fractures, including the plane of principal displacement and subsidiary fractures. They considered a 25 km portion of an 80 km long fault, which developed within Quaternary sediments overlying more competent basement. Tchalenko and Ambraseys (1970) record a left lateral displacement of 450 cm, evident in the disruption of cultural features, for the strike-slip fault, which appears to locally represent a reactivated earlier structure. Near Dasht-e Bayaz township, which was destroyed by the earthquake, the plane of greatest relative displacement steps aside (to the left in the direction of movement) by 500 m and forms what Tchalenko and Ambraseys (1970) describe as a lozenge-shaped graben (Fig. 3.7). Subsidiary fractures link the strike-slip structures within what is herein termed a jog (Fig. 3.7), and are

analogous to dilational ore-hosting fissure veins. Other right stepping bends or flexures in the main fault are compressional or restraining.

2. Application to oblique convergence

Strike-slip structures are rarely single, straight, linear features, but contain irregularities which link fault segments on which movement occurs. The graben delineated by Tchalenko and Ambraseys (1970) is a jog between two faults, and the subsidiary fractures equate to dilatant fissures in many ore systems described in detail below (Figs. 3.5, 3.6; Segall and Pollard, 1980; Sibson, 1989). The subsidiary fractures which link fault segments display angular relationships to the major fault and may form en echelon fracture arrays as sidesteps (steps), or bends which are referred to as releasing or restraining, depending whether they represent extension or compression (Crowell, 1974; Segall and Pollard, 1980). In extensional settings subsidiary fractures form dilational jogs (Sibson 1991 and references therein) or pull-apart basins (Crowell, 1974) and host a variety of ore systems, described below (Figs. 3.8, 3.14). Larger jogs occur in low magnitude displacement faults and act as sites for earthquake rupture termination (Sibson, 1989, 1992; e.g., Dasht-e Bayaz, above) as major strike-slip faults smooth out irregularities in the fault trace (Wesnousky, 1988). Yoshioka (1996) describes strike-slip faults at low angles (about 16°) to the controlling strike-slip faults, which participate in the extinction of pull-apart basins (jogs) and provide a mechanism for smoothing out. Although at a higher angle, the Inglewood fault at Gympie, eastern Australia (Fig. 3.15) may represent such a structure.

Continued reactivation of a fault such as that described above with a consistent direction of movement in settings of oblique convergence may provide a regular opening of the jog and subsidiary fractures. In a model described by Sibson (1987, 1991, 1992), following earthquake rupture, dilational fault systems (jogs) may become the sites of enhanced flow for fluids derived from considerable depths, by a suction pump-like mechanism, and which may vent to the surface as violent eruptions. The concentration of earthquake aftershocks in fault jogs (Sibson, 1989) may reflect rising waters (Sibson, 1987). In Sibson's model, faults in the active geotectonic Pacific rim settings in brittle host rocks may be analogous to ore-forming environments (Sibson, 1986, 1987, 1992). Brittle host rocks such as basement metamorphics fracture well to form ore-systems, whereas clay altered permeable volcanics may undergo more plastic deformation (e.g., Hishikari, Japan; Section 8.vii.c.2).

Fluids rapidly migrate from higher to lower pressure regimes and so travel up the vertical fractures from depth or are sucked from the enclosing rocks (Sibson, 1987). The rapid depressurisation (flashing) of rising fluids promotes phase separation (boiling) and so some fluids may deposit minerals such adularia, chalcedony and platy carbonate, as seen in the pipework of geothermal systems (Section 2). Repeated activation of the strike-slip structural environment results in the formation of the typical banded epithermal veins comprising: silica, adularia and bladed carbonate (generally pseudomorphed by quartz). In strongly dilational environments 'floating clast' breccias (Sibson, 1992) form in which rock fragments are rimmed by banded vein material, commonly at the margin of fissure veins (Fig. 3.17).

In adularia-sericite epithermal vein systems, boiling of meteoric fluids (Henley, 1985; Sibson, 1987) is a favoured mechanism for the deposition of certain gangue minerals (adularia, platy carbonate, commonly pseudomorphed by quartz). Models presented herein focus upon the mixing of rising and locally boiling magmatic-derived fluids with various types of ground waters, as a means of gold deposition (Sections 4 and 8). Different deposit types (Section 1) form as these ground waters, which reside in the fractured host rocks, mix with magmatic fluids rising up the dilatant fissure during activation of the dilational jog. Thus the fissure fracture/veins represent sites of fluid transport and mineral (including ore) deposition. Repeated activation of the dilational structural environment promotes the formation of higher grade ores in a variety of deposit types, best

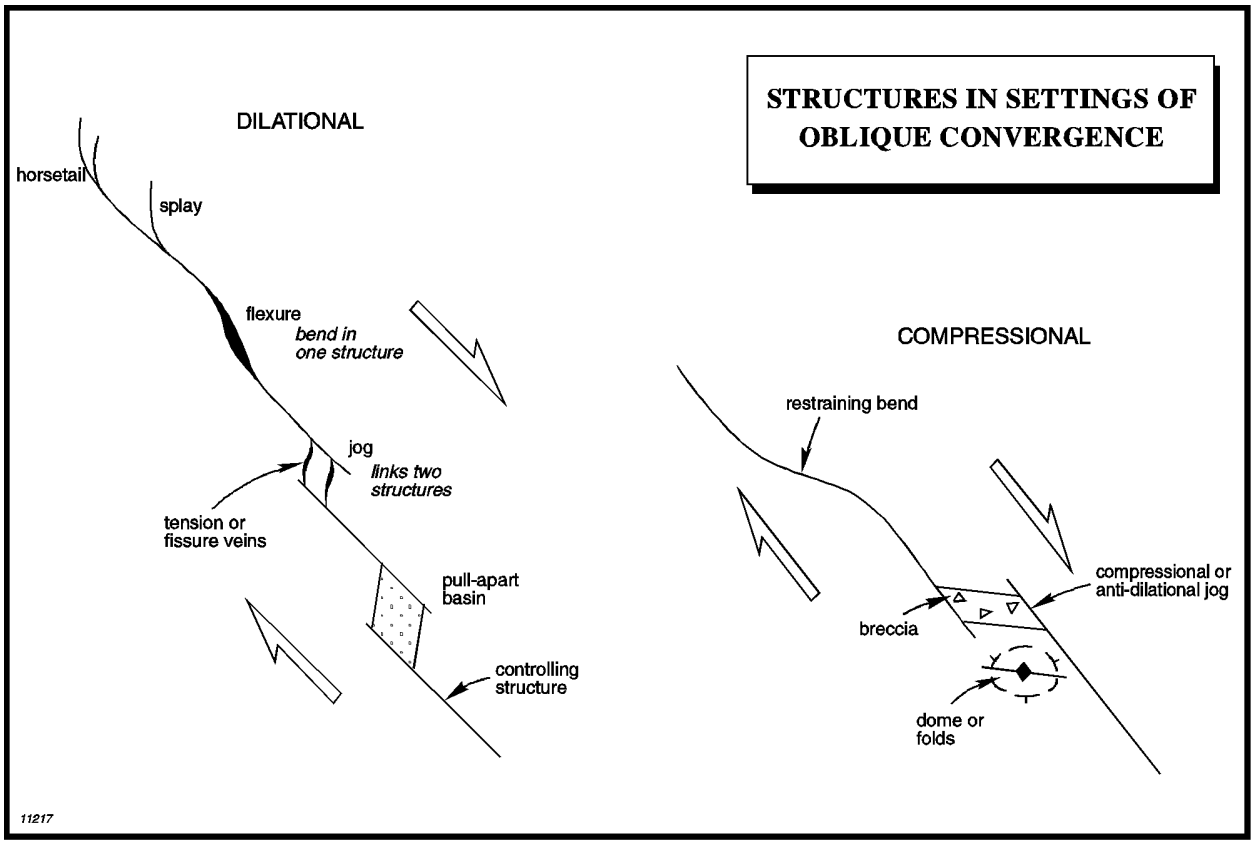
STRUCTURES IN SETTINGS OF OBLIQUE CONVERGENCE
DILATIONAL
horsetail
splay
flexure
bend in one structure
jog
links two structures
tension or fissure veins
pull-apart basin
controlling structure
COMPRESSIONAL
restraining bend
compressional or anti-dilational jog
breccia
dome or folds
11217

FIG. 3.8

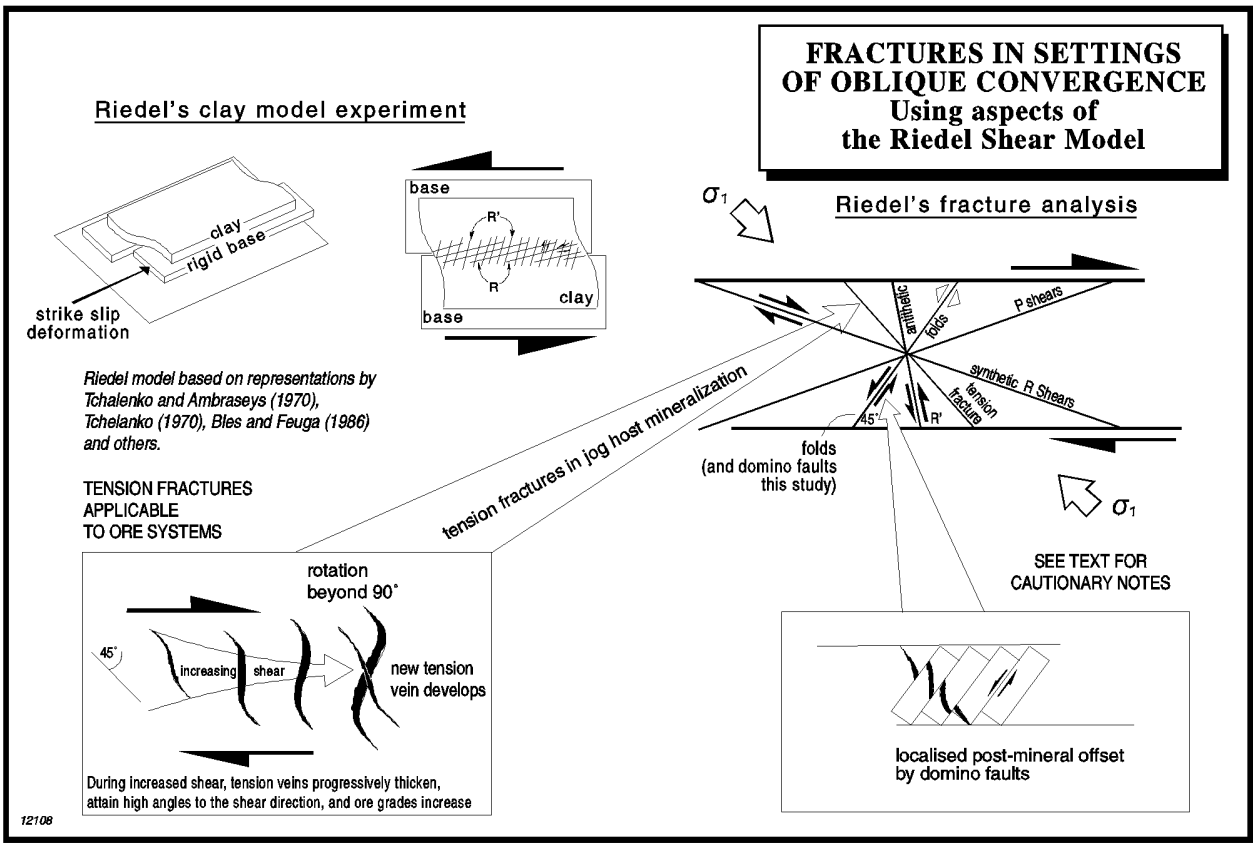
FRACTURES IN SETTINGS OF OBLIQUE CONVERGENCE
Using aspects of the Riedel Shear Model
Riedel's clay model experiment
clay
rigid base
strike slip deformation
base
R'
R
clay
base
Riedel model based on representations by Tchalenko and Ambraseys (1970), Tchelanko (1970), Bles and Feuga (1986) and others.
TENSION FRACTURES APPLICABLE TO ORE SYSTEMS
tension fractures in jog host mineralization
rotation beyond 90°
45°
increasing shear
new tension vein develops
During increased shear, tension veins progressively thicken, attain high angles to the shear direction, and ore grades increase
σ1
Riedel's fracture analysis
antithetic folds
P shears
synthetic R Shears
tension fracture
45°
R'
folds (and domino faults this study)
σ1
SEE TEXT FOR CAUTIONARY NOTES
localised post-mineral offset by domino faults
12108

FIG. 3.9

illustrated in the adularia-sericite epithermal gold-silver vein systems. Dilation is necessary for the transport of considerable quantities of metal-bearing fluids great distances from magmatic sources at depth, to distal and higher crustal level epithermal settings.

3. Riedel shear model

Although many geologists utilize the Riedel shear model (Fig. 3.9) in the analysis of simple shear in brittle conditions, we urge caution with the literal interpretation of essentially experimental data. Riedel (1929) deformed clay overlying a rigid basement, analogous to cover rocks and a strike-slip fault in crystalline basement (Fig. 3.9), and applicable to many settings encountered in oil exploration (Lowell, 1985). This model, as discussed in the geological literature (Riedel, 1929; Tchalenko, 1970; Tchalenko and Ambraseys, 1970; Wilcox et al., 1973; Bles and Feuga, 1986; and many others) defines a set of specific structures which develop during strike-slip deformation of this type (Fig. 3.9). Riedel fractures are well defined in the study of the Dasht-e Bayaz earthquake in Iran in which the Quaternary sediments overlying competent bedrock underwent failure interpreted by Tchalenko and Ambraseys (1970) in terms of Coulomb failure criteria.

Although we briefly describe the Riedel shear model, only the formation and continued dilation of tension veins is of interest to the explorationist, and not the Riedel fractures. The Riedel model (Riedel, 1929; Tchalenko, 1970) suggests that the Riedel shears (R or synthetic shears) form first and take up any early displacement. Conjugate (R' or antithetic) shears form later and display only minor displacements opposite to the overall movement. The Riedel fractures typically form at angles of o/2 (15°) and 90-o/2 (85°) to the shear direction, for R and R' respectively. The P shears form last (at about 15° to the shear direction) but take up much of the overall final shear displacement, especially in major fault zones. Folds form normal to the principle stress direction and tension veins typically form parallel to the principle stress at 45° to shear direction (Fig. 3.9). Tension fractures progressively rotate and continue to dilate as ore-hosts in many mineralized systems as described below.

Another set of fractures not evident in the Riedel fracture analysis which are apparent in some Pacific rim vein systems are termed domino faults (Fig. 3.9; G. Corbett, unpubl. data). These most commonly offset mineralized tension veins as post-mineral fractures and also localize syn-mineral ore shoots. Swanson (1988) describes fractures in a similar orientation which develop during layer parallel extension, and Hanmer and Passchier (1991) also use the term domino for fractures formed in settings characterized by a combination of simple and pure shear. This latter interpretation is consistent with the observation of domino faults as block faults which offset mineralized tension veins at the cessation of dilation (e.g., Mesel, Fig. 7.56; Tolukuma, Fig. 7.50). Similar fractures are noted to facilitate block rotations between faults at the Mesquite mining district California (Willis and Tosdal, 1992). Movement on the domino faults is opposite to that of the bounding strike-slip structures.

4. Tension veins

Tension veins form during orthogonal or oblique convergence. In oblique convergence tension fractures develop as en echelon arrays in brittle to semi-brittle (McClay, 1987) rocks (brittle-ductile, Ramsay, 1967), and fill with minerals to form veins. Continuing movement on strike-slip structures will progressively rotate the tension fractures (Fig. 3.9). Existing segments of the fracture become thickened during progressive rotated (Ramsay, 1967) to an angle > 90° to the shear direction where they enter a compressional regime and new tension fractures form (Durney and Ramsay, 1973). At this point the original tension fracture is no longer in a dilational but a compressional orientation, and may also be offset by domino faults in a compressional regime at the cessation of dilation (Fig. 3.9). During deformation, as the tension fracture continues to grow at the extremities, the central thickened and reoriented portion has been opened for the longest period of time (Fig. 3.9; Hanmer

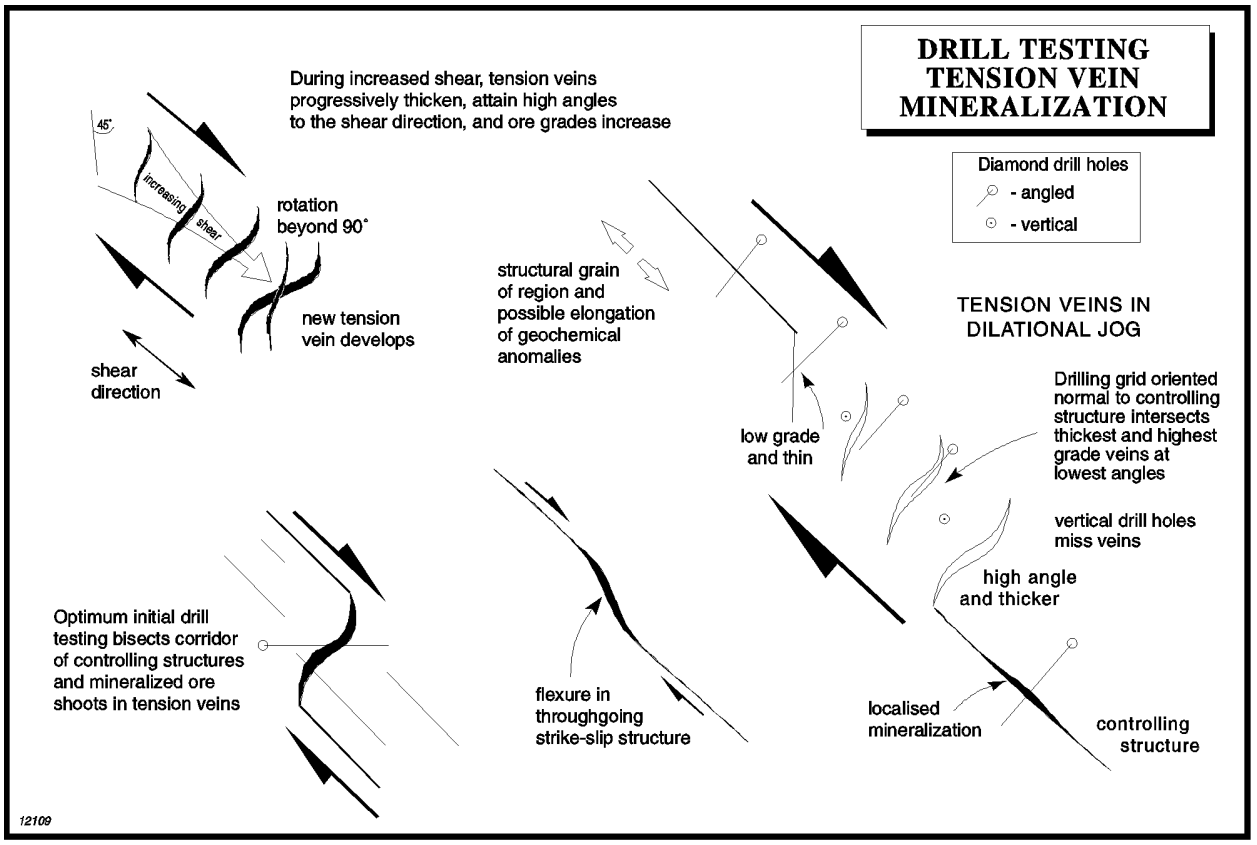

FIG. 3.10

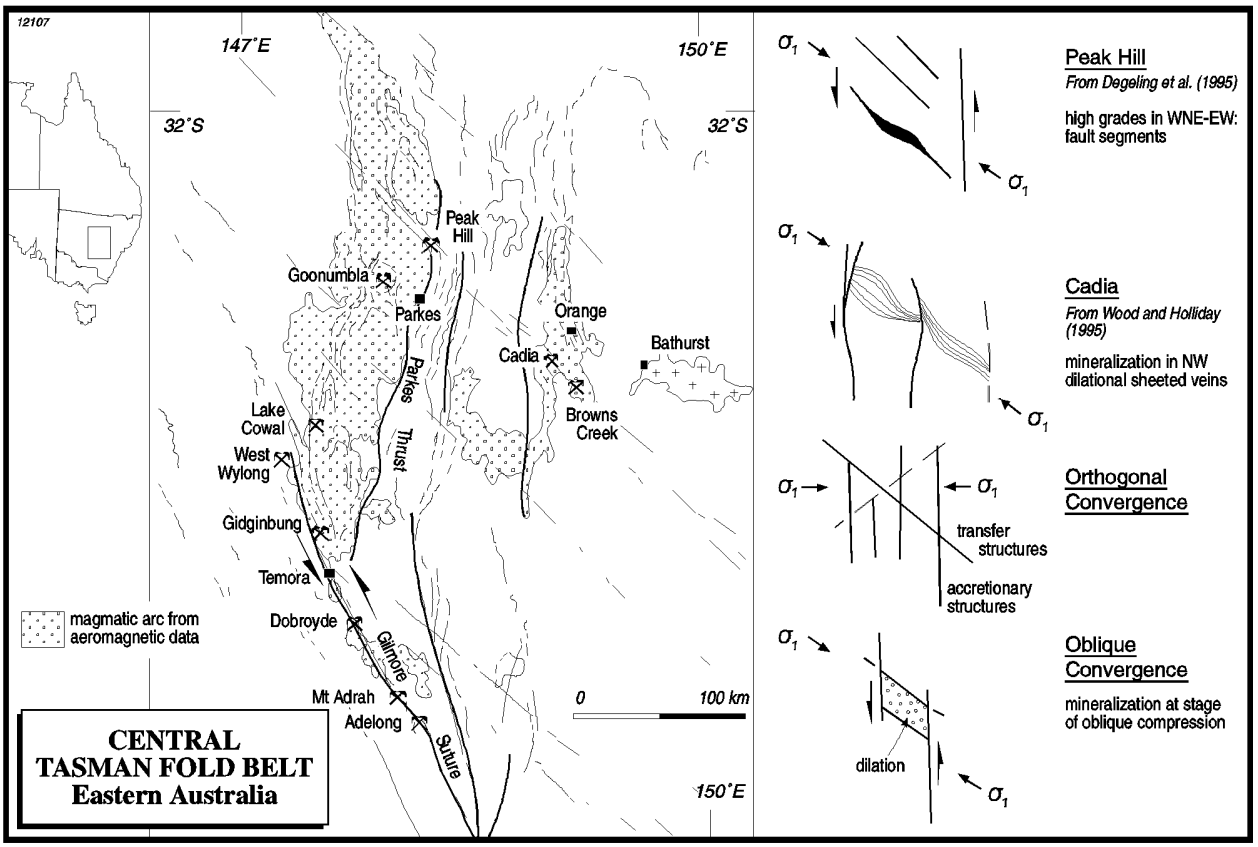

FIG. 3.11

and Passchier, 1991) and so commonly displays higher gold grades (G. Corbett, unpubl. data). Thus the tension veins take on a sigmoidal shape and may be termed tension gash veins. The side step or subsidiary fractures which define dilational jogs are tension fractures, and may therefore also undergo progressive reorientation with associated thickening, to form mineralized fissures. Others occur as ore shoots within fracture/vein systems. Examples of tension veins and importance as ore hosts are discussed below.

5. Drilling directions

Angular relationships of mineralized tension vein systems to controlling strike-slip structures are most important. During strike-slip deformation, tension fractures are initiated at 45° to a controlling strike-slip structure, which may define the shear direction. This is commonly the structural grain of the district. During progressive deformation by the strike-slip structures, tension fractures are rotated to beyond 90° to the controlling structures, and are opened and filled with minerals to form veins (Figs. 3.9. 3.10). The roughly 90° angular relationships between mineralized sheeted tension veins, and controlling structures which lie within the structural grain of the region, are well illustrated at the McLaughlin gold mine, California (Sherlock et al., 1995). The central portion of the fracture which undergoes the greatest rotation remains open the longest and so hosts the thickest and highest grade portion of the vein. However, this portion of the vein undergoes the most rotation to become oriented in a attitude normal to the controlling structure (Fig. 3.10).

Herein lies the problem! It is common for the shear direction to represent a prominent structure which is easily mapped and may contain mineralization. This is generally the structural grain of the district or prospect and elongation of soil geochemical anomaly. Drill testing normal to the orientation of the controlling structure (shear direction) could be at very low angles, or essentially parallel, to the thickest and highest grade tension veins (Fig. 3.10). It is common for drilling programmes of this nature to yield erratic results including anomalously high assays and considerable intercept lengths from the few drill holes which might bore down individual veins, while many more may be bored between veins and so are barren. These problems could be further compounded when vertical drill patterns are used to test vein systems which commonly display sub-vertical orientations. Exploration prospects which have been poorly drill tested in this manner are readily apparent from the low angles of fissure or sheeted veins to the long axis of drill core. The chance of intersecting mineralized veins diminishes rapidly as the drilling orientation approaches that of the veins, and so prospects drill tested in this manner may be downgraded.

Thus it is imperative that fracture vein systems should be carefully mapped prior to the initiation of a drilling programme, even in porphyry copper-gold systems. Not all the relationships may be evident at the initiation of drilling, note how in figure 3.10, drilling is at first oriented to bisect the inferred controlling structure and dilatant fracture systems. This drilling orientation might change as the relationships become clearer. Even without the use of oriented drill core, if mineralized veins are found to occur at low angles to the core axis, then the orientation of the drilling grid should be reconsidered. Care should be taken in any such analyses to utilise the central portions of veins and not 'floating clast' breccias which commonly form at vein margins (Section 3.x.d).

c) Rock competency

Brittle rock failure occurs at <5 km depth passing to ductile at depths of 5-10 km (McClay, 1987) or 10-15 km (Sibson, 1992), suggesting that brittle to semi-brittle regimes apply in the crustal levels under consideration herein. Fissure vein-style gold-silver deposits form within large-scale tension fractures hosted by competent rocks. In the Philippines geothermal systems, while permeable volcanic sequences have undergone pervasive alteration and tend to be unmineralized, fluids which formed carbonate-base metal gold deposits (e.g., Acupan, Antamok) were channelled through fractured competent basement intrusions and metamorphic rocks.

In Japan, although epithermal gold deposits occur in the vicinity of altered volcanic rocks, basement shales host the fissure vein gold mineralization at Hishikari (6.8 M oz Au) and Konomai (2.35 M oz Au), and competent intrusive domes emplaced into volcaniclastic sequences host vein systems at the Sado (2.5 M oz Au) and Chitose (0.9 M oz Au) gold-silver deposits. At Hishikari, the pronounced contrast between the competent Shimanto Group shale, and the overlying clay altered, incompetent volcanic breccias, has constrained mineralization within a 100 m vertical interval at the top of the basement Shimanto Group shales (Izawa, et al, 1990). These ore produce a 80 g/t gold head grade and common bonanza gold grades, typically at the shale/volcanic contact (Section 8.vii.c.2).

In the Coromandel Peninsular of New Zealand, the major fissure vein systems at Martha Hill (>6 M oz Au), Golden Cross (1 M oz Au), and Karangahake (1 M oz Au), are hosted within massive andesite lavas while rhyolitic pyroclastics are poorly mineralized (Brathwaite et al., 1989). The fissure veins at Karangahake pass to sub-economic stockwork veins at the transition from the andesite to the overlying rhyolitic pyroclastic rocks (Brathwaite, 1989). Also in the Coromandel Peninsula, bonanza gold grades in fissure veins of the Thames goldfield (1.4 M oz Au) occur only in the Premier Flow (Merchant, 1986), a more competent lava unit within a largely volcaniclastic sequence.

d) Fracture permeability

Fracture permeability provided by small-scale fracture networks facilitates the flow of hydrothermal fluids through otherwise competent host rocks. Pre-existing alteration such as silicification may promote competency for subsequent fracturing. Recent experimental evidence supports field observations of promoted fracture permeability in extensional settings (Sibson, 1993, 1995; Cox, 1994). Typical fracture networks which promote fluid flow include: fluidized to crackle breccias in structurally controlled high sulfidation systems within jogs in strike slip structures (Sections 3.x.d.4, 6.iv: e.g. Nena, Papua New Guinea; Corbett, 1994; Mt Kasi, Fiji; Corbett and Taylor, 1994), fracture arrays above normal faults including hanging wall splits (Zhang and Sanderson, 1996; e.g. Porgera Zone VII, Corbett et al., 1995), and sheeted and stockwork systems formed in association with porphyry intrusions (Titley, 1990; Section 3.ix). Dilatant fracture permeability formed in this manner may promote the transport of metal-bearing fluids from magmatic sources considerable distances to cooler environments of metal deposition.

v) Changes in Convergence

Localized changes from orthogonal to oblique subduction may promote mineralization, as fluids which were constrained within intrusions during orthogonal compression exsolve along fractures dilated under the influence of strike-slip structures (Fig. 3.5). Fractures developed under the earlier stress environment are commonly utilized in the later conditions. Two styles are apparent:

a) Activation of arc parallel structures

The Frieda River, Papua New Guinea (Corbett, 1994) and Chuquicamata, Chile (Boric et al., 1990), porphyry systems are each interpreted to be localized at splays in regionally significant arc parallel strike-slip faults, formed in arcs characterized by essentially orthogonal compression. It is inferred that changes to oblique convergence have facilitated the formation of these ore systems, including the Nena high sulfidation system at Frieda River (Corbett, 1994; Bainbridge et al., 1994). Fracture orientations within the Frieda porphyry are indicative of formation during extension and in an opposite stress regime to pre- and post-mineralization compression (Asami and Britten, 1980), in this case in an inferred transpressional environment (Corbett, 1994). The dextral movement on the West fault interpreted above for the formation of Chuquicamata (Boric et al., 1990) is the opposite sense to inferred post-mineral offset of the MM mineralization as a possible portion of the Chuquicamata porphyry (Sillitoe et al., 1994). Thus, varying changes in convergence are apparent.

b) Activation of transfer structures

Conjugate transfer structures formed during orthogonal convergence may become activated in a different form and localize mineralization during changes to oblique convergence. Pre-existing fracture sets my undergo dilation to form pull-apart basins, fissure veins, sheeted veins or intrusion-hosting splays, depending upon the level of erosion (Fig. 3.5, 3.14). This is best illustrated by two examples:

1. At the Lachlan fold belt of eastern Australia, many of the gold-copper occurrences display internal structure indicative of formation during episodes of sinistral strike-slip deformation on the NS structures which form within and locally delineate the margins of magmatic arcs (Fig. 3.11). Such a sense of movement is attributed to the Gilmore suture (Scheibner, 1985; Stuart-Smith, 1991) which localizes gold occurrences at Gidginbung, West Wylong, Adleong and Dobroyde (Supple et al., 1986). A sinistral sense of movement on NS arc parallel structures is herein interpreted from the internal structure of many mineral occurrences along the Gilmore suture (e.g., Rosedale; Ryan, 1993: West Wylong; Golden Cross Resources, Prospectus, 1996) and elsewhere (Fig. 3.11; Lake Cowal vein system; North Limited, 1995: sheeted veins at the E48 Goonumbla porphyry copper-gold; G. Corbett, unpubl. report, 1994: Peak Hill high sulfidation gold-copper; Degeling et al., 1995: Bobodah; G. Corbett, unpubl. report, 1994: Cadia; Newcrest Geological Staff, 1996). Although younger, the Peak, New Cobar, New Occidental and Chesney mines in the Cobar district, using the data of Glen (1987), also display the same relationships. By contrast, dextral senses of movement for arc parallel NS structures and inferred by other workers at Browns Creek skarn (Wilkins, 1997) and the E26N porphyry, Goonumbla (Heithersay et al., 1995).

NW-trending transfer structures apparent on the aeromagnetic data (Spencer et al., 1992), developed during EW orthogonal convergence, and are inferred to have been dilated as ore hosts during subsequent sinistral oblique convergence (Fig. 3.11 e.g., Peak Hill, Cadia and others). Perkins et al., (1995) reports a similar age 439-440 Ma age for several (Goonumbla, Lake Cowal, Sheahans-Grants, Glendale) of the magmatic arc gold-copper deposits in this belt, possibly indicative of initiation of emplacement at such a change of tectonism.

2. Mt Muro (Moyle et al., 1996) is one of several gold occurrences (van Leeuwen et al., 1990) localized along a major suture (herein termed the Kalimantan suture), which separates continental basement rocks from shelf sediments and locally delineates the margin of a magmatic arc described by Carlile and Mitchell (1995) in Kalimantan, Indonesia (Fig. 1.2, 3.12). Recent work (G. Corbett, unpubl. report, 1996) suggests that gold mineralization varies progressively from quartz-sulfide to carbonate-base metal and epithermal quartz (Section 7) styles moving away from an inferred magmatic source in the vicinity of argillic and advanced argillic alteration near Mt Muro, and that the most dilational fracture systems host the highest gold grades. Fracture system trends at Mt Muro are represented by the NW Kalimantan suture, a NNW transfer structure, and WNW conjugate fractures, termed accretionary joints. A change in the orientation of convergence from orthogonal to oblique (Fig. 3.12) is inferred to have promoted sinistral strike-slip movement on the NNW transfer structures, which caused the dilation of the pre-existing WNW fractures (G. Corbett, unpubl. report, 1996). These structures host much of the ore, including local high gold-silver grade zones in sigmoidal vein segments apparent on the data of Moyle et al. (1996). Lower grade ores also occur in the NNW transfer structures.

c) Arc reversals

Several gold-copper deposits attributed to back-arc settings by some workers may have developed as a result of arc reversal (Solomon, 1990). These include the caldera-hosted Emperor gold mine, Fiji (Eaton and Setterfield, 1993), classified herein as of the epithermal quartz gold-silver style, the Marian and Didipio porphyry copper-gold prospects, Philippines, and the intrusion-related deposits of the Tabar-Lihir-Feni chain, Papua New

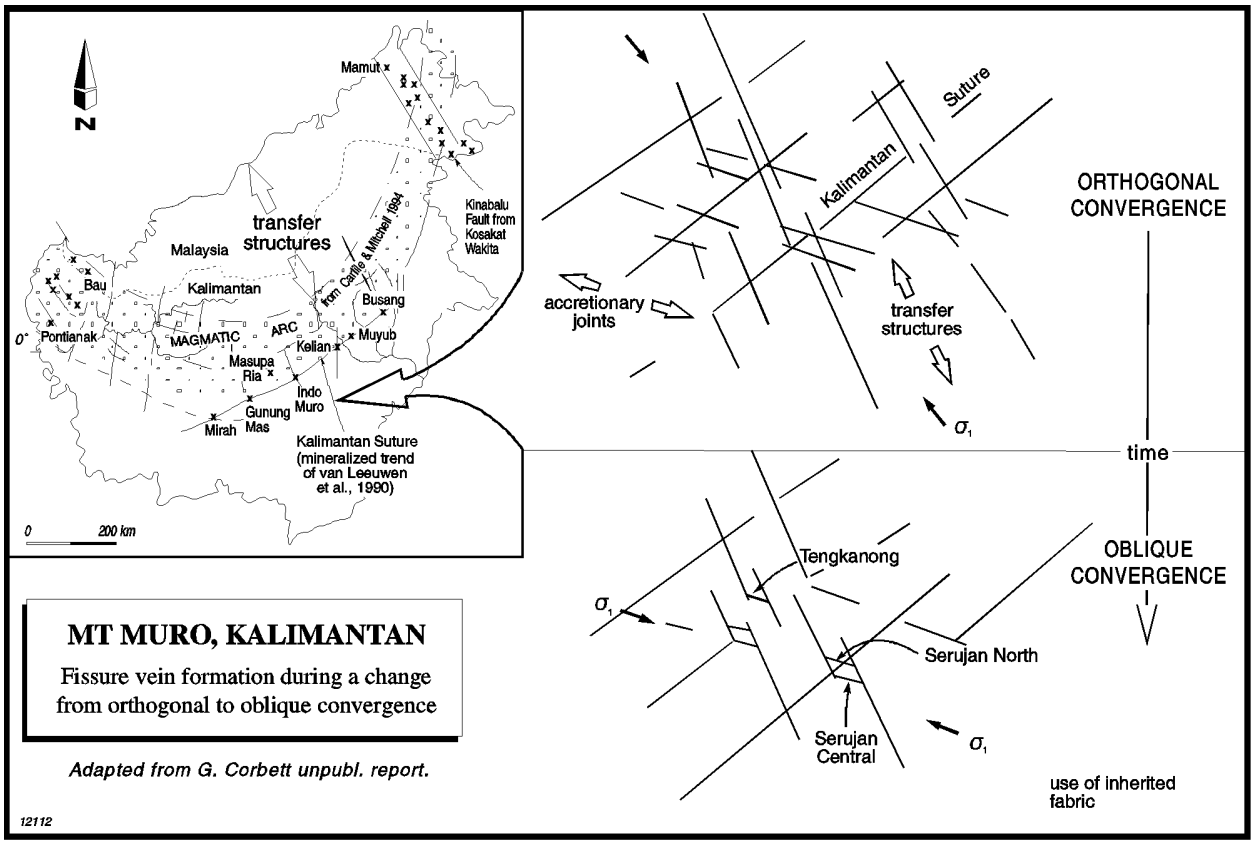

FIG. 3.12

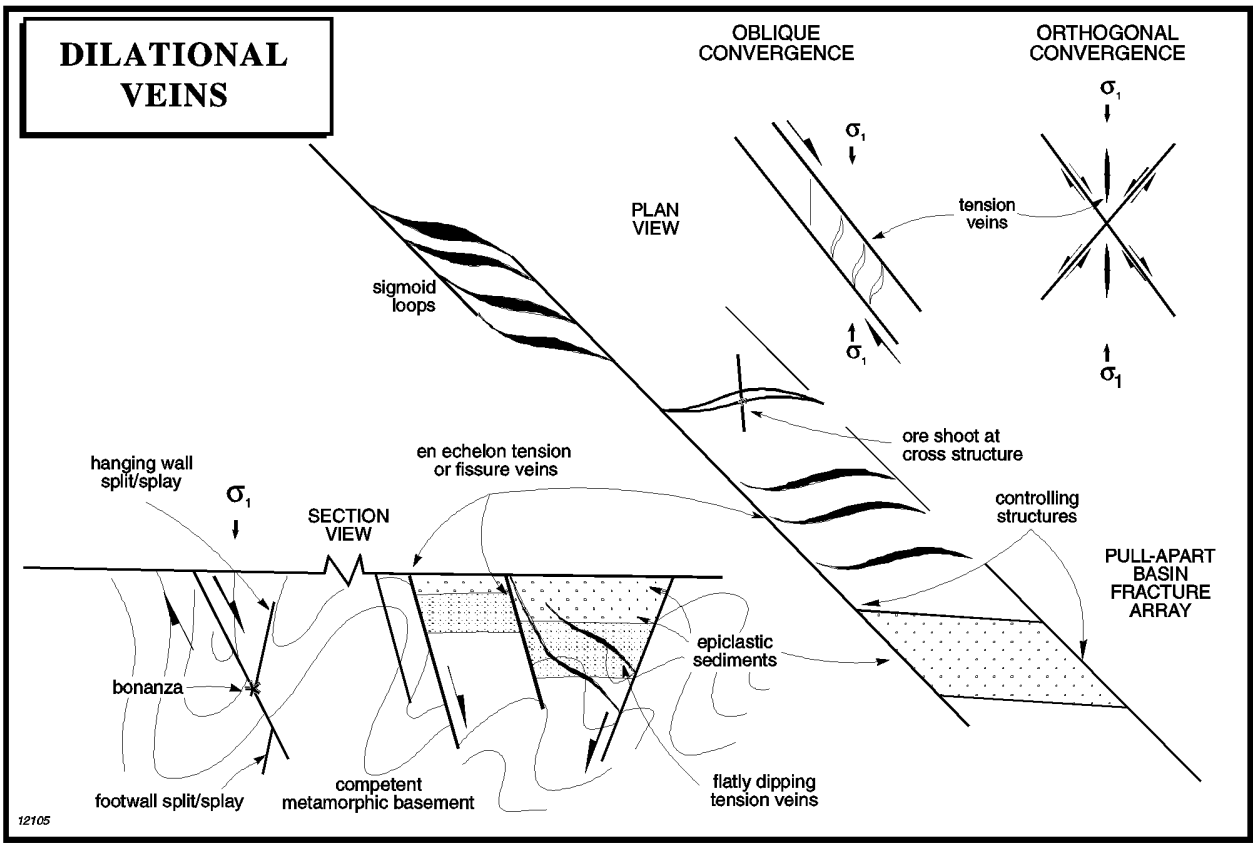

FIG. 3.13

Guinea (Sillitoe, 1992; Section 5.iv). All these mineral occurrences feature alkaline intrusion/extrusion rock suites. Solomon (1990) also extends the arc reversal origin to many Late Miocene to Pliocene porphyry-related systems in mainland Papua New Guinea (e.g., Ok Tedi, Yandera, Frieda River and Porgera).

In northern Papua New Guinea, magmatism associated with southwards subduction of the Pacific plate under the margin of the Australian continental plate from the Oligocene, formed island arcs extending from the Bismarck Archipelago to the Solomon Islands (islands of Manus, New Britain, New Ireland, Bouganville and Guadalcanal). Continent-arc collision and uplift occurred in the Mid Miocene, the thick oceanic Otong Java Plateau jammed subduction, and Late Miocene to Recent magmatic arcs which developed overlying the northward dipping New Britain trench were progressively dismembered to form the current configuration in the Pliocene (Fig. 1.2; Solomon, 1990; Davies, 1991). The Bismarck back-arc basin opened in the Pliocene (Taylor, 1979; Davies, 1991). The NS alignment of the elements of the Pliocene magmatism at Tabar-Lihir-Feni and Talasea arcs are indicative of the exploitation of tear or tension faults (Lindley, 1988; McGinnis and Cameron, 1994). Models which feature remelting of oceanic crust following arc reversal (Johnson, 1987; Solomon 1990, Wyborn, 1992) may account for the alkaline nature of these intrusions.

In Fiji, Colley and Flint (1995) describe a change from island-building magmatism up to the Mid Miocene, to later Pliocene rifting in association with the opening of the Lau and Fiji basins, and development of the North Fiji fracture zone (Fig. 1.2). Porphyry mineralization at Namosi developed in calc-alkaline rocks (6.2 - 5.9 Ma; Gill and McDougall, 1973 in Colley and Flint 1995), followed by Pliocene epithermal gold mineralization in association with shoshonitic magmatism (e.g., Vatukoula, Vuda). After cessation of Miocene subduction on the Vitiaz trench and arc reversal at 5.5 Ma, subduction has continued on the New Hebrides (Solomon, 1990) and Tonga trenches. Although an ENE-trending deep fracture parallel to the North Fiji fracture zone may localize alkaline magmatism and gold mineralization in western Viti Levu (Vatukoula, Vuda), the relationship to subduction remains unclear.

In the Philippines, the Marian and Didipio (Dinkidi) alkaline porphyry copper-gold systems in eastern Luzon may similarly be related to a change in Miocene westward subduction along the North Luzon trench to the eastward Manila trench (Solomon, 1990).
It appears that although many intrusion-related copper-gold systems form in relation to the same tectonic elements as back-arc basin development, deep remelting in response to arc reversal (Solomon, 1990) may produce magmas which rise along major structures. The Porgera transfer structure which is interpreted to represent a deep crustal fracture (Corbett, 1994; Corbett et al., 1995), localizes the Porgera and Mt Kare alkaline gold deposits.

vi) Dilational Ore Environments

Differing styles of dilational ore environments are distinguished and in part display variations indicative of the tectonic setting and levels of erosion of the hydrothermal system (Figs. 3.13, 3.14). These mainly comprise veins, developed as dilatant fractures or other generally linear discontinuities, which have become filled by hydrothermal minerals. These are distinguished from and locally transitional to breccias (Section 3.x). Styles of dilational ore systems include:

a) Tension fracture/veins
b) Jogs
c) Flexures
d) Hanging (foot) wall splits
e) Domes
f) Ore shoots

a) Tension fracture/veins

Although the term 'tension fractures' is utilized by McKinstry (1948) and many field geologists, to describe veins formed at right angles to the direction of extension (Figs. 3.6, 3.9), many other terms (e.g., extension fractures, hybrid shear fractures and shear fractures; Hancock, 1985: others in Etheridge, 1983; Ramsay and Huber, 1983), used in the light of published literature might more correctly describe these veins. Thus, while we as field geologists continue with McKinstry's terminology, readers are referred to more specific texts for detailed discussion of fracture/vein terminology (Hancock, 1985; Etheridge, 1983; Ramsay and Huber, 1983; Bles and Feuga, 1986; and many others).

Tension veins represent extensional fractures or cracks (McKinstry, 1948) which become filled with minerals and develop in settings of orthogonal and oblique convergence (Figs. 3.6, 3.13). In settings of oblique convergence, tension veins may be constrained between strike-slip faults which represent the plane of shearing, commonly as en echelon sets (McKinstry, 1948), and are the predominant style of dilational ore-hosting fractures in epithermal gold-silver vein systems. Examples are well developed in the Coromandel Peninsular of New Zealand (Fig. 3.13; e.g., Waihi, >6 M oz Au; Fig. 8.7: Golden Cross, 1 M oz Au; Fig. 8.4: Thames goldfield, 2 M oz Au; Figs. 7.47, 7.48). Others include Mt Kasi, Fiji (Fig. 6.27); Maniape, Papua New Guinea (Fig. 7.37). These systems most strongly demonstrate the manner in which regional strike-slip (controlling) structures localize ore systems, but are themselves essentially barren (Figs. 3.10, 3.13). Note in these examples, the angular difference between the tension veins and controlling structures as described in section 3.1v.b.4. Tension veins terminate along strike, generally at the controlling structure, and so prospecting should focus on the identification of new veins across strike (Fig. 3.13; e.g., Waihi; Fig. 8.7).

Tension veins formed in settings of orthogonal convergence, locally exploit arc normal transfer structures (Fig. 3.6: e.g., Arakompa, Papua New Guinea; Fig, 7.10). During orthogonal extension tension veins may exploit compressional fractures, formed previously during orthogonal convergence as the structural grain of the district (Fig. 3.6).

Although the term tension veins is preferred here and elsewhere (W. Laing, pers. commun.), a variety of other terms in the geological literature are:

Tension gash vein commonly applies to tension fractures which have been dilated, typically to sigmoidal shapes, and filled with later minerals (McClay, 1987; Figs. 3.9, 3.10).

Fissure vein is utilised herein to emphasise the steeply dipping nature of many mineralized tension fractures, particularly in epithermal environments (Figs. 3.8, 3.13).

Sheeted fractures are closely spaced parallel fracture/veins formed within a stress regime, which are distinguished herein from the more random stockwork fracture/veins which show no pronounced preferred orientation. However, in many instances there is a continuum between sheeted and truly random veins. Many porphyry stockwork vein systems are not truly random but comprise conjugate or radial vein sets in combination with tension and arc parallel fracture fill. Sheeted veins occur at all crustal levels from epithermal (e.g., McLaughlin, western US), mesothermal (e.g., Kidston, eastern Australia) to porphyry (e.g., Cadia and Goonumbla, eastern Australia), and as different to the random stockwork fracture/veins, commonly provide dilational fracture systems for fluid transport as well as sites of mineral deposition. Thus, these fractures are important ore hosts and it is imperative that drill testing be correctly oriented (Fig. 3.10). While sheeted veins at McLaughlin (Sherlock et al., 1995) and Cadia (Newcrest Mining Staff, 1996) formed as tension veins, the Kidston sheeted veins are kinked about the margins of a breccia pipe (Fig. 7.7). The dilation of ore-hosting sheeted veins in porphyry environments is further discussed below (Section 3.ix.b.2).

b) Jogs

Jogs link en echelon fault segments (Sibson, 1989, 1992) by the development of side step fractures (Crowell, 1974), termed tension fractures by Segall and Pollard (1980) and evident in the Dasht-e Bayaz example above (Figs. 3.7, 3.8). Jogs which link two discrete strike-slip structures may be either dilational or compressional (Fig. 3.8). Domes which develop in the latter case are explored as oil traps (Lowell, 1985). A major dilational jog in the Philippine fault hosts the Southern Negros geothermal field which is derived from actively intruding porphyry systems (Fig. 2.6). The Golden Plateau gold mineralization, Cracow, eastern Australia (Fig.7.54), and Umuna lode, Misima Island, Papua New Guinea (Fig. 7.43) are each localized within jogs formed between two major strike-slip structures.

Pull-apart basins (Crowell, 1974) form if jogs are dilational (Sibson, 1989) and by extension form localized fault-bounded depressions which commonly exhibit rhomboid shapes, are filled with epiclastic sediments, and only preserved at surficial to moderate crustal levels, in slightly eroded terrains (Figs. 3.8, 3.13, 3.14. 3.15). Pull-apart basins occur along the Sumatran fault (Pudjowalujo, 1990), and are associated with epithermal gold-silver vein systems (Kavalieris et al., 1987; G. Corbett unpubl. data). The epiclastic sediments which fill pull-apart basins (e.g., Kelian, Indonesia; Figs. 7.18, 7.19: Gympie, eastern Australia; G. Corbett, unpubl. reports, 1993-1996), or flexures may be unique to that portion of a district (e.g., Cinola, British Columbia). Where permeable, these epiclastic rocks may readily undergo hydrothermal alteration, and if rendered more competent, fracture readily.

Elsewhere, epithermal vein systems may form in dilational environments within more competent basement host rocks adjacent to pull-apart basins (e.g., Way Linggo and Semung, South Sumatra, Indonesia; G. Corbett, unpubl. report, 1993), which may display characteristic fracture arrays (below). The rhomboidal shape and atypical epiclastic rocks readily identify pull-apart basins which may then become exploration targets. Structures including growth faults which participate in basin development are subsequently dilated to act as ore hosts (e.g., Gympie, eastern Australia; G. Corbett, unpubl. report; Fig. 3.15; Section 3.vii). Yoshioka (1996) notes intra-basin strike-slip faulting during basin extension, possibly analogous to the Inglewood fault at Gympie, eastern Australia (Fig. 3.15). Careful mapping should distinguish these clastic rocks from phreatomagmatic and phreatic breccias described below (Section 3.x.d.2).

Pull-apart basin fracture arrays are fracture patterns which commonly form within mineralized jogs or pull-apart basins and display elements (Fig. 3.13) categorized as:
* Controlling strike-slip structures form in the shear direction and are generally barren.
* Fissure-style tension veins dip steeply and host most ore, commonly as crustiform/colloform banded veins.
* An additional set of tension veins may display moderate to flat dips.

In many systems steeply dipping tension veins exhibit higher gold grades and act as fluid flow feeders for the flatly dipping veins which tend to contain lower grade ores (e.g., Busai, Woodlark, Papua New Guinea; Figs. 7.34, 7.35; Corbett et al., 1994a). Similarly, gold mineralization at Lake Cowal, eastern Australia (2.44 M oz Au), occurs in a setting of strike-slip deformation in a possible splay from the Gilmore suture, and contains flatly dipping dilational quartz-carbonate-sulfide filled veins adjacent to steeply dipping structures (North Limited, 1995). At Waihi, New Zealand (Fig. 8.7), the Empire vein dips more shallowly than the Martha vein, and is locally parallel to a normal fault. Note the down drop and thickening of the andesite unit as the dilational jog acts as a pull-apart basin in the upper levels (Fig. 8.7). Similarly at Mt Muro, Indonesia, a pull-apart basin fracture array is apparent as: steeply dipping WNW fissure veins, constrained between more linear NNW controlling faults, intervening moderately dipping veins, and local ore shoots at intersections of structures (Moyle et al., 1996; G. Corbett, unpubl. report, 1996; Fig. 3.12).

Sigmoid (cymoid) loops are described by McKinstry (1948), as cam-shaped vein segments which may host ore and as forming within fault jogs (Sibson, 1992). These are evident in plan and cross section in vein systems and

characterized by the thickened sigmoidal shape in the ore-zone (Fig. 3.13). These equate to tension veins in this discussion and so exhibit older and rotated thickened central portions which commonly contain higher grade ores.

Splays or horsetails represent curved fractures, commonly as multiple sets (horsetails), and display angular relationships to a single strike-slip structure from which they are derived (Fig. 3.8), and so form part of a sigmoid loop (McKinstry, 1948). They represent the termination of a fault system and are indicative of a loss of energy (J. Skarmeta, pers. commun). Splays in regional strike-slip faults may localize porphyry intrusions (e.g., Far South East porphyry copper-gold, Philippines; Sillitoe and Gappe, 1984; Sillitoe, 1993a; Baker, 1992; Fig. 6.24: Frieda River porphyry-Nena high sulfidation copper-gold systems; Corbett, 1994; Bainbridge et al., 1994; Fig. 6.18: Chuquicamata porphyry copper, Chile, on the data of Boric et al., 1990). Splays may pass upwards to fissure veins and then pull-apart basins (Fig. 3.14). Splays represent areas of enhanced fluid flow in the Tongonan geothermal field (Fig. 2.6).

c) Flexures

Flexures may represent dilational environments formed at localized bends (Sibson, 1989) in a strike-slip structure and are not characterized by the development of new fracture systems, as in the case of a jog (Fig. 3.8). These are important mechanisms for the formation of ore shoots along mineralized veins (McKinstry, 1948). Large flexures host epiclastic sediments into which ore systems are emplaced (e.g., Cinola, British Columbia; G. Corbett, unpubl. report, 1993).

d) Hanging wall splits (splays)

Hanging wall splits form as discrete fault segments which develop above dipping fault structures and are best propagated in extensional settings characterized by normal faults (Fig. 3.13). Many traditional models for hot spring-style epithermal vein systems (Bonham, 1988a, 1988b), utilise hanging wall splits as settings for ore formation. Hanging wall splits are important loci of mineralization at Porgera (Fig. 7.24; Corbett et al., 1995) and Tolukuma (Fig. 7.51; Corbett et al., 1994c), and in both cases bonanza gold grades occur at the intersection of the normal fault and hanging wall split. Footwall splits also occur but are less common than splits in the hanging wall (e.g., Golden Cross; Caddy et al., 1995; Fig. 8.5). In the Bulolo graben, Papua New Guinea (Fig. 7.28) the Kerimenge, Hamata, Upper Ridges and Hidden Valley ore systems occur in the hanging walls to major structures, including graben-bounding faults.

e) Ore shoots

Ore shoots (McKinstry, 1948) are zones of wider vein segments with higher gold grades, formed by localized increased dilation within vein systems and elevated fluid flow, or preferred settings of ore deposition as:

* Intersections of throughgoing structures with diatreme margins. The G.W. breccias, Acupan mine, Baguio district, Philippines which represent open-space breccias in the enclosing rock are localized by the intersection of fissure veins with the margin of the Balatoc diatreme body, and have been mined for high grade gold ores (Sawkins et al., 1979). High grade ores at the Tolukuma gold-silver mine, Papua New Guinea, occur in the central portion of the vein system at the intersection of the pre-mineral graben structure and milled matrix fluidized breccias (Figs. 7.50, 7.51, 7.53; Corbett et al. 1994c).

* Intersections of dilatant vein/fracture systems in strike-slip settings with cross structures represent sites of higher fluid flow (Fig. 3.13; e.g., Karangahake, New Zealand: Cracow, eastern Australia; Fig. 7.54: Thames goldfield, New Zealand; Fig. 7.48: Bilimoia, Papua New Guinea; Fig. 7.10).

* Intersections of normal faults with hanging wall splits form flatly dipping ore shoots (e.g., the bonanza grades from Zone VII Porgera; G. Corbett, pers. observation, 1991: West Shoot, Serujan North, Mt Muro, Indonesia; Moyle et al. 1996).

* Small scale jogs and flexures in linear veins (McKinstry, 1948), or mineralized shoots (e.g., Bilimoia, Papua New Guinea; Corbett et al., 1994b).

* Intersections of structures which control fluid flow with rock units promote mineral deposition such as carbonaceous units within sedimentary sequences (e.g., Gympie, eastern Australia; Cunneen, 1996: Wattle Gully, eastern Australia; Cox et al., 1995). Typical scenarios of steeply dipping dilational feeder structures and flat bedded sedimentary sequences produce flatly dipping ore shoots (e.g., Gympie).

vii) Structures in Time and Space

Structural elements (faults, fractures, etc) display protracted histories of activity (pre-, syn- and post-mineralization), commonly in response to different stress regimes and at varying crustal levels.

On the regional scale many major structures which localize intrusion-related ore systems are significant crustal discontinuities (e.g., Gilmore suture, Kalimantan suture, Philippine fault) which accommodate continued tectonism. Thus, these structures may act as pre-mineral ore-hosting fractures, by strike-slip movement provide syn-mineral mechanisms for dilatancy, and result in post-mineral offsets of vein systems. Reactivation of existing structures is most common. Ore systems of different ages to be localized by the same structures and so provide apparent telescoping. Major structures need not display the same senses of movement. Different directions of movement described in the Chuquicamata area of the Domeyko (West) fault, northern Chile (Boric et al., 1990; Sillitoe et al., 1994; Yanez et al., 1994), may account for syn-, and post-mineral episodes.

At outcrop scale, structures (fractures, veins, etc) represent a rock fabric defined by discontinuities. Most magmatic arc ore systems are epigenetic; that is, developed in pre-existing rocks, which display an existing fabric. Although metamorphosed sediments are competent rocks which could fracture well as ore hosts, many display existing fabrics which may preferentially open in extensional settings to host mineralization. Pre-existing fractures commonly host mineralization formed proximal to porphyry intrusions and therefore at deeper crustal levels, typically of the quartz-sulfide gold $\pm$ copper style mineralization. At Bilimoia, Papua New Guinea (Fig. 7.10) the regional slaty cleavage changes to a crenulation cleavage within the ore-hosting fracture systems, indicating that these structures formed at depths in the order of 5 km (D. Grey, pers. commun., 1994) and have been exhumed and mineralized at a higher crustal level (Corbett et al., 1994b). At Arakompa (Fig. 7.10), pre-mineral arc normal fractures host mineralization of the quartz-sulfide gold $\pm$ copper ore style in tension fractures. At Batu Hijau, Indonesia, conjugate fractures which are interpreted herein to have formed during orthogonal compression, have been reactivated during porphyry emplacement at a stage of extension, and host gold-bearing veins peripheral to the porphyry copper-gold mineralization (Meldrum et al., 1994).

Different crustal levels characteristically contain different fracture systems and deposit types (Fig. 3.14) in a vertical continuum of dilational structural environments typified by flower structures (Lowell, 1985) formed as dilatant fault segments. Splays at deepest crustal levels localize porphyry intrusions, fissure veins form at intermediate levels, best developed in competent basement rocks, and pull-apart basins form at surficial levels.

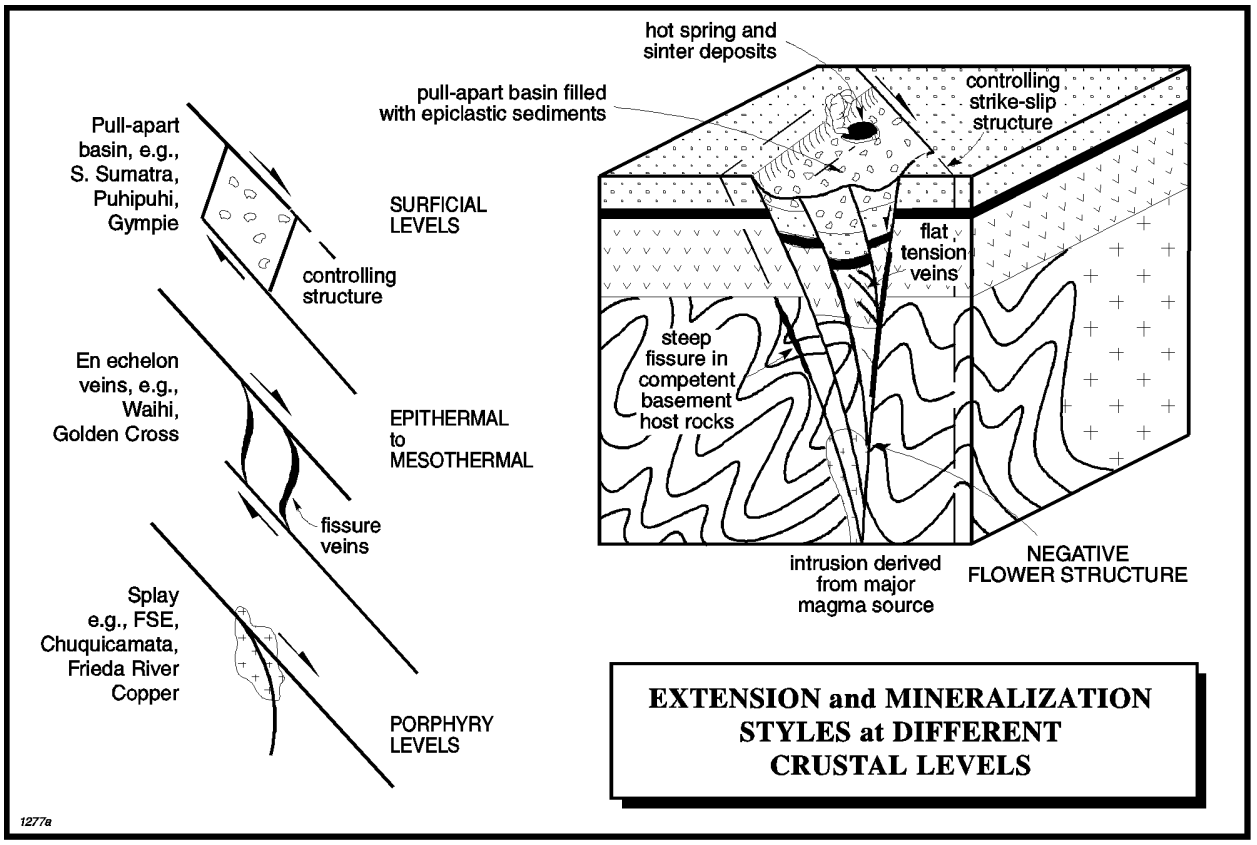

FIG. 3.14

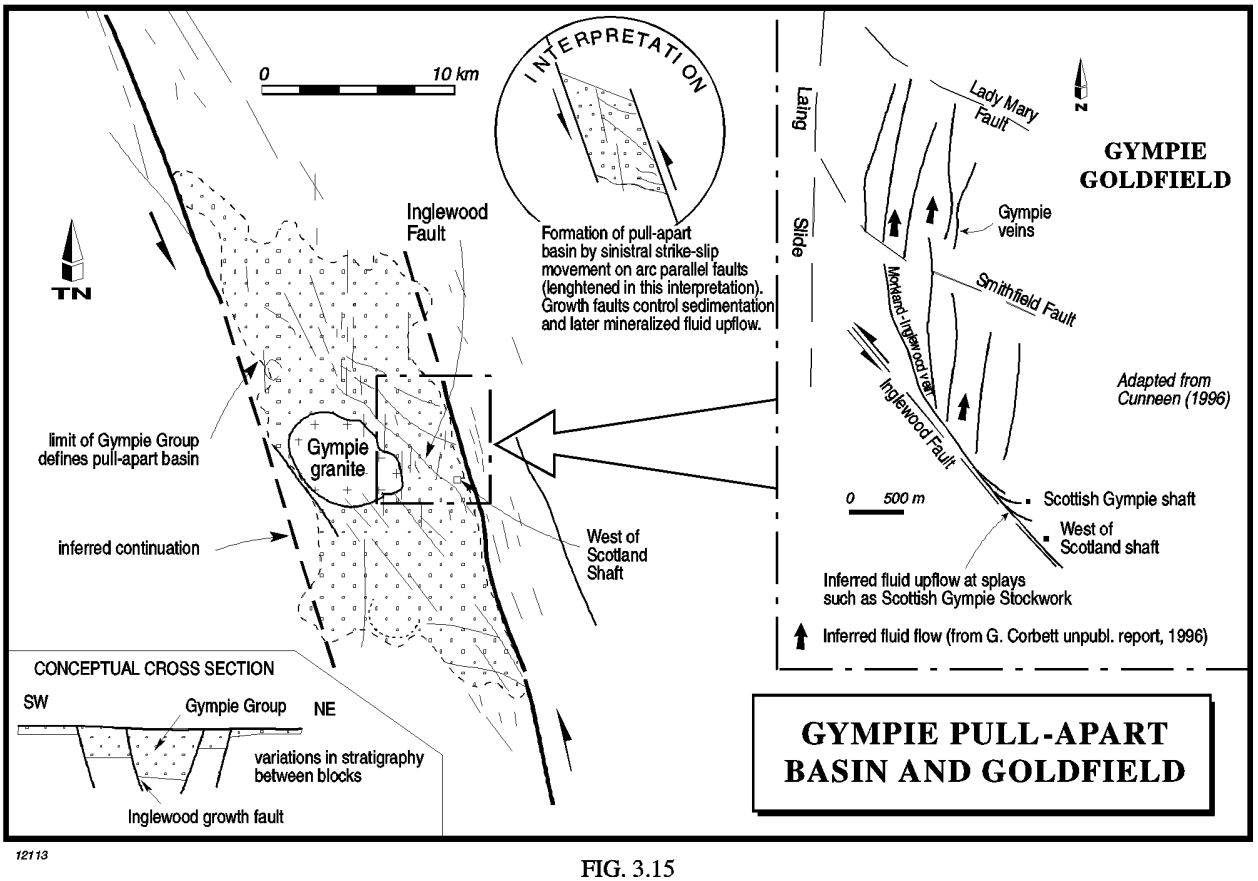

FIG. 3.15

At the Gympie goldfield, eastern Australia, structures demonstrate protracted histories of activity (Cunneen, 1996; G. Corbett, unpubl. report, 1996). Here, sinistral strike-slip movement on arc parallel structures during oblique convergence is inferred to have facilitated the formation of a pull-apart basin filled with epiclastic and volcaniclastic rocks (Fig. 3.15). Intra-basin growth faults separate variations in the basin-hosted sedimentary sequence, which becomes finer grained at higher levels. The pull-apart basin model better accounts for differences between the Gympie Group and the enclosing rock units, than earlier suggested origins, including as an accreted terrain. Continued convergence has activated intra-graben growth faults such as the Inglewood fault to facilitate mineralization. Splays and flexures in this structure are inferred to represent major fluid upflow centres and locally host high grade gold. This fluid flow model further suggests that ore fluids flowed laterally from the upflows into the Gympie veins, as sites of mineral deposition (Fig. 3.15). High and local bonanza gold grades occur at the intersection of Gympie veins and reactive carbonaceous (locally termed favourable) beds (Cunneen, 1996). Thrusts (locally termed breaks) also demonstrate continued pre-, syn-, and post-mineral activation to form and deform veins and also locally host ore.

viii) Shear Sense Indicators

An understanding of the sense of displacements of faults may be an important exploration tool at different scales. However, structures may be reactivated with differing senses of movement, and so the relationship of movement criteria to timing is critical.

On a regional scale, the displacement on many major structures may be predicted from the tectonic setting. For example, in settings of oblique convergence structures parallel to the Philippine, Sumatran, or San Andreas faults are likely to display senses of movement consistent with those major structures, as governed by plate movements (Fig. 3.1). The McLaughlin gold deposit is localized by strike-slip movement on structures parallel to the San Andreas fault (Tosdal et al., 1993; Donnelly-Nolan et al., 1993; Sherlock et al., 1995). A prospecting tool may emerge from an understanding of the regional structure. If the direction of movement on a controlling regional structure is known, it might then be possible from the orientation of subsidiary structures to readily distinguish which subsidiary jogs and flexures are more likely to be dilatant and mineralized, from those which are in compressional orientations and hence unmineralized. This procedure assumes consistent senses of movement for the mineralizing event.

In the Coromandel Peninsula, New Zealand, it has long been recognised that most vein systems trend northeast (Christie and Brathwaite, 1986; Brathwaite, et al., 1989). This is caused by dextral rotation on the Coromandel Peninsula derived from movement of the Pacific plate against the Australian plate (Fig. 7.47). Fissure vein systems such as Martha Hill, Golden Cross, Tui, Thames, and Karangahake are hosted within dilatant subsidiary structures. Similarly, the dilational character of the WNW trending Lepanto fault which hosts the Lepanto high sulfidation system, Philippines, is attributed to sinistral movement on NS-NNW structures derived from plate-scale movements (Fig. 6.24).

At the prospect scale, the sense of movement on major structures is most easily recognised from offsets in faulted rock units. The orientation of dilatant versus compressional subsidiary structures may aid in the development of a fault offset model for testing, but need not establish a sense of movement. Recognition of the direction of movement on weakly mineralized controlling structures may aid in the identification of the orientations of dilational subsidiary fractures and assist in the planning of trenching or drilling programmes (Fig. 3.10). High-grade ore shoots formed within domino fault sets may also represent important exploration targets.

Outcrop scale sense of shear indicators may be indispensable in the determination of offsets of vein-style ore bodies, particularly in underground mines. Slickensides, scratch marks, ploughed striations, or grooves and crystal growths, may indicate whether a fault displays dip-slip or strike-slip movement. However, which block is up/down or left/right as defined by irregularities in the slickensides is more difficult to determine. Petit (1987)

categorised secondary fractures in terms of the Riedel shear model as P, R or T shears to provide direction of movement indicators. These features may be difficult to identify in outcrop. Plough marks or mineral growth fibres provide easily discernible indicators of the direction of movement (Hancock, 1985). The 'smooth-rough' rule, which suggests that when a hand is run over fibres within a fault, the direction which feels smooth indicates block movement (Mawer, 1992), is a reliable method for determination of the sense of fault movement.

ix) Porphyry- and Intrusion-Related Fracture Patterns

We suggest (above) that porphyry intrusions are emplaced in extensional settings which result from relaxation of orthogonal convergence, or in oblique convergence. Typical settings include: splays, horsetails, jogs developed along strike-slip arc parallel faults or intersections of these structures with transfer structures. Many mineralized porphyry intrusions occur as apophyses to larger magma sources at depth (Section 5.i.c.; e.g., Philippines; Sillitoe and Gappe, 1984: Grasberg, Indonesia; MacDonald and Arnold, 1994: Goonumbla, eastern Australia; Heithersay et al., 1990). Much porphyry-style mineralization lies outside the porphyry environment and fluids are most likely to evolve from larger magma sources at depth and form wall rock porphyries (e.g., Cadia, eastern Australia) in settings of oblique convergence. In southwestern USA, Titley (1993) suggests that in 20 of 37 deposits reviewed, ore is mined from sedimentary host rocks adjacent to the source porphyry. Fracture systems transport mineralized fluids into cooler sites of deposition in apophyses to intrusions and wall rocks (Section 5.i.c), and facilitate alteration and also post-mineral supergene enrichment during weathering. Laminated porphyry stockwork and sheeted quartz veins provide evidence of reactivation of the controlling factors of vein formation, and possibly mineralization.

It is possible from an integration of field studies (Titley, 1993; Titley and Heidrick, 1978; Heidrick and Titley, 1982; Pennington and Kavalieris, 1997; G. Corbett, unpubl. data) and theoretical and experimental work (Phillips, 1974; Koide and Bhattacharji, 1975), to categorize styles of fracture/vein systems associated with porphyry ore-systems, according to the tectonic setting during intrusion emplacement, and the current level at which the system is exposed by erosion and mining.

a) <u>Mechanism for fracture development</u>

Fractures which develop during the dynamic process of porphyry emplacement and cooling, under the influence of the local stress environment, host stockwork and sheeted quartz veins and localize subsequent sulfide mineralization (Section 5.i.c.). The exsolution of volatiles due to crystallization of a melt has formerly been described using the terms 'first, second, or retrograde boiling' which are now not recommended (Shinohara and Kazahaya, 1995). Detailed discussions of this process are provided by Phillips (1973, 1986), Burnham (1979, 1985), summarised by Pirajno (1992) and most recently reviewed by Shinohara and Kazahaya (1995). In this process, intrusions form a carapace comprising the chilled margin surrounded by thermally metamorphosed country rock and then progressively cool inwards. The marked reduction in confining pressure, and hence solubility, as a magma is emplaced to a high crustal level, promotes an exsolution of volatiles as 'first boiling' (Pirajno, 1992).

The exsolution of volatiles results in a volume increase as the cooling intrusion separates into crystal and the volatile components. This may be accentuated as volatiles derived from a large body of magma at depth migrate upwards to porphyry copper-gold environments, commonly in the apophyses to larger intrusions (Fig. 3.16). Intrusions forcibly emplaced to high crustal levels will cool more quickly. Although the lithostatic confining pressure is lower at the higher crustal levels, inward cooling may enhance the tensile strength of the carapace which essentially seals the system and encloses the saturated and overpressured fluids. Traditional models (Phillips, 1973; Burnham, 1979) focus upon fracture development when the vapour pressure exceeds load

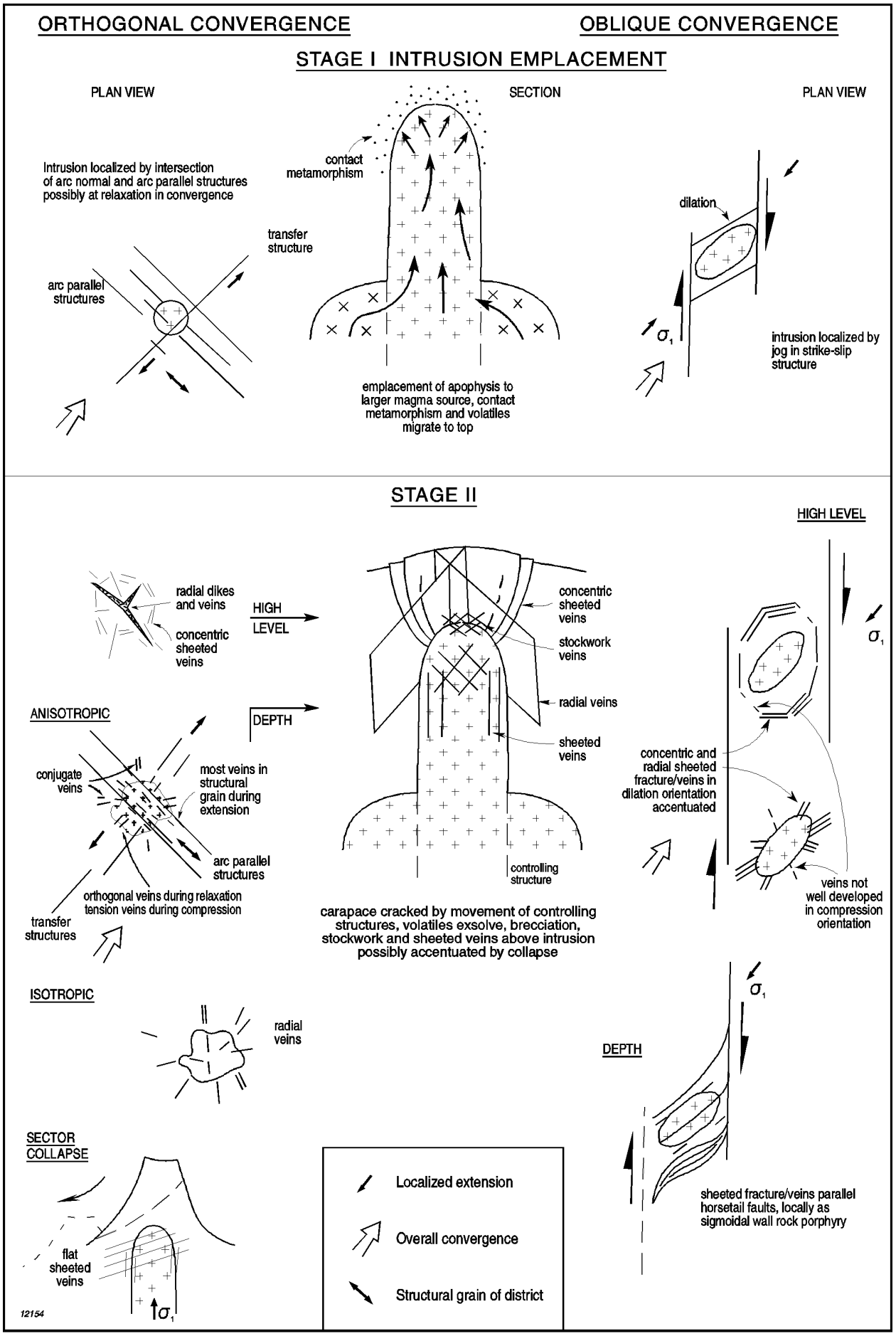
ORTHOGONAL CONVERGENCE
OBLIQUE CONVERGENCE
STAGE I INTRUSION EMPLACEMENT
PLAN VIEW
SECTION
PLAN VIEW
Intrusion localized by intersection of arc normal and arc parallel structures possibly at relaxation in convergence
contact metamorphism
transfer structure
arc parallel structures
dilation
σ_1
intrusion localized by jog in strike-slip structure
emplacement of apophysis to larger magma source, contact metamorphism and volatiles migrate to top
STAGE II
HIGH LEVEL
radial dikes and veins
concentric sheeted veins
HIGH LEVEL
DEPTH
concentric sheeted veins
stockwork veins
radial veins
sheeted veins
controlling structure
ANISOTROPIC
conjugate veins
most veins in structural grain during extension
arc parallel structures
orthogonal veins during relaxation tension veins during compression
transfer structures
carapace cracked by movement of controlling structures, volatiles exsolve, brecciation, stockwork and sheeted veins above intrusion possibly accentuated by collapse
concentric and radial sheeted fracture/veins in dilation orientation accentuated
veins not well developed in compression orientation
ISOTROPIC
radial veins
DEPTH
sheeted fracture/veins parallel horsetail faults, locally as sigmoidal wall rock porphyry
SECTOR COLLAPSE
flat sheeted veins
Localized extension
Overall convergence
Structural grain of district
12154

FIG. 3.16

pressure + surface tension of bubbles + tensile rock strength of the carapace (Phillips, 1986). Disruption by faults which control porphyry emplacement in tectonically active magmatic arcs may also promote fracturing of the overpressured carapace before that point is reached. The disruption of the overpressured carapace dramatically lowers the vapour pressure, prompting additional exsolution of volatiles. The pressurised fluids may escape as varying forms of (hydromagmatic) breccias (Burnham, 1985) or promote hydraulic fracturing of the carapace, possibly as stockwork and sheeted fracture/veins (Phillips, 1973, 1986). The rapid depressurisation associated with the escape of volatiles dramatically lowers the solubility of quartz (Fig. 4.2) which fills the sheeted or hydraulic fractures as veins in what has commonly been termed 'retrograde boiling' (Cf Phillips, 1986; Pirajno, 1992). The distribution of the fractures which host quartz veins and later mineralization is of interest here.

b) Porphyry-related fracture systems

Sheeted and stockwork fracture/veins which develop as a result of intrusion emplacement and cooling are important mechanisms of fluid transport from intrusions at depth to cooler, higher crustal level sites of mineral deposition, in many porphyry copper-gold and porphyry-related breccia gold systems. While the term sheeted fractures has been used to describe parallel fractures which form as flat lying extension joints in granitic rocks (Price, 1966; Hobbs et al., 1976), possibly developed by erosion-induced stress release (Price, 1966), fractures formed by the dynamic emplacement of porphyry intrusions are of interest here. The parallel alignment distinguishes sheeted fractures from the more random stockwork veins or stockworks formed by overprinting (locally conjugate) fracture sets. Heidrick and Titley (1982) classify (after Heidrick and Rehrig, 1972) different fracture (joint) systems in southwestern US porphyry intrusions, and note to importance of J_1 parallel (sheeted) fractures (joints) as mechanisms of fluid flow, while smaller more random fractures influence porosity.

Fracture/vein patterns in porphyry copper-gold systems are dependent upon:
* level of the system exposed by erosion which is in part related to age,
* stress regime into which the intrusion has been emplaced (e.g., oblique convergence),
* nature of the host rocks, in particular any pre-existing rock fabric or structural grain (e.g., fractures of the accretionary prism),
* changes in the stress regime (i.e., convergence) which may promote dilation and fracture formation.

1. High level settings

Mineralized porphyry intrusions are inferred to be forcefully emplaced upwards under the influence of dilational structural settings and the exsolution of volatiles to the apophysis. The dilation is inferred to be provided by a relaxation in orthogonal convergence or dilatant features (e.g, jogs, splays) in strike-slip faults in oblique convergence. Concentric and radial fracture systems which develop above porphyry intrusions (Titley and Heidrick, 1978; Heidrick and Titley, 1982) may vary under orthogonal or oblique convergence, as end members of a continuum.

In orthogonal convergence vertically elongate intrusions might most easily be emplaced upward during a relaxation of the regional stress regime. The vertical stress becomes dominant. Cone-shaped sheeted fractures ring the top of the intrusion and propagate upwards as concentric or kinked straight segments, and display dip variations from moderately inward close to the intrusion, steepening both at higher levels and further from the intrusion (Phillips, 1974; Koide and Bhattachji, 1975; Fig. 3.16). There is a small element of horizontal stress near the intrusion but only a vertical component at higher levels. Concentric (sheeted) fractures propagate above intrusions with high interstitial fluid pressures compared to lithostatic pressures and form concave upward shapes (Koide and Bhattacharji, 1975). Heidrick and Titley (1982) describe radial and concentric fractures developed by hydraulic fracturing in association with the emplacement of 'upward-extending' intrusions in the southwestern US, and elsewhere. These predominate in the host rocks away from intrusions. Concentric

sheeted fractures are inferred herein to preferentially develop above the intrusion margins and stockwork fractures to overlie the carapace. Sheeted fractures overlying intrusion margins are well placed to act as plumbing systems for fluids which migrate towards the margins of the intrusion at depth and then upwards (especially where dilated, see below). Radial and concentric fractures may predominate as dikes (Titley and Heidrick, 1975).

Collapse following venting of magmatic volatiles may accentuate the development of cone shaped sheeted fractures which formed above the intrusion during emplacement. Sheeted kinked concentric fractures overlie an inferred intrusion source at Kidston, eastern Australia (Section 7.ii.d) and define the margins of tourmaline breccia pipes in Chile in which slab breccias are indicative of considerable collapse (Sillitoe and Sawkins, 1971; Fig. 3.19).

In settings of oblique convergence faults which define the structural grain of the district may take on a strike-slip character and intrusions are emplaced into local dilatant settings (e.g., splays, jogs). Tension fractures which develop at the dilatant settings, where the intrusions are emplaced, may form dilatant sheeted fractures. Above a porphyry intrusion, conical and radial fractures aligned in the tension vein orientation will be enhanced, and others in compressional orientations may not be as well developed or mineralized (Fig. 3.16). In strongly transpressional settings fluids may readily evolve from porphyry intrusions at depth and form wall rock porphyry systems dominated by sheeted quartz veins (e.g., Cadia, eastern Australia; Newcrest Mining Staff, 1996). Elsewhere pipe-like intrusions also host mineralization in sheeted quartz-sulfide veins (e.g., Dinkidi, Philippines; Garret, 1996; G. Corbett, unpubl. report, 1995: Goonumbla, eastern Australia; Heithersay et al., 1995). Heidrick and Titley (1982) also describe sheeted fractures as important mediums of fluid transport and mineralization.

2. Deeper levels

At deeper levels of erosion the fractures which overlie the intrusion will be removed to expose fracture systems, generally within the intrusions, formed under the influence not of vertical intrusion emplacement, but the regional stress field and the local rock fabric. Two end member patterns result from settings of orthogonal or oblique convergence.

Settings of orthogonal convergence are further distinguished between those without a pre-existing structural fabric (isotropic) and those in which convergence developed a linear structural fabric (anisotropic) parallel to the trend of the accretionary prism (Fig. 3.16).

A structural grain (anisotropic conditions) developed during orthogonal convergence (compression fractures in Fig. 3.6, Section 5.1.c) will become dilated during a relaxation of convergence to an extensional setting (Fig. 3.16). Quartz-sulfide veins will exploit this pre-existing fabric. Higher angle, commonly orthogonal, fractures may also be present and give the sheeted veins a stockwork appearance. This is particularly evident if porphyry emplacement and degassing occurs during any relaxation of the convergence from which the compressional fabric resulted. Titley (1993) demonstrates a progression from concentric fractures immediately overlying porphyry intrusions, in higher level settings more distal to the intrusion, to a deeper level where fractures are aligned within the structural grain of the region formed by compression, and also a smaller fracture set formed orthogonal to the regional structures (Fig. 3.16). At the Grasberg porphyry copper-gold deposit, Indonesia, a high grade ore zone is aligned in a 120° trend, parallel to the accretionary prism, while other higher angle fractures host lower grade ore (Pennington and Kavalieris, 1996). These workers stress that mineralization is derived from a larger magma source at depth, possibly during a relaxation of compression.

In the absence of an existing structural grain (isotropic conditions), the forceful vertical emplacement of the cylindrical intrusion causes radial fractures to develop, particularly in settings of high fluid pressures (Phillips, 1974). These workers note that radial dikes, inferred herein to be pre-mineral, may extend some distance from

the porphyry source (e.g., Kidston, eastern Australia; Figs. 7.7, 7.8). Titley and Heidrick (1978) describe the downward progression from concentric to radial fractures in this setting. The apparent radial pattern (Fig. 3.16) may result from reactivation of pre-existing fractures formed during orthogonal compression and categorized as: conjugate and tension fractures; or during relaxation of convergence as, orthogonal and reactivated compressional fractures (Fig. 3.16).

In settings of oblique convergence, quartz and sulfide veins exploit dilatant tension fractures and commonly form mineralized sheeted veins, typically at intrusion margins (Fig. 3.16). This is common for porphyry intrusions localized by jogs, splays or horsetails in strike-slip structures. Ore-hosting sheeted fracture/veins will parallel the orientation of other dilational fractures such as horsetails or splays which may be inferred to localize porphyry intrusions (e.g., St Tomas II porphyry copper-gold, Philippines; unpubl. map, R. Baluda, 1996: Frieda River porphyry, Papua New Guinea; Asami and Britten, 1980; Corbett, 1994). Thus oblique convergence during specific time periods provides a mechanism for mineralization. Heidrick and Titley (1982) cite such a scenario to account for the district wide consistency of quartz veins in southwestern US porphyry copper-gold deposits.

Sheeted fracture/veins formed in this manner by dilation, either within, adjacent to, or outside the porphyry environment, are important mechanisms for the transport of mineralization from magma sources at depth to higher level settings of mineral deposition. Many porphyry systems host sheeted veins at and above the margins, while more random stockwork veins predominate at the top of the intrusion. Many vein systems display steep dips and strike directions consistent with the tectonic setting into which the intrusion was emplaced (e.g., St Tomas II, Frieda River, above; Section vi.a). It is imperative that these mineralized fractures be carefully mapped during the planning of drill testing. Angle drill holes bored across the vein strike are favoured to test steeply dipping sheeted veins, which typically host higher grade mineralization (Fig. 5.3).

Sector collapse may promote mineral deposition by sudden depressurisation of porphyry intrusions (Sillitoe, 1994b). In these settings flatly dipping fractures and quartz veins are likely to develop and host ore (e.g., Hinoba-an porphyry copper, Philippines; G. Corbett pers. observation with J. Vasquez, 1996: depth extension of Kidston, eastern Australia; Morrison, et al., 1996). Steeply dipping fractures may transport mineralized fluids into these settings. Sector collapse proposed for Ladolam, Lihir, Papua New Guinea (Sillitoe, 1994b), resulted in the development of a sub-horizontal breccia at the intrusion contact as a host for later gold mineralization.

Conclusion

Intrusion-related fracture/vein patterns pass downward from concentric and radial overlying the intrusion, to commonly display a greater degree of alignment at depth (Titley and Heidrick, 1978), either within pre-existing structural grain, or as new dilatant fractures formed by oblique convergence. The concentric and radial fracture/vein/dike patterns may be modified in oblique settings, such that those in dilational orientations become accentuated and mineralized, while those in compressional orientations are not well developed. Changes from orthogonal to oblique convergence during the mineralizing process are most clearly evident in younger systems of Papua New Guinea (e.g., Frieda River; Asami and Britten, 1980: Yandera, Titley et al., 1978). Oblique convergence is therefore favoured as a mineralizing environment.

x) BRECCIAS

a) Introduction

Practically all magmatic arc gold-copper systems discussed herein contain breccias, and so the processes of breccia and ore formation are intimately related. As exploration geologists we seek to further understand the relationship to mineralization of the wide variety of breccia types. For instance, the mapping of barren diatreme breccias may point towards the mineralization elsewhere in the hydrothermal system (below). Yet the terms used are as numerous as the geologists involved. The aim here is to:

* focus on the processes of formation of breccias,
* to delineate differing breccia types, and
* describe the role of breccias in ore formation.

We attempt to maintain consistency with existing breccia classification and terminology, albeit in the light of our own personal experience, and to some extent, that of our peers. Readers are referred to the following works, on which this discussion draws, for more detailed and in some instances alternative analyses of breccias: Sillitoe (1985), Baker et al. (1986), and Taylor and Pollard (1993).

What is a breccia?

A breccia is a clastic rock composed of fragments held together by matrix and locally containing cavities filled by post-brecciation hydrothermal minerals (Taylor and Pollard, 1993).

Fragments or broken rock clasts become progressively milled with increased deformation (brecciation). Some breccias contain only host-rock fragments while others are characterized by introduced fragments, and fragments undergo varying intensities of alteration. Fragment alignment occurs in some breccia types (below).

Matrix comprises minerals (including ore) deposited from hydrothermal fluids (below) as well as locally-derived and introduced rock material of a finer grain size than the fragments (depending on the degree of milling), which fill the space between fragments. There are local gradational contacts between fragment and matrix, and breccias may be either matrix or fragment (clast) supported. Most of the mineralization within breccias has been introduced as hydrothermal fluid and so occurs within the matrix.

Open space or cavities develop between fragments which are in contact with each other so as to become clast supported. Open space may become filled by hydrothermal minerals, including gold-copper mineralization, during or following brecciation. In the latter case, it may be possible to infer paragenetic sequences of overprinting mineral deposition.

All these fragment and matrix variations contribute towards the development of differing breccia types.

Sampling of breccias should be carried out with great care in order to obtain a representative sample. In surface weathered exposures, softer mineralized matrix may become recessive and so random sampling may be dominated by barren more prominent fragments which are resistive to weathering. The resultant assay values may become downgraded by the inclusion of an unrepresentative quantity of barren material. Underground mines may contain fresh exposures of pre-mineral quartz which has undergone later brecciation and mineralization. Here, softer ore-grade breccias may more readily become part of the sample, than the host resistive quartz of lower gold grade, and the assay value could be upgraded.

b) Classification

In order to map hydrothermal systems breccias must be named (classified). Breccias may be distinguished by classifications which are based upon:

* appearance or a descriptive classification,
* mode of formation or a genetic classification.

Which is appropriate?

As a general rule - it is important to avoid early genetic descriptions and maintain descriptive terms. When studying a breccia it is advisable to start by recognising the differing breccia types or textural variations and map them using descriptive terms. Many subdivisions can be grouped later. This data base will contribute towards the development of a genetic model. Breccia analysis is best carried out at a large scale by extensive geological mapping (e.g., Kidston, eastern Australia; Section 7.ii.d). If one outcrop is confusing, move to the next one and try to stand back in order to obtain a big picture. Analysis of overprinting events within veins, rebrecciated breccia fragments and breccia matrix, may provide information on the paragenesis of the hydrothermal system. Varying styles of breccias have widely different implications in mineral exploration.

1. Descriptive terms

These are most useful in order to provide the data to map a breccia at the initial stages of an investigation. Descriptions should focus on such features as: type and shape of fragments, fragment to matrix ratios, degree of fragment milling and transport, composition of matrix and whether it is locally derived by fragment milling or introduced hydrothermal minerals, degree of rebrecciation, extent of post-breccia vein development, and so on. However, breccias of similar appearance may be derived from different processes. Some examples are:

A mosaic or jigsaw breccia, which is described simply as, 'one in which the fragments can be fitted back together by removal of the matrix', can be derived by a variety of brecciation processes. A mosaic breccia in the carapace to an intrusion may be barren and not point towards higher grade mineralization in the same manner as a mosaic breccia in a high sulfidation system might. Other mosaic breccias are indicative of dilation as a genetic process.

The term milled matrix fluidized breccia describes rocks in which the fragments have been milled (comminuted) to form the matrix and altered during extensive transport (fluidization). Many exploit structures to develop dike-like forms and have been termed tuffisite by some workers (Paull et al., 1990). These breccias are common in the genetic classification of phreatomagmatic breccias and so may occur in association with maar/diatreme complexes. However, the identification of a milled matrix fluidized breccia does not establish the existence of a diatreme as a geological setting, unless the other features of this genetic classification have been established, usually by geological mapping.

As the knowledge of a particular system evolves, an understanding of the geological environment and process of formation may then allow a breccia to be put in a more genetic framework. Rocks described as muddy breccias (as a descriptive term) during original exploration at Kelian, Indonesia (van Leeuwen et al., 1990), have since been placed in a genetic classification as part of maar/diatreme complexes (Sillitoe, 1994a).

2. Genetic terms

A genetic term is based on the interpreted manner in which the breccia formed, and is derived from only the data to hand at that stage of the exploration programme. Recording information using a genetic terminology may result in a loss of the original data base and inhibits later reinterpretation, especially as the knowledge of the

system evolves. Examples may include the dramatic improvement in data quality at progression from geological mapping of trenches in deeply weathered tropical Pacific rim settings, to diamond drilling. The transition from a descriptive terminology to an understanding of the process of formation and geological environment in which genetic terms come into use, may hasten ore discovery (e.g., gold mineralization commonly occurs at diatreme margins).

The genetic term dilational breccias defines a dilated broken rock in which open space has been filled by later ore-bearing fluid, commonly in brittle rocks in high level settings. However, different dilational breccias are delineated by the descriptive terms floating clast breccias, defined below, and mosaic or jigsaw breccias, described above.

c) Primary non-hydrothermal breccias

Magmatic breccias form in association with porphyry intrusions in which there is little mixing of meteoric waters or fluid degassing. Only with later influx of hydrothermal fluid are these breccias inferred to become altered and possibly mineralized. Intrusive or contact breccias develop at the contacts between intrusions and host rocks, while collapse breccias form following the outflow of material from a magma chamber. Many contact breccias represent permeable fluid paths and so display preferential alteration.

Volcanic breccias represent the large group of broken rocks which form in subaerial and subvolcanic environments, locally host volcanogenic massive sulfide deposits, and may also act as host rocks for magmatic-arc copper-gold mineralization. Some permeable host rocks readily become are altered. Readers are referred to texts such as Cas and Wright (1987) and McPhie et al. (1993) for a discussion of these rock types.

Tectonic breccias develop by deformational processes and include fault breccias which vary from milled puggy fault zones, to open space breccias and are usually distinguished by an association with planar fault surfaces. However, many faults are plumbing systems for hydrothermal fluids and so these breccias are transitional to hydrothermal phenomenon.

d) Ore-related hydrothermal breccias

Environments of ore-related breccia formation are categorized as:

1. Magmatic hydrothermal breccias
2. Phreatomagmatic breccias
3. Phreatic breccias
4. Magmatic hydrothermal injection breccias
5. Hydrothermal collapse breccias
6. Dilational breccias
7. Dissolution breccias

These first three environments of formation and associated breccia styles are distinguished using the terminology of Sillitoe (1985) on the basis of crustal level and relationship to porphyry source rocks (Fig. 3.17; Table 3.1). Magmatic hydrothermal breccias typically form at deepest or porphyry levels and are eroded to display pipe-like forms, but need not vent to the surface. Phreatomagmatic (diatreme) breccias typically display associations with high level porphyry intrusions and may vent as diatreme/maar volcanoes or remain as milled matrix fluidized breccias, commonly as dikes which exploit pre-existing structures at varying depths. Phreatic (eruption) breccias form at surficial levels and in this classification do not display a relationship with high level intrusions. For low sulfidation gold deposits, broad correlations are apparent between breccia and mineralization

types, again dependent upon the crustal level and relationship to intrusion source (Figs. 7.1, 7.2). High sulfidation copper-gold deposits form in association with diatreme and less commonly eruption breccias.

Magmatic hydrothermal injection breccias are related to hydraulic breccias and a form by the injection of mineralized magmatic fluids, typically in high sulfidation systems. Hydrothermal collapse breccias form during the retrograde phases of porphyry development as collapsing host acidic fluids overprint the existing prograde alteration, and are not a mineralizing process, but may contain pre-breccia mineralization. Dilational breccias form at varying crustal levels within open space structures (Sections 3.iv and 3.vi), generally within competent host rocks which fracture well (Section 3.iv.c), and are typically filled by hydrothermal minerals. These are most common in low sulfidation adularia-sericite epithermal gold-silver deposits. Dissolution breccias form by the creation of open space either by dissolution of soluble material such as limestone, or the conversion of calcite to dolomite. These breccias are most common in sediment hosted replacement gold deposits (Section 7.v).

1. Magmatic hydrothermal breccias

Magmatic hydrothermal breccias (Figs. 3.17, 3.18) are characterized by a pronounced magmatic involvement in the brecciation process, alteration and composition of the ore fluid (e.g., Kidston, eastern Australia; Baker and Andrew, 1991: Mt Leyshon, eastern Australia; Paull et al., 1990, Orr, 1995: San Cristobal, Chile; G. Corbett, unpubl. report, 1990; Egert and Kasaneva, 1995). The Kidston breccia is described herein as a case study of this type of breccia and associated gold mineralization (Section 7.ii.d.v).

Subvolcanic breccia pipes, which host hydrothermal magmatic breccias typically form at considerable depths (>1 km) in association with high level, commonly felsic, porphyry intrusions, and are generally not expected to have vented to the surface. Breccia pipes commonly overlie apophyses to larger bodies of magma, from which metals at a low tenor may have been concentrated. The analyses during exploration of the architecture of intrusion source rocks, may assist in the identification of settings for breccia pipes. The Kidston breccia pipe is localized at the intersection of a transfer structure and the steeply dipping margin of a buried magmatic arch (Fig. 7.6). Similarly, the Mt Leyshon breccia body is localized by the intersection of a regional structural corridor with the margin of a subvolcanic complex (Paull et al., 1990; Orr, 1995).

The mechanism inferred for breccia formation relies upon the violent explosion of volatiles which rapidly exsolve from a magmatic source. Volatiles, possibly derived from a large magma source at depth, collect and become overpressured in apophyses as intrusions cool. Movement on a controlling structure may fracture the carapace allowing the volatiles to escape explosively (Section 3.ix.a). Metal-bearing fluids utilise sheeted fractures to exsolve from the melt at depth following volatile-driven brecciation. Thus mineralization is inferred to commonly post-date breccia formation. Mineralization predominates in sheeted fractures and open space breccias, particularly breccias close to sheeted veins and at kinks and junctions in the sheeted veins (e.g., Kidston; Morrison et al, 1995). Post-breccia collapse enhances the development of sheeted veins which generally dip steeply and kink around the intrusion margin (e.g., Kidston, Fig. 7.7: Cabeza de Vaca, Chile; Sillitoe and Sawkins, 1971), or form as dilational fissure veins (e.g., San Cristobal, Chile; Egert and Kasaneva, 1995). At Mt Leyshon late-stage and probable syn-mineral tuffisite dikes provide permeability for the transport of gold-base metal mineralization, which is hosted in open space breccias within the dikes and adjacent rocks (Orr, 1995).

An understanding of the anatomy of breccia pipes may assist in the discovery of mineralization. Baker et al. (1986) distinguish different levels of breccia pipes and Sillitoe (1985) describes upper terminations into collapse breccias and the rarely seen lower contacts as; fissures, source intrusions, or shears. Lateral contacts are commonly sharp and exhibit sheeted fracturing (Sillitoe, 1985). As brecciation is generally pre-mineral, ore distribution relates to the plumbing systems (e.g., sheeted veins or tuffisites) and presence of open space in

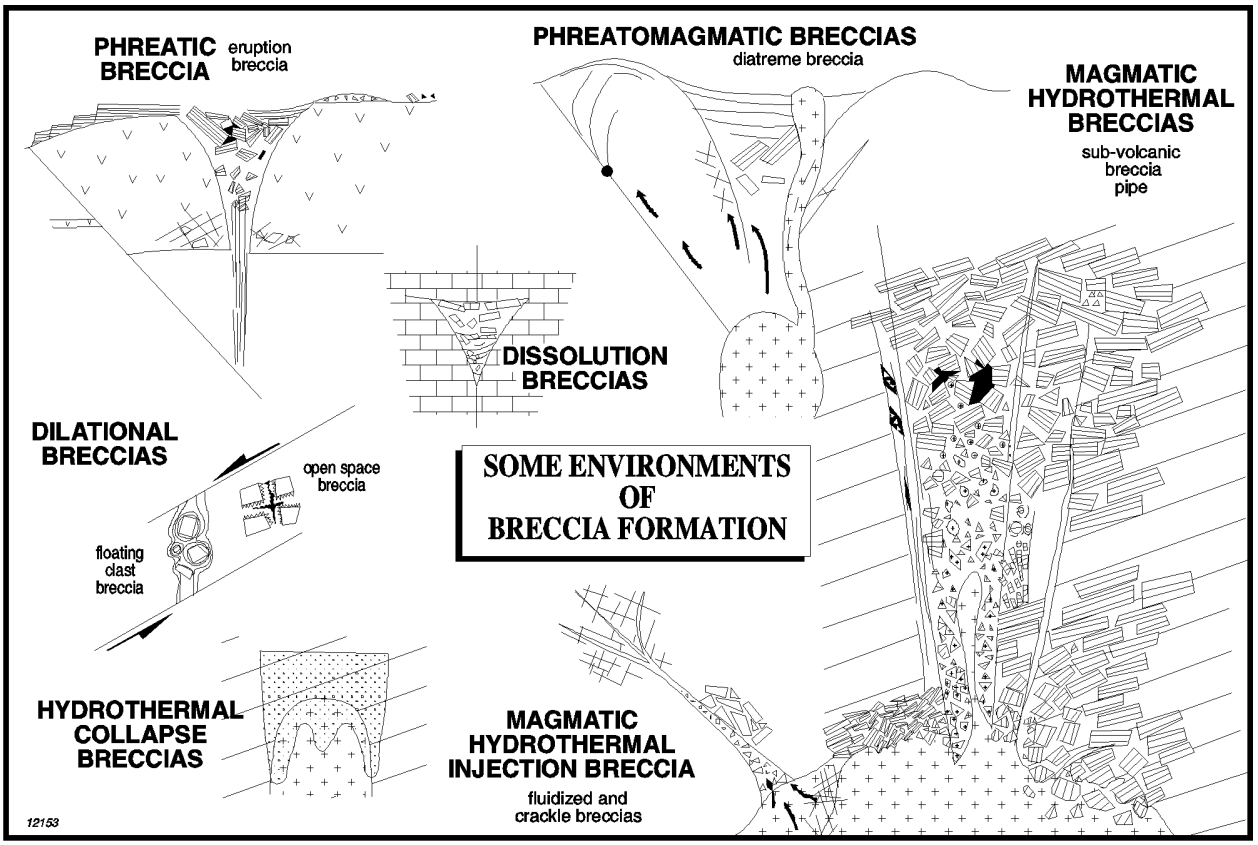

FIG. 3.17

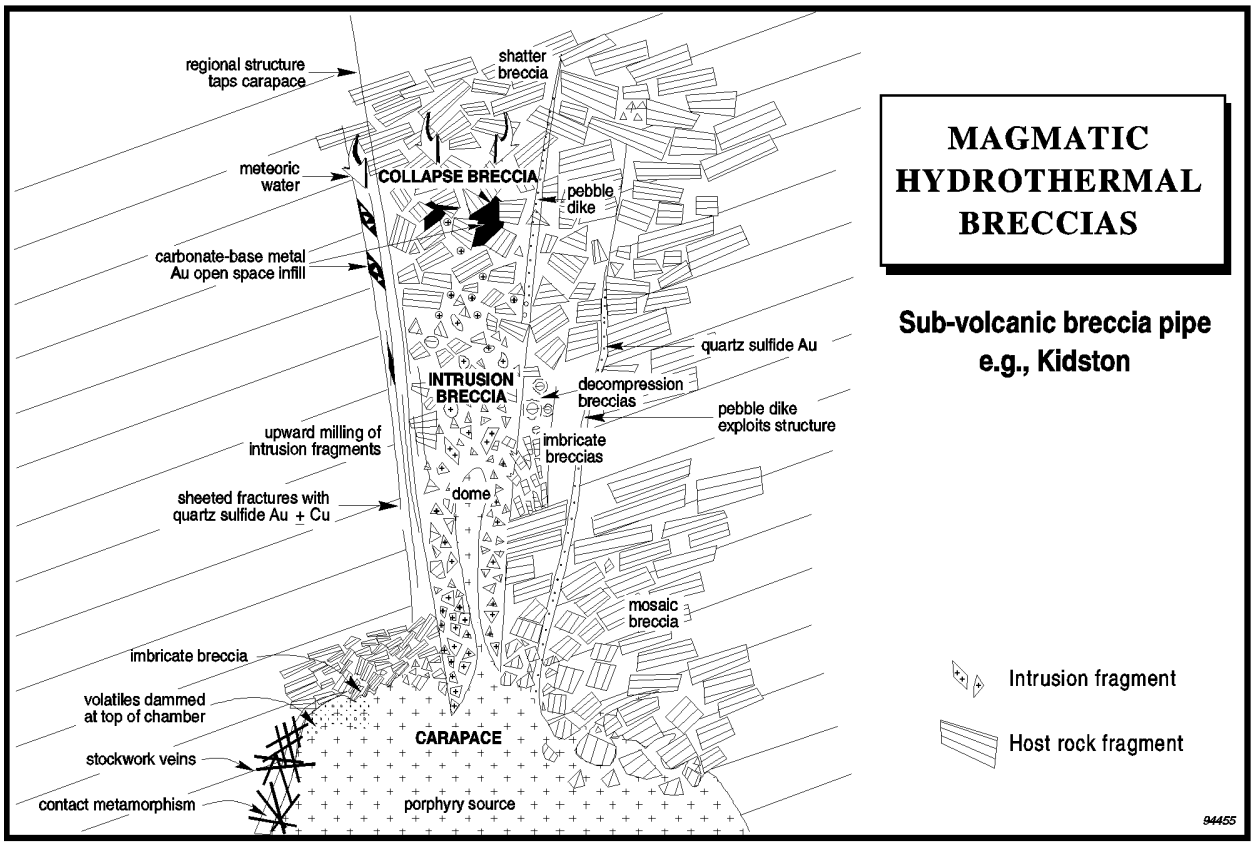

FIG. 3.18

breccias.

Two facies within breccia pipes are related to the mechanism of formation as:

* intrusion breccias
* collapse breccias

The genetic term intrusion breccias describes rocks developed in conditions of intense fluidization during the explosive exsolution of volatiles injected from the intrusion into the overlying host rocks. Breccias which belong to this class include: milled (Baker et al., 1986), or rock flour (Sillitoe, 1985) breccias and locally tuffisites (e.g., Mt Leyshon, eastern Australia; Paull et al., 1990; Orr, 1995; although this term is also used in phreatomagmatic breccias, below). These breccias are generally supported by a matrix of comminuted (milled) rock flour and hydrothermal cement, and represent mixes of rounded, commonly competent, intrusion fragments which have been milled during transport. Milling takes place in highly fluidized environments, and Sillitoe (1985) and Baker and Andrew (1991) also cite hypogene exfoliation as a mechanism of rounding. These rounded breccias may be termed decompression breccias which develop during the rapid depressurisation of venting fluids or rock masses. They exhibit the appearance of spheroidally weathered and rounded fragments, rimmed by curved and tabular (Baker et al., 1986) fragments, separated by minor open space which may be filled with hydrothermal minerals (Fig. 3.18). Other intrusion breccias of this type rim intrusive dikes (e.g., San Cristobal, Chile). At both Kidston and San Cristobal, early fine grained felsic dikes associated with the intrusive breccias are cut by later coarser grained quartz feldspar porphyry intrusions, possibly reflecting a melt derived from deeper within the magma chamber.

The genetic term collapse breccias is applied to a group of open space breccias formed during relaxation following the initial explosive intrusion breccia event, and are typically best exposed about the outer, particularly the upper, portions of breccia pipes. Only small degrees of transport of country rocks are recognised in many typically monomictic jigsaw (Sillitoe, 1985) or shatter (Baker et al., 1986) breccias which can be joined back together by removing the hydrothermal cement, and contrast with the introduced fragment-rich nature of the intrusion breccias. At Kidston, eastern Australia, a country rock geological contact can be traced from outside to within the Kidston breccia pipe, and the presence of large flatly dipping tabular blocks are indicative of a transition to a margin of the system (Fig. 7.7). Early mapping at Kidston (G. Corbett, unpubl. data, 1980) defined a zone dominated by intrusion fragments (termed volcanic breccia in Fig. 7.7), which roughly corresponds to pre-breccia rhyolite and early tourmaline breccias of Baker and Andrew (1991). Moving outwards towards the margin of the pipe, the intrusion breccias are progressively rimmed by polymictic and then collapse breccias. In the metamorphic (collapse, Fig. 7.7) breccias, the pre-breccia metamorphic layering progressively deviates further from the original orientation evident in the country rock outside the breccia pipe, moving inwards away from the pipe margin, as the fragment rotation also increases.

The importance of collapse breccias as ore-hosts is apparent in the copper ± gold-bearing tourmaline breccia pipes of Chile. These breccia pipes form in settings where flatly dipping fractures, resulting from collapse following an escape of (magmatic) volatiles, are exploited by a fluidized breccia matrix of mainly tourmaline and sulfides (Sillitoe and Sawkins, 1971). Breccia pipes display large shingle-like (below) fragments typical of collapse formation at the margins and upper portions, and more rounded, milled and open space breccias in the core zone and closest to the magmatic source (Fig. 3.19; Sillitoe and Sawkins, 1971). The fluidized matrix which exploits the fractures is less well developed in the fragment supported shingle breccias than in the open space-rich core, where sulfides were deposited following the tourmaline. Bimodal fragment sizes are common in the slab breccias, as fluid injection along the fractures between the shatter blocks mills some smaller fragments (Fig. 3.19). Fracture formation by the violent exsolution of volatiles from a magmatic source, followed by later ore-bearing magmatic fluids, is common in intrusion-related ore systems (Section 5).

CHARACTERISTICS of BRECCIA PIPES

	MAGMATIC	PHREATOMAGMATIC	PHREATIC
Common name	• sub volcanic breccia pipes • magmatic hydrothermal breccia pipes	• diatreme breccia • milled matrix fluidized breccia	• eruption breccia
Origin	• violent exsolution of volatiles from intrusion	• venting of volatiles and rapid heating of ground waters	• depressurisation of geothermal waters
Level	• deep at porphyry level • need not vent	• intermediate diatreme vents • milled matrix fluidized breccia exploits structure	• surficial form sinter outflows
Intrustive activity	• porphyry-derived, dykes	• endogenous domes	• none exposed
Style of mineralization	• quartz-sulfide gold ± copper, grading to carbonate-base metal gold	• carbonate-base metal gold • high sulfidation gold-copper	• adularia-sericite epithermal gold-silver
Alteration	• sericite-quartz • biotite, K-feldspar • actinolite, epidote	• illite to smectite • disseminated fine crystalline pyrite	• silica-fine pyrite/marcasite
Form	• intrusion styles dominated by introduced intrusive fragments • collapse styles dominated by local fragments	• vent facies within diatreme • tuff ring facies thrown out of diatreme	• cone-shaped pipes vent and tuff ring facies
Fragments	• magmatic and local • tabular shingle breccias in collapse styles • milled fragments in injection styles	• juvenile intrusion fragments characteristic • local accretionary lapilli • tuffisite are well milled	• locally derived, commonly angular
Matrix	• rock flour, open space	• milled and fluidized clay-pyrite altered	• silica-pyrite
Examples	• Kidston, San Cristobal, Golden Sunlight, Mt Leyshon	• Wau, Kelian, Acupan, Kerimenge, Lepanto, Tolukuma	• Champagne Pool, Puhipuhi, Toka Tindung, McLaughlin

1455

TABLE 3.1

The terms shingle, domino (Sillitoe, 1985) or imbricate (Baker et al., 1986) apply to slab-like breccias formed by regular breaks or sheeting about the margins of breccia pipes (Sillitoe and Sawkins, 1971), typically by collapse. Slab breccias are transitional to the angular shatter breccias of Baker et al. (1986). While these breccias may dip flatly above a pipe, Sillitoe (1985) emphasises the shallowing in dip moving inward from the pipe margin (Fig. 3.19). Collapse along marginal sheeting may promote the formation of fractures which become exploited by fluids to form breccias (Fig. 3.19). Mining has exposed the flat lying slab-like blocks of rebrecciated breccia several tens of metres long on the pit walls, in the collapse portion of the Kidston breccia pipe. Sub-vertical slab breccias occur at the margins of some breccia pipes (Sillitoe and Sawkins, 1971). Vertical slab-like breccias may form by the exploitation by later hydrothermal minerals, of pre-mineral sheeted fractures within structural corridors.

Pebble dikes comprise linear bodies of well rounded, commonly transported fragments in a milled matrix formed by the explosive venting of depressurised volatiles along faults or joints. They are common in porphyry environments (e.g., El Salvador, Chile; Gustafson and Hunt, 1975), may display extensive vertical dimensions (Sillitoe, 1985), and locally provide ground preparation for later gold-bearing quartz-sulfide veins (e.g., Arakompa, Papua New Guinea; Corbett et al., 1994b). Sillitoe (1985) however, cites the association with specific intrusive phases to suggest that pebble dikes are more commonly late- to post-mineral in age (e.g., El Salvador, Gustafson and Hunt, 1975). Pebble dikes are fragment-dominated and fragment-supported and distinguished by the transport of milled fragments, from fluidized breccias (below) which are characterized by transported matrix.

2. Phreatomagmatic breccias

Phreatomagmatic ("phreato" meaning water converted to steam) and magma eruptions are the violent eruptions which develop as a rising depressurised magma exsolves volatiles, and also comes in contact with ground waters, which are rapidly superheated to form steam. The term diatreme is utilised to describe the breccia-filled conduit (Sillitoe, 1985; Sillitoe and Bonham, 1984) which may comprise a surficial maar volcano, endogenous domes and other features described below (Fig. 3.20), although not all breccias formed by this process vent to the surface. The non-genetic field term milled matrix fluidized breccia (defined above) might be utilised during geological mapping to describe phreatomagmatic breccias prior to the identification of sufficient field relationships to place them in a geological environment typical of a diatreme. Some breccias exploit pre-existing structures which may also host volatile-rich apophyses to larger magma sources. Diatreme breccias display a strong association with high level porphyry intrusions, commonly as flow dome complexes. Gold mineralization associated with phreatomagmatic breccias occurs as low sulfidation, most commonly of the carbonate-base metal style (Fig. 7.2; e.g., Kelian, Indonesia; Acupan, Philippines; Kerimenge, Papua New Guinea), as well as high sulfidation gold at higher crustal levels and gold-copper at deeper levels (Fig. 6.1; Wafi, Papua New Guinea; Lepanto, Philippines; Miwah, Indonesia).

Examples of diatreme-related gold/copper mineralization in the southwest Pacific include: in the Philippines at Acupan, 4 M oz Au (Damasco and de Guzman, 1977; Sawkins et al., 1979; Cooke and Bloom, 1990), Lepanto, >3 M oz Au (Section 6.iv; Garcia, 1991), Bulawan Gold (G. Corbett, pers. observations) and Dizon 3 M oz associated with the porphyry copper-gold (Sillitoe and Gappe, 1984); in Papua New Guinea at Wau (Sillitoe et al., 1984), Kerimenge, 1.8 M oz Au (Section 7.iii.i; Hutton et al., 1990), Edie Creek (Section 7.iii.i; Corbett, 1994), and Wafi (Section 6.iii.b; CRA, 1994); in Indonesia, Kelian, 5.7 M oz Au (Section 7.iii.i; van Leeuwen et al., 1990; Sillitoe 1994a); and Miwah, (Williamson and Fleming, 1995), Bawone-Binebase on Sangihe Island (Section 6.v.b; G. Corbett, unpubl. report, 1993), and in the Solomon Islands, Gold Ridge (Section 7.iii.i; Sillitoe, 1989, Fig. 7). Others include: in the USA, Cripple Creek (Thompson et al., 1985), Montana Tunnels (Sillitoe et al., 1985); in the Dominican Republic, Pueblo Viejo, (Vennemann et al., 1993); in eastern Australia, Mt Terrible (G. Corbett, pers. observation; Teale, 1995), Mt Rawdon (Brooker, 1991). Milled matrix fluidized breccias localize gold mineralization in Papua New Guinea at Tolukuma (Section 7.iv.d.3; Corbett et al., 1994a; Semple et al., in review), Busai on Woodlark Island (Corbett et al., 1994a), and Mt Kare (G. Corbett, unpubl. report, 1996).

Diatreme/maar volcano complexes are inferred to be generated by high level porphyry intrusions at depths varying to 1 km, as evidenced by the formation depth of associated carbonate-base metal mineralization and associated alteration. Intrusions of dacitic to rhyodacite compositions are most common. Diatreme breccia/maar volcano complexes range in diameters to many hundreds of metres across, although larger examples have been recognised (e.g., >5 km for Nauti diatreme, Papua New Guinea; G. Corbett, unpubl. report 1985; Section 7.iii.i: and >4 km for Lepanto, Philippines; Baker, 1992; Fig. 6.24). Repeated activation results in rebrecciation and overprinting diatremes. Flared margins are inferred to dip inward shallowly in the upper portions and more steeply at depth, to produce the overall funnel shape (Sillitoe, 1985; e.g., Lepanto, Fig. 6.25).

Diatreme/maar volcano complexes and milled matrix fluidized breccias are commonly localized by major structures along which high level porphyry intrusions have been emplaced and which may have been reservoirs for ground waters. Examples include: the graben structure at Tolukuma (Fig. 7.50, Corbett et al., 1994a); Escarpment fault at Wau, (Figs. 7.28, 7.30; Sillitoe et al., 1984); Kerimenge fault at Wau (Figs. 7.28, 7.31) and the dilational splay represented by the Lepanto fault at Lepanto (Figs. 6.24, 6.25; Baker, 1992).

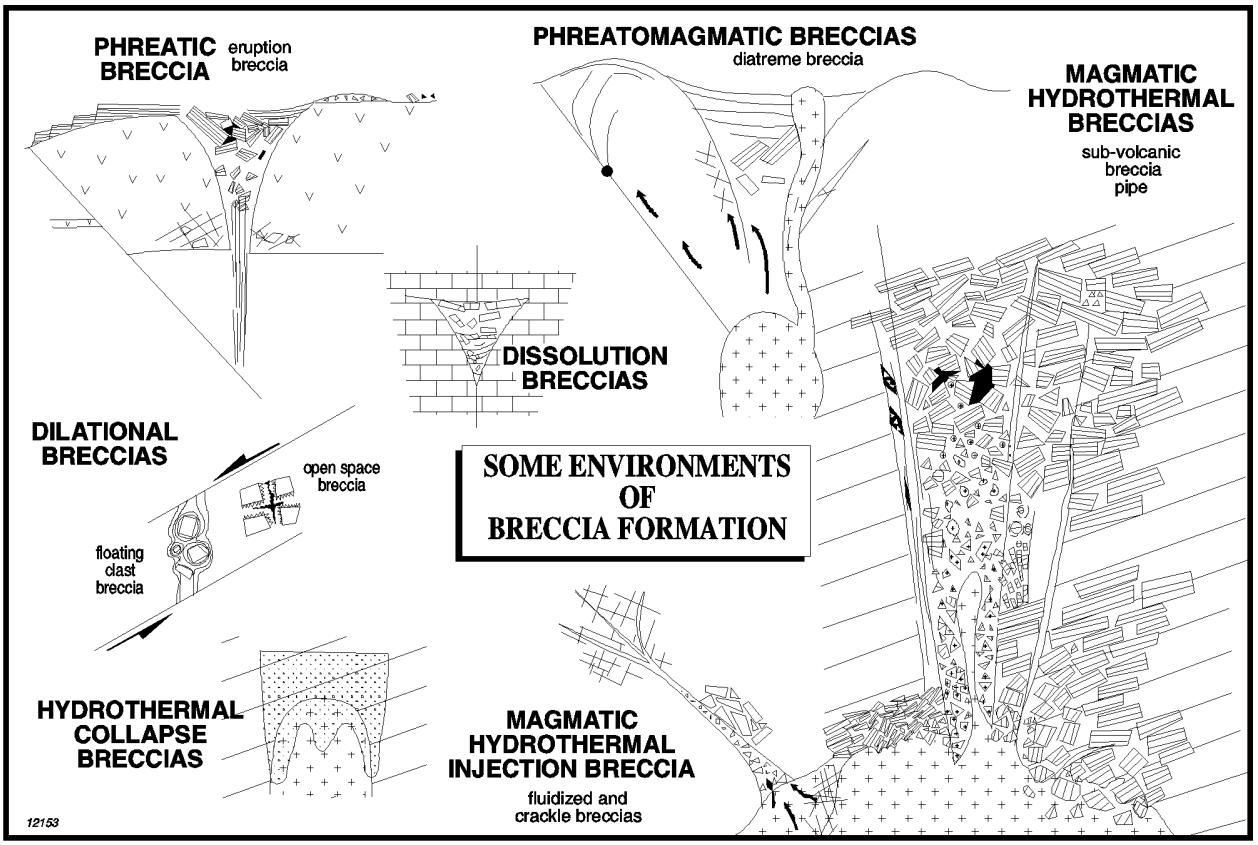

FIG. 3.17

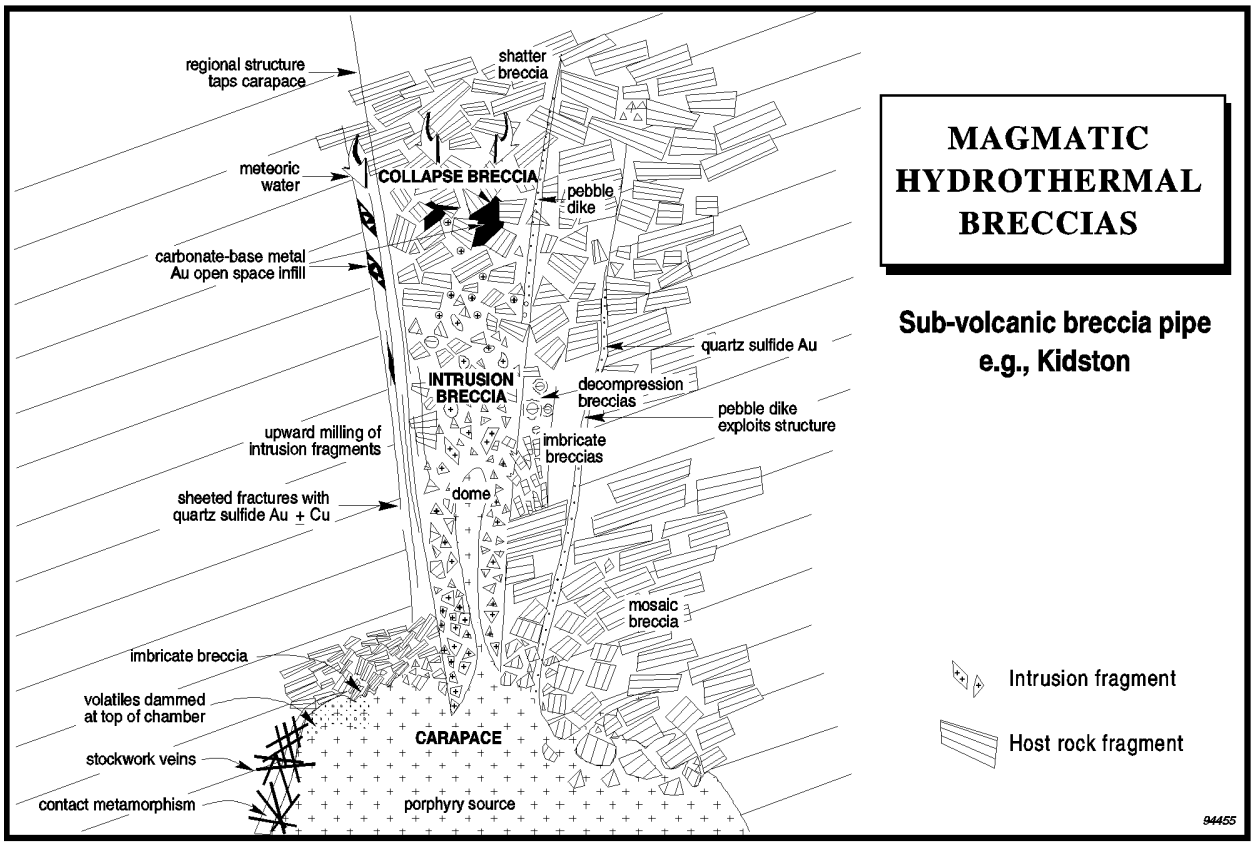

FIG. 3.18

Breccias within diatreme complexes are characterized by milled matrix fluidized breccias. These vary from well milled hetrolithic breccias comprising country rock and introduced porphyry fragments, typically in the most activated central regions of the diatreme pipe, to more angular country rock-rich monolithic breccias, typically towards the diatreme margins. Well rounded massive pyrite fragments, where present, are inferred to be indicative of an early magmatic volatile component. Most breccias are supported by a matrix of comminuted rock material and contain little open space.

Tuffisite rocks (Cloos, 1941, in Sillitoe, 1985) comprising well milled, rounded, intensely altered, bedded to massive, tuffaceous material, are characteristic of diatreme breccia bodies and may represent the dominant rock type. The tuffaceous character is derived from fragmented host and intrusion rock material, rather than eruption of fine grained volcanic material. Some fine grained tuffisites may contain well rounded fragments significantly larger than the host, either in massive or bedded units. Tuffisites are therefore distinguished as a class of strongly comminuted milled matrix fluidized breccias which are commonly massive, although locally bedded, and also occur as dike-like bodies (e.g., Mt Leyshon, eastern Australia; Paull et al., 1990; Orr, 1996). The tuffisite at Mt Leyshon forms as a late stage intrusive dike and provides permeability for the transport of gold-sphalerite-galena mineralization which is also deposited in adjacent open space breccias (Orr, 1996).

Milled matrix fluidized breccias, which display dyke-like forms, represent non-venting phreatomagmatic breccias. These exploit pre-existing structures and may occur adjacent to diatreme breccia complexes. Those at Busai, Woodlark Island (Corbett et al., 1994a), display a gradation from coarser angular fragments at depth to 'flinties' at higher levels, characterized by fine rock flour and chalcedonic silica. These are likened to the 'flinties', comprising chalcedony and pyrite which exploit cross structures and localize the bonanza gold mineralization at the Thames goldfield, New Zealand (Fraser, 1910; Section 7.iv.d.2). Here, nineteenth century miners prospected by following reefs until they intersected the flinties. Breccias at Woodlark Island provide ground preparation for later carbonate-base metal gold mineralization (Section 7.iii.i). Similar well milled breccias at Mt Kare, Papua New Guinea, previously mapped as conglomerates, also transport carbonate-base metal gold mineralization and so are well mineralized (G. Corbett, unpubl. report, 1996).

The distinction between tuff ring and vent facies may be useful when mapping diatreme breccia complexes, as mineralization is commonly localized at diatreme margins within competent fractured host rocks (Fig. 3.20; e.g, Acupan, Kerimenge). Tuff ring facies or tuff apron (Baker et al., 1986), comprises material ejected from the diatreme and deposited outside the actual vent, and is only preserved in systems which are poorly eroded. Various workers (Sillitoe, 1985; Baker et al., 1986; Cas and Wright, 1987) describe base surge deposits derived from the lateral movement of the rapidly expanding depressurised gas cloud venting from the eruptive centre. The resulting deposits may form thin laterally extensive layers containing exotic blocks and exhibit local low angle cross stratification. Finer grained tuffaceous (tuffisite) layers may contain accretionary lapilli developed as the gas cloud condenses and fine grained (mud) particles adhere to a nucleus, possibly a rock fragment. Reverse grading occurs as coarse accretionary lapilli are deposited within individual layers following heavier rock fragments. The recognition of accretionary lapilli has formerly been taken by many workers as evidence for a surficial origin for a particular facies of a diatreme breccia. However, similar features have been generated in subsurface settings in experimental conditions (McCallum, 1985). Accretionary lapilli are recognised in rocks formed in subsurface environments at Nena, Papua New Guinea (T. Leach and G. Corbett, pers. observation), Mount Leyshon, eastern Australia (I. Hodkinson, personal commun.), Porgera Zone VII (T. Leach and G. Corbett, pers. observation) and Tolukuma, Papua New Guinea (G. Corbett, pers. observation). Sillitoe (1985) also stresses that base surge deposits may collapse into diatremes (e.g., Cripple Creek, USA; Thompson et al., 1985).

Vent facies comprise the main pipe or funnel shaped body of the diatreme complex. The maar volcano represents the surficial portion of the vent and is commonly filled with lacustrine sediments. Vent facies diatreme breccias comprise introduced intrusion fragments, milled rock flour, tuffisite (as massive, bedded and dike-like

forms), rebrecciated breccias, and blocks (of tuff ring facies) which slide in from the sides (Fig. 3.20). Instances of considerable collapse are noted by McCallum (1985) and Sillitoe (1985) and include: shale fragments transported 1500 m down into the Mule Ear diatreme Utah (Stuart-Alexander et al., 1972), charcoal fragments occur 650 m below the present surface at the Balatoc diatreme at Baguio, Philippines (Sawkins et al., 1979), from which at least some 400 m has been eroded, and the base surge deposits at >300 m depth at Cripple Creek (Thompson et al., 1985). Well milled hard intrusion fragments reflecting considerable vertical transport may occur as components within breccias dominated by angular, softer, locally derived rocks. Fragment and matrix compositions reflect the host rock provenance and the intrusion from which the diatreme complex has evolved. The recognition of mineralized fragments within diatreme breccias may provide an indication of a target at depth (e.g., the diatreme breccias at Lepanto and the FSE porphyry, Philippines; Sillitoe, 1995c).

Endogenous domes are indicative of the flow dome association for diatreme breccias and typically form about diatreme margins (Fig. 3.21; e.g., Wau, Papua New Guinea; Sillitoe et al., 1984). Many are dismembered and vary to dikes and intrusion fragment-dominated breccias. The felsic, typically dacitic to rhyodacitic, compositions reflect the nature of the inferred source intrusion. Fragments derived from the source intrusion are an essential characteristic of diatreme breccias. Many of these display jagged and resorbed margins indicative of emplacement while molten.

Alteration derived from the hot gasses associated with the eruption of diatreme breccias is most commonly characterized as clay-pyrite alteration of the rock flour breccia matrix in low sulfidation systems. Disseminated fine grained euhedral pyrite is characteristic of diatreme breccias in these systems. Clays vary from higher temperature sericite at depth, through illite and smectite at highest levels, with local kaolinite in surficial acid sulfate alteration. Only diatreme breccias formed at depth and characterized by more competent sericite clays host mineralization in fractures or support open space breccias (e.g., Bulawan; G. Corbett, pers. observation: Montana Tunnels; Sillitoe et al., 1985). High sulfidation alteration may mask alteration derived during diatreme formation. In some high sulfidation systems diatreme breccias provide permeability for hot acidic magmatic fluids and so may be overprinted by intense alteration such as silicification (e.g., Wafi, Section 6.ii.b).

Mineralization follows the pre-mineral phreatomagmatic diatreme eruption which taps the top of the magma chamber at depth and fractures the country rocks overlying the intrusion and adjacent to the diatreme breccia. Ore-bearing fluids which evolve from the source magma as it cools and degasses, rise into the fractured overlying country rocks, and locally to the lower portion of the diatreme. The setting of diatreme-associated mineralization is in part governed by the level of erosion and structural environment. Diatremes formed at higher crustal levels are dominated by incompetent low temperature clay alteration which does not fracture well, and so these rocks tend to be poorly mineralized internally (e.g., Gold Ridge). In low sulfidation systems, diatremes eroded to deeper levels expose sericite clays which tend to fracture or support breccias, and are more proximal to the magmatic source. Thus, these diatreme systems may host fracture/disseminated gold mineralization (e.g., Montana Tunnels; Sillitoe et al., 1985: Bulawan; G. Corbett, pers. observation: Mt Rawdon, Brooker, 1991). Low sulfidation carbonate base-metal gold mineralization is most commonly associated with diatreme breccias, typically at elevated crustal levels within competent fractured country rocks about the diatreme margins, commonly at the intersection with throughgoing structures (e.g., Kerimenge; Figs. 7.28, 7.31). The GW breccia pipes which rim the Balatoc diatreme, Acupan, occur at the intersection of throughgoing vein systems and demonstrate an increased fluid flow along the diatreme margin (Damasco and de Guzman, 1977; Sawkins et al., 1979). High grade ore occurs close to the milled matrix fluidized breccias at Tolukuma (Section 7.iv.d.3). In high sulfidation gold and gold-copper deposits, mineralization may occur within the permeable diatreme rocks (e.g., Pueblo Viejo, Wafi) or at the fractured contact within competent host rocks, typically at the intersection of throughgoing structures (e.g., Lepanto, Wafi). Note two ore styles occur at Wafi (Section 6.iii.b).

Both high and low sulfidation gold-silver mineralization associated with diatreme breccia complexes or milled matrix fluidized breccias vary as:

* Banded fissure veins at Tolukuma (Section 7.iv.d.3, Corbett et al., 1994c); Wau (Sillitoe et al., 1984; Denwer, et al., 1995); and Edie Creek, (Section 7.iii.i; Lowenstein, 1982; Neale and Corbett, in prep).
* Breccia fill at diatreme contacts, in the GW breccias, Acupan (Damasco and de Guzman, 1977; Sawkins et al., 1979); and Lepanto (Section 6.iv.b, Garcia, 1991);
* Sheeted vein/breccias at Kerimenge (Section 7.iii.i, Hutton et al. 1990), or
* Disseminated within the diatreme at Montana Tunnels (Sillitoe et al., 1985), Gold Ridge (Section 7.iii.i; Fig. 7 in Sillitoe, 1989) and Bulawan, (G. Corbett, pers. observations), Mt Rawdon (Brooker, 1991).

3. Phreatic breccias

Phreatic (meaning water converted to steam) breccia systems occur as vapour-driven explosions at shallow crustal levels (Fig. 3.21), and are broadly equivalent to the hydrothermal explosion breccia of Baker et al. (1986), and eruption breccia of Nelson and Giles (1985), and Hedenquist and Henley (1985a). The term eruption breccia is preferred herein. Most workers (Phillips, 1973; Sillitoe, 1985; Nelson and Giles, 1985; Baker et al., 1986; Hedenquist and Henley, 1985a) provide a mechanism for brecciation based upon violent release following a build up of gas pressure, and suggest that these breccias are common within geothermal terrains. Their models mostly focus upon the development and later disruption of impermeable barriers of silica deposed by rapid cooling of upwelling fluids. Eruption will occur when the gas pressure beneath impermeable barriers exceeds the hydrostatic at that depth (Hedenquist and Henley, 1985). Reactivation of existing dilational structures which focus geothermal fluids during earthquakes (Section 3.iv) may also initiate eruption by fracturing the silicified cap to the overpressurised hydrothermal fluids (Sillitoe, 1985). Crack-seal brecciation featuring multiple and overprinting silica deposition within vein/breccias, formed at each eruption event, may develop in this manner.

Examples of phreatic or eruption breccias in the southwest Pacific are confined to young, poorly eroded terrains where surficial and near-surficial features are preserved. These include the active geothermal districts of the Taupo Volcanic Zone, New Zealand, and associations with adularia-sericite epithermal gold-silver mineralization are described more fully in Section 8.vii.a.2. Anomalous gold and other metals occur at eruption breccia vents at Champagne Pool, New Zealand (Hedenquist and Henley, 1985a), and the Beppu district (Austpac Gold; unpubl. report, 1987) and Osorezan, Japan (Section 8.vii.a.2; Aoki, 1991). Unmineralized eruption breccias at the Ladolam deposit Lihir Island, Papua New Guinea, probably relate to the recent geothermal activity, whereas the diatreme breccias are associated with earlier gold mineralization (Carmen, 1995; Fig. 7.5). Fossil geothermal terrains host gold-silver mineralization associated with eruption breccias (Section 8.vii): at the McLaughlin mine (Lehrman, 1986; Sherlock, et al., 1995) and other hot spring gold deposits (Nelson and Giles, 1985) in the western USA, Puhipuhi, New Zealand (White, 1986; Section 8.vii.a.2), the Yamada veins, Hishikari, Japan (Izawa et al., 1993; Section 8.vii.c.2), Toka Tindung, North Sulawesi (Wake et al., 1996) and the 309 anomaly, Twin Hills, eastern Australia (Section 8.viii.c.2).

Eruption craters or eruption breccia vents vary from tens to hundred of metres wide, by up to several hundreds of metres deep and commonly lie on regional structures (Fig. 3.21). Many craters act as outflows for typically neutral chloride fluids, which mix with cool surficial waters to promote the deposition of siliceous sinters (Fig. 8.1). Thus sinter fragments predominate in many eruption breccias (below). The Champagne Pool, New Zealand, eruption breccia vent is localized on fractures which display angular relationships to regional structures and are interpreted to have been dilated by regional transpression consistent with the tectonic setting (Fig. 8.2).

Eruption breccias vary from ejecta projected considerable distances from the vent, to in situ brecciation and introduce hydrothermal fluid matrix, much like hydrothermal injection breccias of magmatic origin (above). In the

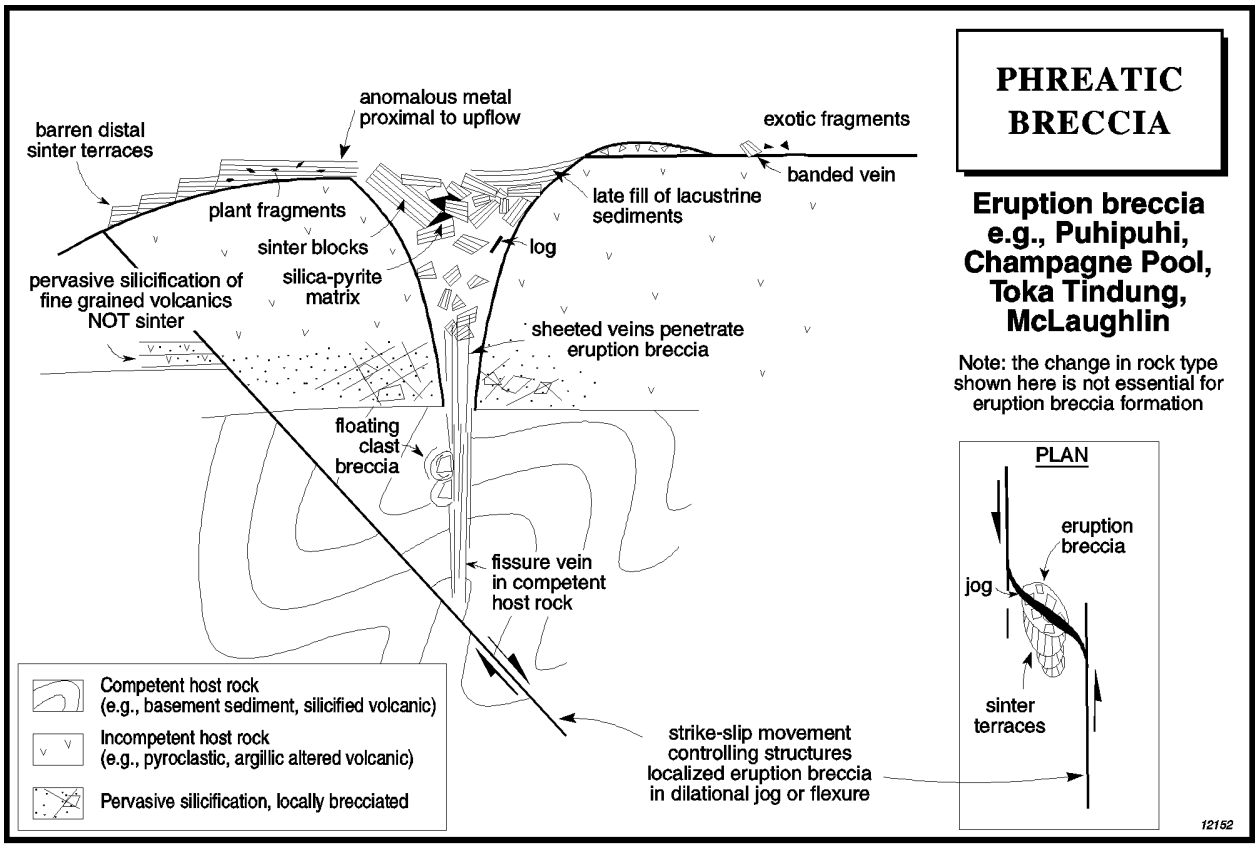

FIG. 3.21

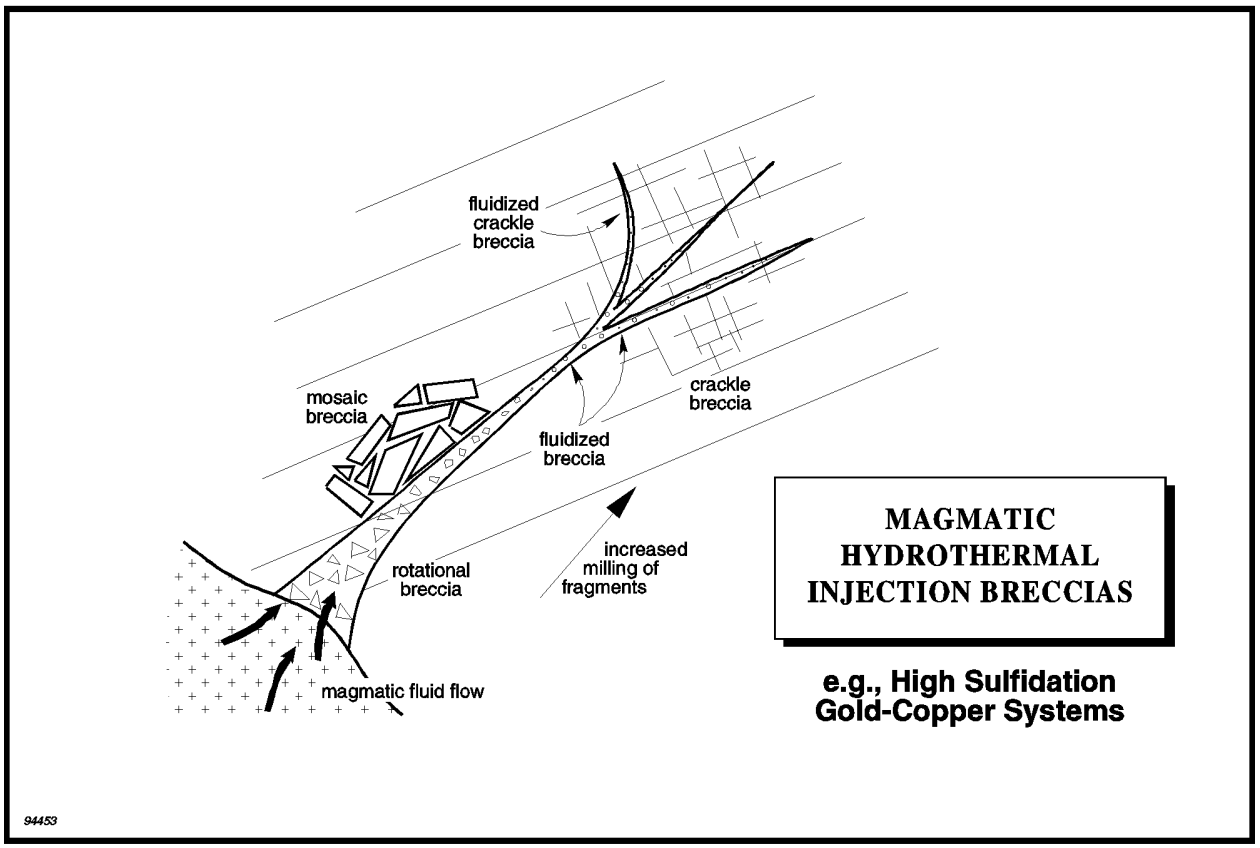

FIG. 3.22

former case, breccias tend to be massive, poorly sorted (vent breccias of Nelson and Giles, 1985, Fig. 1, A and B) and supported by a matrix of milled rock material (Hedenquist and Henley, 1985a). Hydrothermal injection breccias exhibit matrix of rock flour, silica and sulfides such as pyrite. Angularity is dependent upon the degree of milling during transport, and fragment styles are dominated by the rocks through which the eruption has passed. Rebrecciation is common, with increasing rounding of rebrecciated fragments. Although lacking the juvenile porphyry fragments which characterize diatreme breccia bodies, eruption breccias may host exotic and locally mineralized ejecta such as fragments of fissure veins formed in inferred feeder structures (e.g., Sappes, Greece; G. Corbett, pers. observation, 1996: Osorezan, Japan; Aoki, 1992). At Osorezan, Japan, where precipitates from recent drilling contain antimony, arsenic and mercury, eruption breccias contain ejected fragments of bladed stibnite and auriferous banded quartz (Aoki, 1992; Section 8.vii.a.2). Many more locally-derived breccias exhibit monolithic and angular fragments. Eruption breccias which form fluid outflows in settings of adularia-sericite gold-silver mineralization are characterized by a predominance of sinter fragments, lacustrine sediments and plant fragments (e.g., Puhipuhi, New Zealand; Toka Tindung, Indonesia; McLaughlin, USA; Section 8.vii.a.2).

Alteration in eruption breccias associated with low sulfidation adularia-sericite gold-silver mineralization characteristically occurs as a flooding of silica and varying degrees of fine grained, commonly massive, locally sooty pyrite. This silicification, which is most common in fluid outflows, contrasts with the clay and disseminated crystalline pyrite alteration in low sulfidation diatreme breccias. Near surface oxidation of SO_2-rich volatiles results in the formation of acid waters which promote collapsing advanced argillic and argillic (herein termed acid sulfate alteration), common in the vicinity of many eruption breccias (e.g., Osorezan, Champagne Pool; Section 8.vii.a.2). In high sulfidation systems eruption breccias provide permeable host rocks and so may display intense alteration grading outwards from silica to alunite and clay (Section 6).

Mineralization associated with eruption breccias is typically of the adularia-sericite epithermal gold-silver style, although high sulfidation styles also occur (e.g., Nansatsu deposits, Japan; Izawa and Cunningham, 1989). In the low sulfidation adularia-sericite systems, sinter deposits represent surficial fluid outflows which may occur some distance from the fluid upflow represented by the eruption breccia, and gold-silver mineralization predominates as banded fissure veins below the eruption breccias. The dilatant structures which localize the fluid upflow and eruption breccia therefore host mineralized fissure veins. Sinter deposits formed as fluid outflows may occur some distance from the eruption breccia. Anomalous As, Hg, Sb, W, Tl, Au, and Ag are recognised in proximal settings to eruption breccia vents, whereas sinter deposits further from the vent tend to be barren. The precipitate adjacent to Champagne Pool, New Zealand has yielded anomalous gold to 80 ppm and silver to 175 ppm (Weissberg, 1969) and eruption breccia-related sinter deposits from the Kinruyu Hot Spring, Beppu, Japan yielded; 0.47 ppm Au, <1 ppm Ag, 12.2 percent As, 1290 ppm Sb and 9990 ppm W (Austpac Gold, unpubl. data). The McLaughlin gold mine, USA (Tosdal et al., 1993) and Puhipuhi gold prospect, New Zealand (Brown, 1989; White, 1986) each have recorded histories of mercury production from sinter deposits adjacent to eruption breccia vents and have since undergone exploration for underlying gold mineralization, leading to production in the ease of McLaughlin (Section 8.vii.b).

Much of the gold mineralization mined at McLaughlin lies mostly within sheeted veins below the eruption breccia (Sherlock et al., 1995 and references therein). Similarly, the setting of the Yamada veins, Hishikari, Japan, immediately underlying the eruption breccia (Izawa et al., 1993), may have promoted downward movement of ground waters and mineral deposition by quenching (Section 8.vii.c). Vein mineralization is interpreted to also underlie eruption breccias at Osorezan, Japan (Aoki, 1992), from which fluid venting from diamond drill holes contained anomalous As Sb, Hg and W (Austpac Gold, unpubl. data; Aoki, 1992), and is subjacent to the eruption breccias at Toka Tindung, North Sulawesi (Wake et al., 1996; G. Corbett, unpubl. report, 1996; Section 8.vii.a). Here, drill testing of an adularia-sericite epithermal vein system has recently yielded best gold grades closest to the eruption breccia (Aurora Gold, press release).

4. Dilational breccias

Dilational breccias are described above as a genetic group of breccias in which dilational structural environments create open space which is commonly filled by hydrothermal minerals (Fig. 3.17). Typical settings might include fissure or sheeted fracture systems formed in association with strike-slip structures during oblique convergence (Sections 3.iv.b, 3.vi; Figs. 3.8, 3.13). Although hosts to hydrothermal mineralization, these breccias form by tectonic processes. Hydrothermal fluids enter the breccia during brecciation as part of the activation of the dilatant structure (Section 3.iv.b), and so fragments may be entirely supported by a matrix of hydrothermal minerals.

A colloform/crustiform banded breccia matrix may indicate repeated fracture opening and filling by silica as the hydrothermal fluid is cooled rapidly (quenched), whereas slower cooling will result in banded crystalline breccia matrix. Note that in the colloform banded breccias, opening must have been relatively uniform for the banding between each fragment to continue to expand. Rebrecciation and cross-cutting breccia matrix minerals, formed by reactivation of the dilational environment, are characteristic of dilatant breccias which commonly form in fissure veins. The dilatant structural environment, rather than only not fluid pressure, is inferred to promote brecciation. Sibson (1992) utilises the term floating clast breccia to delineate a class of dilational breccias formed in adularia-sericite epithermal vein systems, in which colloform mineral banding rims fragments, commonly at the margins of fissure veins (G. Corbett, pers. observations). Here, the banding is locally not oriented in the overall trend of the fissure vein.
Sub-surface sedimentary structures form in some dilatant breccia environments, by the filling of open space in a fissure, with collapsing rock fragments, much like stope fill in an underground mine. These may contain layers of broken rock fragments, quenched hydrothermal minerals, cooled suddenly in the open space, or locally accretionary lapilli. Mosaic and jigsaw breccias (below) may also form by dilational processes as hydrothermal minerals fill dilatant open space.

5. Magmatic hydrothermal injection breccias

These breccias comprise host rock fragments set in a matrix of essentially magmatic hydrothermal fluid and rock flour derived from comminuted fragments. The terminology for hydrothermal breccias parallels with the term hydraulic breccia used in the literature to describe breccias formed by breaking under the influence of pressurised hydrothermal fluids. Many of these breccias form in dilational structural environments derived by movement on controlling structures (Section 3.iv), and so display transitional relationships to the dilational breccias. Tectonic faulting assists fluid pressures in fracturing host rocks and the creation of open space which becomes filled by hydrothermal minerals. Thus structural processes promote brecciation formerly attributed to only a build up of fluid pressures. Magmatic hydrothermal injection breccia styles may vary according to the degree of fluid input and therefore, if mineralized, there is a proportional relationship between matrix content and metal grades (Figs. 3.20, 6.2: e.g., Mt Kasi, Fiji; Corbett and Taylor, 1994; Fig. 6.17).

These breccias are classified as:
Rotational breccias which are characterized by substantial fragment rotation or transport in association with considerable fluid injection, and display the highest metal grades. These pass with smaller quantities of injected fluid to mosaic or jigsaw breccias, characterized by fragments which are separated but have not undergone substantial transport. Rock fragments in these breccias may be joined back together by removal of the matrix component. Fluidized breccias are distinguished on small scales as containing milled fragments in a transported and exotic matrix, and commonly exploit fractures, to form dike-like bodies. These may transport considerable mineralization in some ore systems (e.g., Ladolam, Lihir Island, and Nena at Frieda River Copper, in Papua New Guinea). Where only minor matrix introduction is recognised within fractures, then mosaic-like crackle breccias are recognised (also termed hydraulic breccias). Many slab breccias described above form as elongate crackle breccias. If crackle breccias are opened and exploited by fluid flow, then a fluidized crackle breccia may result.

Thus a pattern emerges where copper-gold grades may be directly proportional to matrix content in breccias, which change with increasing distance from the magmatic source from; rotational --> mosaic (jigsaw) --> fluidized --> fluidized crackle --> crackle breccias (Fig. 3.22). Mapping zones of breccia types may point towards higher grade ores or magmatic source rocks, particularly in high sulfidation copper-gold systems (Fig. 6.2).

6. Hydrothermal collapse breccias

Hydrothermal collapse breccias are herein defined as forming during the retrograde phases of porphyry copper development. Magmatic vapours rise above the porphyry environment, condense, and mix with ground waters to collapse as low pH fluids (Section 5.i.c.2). Pressure draw down during the waning stages of cooling porphyry may assist in the fluid collapse. The resulting overprinting phyllic to argillic alteration forms clay matrix breccias in which sericite and clays grade from fractures or crackle breccias into the host rock, typically adjacent to structures. Remnants of original rock type remain as breccia fragments, characterized by hypogene alteration in a matrix of retrograde alteration minerals.

Where undeformed, breccia fragments remain in the original position and generally display no rotation. Fluids commonly migrate down feeder structures which, having formed as zones of incompetent clay alteration, may be reactivated during later faulting. Many clay matrix breccias grade to shear zones in which fragments may display progressively more intense rotation, and locally alteration or milling grading towards areas of high strain.

7. Dissolution breccias

These breccias form in limestone and other carbonate rocks by the removal of carbonate (typically calcite) and subsequent collapse, and may therefore be related to slump and karst development (Fig. 3.17). Dolomitization of calcite in sediment hosted replacement gold deposits is categorized by a volume decrease, and so promotes collapse (Section 7.v). Dissolution breccias feature remnant carbonaceous material remaining after dissolution of carbonate. Large cavities are commonly filled by detritus containing sedimentary structures formed in subsurface settings. In these environments, eruption breccias may result from depressurisation of hydrothermal fluids upon entering open space, and phreatomagmatic breccias by the contact of high level intrusions with water-filled cavities.

ix) Conclusion

Pacific rim gold-copper systems require fractured rocks to provide open space for the flow of magmatic mineralized fluids.
Intrusions sources for of copper-gold mineralization are localized by major structures, and continued movement on these structures may create ore-hosting subsidiary fractures. Major and subsidiary structures may be considered in terms of the style of convergence and demonstrate recognisable patterns. Differing styles of fractured host rocks may be modelled by comparisons with: active fault systems, experimental data, and field observations. Repeated activation of existing structures is common in many ore systems. Different breccia styles are classified according to features such as crustal level, relationship to magma source, and tectonic environment. There are broad relationships between some breccia and mineralization styles. Careful study of field relationships may point towards the better mineralized portions of hydrothermal systems and the best orientation for drill testing.

4 CONTROLS ON HYDROTHERMAL ALTERATION AND MINERALIZATION

i) Introduction

A large number of variables influence the formation of alteration minerals in hydrothermal systems. These are grouped into seven main categories (Browne, 1978):

1. Temperature
2. Fluid chemistry
3. Concentrations
4. Host rock composition
5. Kinetics of reactions
6. Duration of activity or degree of equilibrium.
7. Permeability

Although these are all more or less interdependent, temperature and fluid chemistry probably have the strongest influence on the styles of hydrothermal alteration developed in Pacific rim porphyry-related copper-gold systems.

Increasing temperature favours the stability of progressively more dehydrated mineral species. This is especially evident in clay/sheet silicate mineralogy in which progressively higher temperatures result in the formation of the mineral sequence: smectite --> interlayered smectite-illite (with gradually decreasing smectite content) --> illite --> white mica. Similarly, zeolites become more dehydrated under hotter conditions, as illustrated by the sequence clinoptilolite --> mordenite --> stilbite --> laumontite --> wairakite.

Temperature also influences the degree of ordering or crystallinity of minerals. Higher temperatures favour the formation of more crystalline minerals. Disordered kaolinite and halloysite, for instance, form under ambient conditions, whereas more ordered kaolinite occurs under elevated hydrothermal temperatures, and well crystalline dickite develops under still hotter conditions.

It can be seen from activity diagrams that fluid composition also has a strong influence on the alteration mineralogy, whereas temperature has a marked influence on the actual position of phase boundaries. The ratios of constituents e.g., $a_{Na}+/a_{H}+$, $a_{K}+/a_{H}+$ are more important than absolute concentrations. For example, in active hydrothermal systems, highly saline brines of the Salton Sea geothermal field (approximately 250,000 ppm total dissolved solids) produce the same alteration assemblages at most temperature ranges as the very dilute fluids (around 3,000 ppm total dissolved solids) of New Zealand, and some Icelandic geothermal fields (Weissberg et al., 1979).

Absolute concentrations of components in hydrothermal fluids have some effect on the nature of the alteration minerals produced, as this influences the degree of saturation of the fluid with respect to certain minerals. For example, sulfur, sulfides, and/or sulfates are associated with solfataras, and lepidolite is encountered in the Yellowstone geothermal fields where fluids have high concentrations of lithium (Browne, 1978).

The host rock composition to some extent controls the alteration mineral assemblages. Skarn mineralogy forms in calcareous host rocks. The secondary K-feldspar mineral adularia is preferentially encountered where host and/or source rocks are potassium-rich (e.g., rhyolite or shoshonite). Paragonite (Na-mica) under certain conditions forms as an alteration product of albite, whereas muscovite forms from altered potassium feldspars.

The kinetics or rates of alteration/mineral deposition more commonly affect the crystallinity of the minerals rather than the species formed. Amorphous silica can form at moderately high temperatures where silica-saturated

fluids are quenched (e.g., geothermal surface pipework), whereas coarse crystalline quartz forms at the same temperature but under static conditions, which permit slow crystal growth.

The duration of the hydrothermal system, or the period during which permeability has remained open, determines whether equilibrium has been established between the circulating fluid and host rocks. Minerals may form under metastable conditions if equilibrium has not been attained.

Permeability, commonly as dilational fracture systems (Section 3) and locally as permeable lithologies, brings the host rock into contact with hydrothermal fluids. Phyllic and argillic alteration are commonly encountered immediately adjacent to major structures or vein systems where the fluids are at less than neutral pH; whereas propylitic alteration is usually encountered in host rocks in conditions of decreased permeability further from the main fluid channelway.

ii) Temperature and pH Controls to Alteration Mineralogy

Temperature and fluid pH are the most important of the many factors which influence the mineralogy of hydrothermal systems. Under saturated, hot, hydrostatic conditions, pressure is directly related to temperature (Browne, 1978), whereas the gas pressure and the ratios of elemental concentrations are reflected in the fluid pH (Henley et al., 1984). The other variables (with the local exception of perhaps host rock composition and absolute fluid compositions) have only minor influence on alteration mineralogy.

The stability ranges for the common hydrothermal minerals encountered in Pacific rim active geothermal and hydrothermal ore systems, are plotted in terms of temperature and fluid pH in Figure 4.1. This figure is derived from a compilation of data from geothermal systems in the Philippines, Japan, USA, Iceland, and New Zealand, in combination with thermodynamic and laboratory experimental work on various mineral phases. The main references for this data are Steiner (1977), Browne (1978), Hemley et al. (1980), Elders et al. (1979), Leach et al. (1985) and Reyes (1990b).

Fluid element concentrations and ratios, and pressures (partial pressure of gases, hydrostatic and lithologic pressures) are constant in Figure 4.1. However, in many cases these factors can substantially effect the temperature and pH stability ranges of the various mineral phases (Henley et al., 1984). Discussions of variations in these factors, which would add further axes to this diagram, is beyond the scope of this review. Absolute temperature and pH values are not shown in Figure 4.1 because of the influence other factors (above) could have upon the positions of the boundaries between mineral phases. In addition, it is more important in mineral exploration to determine, from alteration mapping, the relative, rather than absolute changes, in fluid conditions. The following discussions include the approximate temperature and pH ranges for most of these mineral phases. Different mineral groups categorized by increasing pH of formation on Figure 4.1 are:

a) Silica group minerals

Silica minerals are the only significant stable alteration minerals to occur at very low fluid pH (generally below pH 2, Stoffregen, 1987), where they are commonly associated with small quantities of titanium-iron phases such as rutile. Under these extremely acid conditions, opaline silica, cristobalite, and tridymite are encountered within surficial environments above the upper level of the chloride hydrothermal system, typically at temperatures of <100°C (Leach et al., 1985). Quartz is the main silica mineral at high temperatures. In Figure 4.1, quartz or silica (cristobalite, tridymite or amorphous silica) has been included in all mineral assemblages because hydrothermal fluids (in active geothermal systems) are most commonly saturated with respect to SiO_2 (Henley et al., 1984).

Under higher fluid pH conditions, amorphous silica is encountered at temperatures <100°C. Quartz is almost present at higher temperatures, whereas chalcedony locally occurs at intermediate temperatures (generally in the range of 100-200°C), especially under conditions of rapid deposition. The type of silica phase is also effected by the kinetics of deposition. For example, amorphous silica may form at temperatures up to 200°C in rapidly quenched environments (e.g., scales in geothermal surface pipeworks; Brown, 1986).

b) Alunite group minerals

At fluid pH slightly higher than 2, alunite forms together with the silica minerals over a wide temperature range (Stoffregen, 1987). It occurs in association with andalusite at high temperatures (typically >350-400°C; Sverjensky et al., 1991), and with corundum at still higher temperatures (>400-450°C; Hemley et al., 1980).

The following four environments of alunite formation have been identified by Rye et al., (1992), using sulfur and oxygen isotope data. The conditions of formation of alunite in these environments can also be inferred from its crystal form, as well as from the geological setting and mineral paragenesis.

1. Steam-heated alunite develops under surficial environments by the oxidation of acid sulfate fluids from H_2S gas which evolved from a boiling hydrothermal system at depth. Alunite deposited from these low pH steam-heated waters commonly occurs as very fine-grained pseudo-cubic crystals. This steam-heated alunite may be encountered down to 1-1.5 km depths, in settings where acid sulfate fluids descend into waning hydrothermal systems (Reyes, 1990b).

2. Supergene alunite develops from the production of sulfuric acid by weathering of massive sulfide deposits and exhibits a poorly crystalline, very fine pseudo-acicular habit.

3. Magmatic alunite is derived from magmatic-dominated liquids and forms well crystallized, commonly coarse-grained tabular to lath-like crystals which fill fractures, cement breccias, and deposit in leached vughs pseudomorphing phenocrysts or lithic clasts. Alunite formed at higher temperatures, where it is intergrown with well crystalline muscovite and/or andalusite, can also occur as large irregular crystals poikilitically enclosing quartz and other phases, or as euhedral pseudo-rhombic crystals.

4. Magmatic vein/breccia alunite occurs in veins and breccias and is inferred to have been deposited directly from volatile-rich fluids which are ascending from a crystallising melt (Rye et al., 1992). In this environment alunite can occur as radiating prismatic crystals.

c) Kaolin group minerals

The kaolin group of minerals (Fig. 4.1) are derived from moderately low pH fluids (approximately pH 4; Reyes, 1990b), and co-exist with the alunite group of minerals under a transitional fluid pH range (pH 3-4; Stoffregen, 1987). Halloysite occurs mainly as a supergene weathering product, although there is some evidence (Harvey and Browne, 1991) that halloysite forms under very low temperature hydrothermal conditions. Zonations of hydrothermal kaolin group minerals with increasing depth and temperature have been identified in Philippine geothermal systems by Reyes (1990b) and Leach et al. (1985). Kaolinite is formed at shallow depths under low temperature conditions (<150-200°C), and pyrophyllite forms at greater crustal depths, under higher temperature conditions (<200-250°C). Dickite forms in a transitional setting between these two crustal levels and temperature ranges.

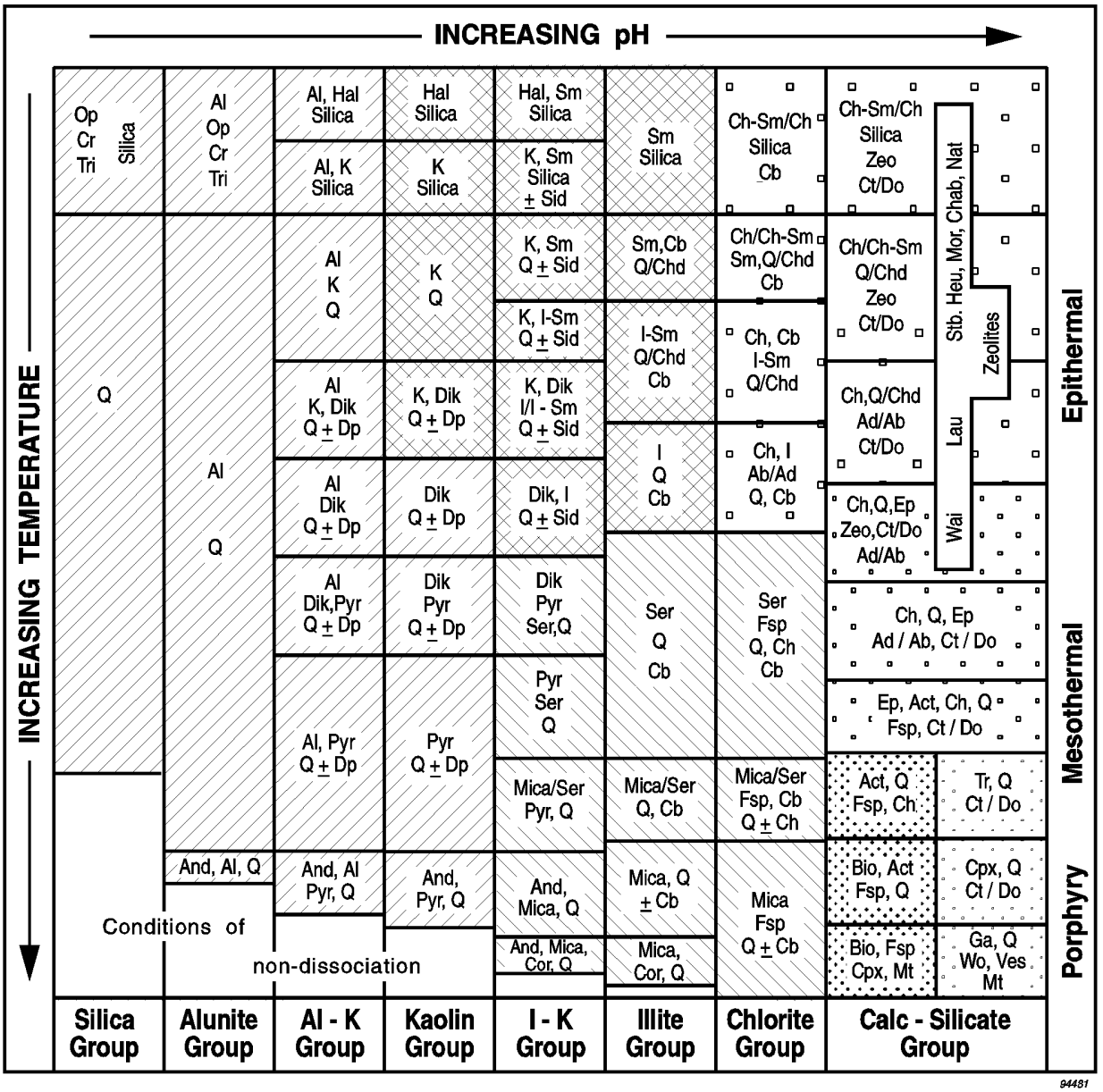

Mineral Abbreviations :

Ab - albite; Act - actinolite; Ad - adularia; Al - alunite; And - andalusite; Bio - biotite; Cb - carbonate (Ca, Mg, Mn, Fe); Ch - chlorite; Chab - chabazite; Chd - chalcedony; Ch-Sm - chlorite-smectite; Cor - corundum; Cpx - clinopyroxene; Cr - cristobalite; Ct - calcite; Do - dolomite; Dik - dickite; Dp - diaspore; Ep - epidote; Fsp - feldspar; Ga - garnet; Hal - halloysite; Heu - heulandite; I - illite; I-Sm - illite-smectite; K - kaolinite; Lau - laumontite; Mt - magnetite; Mor - mordenite; Nat - natrolite; Op - opaline silica; Pyr - pyrophyllite; Q - quartz; Ser - sericite; Sid - siderite; Sm - smectite; Stb - stilbite; Tr - tremolite; Tri - tridymite; Ves - vesuvianite; Wai - wairakite; Wo - wollastonite; Zeo - zeolite

Potassic
Propylitic
Outer / Sub Propylitic
Skarn
Argillic
Advanced Argillic
Phyllic

Common Alteration Mineralogy in Hydrothermal Systems

FIG. 4.1

Diaspore is locally encountered with alunite and/or kaolinite group phases, commonly in zones of intense silicification, where it forms at the expense of pyrophyllite by the reaction:

quartz + diaspore <--> pyrophyllite (Hemley et al., 1980).

d) Illite group minerals

Where the fluids are at a fluid pH in the range of 4-6, the illitic group of minerals dominate (Fig. 4.1), and co-exist with the kaolin group minerals at fluid pH 4-5, depending on the temperature and fluid salinity (Hemley et al., 1980; Reyes 1990b). Depth/temperature relationships of the illite group minerals are well documented from both sedimentary basins and active geothermal systems (Steiner, 1977; Browne, 1991; Harvey and Browne, 1991). Smectite occurs at low temperatures (<100-150°C), interlayered illite-smectite at around 100-200°C, illite at approximately 200-250°C, and muscovite at >250°C. Sericite is a fine grained muscovite which may contain some illite, and is encountered at levels which are transitional between illite and coarser well crystalline muscovite (e.g., Frieda River porphyry copper deposit, Papua New Guinea; Britten, 1981).

The smectite content within the interlayered illite-smectite clays progressively decreases with increasing temperature over the 100-200°C range (Harvey and Browne, 1991). The crystallinity of illite and sericite increases with increasing temperature, and can be monitored by XRD analyses of the peak width, at half the peak height, of the {001} reflection, (i.e., the Kubler Index; Dunoyer de Segonzac, 1968). The changes in muscovite crystallinity can also be monitored by XRD analyses. With increasing temperature there is a progressive change from a disordered 1M mica to a well crystallized 2M muscovite. Although muscovite is the common mica mineral present in copper-gold hydrothermal systems, the sodic mineral phase paragonite is encountered in some systems where the host rock has a high Na:K ratio (e.g., albite as the plagioclase mineral). The vanadium mica roscoelite, and the chromium mica fuchsite, are also locally common and are deposited from fluids sourced by migration through mafic volcanic rocks/intrusions.

e) Chlorite group minerals

Under slightly acid to near neutral pH conditions, chlorite-carbonate (Fig. 4.1) minerals become dominant, coexisting with illite group minerals in environments where fluid pH is 5-6 (Leach and Muchemi, 1987). Interlayered chlorite-smectite occurs at low temperatures, grading to chlorite at higher temperatures (Kristmannsdotter, 1984). In active geothermal systems, this transition occurs at significantly lower temperatures in rift environments (e.g., Iceland, Kristmannsdotter, 1984) than in volcanic island terrains (e.g., Philippines, Reyes, 1990a), and possibly reflects a response to either fluid or host rock chemistry.

f) Calc-silicate group minerals

The calc-silicate group of minerals (Fig. 4.1) form under neutral to alkaline pH conditions. Zeolites-chlorite-carbonate are formed under cool conditions, and epidote, followed by secondary amphiboles (mainly actinolite) progressively develop at higher temperatures. Zeolite minerals are particularly temperature sensitive. Hydrous zeolites (natrolite, chabazite, mesolite, mordenite, stilbite, heulandite) predominate under cool conditions (<150-200°C), while less hydrated zeolites such as laumontite (150-200°C), and wairakite (200-300°C) occur at progressively deeper and hotter levels in the hydrothermal system (Steiner, 1977; Leach et al., 1983). In some systems prehnite and/or pumpellyite are encountered at temperatures of around 250-300°C (Elders et al., 1979) in association with, or in some instances in place of, epidote.

Epidote occurs as poorly crystalline incipient grains at temperatures of around 180-220°C, and as well crystalline phases at higher temperatures (>220-250°C; Reyes, 1990b). Secondary amphiboles (mainly actinolite) appear to be stable in active hydrothermal systems at temperatures >280-300°C (Browne, 1978). Biotite predominates within, or immediately adjacent to, porphyry intrusions. In active systems secondary biotite develops at

temperatures of >300-325°C (Elders et al., 1979). Active porphyry environments are characterized by clinopyroxene (>300°C) and garnet (>325-350°C) assemblages (Elders et al., 1979). However, hydrated garnets are locally encountered at significantly lower temperatures (250-300°C) in the Tongonan geothermal field (Leach et al., 1983). The zonations in skarn mineralogy with respect to temperature are in many ways comparable to those in porphyry copper environments, and are discussed in more detail in Section 5.ii.

g) Other minerals

Carbonate minerals are encountered over a wide range of pH and temperatures, and are associated with kaolin, illite, chlorite and calc-silicate phases. A zonation in carbonate species with increasing fluid pH is encountered in many hydrothermal systems (Leach and Corbett, 1993, 1994, 1995). Fe-Mn carbonates (siderite-rhodochrosite) coexist with kaolin and illitic clays, while mixed Ca-Mn-Mg-Fe carbonates (rhodochrosite-ankerite-kutnahorite-dolomite) occur with illitic and chloritic clays, and Ca-Mg carbonates (dolomite-calcite) coexist with chlorite-calc-silicate mineralogy. This zonation is interpreted to reflect the decreasing mobility of Fe, Mn and Mg at progressively increasing fluid pH (Leach et al., 1985). Carbonate minerals typically extend throughout all levels in hydrothermal systems, from surficial to porphyry-related skarn environments.

Feldspar minerals are associated with both chlorite and calc-silicate mineral phases. Secondary feldspars are generally stable under near neutral to alkaline pH conditions. Albite occurs where fluids have a high aNa+/aK+ ratio and potassium feldspar a low aNa+/aK+ ratio (Browne, 1978). Adularia occurs as a low temperature secondary potassium feldspar species, whereas orthoclase is encountered at high temperatures within the porphyry environment. Browne (1978) demonstrated that adularia preferentially occurs within high fluid flow permeable conditions, and albite under low permeability conditions.

Sulfate minerals are encountered over most temperature and pH ranges in hydrothermal systems. Whereas alunite forms under low pH (<3-4) conditions, anhydrite forms at a higher pH (Reyes, 1985) and temperatures greater than 100-150°C, and gypsum develops in cooler environments (Harvey et al., 1983). Although jarosite commonly forms as a weathering product of sulfides, it also occurs at shallow levels in acid environments in some Philippine active geothermal systems (Leach et al., 1985).

Various hydrothermal mineral phases contain halogen elements (e.g., boron in tourmaline; and fluorine, chlorine and phosphorous in apatite), which is inferred to indicate that the fluids contain a significant component of magmatic volatiles. These phases are commonly associated with sericite/mica formed at high temperature under moderately low pH conditions.

iii) Alteration Zones Associated with Ore Systems

Although it is considered preferable to use the alteration mineral assemblages themselves to define the style of alteration, a classification of broad alteration types can be beneficial in describing overall characteristics of zoned alteration systems. Alteration styles in most alumino-silicate rocks have been classified by Meyer and Hemley (1967) as: propylitic, intermediate argillic, advanced argillic, sericitic, and potassic types. Rose and Bart (1979) indicate that the sericitic type is identical to the phyllic alteration of Lowell and Guilbert (1970). The term argillic, which is now in common use, is synonymous with intermediate argillic.

The mineral assemblages within these five alteration zones are shown in Figure 4.1 and may be summarised as:

Advanced argillic alteration comprises mineral phases which are formed under low pH (≤4) conditions (i.e., silica and alunite group minerals) in addition to assemblages which contain both alunite and kaolinite group minerals. Meyer and Hemley (1967) include high temperature kaolin group phases (i.e., dickite and pyrophyllite without alunite group minerals) in advanced argillic alteration, and this convention has been followed in Figure 4.1.

Argillic (intermediate argillic) alteration assemblages consist of those formed at relatively low temperatures (> 200-250°C) and moderately low fluid pH (approx. 4-5). Rose and Bart (1979) defined this type of alteration as encompassing those assemblages dominated by kaolinite and smectite. However in Figure 4.1, other low temperature kaolin (halloysite) and illite (interlayered illite-smectite, illite) group minerals, which are not included in phyllic/sericitic zones, are placed within the argillic type of alteration. The argillic alteration assemblage may also contain chlorite group minerals subordinate to the illite group minerals.

Phyllic alteration forms at similar pH ranges to the argillic alteration minerals, but higher temperatures (>200-250°C), and is characterized by the presence of sericite (or muscovite). The phyllic zone can also include higher temperature members of the kaolin (pyrophyllite-andalusite) and chlorite group minerals where they are subordinate to sericite/muscovite.

Propylitic alteration forms under near neutral to alkaline conditions characterized by the presence of epidote and/or chlorite (Meyer and Hemley, 1967). At relatively low temperatures (<200-250°C), where alteration assemblages are dominated by zeolites in place of epidote, the term sub-propylitic may be applied. The occurrence of secondary amphiboles (generally actinolite) at high temperatures (>280-300°C) may be used to characterize an inner-propylitic alteration zone. Secondary albite and/or K-feldspars are commonly encountered in propylitic alteration assemblages.

Potassic alteration forms at high temperature, under neutral to alkaline conditions and is characterized by biotite and/or K-feldspar + magnetite ± actinolite ± clinopyroxene. Where the host rock is a calcareous sediment, skarn mineralogy forms under similar conditions, and consists of zoned calc-silicate minerals such as Ca-garnet, clinopyroxene, and tremolite.

iv) Controls on the Deposition of Gangue Mineral Phases

The main non-ore or gangue components, which are deposited directly from solution in ore-forming systems, are silica minerals (predominantly quartz) and carbonate minerals, with local abundances of sulfate mineral species. The following sections outline the main factors which control the deposition (and dissolution) of these mineral phases in hydrothermal systems.

a) Silica minerals

Temperature is the major control on the deposition of silica mineral species, however subordinate factors include pressure, salinities, pH, kinetics of deposition, and complexing agents (Fournier, 1985a). In dilute, epithermal to mesothermal environments (i.e., <300-350°C) quartz will deposit upon cooling, with maximum solubility occurring around 350°C (Fig. 4.2). Therefore, rapid quenching of high temperature fluids in the upper regions of a fluid upflow conduit will produce a silica cap to that system. Between 300-350°C, decreases in pressure and salinity have a moderate influence on quartz deposition; whereas below 300°C, these effects are minor, except under rapidly changing conditions.

At shallow levels in an epithermal system (<100-150°C) the various silica minerals deposited include: amorphous silica, cristobalite, tridymite, chalcedony and quartz. Although quartz is the least soluble of all the mineral phases, the rates of temperature change control the mineral species formed (Saunders, 1994). For example, amorphous silica is deposited as silica sinters under rapidly cooling conditions, where boiling hydrothermal fluids at <200°C rapidly cool to less than 100°C in surficial environments. Cristobalite and

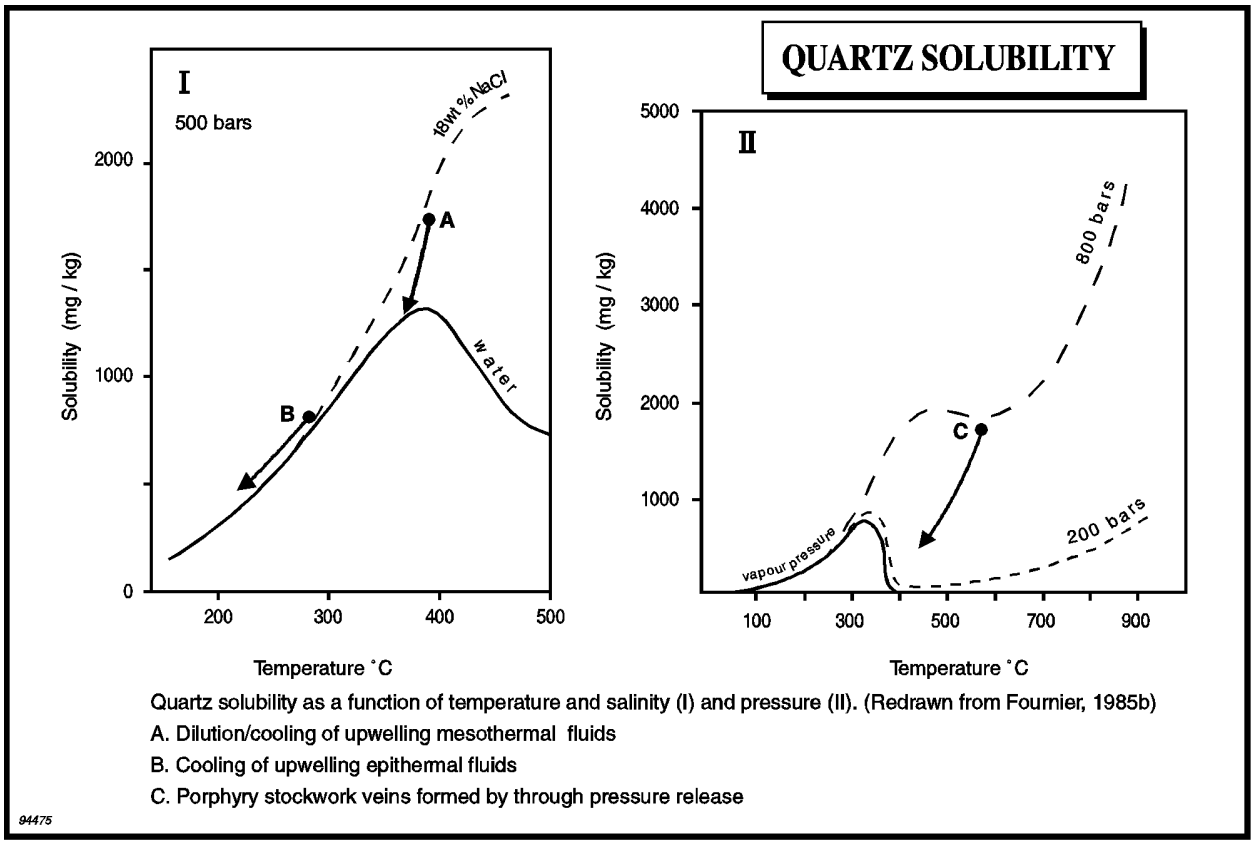

Quartz solubility as a function of temperature and salinity (I) and pressure (II). (Redrawn from Fournier, 1985b)
A. Dilution/cooling of upwelling mesothermal fluids
B. Cooling of upwelling epithermal fluids
C. Porphyry stockwork veins formed by through pressure release

FIG. 4.2

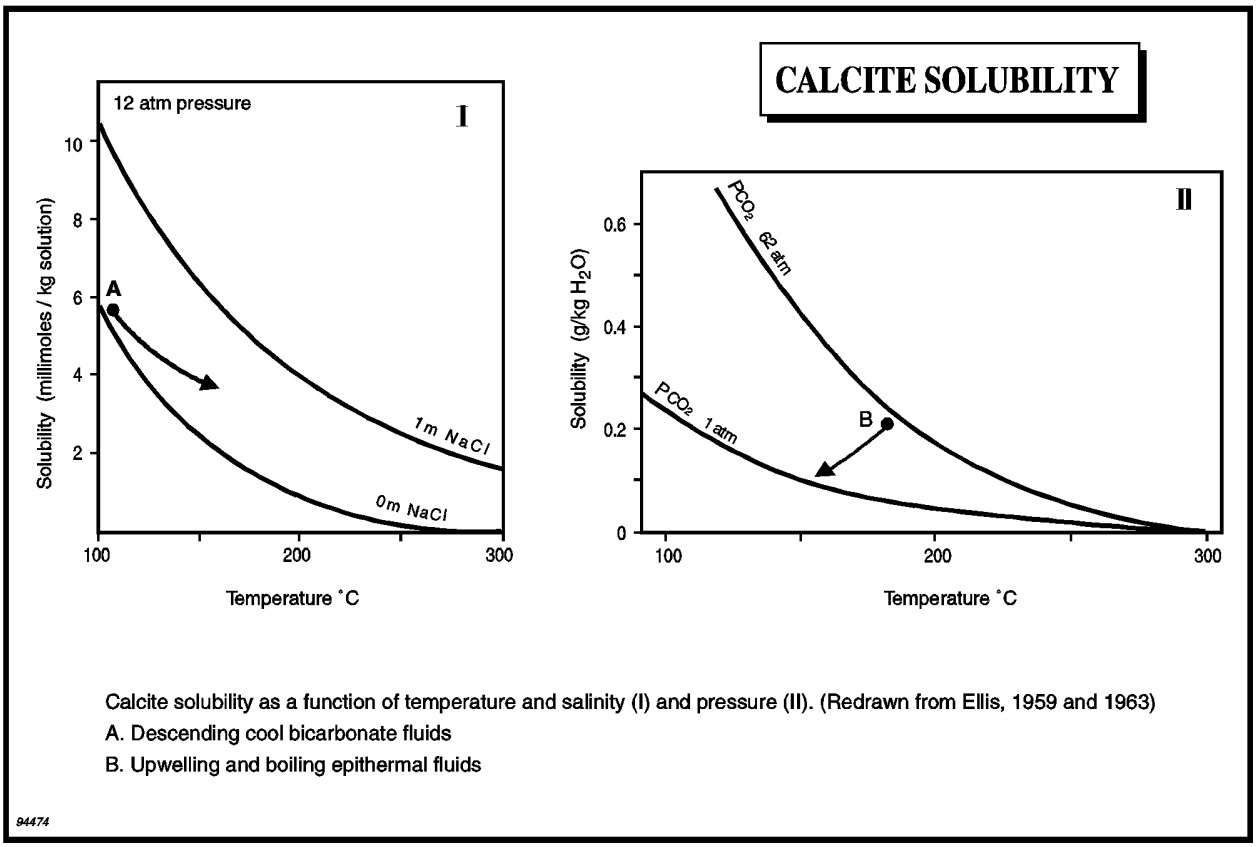

Calcite solubility as a function of temperature and salinity (I) and pressure (II). (Redrawn from Ellis, 1959 and 1963)
A. Descending cool bicarbonate fluids
B. Upwelling and boiling epithermal fluids

FIG. 4.3

chalcedony form under progressively slower cooling environments. The other silica minerals recrystallize to quartz with time and/or increasing temperature (and pressure) along the following path: opal-A --> beta cristobalite --> gamma cristobalite --> chalcedony --> quartz (Fournier, 1985b). Fine-grained silica, especially thin colloform banding, forms under rapid quenching conditions; whereas well-formed crystalline (druzy, crystalline, cockscomb, dog tooth) quartz forms where temperature drops are less rapid, commonly within open spaces (Saunders, 1994).

Alteration under acidic conditions commonly results in the formation of an intensely silicified host rock. At fluid pH <2, almost all cations except silica (and minor Fe, Al and Ti) are leached from the rock (Stoffregen, 1987), and this results in the formation of a vughy, residual quartz (White, 1991). In addition, sulfate-silica complexes in low pH fluids may cause silica supersaturation (Fournier, 1985a), and therefore deposition of sulfate minerals, such as alunite or barite, from these fluids can result in the precipitation of silica group minerals.

At high temperatures (>300-400°C), pressure, fluid salinity, as well as temperature have a significant influence on silica deposition (Fig. 4.2), such that quartz solubility increases substantially with increasing pressure and temperature. Therefore, rapid pressure drops, possibly associated with a change from lithostatic to hydrostatic pressures in a porphyry environment (Sections 5.i.c.2, 3.ix.a), can result in silica oversaturation, and give rise to the development of quartz stockwork vein development (Fig. 4.2). Quartz deposition may also result from the dilution of this saline fluid by mixing with circulating dilute meteoric-dominated waters.

b) Carbonate minerals

The solubility of carbonate minerals in an aqueous solution (at pH 4-8) may be represented by the equation:

$$MCO_3 + CO_2 + H_2O = M^{2+} + 2HCO^{3-}$$

(where M = Ca, Mn, Mg, Fe).

The dominant control on carbonate deposition is increasing temperature; whereas dilution and pressure drops are only secondary factors (Fig. 4.3; Fournier, 1985b). Therefore, carbonate deposition occurs at shallow levels by the heating of descending CO_2-rich waters.

On the other hand, if a fluid, which contains significant concentrations of dissolved CO_2, boils rapidly, then release of CO_2 promotes carbonate deposition (Fig. 4.3), typically as bladed carbonate (Simmons and Christenson, 1994). This release of CO_2 is accompanied by an increase in fluid pH which will inhibit quartz deposition. Bladed carbonate is therefore commonly replaced by quartz. This is interpreted to result from dissolution of carbonate and deposition of silica in response to the decrease in fluid temperatures upon boiling (Simmons and Christenson, 1994). Thus many epithermal systems contain quartz which pseudomorphs platy carbonate.

At pH <4 carbonates are dissolved. At temperatures of <100°C and neutral conditions (pH>6-7), HCO^{3-} dominates over dissolved CO_2 (Ellis and Mahon, 1977), and therefore travertine deposits are encountered at the surface in some geothermal systems (e.g., Amacan, Philippines; PNOC-EDC, 1985a).

The controls on carbonate solubility under high temperature, saline conditions are not well documented. However, comparisons with sulfate solubility, and the observed deposition of carbonate minerals from magmatic brines in porphyry environments (Section 5), suggest that under hot, saline conditions, carbonate solubility may similarly decline with decreasing temperature.

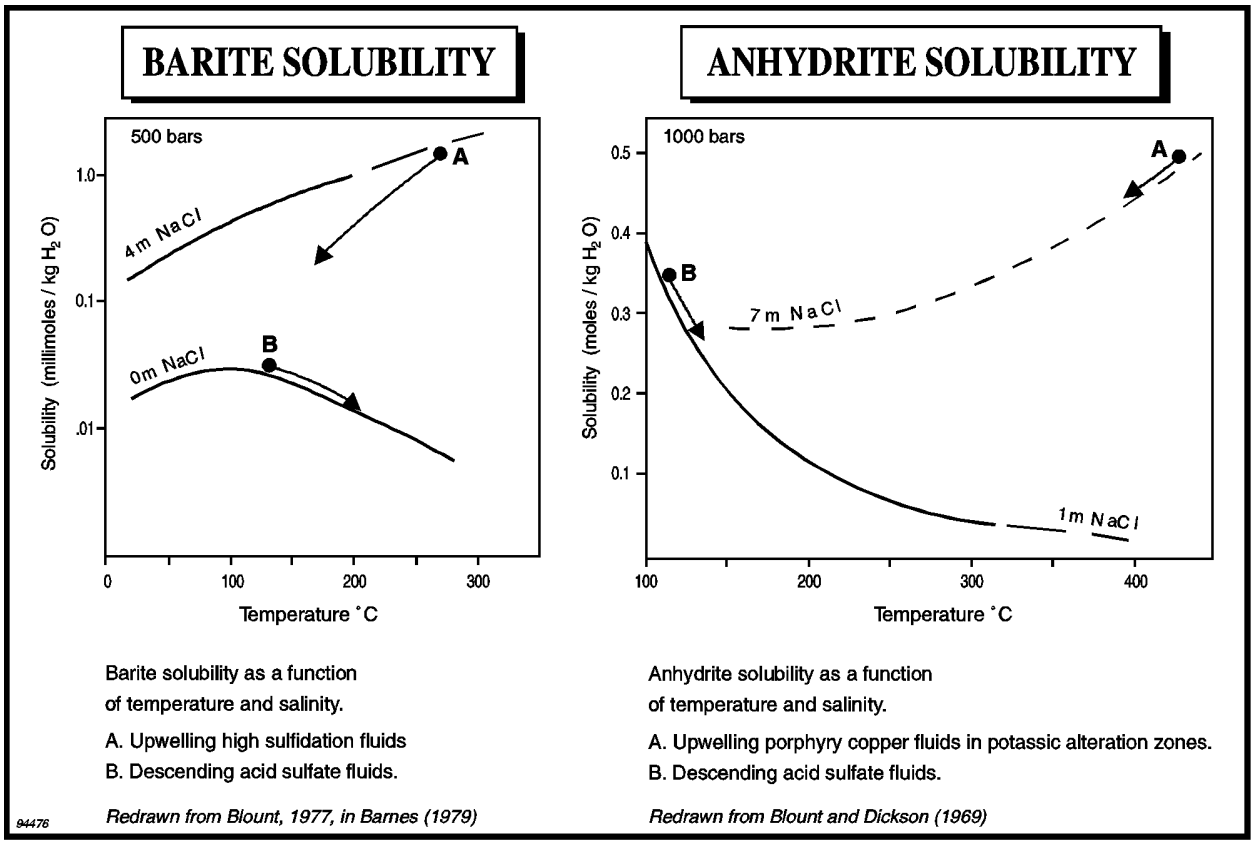
BARITE SOLUBILITY
500 bars
4m NaCl
0m NaCl
A
B
Solubility (millimoles / kg H2O)
1.0
0.1
.01
0
100
200
300
Temperature °C
ANHYDRITE SOLUBILITY
1000 bars
7m NaCl
1m NaCl
A
B
Solubility (moles / kg H2O)
0.5
0.4
0.3
0.2
0.1
100
200
300
400
Temperature °C
Barite solubility as a function
of temperature and salinity.
A. Upwelling high sulfidation fluids
B. Descending acid sulfate fluids.
Redrawn from Blount, 1977, in Barnes (1979)
Anhydrite solubility as a function
of temperature and salinity.
A. Upwelling porphyry copper fluids in potassic alteration zones.
B. Descending acid sulfate fluids.
Redrawn from Blount and Dickson (1969)
94476

FIG. 4.4

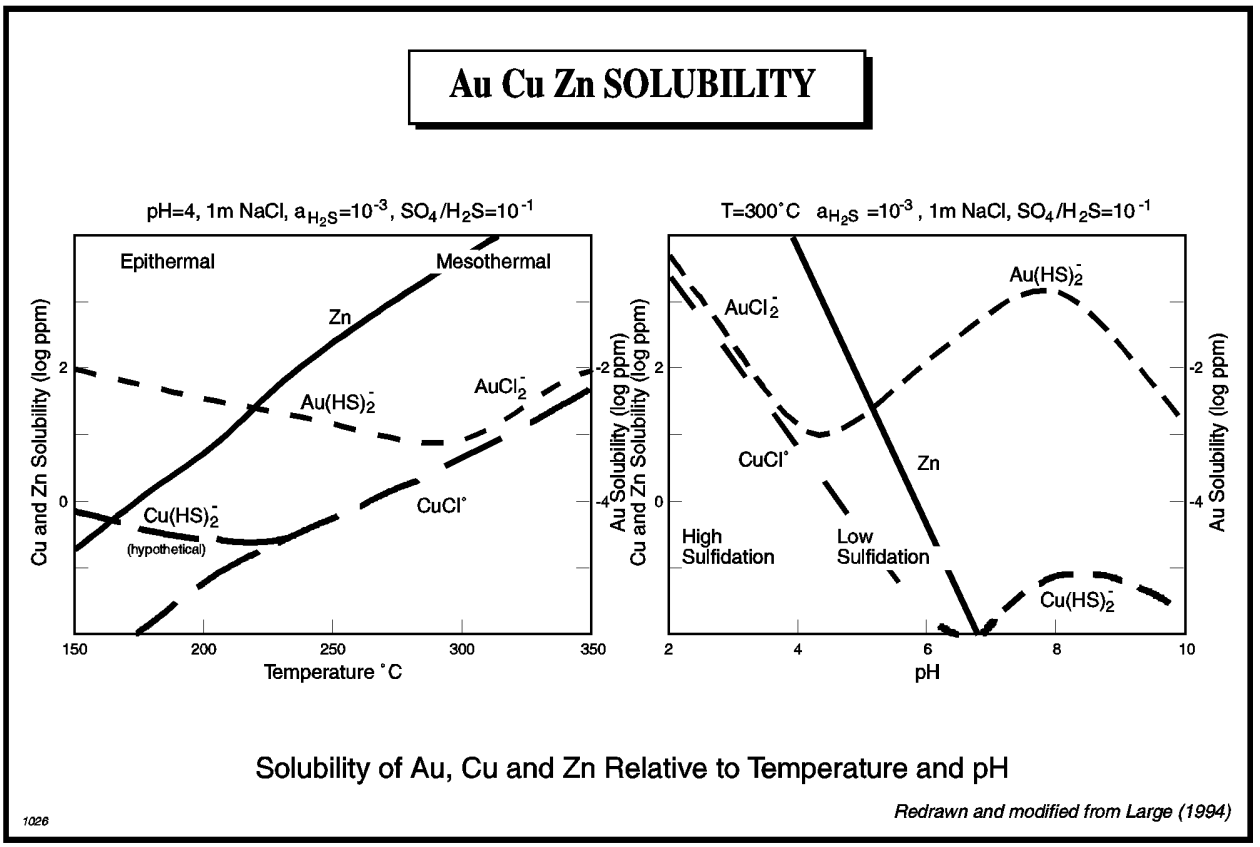
Au Cu Zn SOLUBILITY
pH=4, 1m NaCl, aH2S=10-3, SO4/H2S=10-1
Epithermal
Mesothermal
Zn
Au(HS)2-
AuCl2-
CuCl°
Cu(HS)2-
(hypothetical)
Cu and Zn Solubility (log ppm)
Au Solubility (log ppm)
2
0
-2
-4
150
200
250
300
350
Temperature °C
T=300°C aH2S =10-3 , 1m NaCl, SO4/H2S=10-1
AuCl2-
Au(HS)2-
CuCl°
Zn
High
Sulfidation
Low
Sulfidation
Cu(HS)2-
Cu and Zn Solubility (log ppm)
Au Solubility (log ppm)
2
0
-2
-4
2
4
6
8
10
pH
Solubility of Au, Cu and Zn Relative to Temperature and pH
Redrawn and modified from Large (1994)
1026

FIG. 4.5

c) Sulfate minerals

The solubilities of sulfate minerals are also strongly controlled by temperature, and like carbonate minerals exhibit an inverse relationship with increasing temperature under dilute conditions (Fig. 4.4; Blount and Dickson, 1969). Gypsum deposits in preference to anhydrite at low temperatures (<100-150°C; Leach et al., 1985). In highly saline porphyry environments, anhydrite solubility decreases proportionally with decreasing temperature (Blount and Dickson, 1969), and as a consequence, anhydrite is commonly deposited in porphyry environments. At high activities of sulfur, and/or low fluid pH, alunite will deposit in preference to anhydrite (Reyes, 1985).

Barite is the least soluble of the sulfate minerals and will preferentially deposit, from a dilute solution, upon heating at temperatures above about 100°C (Fig. 4.4; Blount, 1977 in Barnes, 1979). Under saline conditions, barite solubility decreases with temperature (Fig. 4.4). Therefore, the common occurrence of barite in the central zones of high sulfidation systems is inferred to result from the cooling of hot magmatic derived fluids (e.g., Nena, Frieda River Copper, Papua New Guinea; Section 6).

v) Controls of Metal Deposition

a) Gold

Gold is probably transported as a chloride complex ($AuCl^-$) under deep mesothermal and porphyry environments, and its deposition is controlled by decreases in temperature, pressure, and salinities (Henley, 1973; Fig. 4.5). In low sulfidation mesothermal and epithermal systems (<300-350°C), gold is preferentially transported in near neutral fluids as a bisulfide complex ($Au(HS)^{2-}$; Seward, 1982). In this case the controls to gold deposition are more complex, and dependent upon a wide range of factors, which are dominated by: changes in fugacity of oxygen, activity of sulfur, and pH, as well as temperature and salinity (Seward, 1982).

The influence of temperature and fluid pH (under dilute, reducing conditions) on gold mineralization is illustrated in Figure 4.5. The solubility of the gold complex $Au(HS)^{2-}$, increases with decreasing temperatures, but decreases with decreasing fluid pH (Seward, 1973).

The deposition of gold at epithermal/shallow mesothermal levels can be summarised by the equation (Brown, 1986):

$$Au + H_2S_{(aq)} + HS^- = Au(HS)_2^- + 1/2H_{2(g)}$$

In these environments, gold deposition from a chloride hydrothermal fluid can result from boiling, mixing with oxygenated meteoric waters, or mixing with an acid sulfate fluid (Brown, 1989; Spycher and Reed, 1989). Figure 4.6 illustrates the hypothetical changes in the fluid pH and fO_2 which could be expected in each of these scenarios and are represented by paths A, B and C respectively.

A. <u>Boiling</u>
The exsolution of H_2S upon boiling is an efficient mechanism for gold deposition at shallow, epithermal levels (Seward, 1982); however boiling also causes an increase in pH and decrease in temperature, both of which increase gold solubility (path A in Fig. 4.6.i). Brown (1986) showed that flashing (i.e. sudden pressure release and associated boiling) of deep hydrothermal fluids to atmospheric pressure at Broadlands geothermal field, New Zealand, deposited high concentrations of gold, silver and copper in scales in surface pipework (Section 2.iii.c). He calculated that the amount of gold deposited represents a decrease in solubility of approximately three orders of magnitude between the deep hydrothermal system at 260°C, and 100°C at atmospheric pressure.

Quartz, adularia and quartz pseudomorphed by bladed carbonate commonly occur in mineralized epithermal veins, and their presence is taken as evidence for boiling as a mechanism for gold deposition in epithermal environments (Hedenquist, 1991). However, as illustrated in Section 8, although gold-silver mineralization is hosted in the banded quartz, adularia and locally bladed carbonate veins, most gold typically occurs in thin sulfide bands which commonly contain low temperature clays (e.g., smectite, kaolinite or chlorite). Therefore the presence of adularia and/or bladed carbonate in auriferous banded epithermal veins cannot, in themselves, be used as evidence for gold mineralization as a result of boiling.

B. Mixing with oxidized waters

A change in the oxidation state of a mineralized fluid, caused by the mixing of a deep hydrothermal fluid with an oxidizing surficial water, has been shown experimentally to promote gold deposition (Brown, 1989). The solubility of gold (as a bisulfide complex) in a near neutral pH fluid at 260°C relative to changing f_{O2} conditions is illustrated in Figure 4.6.ii. Increases in fO_2 of a fluid in equilibrium with pyrite + pyrrhotite will initially be accompanied by an increase in gold solubility (path B, Fig. 4.6.i), however in the region of the pyrite/hematite or chlorite phase boundaries, small increases in oxidation can decrease gold solubility by many orders of magnitude (Romberger, 1988; path D, Fig. 4.6.ii).

In several southwest Pacific rim low sulfidation gold deposits, there is a close association of hypogene hematite and gold mineralization (White et al., 1995; Sections 7 and 8), and chlorite and/or chlorite-smectite occur in sulfide bands which host most of the gold mineralization in some banded epithermal deposits (e.g., Cracow, eastern Australia; Section 7: Hishikari, Section 8). These are taken as evidence that the increase in the oxidation state may be a significant mechanism for gold deposition and formation of bonanza gold deposits.

C. Mixing with low pH fluids

Experimental and computer modelling studies (Brown, 1989; Spycher and Reed, 1989) illustrate that mixing of near neutral pH chloride hydrothermal fluids with acid sulfate waters can be an efficient mechanism for the deposition of gold in epithermal systems (path C, Fig. 4.6.i); however the effects of dilution and cooling counterbalance this decrease in solubility. Gold mineralization in some New Zealand and Philippine geothermal systems may be related to the mixing of deep hydrothermal fluids with surface acid sulfate waters (Section 2.iii.c). The recognition of sulfate minerals in some low sulfidation epithermal gold systems (White et al., 1995; Sections 7 and 8) also suggests that acid sulfate waters may locally have been involved in gold deposition.

In high sulfidation systems, gold is interpreted to be transported either as $HAu(SH)_2$ or the chloride complex $AuCl_2^-$ (Giggenbach, 1992). It has been proposed (Hedenquist et al., 1994) that $AuCl_2^-$ is the dominant complex for gold under the low pH (<3), oxidizing and saline (>1 percent Cl^-) conditions of high sulfidation systems. The common association of copper and gold mineralization in high sulfidation systems is interpreted (Hedenquist et al., 1994) to support the concept that $AuCl_2^-$ and $HAu(SH)_2$ are the main complexing agents for gold in these environments, because copper is probably also transported as a chloride complex ($CuCl^o$). Cooling, possibly due to mixing with ground water, is likely to be the main mechanism of gold deposition from these complexes (Hedenquist et al., 1994).

Other complexes which transport gold in high sulfidation systems have also been proposed. $AuHS^o$ has been identified as a possible gold complex in high temperature acidic solutions (Bening and Seward, 1994; Arribas, 1995); and elsewhere (Seward, 1982) it has been postulated that under low pH (<3-4) conditions gold may be transported as either a thio-bisulfide complex [$HAu(HS)_2^-$] or as a combined chloride-bisulfide complex [$AuCl_2^-$-$Au(HS)_2^-$].

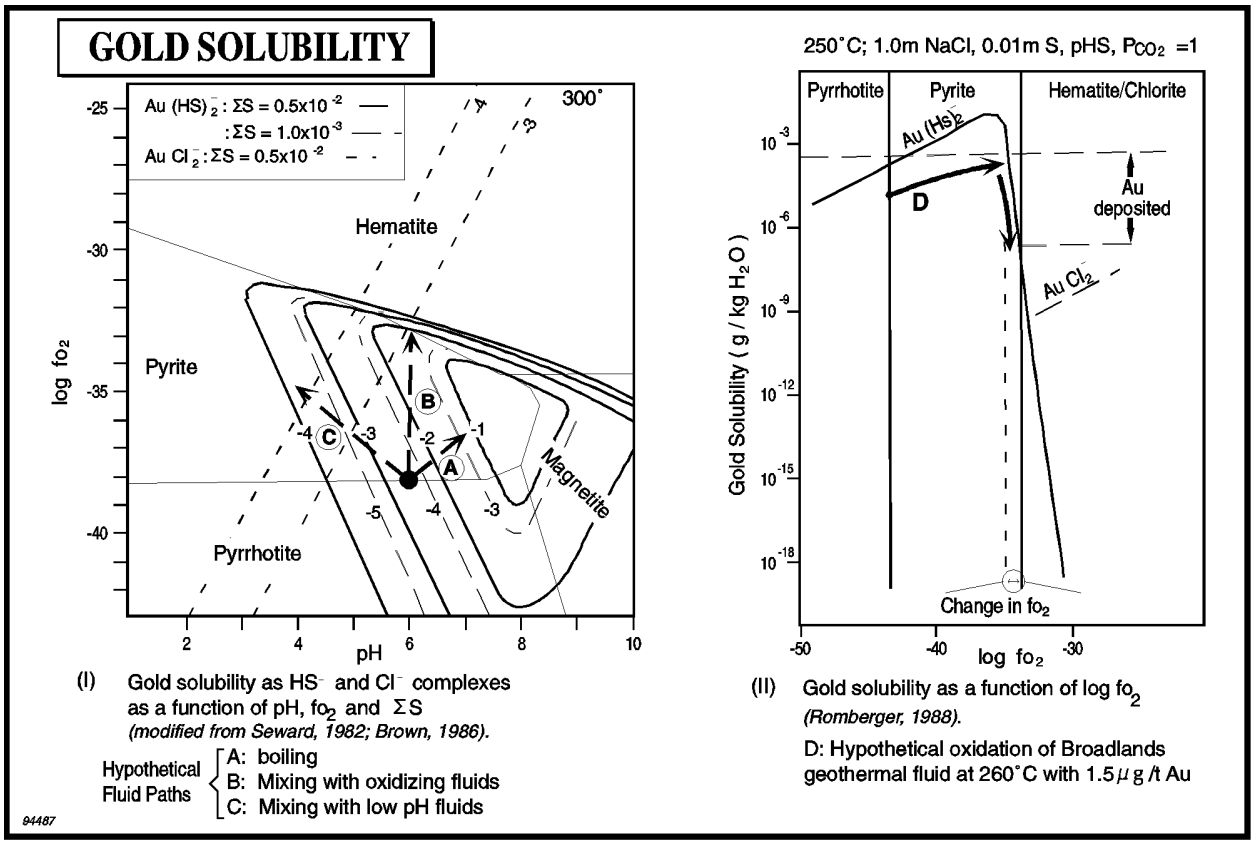
GOLD SOLUBILITY
Au (HS)$_2^-$: ΣS = 0.5x10^{-2}
: ΣS = 1.0x10^{-3}
Au Cl$_2^-$: ΣS = 0.5x10^{-2}
300°
Hematite
Pyrite
Pyrrhotite
Magnetite
log fo$_2$
pH
(I) Gold solubility as HS$^-$ and Cl$^-$ complexes as a function of pH, fo$_2$ and ΣS
(modified from Seward, 1982; Brown, 1986).
Hypothetical Fluid Paths
A: boiling
B: Mixing with oxidizing fluids
C: Mixing with low pH fluids
250°C; 1.0m NaCl, 0.01m S, pHS, P$_{CO_2}$ =1
Pyrrhotite
Pyrite
Hematite/Chlorite
Au (Hs)$_2^-$
Au deposited
Au Cl$_2^-$
Change in fo$_2$
Gold Solubility (g / kg H$_2$O)
log fo$_2$
(II) Gold solubility as a function of log fo$_2$
(Romberger, 1988).
D: Hypothetical oxidation of Broadlands geothermal fluid at 260°C with 1.5μg /t Au
94487

FIG. 4.6

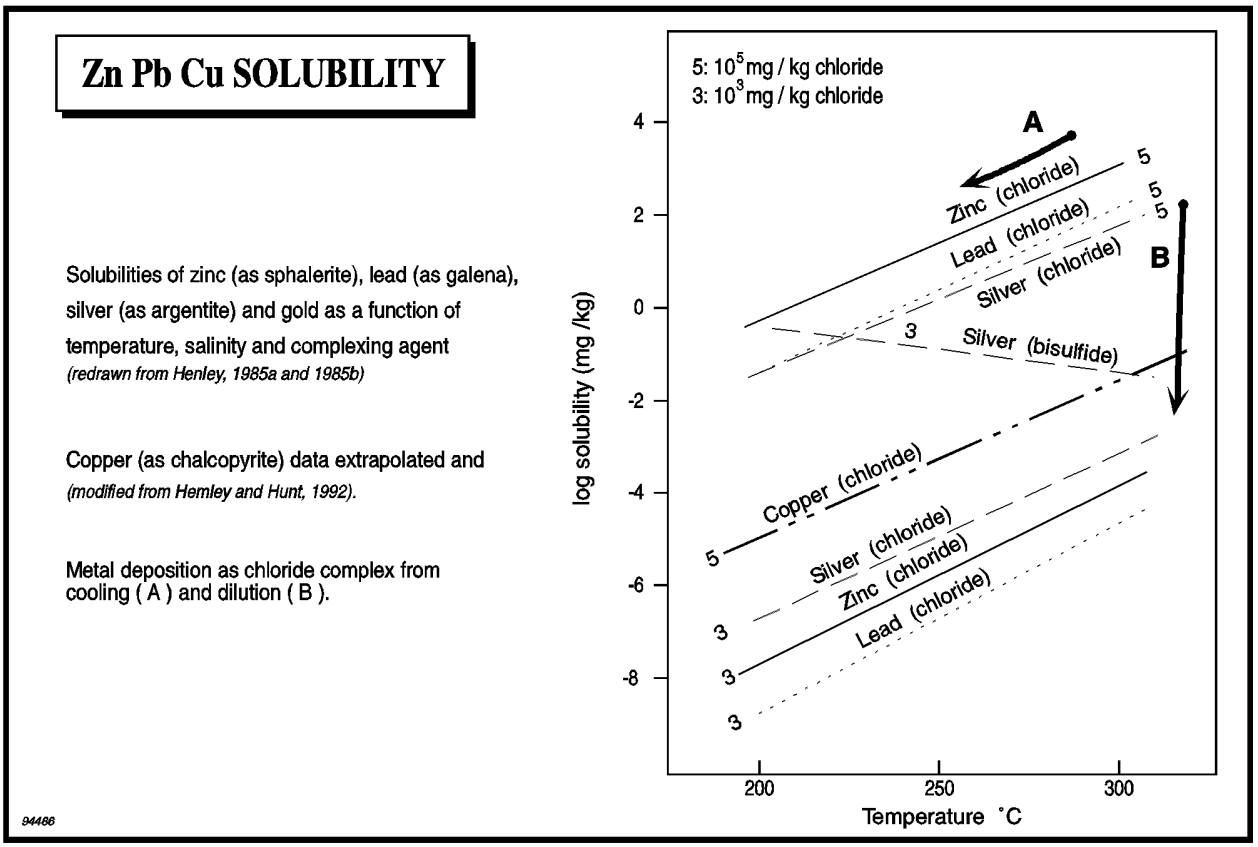
Zn Pb Cu SOLUBILITY
Solubilities of zinc (as sphalerite), lead (as galena), silver (as argentite) and gold as a function of temperature, salinity and complexing agent
(redrawn from Henley, 1985a and 1985b)
Copper (as chalcopyrite) data extrapolated and
(modified from Hemley and Hunt, 1992).
Metal deposition as chloride complex from cooling (A) and dilution (B).
5: 10^{5}mg / kg chloride
3: 10^{3}mg / kg chloride
Zinc (chloride)
Lead (chloride)
Silver (chloride)
Silver (bisulfide)
Copper (chloride)
log solubility (mg /kg)
Temperature °C
94486

FIG. 4.7

b) Copper

Copper is probably transported as a chloride complex (either as $CuCl^0$ or $CuCl_3^{2-}$) over temperature and pH ranges which are encountered in most hydrothermal systems (Crerar and Barnes, 1976; Barnes, 1979; Fig. 4.5). Copper deposition is controlled by decreases in temperature, salinity, pH and increases H_2S concentration (Barnes, 1979). However, it has been postulated (Barnes 1979; Henley and Brown, 1985; Brown, 1986) that copper may be preferentially transported as a bisulfide complex at low temperature (<200-250°C), epithermal environments and under dilute and near neutral conditions. This is supported by the common occurrence of low grade, but significant, copper which accompanies gold mineralization in many epithermal quartz vein deposits (Section 8).

c) Lead and Zinc

These metals are transported as chloride complexes under most hydrothermal conditions (Barnes, 1979), and their deposition results from decreases in temperatures (path A, Fig. 4.7), salinities (path B in Fig. 4.7) and pressure (Henley, 1985a, 1985b).

d) Silver

Silver is transported mainly as a bisulfide complex in dilute conditions, and as a chloride complex in hotter more saline conditions (Seward, 1976; Barnes 1979; Fig. 4.7). Therefore, silver mineralization mimics base metal phases at deeper levels of hydrothermal systems, and gold at shallower, epithermal levels. Many southwest Pacific rim high sulfidation systems are remarkably low in silver, inferring that either hot, very acidic fluids are Ag-depleted, or as is more likely the case, that Ag-complexes are much more soluble than gold under low pH conditions (Fig. 4.7).

e) Gold fineness

The silver content of gold is commonly given as fineness (= Au/Au+Ag x 1000). Previous workers (Morrison et al., 1991) showed that Archean, Slate Belt and Plutonic gold systems have high and consistent finenesses, however their porphyry, volcanogenic and epithermal classes exhibit wide fineness ranges within each class. These apparent wide variations may be explained by:
* The attribution of deposits from widely differing geological environments in a single class, such as both high sulfidation gold (e.g., Mt. Kasi, Fiji) and adularia-sericite epithermal gold-silver (e.g., Hishikari, Japan) grouped within the epithermal class, and shallow level carbonate-base metal gold (e.g., Wau, Papua New Guinea) and porphyry copper-gold (e.g., Guinaoang, Philippines) grouped within the porphyry class.
* The comparison of bullion data (e.g., Waihi, New Zealand), which also incorporates silver from phases other than gold, with microprobe determinations from gold grains.

Figure 4.8 presents histograms of the finenesses of hypogene gold from selected southwest Pacific gold and copper-gold prospects and deposits, based on the classification used for these systems in this volume. The data is derived from unpublished microprobe analyses by Ken Palmer (Victoria University, Wellington, New Zealand) for T. Leach, except where indicated.

Figure 4.8 indicates that there is a systematic decrease in gold fineness at progressively cooler and shallower crustal levels (or distal to the intrusive source), from:
* porphyry copper-gold/skarn (average = 920),
* through quartz-sulfide gold $\pm$ copper (average = 850) and
* carbonate-base metal gold (average = 765), to

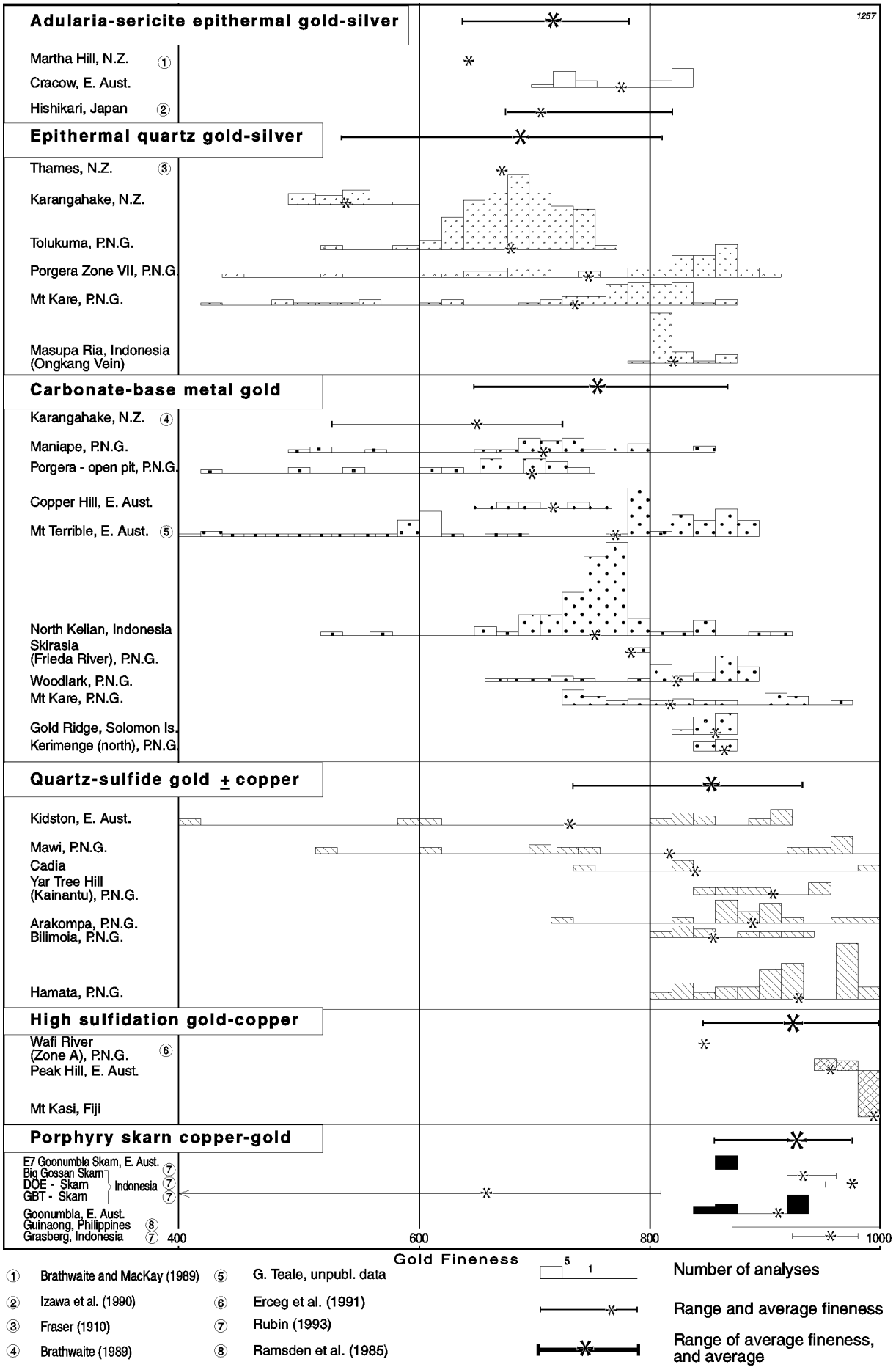

Histograms of gold fineness in southwest Pacific gold - copper prospects and deposits (microprobe analyses by Ken Palmer except where indicated)

FIG. 4.8

*

epithermal quartz silver-gold systems (average = 685).

White (1981) also noted that gold commonly occurs at a lower fineness in deposits formed at shallow epithermal levels, and computer modelling (Spycher and Reed, 1989) suggests that this may be related to decreases in temperature in the absence of other silver minerals. These zonations therefore indicate that temperature is probably the most important control on gold fineness in intrusion-related gold-copper systems. Wide ranges in gold fineness within a single deposit is interpreted to reflect wide temperature ranges during mineralization. For example, at Kidston, eastern Australia, gold is associated with both quartz-sulfide and carbonate-base metal vein styles; and at Mt. Kare, Papua New Guinea, gold in the roscoelite-bearing epithermal quartz silver-gold mineralization was deposited over a wide temperature range of approximately 250°C to <100-150°C (Section 7.iv.d.1).

The fineness of gold in intrusion-related epithermal quartz silver-gold systems, and adularia-sericite epithermal gold-silver systems is closer to the fineness of gold in carbonate-base metal gold systems, than would be expected from only the generally cooler conditions of mineralization. This may be a function of:
* Many carbonate-base gold metal systems form at very shallow epithermal levels (e.g., Maniape, Papua New Guinea; Karangahake, New Zealand) and therefore the gold is silver-rich,
* The preferential partitioning of silver into other minerals (Ag-sulfosalts, sulfides and tellurides) in epithermal systems could result in less silver being available to be incorporated into the native gold/electrum (Afifi et al., 1988).

Spycher and Reed (1989) showed that gold deposited under low pH conditions is at a very high fineness. This is supported by the data on high sulfidation systems in the southwest Pacific rim (Fig. 4.8). Free gold in high sulfidation systems is only observed in very shallow, epithermal environments, however even under these cool conditions the fineness of gold is very high (average of 935 for Mt. Kasi, Fiji; Peak Hill, eastern Australia; Zone A at Wafi River, Papua New Guinea). The low silver content of southwest Pacific rim high sulfidation systems contrasts with the high silver systems in South America (e.g., La Coipa; Oviedo et al., 1991).

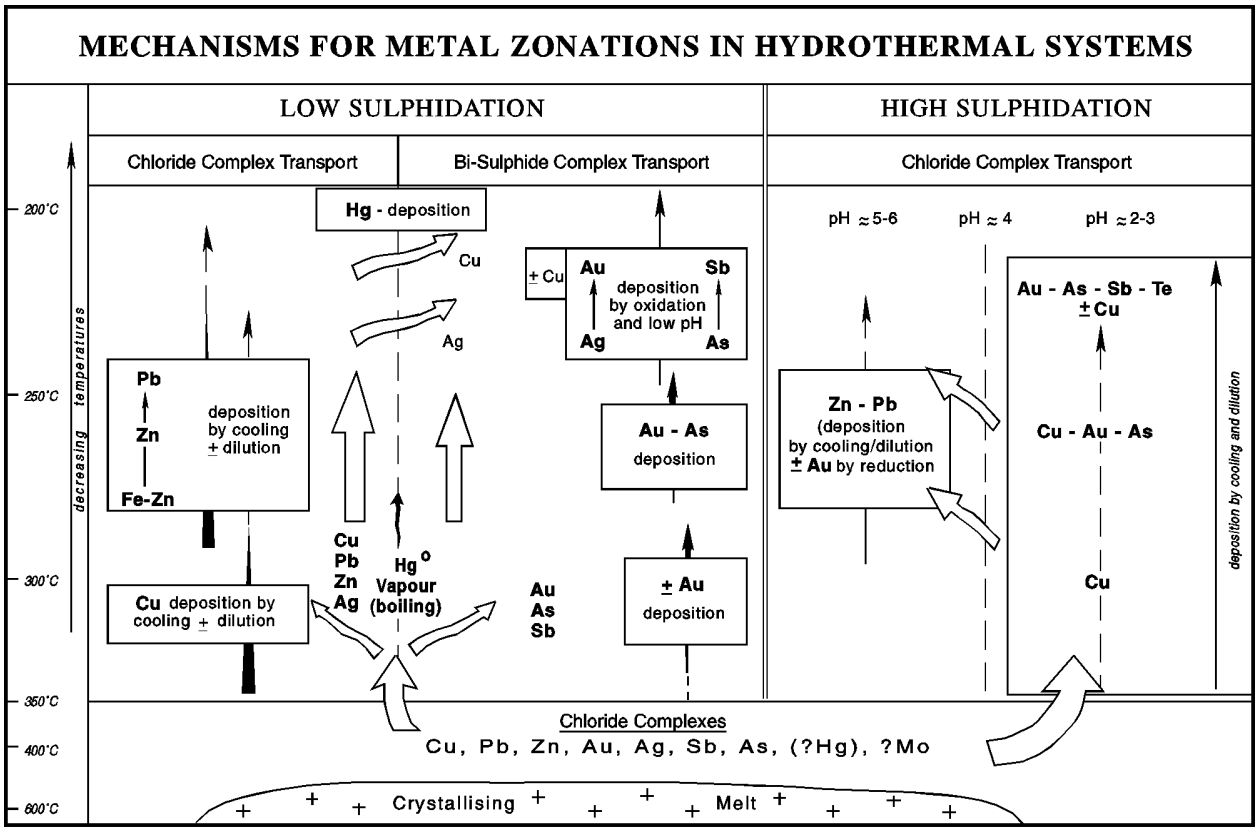
MECHANISMS FOR METAL ZONATIONS IN HYDROTHERMAL SYSTEMS
LOW SULPHIDATION
HIGH SULPHIDATION
Chloride Complex Transport
Bi-Sulphide Complex Transport
Chloride Complex Transport
200°C
250°C
300°C
350°C
400°C
600°C
decreasing temperatures
Hg - deposition
Cu
Ag
± Cu
Au
Sb
deposition by oxidation and low pH
Ag
As
Pb
Zn
Fe-Zn
deposition by cooling ± dilution
Au - As deposition
Cu Pb Zn Ag
Hg° Vapour (boiling)
Au As Sb
± Au deposition
Cu deposition by cooling ± dilution
pH ≈ 5-6
pH ≈ 4
pH ≈ 2-3
Au - As - Sb - Te ±Cu
Zn - Pb (deposition by cooling/dilution ± Au by reduction
Cu - Au - As
Cu
deposition by cooling and dilution
Chloride Complexes
Cu, Pb, Zn, Au, Ag, Sb, As, (?Hg), ?Mo
Crystallising
Melt

FIG. 4.9

5 GOLD-COPPER SYSTEMS IN PORPHYRY ENVIRONMENTS

i) Porphyry Copper-Gold Systems

a) Structure

1. Setting

The structural setting of southwest Pacific rim porphyry systems is outlined in sections 3.ii, 3.iii and 3.v. The major portion of the gold and most of the copper resources of the southwest Pacific rim occur within porphyry copper-gold deposits (Fig. 1.3), formed in subduction related I-type volcanoplutonic arcs (Sillitoe, 1992). A variety of subduction-related arc settings for porphyry emplacement at plate margins are distinguished by Sillitoe (1992) and described in detail in Section 3.ii. Although magmatic arcs which host porphyry intrusions are typically described as having formed during orthogonal or oblique convergence and associated subduction, many arcs demonstrate changes in style through time, and these changes may promote intrusion emplacement. Porphyry emplacement is inferred to have been promoted by changes from orthogonal to oblique convergence and periodic relaxation in orthogonal convergence (Section 3.v). The Chuquicamata porphyry copper in northern Chile is localized by a splay which is indicative of a component of strike-slip deformation on the Falla Oeste (West Fault) (Boric et al., 1990). The structure of many of the Ordovician porphyry-related gold-copper occurrences in New South Wales suggests that these formed during an episode of sinistral oblique compression (Section 3.v.b).

Major structures localize porphyry intrusions within magmatic arcs (Section 3.iii; Figs. 3.3, 3.4, 3.5, 3.11). Transfer structures which account for variations in the dip of subducting plates and rates of subduction, localize melts derived from deep crustal settings and focus overprinting intrusions (Fig. 3.3). A series of transfer structures which transect the island of New Guinea localize porphyry intrusions (e.g., Grasberg, Indonesia; Porgera, Wafi, and Bilimoia in Papua New Guinea; Fig. 3.4; Corbett, 1994). Arc-parallel or accretionary structures localize porphyry intrusions at splays (e.g., Far South East and others in the Philippines; Sillitoe and Gappe, 1984; Fig. 6.24: Chuquicamata, Chile; Boric et al., 1990: Frieda River, Papua New Guinea; Corbett, 1994; Fig. 6.18), typically in settings of oblique convergence, or at intersections with transfer structures (Porgera, Papua New Guinea; Corbett et al., 1995; Fig. 7.23).

2. Vein/fracture patterns

Fracture/vein patterns associated with porphyry intrusions are described in sections 3.iv. and 3.ix. Although stockwork fracture/veins are assumed to represent essentially random patterns, alignment of fracture veins in mineralized systems is common (Heidrick and Titley, 1982; Section 3.ix). Parallel, co-planar or sheeted veins may represent dilatant fracture systems which transport and host porphyry copper-gold mineralization. These must be carefully accessed in order to correctly plan drilling directions. Random stockwork veins predominate over the carapace of intrusions and sheeted or co-planar veins may occur near and above the margins. Fracture/vein patterns are categorized in terms of convergence and levels in the porphyry system, and adjacent mineralized host rocks (Fig. 3.16).

High level settings commonly result from the (Titley, 1993) development of mineralization in country rocks above and peripheral to the source intrusion, particularly in strongly dilatant structural environments. Concentric and radial fractures form above cylinder-shaped intrusions which have been emplaced upward into the host rocks with considerable force. Post-intrusion collapse may enhance the development of concentric sheeted fractures. In settings of oblique convergence the fracture/veins concentric and radial in dilational orientations will be enhanced and mineralized, and those in compressional orientations not well developed (Fig. 3.16). The Cadia wall rock porphyry occurs as a sheeted vein system removed from the source porphyry environment (Newcrest

Geological Staff, 1996; Fig. 3.11). The shapes of vein systems formed peripheral to many porphyry intrusions are indicative of emplacement during a relaxation of orthogonal compression resulting in localized extension (e.g., Batu Hijau, Indonesia; Meldrum et al., 1994). In these settings the exploitation of conjugate, and pre-existing arc parallel and arc normal fractures, may contribute towards the formation of apparent radial fracture patterns.

At depth fracture veins commonly display coplanar arrays which are controlled by the regional stress field. Many porphyry intrusions are emplaced in settings of oblique convergence, typically at splays, horestails and jogs in strike-slip structures. Sheeted veins formed parallel to the dilatant structural environment defined by these structures assist in the evolution of magmatic fluids from source intrusions and host mineralization (e.g., St Tomas II, Philippines; Goonumbla, eastern Australia: Dinkidi, Philippines; Garrett, 1996; southwestern US; Heidrick and Titley, 1982). Tectonic environments characterized by oblique convergence and settings within splays are ideal loci for the formation of ore-hosting sheeted quartz veins in porphyry environments (Section 3.ix.b; Fig. 3.16). Porphyry systems emplaced during relaxation of orthogonal convergence may also exploit the (now dilated) pre-existing structural grain formed during convergence (Fig. 3.16; e.g., Grasberg; Pennington and Kavalieris, 1997).

b) Early models of alteration and mineralization zonation

Extensive exploration for porphyry copper deposits took place during the 1960-80 period prior to the gold boom of the 1980s. The application of alteration zonation models developed at that time contributed towards the discovery of the Kalamazoo, southwestern USA (Lowell, 1991a) and La Escondida, Chile (Lowell, 1991b) porphyry copper deposits.

The temporal and spatial zonations in alteration and mineralization associated with porphyry copper deposits is commonly attributed to a progressive change from a hydrothermal system dominated by magmatic fluids, to one which is dominated by meteoric waters (e.g., Gustafson and Hunt, 1975; Beane and Titley, 1981; Reynolds and Beane, 1985). The interaction of these two cogenetic yet chemically different fluids is believed to result in mineral deposition in response to decreasing temperature and salinity as well as variations in pH and oxygen and sulfur fugacity (Barnes, 1979; Hemely and Hunt, 1992). Copper mineralization in porphyry copper deposits in southwest USA takes place in response to this fluid mixing at temperatures of <350°C (Nash, 1976; Beane and Titley, 1981; Reynolds and Beane, 1985).

While many of the porphyry copper deposits which occur in Chile and the western USA are primarily copper deposits, most southwest Pacific rim examples such as Dizon in the Philippines, Grasberg in Indonesia and Ok Tedi and Panguna in Papua New Guinea, are gold-rich (Titley, 1978), and so are described as porphyry copper-gold deposits (Sillitoe, 1993a). Although many porphyry copper deposits in the southwest Pacific do not contain recoverable molybdenum, it may occur at appreciable levels (e.g., Yandera, Papua New Guinea; Titley, 1978; Titley, et al., 1978).

No single model can adequately portray the alteration and mineralization processes that have produced widely different styles of porphyry copper deposits (McMillan and Panteleyev, 1980). Because of this, a number of models have been put forward to illustrate the alteration and mineralization encountered in porphyry copper systems in different geological settings.

From their work on the San Manuel-Kalamazoo porphyry copper deposit in the southwestern USA, Lowell and Guilbert (1970) suggest that this porphyry copper system exhibits zoned hydrothermal alteration assemblages which grade from centre to periphery (Fig. 5.1) as:

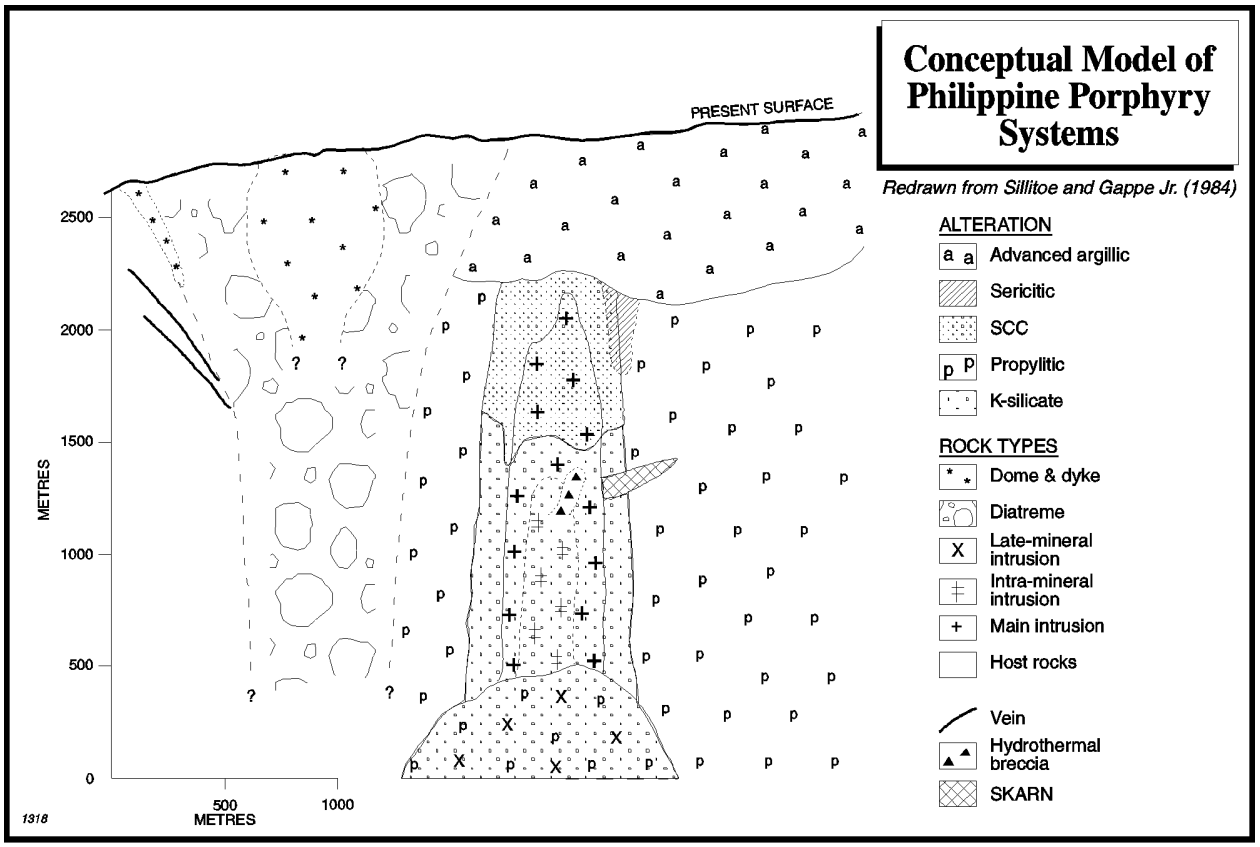

FIG. 5.1

* quartz core: quartz, sericite, chlorite, K-feldspar,
* potassic zone: quartz, K-feldspar, biotite, + sericite, + anhydrite,
* phyllic zone: quartz, sericite, pyrite,
* propylitic zone: chlorite, epidote, carbonate, adularia, albite.

Sulfides are also zoned within the shell-like alteration zones and grade outwards from the core as:
* ore shell: pyrite, chalcopyrite, magnetite on the periphery of the potassic alteration in contact with the phyllic alteration,
* low grade core: central lower grade equivalent of the ore shell,
* pyrite shell: pyrite >> chalcopyrite which rims the ore shell within the phyllic alteration,
* low pyrite shell at the periphery.

Sillitoe and Gappe (1984) developed a model based on the study of 48 variably eroded Philippine porphyry systems which are hosted in calc-alkalic intrusions and volcanic rocks (Fig. 5.1). While the setting of copper-gold mineralization is much the same as in the Lowell and Guilbert model, the Sillitoe and Gappe model includes features characteristic of the southwest Pacific rim environment. These include:
* caps of advanced argillic alteration,
* diatreme breccia associations,
* intra-mineral intrusions,
* vertically elongate porphyry system,
* the SCC alteration (defined as sericite, clay, chlorite) which occurs in place of the phyllic (sericitic) alteration and appears to represent transition from the potassic (K-silicate) to advanced argillic alteration zones.

Porphyry copper deposits form within dynamic hydrothermal systems in which continually changing conditions create multiple overprinting events (Gustafson, 1978). This is implicit in the Sillitoe and Gappe model, since the low temperature clays and higher temperature sericite in the SCC zone indicate that several distinct overprinting stages of alteration took place under significantly different physical and chemical conditions.

Gustafson and Hunt (1975) developed a model for the progressive evolution of the El Salvador porphyry copper deposit in Chile. They postulated that initial emplacement of mineralizing porphyries at approximately 2 km depth under lithostatic pressures, facilitated the formation of potassic alteration and the development of quartz stockwork veins under very hot (>400-500°C), highly saline conditions. In order to explain the subsequent progressive changes to lower temperature conditions during phyllic and argillic to advanced argillic alteration, they proposed a change from lithostatic to hydrostatic conditions. This change was interpreted to have been brought about by the influx of deep circulating meteoric dominated fluids.

c) Model of polyphasal overprinting events in southwest Pacific rim porphyry copper-gold systems

Studies in active porphyry systems in the Philippines (Mitchell and Leach 1991; Section 2) indicate that magmatic hydrothermal systems form over prolonged time periods, and are characterised by: initial intrusion emplacement, exsolution of fluids from the cooling melt, followed by influx of meteoric waters at progressively lower temperatures. Some of the overprinting events of mineral deposition and alteration in the Philippine active porphyry systems result from the descent of fluids of different chemistries and temperatures from shallow levels, rather than the in situ development of these fluids (Reyes, 1990b; Mitchell and Leach, 1991). The descent of these fluids is interpreted to have been brought about by the pressure draw down during waning of the hydrothermal system (Section 2).

The following section describes a conceptual model for the progressive development of porphyry copper-gold systems in the southwest Pacific (Figs. 5.2, 5.3). A generalized paragenetic sequence of alteration and mineralization in southwest Pacific porphyry copper-gold systems is illustrated in Figure 5.4.

It is not possible to present a suitable static model which illustrates the features encountered in all the southwest Pacific porphyry copper-gold systems. Rather, it is considered more beneficial to describe possible processes which are involved in the evolution of a porphyry copper-gold system, and then to apply these processes to the development of a genetic model which can satisfy the individual characteristics of each system.

In a similar manner to Beane and Titley (1981) and Reynolds and Beane (1985), it is proposed that there are two major stages during the evolution of southwest Pacific porphyry copper-gold systems. These are:

* A <u>prograde</u> sequence of events is associated with emplacement and cooling of a melt at shallow (<2 km depth) crustal levels, as an apophysis to a larger magma source, and the exsolution of magmatic fluids and metals from the upper levels of that porphyry stock. These prograde events have here been divided into the initial formation of zoned potassic-propylitic alteration (Stage I; Fig. 5.2), followed by later quartz vein development and advanced argillic alteration (Stage II; Fig. 5.2).

* A <u>retrograde</u> stage involves the subsequent cooling of the intrusion, to the extent that the porphyry stock and its host rocks become an environment of metal deposition (Stage III; Fig. 5.3). The vast bulk of mineralization in southwest Pacific porphyry copper-gold systems (and southwest USA porphyry deposits e.g., Cathles, 1977; Beane and Titley, 1981; Reynolds and Beane, 1985) is interpreted to have developed during this retrograde event at temperatures of around 250-350°C.

The changes in alteration related to variations in temperatures and fluid pH during these events are illustrated in Figure 5.5.

The following conceptual model of the evolution of porphyry copper systems in the southwest Pacific is therefore presented as a framework to develop site-specific models for each individual prospect or deposit.

1. Stage I: Heat transfer and zoned alteration

Initial emplacement of melts at shallow crustal levels and the associated cooling and crystallization is accompanied by the formation of zoned alteration assemblages formed in response to the transfer of heat from the melt into host lithologies (McMillan and Panteleyev, 1980). This zoned alteration mineralogy, in many of the southwest Pacific porphyry copper-gold systems, grades from an inner potassic zone progressively outward to cooler propylitic alteration assemblages (Fig. 5.2; e.g., Yandera, Papua New Guinea; Watmuff, 1978: Panguna, Papua new Guinea; Ford, 1978: also for El Salvador, Chile; Gustafson and Hunt, 1975). A similar zonation in alteration mineralogy is associated with the initial emplacement of high level intrusions in active Philippine geothermal systems (Section 2).

1.1. Potassic alteration

In calc-alkaline magmatic arcs, the potassic alteration is dominated by biotite. In some systems (e.g., Yandera, Papua New Guinea), biotite varies from brown at the core to green at the margin of the potassic alteration, as a result of an increase in Mg/Fe content (Watmuff, 1978) and is indicative of increasingly cooler conditions towards the margins (see also garnet compositions in skarns; Section 5.ii). In areas of crustal rifting, emplacement of more felsic/silicic intrusions, the potassic alteration is dominated by K-feldspar (e.g., Goonumbla, eastern Australia; Heithersay and Walshe, 1996: Cadia, eastern Australia; Newcrest Geological Staff, 1996: Dinkidi, Philippines; Garrett, 1996). In both environments, secondary quartz and plagioclase are subordinate to the biotite. Secondary clinopyroxene is intergrown with biotite in the central potassic zones in the St. Tomas II porphyry copper deposit, Philippines (Philex, unpubl. reports) and the Palinpinon active porphyry copper system, Philippines (Reyes, 1990a). Magnetite occurs in most potassic alteration, and is interpreted to reflect neutral to alkaline reducing conditions.

The early potassic alteration commonly exhibits hornfelsic textures (McMillan and Panteleyev, 1980) and has a composition similar to that of primary magmatic biotites (Watmuff, 1978). Isotopic studies (Sheppard et al., 1971; Ford and Green, 1977) illustrate that the biotite is formed from magmatic fluids, and may have developed in response to reaction between the melt and primary hornblende (Burnham, 1979). Later biotite occurs in veinlets and is more Mg-rich (Watmuff, 1978). This change in the style and composition of alteration is herein inferred to indicate that there is a gradation from heat transferral from the melt initially by conduction (contact metamorphism), to later hydrothermal convection, possibly associated with the early exsolution of magmatic fluids.

1.2. Propylitic alteration

Alteration zones distal to the central potassic core reflect progressively cooler conditions (Fig. 5.5). Secondary amphiboles, typically actinolite in calc-alkaline environments, locally occur with biotite in the outer potassic alteration zones, and with epidote in the inner propylitic alteration zones (e.g., Philippine systems; Sillitoe and Gappe, 1984: Mamut, Sabah, Malaysia; Kosaka and Wakita, 1978: Grasberg, Indonesia; MacDonald and Arnold, 1994). At shallower levels, propylitic alteration assemblages of epidote-chlorite-albite-carbonate grade upward and outward into zones dominated by chlorite and progressively more hydrated zeolites which form under low temperature conditions (e.g., Yandera, Papua New Guinea; Watmuff, 1978). Prehnite (e.g., Cadia, eastern Australia; T. Leach, unpubl. data), and very rarely pumpellyite (T. Leach, unpubl. reports), are

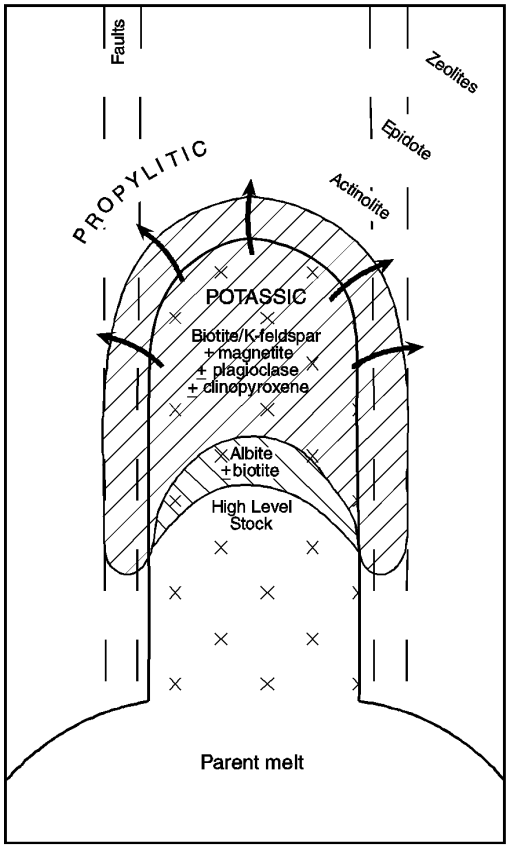

Stage I : Heat transfer and zoned potassic - propylitic alteration

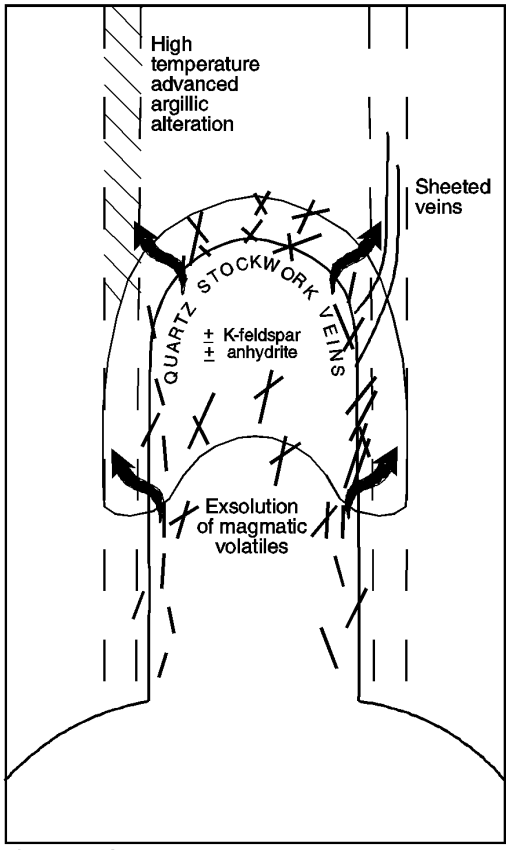

Stage II : Crystallization of stock, exsolution of magmatic volatiles; stockwork and sheeted veins and advanced argillic alteration.

Fig. 5.2 Early stages of development of southwest Pacific porphyry copper-gold systems.

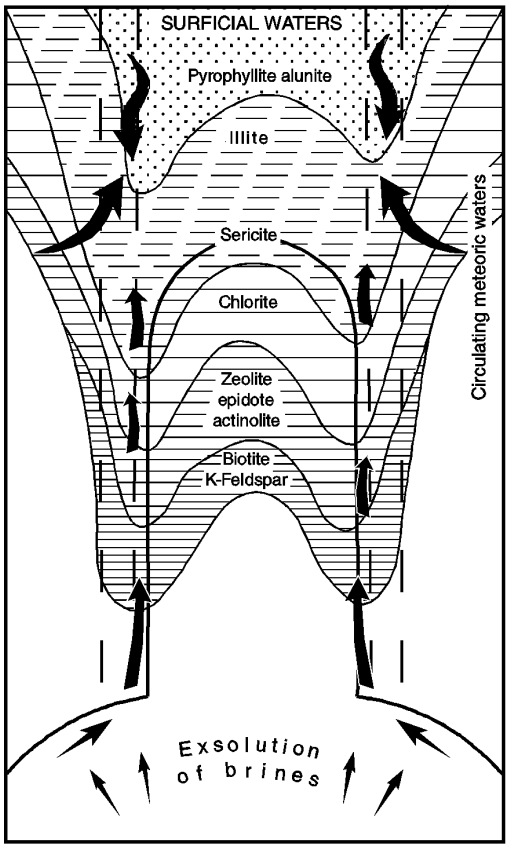

Stage IIIa : Cooling of shallow levels of stock and development of zoned alteration and veins

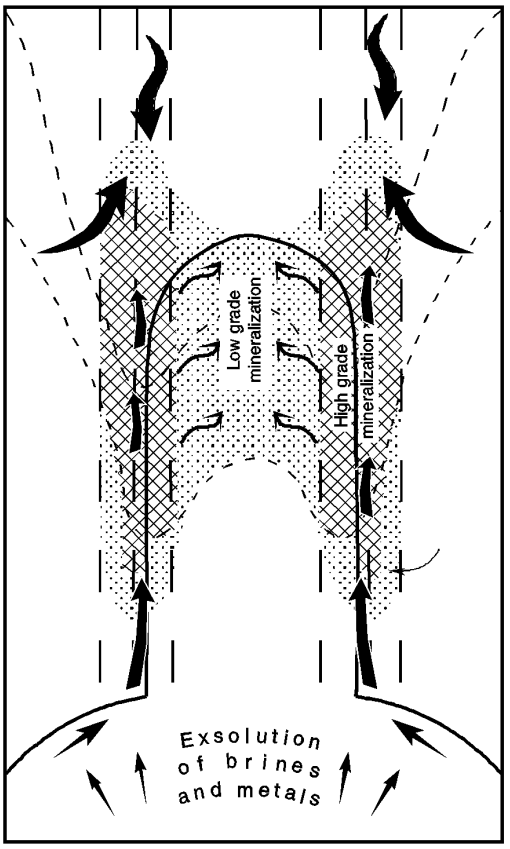

Stage IIIb : Exsolution of metals from deep levels of stock and/or parent metal and copper-gold mineralization

Fig. 5.3 Late stages of cooling and mineralization in southwest Pacific porphyry copper-gold systems. encount

encountered in some epidote-bearing propylitic assemblages. Although magnetite is locally abundant in the propylitic zones, pyrrhotite (e.g., Mamut, Sabah, Malaysia; Kosaka and Wakita, 1978) and/or pyrite dominate in these cooler, less reducing, and locally lower pH environments. In places magnetite and/or pyrrhotite produce significant geophysical magnetic anomalies within the propylitic alteration zones (e.g., Batu Hijau, Indonesia; Meldrum et al., 1994), although most magnetic anomalies are derived from magnetite in the cental zone of potassic alteration (Sillitoe, 1993a).

1.3. Albitization

In the central portions of many of the intrusions, potassic alteration grades with increasing depth through zones of propylitic alteration (commonly with actinolite) to zones of increasingly weaker alteration, and in some cases to a relatively unaltered core (e.g., Dinkidi, Philippines; Garrett, 1996). Elsewhere, the deep propylitic alteration assemblage is dominated by albite (e.g., Yandera, Papua New Guinea; Watmuff, 1978: Batu Hijau, Indonesia; Meldrum et al., 1994). This albitization of plagioclase has been interpreted to have formed during the late stage crystallization of the melt (Watmuff, 1978), as all other alteration events post-date the albite. Albitization of plagioclase at deep levels in porphyry systems has also been documented at the Ann-Mason deposit, Nevada, although there it is documented to occur late in the sequence of events, and is inferred to be related to the incursion of non-magmatic fluids (Dilles and Einaudi, 1992).

2. Stage II: Exsolution of magmatic fluids

Cooling and crystallization of the melt results in fracturing, especially around the carapace of the intrusion, accompanied by the exsolution of magmatic volatiles (Henley and McNabb, 1978). The build up of gas pressure within the cooling magma may initiate fracturing in the brittle host rocks (Burnham, 1979). In many instances tectonic movements are inferred to facilitate fracturing of the carapace and associated sudden pressure drops (Section 3.ix.b). As outlined in Section 4.iv.a, a change from lithostatic to hydrostatic pressures at 2 km depth, and an accompanying drop in pressure upon exsolution of volatiles, can result in the deposition in the fractured carapace of quartz from the magmatic fluids.

2.1. Quartz-dominated stockwork and sheeted vein development

2.1.a. Distribution

Quartz can therefore be deposited within the fracture network and result in the formation of a stockwork quartz vein system around the carapace of the intrusion (Fig. 5.2). As outlined in Section 3.ix, quartz is also commonly deposited in sheeted fracture systems, typically at the fault controlled margins of the intrusion (e.g., Mamut, Sabah, Malaysia; Kosaka and Wahila, 1978). In some cases the sheeted quartz veins cross cut the host intrusion or extend up to many hundreds of metres into the host sediments or volcanics (e.g., Cadia, eastern Australia; Newcrest Geological Staff, 1996). Elsewhere, the development of these sheeted veins are interpreted to relate to continued reopening of the dilational faults which facilitated the initial emplacement of the intrusion into shallow crustal levels (e.g., Frieda River, Papua New Guinea; T. Leach, unpubl. reports). These dilational plumbing systems are here inferred to be important in subsequent metal transport.

This Stage II quartz is deposited from a hot, hypersaline two phase fluid and is commonly a murky light grey-white colour due to the large number of both primary and secondary fluid inclusions and minute inclusions of gangue and ore phases. This early quartz is distinguishable from the clearer and whiter quartz veins formed under cooler, more dilute conditions (Stage III) and which contain fewer fluid and mineral inclusions.

At Batu Hijau, Indonesia, average fluid inclusion homogenisation temperatures in the quartz are highest towards the carapace of the mineralized tonalite, and decrease both with depth and at shallower levels outside the intrusion (A. Coote, unpubl. Newmont petrology report). This distribution implies that fracturing and quartz vein development initially took place around the upper margins of the intrusion, then later extended out into the country rock, and inward to the core of the intrusion.

2.1.b. Fluid conditions

In some systems, the stockwork quartz veins near the carapace of the intrusion locally comprise >20-30 percent of the intrusion (e.g., Grasberg, Indonesia; MacDonald and Arnold, 1994: Batu Hijau, Indonesia; Irianto and Clarke, 1995). This high density of quartz veins implies that a significant quantity of volatiles were released from the melt. In these cases the interpreted original enrichment in volatiles, possibly during melt ascent (Lowenstein, 1994), may have provided the buoyancy necessary to facilitate intrusion emplacement at relatively shallow crustal levels.

Two stages of early quartz veins recognised in southwestern USA porphyry copper systems (Nash, 1976; Reynolds and Beane, 1985), also occur in porphyry copper systems in the southwest Pacific. Early quartz veins at Goonumbla, eastern Australia (Heithersay and Walshe, 1996) formed during late stages of melt crystallization as evidenced by their local discontinuous ptygmatic morphology which merge with the host intrusion. These are equivalent to the 'A'-type quartz veins of Gustafson and Hunt (1975). Fluid inclusion analyses at Panguna and Frieda River in Papua New Guinea (Eastoe, 1978) as well as at Goonumbla (Heithersay and Walshe, 1996), indicate that these early veins formed at temperatures of >600-800°C, similar to crystallization temperatures of the melt, and from brines with salinities of >35-40 weight percent NaCl.

The vast majority of the quartz veins commonly exhibit multiple phases of fracturing and sealing within a brittle, fractured, host intrusion (e.g., Panguna, Papua New Guinea; Eastoe, 1978), and therefore post-date crystallization of the melt at that level. They also cross-cut the earlier formed potassic and inner propylitic alteration zones, and may be accompanied by K-feldspar alteration of the adjacent wall rock plagioclase and Stage I biotite (Watmuff, 1978). These are equivalent to the 'B'-type quartz veins of Gustafson and Hunt (1975). Magnetite, K-feldspar, biotite and/or albite are locally intergrown with the quartz, and may form as vein selvages to quartz stockwork veins (e.g., Goonumbla, eastern Australia; Heithersay and Walshe, 1995). Minute biotite and anhydrite inclusions are also encountered in some quartz stockwork veins (Britten, 1981). In systems associated with alkali intrusions, K-feldspar and/or magnetite represent significant components in both the stockwork and the sheeted veins (e.g. Goonumbla, eastern Australia; Heithersay and Walshe, 1995: Dinkidi, Philippines; Garrett, 1996).

Fluid inclusion studies (e.g., Eastoe, 1978; Heithersay and Walshe, 1995) indicate that the majority of the stockwork and sheeted quartz veins were typically deposited from a hot (> 300-500°C), hypersaline (>25-30 wt % NaCl equiv), two phase (i.e., boiling) brine. Recent work from porphyry systems in the southwestern USA (e.g., Cline and Bodnar, 1994) has shown that during the formation of such quartz veins, the vapour and brine fluids partition separately from the cooling melt. Therefore, the salinity of the liquid-rich brine, as determined from fluid inclusion data, may be an over-estimation of the true salinity of the fluids which exsolved from the melt.

2.1.c. Metal contents of fluids

Fluids which formed the stockwork quartz veins were significantly enriched in metals. Hematite, magnetite and copper minerals commonly occur as minute minerals in the primary saline-rich fluid inclusions (Roedder, 1984). Based on the volume percentage of chalcopyrite daughter crystals, Eastoe (1978) estimated a copper

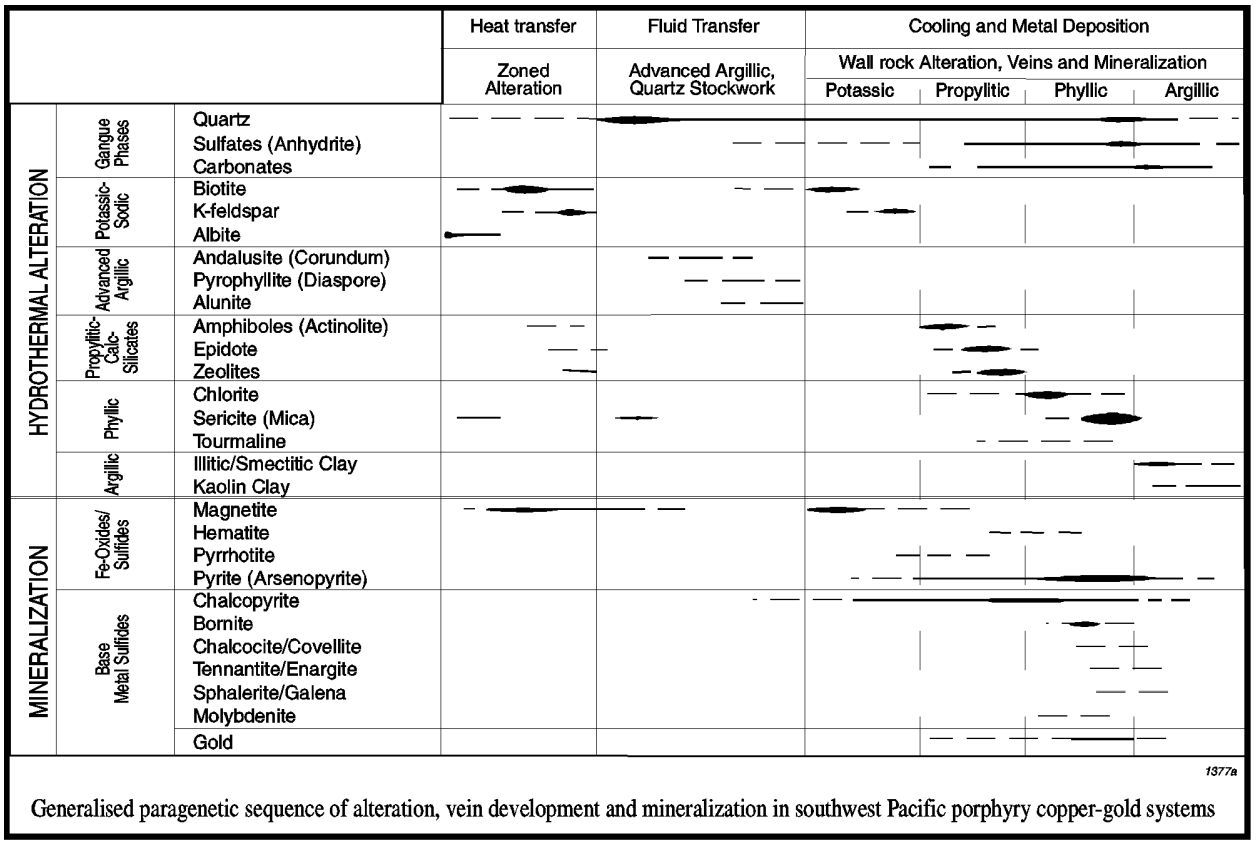

Generalised paragenetic sequence of alteration, vein development and mineralization in southwest Pacific porphyry copper-gold systems

FIG. 5.4

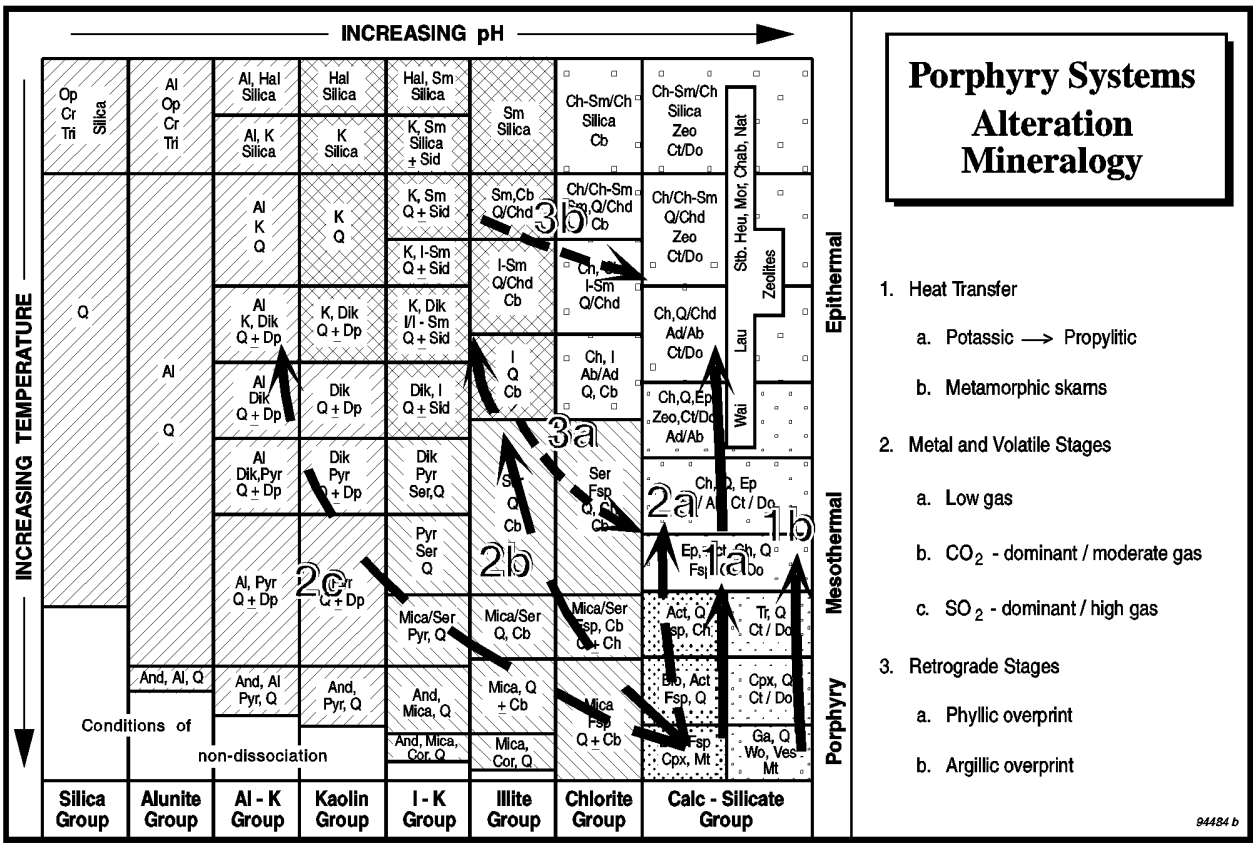

FIG. 5.5

concentration of 1,900 ppm from one liquid inclusion in a quartz vein at Panguna, Papua New Guinea. Similar concentrations of copper (average approx. 2,000 ppm Cu), in addition to high concentrations of other metals (up to 35,000 ppm Fe, 2700 ppm Zn, and 940 ppm Pb) have been detected in hypersaline brines in primary inclusions in the Questa porphyry molybdenum system, southwestern USA (Cline and Vanko, 1995).

However, experimental work (Hemley et al., 1992) has illustrated that solutions at temperatures of 500°C and 1 kbar pressure are as saturated at similar concentrations (average approx. 1300 ppm Cu) as the fluids which deposited the sheeted and stockwork quartz veins, but at much lower salinities (5.8 wt % NaCl equiv). As the solubility of copper as a chloride complex increases at higher salinities (Crerar and Barnes, 1976), the hot hypersaline (>25-30 wt % NaCl) solutions from which the quartz veins deposited, were therefore probably significantly undersaturated with respect to copper (Roedder, 1984).

This experimental work is supported by detailed petrology on porphyry copper systems in the southwestern USA (Beane and Titley, 1981; Reynolds and Beane, 1985), which indicates that copper mineralization is not associated with deposition of the quartz veins from these hot (>350-400°C) hypersaline magmatic fluids. This is also the case for southwest Pacific porphyry copper-gold systems. Quartz-magnetite stockwork veins at Yandera, Papua New Guinea form a barren core, whereas mineralization is here associated with later structurally controlled sericite and zeolite veins (Titley et al, 1978; Watmuff, 1978). Early quartz veins at Frieda River, Papua New Guinea, which were deposited at temperatures of >400-500°C from hypersaline brines, are barren and merely provide a brittle host for later mineralization. Similarly, copper mineralization at Copper Hill, eastern Australia, is associated with late sericite-chlorite veins which cross cut the stockwork quartz veins (Scott, 1978).

Therefore, although the early hypersaline fluids contained ore metals when they exsolved from the crystallizing magma (Bodnar, 1995), these fluids did not deposit copper (or gold) during the formation of quartz veins. However, the high concentrations of iron in both fluid inclusions (Cline and Vanko, 1995) and high temperature, saline solutions (Hemley et al., 1992), implies that these brines were near saturation with respect to iron oxides as they exsolved from the cooling intrusion. This is supported by the abundance of magnetite found associated with early potassic-propylitic alteration, and with later quartz and K-feldspar stockwork and sheeted veins (and also as metasomatic skarns, Section 5.ii).

Magmatic fluids outflow laterally and vertically along regional fracture/fault systems (Henley and McNabb, 1978). It is proposed here that these magmatic fluids are entrained into circulating waters and deposit quartz and K-feldspar/adularia in veins which act as hosts to later gold and base metal mineralization (Section 7).

2.2. High temperature advanced argillic alteration

The intense silicification and advanced argillic alteration along the upper margins of some southwest Pacific porphyry systems are herein interpreted to have formed during the exsolution of magmatic volatiles from the crystallizing high level stock (Fig. 5.2). These zones of high temperature advanced argillic alteration, herein termed barren high sulfidation shoulders (Section 6.ii), have been documented in a number of southwest Pacific porphyry copper-gold systems (e.g., Batu Hijau, Indonesia; Meldrum et al, 1994: Horse Ivaal, Frieda River, Papua New Guinea; Britten, 1991; Section 6.ii.b: Dizon, Philippines; Sillitoe and Gappe, 1984: Cabang Kiri, Indonesia; Carlile and Kirkegaard, 1985; Lookout Rocks, New Zealand; Section 6.ii.b) and are also termed lithocaps which overlie buried porphyry intrusions by Sillitoe (1995b).

High temperature advanced argillic alteration, which is distributed along the margins of the mineralized intrusions, is strongly aligned within bounding structures. Evidence from the Palinpinon active porphyry system, and the solfataras at Biliran (Mitchell and Leach, 1991) indicate that the silicification and advanced argillic alteration may extend from porphyry depths to the surface where they form magmatic solfataras. At Palinpinon,

the advanced argillic alteration post-dates the formation of zoned potassic-propylitic alteration and skarn assemblages, but pre-dates later phyllic and argillic alteration. In the Alto Peak geothermal field, the acidic alteration has been shown to relate to a hot (<400°C) magmatic-dominated vapour-plume, which is inferred to be currently exsolving from a crystallising magma at depth, and overprints earlier potassic-propylitic alteration (Reyes et al., 1993).

High temperature advanced argillic alteration marginal to high level porphyry intrusions is zoned from: biotite in the potassic zone, through zones of K-feldspar and chlorite, sericite-andalusite ± corundum ± tourmaline, pyrophyllite-diaspore, to alunite + kaolinite (e.g., Cabang Kiri, Indonesia; Lowder and Dow, 1978: Frieda River, Papua New Guinea; Britten, 1981; T. Leach, unpubl. data). This zonation is interpreted to reflect an increase in fluid acidity as reactive magmatic volatiles (mainly SO_2 and HCl, and subordinate but locally significant HF) disproportionate and disassociate at progressively cooler conditions away from the crystallizing melt (Rye et al., 1992; Fig. 6.3). These features are discussed in more detail in high sulfidation systems (Section 6).

3. Stage III: Late stage cooling and metal deposition

3.1. Cooling and alteration

As discussed above, copper-gold mineralization in many porphyry copper systems in both the southwest USA (e.g., Beane and Titley, 1981; Reynolds and Beane, 1985; Dilles and Einaudi, 1992) and the southwest Pacific (e.g. Watmuff, 1978; Leach, unpubl. data), post-date Stage I potassic/propylitic alteration, quartz vein formation and advanced argillic alteration (Fig. 5.3). This mineralization is attributed by many authors to be a result of a progressive change from an environment dominated by magmatic fluids to one that is dominated by cooler and more dilute meteoric waters (e.g., Gustafson and Hunt, 1975; Reynolds and Beane, 1985).

The general sequence of events associated with cooling (Stage IIIa) and metal deposition (Stage IIIb) in southwest Pacific porphyry systems is illustrated in Figure 5.6 and may be summarised as: quartz --> silicate minerals (potassic, propylitic, phyllic alteration) --> Fe-oxides/sulfides --> mineralization (Cu-Au ± Mo, Pb, Zn) --> sulfates/carbonates. These minerals occur:
i) in newly formed fractures which cross cut Stage I alteration and Stage II quartz veins,
ii) in older reopened fractures,
iii) in open spaces in Stage I quartz veins (commonly along partings in the centre of veins),
iv) associated with the alteration of primary and pre-existing secondary feldspars and mafic minerals in the wall rock (disseminated mineralization).

The quartz is commonly clear to white, and from fluid inclusion analyses (Eastoe 1978; Watmuff, 1978) was deposited from a fluid significantly more dilute (<15 wt % NaCl, and typically <5 wt % NaCl) and cooler (<300-400°C) than the fluid that deposited Stage I quartz. Where these quartz veins are associated with sericite-chlorite assemblages they are equivalent to the 'D'-type veins of Gustafson and Hunt (1975).

The silicate phases are intergrown with, or commonly overgrow the quartz, and are zoned from early and deep to shallow and late (Fig. 5.6) as: potassic alteration minerals (biotite then K-feldspar) --> calc-silicate minerals (actinolite, epidote and zeolites) --> chlorite --> sericite --> illitic clay --> kaolin clay. Some or all of these minerals may be present in any one system. Mineralization is intimately associated with these silicate phases, although the ore phases commonly overgrow the silicates (T. Leach, unpubl. data). This spatial and temporal zonation is indicative of progressive cooling and a decrease in the pH of the fluids during mineralization (Fig. 5.5; Beane and Titley, 1981).

STAGE II - PRE-MINERAL PORPHYRY VEINS				
Melt Composition	CALC - ALKALINE		ALKALINE	
INTRUSION TYPE	DIORITE	QUARTZ DIORITE TONALITE/ GRANODIORITE DACITE	MONZONITE QUARTZ-MONZONITE	SYENITE QUARTZ-SYENITE
VEIN MINERALS ↓ decreasing abundance	Biotite Anhydrite Quartz Magnetite	Quartz Biotite K-Feldspar Magnetite	K-Feldspar Quartz Biotite Magnetite Actinolite	K-Feldspar Biotite Magnetite Quartz Actinolite Epidote Garnet Clinopyroxene

FIG. 5.6
Spacial and temporal distribution of minerals during copper-gold mineralization in southwest Pacific porphyry copper-gold systems

3.1.a. Potassic alteration assemblages

Biotite and K-feldspar form as early Stage III minerals, commonly deposited in thin veinlets (generally <5 mm in width) with quartz, magnetite and/or pyrite, and are associated with variable abundances of chalcopyrite (e.g., Yandera, Papua New Guinea; Titley et al., 1978). The occurrence of biotite indicates that the veins and alteration formed under neutral to alkaline conditions at temperatures of >300-350°C (Section 4.ii.f). Although K-feldspar is locally intergrown with biotite, it may also occur in thin veinlets which cut biotite (Titley et al., 1978). Magnetite, which is intergrown with, but commonly overgrows the biotite, may contain inclusions of chalcopyrite and can therefore be distinguished from magnetite that formed during Stage I potassic alteration and primary igneous magnetite (e.g., Taysan, Philippines; T. Leach, unpubl. data). Similar K-feldspar-quartz-magnetite-chalcopyrite veinlets in southwest USA porphyry copper deposits were deposited from less saline fluids (<15 wt % NaCl) and under cooler conditions (200-450°C) than those for stockwork quartz veins. Isotopic data has shown that these minerals were deposited from mixed magmatic-meteoric fluids (Beane and Titley, 1981; Sheppard et al., 1971; Reynolds and Beane, 1985).

3.1.b. Propylitic alteration assemblages

The calc-silicate mineral phases (actinolite, epidote and zeolites) which occur in fractures and in open spaces, replace wall rock minerals (mainly mafic phases), and post-date the biotite and K-feldspar (Sillitoe and Gappe, 1984; Chivas, 1978; Watmuff, 1978). The paragenetic sequence of actinolite --> epidote --> zeolites (e.g., Cadia, eastern Australia; T. Leach, unpubl. data; Taysan, Philippines; T. Leach, unpubl. data) is indicative of progressive cooling under near neutral fluid pH conditions (Fig. 5.6). The zeolites typically comprise laumontite (e.g., Mamut, Sabah, Malaysia; Kosaka and Whila, 1978: Cadia, eastern Australia; T. Leach, unpubl. data). In

some systems prehnite forms early and occurs at deeper levels than laumontite (e.g., Cadia; T. Leach, unpubl. data). Elsewhere, more hydrated and lower temperature zeolites such as stibnite (Yandera, Papua New Guinea; Watmuff, 1978) and chabazite (Panguna, Papua New Guinea; Eastoe, 1978) form as late, post-mineral phases associated with barren calcite veins. Chlorite is typically associated with the above calc-silicate minerals and in many cases replaces early Stages I and II biotite (Sillitoe and Gappe, 1984).

3.1.c. Phyllic alteration assemblages

Most of the copper-gold mineralization in the southwest Pacific systems is intimately associated with late chlorite (e.g., Batu Hijau, Indonesia; Irianto and Clark, 1995) and/or sericite or illitic clay deposition and wall rock alteration (e.g., Copper Hill, eastern Australia; Scott, 1978: North Sulawesi, Indonesia; Lowder and Dow, 1978: FSE, Philippines; Garcia, 1991: Frieda River, Papua New Guinea; T. Leach, unpubl. data). Copper-gold mineralization is also predominantly associated with sericite-chlorite alteration in porphyry copper deposits in southwestern USA (Beane and Titley, 1981). In this phase of deposition/alteration, chlorite dominates at depth and is early, whereas sericite dominates at shallower levels and is late (e.g., Frieda River; T. Leach, unpubl. data). The upwards zonation of chlorite to sericite is indicative of a progressive decrease in fluid pH at shallower levels. A change from calc-silicate minerals to chlorite and then to sericite also reflects a decrease in fluid pH during progressively later stages of mineralization (Figs. 5.4, 5.5, 5.6). Isotopic analyses indicate that the sericite in many porphyry systems (Sheppard et al, 1971; Ford and Green, 1977; Eastoe, 1978) is derived from meteoric dominated waters. However, Wolfe (1994) interpreted from isotope analyses, that the sericite associated with mineralization at the E48 stock at Goonumbla, eastern Australia, was derived from magmatic-dominated fluids, whereas post-mineral sericite was probably formed from a meteoric-dominated water.

3.1.d. Argillic alteration assemblages

Argillic alteration overprints the sericite-chlorite alteration in a number of porphyry copper deposits (e.g., Batu Hijau; Meldrum et al., 1994: Grasberg; MacDonald and Arnold, 1994: Frieda River; T. Leach unpubl. report, 1995) and is equivalent to the clay in the sericite-clay-chlorite alteration at shallow levels in many Philippine porphyry systems (Sillitoe and Gappe, 1984). Clays at Yandera, Papua New Guinea are zoned from illite in the central part of the deposit, to illite-smectite in outer zones (Watmuff, 1978). Late quartz-clay-chlorite veinlets cut sulfide veinlets at Yandera, although some may be related to late copper mineralization (Watmuff, 1978). High grade copper-gold mineralization in late chalcopyrite-filled fractures at Grasberg is intimately associated with illitic clay deposition (T. Leach, unpubl. data).

3.2. Copper-gold mineralization

Magnetite is the main ore phase associated with biotite and K-feldspar alteration, although in some cases pyrite dominates over magnetite (e.g. Wafi River; Tau-Loi and Andrew, in prep). Chalcopyrite rarely occurs as inclusions in the magnetite or overgrows magnetite and pyrite in association with these potassic assemblages (Watmuff, 1978).

Magnetite, locally with chalcopyrite inclusions and/or pyrrhotite, is in places associated with early actinolite and epidote deposition. However, pyrite generally occurs as the dominant iron mineral in the calc-silicate mineral assemblages (Watmuff, 1978; Chivas, 1978; T. Leach, unpubl. data). The association of actinolite with copper minerals indicates mineralization occurred at temperatures >280-300°C. Hematite alteration of magnetite is inferred to have occurred during chlorite alteration of biotite at Taysan, Philippines (T. Leach, unpubl. data) and Frieda River, Papua New Guinea (T. Leach, unpubl. data).

Chalcopyrite and minor bornite are commonly associated with calc-silicate minerals. In many Philippine porphyry copper systems (Sillitoe and Gappe, 1984), at Yandera, Papua New Guinea (Watmuff, 1978) and some

southwestern USA deposits (e.g., Ann-Mason, Nevada; Dilles and Einaudi, 1992), the bulk of the copper mineralization is associated with late stage chlorite-epidote veins and wall rock alteration. The association of epidote and laumontite with copper sulfides indicates that mineralization took place under conditions of near neutral fluid pH at temperatures of 150-300°C (Section 4.ii.f).

Chalcopyrite is more abundant than bornite in chlorite-dominated assemblages, whereas bornite is locally more abundant than chalcopyrite in sericitic assemblages. Bornite is commonly intergrown with, and locally overgrows chalcopyrite. Mineral phases of the intermediate solid solution series (ISS; e.g., idaite) are rare and commonly late, possibly formed under lower temperature conditions (e.g., Wafi River, Papua New Guinea; T. Leach, unpubl. data). Hypogene chalcocite, covellite, enargite and tennantite generally post-date bornite formation, and are restricted to sericitic assemblages at shallow levels in some systems (e.g., Cadia, eastern Australia; T. Leach, unpubl data: Goonumbla, eastern Australia; Wolfe, 1994: Frieda River, Papua New Guinea; T. Leach, unpubl. data), and in peripheral zones of pyrophyllite and diaspore at Dizon, Philippines (Malihan, 1987).

Molybdenite is generally associated with chlorite-epidote-carbonate deposition and alteration (Watmuff, 1978; Sillitoe and Gappe, 1984). Galena and sphalerite typically form very late in the development of porphyry systems, commonly in association with sericite (e.g., Goonumbla; Wolfe, 1994) and carbonate (e.g., Copper Hill; Scott, 1978) veins and shears which post-date copper mineralization (Fig. 5.6).

Gold occurs in porphyry copper-gold systems as the native metal, typically as minute (<10-15 micron) inclusions in copper sulfides. More gold occurs with bornite than chalcopyrite (Sillitoe and Gappe, 1984) and in places is enriched within hypogene covellite and chalcocite (e.g., Goonumbla, eastern Australia; Wolfe, 1994). It is also more commonly associated with sericite alteration and related veins rather than with chlorite, calc-silicate or potassic assemblages (T. Leach, unpubl. data). Gold generally displays a high fineness (>900, Fig. 4.8), although where cooler conditions are evident (e.g., locally at Goonumbla; T. Leach, unpubl. report, 1995) the fineness is lower and more comparable to that encountered in mesothermal vein systems. Higher gold grades commonly, but not always, occur at shallow levels (e.g., Ok Tedi, Papua New Guinea; Rush and Seegers, 1990) or in fault controlled porphyry margins (e.g., Horse Ivaal, Frieda River, Papua New Guinea; T. Leach, unpubl. report, 1995: Didipio, Philippines; Garrett, 1996) and in these settings is associated with extensive sericite alteration and deposition. High grade gold at Copper Hill is associated with late carbonate-base metal veins, which cross cut porphyry-related quartz veins and pyrite-chalcopyrite-chlorite/sericite alteration and mineralization (T. Leach, unpubl. report; Section 7). Gold grades are generally higher in porphyry systems associated with alkaline intrusions, although copper grades are comparable to those reported for calc-alkaline systems.

3.3. Sulfate and carbonate deposition

Anhydrite, calcite and locally dolomite commonly overgrow sulfides in veins/veinlets and wall rock alteration (T. Leach, unpubl. data), although in some instances sulfide mineralization extends into the sulfate and carbonate phases of alteration (e.g., Frieda River; T. Leach, unpubl. report, 1995). Fluid inclusion data from Frieda River (Eastoe, 1979; T. Leach, unpubl. report, 1995) indicate that quartz and anhydrite, associated with copper mineralization, were deposited from fluids at significantly lower temperatures (100-400°C; average 230°C) and which were more dilute (<20-25 wt % NaCl) than those that deposited the Stage I quartz (Th average 440°C; salinity >35-40 wt % NaCl). Isotope analyses indicate that sulfide and anhydrite from Panguna and Frieda River in Papua New Guinea (Eastoe, 1983) are in isotopic equilibrium, and the sulfur in anhydrite is of probable magmatic origin. It is suspected here that the carbonates in southwest Pacific porphyry copper-gold systems were deposited in response to mixing of magmatic- and meteoric-derived fluids. This is supported by isotopic studies by Zaluski et al. (1994) on calcite associated with sericite and copper mineralization in the Babine porphyry copper deposit, British Columbia.

4. Stage IV: Post-mineral phyllic, argillic and advanced argillic overprint

Pervasive quartz-sericite-pyrite alteration which displays an increasing abundance of chlorite at depth, and post-dates copper-gold mineralization, overprints other alteration assemblages and veins at shallow levels and along the margins of a number of southwest porphyry copper-gold intrusions (e.g., Yandera, Papua New Guinea; Watmuff, 1978: Frieda River, Papua New Guinea; Britten, 1981: Batu Hijau, Indonesia; Meldrum et al., 1994: Goonumbla, eastern Australia; Heithersay and Walshe, 1996). Isotopic data from southwest Pacific porphyry systems (e.g., Ford and Green, 1977; Wolfe, 1994; Heithersay and Walshe, 1996) indicate that this sericite is derived from a fluid dominated by meteoric water.

Smectite and/or kaolinite ± siderite alteration and deposition in open spaces and fractures in many of the porphyry copper systems (e.g., Cadia, eastern Australia; T. Leach, unpubl. report, 1995: Taysan, Philippines; T. Leach, unpubl. report, 1995) are inferred from X-ray diffraction data, to have formed as late hydrothermal alteration minerals, although in some cases these clays are of supergene origin. Isotope studies on late argillic alteration in the Babine porphyry copper deposit, British Columbia (Zaluski et al., 1994) indicate that the clay is derived from the reaction of host rocks with meteoric waters circulating within a hydrothermal system.

In some porphyry copper systems, renewed igneous activity has taken place during the later stage of meteoric water incursion (Sillitoe and Gappe, 1984). The emplacement of late stage stocks has locally resulted in the formation of diatreme breccia complexes proximal to the mineralized porphyry, and these may post-date and cross cut copper-gold mineralization (e.g., Dizon, Philippines; Malihan, 1987). In some circumstances, exsolution of magmatic volatiles from these late stocks may result in overprinting of the mineralized porphyry by hot acidic fluids (e.g., Wafi River, Papua New Guinea; Erceg et al., 1991). Elsewhere, the advanced argillic alteration has occurred late and is metal destructive (e.g., El Salvador, Chile; Gustafson and Hunt, 1975: Island Copper, western Canada; Mathias et al., 1995). The relationship between advanced argillic alteration and copper-gold mineralization is discussed in more detail in the following section on high sulfidation systems.

d) Summary

The emplacement of melts at shallow crustal levels is inferred to occur at dilatant portions of regional structures and is herein interpreted to produce initial zoned potassic-propylitic alteration within a magmatic-dominated regime. Hypersaline brines (> 25-30 wt % NaCl) and volatiles were released from the melt as the upper levels cool and crystallize, to deposit quartz and/or K-feldspar within stockwork and dilatant sheeted fracture systems at temperatures of >400-600°C. The release of the fluids from the melt may have been facilitated by the reactivation of the dilational structures during tectonic movement. The cooling of these fluids at shallower levels is inferred to result in the dissociation of dissolved magmatic volatiles and the progressive formation of hot acidic fluids (Rye et al., 1992), and subsequent high temperature advanced argillic alteration through rock reaction. It is inferred that although metals exsolve from the melt at this stage, the intrusion and immediate host rocks remain too hot and the fluids too saline for metal deposition to occur.

Copper-gold mineralization in porphyry environments takes place at temperatures of around 200-350°C. Metal deposition is preceded by potassic and calc-silicate alteration and Fe-oxide/sulfide mineral deposition, and is overgrown by later anhydrite and calcite/dolomite. These minerals fill pre-existing fractures/veins, open cavities and vein partings, or new fracture sets, and develop as wall rock alteration. The zonation from early to late and deep to shallow of the silicate minerals of: biotite --> K-feldspar --> actinolite --> epidote --> zeolites --> chlorite --> sericite --> pyrophyllite --> kaolin/illitic clay, is indicative of progressive cooling and decrease in fluid pH during copper-gold mineralization (Figs. 5.4, 5.5, 5.6).

This cooling may have taken place entirely through heat conduction to the country rock in small mineralized intrusions (e.g., Goonumbla, eastern Australia). In active porphyry systems in the Philippines, CO_2-rich and

dilute ground waters have been encountered down to depths of up to 1.5-2 km from the surface. These waters react with the host rocks to form similar zoned phyllic and argillic alteration (Section 2) as described above for porphyry copper-gold systems. The model of an incursion of surficial waters to facilitate the cooling of the upper levels of a larger mineralized porphyry intrusion is also supported by the meteoric isotopic signature for sericite, and the dilute conditions determined from fluid inclusion data. The information from active hydrothermal systems suggests that the meteoric waters may have migrated down the same structures which initially facilitated the emplacement of the intrusion to shallow levels (e.g., Bacon Manito geothermal field, Section 2.iv.a.3.ii). It is speculated that this can only take place once the intrusion has cooled significantly. Pressure draw down along these structures may have been initiated by renewed intrusion elsewhere within the immediate vicinity (e.g., from Cawayan to Pangas-Pulog in the Bacon-Manito Geothermal Field, Philippines; Section 2.iv.a.3.ii). Other authors (e.g., Gustafson and Hunt, 1975) and computer modelling (Norton and Knight, 1977) suggest that the meteoric waters may have migrated towards the margins of the intrusion (see also Fig. 2.12, Southern Negros Geothermal field).

Copper-gold mineralization therefore takes place at some significant time period after the intrusion has cooled and crystallized. K/Ar age dating at FSE, Philippines, has indicated the time span between early biotite alteration and late illite associated with copper mineralization may have been up to 200,000-300,000 years (Arribas et al., 1995). It is therefore speculated that the magmatic fluids and metals associated with mineralization in porphyry copper systems have probably been exsolved from the cooling and crystallizing of deeper portions of the host shallow level intrusion, or of a much larger parent melt (Fig. 5.3).

The metal-bearing magmatic fluids are therefore interpreted to have migrated from the deeper melts along reactivated fractures, including sheeted veins, typically at the margin of the intrusion. Metal deposition takes place as these fluids enter environments which have cooled to <300-350°C, in fractures which may be saturated with cool and dilute meteoric-derived waters. The cooling of magmatic-derived fluids results in progressive decrease in fluid pH in response to the dissociation of dissolved gases. This change in fluid pH is reflected in the progression in the silicate species of: potassic/calc-silicate minerals --> chlorite --> sericite --> pyrophyllite/kaolinite (Fig. 5.8). The decrease in fluid pH may also have been facilitated by the mixing of low pH CO_2-rich waters with the metal-bearing magmatic brines.

Southwest Pacific porphyry copper deposits are typically gold-rich (Sillitoe, 1993a). Variations in the Cu:Au ratios of the porphyry copper systems are herein interpreted to reflect, in part, a change from hotter environments of mineralization (more copper-rich) associated with potassic and calc-silicate alteration assemblages (e.g., Yandera, Papua New Guinea), to cooler environments (gold-rich) associated with sericite, chlorite or clay alteration assemblages (e.g., Dizon and Didipio, Philippines; Grasberg, Indonesia).

ii) Skarn Deposits

a) Introduction

Skarns are rocks comprising Ca-Fe-Mg-Mn silicates formed by the replacement of carbonate-bearing rocks during regional or contact metamorphism and metasomatism (Einaudi et al., 1981), in response to the emplacement of intrusions of varying compositions. Skarns can therefore be regarded as a specific type of alteration within a porphyry environment.

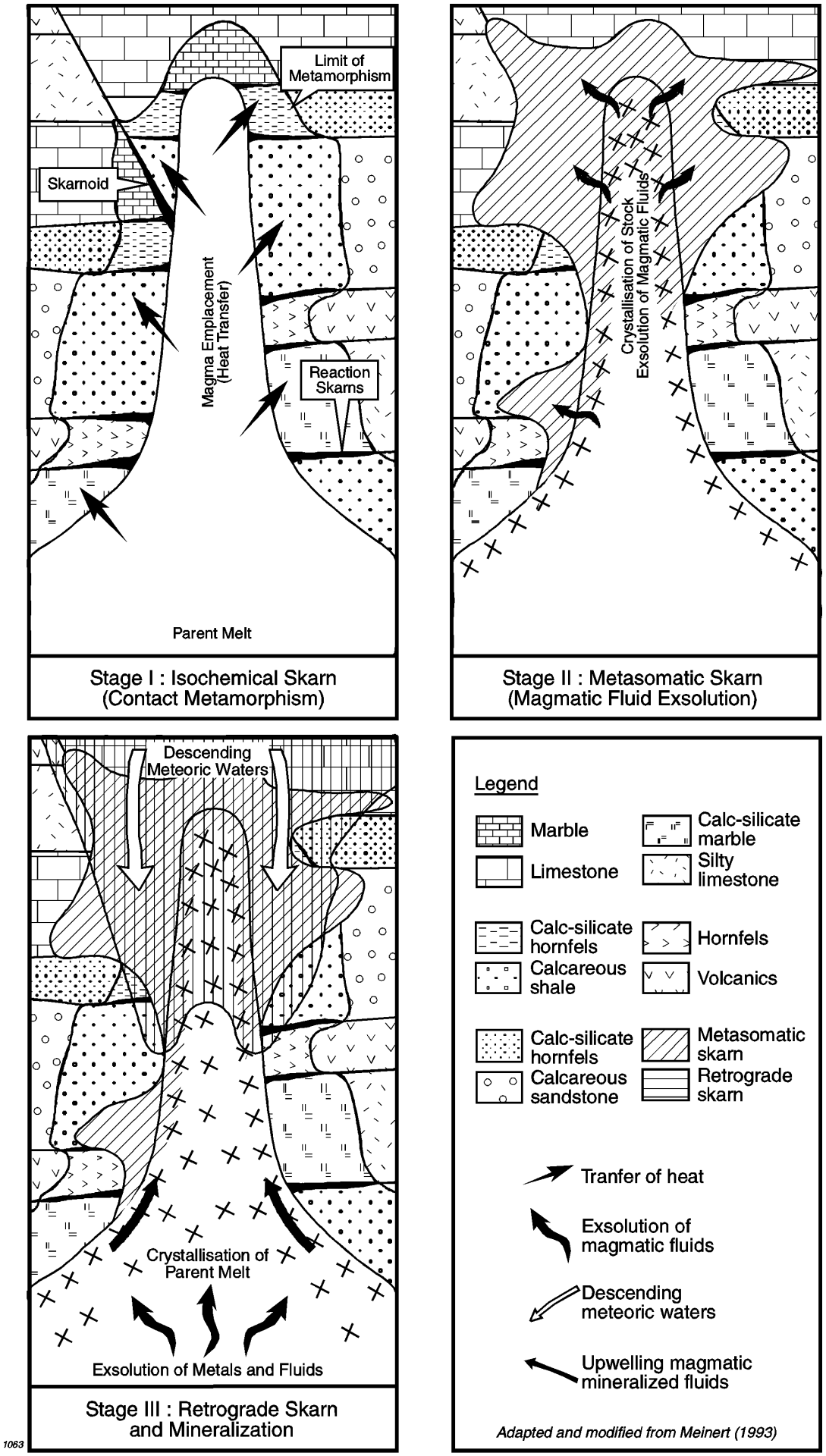

Fig. 5.7 Processes in the evolution of skarn deposits

The terms

exoskarns and endoskarns are used to describe deposits derived from sedimentary and igneous/intrusion protoliths respectively. Veins of skarn mineralogy may be present in both intrusions and carbonate sediments. Calcic skarns form by replacement of limestone and produce Ca-rich alteration products such as garnets (grossular-andradite), clinopyroxene (diopside-hedenbergite), vesuvianite, and wollastonite. Magnesian skarns form by the replacement of dolomite, and produce Mg-rich alteration minerals such as diopside, forsterite and phlogopite. Magnetite is common in magnesian skarns because iron is not taken up by the Mg-rich silicates.

Skarns typically display complex mineral assemblages and are polyphasal. Early alteration formed at high temperatures is typified by assemblages of anhydrous silicates + iron oxides. These are overprinted by later hydrous silicates and sulfides which are formed at lower temperatures. Spatial mineralogical zonations are related to both the lateral and vertical distance from the intrusion (i.e., to chemical potential and temperature gradients) and to depth (i.e., to these gradients plus pressure; Meinert, 1992).

Detailed mapping of the distribution of alteration and ore mineral phases provides information about the overall size, characteristics and genesis of a skarn system, and mineral zonations may point towards exploration targets. Models of skarn zonation are particularly useful in evaluating incompletely exposed or inadequately explored skarn systems.

Skarn deposits are not common in the southwest Pacific, although significant copper-gold skarn ore bodies occur in the Guning Bijih District, Indonesia (Ertsberg, GBT, IOZ, DOZ, DOM and Big Gossan; Mertig et al., 1994), Ok Tedi, Papua New Guinea (Rush and Seegers, 1990), Red Dome, eastern Australia (Ewers et al., 1990) and Browns Creek, eastern Australia (Creelman et al., 1990).

As skarns represent a specific class of porphyry system, they exhibit the same processes of formation described previously for porphyry copper-gold deposits. However, because the host rocks have a specific chemistry, these processes are manifest in a different manner. The following discussion is taken from detailed discussions of copper-gold skarns by Meinert (1989, 1992), Einaudi (1982a, 1982b), Einaudi et al. (1981), and T. Leach (unpubl. data).

b) Processes of skarn formation

Skarn evolution occurs in response to three main sequential processes described as: prograde isochemical, prograde metasomatic, and late stage retrograde events (Fig. 5.7). The isochemical skarn event is equivalent to the formation of zoned potassic-propylitic alteration in response to the conductive transfer of heat in porphyry copper systems. The metasomatic skarn event is comparable to the formation of quartz stockwork veins and high temperature advanced argillic alteration (barren shoulders of high sulfidation alteration) during exsolution of magmatic fluids from the crystallizing porphyry stock. Retrograde skarns are analogous to the collapse of meteoric waters and contemporaneous mineralization events outlined in section 5.ii.c.

1. <u>Prograde isochemical</u> (metamorphic, contact metamorphic, calc-silicate hornfels) <u>skarns</u>:

<u>Isochemical</u> skarns develop in settings in which intrusions are emplaced into calcareous sediments with little or no introduction of chemical components. H_2O is derived from the intrusion and CO_2 from the calcareous sediments. The skarn development is controlled predominantly by temperature and host rock composition and texture, within a predominantly conductive regime.

This contact metamorphism forms zoned thermal alteration aureoles comprising: Ca-Al silicates/hornfels in calcareous shale or marl, Ca-Mg silicates in silty dolomites, and calc-silicate marble and/or wollastonite in limestone. Metamorphic minerals are generally fine grained and the metamorphism is likely to be more extensive and/or higher grade around a skarn formed at relatively greater depth than one formed at shallower

levels. Isochemical skarns are characteristically confined to the host lithologies, and the bulk compositions for any given rock type are identical for all alteration zones. These skarns display a wide variety of mineralogy for a given number of elements. The metamorphic stage of skarn development is essentially barren of ore mineralization (Einaudi et al., 1981).

Zonations in mineralogy formed in response to decreasing temperature, and increasing concentrations of CO_2, (i.e., progressively away from the intrusion), can be generalised as:

in dolomite -
garnet -----> pyroxene -----> tremolite -----> talc/phlogopite;

in limestone -
garnet -----> vesuvianite + wollastonite -----> marble.

These changes reflect an increase in the abundance of quartz and calcite as well as a progression to a more hydrous mineralogy moving away from the source intrusion.

The iron content of garnet increases toward the intrusion, whereas the Fe:Mg ratio of pyroxene decreases. Garnet is therefore commonly dark red-brown proximal to the intrusion, and becomes lighter brown in more distal settings, and pale green within fringe marbles (Meinert, 1992).

Reaction (also termed local exchange, bimetasomatic, or calc-silicate banded) skarns form during the metamorphic event by the mass transfer of non-volatile components on a local scale between adjacent lithologies. Skarnoids result from metamorphism of impure lithologies with some mass transfer by small-scale fluid movement (Meinert, 1992).

2. Prograde metasomatic (infiltration, replacement) skarns:

The formation of isochemical skarns is followed by the development of a metasomatic or hydrothermal stage of alteration characterized by the exchange of H_2O, silica, aluminium and iron, exsolved from the crystallizing intrusion, with CO_2, calcium, and magnesium derived from the calcareous sediments (Fig. 5.10). Hydrofracturing within the cooling pluton and previously formed hornfels/isochemical skarn, is accompanied by release of magmatic fluids. The magmatic-dominated fluids ascend along the intrusion contacts, fractures, fissures, faults, sedimentary contacts, pre-skarn dikes and sills, and other zones of permeability (Meinert, 1992).

Minerals formed during metasomatic processes overprint, and commonly replace, earlier metamorphic mineral phases, and are characteristically coarser grained. Metasomatic skarns typically contain very few mineral phases for the number of components (mono- or bimineralic assemblages). Composition of alteration mineralogy need not reflect the composition or texture of the host lithologies.

Zonations in mineralogy are similar to those encountered in isochemical skarns. Garnets and pyroxenes progressively become more iron-enriched and magnesium-depleted with time. Lower temperature minerals commonly overgrow and replace mineral assemblages formed under earlier higher temperature regimes (e.g., pyroxene replaces garnet).

Einaudi et al. (1981) suggest that oxide and some sulfide deposition commence during the latter stages of metasomatic skarn development. Magnetite mineralization greatly dominates over sulfides, forming either by replacement of garnet or pyroxene at the intrusion-skarn contact, or in outer zones at the marble-skarn contacts.

The influx of acidic fluids may inhibit skarn formation in favour of the development of massive pyrite-sulfide replacement bodies and breccia pipes (e.g., Brisbee, USA; Einaudi, 1982a). In this case pervasive silicification has been superimposed upon earlier calc-silicate skarns.

3. Retrograde skarns

The previously discussed skarns are commonly referred to as prograde skarns, and form end members of a continuum which shows a progressive transition from early metamorphic to late metasomatic-dominated alteration. Retrograde skarns form in settings in which temperatures decline and fluid compositions become dominated by meteoric waters, especially where skarns develop at shallow crustal levels (Fig. 5.7).

Retrograde alteration is characterized by the replacement of earlier prograde anhydrous minerals by late stage hydrous mineral phases such as epidote, amphiboles, chlorite and clays. This reflects the leaching of calcium, and introduction of volatiles. Unlike metasomatic skarns, retrograde skarns have complex multiphase mineral assemblages. Einaudi et al., (1981) list the following as typical retrograde alteration mineralogies:

grossular garnet ---> low Fe-epidote + chlorite + calcite
andradite garnet ---> quartz + iron oxide + calcite
almandine garnet ---> biotite + hornblende + plagioclase
diopside ---> tremolite/actinolite ---> talc
forsterite ---> serpentine

This is the main mineralization event. Sulfides and minor iron oxides occur as disseminations, or within veins which transect prograde skarns, and may form massive replacements of marble. The structural control of sulfide veins and retrograde alteration is similar to that outlined for porphyry copper systems (above, Section 3.ix), and in some cases extends beyond the skarn alteration. Sulfide assemblages of pyrite-chalcopyrite (±magnetite occur proximal to intrusions, and bornite-chalcopyrite dominate in distal settings. This reflects a decrease in total iron concentration during later stages of skarn development. The sulfides are interpreted to have been deposited in response to either decreasing temperatures, neutralization of the hydrothermal solution (especially at the marble contact), or changes in oxidation state of the fluids. The association of most ore phases with late stage retrograde assemblages is interpreted to indicate that:
i) either the prograde skarn is merely a reactive host rock for later mineralizing fluids derived from a deep parent melt, or
ii) that there has been remobilization of sulfides which were deposited during prograde alteration events. However, the absence of copper-gold mineralization within prograde alteration assemblages makes this unlikely.

c) Skarn ore deposits

Ore deposits hosted in skarns are classified as skarn deposits. The following common classification of skarn deposit types is based on the dominant metal content, i.e., Cu, Au, Pb-Zn, Fe, Mo, W and Sn (Einaudi et al., 1981; Meinert, 1992; Einaudi, 1982a; Einaudi, 1982b).

Copper-gold skarns (e.g., Ertsberg, Indonesia; Ok Tedi, Papua New Guinea) and gold skarns (e.g., Red Dome, eastern Australia) represent the most economically significant skarn deposits in the southwest Pacific rim, and are associated with shallow level alkaline and calc-alkaline porphyry intrusions.

Copper skarns are typically dominated by andradite (Fe-rich) garnets, and massive garnet formation proximal to the intrusion, which grades outward via zones which contain an increasing abundance of pyroxene (Fe-poor), to distal vesuvianite and/or wollastonite near the marble contact. Garnet colour grades from red-brown, to light brown, to green, and yellow with increasing distance from the intrusion. Chalcopyrite dominates mineralization

close to the intrusion, whereas bornite occurs in wollastonite alteration zones near the marble contact. Intense retrograde alteration is common and epidote-actinolite/tremolite typically replaces prograde garnet. The presence of specular hematite may reflect a shallow oxidizing environment of formation.

Gold skarns (e.g., Red Dome, eastern Australia; Ewers et al., 1990: Gunung Bijih [Ertsberg] District, Iran Jaya, Indonesia; Mertig et al., 1995: Wabu, Iran Jaya, Indonesia; Allen et al., 1995) are associated with diorite-granodiorite plutons and commonly contain sub-economic Cu, Pb, and Zn mineralization. Potassium-feldspar, scapolite, vesuvianite, apatite and Cl-rich amphiboles are common. The presence of arsenopyrite and pyrrhotite as the main sulfide minerals is indicative of formation in a reducing environment. Most of the gold occurs as electrum in close association with bismuth and telluride minerals. Gold skarns can form in portions of large skarn deposits furthest from the intrusion. The parts of gold skarns close to the intrusion grade into copper-gold skarn deposits, and display similarities to low sulfidation quartz-sulfide gold ± copper deposits (Section 7.ii).

Lead-zinc skarns occur in distal settings relative to the source intrusions, and commonly display a decline in the intensity of skarn mineralogy development, moving away from the intrusion. In places, skarn mineralogy may be almost totally absent. Almost all minerals in lead-zinc skarns are manganese-rich. The pyroxene:garnet ratio and the manganese content of pyroxenes increase away from the intrusion. These skarns are therefore closely related to the porphyry-related carbonate-base metal-style gold systems outlined in Section 7.iii.

Elsewhere in the world, iron skarns form the largest known skarn deposits, and although mined principally for the magnetite content, many contain sub-economic amounts of Cu, Co, Ni, and Au. Some display transitional relationships to copper skarns. Iron skarns typically form in back-arc basins to island arcs in association with iron-rich diabase to diorite intrusions (Meinert, 1992). Molybdenum and tin skarns are not recognised in the southwest Pacific rim, but occur in continental rift environments associated with leucocratic and high-silica granites respectively. Tungsten skarns occur in deeply eroded calc-alkaline granodiorite to quartz monzonite batholiths.

iii) Breccia-Hosted Gold Deposits

Gold-bearing magmatic hydrothermal breccias form in volcanoplutonic terrains and display characteristics indicative of a magmatic association. Deposits of this type generally represent large tonnage low grade gold resources. Discrete breccia bodies include: in eastern Australia, Kidston (Baker and Tullemans, 1990; Baker and Andrew, 1991), Mt Leyshon (Paull et al., 1990; Orr, 1995), and Mt Rawdon (Brooker and Jaireth, 1995); in USA, Golden Sunlight (Porter and Ripley, 1985); and in Chile, San Cristobal (Corbett, unpubl. reports; Egert and Kaseneva, 1995). Sillitoe (1991b) distinguishes breccias which are derived from a higher temperature magmatic fluid (e.g., Kidston and Golden Sunlight), from phreatomagmatic (diatreme) breccias which commonly host carbonate-base metal gold deposits (Section 7.iii: e.g., Montana Tunnels, USA, Sillitoe et al., 1985; Wau, Papua New Guinea; Sillitoe et al., 1984). Mineralization associated with the magmatic hydrothermal breccias described above (Kidston, San Cristobal) therefore corresponds to the deeper low sulfidation quartz-sulfide gold ± copper style (Section 7.ii: e.g., Kidston; Section 7.ii.d) and grades upwards to the higher crustal level carbonate-base metal gold style (Section 7.iii).

Magmatic hydrothermal breccias provide pre-mineral ground preparation overlying porphyry environments from which mineralized fluids are channelled. Sheeted fracture/vein systems commonly assist in fluid transport.

iv) Porphyry-Related Alkaline Gold-Copper Deposits

Bonham (1988b) proposed the alkaline class for volcanic hosted epithermal gold-silver deposits associated with rocks in the potassium-rich composition range of syenite, trachyte, phonolites and shoshonite, and noted the

common occurrence of telluride in the ores (similar to the epithermal quartz gold-silver deposits herein, Section 7.iv). Rock et al. (1988) extended this class to include the textural term lamprophyre, to group geochemically similar calcalkaline-alkaline rocks occurring through a wide range of geological time, and suggested that these magmas could display primary gold enrichments (Rock, 1991), although subsequently disputed by some workers. Sillitoe (1996) notes that 6 of the 20 giant gold deposits in the Pacific rim are associated with the relatively uncommon alkaline or shoshonitic rock compositions, and emphasises the alkaline compositions of some gold-rich porphyry systems (Sillitoe, 1991b, 1993a). Readers are referred to recent reviews (Muller and Groves, 1993, 1995; Mutschler and Mooney, 1993; Lang et al., 1995; Richards, 1995) for detailed discussions of gold-copper mineralization associated with this group of rocks.

The identification of gold mineralization in the Tabar-Lihir-Tanga-Feni Island Chain in Papua New Guinea (Moyle et al., 1990, 1991; Licence et al., 1987; McGinnis and Cameron, 1994), which Wallace et al. (1983) describe as shoshonitic, and the similarity to host rocks at Emperor gold mine (Anderson and Eaton, 1990; Eaton and Setterfield, 1993); Porgera, Papua New Guinea (Richards, 1990) and Goonumbla, eastern Australia (Heithersay et al., 1990), and the association of many other gold-copper occurrences with potassium-rich rock types (Muller, and Groves 1993, 1995), prompted the use of exploration models based upon shoshonitic compositions during the 1980's.

Recent models (Johnson, 1987; Solomon, 1990; Wyborn, 1992; Solomon and Groves, 1994) suggest that shoshonites are derived from the remelting of mantle derived material, which Solomon (1992) associates with arc-reversal for the Tabar-Lihir-Tanga-Feni arc, and Fiji (Section 3.v.c). Sillitoe (1989, 1992) suggests that alkaline intrusions are associated with advanced extension in back-arc settings. The importance of major structures as conduits for mantle-derived melts to rise to elevated crustal positions is emphasised here. Examples include: the Porgera transfer structure localizes Porgera and Mt Kare, Papua New Guinea; the Lihir and Tabar Island chains, Papua New Guinea occur along NS rifts; the Viti Levu lineament formed parallel to the offshore North Fiji fracture zone localizes the Tavua caldera which hosts the Emperor gold mine, and the Kingston, Vuda, Tavatu, and Faddy's gold prospects, Fiji (Eaton and Setterfield, 1993).

Porphyry copper deposits hosted in alkalic igneous rocks in British Columbia display alteration and mineralization distinguished from the more common associations with calc-alkalic intrusions and volcanic rocks (Lang et al., 1995) as:
i) dominated by alteration described as albitic (sodic) and calc-silicate (garnet, diopside, actinolite, epidote) minerals in addition to biotite and K-feldspar,
ii) there is a paucity of sericitic/phyllic, argillic and advanced argillic alteration,
iii) there is an abundance of magnetite associated with mineralization,
iv) there is a near absence of quartz and the abundance of carbonate as alteration minerals.

Like southwest Pacific porphyry systems, the alkalic porphyry systems of British Columbia, are molybdenum-poor and gold-rich. Lang et al. (1995) suggest that the differences in alteration styles between the calcalkaline- and alkali-hosted porphyry systems may be related to differences in the composition of the fluid which is derived from magmas of different compositions. The Dinkidi porphyry copper-gold deposit, Didipio, Philippines (Figs 1.2, 2.1) is also hosted in alkali intrusions and exhibits some of the features described above (Garrett, 1996). Elsewhere in the southwest Pacific the silica-poor and potassium-rich compositions of shoshonitic host rocks are reflected in the alteration associated with mineralization (e.g., abundant secondary K-feldspar formerly identified as adularia and lack of quartz at Ladolam, Lihir Island [Section 7.ii.d] and Tabar Islands).

Deposit types associated with alkaline magmatism extend from porphyry environments (e.g., in the Philippines, Marian; Sillitoe, 1989; Didipio; Garrett, 1996: in eastern Australia, Goonumbla; Heithersay and Walshe, 1995: in Papua New Guinea, Ok Tedi; Rush and Seegers, 1990), to quartz-sulfide gold $\pm$ copper (e.g., in Papua New

Guinea; lower parts of Porgera and Ladolam, Lihir Island [although quartz-poor and K-feldspar-rich]); to carbonate-base metal gold (e.g., in Papua New Guinea, Porgera Zone VII, Mt Kare; Section 7.iii.i: in eastern Australia, Mt Terrible; Teale, 1995) and epithermal quartz gold-silver (e.g., in Papua New Guinea, Porgera, Mt Kare; Section 7.iv.d.1: in Fiji, Emperor gold mine; Section 7.iv.d.2). This latter group are commonly telluride-bearing (Section 7.iv). Arribas et al. (1995) note that no high sulfidation copper-gold mineralization occurs in association with these intrusive compositions. Thus alkaline gold deposits represent a group of porphyry-related gold, and gold-copper systems, which demonstrate an association with a similar style of magma source, which may be more prospective. Gold-rich porphyry deposits may form by pronounced telescoping in these systems.

We speculate that the presence of lamprophyre and other mafic dikes at many gold deposits may be indicative of a genetic association between gold mineralization of varying styles and alkaline intrusion source rocks. Lamprophyre dikes are spatially associated with mineralization in the Goldstrike District (Volk et al., 1995), Misima, Papua New Guinea (Appleby et al., 1996), dolerite (alkaline; G. Arnold, unpubl. report) dikes are intimately associated with ore at Gympie, eastern Australia (Cunneen, 1996), mafic dikes occur in the Reefton district, New Zealand (Brathwaite and Pirajno, 1993; Corbett et al., in prep). In addition, lamprophyre dikes are described as post-mineral at the Wattle Gully (Cox et al., 1995) and Hill End (Windh, 1995) slate-belt style gold deposits in eastern Australia. However, we infer that gold mineralization post-dates the host quartz reefs in many slate belt deposits, and so a genetic association between gold mineralization and lamprophyre dikes, although speculative, cannot be ruled out. The dolerite dikes at Gympie, and a mafic dike at the Blackwater mine, Reefton (above), have each been intruded along structures which host remarkably similar gold-bearing quartz reefs to those of slate belt deposits.

6 HIGH SULFIDATION GOLD-COPPER SYSTEMS

i) Characteristics

a) Classification

High sulfidation (also termed acid sulfate, quartz-alunite-enargite gold, and silica-alunite-kaolinite ± pyrophyllite gold) gold-copper systems are formed where acidic fluids dominated by reactive magmatic-derived gases, migrate vertically and laterally along structures and permeable country rock (i.e., porous lithologies, secondary fracture permeability), and undergo rock reaction and fluid mixing. These systems have the following unique characteristics (Bonham, 1986):

1. Zoned central advanced argillic, to argillic, to peripheral propylitic alteration.
2. Copper-gold-arsenic mineralization commonly, but not exclusively, with enargite/luzonite as the dominant copper mineral phase.
3. An association with calc-alkaline volcanism.

We suggest that the term acid sulfate only be used for alteration formed by collapsing low pH, surficial fluids discussed in Sections 1 and 4.

Although traditionally regarded as epithermal, high sulfidation alteration and mineralization extend with increasing depth from epithermal through mesothermal to porphyry environments (Fig. 6.1). The depths of formation of high sulfidation systems may be inferred from the alteration mineralogy in both the central silica zone (indicating the temperature of the upwelling acid fluid), and peripheral clay zones, which provide an indication of the conditions which prevailed in the host rock. The recognition of andalusite or corundum in high sulfidation advanced argillic alteration (e.g., Horse-Ivaal, Frieda River, Papua New Guinea; Lookout Rocks, New Zealand; Cabang Kiri, Indonesia) suggests that some systems formed under very hot conditions, proximal to the magmatic source. Central alunite-pyrophyllite alteration (e.g., Nena, Frieda River and Wafi River, Papua New Guinea; Gidginbung (Temora), eastern Australia) is indicative of shallow mesothermal to epithermal conditions. The predominance of low temperature alteration minerals such as dickite/kaolinite and illitic clays in other systems (e.g., Lepanto, Philippines; Maragorik, Papua New Guinea; Mt. Kasi, Fiji; Peak Hill and Dobroyde, eastern Australia), demonstrate that these systems formed at shallow epithermal levels (Figs. 6.1, 6.3).

White (1991) described high sulfidation systems on the basis of morphology and alteration mineralogy/zonations, to define differing styles characterized by type examples as: vein or El Indio, disseminated or Temora, and disseminated with local veins or Nansatsu styles. A similar classification can be applied to southwest Pacific rim high sulfidation systems, based on the styles and zonations in alteration mineralogy and the main controls on fluid flow. Three distinct end member high sulfidation styles are recognised and discussed in a later section as:
* porphyry related (termed shoulders to porphyry intrusions),
* lithologically controlled,
* structurally controlled.

Many systems are in part both structurally and lithologically controlled and so the above classification should be regarded as end members of a continuum. Many appear to be structurally controlled at depth and become lithologically controlled at higher levels where permeable lithologies are intersected and exploited by rising fluids. Lateral fluid flow is common either within permeable horizons, dilational structures, or typically at the intersection of the two. These systems may appear to be rootless during early exploration, until explored down dip of the original drill intersections or exposures (e.g., Nena, Lepanto, Mt Kasi, Gidginbung). Hybrid high-low

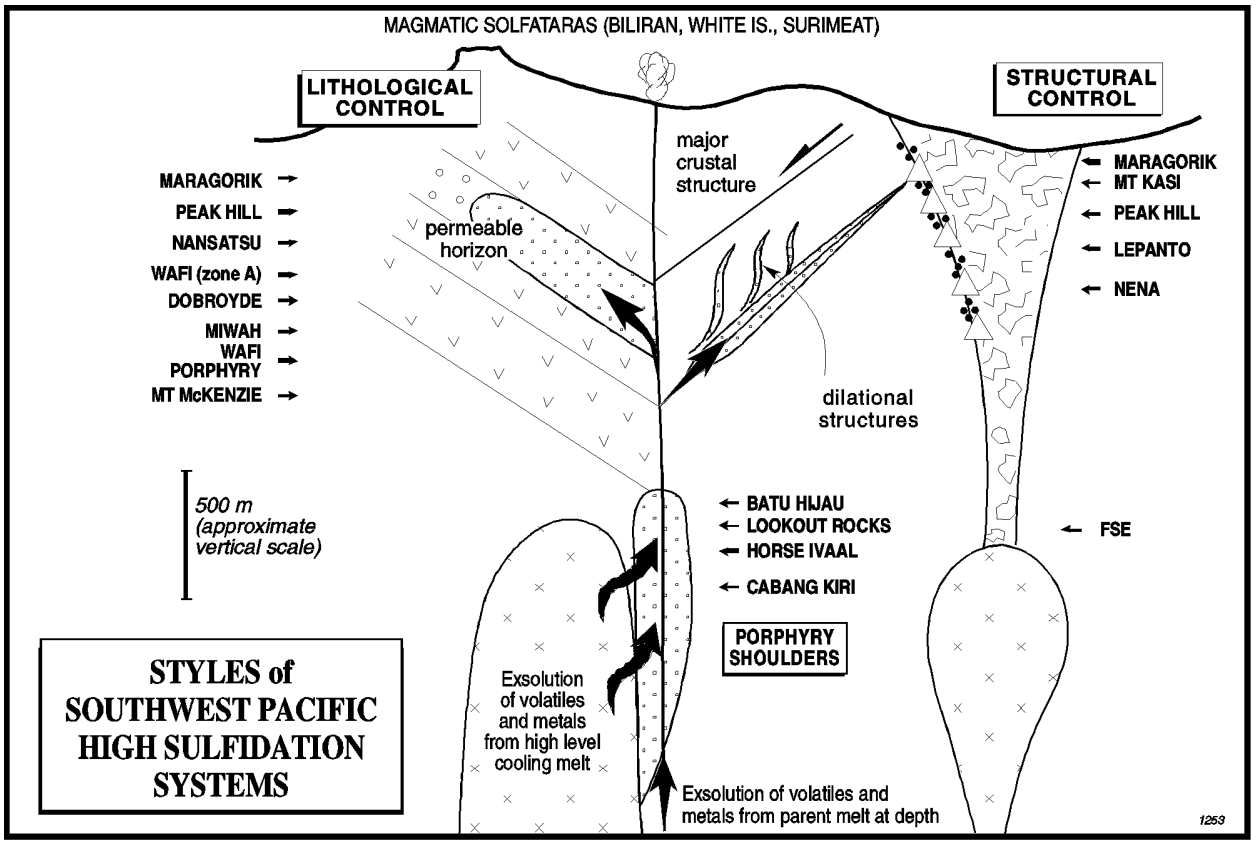
MAGMATIC SOLFATARAS (BILIRAN, WHITE IS., SURIMEAT)
LITHOLOGICAL CONTROL
STRUCTURAL CONTROL
MARAGORIK
PEAK HILL
NANSATSU
WAFI (zone A)
DOBROYDE
MIWAH
WAFI
PORPHYRY
MT McKENZIE
permeable horizon
major crustal structure
dilational structures
MARAGORIK
MT KASI
PEAK HILL
LEPANTO
NENA
500 m (approximate vertical scale)
BATU HIJAU
LOOKOUT ROCKS
HORSE IVAAL
CABANG KIRI
PORPHYRY SHOULDERS
FSE
STYLES of SOUTHWEST PACIFIC HIGH SULFIDATION SYSTEMS
Exsolution of volatiles and metals from high level cooling melt
Exsolution of volatiles and metals from parent melt at depth
1253

FIG. 6.1

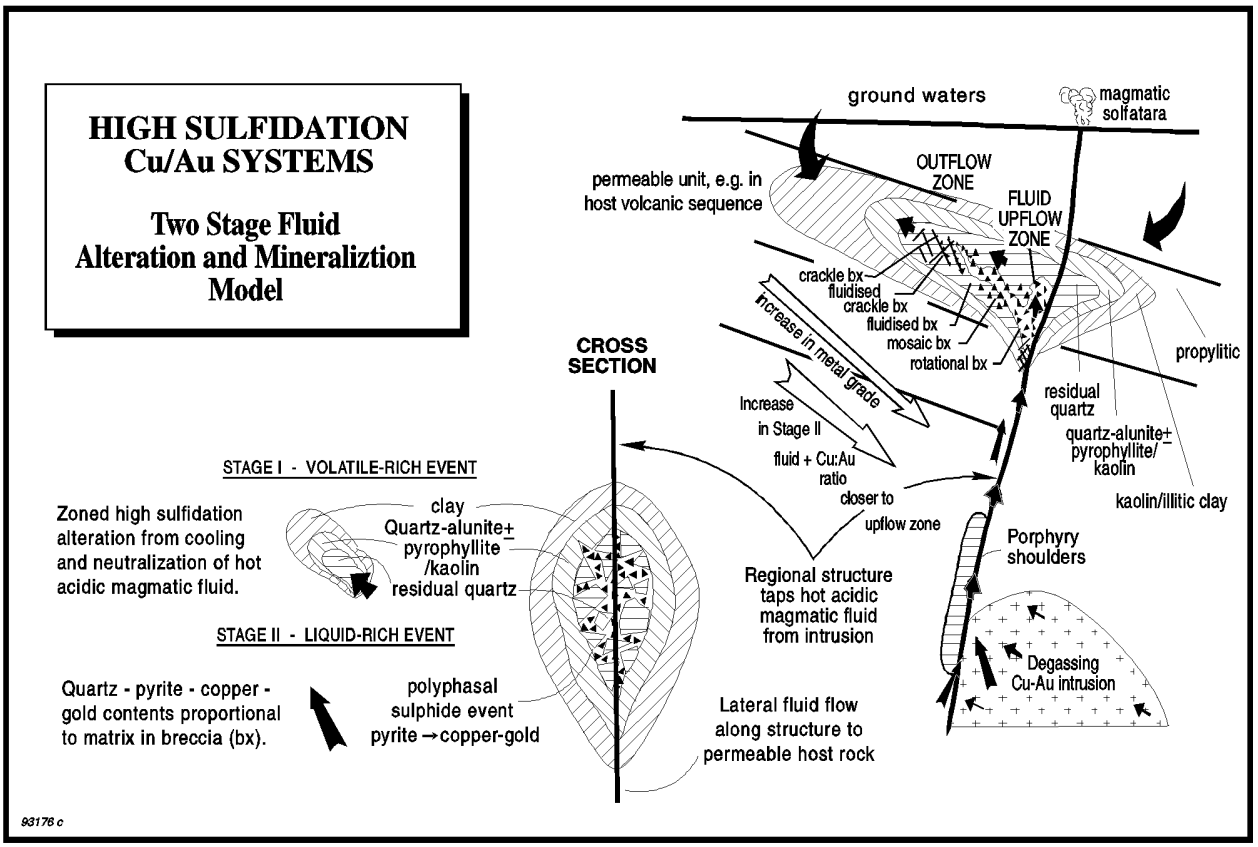
HIGH SULFIDATION Cu/Au SYSTEMS
Two Stage Fluid Alteration and Mineraliztion Model
ground waters
magmatic solfatara
permeable unit, e.g. in host volcanic sequence
OUTFLOW ZONE
FLUID UPFLOW ZONE
crackle bx
fluidised crackle bx
fluidised bx
mosaic bx
rotational bx
increase in metal grade
propylitic
residual quartz
quartz-alunite+ pyrophyllite/ kaolin
kaolin/illitic clay
CROSS SECTION
Increase in Stage II fluid + Cu:Au ratio closer to upflow zone
STAGE I - VOLATILE-RICH EVENT
Zoned high sulfidation alteration from cooling and neutralization of hot acidic magmatic fluid.
clay
Quartz-alunite+ pyrophyllite /kaolin
residual quartz
Porphyry shoulders
Regional structure taps hot acidic magmatic fluid from intrusion
STAGE II - LIQUID-RICH EVENT
Quartz - pyrite - copper - gold contents proportional to matrix in breccia (bx).
polyphasal sulphide event pyrite → copper-gold
Degassing Cu-Au intrusion
Lateral fluid flow along structure to permeable host rock
93176 c

FIG. 6.2

sulfidation and exhalative systems are also discussed.

b) Active analogues

Volatiles (H_2O, CO_2, SO_2, HCl, HF) which are channelled up major crustal faults can migrate directly from a degassing magma to the surface and vent as magmatic solfataras (Fig. 6.1). At Biliran Island, Philippines, magmatic volatiles (superheated steam and magmatic gases) vent to the surface at the Vulcan solfatara, and produce liquid sulfur flows up to 1-2 km long (Mitchell and Leach, 1991), and elsewhere have ascended into a meteoric-dominated circulating geothermal system. The presence of significant fluorine contents in geothermal waters, at an order of magnitude higher than other Philippine geothermal systems (PNOC-EDC, unpubl. data), suggests that the circulating hydrothermal system has incorporated some of the magmatic volatiles. Feeders to the magmatic solfatara were intersected by drilling at depths of 1 km, and these structures produced fluids at >310°C and pH <2 (Table 2.1).

These magmatic-derived volatiles may also contain significant metal contents. It has been interpreted (Hedenquist et al., 1993) that the magmatic discharge from the 1988 eruption at White Island, New Zealand had a metal flux of 110 tons/year copper and >350 kg/year gold. Altered rocks adjacent to the Surimeat active magmatic solfatara on Vanu Lava Island, Vanuatu, contain thousands of ppm copper and arsenic, and anomalous gold (T. Leach, unpubl. data).

c) Two stage alteration and mineralization model

A two stage model was proposed by White (1991) to explain the overprinting alteration and mineralization features encountered in many high sulfidation systems. This model is characterized by early volatile-rich and later liquid-dominated alteration/mineralization events. Features of this model (Fig. 6.2) are:

1. <u>Volatile-rich event</u>

Magmatic fluids which exsolve from a melt emplaced at shallow crustal levels ($\leq$1 kb pressure) are postulated to partition into a low density vapour (containing H_20, CO_2, SO_2, H_2S, HCl, etc.) and a hypersaline liquid (Hedenquist and Lowenstern, 1994). It has been proposed (Henley and McNabb, 1978) that the density contrast between the vapour and hypersaline liquid results in separation of the two phases within the magma chamber. The vapour phase is inferred to be more mobile than the saline liquid due to relatively low viscosity and density, and quickly ascends to shallow levels, even under lithostatic pressures (Hedenquist et al., 1994). The low density phase is interpreted to contain relatively low metal concentrations, whereas the dense hypersaline liquid may be enriched in gold, copper and other chalcophile elements (Hemley and Hunt, 1992).

The magmatic vapours are interpreted to become absorbed into ground water or circulating meteoric waters. The SO_2 disproportionates to H_2S and H_2SO_4 at temperatures below approximately 400°C (Rye, 1993), and at lower temperatures (<300-350°C; Hedenquist and Lowenstern, 1994) HCl and H_2SO_4 progressively disassociate to form hot acidic fluids (Section 1.iv, Fig. 1.4). Alteration minerals which form in rocks immediately adjacent to inferred source intrusions for the acid fluids reflect this gradual decrease in fluid pH (Fig. 6.2). These minerals are commonly zoned moving away from the degassing melt, to shallower and/or more distal settings as: mica-andalusite $\pm$ corundum, through pyrophyllite-diaspore, to quartz-alunite. The presence of andalusite, and locally of corundum, in these assemblages suggest that dissociation to form the hot acidic fluids may be initiated at temperatures of greater than 340-390°C (Hemley et al., 1980).

At shallower levels, alteration zonation in high sulfidation systems is formed in response to the progressive neutralization and cooling of hot acidic magmatic-derived fluids mainly by wall rock reaction (Steven and Ratte, 1960; Stoffregen, 1987; Fig. 6.3), and possibly to a lesser extent by mixing of the hydrothermal fluids with

locally-derived neutral, meteoric waters. Zoned alteration assemblages occur in all structurally and lithologically controlled high sulfidation systems. While overprinting may complicate these relationships, alteration assemblages can be divided into three main alteration zones: central quartz-alunite, marginal phyllic or argillic, and peripheral propylitic zones.

The quartz-alunite zone usually comprises a characteristic core of silica group minerals, mainly quartz (but at shallow levels possible cristobalite, tridymite and/or opaline silica), which typically display a vughy texture, indicative of intense acid leaching. It is interpreted (Giggenbach, 1992) that only at temperatures of <250°C can the fluid acidity become high enough (pH <2; Stoffregen, 1987) to promote complete rock destruction. Thus, while vughs form after leached pheoncrysts or rock fragments, many develop by a destruction of the primary rock texture. The quartz (and at low temperatures other silica minerals; Section 4.ii.a) is virtually the only residual mineral following the leaching of other rock components, and so this alteration is commonly termed residual quartz (silica). Lower temperature high sulfidation systems formed as high crustal levels may feature extensive silica mineral deposition. The central residual (vughy) quartz zone grades out to a silicified zone which contains alunite group minerals formed under a slightly higher (2-3) fluid pH range, as the fluid becomes progressively neutralized in response to reaction with the host rocks and/or fluid mixing.

The central silica-alunite zone is typically surrounded by marginal argillic/advanced argillic alteration assemblages of kaolin group (pyrophyllite, dickite, kaolinite) minerals which are indicative of formation at a pH of around 4. These grade outwards into illite group (sericite, illite, illite-smectite, smectite) minerals, as the fluid becomes progressively more neutralized to a pH of around 5. The mineral assemblages formed in each zone are dependent upon the temperature and pH of the upwelling acid fluid, the composition of the host rock, and the physico-chemical conditions of waters residing in the host rock. The illite group minerals grade outward to peripheral sub-propylitic chlorite-carbonate alteration assemblages, or at deeper high temperature conditions, propylitic epidote/actinolite-albite-chlorite-carbonate alteration assemblages.

The alteration zonation which forms in response to upwelling hot acidic magmatic-derived fluids, is distinct from the alteration zonation formed by descending acid sulfate waters. The latter produces alteration zones which reflect a change from surficial cool and acid, to hot and neutral conditions, with increasing depth (Fig. 6.3).

2. Liquid-rich event

It is interpreted that the dense, hypersaline and metal-rich liquid remains at depth until pressures drops are promoted by tectonic fracturing of the carapace (Section 3.ix.a), and/or crystallization of the melt, to facilitate expulsion to shallower crustal levels (Hedenquist et al., 1994). The cooling and dilution of these metal-bearing fluids, in response to wall rock reaction and mixing with ground water and/or circulating meteoric water, results in mineralization which overprints the zoned alteration formed by the earlier vapour phase.

The dense, liquid-rich phase utilises the same plumbing system as the earlier volatile-rich phase and focuses mineralized fluids into the residual or vughy quartz at the core of the zoned alteration. Competent residual quartz and quartz-alunite rocks brecciate well and so commonly host mineralization (e.g., Nena, Frieda River, Papua New Guinea; Bainbridge et al., 1994). Continuing deformation of dilational structures which channel the liquid-phase fluids may enhance breccia formation and mineralization. The metal grades of ores are commonly proportional to the degree of brecciation and introduction of sulfide matrix (Section 3.x.d.4, Fig. 3.22). The enclosing incompetent clay alteration generally displays more plastic deformation, does not fracture, and so is commonly not mineralized. A skin of barren silica-alunite alteration may rim the mineralized silica core and mask mineralization, especially if this material is relatively hard (e.g., Nena, Figs. 6.21, 6.22). In some systems the clay alteration has a damming effect and so the interface between the competent and incompetent rocks may represent a locus for higher metal grades (e.g., Binebase, Sangihe Is, Indonesia).

Although in most high sulfidation systems copper-gold mineralization post-dates the formation of the zoned alteration, significant gold and copper mineralization is locally encountered in the clay zones formed during the initial vapour dominated alteration event (e.g., Zone A, Wafi River, Papua New Guinea; Leach and Erceg, 1990: Peublo Viejo, Dominican Republic; Muntean et al., 1990). It has been postulated that some metals may partition into the volatile phase with time (Candela and Piccoli, 1995), and also that under unusually high pressures the vapour phase can contain significant metal concentrations (Hemley et al., 1992).

d) Mineralization

During the liquid-rich event, sulfide mineralization fills leached vughs and additional open space in fractures and breccias, and is commonly associated with sulfate (alunite or barite) deposition. The grade of the gold-copper mineralization may be proportional to the quantity of sulfide breccia matrix in styles of hydrothermal injection breccias, which grade from fluid upflow to outflow settings as: rotational --> mosaic --> fluidized --> fluidized crackle --> crackle breccias (Section 3.x.d.4. Fig. 3.22: e.g., Mt Kasi, Fiji; Corbett and Taylor, 1994).

The common sequence of deposition is: sulfate --> iron sulfide --> copper sulfide. The initial liquid-rich brine may be oxidized and buffered mainly by magmatic gases to deposit early sulfates, whereas sulfides are deposited from a later, more reducing liquid which is buffered predominantly by the wall rock (Giggenbach, 1991). Sulfide deposition may display a polyphasal character in which the early deposition of iron sulfides is followed by the deposition of copper sulfide minerals. A similar sequence of initial iron sulfides and later base metal sulfides is also characteristic of low sulfidation intrusion-related gold-copper mineralization, especially the deep level quartz-sulfide gold $\pm$ copper systems. This sequence of metal deposition is inferred by the authors to reflect either selective metal partitioning during melt crystallization, or preferential early precipitation of the iron sulfides from solution relative to the copper sulfides.

Pyrite represents the predominant iron-sulfide mineral phase at all depths, whereas marcasite and melnicovite-pyrite are common only at shallow levels. Arsenean pyrite is encountered only in marginal argillic and propylitic alteration zones. In some systems polyphasal pyrite is evident as early coarse pyrite overprinted by later fine pyrite-quartz, commonly as banded massive sulfide veins or as the matrix to breccias. Copper deposition typically occurs as the last event, filling vughs, fractures and breccias, generally as overgrowths to earlier pyrite and sulfates.

High sulfidation systems exhibit zonations in metals and sulfide minerals, both vertically from deep levels proximal to intrusion source rocks, grading to higher crustal levels, and laterally from silicic core zones, to marginal argillic-propylitic alteration zones (Fig. 6.4). The Cu:Au ratios decrease from deeper porphyry to higher epithermal levels. At intermediate depths high sulfidation systems display arsenic-rich compositions, and at very shallow near surface levels, enrichments in tellurium, antimony and locally mercury are common. The central quartz-alunite alteration zones are copper-arsenic-rich, whereas the adjacent quartz-pyrophyllite/dickite/kaolinite alteration commonly contains lead-zinc mineralization.

The zonation in the sulfide minerals reflects that of metals (Fig. 6.4). Hypogene covellite is commonly the main copper sulfide mineral at deeper levels proximal to the intrusion source (e.g., porphyry zone at Wafi River, Papua New Guinea), whereas enargite and luzonite occur in more distal environments as the main copper-bearing minerals in high sulfidation systems (e.g., Zone A, Wafi River and Nena, Frieda River, Papua New Guinea; Lepanto, Philippines). A transition from enargite to the lower temperature polymorph luzonite occurs in cool outflow zones (e.g., Nena, Fig. 6.23). Antimony, tellurium, vanadium and mercury substitute for copper and arsenic at shallow epithermal levels, and form mineral phases such as stibioluzonite, goldfieldite, sulvanite and

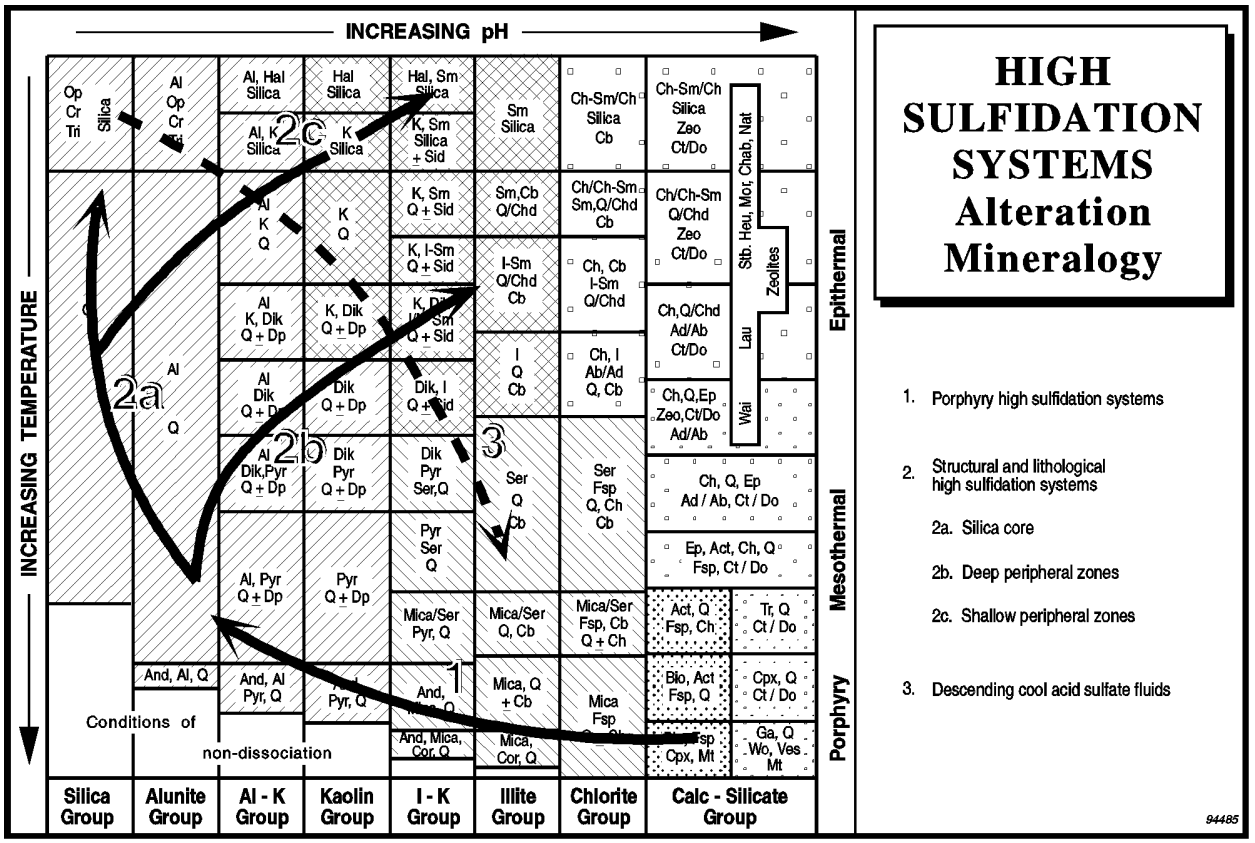

FIG. 6.3

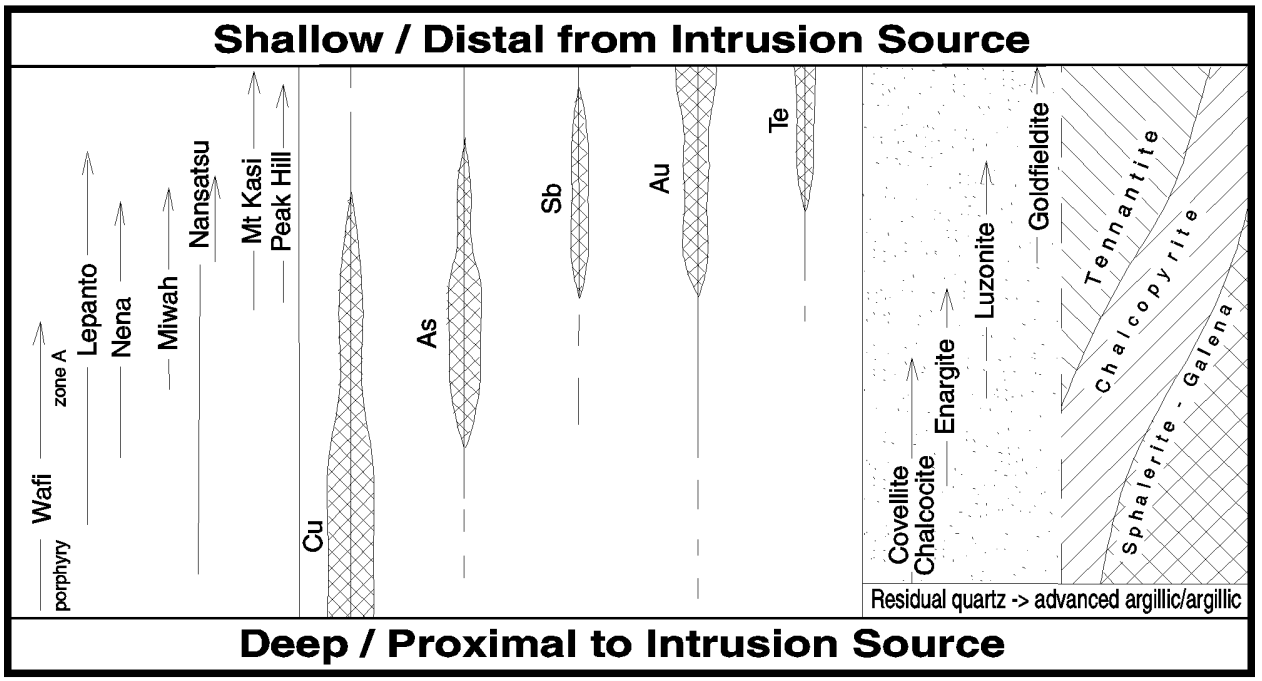

Zonations in Metals and Copper Sulfides in High Sulfidation Systems

FIG. 6.4

schwazite respectively (e.g., Mt. Kasi, Fiji; shallow levels at Nena). The occurrence of antimony-, vanadium-, tellurium- and mercury-bearing mineral phases at epithermal levels in high sulfidation systems is comparable to shallow levels in many intrusion-related low sulfidation gold deposits.

Generally, the copper sulfide phases become progressively more iron-rich moving from the central quartz zones to more distal advanced argillic/argillic zones (Fig. 6.4). This zonation is: covellite --> chalcopyrite, at deep levels (e.g., Wafi River, Papua New Guinea); and enargite/luzonite --> tennantite --> chalcopyrite, at shallow levels (e.g., Peak Hill, eastern Australia). Galena and sphalerite are common clay-rich zones marginal to the quartz-alunite cores.

High sulfidation systems in the southwest Pacific are commonly silver-poor (Section 4.e). Gold typically displays very high fineness (> 900), and occurs at deeper level systems as submicroscopic inclusions in sulfides, in the lattice of sulfides, or as free native gold or Au-tellurides at shallower level gold deposits. Gold is commonly associated with the copper minerals, however in some systems significant quantities of gold occur in association with, and are locally encapsulated within pyrite (e.g., Zone A, Wafi), especially those where it immediately pre-dates copper mineralization.

ii) High Sulfidation Systems Formed as Shoulders to Porphyry Intrusions

a) Characteristics

Porphyry-related high sulfidation alteration may occur immediately adjacent to the inferred porphyry source for the acidic fluids (e.g., Horse-Ivaal, Frieda River, Papua New Guinea; Lookout Rocks, New Zealand; Cabang Kiri, Indonesia). Although also referred to as lithocaps (Sillitoe, 1995b), the term shoulder is preferred here to account for the exploitation by acidic fluids of fracture permeability at intrusion margins, and adjacent dilational structures (e.g., Batu Hijau, Indonesia; Lookout Rocks, New Zealand; Horse Ivaal, Frieda River, Papua New Guinea).

Advanced argillic zones marginal to high-level intrusions are interpreted to form early in the development of the porphyry-related hydrothermal system. In active porphyry systems in the Philippines (Section 2), hot acidic fluids form after the zoned propylitic-potassic alteration (e.g., Alto Peak), but pre-date the collapse of surficial waters (e.g., Palinpinon, Southern Negros).

As outlined above, the progressive increase in acidity upon cooling results in a zonation of alteration mineralogy away from the intrusion as: mica-andalusite --> pyrophyllite-diaspore --> quartz-alunite. This zonation may be evident in the topography as silicified (quartz-alunite) ridges distal to the intrusion, and more deeply eroded valleys in the mica-andalusite alteration proximal to the intrusion. Dilatant fractures at the intrusion contacts typically act as fluid conduits (e.g., Horse-Ivaal, Frieda River, Papua New Guinea: Lookout Rocks, New Zealand: Batu Hijau, Indonesia; Meldrum et al., 1994). The term ledges is commonly used to describe silicified zones which display tabular either vertical or flatly dipping morphologies.

The high alteration temperature in porphyry environments inhibits formation of extremely acidic fluids (Giggenbach, 1992). Therefore, the silicification formed at depth, lacks the vughy character of residual quartz formed from rock leaching by very acidic fluids (pH<2) in shallower level ore-related high sulfidation systems. Corundum is locally encountered in these high temperature alteration zones immediately adjacent to some intrusions (e.g., Cabang Kiri, Indonesia; Lowder and Dow, 1978). Very coarse grained muscovite may be associated with advanced argillic alteration, and the intergrowth with alunite is diagnostic of high sulfidation systems at porphyry depths (T. Leach, unpubl. data). Some high sulfidation systems proximal to source intrusions are enriched in halogens derived from the magmatic volatiles. This is pronounced in those systems sourced from more felsic intrusions, and in which mineral phases include topaz (e.g., Bilimoia, Corbett et al.,

1994b), dumortierite (after tourmaline, e.g., Island Copper, Mathias et al., 1995), apatite, and zunyite (e.g., Wild Dog, Section 6.iv.b.1).

Porphyry-related shoulders of high sulfidation (advanced argillic) alteration are typically barren of significant gold-copper mineralization. It is speculated that the formation of acidic fluids may be initiated under these deep, high temperature conditions (>300-350°C), but this is not interpreted to represent a favourable environment for metal deposition which occurs at lower temperatures (<300°C; Hedenquist et al., 1994).

b) Examples

1. Horse-Ivaal, Frieda River Copper, Papua New Guinea

The Horse-Ivaal porphyry copper deposit, within the Frieda River porphyry complex of northwest Papua New Guinea, is described in detail by Britten (1981) and Leach (unpubl. reports, 1992-1996) and summarised by Asami and Britten (1980) and Hall et al. (1990). The Horse-Ivaal deposit is centred around the fine grained Horse microdiorite which has been emplaced into an older diorite porphyry and andesite volcanics. Copper mineralization, mainly as chalcopyrite, is associated with late sericite-chlorite + anhydrite alteration and veins, which post-date the formation of quartz stockwork veins and zoned advanced argillic, potassic (biotite + K-feldspar) and propylitic alteration.

Two zonations in alteration mineralogy are evident at Horse-Ivaal (Figs. 6.5, 6.6):
1. There is a progressive change from potassic alteration characterized by biotite and K-feldspar, laterally to propylitic alteration characterized at higher levels by actinolite-epidote-albite and albite-biotite at depth. These alteration assemblages, formed during early stages of development of the hydrothermal system, are indicative of a progressive temperature decrease (possibly by conduction) away from the intrusion heat source.
2. Phyllic - advanced argillic alteration along the western contact of the Horse microdiorite is zoned from deeper to shallow levels as: quartz-andalusite-mica/sericite --> quartz-andalusite-diaspore --> quartz-pyrophyllite-diaspore --> quartz-alunite-pyrophyllite-diaspore. Figure 6.3 illustrates that this zonation is indicative of a progressive decrease in fluid pH, interpreted to result from gradual disproportionation of magmatic volatiles, which evolved from the crystallising melt, and migrated along the same structures that facilitated the emplacement of the pluton.

The shoulder of advanced argillic alteration formed peripheral to the Horse-Ivaal porphyry copper-gold deposit, is typical of many other similar zones of high sulfidation alteration in the southwest Pacific rim, in which the fluid chemistry is dominated by sulfur in the form of SO_2. The unmineralized nature of the Horse-Ivaal high sulfidation alteration may result from the high alteration temperature (>350-400°C, based on andalusite; Sverjensky et al., 1991), which would prohibit the deposition of mineralization (Hemley et al., 1992). Local copper mineralization hosted in advanced argillic alteration at Ivaal is associated with later cross cutting chalcopyrite-sericite veinlets (T. Leach, unpubl. data).

2. Lookout Rocks, New Zealand

A jog in the Hauraki graben fault which separates the Hauraki graben from the Coromandel Peninsula hosts the Ohio Creek copper-gold porphyry, the Lookout Rocks high sulfidation shoulder, and the Thames 1.3 million oz gold deposit (Figs. 7.47, 7.48). Dextral movement on the graben structures, associated with oblique convergence, has produced a series of dilational fractures which host ledges of high sulfidation alteration formed as shoulders adjacent to the Ohio Creek porphyry and the auriferous quartz veins in a more distal setting at Thames (Fig. 7.48).

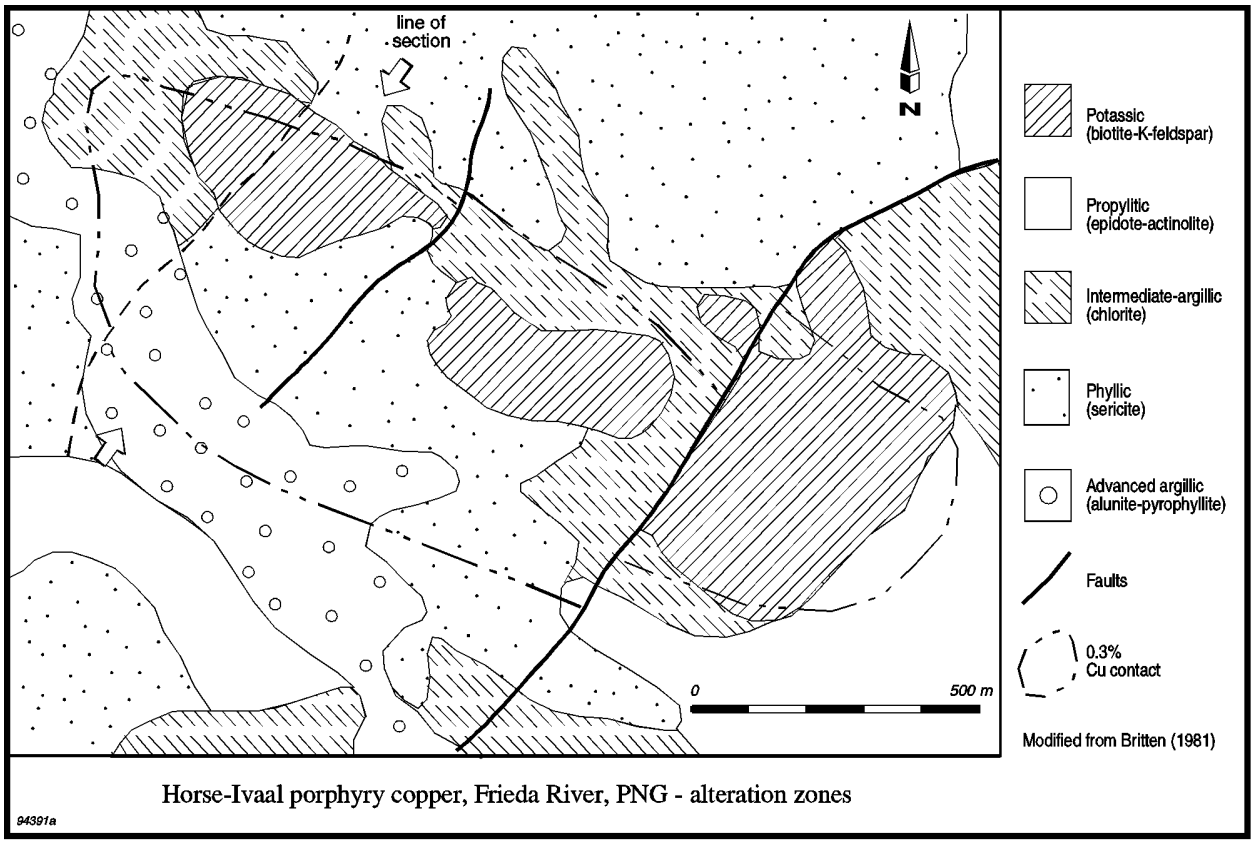
line of section
N
0
500 m
Potassic (biotite-K-feldspar)
Propylitic (epidote-actinolite)
Intermediate-argillic (chlorite)
Phyllic (sericite)
Advanced argillic (alunite-pyrophyllite)
Faults
0.3% Cu contact
Modified from Britten (1981)
Horse-Ivaal porphyry copper, Frieda River, PNG - alteration zones
94391a

FIG. 6.5

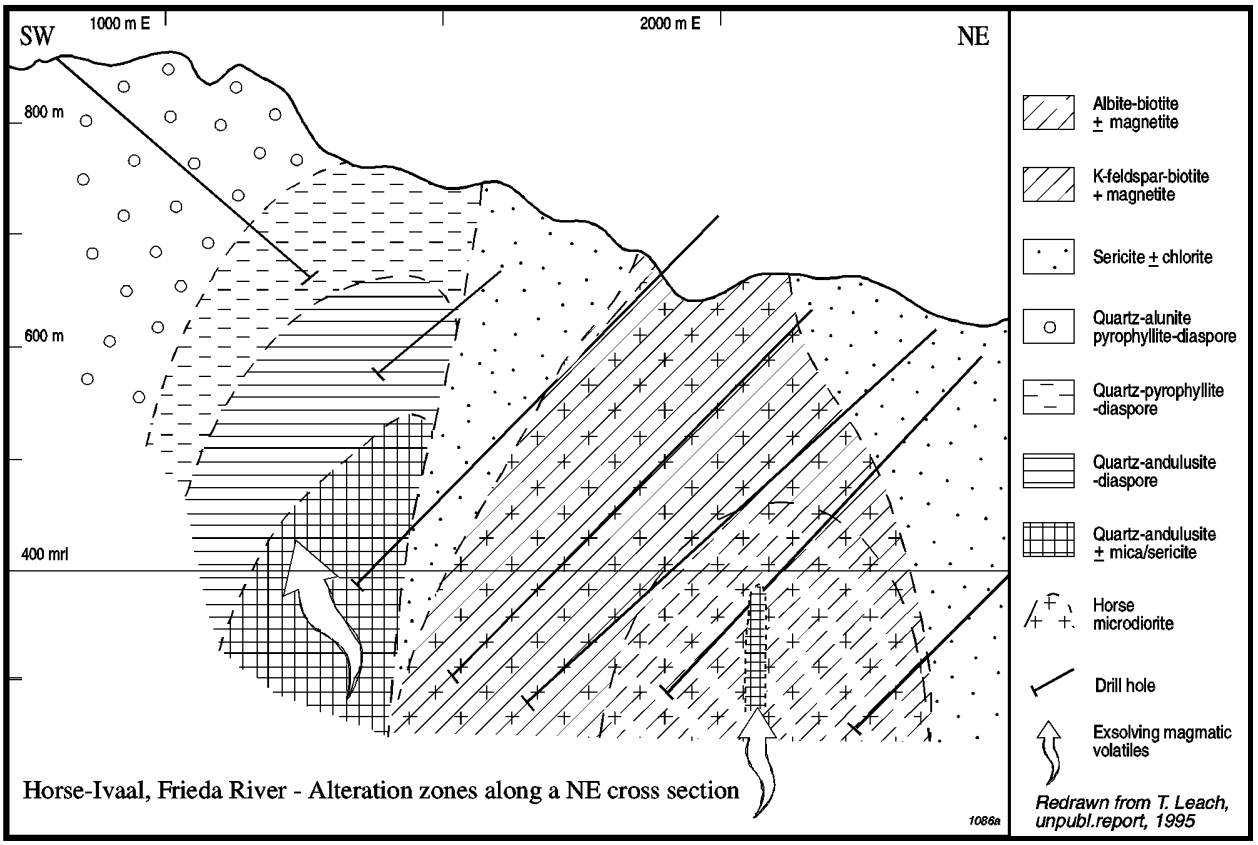
SW
1000 m E
2000 m E
NE
800 m
600 m
400 mrl
Albite-biotite ± magnetite
K-feldspar-biotite + magnetite
Sericite ± chlorite
Quartz-alunite pyrophyllite-diaspore
Quartz-pyrophyllite -diaspore
Quartz-andulusite -diaspore
Quartz-andulusite ± mica/sericite
Horse microdiorite
Drill hole
Exsolving magmatic volatiles
Horse-Ivaal, Frieda River - Alteration zones along a NE cross section
1086a
Redrawn from T. Leach, unpubl.report, 1995

FIG. 6.6

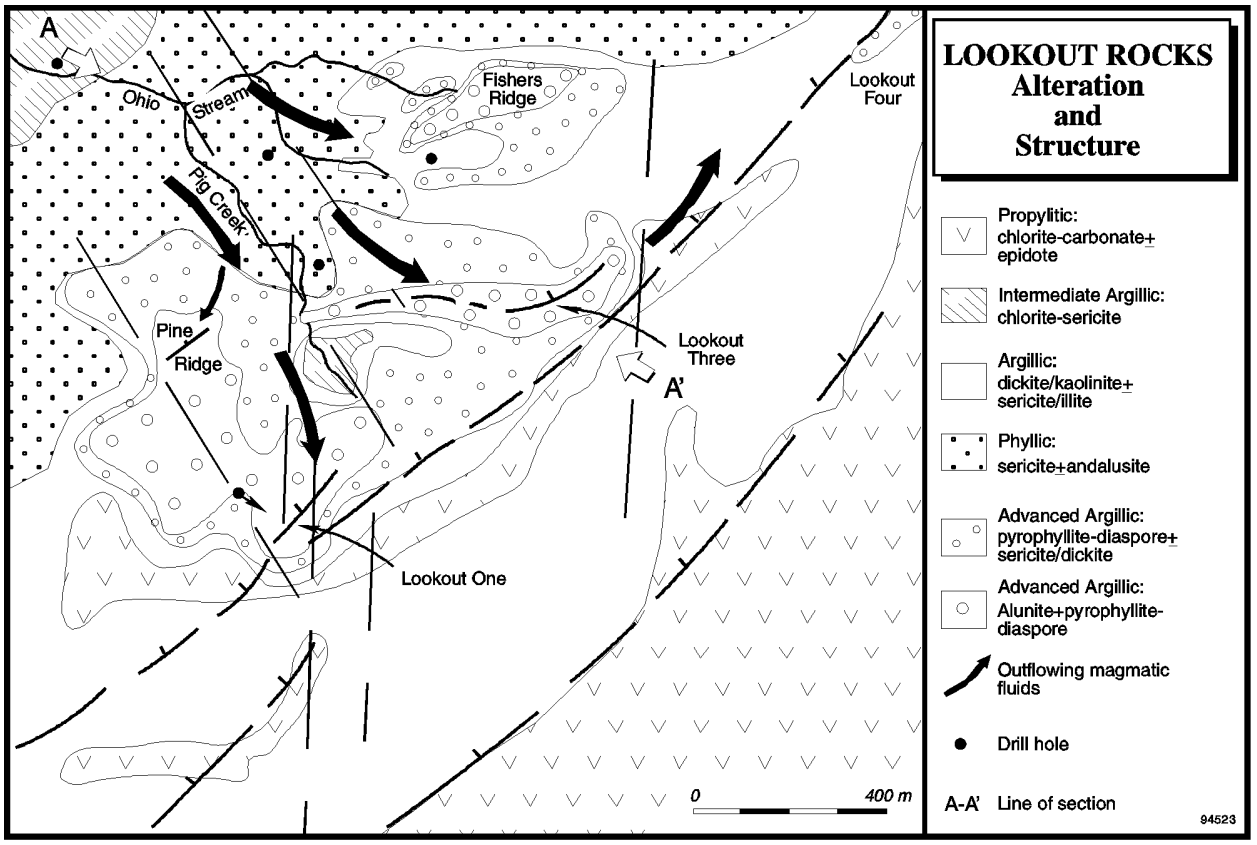
LOOKOUT ROCKS
Alteration
and
Structure
A
A'
Ohio Stream
Pig Creek
Fishers Ridge
Lookout Four
Pine Ridge
Lookout Three
Lookout One
0
400 m
Propylitic: chlorite-carbonate± epidote
Intermediate Argillic: chlorite-sericite
Argillic: dickite/kaolinite± sericite/illite
Phyllic: sericite±andalusite
Advanced Argillic: pyrophyllite-diaspore± sericite/dickite
Advanced Argillic: Alunite+pyrophyllite-diaspore
Outflowing magmatic fluids
Drill hole
A-A' Line of section
94523

FIG. 6.7

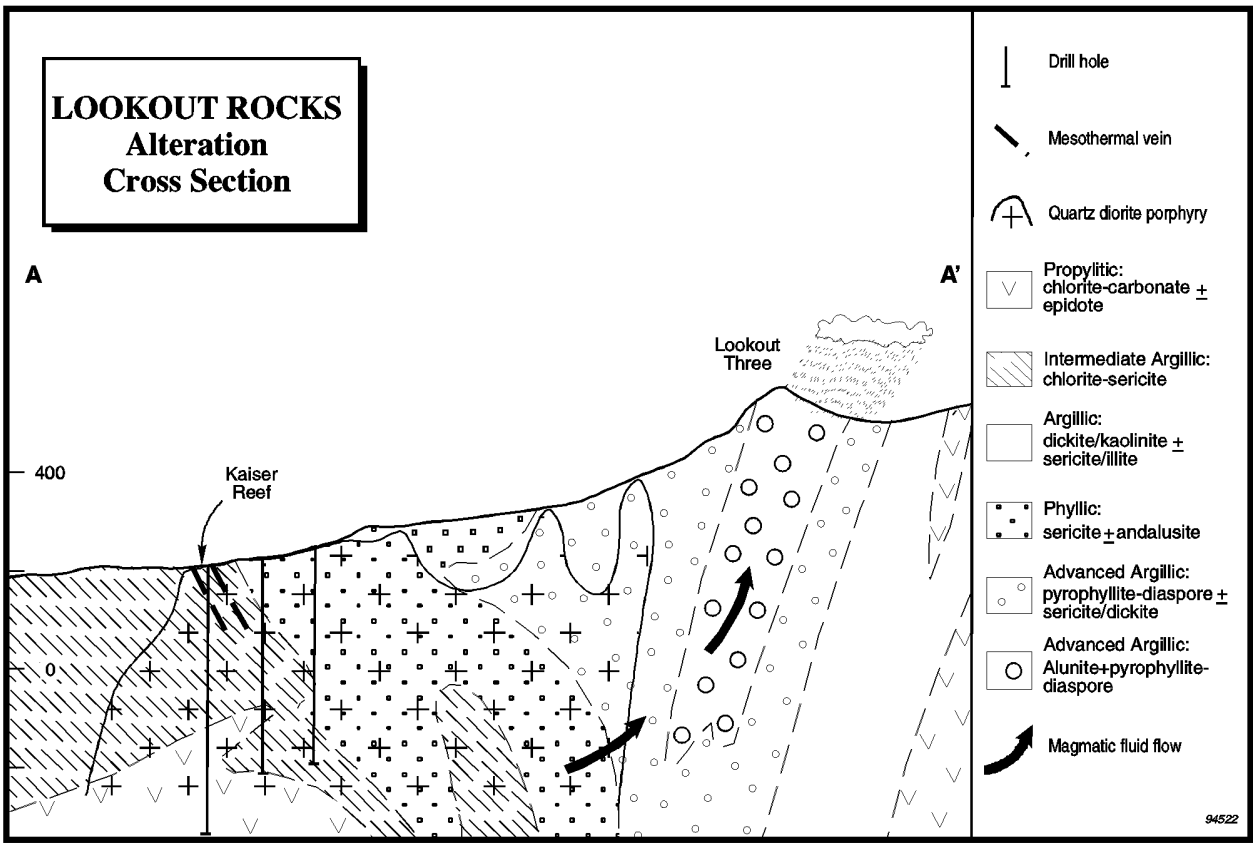
LOOKOUT ROCKS
Alteration
Cross Section
A
A'
Lookout Three
400
Kaiser Reef
0
Drill hole
Mesothermal vein
Quartz diorite porphyry
Propylitic: chlorite-carbonate ± epidote
Intermediate Argillic: chlorite-sericite
Argillic: dickite/kaolinite ± sericite/illite
Phyllic: sericite ± andalusite
Advanced Argillic: pyrophyllite-diaspore ± sericite/dickite
Advanced Argillic: Alunite+pyrophyllite-diaspore
Magmatic fluid flow
94522

FIG. 6.8

Scout drilling in the 1970's defined copper-gold-molybdenum mineralization associated with the Ohio Creek porphyry (Merchant, 1986). The copper mineralization occurs in narrow quartz stockwork veins typically hosted near intrusion contacts of the quartz diorite porphyry stock and host andesitic volcanics. The mineralization does not extend into the Lookout Rocks high sulfidation alteration to the southeast (Fig. 6.7). Auriferous quartz-sulfide veins (e.g., Kaiser Reef) occur in the andesitic host rocks adjacent to the Ohio Creek porphyry (Merchant, 1986) and were the target of small scale mining last century.

Immediately southeast of the Ohio Creek porphyry, a number of discrete dipping ledges of advanced argillic alteration which form the Lookout Rocks occur as an arcuate series of silicified ridges extending over an elevation of several hundred metres, and for a strike distance of over 1000 m (Figs. 7.48, 6.7). The alteration mineralogy comprises assemblages which are zoned from depth adjacent to the Ohio Creek porphyry towards the southeast and higher elevations in the volcanic rocks (Fig. 6.7) as: epidote-chlorite (propylitic), chlorite-sericite (intermediate argillic), sericite-andalusite-quartz ± tourmaline-apatite-pyrophyllite (phyllic), pyrophyllite-diaspore-quartz (advanced argillic). Further to the south and east, the pyrophyllite-diaspore assemblages grade into intensely silicified zones dominated by progressively more abundant alunite as alunite ± pyrophyllite-diaspore alteration (Figs. 6.7, 6.8). These zonations in alteration mineralogy are indicative of a gradual decrease in fluid pH from deeper porphyry levels to shallow levels at Lookout Rocks (Fig. 6.3).

Cooling and neutralization of this hot acidic fluid continued towards the southeast and formed dickite-kaolinite, illitic clays, and chlorite-carbonate + illitic clays (outer propylitic) alteration assemblages. The presence of andalusite, tourmaline and apatite demonstrate that the alteration at Lookout Rocks took place at high temperatures from fluids containing a significant magmatic component. It is interpreted that changes in fluid pH resulted from the progressive disproportionation of reactive magmatic volatiles emanating from the magmatic source. These volatiles were channelled along ring fractures and then into the dilatant structures to form the ledges by reaction with ground waters. Quartz-sulfide veins occur adjacent to the Ohio Creek porphyry which is cut by late stage andesite dikes (Merchant, 1986). Gold mineralization in the distal quartz reefs is discussed in Section 7.iv.d.2.

3. Vuda, Fiji

High sulfidation alteration in the Vuda Valley, eastern Viti Levu, Fiji (Figs. 1.2, 6.9), has been explored for porphyry copper and epithermal gold mineralization (Colley and Flint, 1995). Minor gold production is recorded from several small, mainly pre-World War II mines located outside the high sulfidation alteration. Some of the early exploration data (G. Corbett, unpubl. data, 1985; Austpac Gold Prospectus, 1986) has been reinterpreted in the light of new models.

Late Miocene shoshonitic lavas and autoclastic breccias dominate as host rocks, and recent gravity data is consistent with a continuation of outcropping intrusive rocks, to depth below the alteration zone (Colley and Flint, 1995). The alteration is zoned about feeder structures which occur as arcuate siliceous ridges and may represent caldera ring fractures. Alteration grades laterally through: quartz-alunite, to pyrophyllite, coarse grained euhedral diaspore, and clay dominant assemblages (Figs. 6.9, 6.10). Zonation to lower temperature high sulfidation alteration to the north and a propylitic altered intrusion to the south combined with the overall shape of the alteration system, are indicative of possible northward tilting (Fig. 6.9).

Extensive trenching and drilling in 1985-87 showed that the acid alteration is essentially barren, and from the style and nature of the alteration, the system formed at too high a temperature to be regarded as epithermal (in the then terminology). Most gold mineralization in the district occurs outside the high sulfidation alteration, typically with adularia, on fractures and within vughs, in relatively fresh rock. Minor gold in the altered areas may have formed by the overprinting of clay alteration on existing mineralization. The Natalau was the most

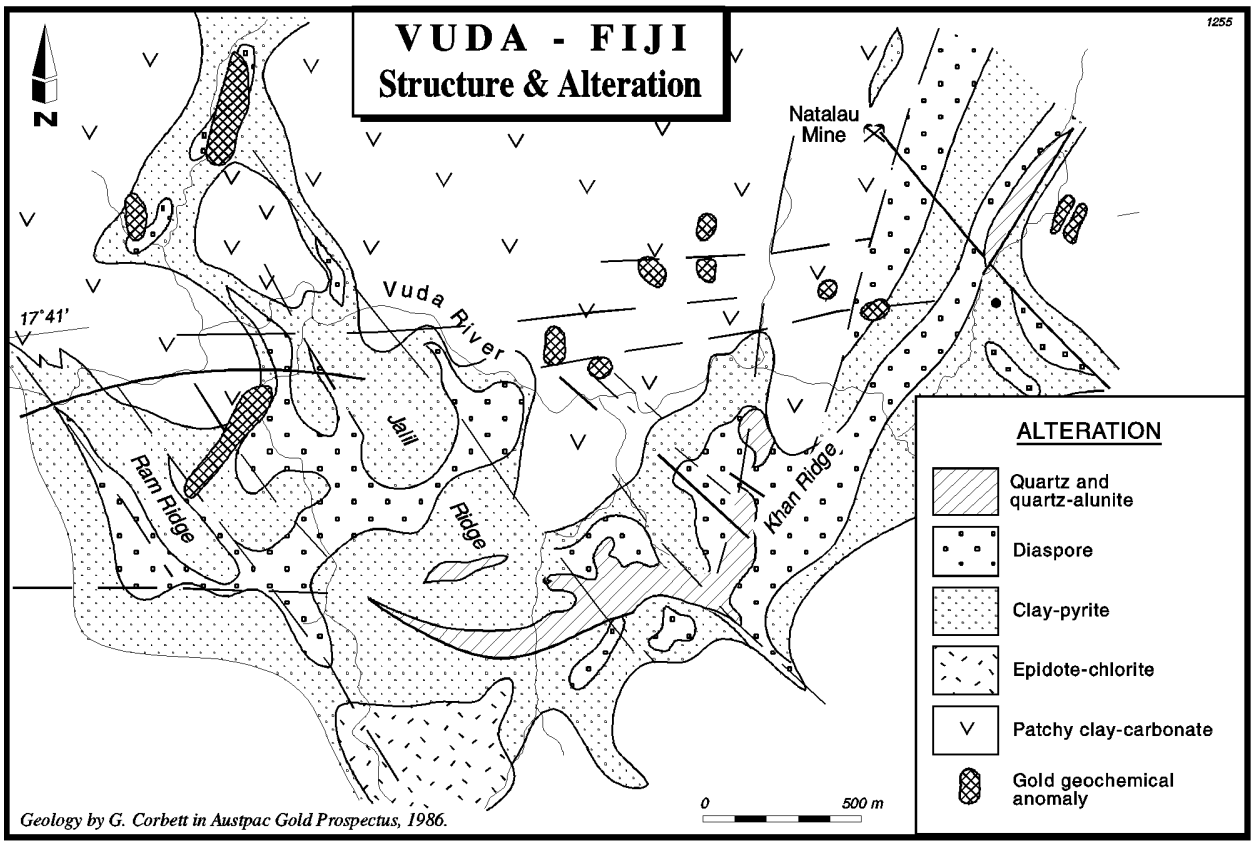

FIG. 6.9

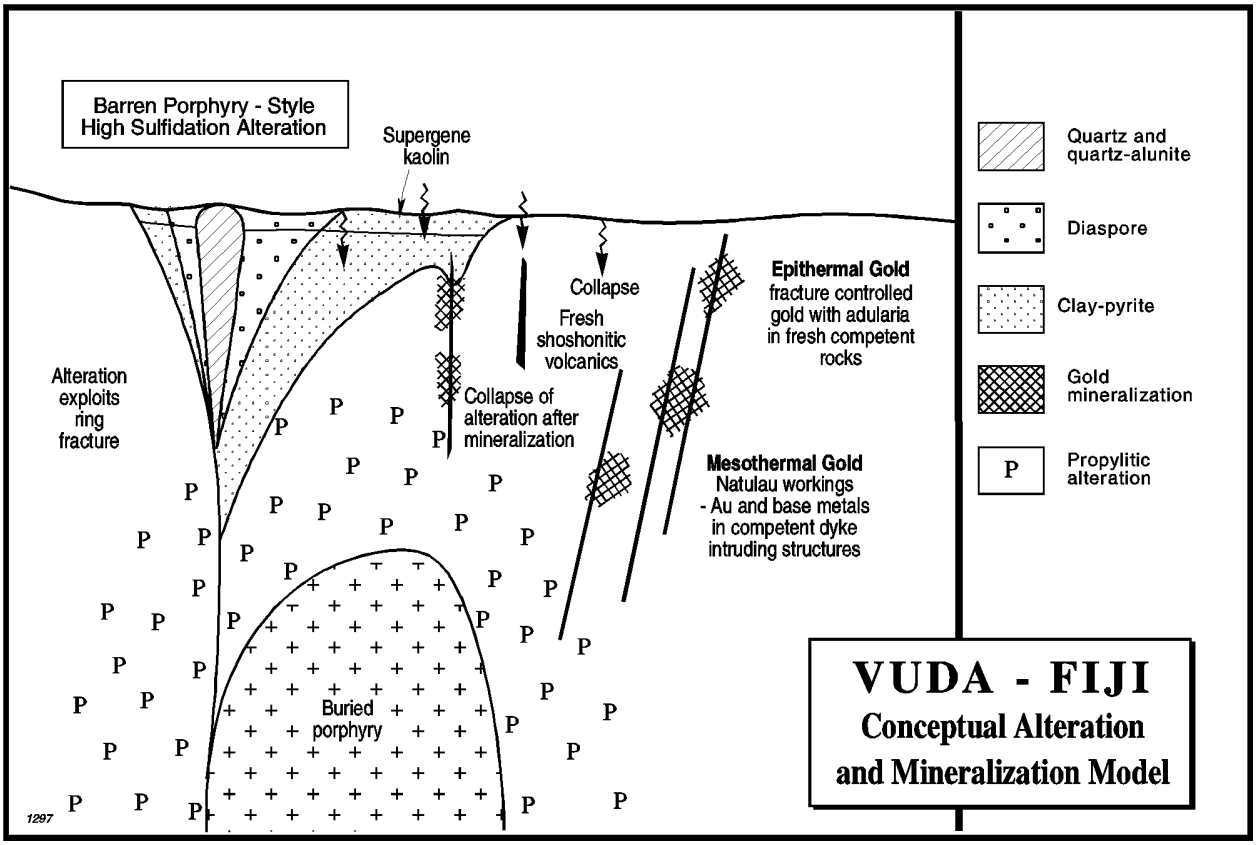

FIG. 6.10

significant mine with a production of 880 ounces of gold to 1954 (Colley and Flint, 1995). Here, gold mineralization is associated with pyrite and base metal sulfides, which have exploited pre-existing structures on the margins of a mafic dike (S. Henderson, pers commun., 1993). Lawrence (1984) describes the fineness of the Natalau gold as 850, which along with the mineralogy, is typical of gold found in low sulfidation quartz-sulfide gold ± copper style mineralization formed peripheral to porphyry intrusions, rather than in the low sulfidation epithermal environment (Fig. 4.8). Drilling intersected porphyry-related phyllic (sericite-anhydrite-quartz), argillic altered clay matrix breccias, and propylitic alteration in the footwall of the feeder structures for the high sulfidation alteration.

It is proposed herein (Fig. 6.10) that the high sulfidation alteration formed within feeder structures above and subjacent to a shallow intrusion, now evident on the gravity data (Colley and Flint, 1995). Gold mineralization at the Natalau mine is interpreted to be of the quartz-sulfide ± copper style (Section 7.ii), which typically forms peripheral to many Pacific rim porphyry intrusions, and grades to localized distal low sulfidation porphyry-related epithermal gold mineralization (Section 7.iv). Vuda was targeted as epithermal style gold mineralization from the association of gold, adularia and alunite (Austpac Gold Prospectus, 1986). However, potassium-rich shoshonitic host rocks readily deposit secondary K-feldspar, and so adularia need not be indicative of gold deposition by boiling in an epithermal environment. The alunite is now interpreted to be of a high temperature, rather than a low temperature acid sulfate origin, typical of epithermal settings (Section 8).

4. Cabang Kiri, Indonesia

Copper mineralization at Cabang Kiri in the Tombulilato district, North Sulawesi, Indonesia (Fig. 1.2) is hosted in quartz stockwork veins which extend out from cylindrical quartz diorite porphyry stocks into surrounding metavolcanics (Carlile and Kirkegaard, 1985). Pervasive advanced argillic alteration occurs within the porphyry intrusions, and in structurally-controlled zones in the andesitic host rocks. It grades as zones outwards from an inner core as: andalusite-corundum-muscovite, andalusite-pyrophyllite/muscovite, andalusite-pyrophyllite-diaspore, diaspore-pyrophyllite, diaspore-pyrophyllite-alunite, alunite-kaolinite-pyrophyllite, and peripheral silica-alunite-kaolinite (Lowder and Dow, 1978). This zonation in high sulfidation-style alteration is indicative of progressive cooling and decrease in fluid pH away from the porphyry intrusions (Fig. 6.3).

iii) Lithologically Controlled High Sulfidation Gold-Copper Systems

a) Characteristics

Lithologically controlled high sulfidation alteration forms as magmatic fluids migrate up dilatant structures then pass laterally along permeable host rocks such as coarse grained pyroclastics (e.g., Nansatsu deposits, Japan; Gidginbung, Dobroyde, and Mt. MacKenzie, eastern Australia) or permeable sediments and diatreme breccias (e.g., Pueblo Viejo, Dominician Republic; Wafi River, Papua New Guinea). In many systems diffusion of the upwelling hot acidic fluids within the permeable host rocks creates relatively broad alteration zones (e.g., Wafi River), whereas sharp alteration zones are present at the contacts with less permeable host rocks (e.g., Nansatsu Deposits). In most cases mineralization post-dates alteration and is concentrated in the fractured and brecciated core residual and silica-alunite alteration (e.g. Nansatsu deposits; Hedenquist et al., 1994). In some systems (e.g., Zone A, Wafi River) mineralization occurs initially during the progressive cooling and neutralization of the fluids as a halo to the zoned alteration system. Sites of high fluid flow or rapid quenching may produce the higher grade zones.

b) Examples

Several high sulfidation systems occur in the Lachlan fold belt of eastern Australia. Mt. Mackenzie and Clive Creek exhibit predominantly lithological controls to high sulfidation alteration and mineralization and are hosted

in Devonian, shallow dipping coarse grained andesite to dacite pyroclastics (T. Leach, unpubl. data). The Gidginbung (Temora) high sulfidation deposit (Thompson et al., 1986) displays a predominantly lithological control to the alteration within a volcaniclastic breccia unit (Lawrie et al., 1997), although elongate along an arc parallel structure or shear zone (Allibone et al., 1995). Dobroyde (White 1991; T. Leach, unpubl. data) and Peak Hill (below) display composite structural-lithological controls to the high sulfidation alteration and mineralization.

1. Wafi River, Papua New Guinea

The Wafi Project comprises high sulfidation gold and porphyry copper-gold mineralization (Fig. 6.12). The following discussion of the Wafi River lithologically controlled high sulfidation gold system is taken from Leach and Erceg (1990), Erceg et al. (1991), and CRA (1994). The discussion on the Wafi River porphyry copper-gold system is taken from Tan-Loi and Andrews (in review) and T. Leach, unpublished reports (1990-1995).

The Wafi Transfer Structure, a major crustal structure, localized overprinting microdiorite and quartz diorite porphyry intrusions, and a diatreme-flow dome complex which were emplaced into low grade Mesozoic Owen Stanley metamorphics comprising siltstones, litharenites and conglomerates (Figs. 6.11, 6.12). The magnitude of the Wafi Transfer Structure is evident in the manner in which it separates the western and eastern segments of the New Guinea Orogen and provides a sinistral offset to the Markham fault, a plate boundary to the north of Wafi (Fig. 6.11; Corbett, 1994).

In the Wafi River lithologically controlled high sulfidation gold system, surface alteration comprises concentric zones of advanced argillic and argillic alteration which are elongated roughly parallel to the transfer structures and extend over an area of 4 square km (Fig. 6.12). Permeability provided by the clastic metasediments, enhanced by fracturing in association with diatreme emplacement and also the diatreme and intrusion breccias, has allowed dispersion of hot acidic fluids over a large area. Alteration assemblages grade outwards as zones of: residual quartz, quartz-alunite, alunite-pyrophyllite or alunite-dickite, pyrophyllite or dickite, dickite/kaolinite-illitic clay zones, to peripheral interlayered clay and/or chlorite. This zonation has been interpreted (Leach and Erceg, 1990) to be indicative of progressive cooling and neutralization of a hot acidic fluid, sourced from the east at depth and radiated outward, to define the elongate alteration (Figs. 6.12, 6.13).

Although low grade gold is disseminated throughout much of the alteration, zones of more significant gold mineralization occur around the margins of the diatreme complex (Zones A, B, and D, Fig. 6.12), in structurally controlled breccias (Zone C) which cross cut the diatreme complex, and in distal settings (Malaria and Hesson Creek Zones) aligned along the NNE-NE trending transfer structures. Gold in these zones occurs in two settings, interpreted to be related to two separate events of the same high sulfidation system as:
i) Disseminated auriferous pyrite mineralization within alunite-dickite and clay alteration zones is inferred to be related to the initial formation of the zoned advanced argillic alteration, and associated with the influx of hot acidic volatile-dominated fluids.
ii) A later phase is hosted in pyritic fractures and breccias which cross cut the zoned alteration and was deposited from mineralized brines.

The occurrence of two distinct styles of gold mineralization at Wafi is unusual in high sulfidation systems, but not unique. Gold mineralization in the Pueblo Viejo high sulfidation system, Dominican Republic, is similarly attributed to two pulses of mineralized magmatic fluids: one associated with disseminated pyrite in clay-alunite alteration zones at depth, and the other hosted in pyritic veins at shallower levels (Muntean et al., 1990). Gold in Zone A at Wafi (>15 Mt at 2.6 g/t Au; Erceg et al., 1991) is refractory and generally submicroscopic, although a few minute (1-3 micron) inclusions have been observed in pyrite both disseminated in the altered

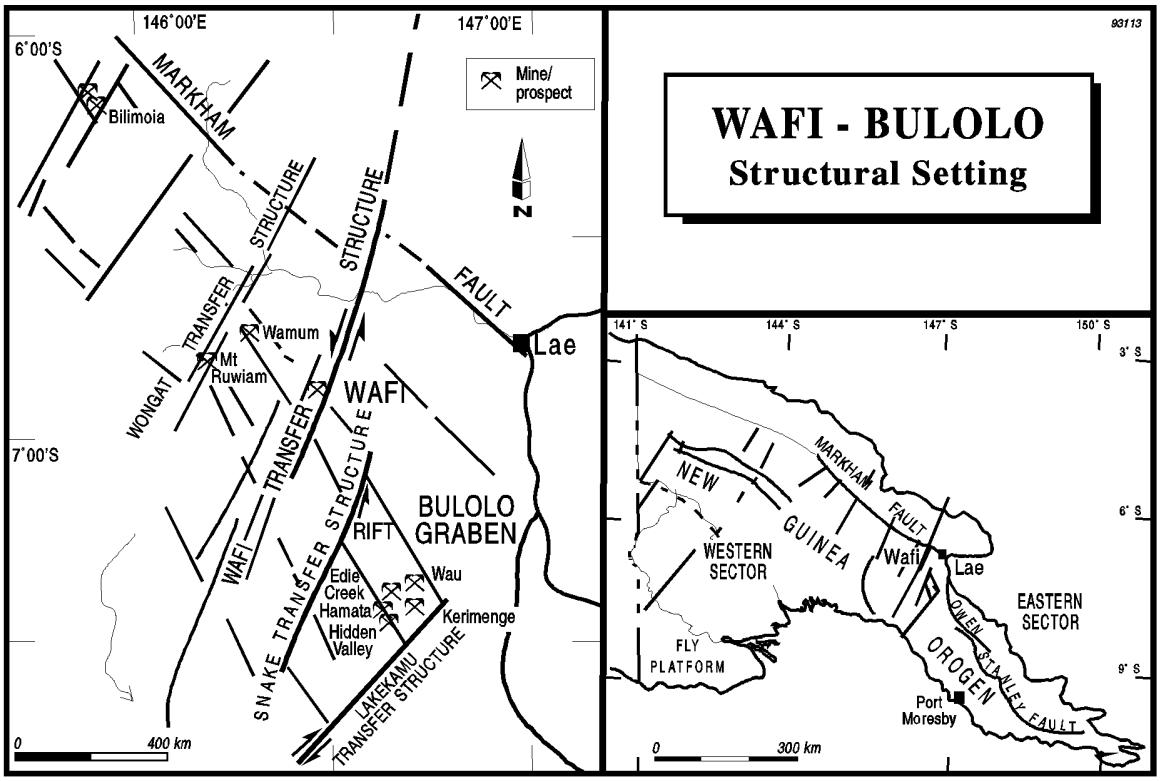

FIG. 6.11

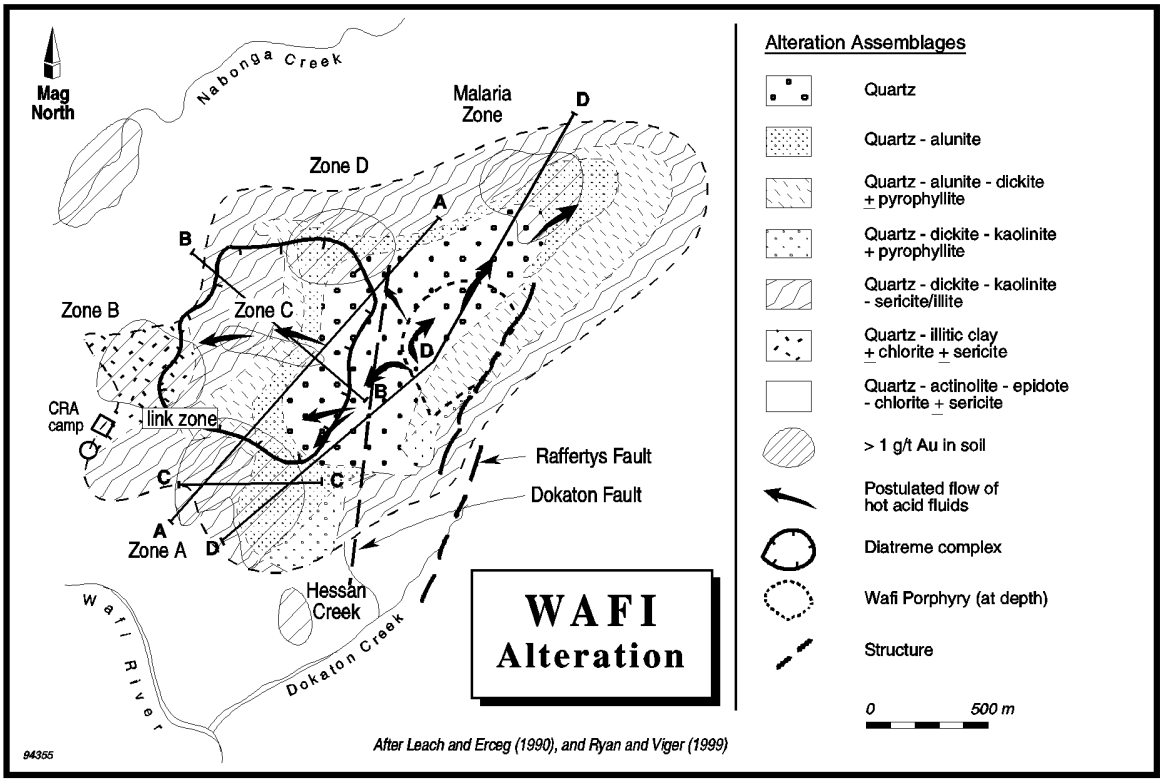

FIG. 6.12

sediments, and filling fractured and brecciated metamorphic quartz veins. Copper mineralization in Zone A occurs in trace amounts as enargite and luzonite in the quartz-alunite-dickite alteration, and as tennantite, with base metal sulfides, in the peripheral argillic alteration. Fluid inclusion data on sphalerite associated with the acidic alteration indicates that mineralization took place under cool (200-220°C) epithermal conditions.

A blind mineralized diorite to quartz diorite porphyry stock was encountered at Wafi 800 m NE of Zone A, beneath a leached cap during a conceptual drill programme which targeted a potential fluid upflow for the high sulfidation alteration and mineralization (G. Corbett, unpubl. report, 1990; Erceg et al., 1991). The initial drill intercept in the porphyry copper intrusion, drill hole WR 95, yielded published results of 263 m at 1.86 percent Cu and 0.27 g/t Au (Elders Resources, press release, 1990).

The Wafi porphyry copper-gold project comprises an early porphyry copper-gold system similar to other southwest Pacific porphyry systems (Section 5.i) which has been overprinted by a later a high sulfidation gold system. The porphyry copper-gold system consists of early alteration which is zoned outward from the porphyry stock to host sediments as: potassic (biotite-quartz-K-feldspar) --> inner propylitic (actinolite-epidote) --> propylitic (chlorite ± epidote). Porphyry-related quartz veins form a dense stockwork around the intrusion carapace (up to 90% of the rock), as sheeted fractures along the intrusion margin, and rare as veins in the core of the stock, and diminish in intensity outward into the altered sediments. K-feldspar selvages are common adjacent to the quartz veins which cut biotite altered sediments. Porphyry-style chalcopyrite ± bornite ± gold ± molybdenite mineralization is associated with late stage veinlets and wall rock alteration which range from: early biotite-K-feldspar ± quartz ± pyrite ± magnetite, to chlorite-pyrite ± magnetite, to late sericite-quartz-pyrite.

The high sulfidation system has produced vertically zoned advanced argillic, phyllic and argillic alteration which overprinted the earlier porphyry-related alteration. The high sulfidation alteration is zoned from shallower levels and to the southeast to deeper levels and to the northwest as: residual quartz --> quartz-alunite --> quartz-alunite-dickite --> quartz-dickite-sericite --> kaolinite-illitic clay-quartz --> smectite ± chlorite ± siderite (Fig. 6.14). This zonation reflects progressive cooling and neutralization of a hypogene hot acidic fluid, probably in response to rock reaction. The earlier porphyry-related alteration is totally masked by the very intense advanced argillic alteration at shallow levels, whereas relict potassic and propylitic alteration are evident at depth in the less intense overprinting argillic alteration.

Copper mineralization associated with the high sulfidation system occurs in late fractures and as disseminated grains in the altered wall rock. This mineralization is zoned as: enargite-tennantite in the shallow quartz and alunite alteration, covellite in the dickite-sericite alteration, and chalcopyrite in the deeper kaolinite-illitic clay-smectite alteration. Pyrite occurs in all alteration assemblages and preliminary metallurgical tests indicate that approximately 50 percent of the gold mineralization is associated with the high sulfidation pyrite.

Two main episodes of hydrothermal alteration and mineralization are therefore recognised at Wafi as:

i) A porphyry copper system with classical temporally and spatially zoned alteration and mineralization. K/Ar dating on K-feldspar gave 14 Ma age for this event.

ii) High sulfidation alteration and mineralization overprinted the porphyry event around 1 m.y. later (13 Ma K/Ar age on alunite). It is interpreted that the high sulfidation system caused the remobilization of pre-existing porphyry-related copper into zoned enargite-tennantite, covellite and chalcopyrite mineralization in a similar manner to that proposed for Butte, Montana (Brimwall and Ghiorso, 1983) and El Salvador, Chile (Gustafson and Hunt, 1975). Gold has been introduced during the high sulfidation event as pyrite within the porphyry stock and in the surrounding gold zones (Zone A, B, C, etc.).

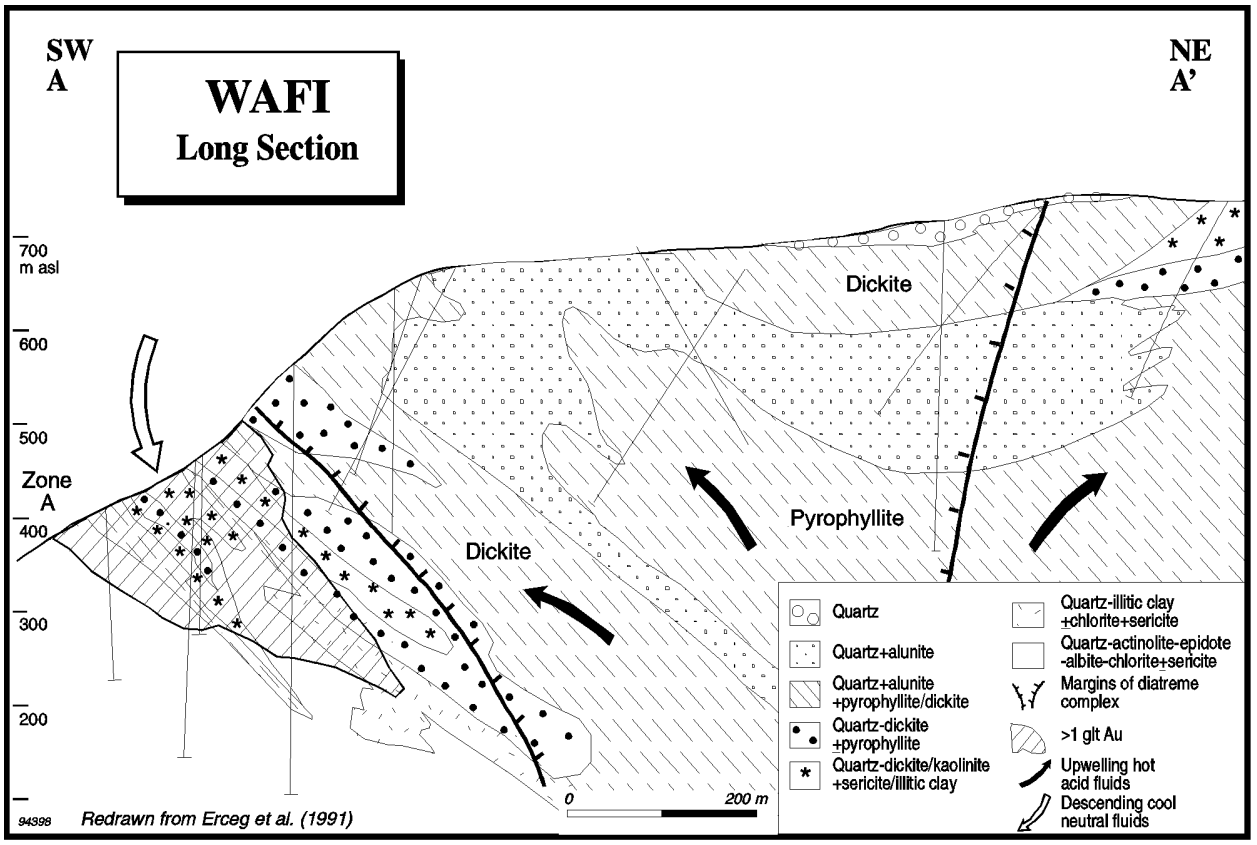

FIG. 6.13

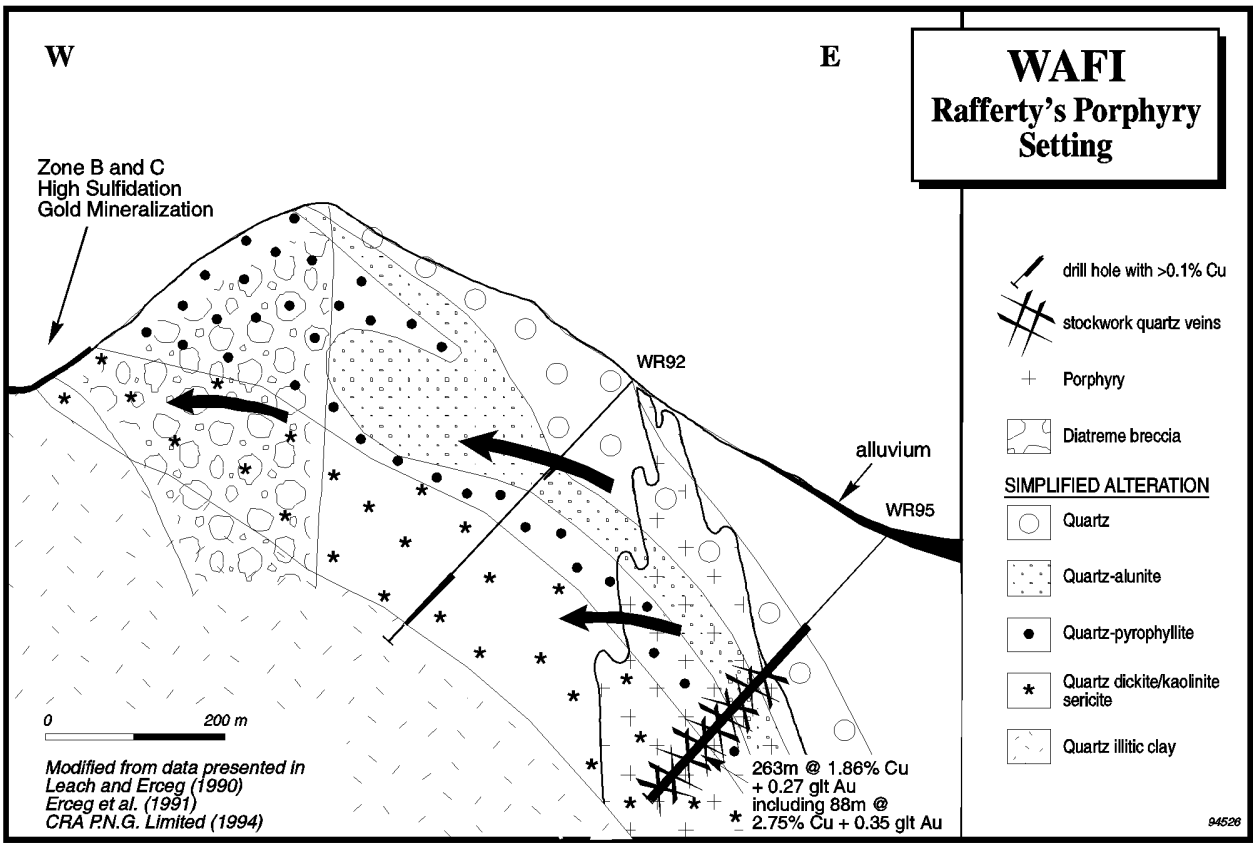

FIG. 6.14

2. Nansatsu deposits, Japan

The following discussion of the Nansatsu deposits in southern Kyushu, Japan, is derived from reviews (Hedenquist et al., 1988, 1994; Matsuhisa et al., 1990; White 1991; Izawa and Cunningham, 1989) and personal observations (G. Corbett, unpubl. report, 1987). The deposits are characteristically small, mushroom-shaped bodies, and there are three recent producers: Kasuga (0.15 M oz Au), Iwato (0.21 M oz Au) and Akeshi (0.22 M oz Au). All have low gold grades in the order of 3-4 g/t Au, but locally contain higher grades within feeder structures, as at Kasuga (Hedenquist et al., 1988), or breccias (Izawa and Cunningham, 1989). The silica-rich ores are used as fluxes in copper smelters.

The Nansatsu deposits are interpreted to have formed within 150-300 m below the paleowater table (Hedenquist et al., 1994) based on: the slightly younger (0.5 m.y.; Hedenquist et al., 1994) age of the alteration than the host Upper Miocene-Pliocene host volcanic sequence, presence of low temperature (kaolinite, smectite) alteration at shallow levels, and interpreted eruption breccias (Izawa and Cunningham, 1989).

Hot acid magmatic-sourced fluids migrated from feeder structures into more permeable pyroclastic units in a volcanic sequence dominated by andesite flow units, and formed tabular-shaped silicified bodies (Fig. 6.15). Cooling and neutralization of those fluids by rock reaction is reflected by a characteristic zoned alteration pattern from: a core of residual quartz through alunite-kaolinite, to a rim of illite, illite-smectite, and smectite clays, commonly with sharp contacts (Fig. 6.15). Ore-related sulfides and sulfosalts occur in fissures and breccias which cross cut the central quartz zone, and fill vughs (Hedenquist et al., 1994). Gold occurs within the residual silica with pyrite, enargite (luzonite), covellite, native sulfur and later iron oxides. Fluid inclusion and clay alteration studies suggest mineralization temperatures of 170-210°C (Hedenquist et al., 1994; Izawa and Cunningham, 1989), which are consistent with a shallow epithermal setting. The fluid inclusion temperatures are locally higher (250-300°C) within deeper levels at Kasuga (Hedenquist et al., 1994).

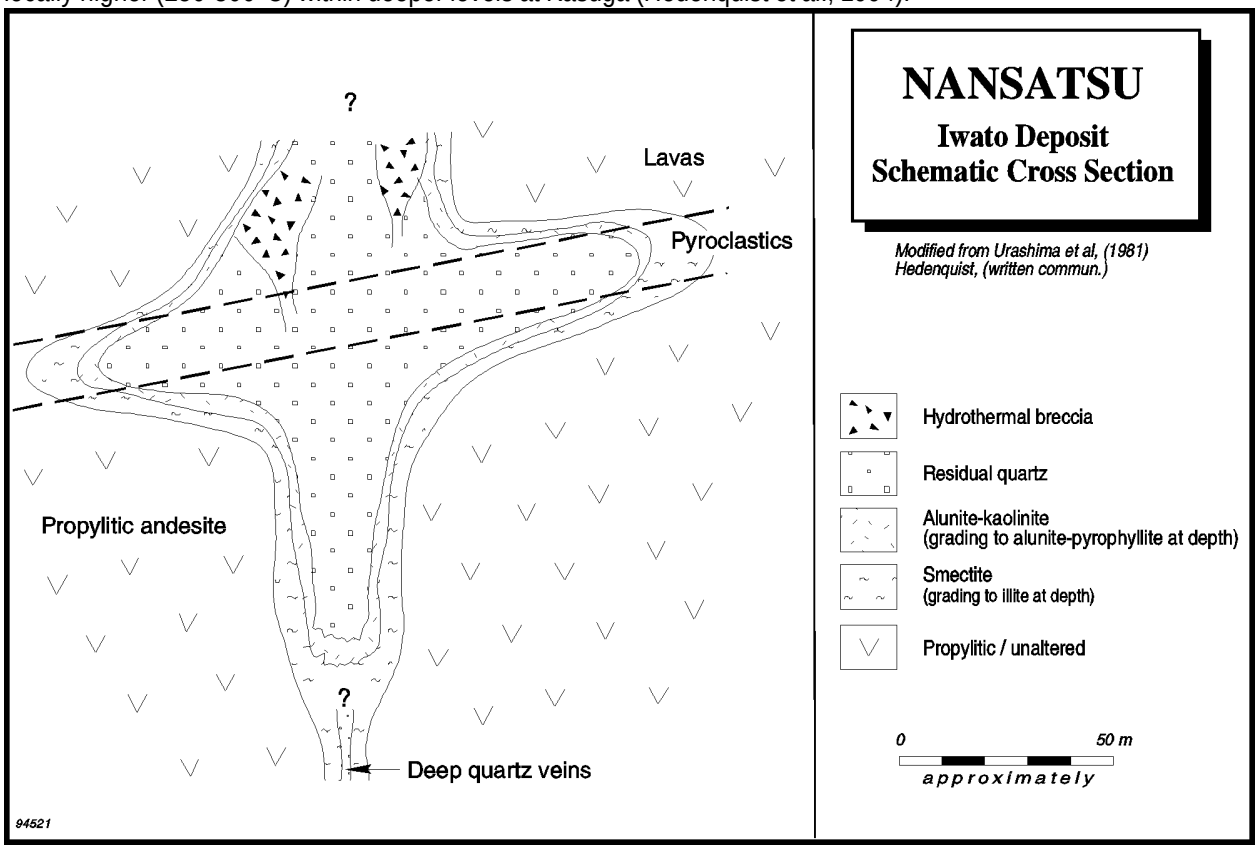

FIG 6.15

3. Miwah, Indonesia

The Miwah lithologically controlled high sulfidation system shows some similarities to Wafi and also the Lepanto structurally controlled high sulfidation gold-copper system. It is located in northern Sumatra, Indonesia, in a region of dextral strike-slip faulting related to movement on the Sumatra fault system (Fig. 1.2). The following discussion on Miwah is taken from Williamson and Fleming (1995) and unpublished reports (T. Leach, Graham Corlett).

Alteration and gold mineralization are hosted in a sequence of andesitic to dacitic lavas and tuffs of the Pliocene Leuping Volcanics. These volcanics are aligned ENE along the Miwah lineament, and are paralleled by a similar trend of recent to active volcanism to the north. Dilation on ENE structures is inferred from dextral movement on the Sumatra fault system. The Leuping Volcanics have been intruded by porphyritic andesite to rhyodacite dikes and domes (Fig. 6.16), which are dated by K/Ar methods at 2.9 Ma. These intrusions contain a wide variety of xenolith clasts which range from andesite and diorite porphyry, to K-feldspar-magnetite altered volcanics. In the south and west regions of the prospect, the volcanics are intruded by a diatreme breccia complex which contains local dacitic material and quartz-veined andesite clasts. Some of the quartz in the veins contain inclusions of anhydrite and halite daughter crystals associated with liquid-and vapour-dominated fluid inclusions, which suggest formation in an environment proximal to a high level intrusion.

The volcanics, domes, dikes and diatremes have been altered by extensive advanced argillic - argillic alteration which is zoned from: central vughy to dense quartz-rutile-pyrite, quartz-alunite, through marginal zones of quartz-kaolinite, low temperature illite-smectite, to peripheral chlorite/chlorite-smectite assemblages. This alteration overprints earlier propylitic, and locally phyllic, alteration. The quartz and quartz-alunite alteration (Figs. 6.16, 6.17) occur as:
i) Restricted zones within inferred NNW trending structures which parallel the Rusa fault and crop out on the eastern margins of the prospect.
ii) Less dominant NNE trending structures which crop out as thin ridges, parallel to the Camp fault.
iii) Broad zones within the diatreme breccias, possibly as a reflection of the high permeability in the breccia matrix.
iv) Shallow (up to >100 m thick) north to northeast dipping ledges, hosted in volcanics.

The quartz and quartz-alunite alteration have acted as brittle host rocks during subsequent fracturing and brecciation associated with mineralization which changes from early pyrite-rich quartz veins, to later breccia zones and veins composed of brassy pyrite, overgrown by copper sulfide minerals. Copper minerals are dominated by luzonite at shallow levels to the south, and enargite at deeper levels to the north. Hypogene covellite occurs locally at depth, whereas tennantite occurs in more distal settings to the east. The copper minerals are intergrown with quartz and banded chalcedony, and locally at depth with alunite. Native sulfur commonly fills open cavities and fractures. The alteration and mineralization are indicative of relatively cool conditions for the high sulfidation alteration and mineralization.

Although there is a close relationship between gold, copper and arsenic, gold is not always associated with enargite/luzonite, and is locally inferred (T. Leach, unpubl. reports) to have been deposited with earlier pyrite. The assay data from recent drilling indicate that the Cu:Au ratios increase with depth and to the north. Information from the structure, alteration and mineralization suggest that a possible source for hot acidic, mineralized fluids was from the north and at depth below the diatreme breccia, and fluid outflow occurred towards the south (Figs. 6.16, 6.17).

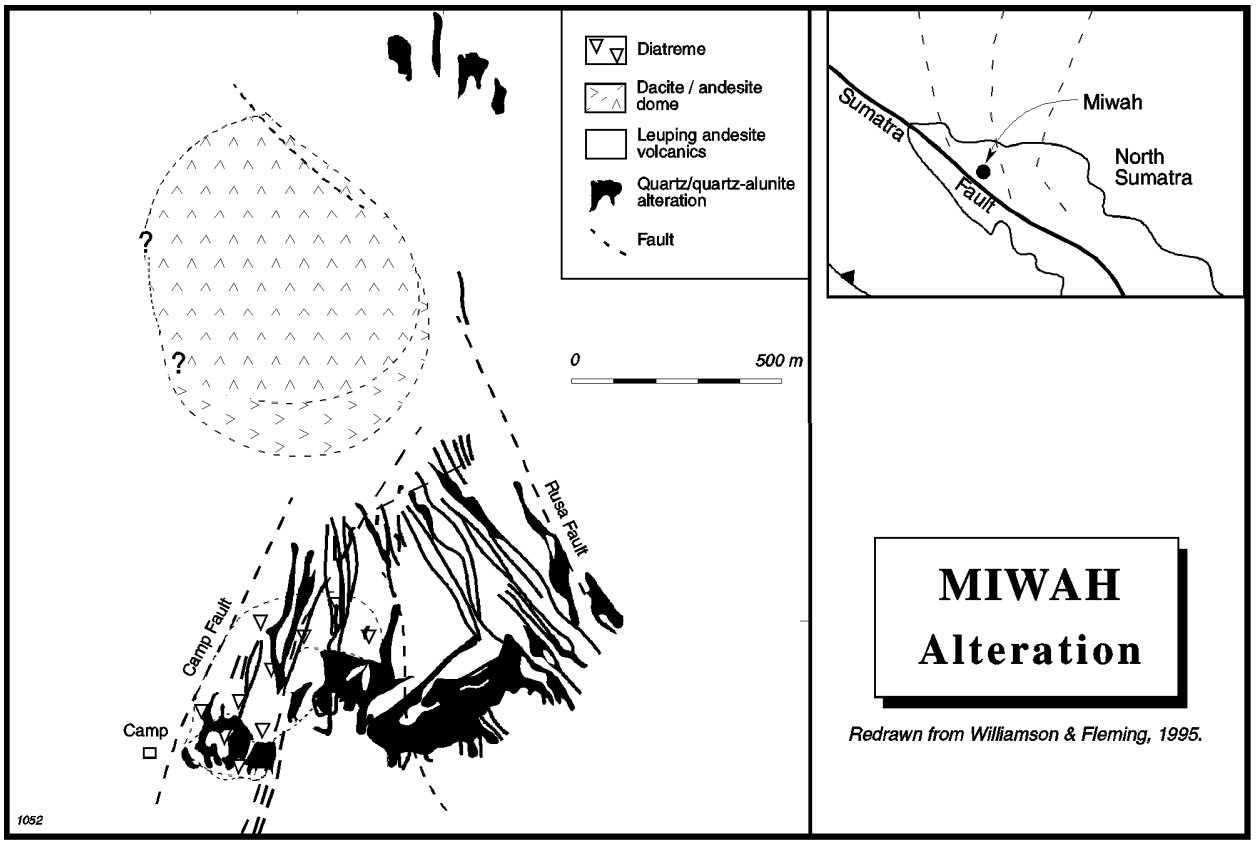

FIG. 6.16

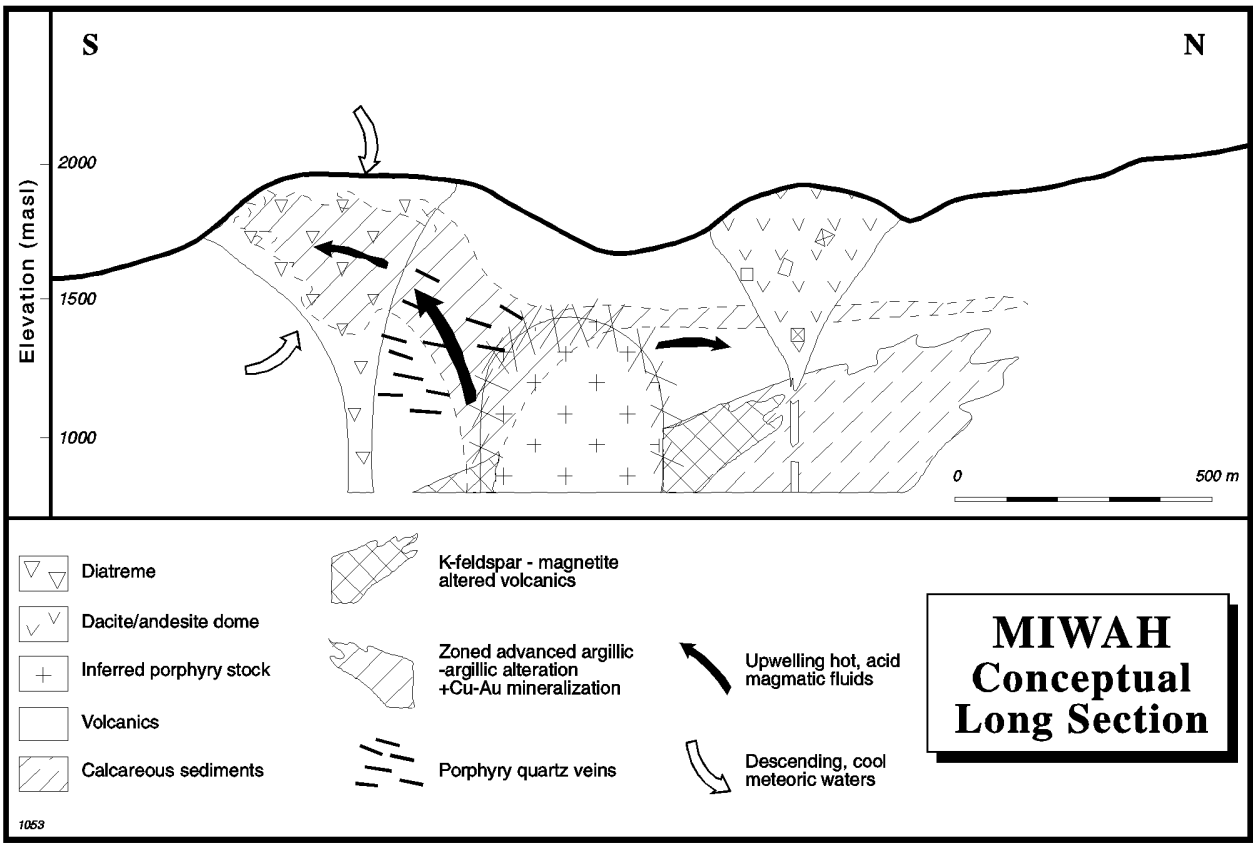

FIG. 6.17

iv) Structurally Controlled High Sulfidation Gold-Copper Systems

a) Characteristics

High sulfidation systems which display a predominantly structural control form if the permeability for lateral fluid flow is provided by dilational fault/fracture systems (e.g., Nena, Frieda River, Papua New Guinea), and/or breccias (e.g., Mt Kasi, Fiji), including diatreme breccia margins (e.g., Lepanto, Philippines). In most structurally controlled high sulfidation systems, central residual (vughy) quartz and marginal quartz-alunite assemblages, form bulbous alteration zones surrounded by thin argillic zones, which grade out into regional propylitic alteration, when viewed in cross section. The thin outer alteration zones are indicative of rapid changes in fluid conditions, moving away from the dilational structures which control fluid flow. Many systems are elongate along dilational structures (e.g., Lepanto), commonly as resistive ridges of silica-alunite (e.g., Nena). The overprinting relationship of the vapour-derived alteration and the subsequent liquid-derived mineralization is generally more clearly evident in the structurally than lithologically controlled high sulfidation systems. The utilization of the same plumbing system focuses mineralized fluid into the core of the zoned alteration where the competent residual silica readily brecciates. The surrounding clay alteration is less competent and impermeable and so commonly remains unmineralized and may mask mineralization (e.g., Nena, Papua New Guinea). Breccias, categorised as rotational, grading to mosaic (jigsaw) and fluidized breccia dikes (Section 3.x.d.4, Fig. 3.22), are indicative of fluid transport in feeder structures, and commonly grade to crackle breccias towards the periphery of the mineralized zones. Metal contents decline moving away from the feeder structures in proportion to the sulfide content.

b) Examples

1. Nena, Frieda River Copper, Papua New Guinea

The Nena Prospect at Frieda River Copper is an example of a structurally controlled high sulfidation system, recently described by Bainbridge et al. (1993, 1994), from which this discussion is taken. A total sulfide resource of 60 Mt at 2.0 percent Cu and 0.6 g/t Au, and an oxide gold resource of 14.5 Mt at 1.4 g/t Au has been defined for Nena (Holtzberger et al., 1996).

Exploration at Frieda River up to 1983 inferred a porphyry copper resource of 860 Mt at 0.47 percent Cu and 0.31 g/t Au within the Koki and Horse-Ivaal deposits, and 32 Mt at 2.35 percent Cu and 0.58 g/t Au within the Nena high sulfidation deposit, located 6 km northeast of the porphyry deposits (Hall et al., 1990). A better understanding of high sulfidation gold-copper mineralization and the relationship to buried porphyry copper intrusions, in particular Lepanto, Philippines (Garcia, 1991; Arribas et al., 1995) and Wafi, Papua New Guinea (Leach and Erceg, 1990; Erceg et al., 1991), led to a re-evaluation of the Nena mineralization in the early 1990's (G. Corbett, unpubl. reports, 1990-1993; T. Leach, unpubl. reports, 1990-1996; Bainbridge et al., 1993, 1994).

The Nena Prospect occurs on the margin of the Frieda River porphyry copper intrusion complex which is inferred to have been localized by the NW trending Frieda fault, formed as a splay fault from the more regional EW trending Leonard-Schultz fault (Corbett, 1994; Fig. 6.18). An inferred dextral movement has imparted a dilational character to the set of NW-trending structures between the Frieda and Leonard-Schultz faults, and this is termed the Nena structural corridor (Corbett, 1994; Figs. 6.18, 6.19). These structures host a series of quartz and quartz-alunite ridges which extend for over 10 km from the Horse-Ivaal porphyry copper deposits and include the Nena high sulfidation system (Figs. 6.19, 6.20). This comprises an elongate NW trending characteristic bulbous alteration (in cross section) which, at grid 4700N, grades outward as zones of: central mineralized residual (vughy) quartz, barren quartz-alunite (locally sulfur-bearing), thin zones of pyrophyllite-dickite-kaolinite, interlayered illite-smectite and carbonate-gypsum-chlorite (Fig. 6.21). The concentric

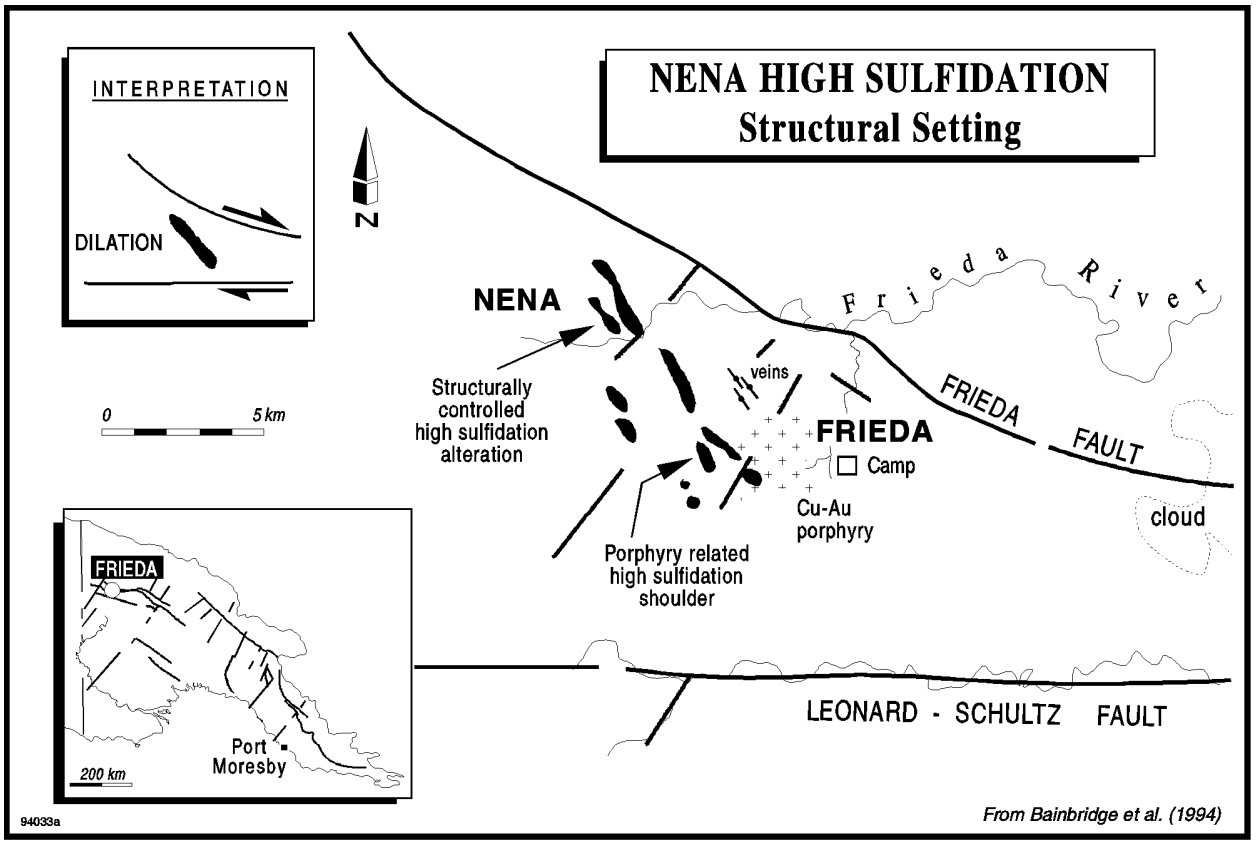

FIG. 6.18

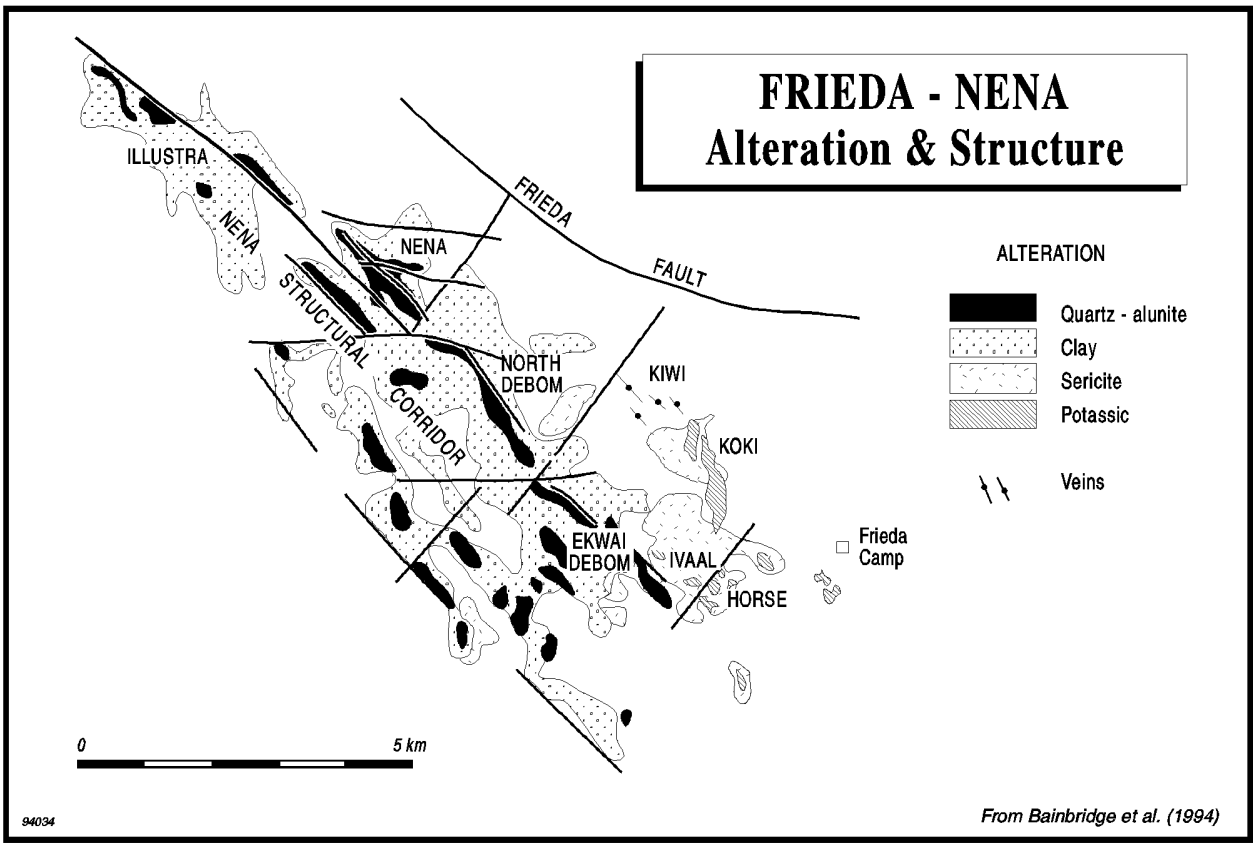

FIG. 6.19

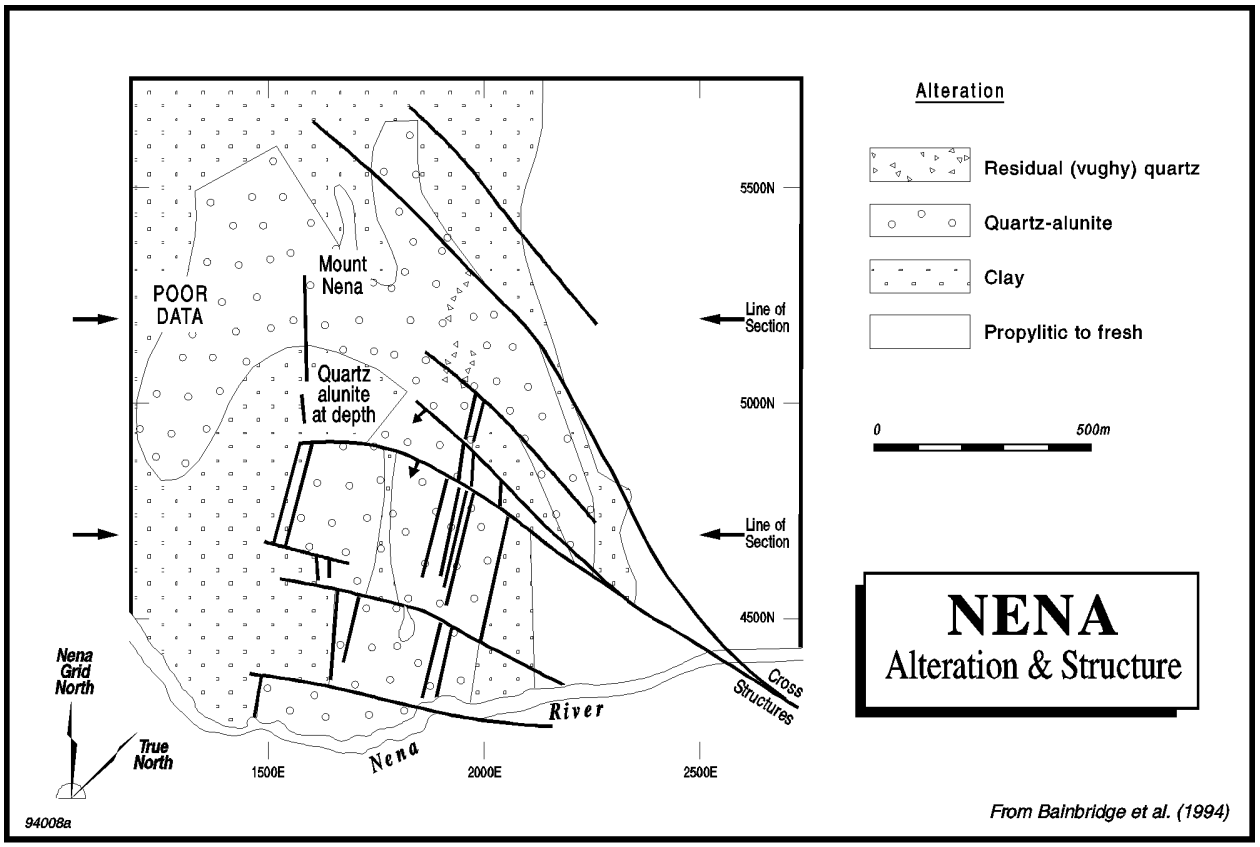

FIG. 6.20

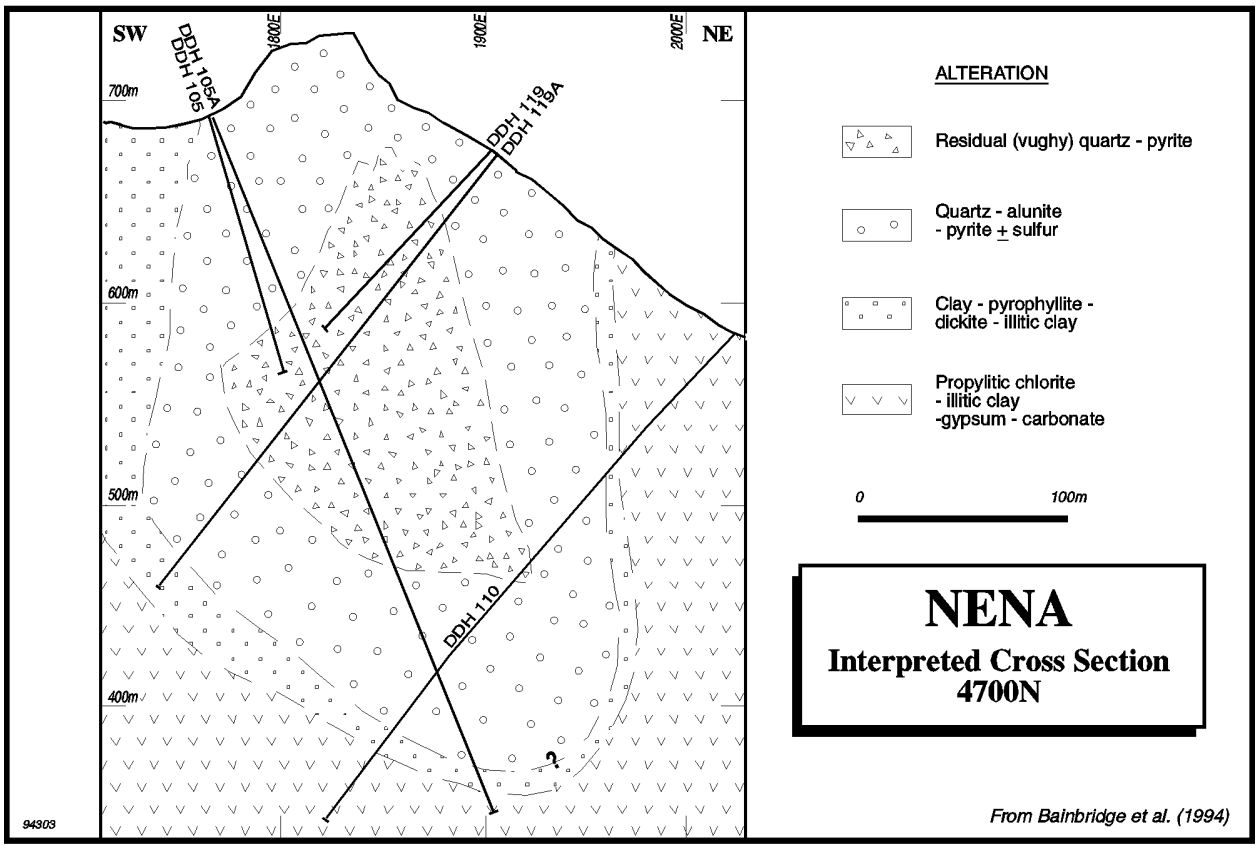

FIG. 6.21

morphology of the alteration (in cross section) is consistent with lateral fluid flow along the controlling structure. However, at 500 m to the northeast (grid 5200N, Fig. 6.22), steeply dipping sheeted zones of quartz and quartz-alunite are indicative of near vertical fluid flow.

The alteration is interpreted to be derived from acid leaching by an initial vapour-rich magmatic fluid phase which migrated upwards and then laterally southeast along the NW-trending dilational feeder structures. The gradation from broad central zones of residual (vughy) quartz outward to quartz-alunite alteration is postulated to be derived from the progressive cooling and neutralization of this acidic fluid by rock reaction. The thin zones of peripheral clay alteration are inferred to result from the rapid change in fluid physico-chemistry upon mixing with circulating meteoric-dominated fluids. The permeable volcaniclastic units within a sequence interlayered with lavas are preferentially silicified, suggesting that the intersection of the Nena structure with the pyroclastic units may represent the locus of fluid flow.

Copper and gold mineralization are associated with a later, magmatically-derived fluid which has used the same feeder structures as the earlier phase, and brecciated the competent residual (vughy) quartz. Fractures, and open space in breccias and vughs, were initially sealed by multiple phases of pyrite. Copper mineralization occurs in cavities and fractures in the pyrite, in places intergrown, and locally rhythmically banded with, barite. Intense brecciation, and local fluidized breccias, accompany high grade copper mineralization within the central residual (vughy) silica alteration, whereas mineralization in the peripheral quartz-alunite alteration, is more fracture controlled and displays lower metal grades.

Initial fluid inclusion studies (Bainbridge et al., 1994) on barite associated with copper mineralization indicate that the mineralized fluid was two phase, relatively hot (>300-350°C) and moderately saline (>9-10 wt % equiv. NaCl), and that mineralization probably resulted from rapid cooling upon mixing with low temperature (<150-200°C), dilute (<1-2 wt % NaCl) meteoric waters.

The copper minerals vary laterally (Fig. 6.23), from Mount Nena in the NW to the SE as zones of: hypogene covellite + enargite, enargite, luzonite > enargite, and only luzonite at shallow levels. Covellite formed early in the paragenetic sequence and is locally altered to enargite. Cu:Au ratios in the sulfide zone decrease from NW to SE, and from deeper to shallow levels in the southern regions. Luzonite becomes progressively Sb- and Te-rich at shallow levels implying solid solution series with stibioluzonite and goldfieldite. Gold is inferred to occur in association with luzonite-goldfieldite as well as with late stage pyrite. These changes in metals and ore phases, together with the change in the morphology of alteration outlined above, suggest that magmatic-derived vapours and brines, which produced the alteration and mineralization, possibly ascended from depth in the region beneath Mount Nena and flowed laterally to the southeast (Fig. 6.20).

Supergene leaching formed an oxidized zone of gold enrichment and copper depletion which overlies supergene covellite-chalcocite enrichment. Supergene native gold displays a very high fineness and occurs as minute grains which fill fractures in the gold-rich oxide zone.

2. <u>Lepanto-Far South East (FSE)</u>, Philippines

The Lepanto high sulfidation enargite gold deposit (production and reserves of 33 million tonnes at 2.2% Cu, 3.5 g/t Au, and 11 g/t Ag; Sillitoe, 1995c) in the Philippines is located 200-400 m to the northwest (Fig. 6.24) and 400 m above (Fig. 6.25) the high grade Far Southeast (FSE) porphyry copper deposit (356 million tonnes at 0.73% Cu, and 1.24 g/t Au; Concepcion and Cinco, 1989).

The Lepanto high sulfidation system is localized by the intersection of the dilatant Lepanto fault with the fractured contact between the diatreme breccia and host rocks, to give an oval plate-like shape (Figs. 6.24,

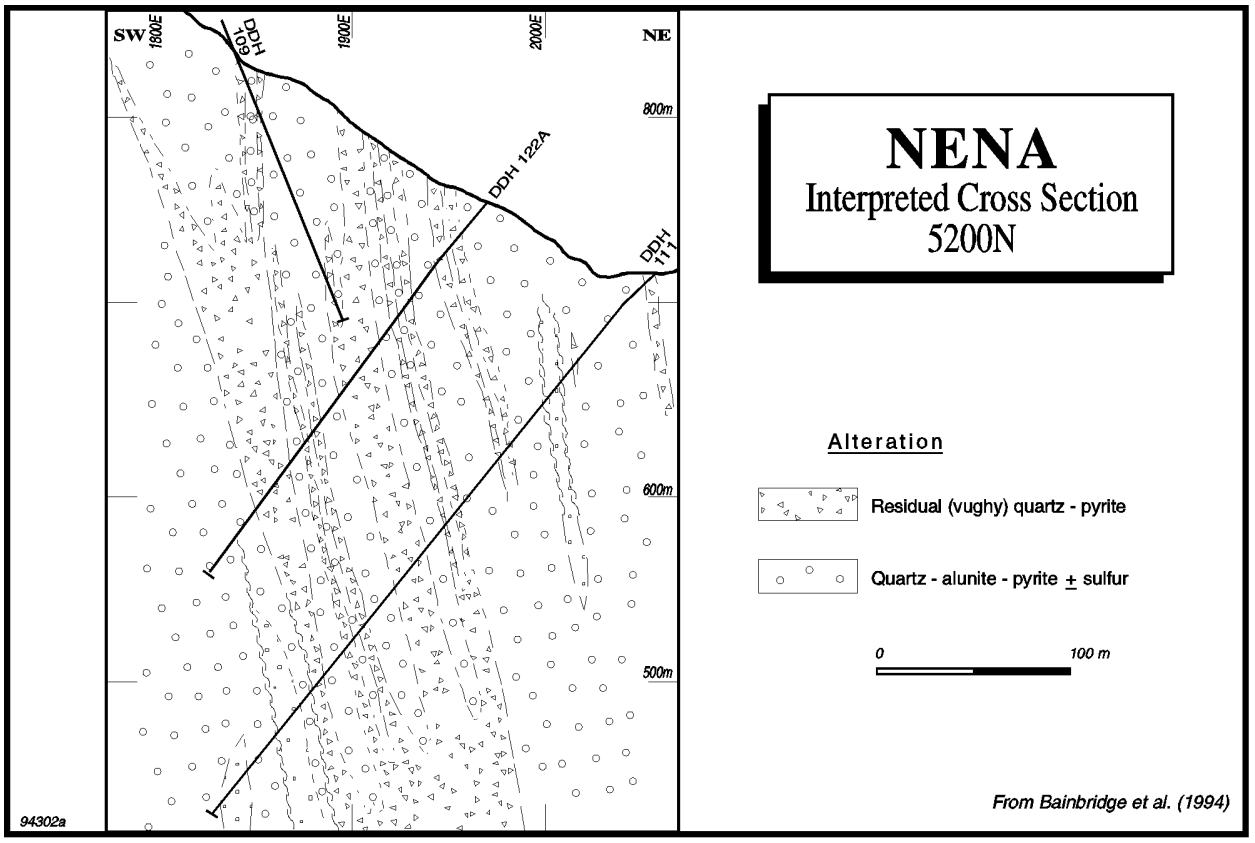

FIG. 6.22

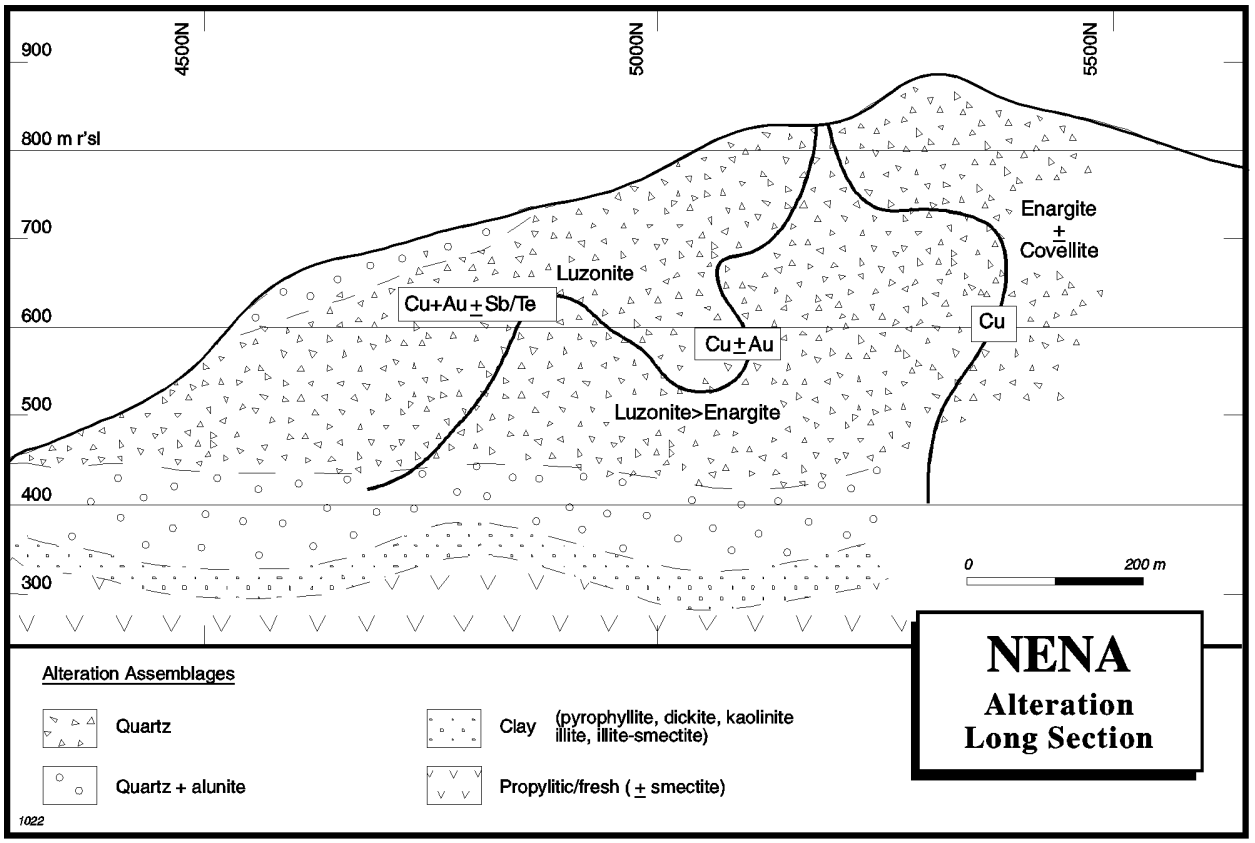

FIG. 6.23

6.25). The Philippine fault, a major sinistral transpressional terrain boundary with a protracted history of activity, breaks up into several splays which parallel the magmatic arc in Luzon (Figs. 1.2, 2.5; Mitchell and Leach, 1991). NS trending inferred splays, the Abra and Pseudo faults (Baker, 1992) constrain NW trending structures (Garcia, 1991) in the mine area (Fig. 6.24). The sinistral movement presented by Baker (1992) for the Pseudo fault coupled with the Abra fault are interpreted to have dilated the subsidiary Lepanto fault (Fig. 6.24), for which Baker (1992) also records a sinistral sense of movement. The pyroclastic and dacite porphyry rocks of Garcia (1991) are interpreted as diatreme breccias and endogenous domes respectively (Baker, 1992), and it is possible that there are both pre- and post-mineralization diatremes in the area (Figs 6.24, 6.25).

The FSE porphyry may be localized at the intersection of the Lepanto fault formed as a splay, with the arc parallel Pseudo fault (Fig. 6.24), similar to the inferred localization of porphyry mineralization at Frieda, Papua New Guinea (Fig. 6.18), and at Chuquicamata, Chile (Boric et al., 1990). Porphyry copper-gold mineralization at Guinaoang (Fig. 6.24), 6 km to the southeast of FSE, is hosted at depth in a chlorite-sericite altered quartz diorite stock, and at shallow levels in advanced argillic altered volcanics, a post-mineral diatreme locally cuts altered volcanics at shallow levels (Sillitoe and Angeles, 1985).

Three phases of intrusion inferred for Lepanto-FSE are:
i) The emplacement of the funnel shaped Imbanguila dacite porphyry and associated diatreme breccia which flares at shallow levels to the NW (Garcia, 1991; Baker, 1992), and is dated at 1.8-2.9 Ma (Sillitoe and Angeles, 1985; Arribas et al., 1995).
ii) Narrow dikes and irregular bodies of quartz diorite porphyry (the FSE porphyry) were emplaced at depth (2 km below the current surface) into mid Miocene volcaniclastics. Associated biotite alteration extends for 100 m from the diorite contact, and grades outwards to propylitic epidote-calcite-chlorite alteration (Garcia, 1991). The age of biotite (1.34-1.45 Ma, average 1.41 Ma; Arribas et al., 1995) suggests that the emplacement of the FSE porphyry stock postdates the Imbanguila diatreme-dome complex. Quartz veins associated with crystallization of these intrusions were deposited from hot (>500°C) and hypersaline brines (Mancano and Campbell, 1995).
iii) The barren Bato dacite dome and associated tuffaceous diatreme breccias are dated at 0.96 and 1.18 Ma (Arribas et al., 1995).

Three styles of alteration and mineralization recognised at Lepanto-FSE are:

i) <u>High sulfidation enargite-luzonite</u> mineralization is hosted within central vughy to massive quartz zones of advanced argillic alteration localized at the intersection of faults and fractures (of the Lepanto fault) and the contact between the diatreme and underlying volcaniclastics. Zoned alteration and mineralization at Lepanto have been described in detail by Garcia (1991) as: central vughy to massive quartz alteration which grades outward through zones of quartz-alunite-kaolinite, kaolinite, to peripheral smectite-illite and chlorite alteration. The dacite porphyry displays quartz-pyrite-anhydrite grading outward to marginal quartz-alunite-kaolinite alteration at intrusion margins and cross cutting faults.

A steep hydrothermal breccia pipe cuts the FSE diorite and the Imbanguila dacite and exhibits alteration grading from sericite-tourmaline at depth, to anhydrite-alunite (+ diaspore, pyrophyllite, zunyite and illite) at shallow levels. This advanced argillic alteration extends beyond the breccia and grades laterally from: central quartz-alunite-zunyite, through pyrophyllite-diaspore, to marginal illite-chlorite. K/Ar dating (Arribas et al., 1995) on five wall rock alunites gave ages of 1.34-1.56 Ma (average of 1.43 Ma), which are close to the age of formation of the hydrothermal biotite (above).

High sulfidation enargite-luzonite mineralization at Lepanto (Fig. 6.25) is hosted within the: central vughy to massive quartz of the zoned advanced argillic alteration, alunite-anhydrite hydrothermal breccia, along the intersection of the Lepanto fault and diatreme-metavolcanic contact (branched veins or classical ore), flat lying

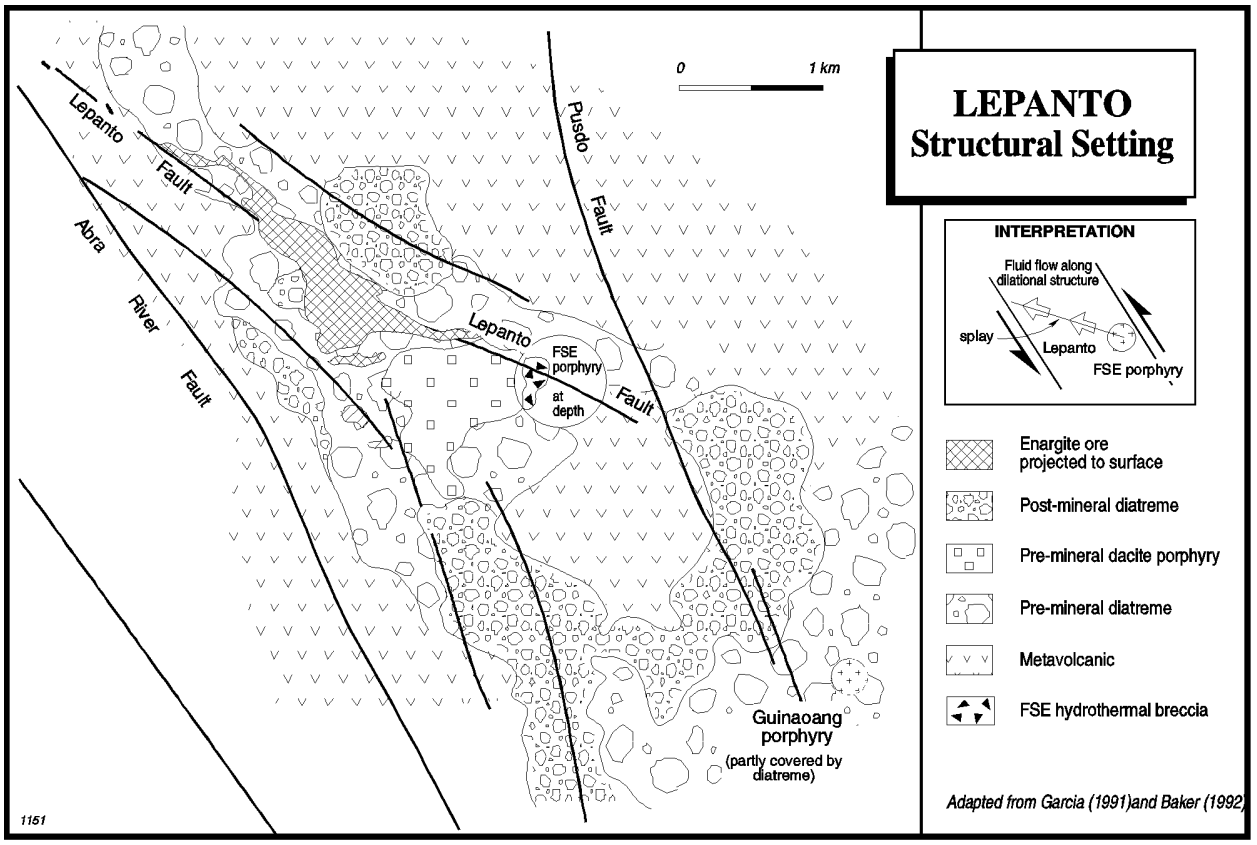

FIG. 6.24

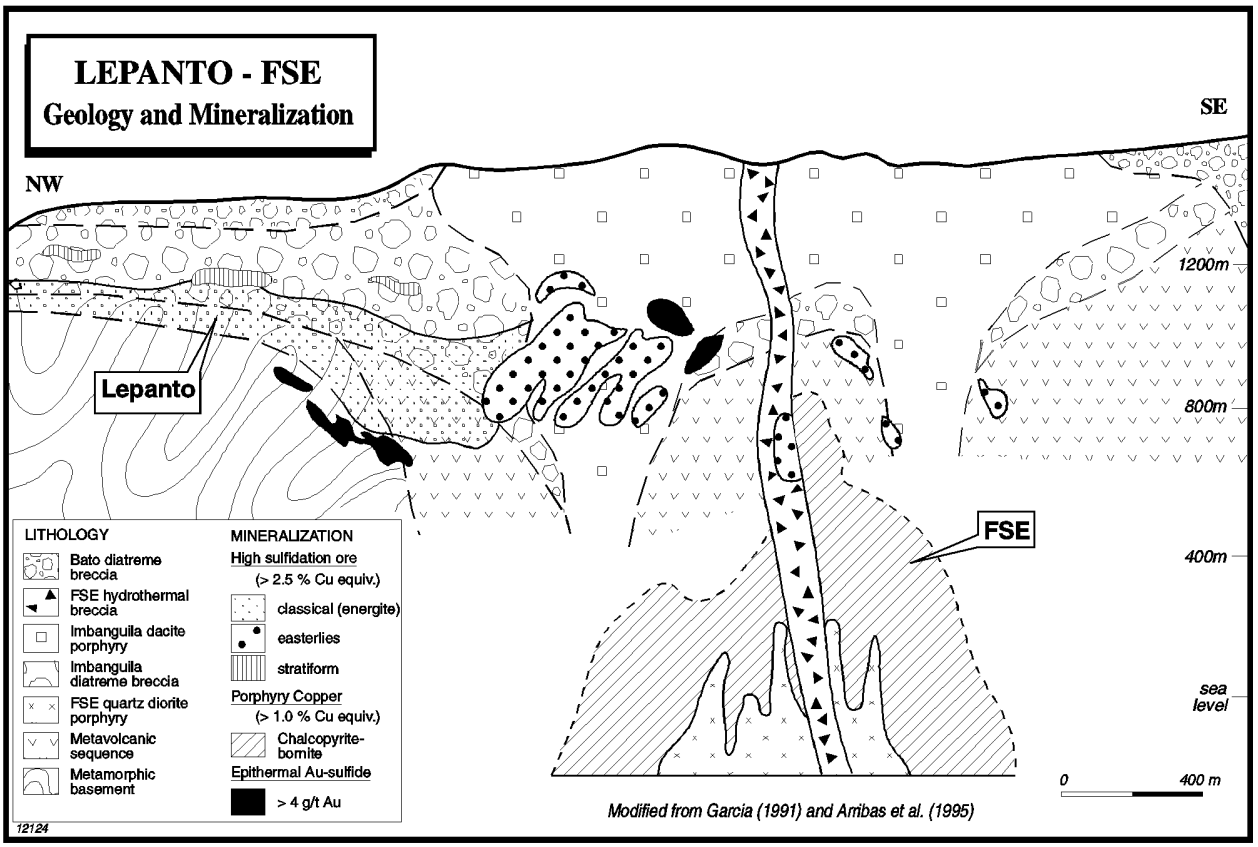

FIG. 6.25

bodies which replace calcareous sediments (stratabound ore), fault-controlled zones which cut the Imbanguila dacite (Easterlies), and silicified lenticular to pod-like bodies which are hosted in permeable breccias (stratiform ore). Two alunite samples from sulfide veins gave average ages of 1.26 Ma (Arribas et al., 1995). Gold developed late and in association with tennantite, chalcopyrite, stibnite and tellurides (Garcia, 1991).

Homogenisation analyses on fluid inclusions in enargite/luzonite from Lepanto (Mancano and Campbell, 1995) range from an average of 285°C within the hydrothermal breccia proximal to the FSE porphyry dikes, to an average of 166°C distal (>2 km) from the FSE porphyry deposit. These authors concluded that enargite/luzonite mineralization at Lepanto resulted from metal-bearing high temperature (>300°C) moderately saline (>4.5 wt % NaCl) waters mixing with ground waters. The fluid inclusion data suggest that the high temperature, hypersaline brines, which formed the early quartz stockwork veins at FSE, were not directly associated with enargite mineralization at Lepanto.

ii) Porphyry copper-gold chalcopyrite-bornite mineralization hosted within and adjacent to the FSE quartz diorite is related to chlorite-illite/sericite-clay alteration which postdates the quartz veins and biotite alteration (Garcia, 1991). Gold occurs as inclusions within, and overgrowing, copper sulfides. K/Ar dating (Arribas et al., 1995) on illite gave ages of 1.22-1.37 Ma (average of 1.30 Ma), generally younger than the formation of the hydrothermal biotite and wall rock alunite alteration (average 1.41 Ma and 1.43 Ma respectively), but close to the average age of vein alunite associated with the high sulfidation enargite/luzonite mineralization (1.26 Ma).

iii) Low sulfidation gold pyrite- and base metal-quartz veins and stringers locally postdate the high sulfidation mineralization (Garcia, 1991).

In conclusion, from the above data, it is herein postulated that cooling and crystallization of the FSE quartz diorite porphyry bodies was accompanied by potassic (biotite) alteration, the exsolution of magmatic volatiles and the formation of quartz stockwork and sheeted veins. The change in alteration in the hydrothermal breccia pipe from sericite-tourmaline at depth to alunite-pyrophyllite-diaspore (+ zunyite) at shallower levels suggests that magmatic volatiles ascended to shallow and cooler levels and were absorbed into meteoric water to progressively form hot acidic fluids. It is postulated that these fluids then migrated laterally along the intersection of the Lepanto fault and the diatreme-metavolcanic contact to develop the zoned high sulfidation alteration by rock reaction. K/Ar age dating suggests that the porphyry-related biotite and the high sulfidation alteration events were roughly contemporaneous (biotite, 1.34-1.45 Ma, average 1.41 Ma; alunite, 1.34-1.56 Ma, average 1.43 Ma).

Age dating also suggests that copper-gold mineralization associated with chlorite-illite alteration in the FSE porphyry copper environment, and with alunite deposition in the Lepanto high sulfidation environment took place more or less contemporaneously (illite, 1.22-1.37, average 1.30; alunite 1.26). It is therefore postulated that mineralization at FSE-Lepanto occurred approximately 0.11-0.17 m.y. after the potassic and zoned high sulfidation alteration, within which time the hydrothermal system had cooled significantly (as indicated by the fluid inclusion data). The mineralizing waters are inferred to have migrated laterally along the Lepanto fault within fractured and brecciated, pre-existing quartz-alunite alteration. Copper-gold mineralization formed as a result of progressive mixing of the metal-bearing waters with cool and dilute ground waters. A deeper parent melt to the known porphyry intrusions is speculated to represent a possible source of the late metal-bearing fluids (Arribas et al., 1995).

Garcia (1991) concluded that some base metal-gold mineralization is related to neutralization of low pH magmatic-derived waters during the last stages of activity.

3. Mt Kasi, Fiji

The Mt. Kasi Prospect, Fiji (Fig. 1.2) is a poorly eroded, structurally controlled high sulfidation system in which gold-copper mineralization formed at a high crustal level. The following discussion is taken from Corbett and Taylor (1994) and Leach (unpubl. report 1994). Production began in 1996 to extract a resource comprising: 1,048,000 t of eluvial Au @ 1.9 g/t, and 1,240,000 t of hard rock @ 3 g/t Au (total of 180,000 oz Au). Workings from 1932 to 1948 produced 261,000 t @ 7.5 g/t Au (63,000 oz Au).

Host rocks comprise Late Miocene lavas and pyroclastics which are intruded by dacite domes. An aeromagnetic high in the vicinity of the Mt. Kasi Prospect, which may be indicative of a magnetite-bearing altered intrusion at depth, appears to be offset with a sinistral displacement, by a NNW trending corridor of structures termed the Mt. Kasi fault system (MKFS) (Fig. 6.26). The high contrast between the resistive silicification and the enclosing conductive clay alteration has facilitated the subsurface mapping of the Mt. Kasi alteration system by CSAMT (controlled source audiomagnetictelluric) geophysics (Corbett and Taylor, 1994).

Zoned alteration extends from localized steeply-dipping silicification, formed as interpreted fluid upflow features, laterally into interpreted fluid outflows, which were identified in early drilling to be rootless. Upflows tend to be localized at intersections of cross structures with the MKFS, and paleo-flow directions are apparent from the shapes of upflow-outflow relationships (Figs. 6.26, 6.27). The cross faults may produce late- to post-mineral offsets of the alteration in a configuration similar to domino structures (Fig. 3.9). The 1100 workings are therefore inferred to occur within a fluid upflow feature which becomes an outflow at the open pit workings. Another upflow zone is evident in the Done Creek area.

The overprinting of alteration by mineralization is apparent at Mt. Kasi. The individual fluid upflow-outflow centres derived from an initial interpreted vapour-dominated fluid display alteration zonation grading outward from: cores of residual (vughy) quartz grading outward to quartz-alunite, and kaolin alteration. Gold and copper mineralization associated with the later, inferred liquid-dominated fluid, exploited the same plumbing system during continued deformation on the MKFS. Ore forms the matrix to breccias within the competent residual silica, and gold/copper grades are proportional to the matrix content of the breccias. Matrix supported rotational breccias proximal to the fluid upflow zones contain higher gold grades than the peripheral fluidized and crackle breccias in the outflow zones (Corbett and Taylor, 1994; Fig. 6.27). NW trending fractures, slickensided faults and sigmoidal-shaped fluidized breccia zones occur as dilational ore-hosting features, indicative of a continued sinistral movement along the MKFS during ore formation (Fig. 6.27; Corbett and Taylor, 1994).

Alteration at Done Creek grades outwards as concentric zones of: central residual (vughy) silica in which cavities are filled by kaolinite + dickite, quartz-kaolinite-interlayered illite-smectite, and peripheral sub-propylitic chlorite-carbonate. Local alunite fills leached vughs and has been replaced by later kaolinite.

Breccia-hosted gold mineralization consists of early pyrite-quartz and followed by later copper-gold. Ore was deposited in open fractures and leached vughs adjacent to fractures and overgrows earlier quartz and barite. Mineralization grades from luzonite-tennantite-chalcopyrite at depth to goldfieldite-tennantite at shallow levels (and in eroded float boulders), and elsewhere at Mt. Kasi (Turner, 1986) laterally to chalcopyrite-tennantite-galena-sphalerite in peripheral argillic zones. Bonanza grade gold mineralization (locally >1% Au) in float at Done Creek occurs as high fineness (>900) native gold, which was deposited as inclusions in, and overgrowing tennantite and goldfieldite, overgrowing pyrite, and filling vughs in earlier quartz-pyrite veins. Trace gold-tellurides (mainly calaverite) occur as minute inclusions in goldfieldite and tennantite. Inclusions of copper-tin sulfide minerals (colusite and hemusite), which contain appreciable vanadium and molybdenum contents respectively, have been recognised in some high gold grade silicified float.

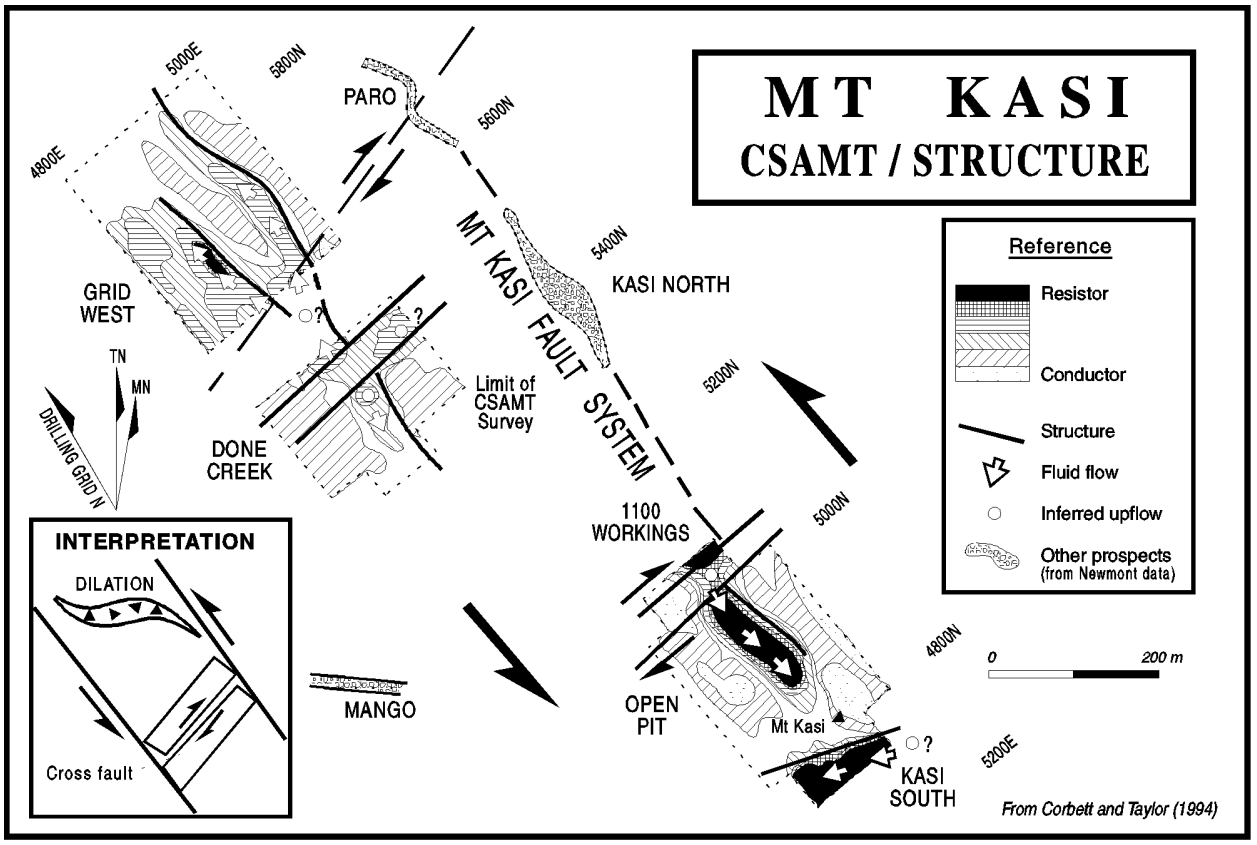

FIG. 6.26

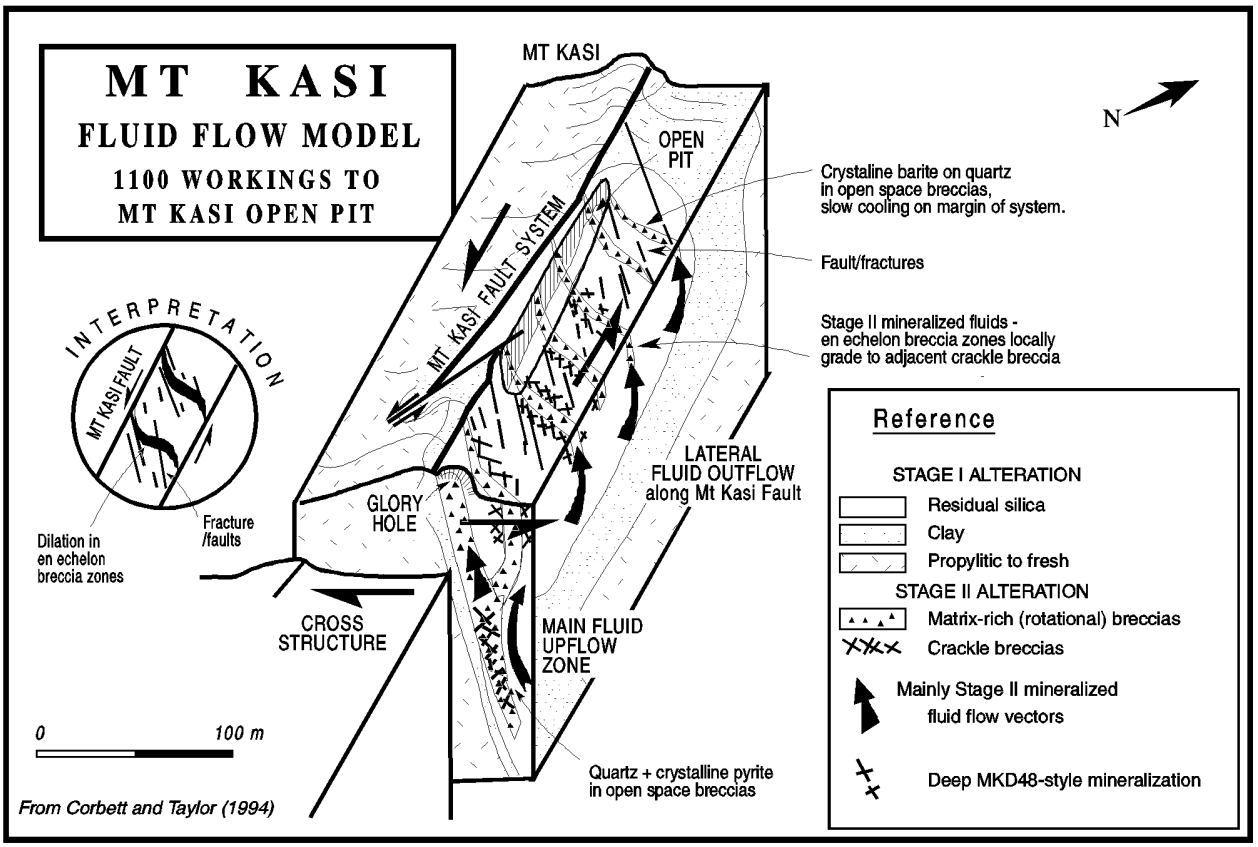

FIG. 6.27

Mt. Kasi is a high sulfidation system which is exposed at very shallow, epithermal levels. Recent mining has exposed features typical of hot spring deposits (G. Taylor, pers. commun.). This is consistent with the dominance in the alteration and mineralization mineralogy of quartz-kaolinite-dickite and luzonite-tennantite-goldfieldite respectively, and low homogenisation temperatures in barite within mineralized zones (averages of 165-220°C; Turner, 1986). The association of bonanza grade gold mineralization with tellurium (+ vanadium) in this epithermal high sulfidation system is comparable to the bonanza grade deposits in low sulfidation, intrusion-related, epithermal systems (e.g., Zone VII at Porgera, Papua New Guinea).

Paleo-fluid flow is apparent as the several centres of fluid upflow and outflow, which suggest that fluid has flowed away from an inferred dilational jog in the Mt Kasi fault system at the central portion of the prospect (Fig. 6.26). Minor dacite in this area may be indicative of a magmatic source at depth for the high sulfidation alteration and mineralization.

v) Composite Structurally and Lithologically Controlled Gold-Copper High Sulfidation Systems.

a) Characteristics

Most high sulfidation gold-copper systems display both lithological and structural control, and those classified above as either lithologically or structurally controlled are in essence part of a continuum. These controls may vary from one part of a system to another or with time. A diatreme margin could be classed as a permeable lithological contact by some, or as a structural contact by other workers. Dilatant structures which tap the magmatic source, typically control the fluid flow at depth. Upon contact with permeable host rocks, a lithological control may become evident, particularly in the upper portions of many systems.

Examples of systems which display approximately equal structural and lithological control include: Maragorik, East New Britain, Papua New Guinea (G. Corbett et al., 1991; Corbett and Hayward, 1994); Peak Hill, eastern Australia (Degeling et al., 1995); Bawone-Binebase, Sangihe Is, Indonesia (Corbett unpubl. report, 1993).

b) Examples

1. Peak Hill, eastern Australia

Although occurring in a Late Ordovician magmatic arc of the Lachlan fold belt, eastern Australia (Walshe et al., 1995), Peak Hill displays features typical of younger high sulfidation gold-copper systems, as summarised from Degeling et al., (1995).

On a regional scale, the inferred magmatic source for the high sulfidation alteration and mineralization may have been localized by the intersection of NW-trending transfer structures which offset the magmatic arc to form an inferred graben, and the arc parallel Parkes thrust (Fig. 3.11). Host rocks comprise andesitic volcanic and epiclastic rocks. An initial lithological control to the high sulfidation alteration is evidenced by the localisation of silicification at the intersections of NW trending structures (parallel to the graben trend) and permeable host rocks (e.g., Bobby Burns workings, Fig. 6.28). These structures also create post-mineral offsets of the alteration (e.g., Crown workings, Fig. 6.28), and host possible earlier low sulfidation quartz veins. In addition, NW structures localize fracture controlled mineralization which is best developed in portions of the NW structures which deviate to WNW trends (e.g., Proprietary open pit, No. 2 and Mingelo stopes, Fig. 6.28). The model presented by Degeling et al. (1995) suggests that regional sinistral movement on the NS-trending arc parallel structures similar to the sinistral Gilmore suture (Section 3.v.b), has facilitated the formation of local dilational ore-hosting WNW-trending flexures where the NW fractures transgress the competent silicification.

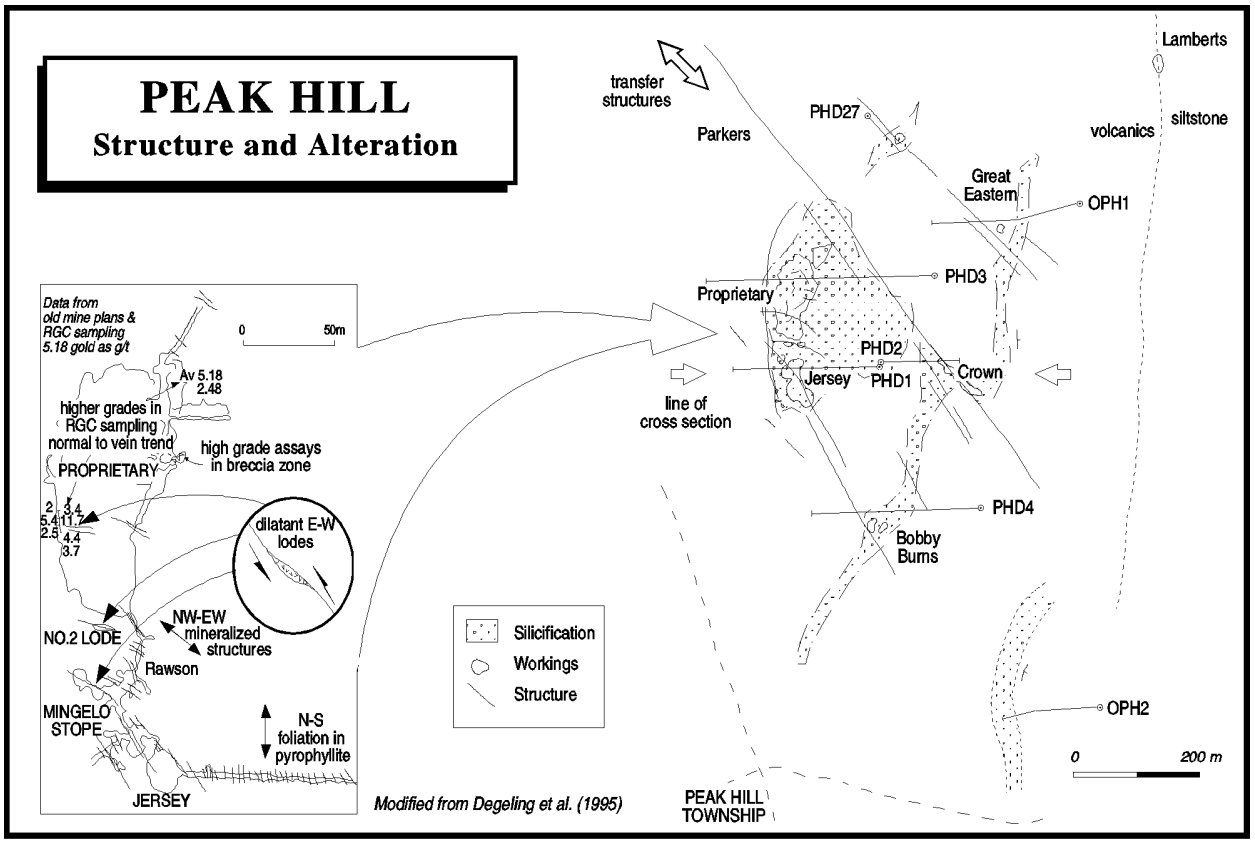

FIG. 6.28

MESO-THERMAL	HIGH SULFIDATION			DEFORM-ATION	RETROGRADE COLLAPSE
STAGE I	STAGE II			STAGE III	STAGE IV
Buck quartz	Zoned alteration	Massive sulfide	Mineralization and gangue	Foliation alteration	Overprint
Massive quartz veins (blows)	Residual quartz ⇨ Quartz-alunite ⇨ Quartz-mica -kaolinite ⇨ Mica-chlorite ⇨ Epidote-chlorite-carb	Pyrite	Initial barite and /or alunite Later Cu-sulfides zoned Enargite/luzonite ⇨ tennantite	Deformation and foliation Zoned pyrophyllite -sericite	Alunite + kaolinite

Peak Hill - Paragenetic sequence of alteration and mineralization

From Degeling et al. (1995)

FIG. 6.29

Four distinct stages of hydrothermal activity have been recognised at Peak Hill (Fig. 6.29):

Stage I: Massive white quartz veins host gold mineralization at Myall United or McPhails workings north of Peak Hill, and at the Crown workings at Peak Hill, and are herein inferred to predate the high sulfidation mineralization. These veins strike NW and exhibit locally higher gold grades in WNW-trending segments.

Stage II: This is the main high sulfidation alteration and mineralization which developed progressively as:

i) The initial lithologically controlled alteration exploits the permeable epiclastic units within the volcanic sequence over a 500 x 1000 m area. At the Proprietary workings (Fig. 6.29), alteration comprises a central core of residual (vughy) and massive quartz which is hosted in a steeply dipping fine grained pyroclastic and rimmed by silica-alunite (Fig. 6.30). The silicified zones grade to silica-micaceous clay alteration which is broad on the east and narrow to the west. The micaceous clays are interpreted to have been formed during post-high sulfidation deformation, and grade from sericite at depth and in the south, to pyrophyllite at shallow levels and to the north. Trace andalusite co-exists with pyrophyllite at Great Eastern. The less permeable andesitic volcanics host alteration, which grades westward from the central silica-micaceous clay as zones of: silica-paragonite, paragonite-chlorite, chlorite-albite and epidote-albite-chlorite (Fig. 6.30). The alteration zonation reflects the progressive neutralization and cooling of a hot acidic fluid as it migrates away from permeable lithologies (Fig 6.3). The silicification is more extensive closer to the inferred NW feeder structures and dies out moving along the strike of the permeable units (e.g., Parkers, Fig. 6.28).

ii) The zoned alteration, and especially the more brittle quartz and quartz-alunite zones, displays fracturing and local brecciation, accompanied by deposition of quartz-barite + alunite. In drill hole OPH2, south Peak Hill (Fig. 6.28), silicified vughy volcanics are intensely fractured and brecciated, and sealed in a vein breccia of bladed coarse tabular alunite. This type of alunite vein/breccia is common in high sulfidation systems proximal to source intrusions (Section 4.ii).

iii) Further fracturing and brecciation was accompanied by sulfide deposition as early massive pyrite, followed by later copper-gold ore minerals. Copper-gold mineralization at Proprietary is localized at the intersection of the central residual silica zones and the NW trending feeder structures. Sub-economic copper mineralization at Proprietary, and to a lesser degree at Parkers, is restricted to a zone of quartz-pyrite-barite alteration, and is dominated by tennantite and minor luzonite (Fig. 6.28). Tennantite is locally enriched in Te, and trace minute Au-tellurides (calaverite) have been reported as inclusions in some pyrite (Allibone, 1993). High fineness (943-968) native gold occurs with tennantite filling fractures cutting pyrite. The occurrence of Te-rich mineralogy, tennantite-luzonite copper mineralization, and free gold are indicative of formation at shallow epithermal levels in a high sulfidation system. Chalcopyrite-enargite + bornite mineralization predominate at Bobby Burns, closer to the inferred intrusion source (below).

Stage III: This is the main phase of post-alteration/mineralization deformation and shearing. The zonation in micaceous clays outlined above is inferred to indicate lower pH conditions to the north during deformation.

Stage IV: The presence in open cavities and breccia zones, of late stage kaolinite and gypsum and fine grained pseudo-cubic alunite at depth, implies that cool, acidic fluids collapsed onto the earlier alteration. In places the pseudo-cubic alunite is slightly deformed, however in most cases it is undisturbed, indicating that most of the Stage IV retrograde activity occurred after deformation/shearing.

Information from structure, alteration and mineralization suggest that hot acidic magmatic fluids may have been derived from an intrusion source in the vicinity of a magnetic high about 1.5 km to the southeast of Peak Hill. It is interpreted that volatile-rich magmatic fluids migrated along the NW transfer structures, resulting in the

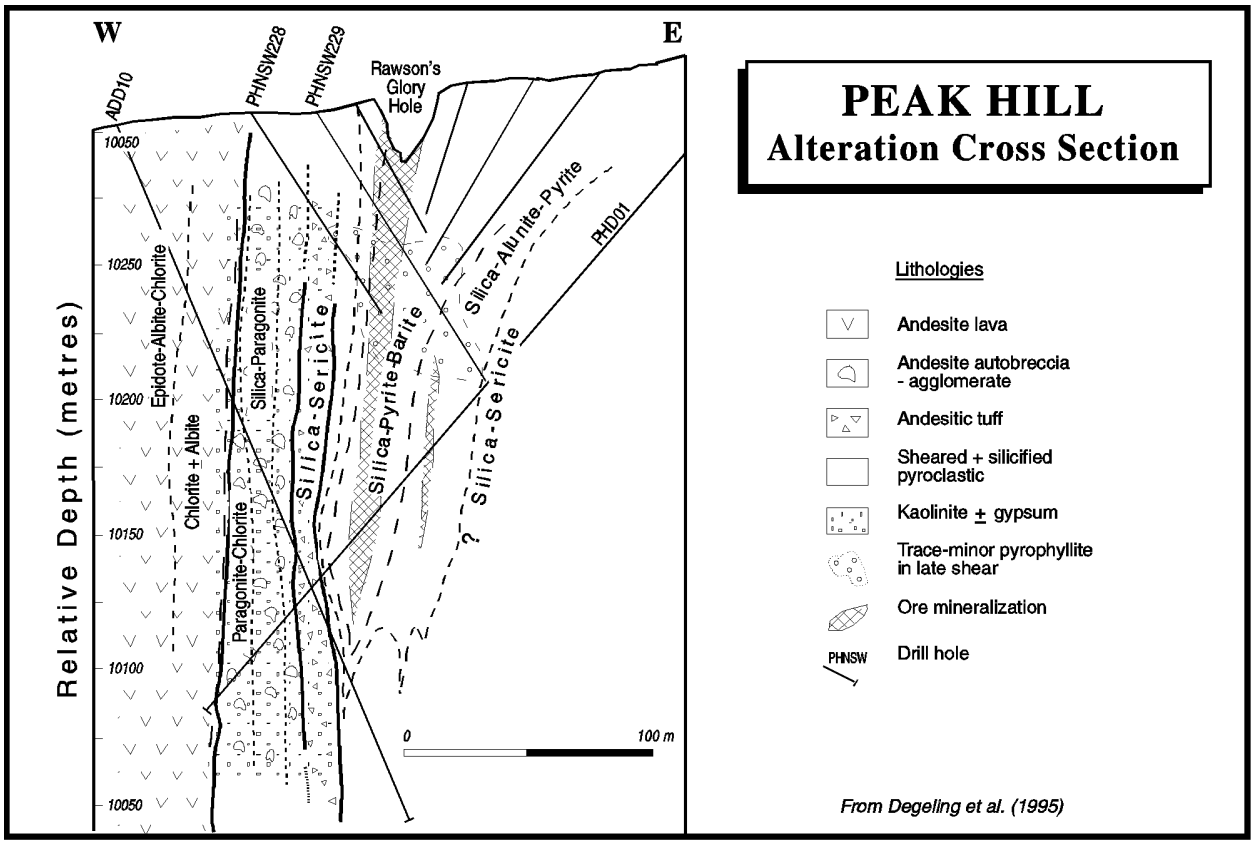

FIG. 6.30

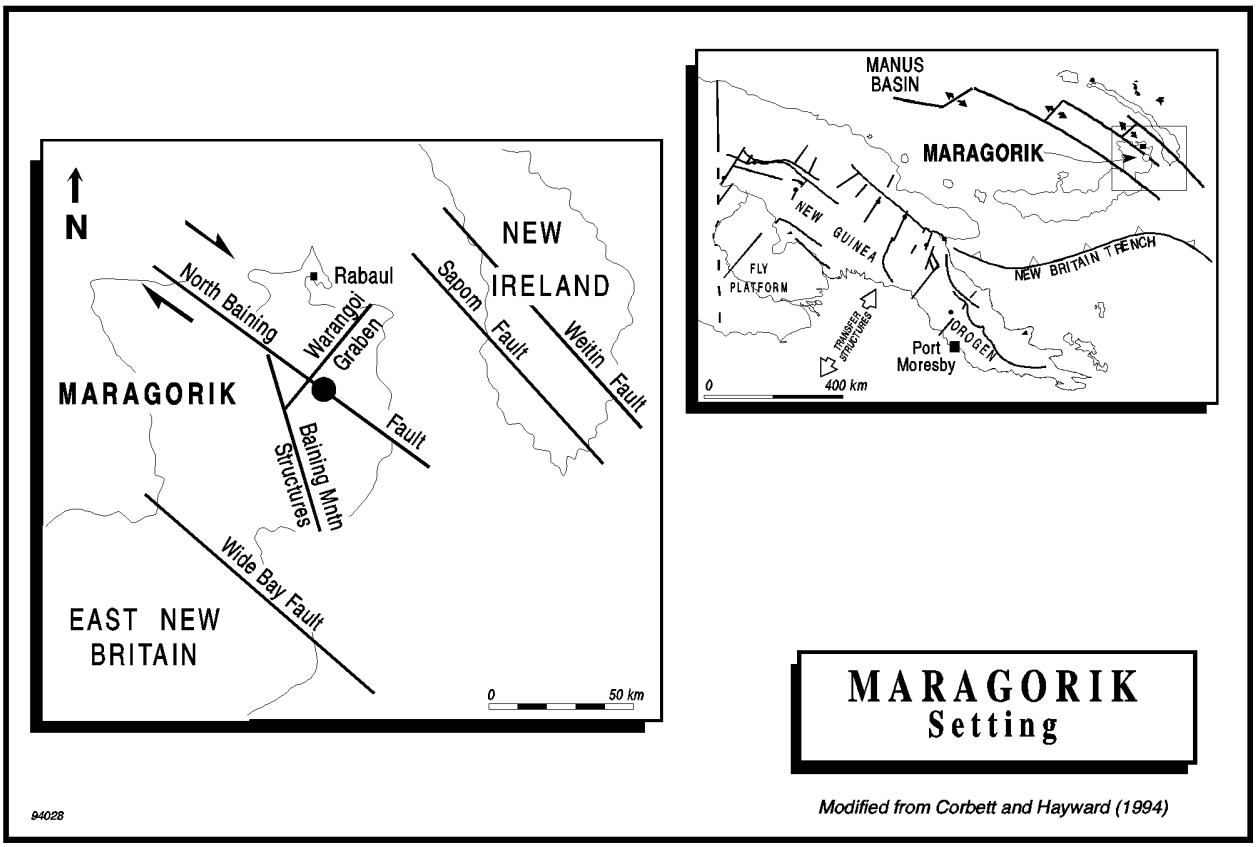

FIG. 6.31

formation of zoned alteration centred in permeable pyroclastic units. Later mineralized fluids moved northwesterly along the same regional structures, and deposited gold-copper mineralization within dilational WNW-EW trending fractures hosted in brittle silicified zones. Extensive shearing and deformation at Peak Hill (Allibone, 1993; Allibone et al., 1995) is interpreted herein to predominantly post-date the development of the high sulfidation system, and to have resulted in the recrystallization of much of the peripheral clay alteration into sericite or pyrophyllite.

2. Maragorik, East New Britain, Papua New Guinea

The Maragorik Prospect, East New Britain, Papua New Guinea, is a poorly eroded high sulfidation gold-copper system (Corbett et al., 1991; Corbett and Hayward, 1994). As extensive ash deposits blanket East New Britain, CSAMT geophysics, in conjunction with bulldozer trenching, were used to delineate the subsurface geology. This geophysical tool, which delineates alteration of differing resistivity (Fig. 6.33), is applicable to high level high sulfidation systems characterized by sharp boundaries between silica and clay alteration (e.g., Mt Kasi, Fiji; above).

As typical of southwest Pacific rim high sulfidation systems, alteration and mineralization at Maragorik are inferred to have been derived from a two stage vapour- and liquid-dominated hydrothermal fluid (Section 6.i.c). At deeper levels fluid upflow occurred along EW structures dilated by the rotation on the bounding major NW linear structures (Figs. 6.31, 6.32). At higher levels, the rising hydrothermal fluids flowed laterally along permeable horizons which intersect the upflow structures. Lapilli tuff units within a dominantly lava sequence controlled the vapour-dominated fluid flow to form flatly dipping ledges of silicification and peripheral clay alteration, while the feeder structures are evident as steeply dipping ledges (Fig. 6.33). Mineralization occurs as the sulfide matrix to breccias within the earlier formed competent silicified flatly dipping ledges, best developed proximal to the steeply dipping feeder structures. The rimming incompetent clay alteration did not fracture and so is barren.

Alteration and mineralization, indicative of a very low temperature and hence high level system, are characterized by opaline silica, smectite dominated clays (Figs. 6.32, 6.3), and luzonite as the low temperature polymorph of enargite (Fig. 6.4). Although high sulfidation systems are inferred to develop from porphyry-related magmatic fluids, such a source at Maragorik is interpreted to be very deeply buried.

3. Bawone-Binebase, Sangihe Island, Indonesia

At Bawone-Binebase on Sangihe Island, Indonesia, both structurally and lithologically controlled high sulfidation gold-copper mineralization are interpreted to have been derived from the one fluid source (Fig. 6.34; G. Corbett, unpubl. report, 1993). Low grade (propylitic/phyllic) porphyry-style alteration and mineralization occur at Binebase and elsewhere on Sangihe Island. Low sulfidation mesothermal quartz-sulfide veins are the interpreted hypogene source for supergene gold recovered by illegal miners at Taware Ridge, south Sangihe Island. The inferred magmatic source for the Bawone-Binebase high sulfidation system, north Sangihe Island, is localized on the margin of an inferred NNW trending graben by the intersection of thoroughgoing NNE lineaments (Fig 6.34). Sinistral movement on the NNW graben-bounding structures has dilated ESE fractures (Fig. 6.34) which are interpreted to tap the magmatic source and form a fluid upflow feature.

At Bawone, a fluid flow model can be deduced from the zoned alteration and gold-copper distribution in several cross sections (Fig. 6.34). Hot magmatic fluids are inferred to have flowed upward in the vicinity of late stage diatreme breccias, and then laterally along the dilatant structures towards the SE. The size of the alteration zones, temperature of formation and metal grades all decline moving from the upflow to outflow settings. The zonations and paragenetic sequences of overprinting alteration and mineralization are typical of high sulfidation

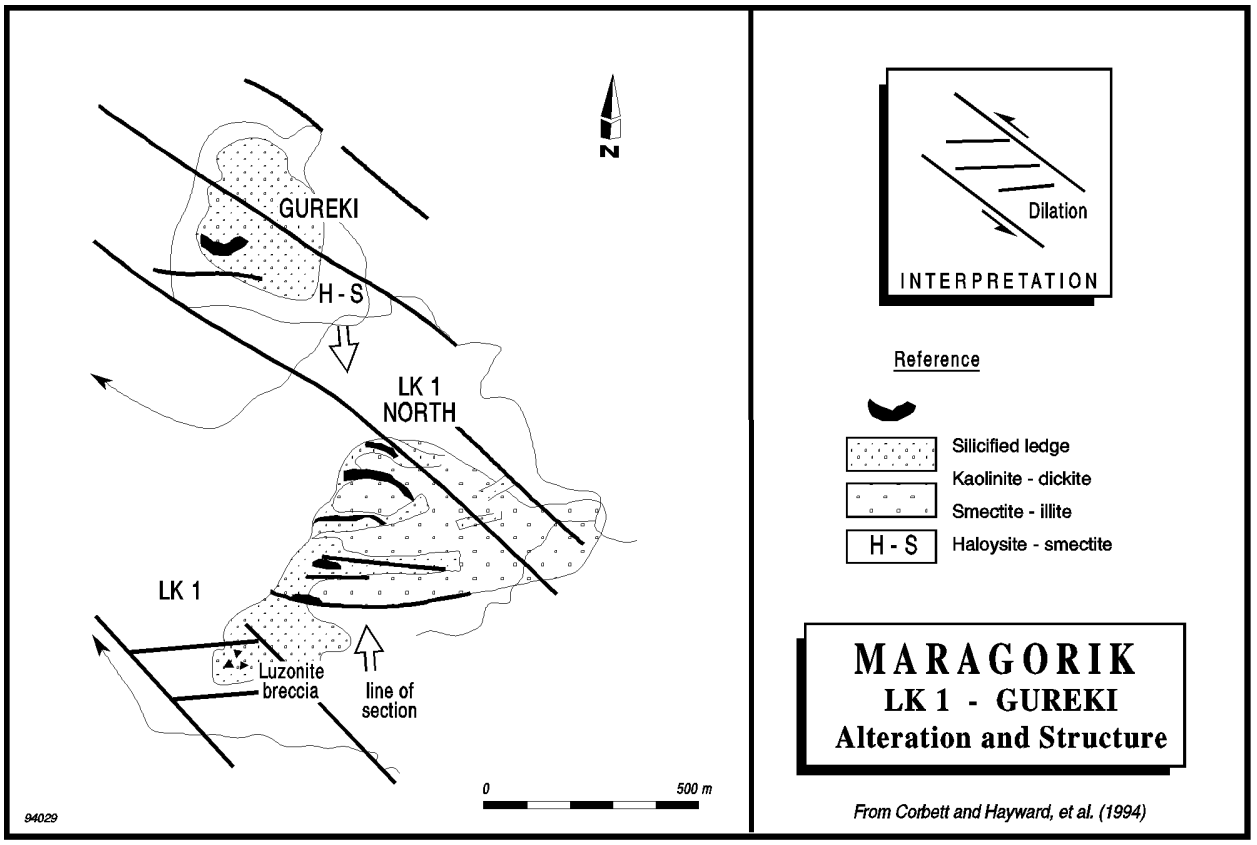

FIG. 6.32

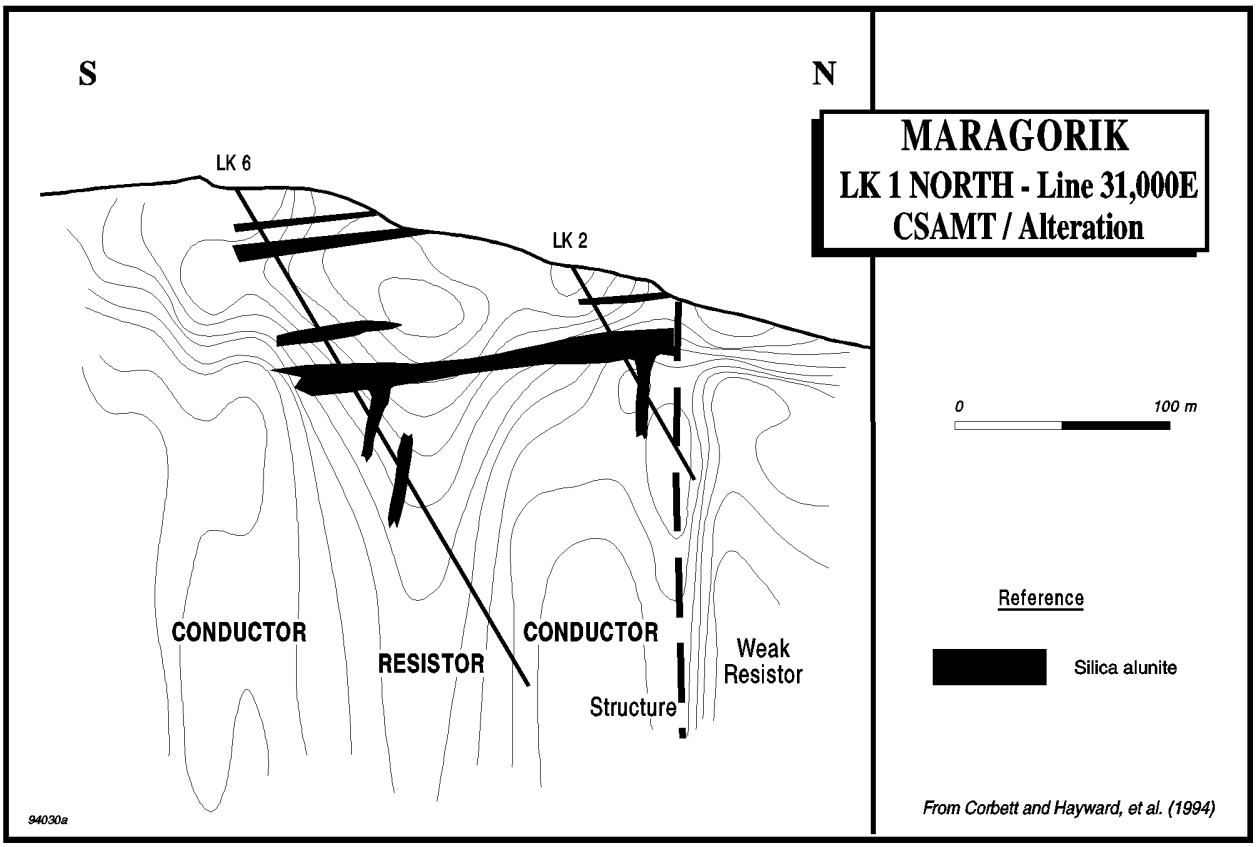

FIG. 6.33

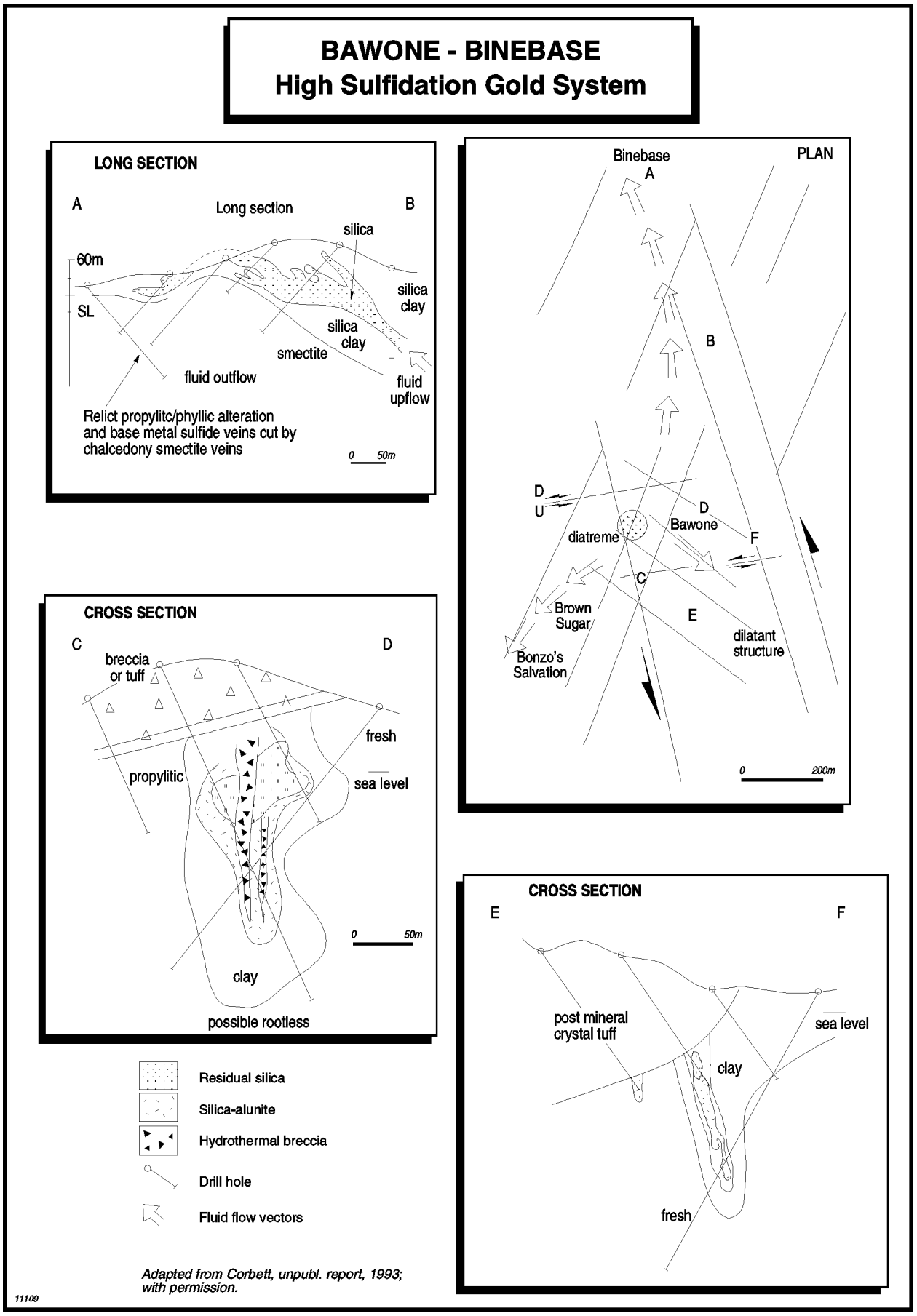
BAWONE - BINEBASE
High Sulfidation Gold System
LONG SECTION
A
Long section
B
silica
60m
SL
silica
clay
silica
clay
smectite
fluid outflow
fluid
upflow
Relict propylitc/phyllic alteration
and base metal sulfide veins cut by
chalcedony smectite veins
0 50m
Binebase
A
PLAN
B
D
U
D
Bawone
diatreme
F
C
Brown
Sugar
E
dilatant
structure
Bonzo's
Salvation
0 200m
CROSS SECTION
C
D
breccia
or tuff
fresh
propylitic
sea level
0 50m
clay
possible rootless
CROSS SECTION
E
F
post mineral
crystal tuff
sea level
clay
fresh
Residual silica
Silica-alunite
Hydrothermal breccia
Drill hole
Fluid flow vectors
Adapted from Corbett, unpubl. report, 1993;
with permission.
11109

FIG. 6.34

systems. The local sharp contacts between; residual (vughy) silica, silica-alunite and peripheral clay alteration, indicate formation at a high crustal level or distal to the inferred magmatic source, and are typical of an outflow portion of the hydrothermal system. Mineralization occurs as filling of vughs in the residual silica as sulfide matrix to the brecciated competent residual silica and silica-alunite alteration.

While the bulk of the hydrothermal fluids flowed to the SE along the dilatant structures, relatively small structurally controlled high sulfidation mineralization occurs to the SW at Brown Sugar and Bonzo's Salvation. Here, observed rapid changes in alteration zonation are consistent with fluid quenching. This, and the presence of low temperature alteration minerals, reflect a distal setting to the inferred fluid upflow in the vicinity of the diatreme breccia (Fig. 6.34).

At Binebase, alteration and mineralization are interpreted to have been derived from fluids which flowed northward along the throughgoing NNE and then NNW structures and then intersected a permeable lapilli tuff unit (Fig. 6.34). Low temperature alteration assemblages are consistent with the distal relationship to the inferred fluid source at Bawone. Chalcedonic quartz becomes increasingly vughy down dip and to the south towards the inferred upflow. As seen in some other lithologically controlled high sulfidation systems (e.g., Wafi, Papua New Guinea), there is little distinction between alteration and mineralization resulting from the early vapour-dominated fluid phase, and the later liquid-dominated mineralized fluid. The abundant gypsum and barite suggest that incursion of sea water could have occurred, possibly from the NW.

iv) Hybrid High-Low Sulfidation Systems

a) Introduction

Giggenbach (pers. commun., in Hedenquist, 1987) states that "ascent of volcanic (magmatic) gases and their transition from an oxidized (sulfur as SO_2 - high sulfidation) to reduced (sulfur as H_2S - low sulfidation) state is 'a battle of the buffers' (i.e., between the fluid and wall rock), in which each achieves a partial victory". Hedenquist (1987) postulated that there is a continuum from high to low sulfidation systems, and this is dependent on the degree of access of these upwelling fluids to neutralization (and cooling) through reaction with the wall rock and/or circulating surficial waters.

All high sulfidation systems exhibit zoned alteration, which indicates that this process of cooling and neutralization occurs within subsidiary structures or permeable lithologies. In this environment the magmatic-derived fluids can be modified away from the major fluid feeder structures. However, in certain cases, the upwelling hot acidic, magmatic-derived high sulfidation fluids become cooled and neutralized while remaining within the major feeder structures. This results in a transition from high to low sulfidation type fluids, and the formation of a hybrid style of gold deposit (e.g., Wild Dog, Papua New Guinea). Elsewhere, the initial hydrothermal fluid may be dominantly high sulfidation, but later fluids of a low sulfidation nature (e.g., Lepanto; Garcia, 1991: El Indio, Chile; Jannas et al., 1990). This may result from: extensive mixing of the magmatic hydrothermal fluid with circulating meteoric water to form a more reduced and/or neutralised liquid, or changes in the chemistry of the volatiles and liquids, which exsolve from the magmatic source during late stage of melt crystallization.

b) Examples

The Wild Dog Prospect, Papua New Guinea (Lindley, 1987, 1988, 1990) displays characteristics of both high and low sulfidation gold systems, and Arribas (1995) notes that Masupa Ria, Indonesia (Thompson et al., 1994) and the Kelly Mine, Philippines (Comosti et al., 1990) are examples of overprinting hydrothermal systems. Superimposed high and low sulfidation alteration and mineralization are apparent as the base metal-gold veins which are reported to cut the high sulfidation system at Lepanto, Philippines (Garcia, 1991). High sulfidation

alteration and mineralization on Wetar Island, Indonesia, described below as an exhalative style of system, also displays an inferred evolution from a high to low sulfidation system.

1. Wild Dog, East New Britain, Papua New Guinea

The Wild Dog Prospect in northern New Britain was discovered in 1983 during a regional stream sediment exploration programme which investigated the earlier identification of altered float and pannable gold (Lindley, 1987). Evaluation of the project by Esso (Papua New Guinea), City Resources and Highlands Gold Limited continued until the early 1990's. Host rocks comprise andesitic to dacitic lavas and tuffs to which Lindley (1987, 1988) attributes a probable Mio-Pliocene age. Recent ash partly blankets the area.

Wild Dog is one of several alteration systems hosted within the Warangoi structural corridor, which cuts an inferred Nengmutka caldera (Lindley, 1987, 1990). The caldera is localized within the Baining Mountain graben structures which, based on data showing the depth to the mantle (Wiebenga, 1973), may represent the margin of a deep rift (Fig. 6.35; G. Corbett, unpubl. report, 1990). At the prospect scale, three NNE trending and west dipping silicified zones occur within the Warangoi structural corridor as a prominent ridge (Lindley, 1986). NW trending cross structures apparent on outcrop scale, are exploited by the drainage pattern, and locally offset the silicified zones, as slickensided faults, and localize gold mineralization (G. Corbett, unpubl. report, 1990; Fig. 6,36).

Two main hydrothermal events are recognised as (Fig. 6.37):

i) Replacement silicification of regionally propylitic (epidote-pyrite-chlorite) volcanics produced a dense, grey, fine grained chert-like alteration (Lindley, 1990). These steeply dipping silicified zones are unmineralized, pinch and swell up to true widths of 50-70 m, and are aligned NNE parallel to the Warangoi structural corridor and assumed to be structurally controlled. Alteration mineralogy in the silicified zones and the immediate wall rock is vertically zoned from deeper to shallower levels as: sericite + pyrophyllite, through sericite, to local sericite + chlorite (T. Leach, unpubl. report, 1990). Trace molybdenite mineralization is associated with the silicification.

Similar structurally controlled silicification occurs locally along the Warangoi structure at Keamgi Hill, 2 km SSW of Wild Dog, and Kasie Ridge, 4 km to the NNE (Fig. 6.35). At Kasie Ridge, 300 m lower in elevation than Wild Dog, sub-parallel NNE trending silicified ridges are zoned outwards as zones of: central quartz-alunite + zunyite + pyrophyllite + diaspore, through pyrophyllite-sericite + kaolinite/dickite and sericite + illitic/kaolin clay, to peripheral chlorite-illitic clay, and regional propylitic alteration (T. Leach, unpubl. report, 1990). This zonation is comparable to high sulfidation systems encountered elsewhere in the southwest Pacific.

ii) At Wild Dog polyphasal steeply dipping quartz tension veins cross cut the more moderately dipping NW trending silicified zones, commonly as hanging wall splits, and are best developed near the cross structures (Lindley, 1990; G. Corbett unpubl. report, 1990). Later mineralization fills open fractures and cavities in the quartz veins as dark sulfide stringers comprising copper minerals (chalcopyrite and minor bornite, chalcocite and tennantite), with local occurrences of a wide variety of Cu-Bi-Pb-Ag sulfide, telluride and sellenide minerals (Lindley, 1990). Gold is generally restricted to Au-Ag telluride minerals (Lindley, 1990), and native 'mustard' gold occurs as an alteration (weathering) product of these tellurides. (Also see Bilimoia low sulfidation mineralization, Section 7.ii.d)

Zonations in illite and smectite clays and fluid inclusion data for the late quartz veins are interpreted to indicate that copper-gold mineralization took place in response to the mixing of cool (<200°C) and dilute (<2.0 wt % NaCl) meteoric waters, with upwelling hot (>280°C) and saline (>15 wt % NaCl) fluids (T. Leach, unpubl. report,

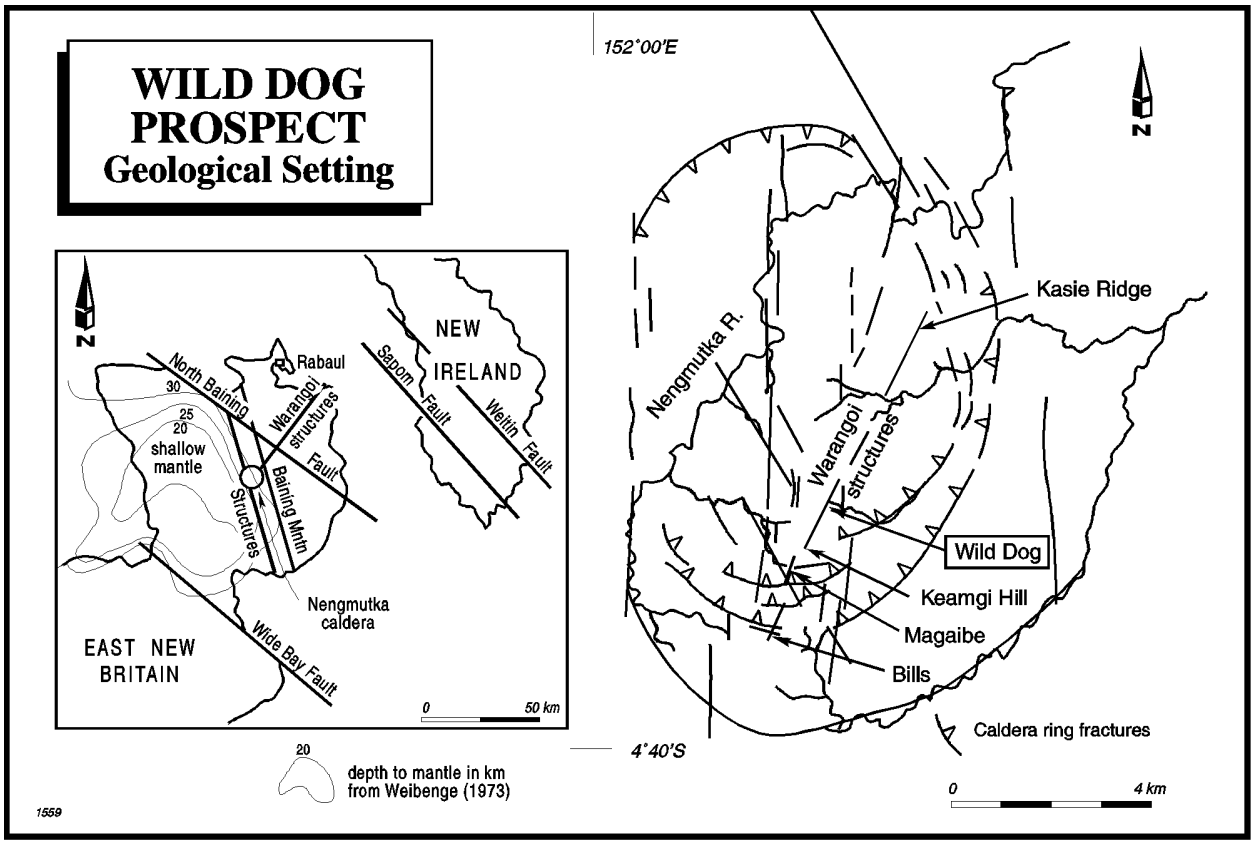

FIG. 6.35

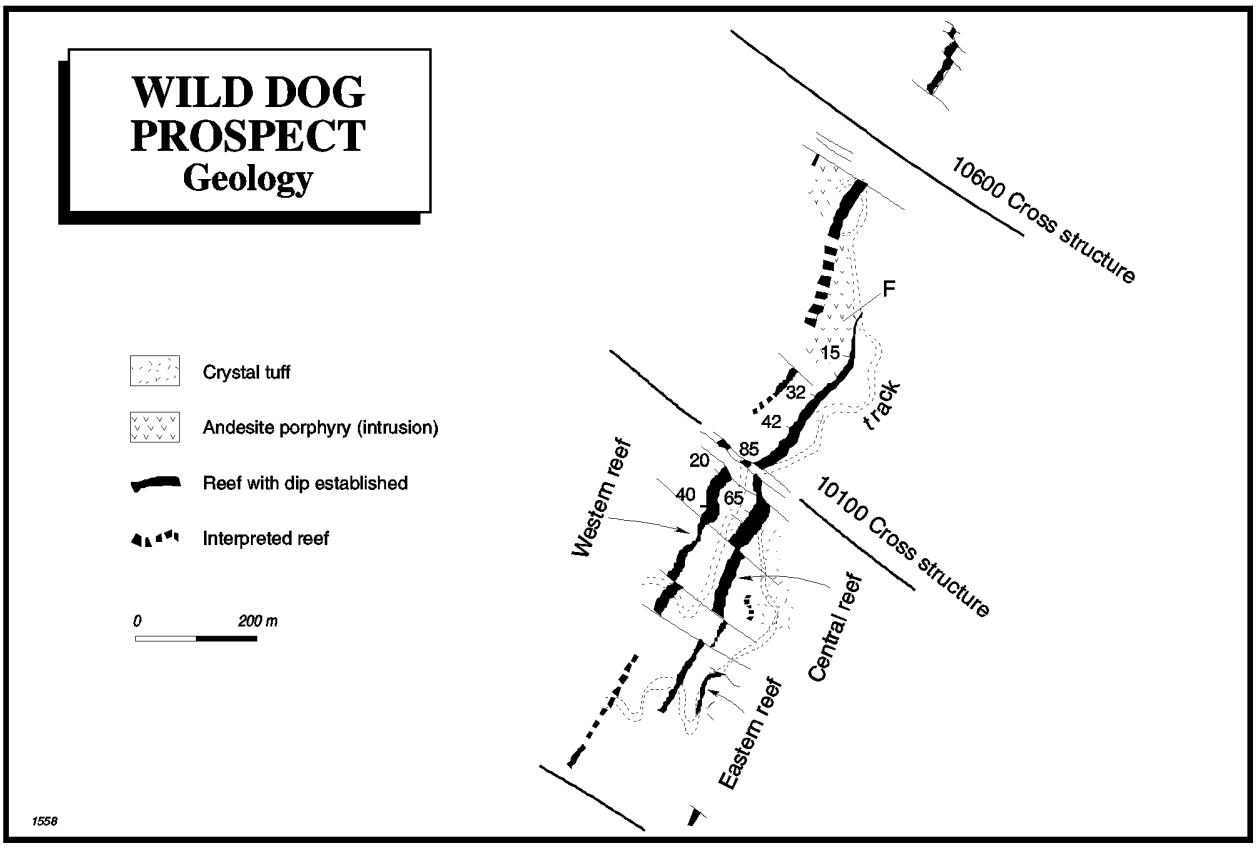

FIG. 6.36

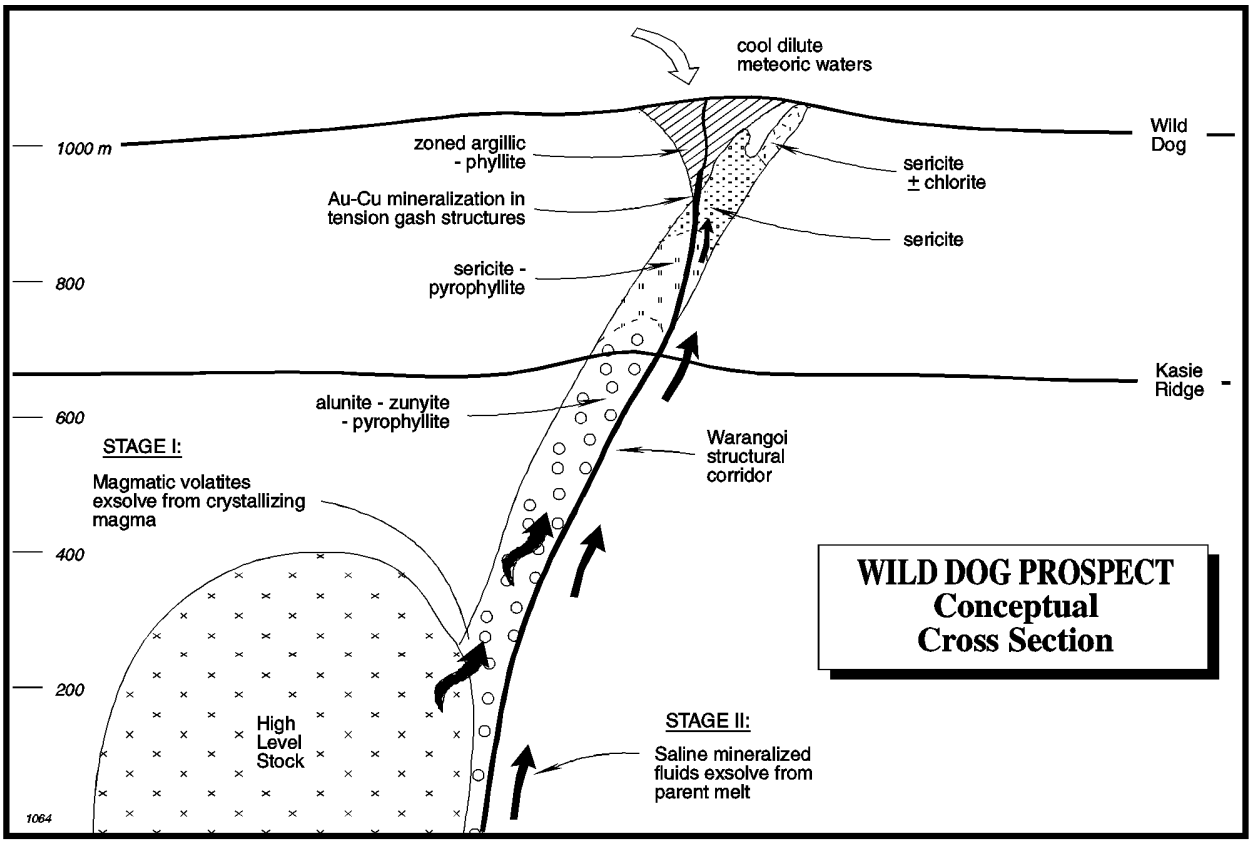

FIG. 6.37

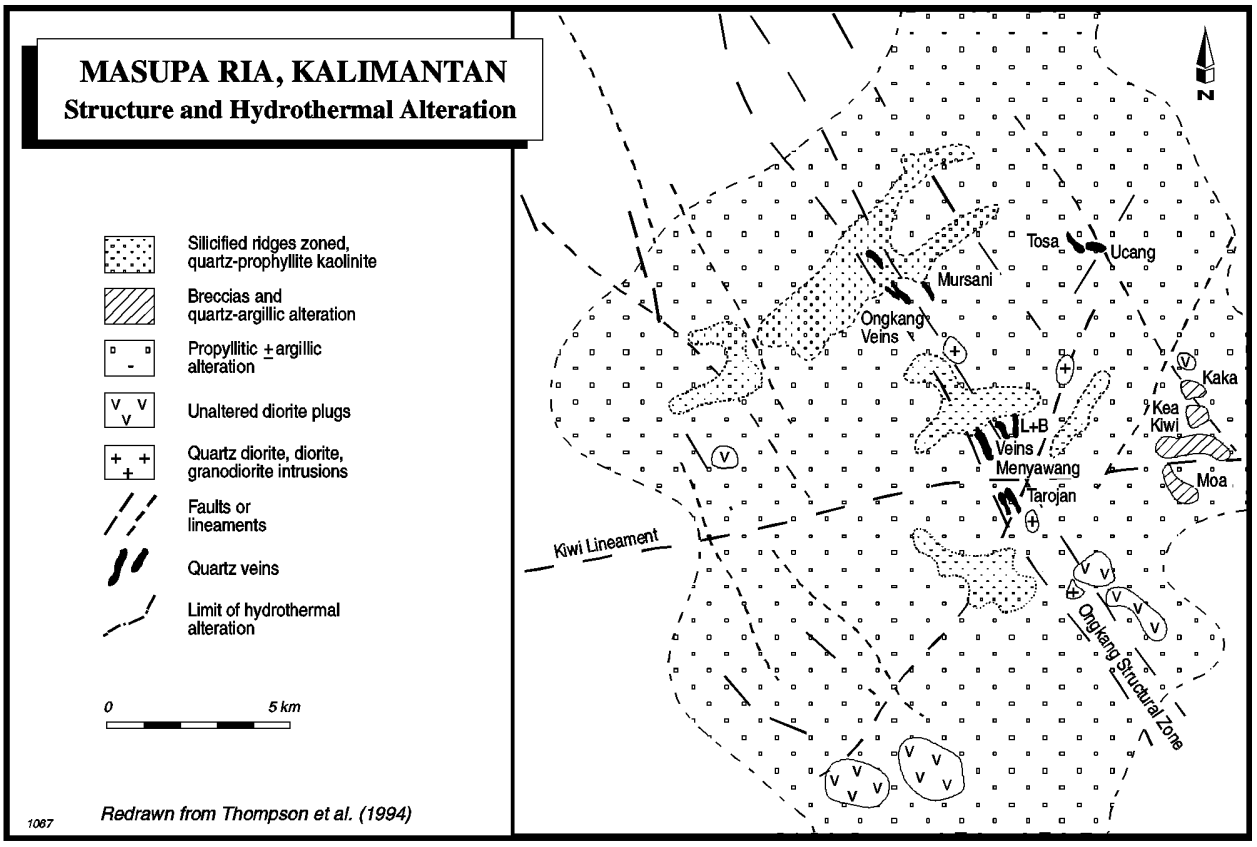

FIG. 6.38

1990).

It is interpreted herein, that the prospects in the Wild Dog region formed as composite high- and low-sulfidation systems. Initial silicification was caused by hot acidic fluids which exsolved from a crystallising high level intrusion into the Warangoi structural corridor (Fig. 6.35). These acidic fluids progressively became neutralized at shallower levels as indicated by the zonation from alunite-zunyite-pyrophyllite at Kasie Ridge, through pyrophyllite and sericite, to near surface sericite-chlorite at Wild Dog and Keamgi Hill (Fig. 6.37). This is comparable to the initial stage of vapour-rich leaching in high sulfidation systems. Later gold mineralization is related to fracturing of the silicified zones and inferred contemporaneous release of magmatic-derived, mineralized fluids from depth (e.g., the parent melt). These fluids mixed with cool dilute meteoric waters within tension veins, and resulted in the Cu-Bi-Pb-Te-Au mineral deposition, typical of low sulfidation quartz-sulfide lodes (Section 7.ii).

2. Masupa Ria, Central Kalimantan, Indonesia

Overprinting low and high sulfidation systems at Masupa Ria have been described by Thompson et al., (1994) and T. Leach (unpubl. reports, 1987-1989). Flat lying ridges of zoned quartz and advanced argillic alteration at Masupa Ria are localized at the intersection of NW transfer structures and NE structures which form part of the magmatic arc (Figs. 3.12, 6.38). These ridges comprise massive to vughy quartz which passes with increasing depth to alteration categorized as: pyrophyllite-kaolinite-dickite, quartz-sericite, and regional epidote-chlorite-calcite (propylitic). This alteration is hosted in flat lying pyroclastic units which are interpreted to have acted as permeable host rocks for outflowing high sulfidation-style acidic fluids.

Although barren of mineralization, the silica-alunite ridges have fractured as brittle host rocks to later low sulfidation style vein mineralization. The Ongkang vein system trends parallel to northwest transfer structures, and swells at the intersection with Masupa Ria silica ridge. Veins comprise colloform banded quartz (local quartz pseudomorphing bladed carbonate), typical of intrusion-related low sulfidation gold-silver quartz vein systems formed at epithermal levels (Section 8.v). Fluid inclusion analyses indicate that coarse quartz was deposited at 250-300°C from dilute (<3 wt % NaCl) fluids. Mineralization is restricted to thin sulfide bands composed of fine quartz, low temperature illite and chlorite, rare base metal sulfides and trace silver sulfosalts and sulfides. Gold occurs as minute free grains in the sulfide bands and in fractures cutting the banded quartz, and has an average fineness of around 820. Fractures and cavities are filled by barite, gypsum, kaolinite and smectite clays. Gold mineralization is interpreted to have developed in response to the mixing of hot mineralized liquids with cool meteoric waters.

It is not clear whether the silica ridges formed by high sulfidation fluids, and the auriferous quartz veins deposited by low sulfidation fluids, are different phases of the same magmatic-related hydrothermal system, or completely separate overprinting hydrothermal systems.

vi) High Sulfidation Exhalative Systems

a) Characteristics

The high sulfidation systems outlined above are interpreted to have formed in a subaerial environment by the modification of hot acidic fluids produced from the absorption of magmatic-derived volatiles and brines into circulating meteoric waters. However, there are a number of high sulfidation systems formed in a submarine environment, where magmatic-derived fluids are interpreted to condense into circulating seawater (Sillitoe et al., 1996). These are classified as high sulfidation deposits in a volcanogenic massive sulfide (VMS) environment (Sillitoe et al., 1996). These authors have characterized the high sulfidation VMS deposits as:
i) related to submarine intermediate to felsic intrusions,

ii) associated with advanced argillic alteration and capped by barite-rich zones,
iii) containing copper and/or gold mineralization within pyrite-rich zones and associated with several of: bornite, enargite, luzonite, tennantite, covellite as well as low Fe-sphalerite, orpiment and realgar.

Sillitoe et al. (1996) postulate that the copper-gold high sulfidation exhalative deposits are formed proximal to the intrusion source of the magmatic fluids, whereas the more classical Zn-Pb-Cu VMS deposits are equivalent to low sulfidation systems and develop more distal settings.

b) Active Analogue

An active analogue of high sulfidation exhalative systems in the southwest Pacific occurs in a back arc environment along the Valu Fa Ridge, southern Lau Basin, Fiji (Fig. 1.2; Herzig et al., 1993). Low temperature and inactive vents at 1,850-1,900 m depth in the Hine Hina region of the Lau Basin contain gold-rich barite-silica-sulfide precipitates which are hosted in andesite domes (Herzig et al., 1993). These authors describe the precipitates as being associated with advanced argillic alteration characterized by: pyrite-cristobalite-barite, alunite, pyrophyllite, native sulfur and opal C-T advanced argillic alteration.

c) Example

1. Wetar Island, Indonesia

A number of small, silver-rich copper-gold high sulfidation deposits on Wetar Island, east Indonesia have been described in detail by Sewell and Wheatley (1994), from which the following discussion is taken. These authors interpret the deposits to have formed in a submarine environment at depths of 600 m, and have been interpreted (Sillitoe et al., 1996) to represent high sulfidation VMS systems. The deposits currently occur at >400 m above sea level, which is indicative of some 1000 m of recent uplift.

Alteration and mineralization at the Lerokis and Kali Kuning deposits on Wetar Island are hosted in a sequence of subvolcanic dacite intrusions, which are overlain by submarine basaltic andesite pillow lavas and volcanics grading upwards into more felsic lavas, tuffs, breccias and domes. The sequence is capped by sedimentary rocks and epiclastic mudflows. The dacites have undergone silicification to quartz, opaline silica, cristobalite or tridymite. Variable kaolinite, smectite, interlayered illite-smectite, illite and zeolite and chlorite alteration occur around a central core of silicification. Alunite reported by Sewell and Wheatley (1994), has not been substantiated by later detailed petrology (G. Hedenquist, pers. commun., 1995).

The silicified dacites display pervasive quartz-pyrite stockwork veins and breccia fill, which grades upwards into a thick (up to >50 m) zone of massive pyrite + barite ± diaspore. Brecciation of the massive sulfide is accompanied by deposition of barite-silica-colloform banded pyrite-marcasite with minor disseminated copper mineralization which exhibits a depositional sequence of chalcopyrite --> chalcocite --> covellite-digeneite-enargite-tennantite. Massive pods of barite sand overlie the pyrite zones and are contiguous with the barite-silica breccia. Barite is cemented by iron oxides, opaline silica, minor carbonate and trace anhydrite. Native gold occurs as inclusions in barite, whereas electrum is intergrown with the iron oxides. High levels of mercury (average of 18 ppm) and lead (locally >1 %) are also recorded.

The sequence of early development of silicification and argillic alteration, followed by pyrite and then gold-copper mineralization associated with barite deposition, is common in the southwest Pacific high sulfidation systems described above. However, the Wetar deposits are unusually silver-rich for southwest Pacific rim high sulfidation systems (Au:Ag approx. 0.03-0.04), where the silver is associated with tetrahedrite and other sulfosalts. The paucity of extensive advanced argillic alteration is herein interpreted to suggest that these

deposits may be transitional to low sulfidation style hydrothermal systems, in which magmatic-derived volatiles condensed into circulating sea water to form only moderately low pH waters. These waters are speculated to have produced zoned silicification and argillic alteration in the felsic volcanics. Mineralization is postulated to be related to a subsequent influx of magmatic-derived, metal-bearing fluids which ascended along fractured silicified volcanics and mixed with sea water in a sub-sea floor environment.

7 PORPHYRY-RELATED LOW SULFIDATION GOLD SYSTEMS

i) Classification

a) Introduction

Intrusions emplaced in magmatic arcs provide heat sources to drive deep circulating hydrothermal systems which are composed of varying proportions of magmatic and meteoric fluids (Hedenquist and Lowenstern, 1994). Magmatic volatiles which evolve from the cooling magma, become entrained at the base of the circulating fluids (Giggenbach, 1991). Rock reaction and fluid mixing reduce gases such as SO_2 to H_2S, and HCl to dissolved salts, mainly NaCl (Giggenbach, 1992). As outlined in Section 1.iv, low sulfidation state sulfides are deposited from these reduced, near neutral fluids (Barton and Skinner, 1979) and such systems are correspondingly referred to as low sulfidation systems (Hedenquist et al., 1994).

In crustal settings where the intrusions are emplaced into thick permeable volcanic piles, the magmatic fluids become diffused within large circulating hydrothermal systems. This diffusion results in the formation of broad alteration zones, characteristic of many active porphyry-related geothermal systems (Section 2.iv.a), and commonly encountered in porphyry-copper systems (Section 5). Regional structures provide enhanced permeability, and channel outflows considerable distances from the intrusion heat source (e.g., 15-20 km at Bacon-Manito, Philippines).

However, in magmatic arcs at continental margins, high level intrusions are commonly emplaced into impermeable host rocks such as older plutons, sediments and metamorphic basement rocks (Section 2.iv.b). In these environments circulating hydrothermal fluids migrate along zones of permeability in competent host rocks which are generally provided by structures (e.g., dilational jogs, flexures or splays in major structures, sheeted fractures, and fracture permeability), breccias (e.g., diatreme margins, intrusive fluidized breccias), or geological contacts (e.g., fractured dome or dike margins). This focusing of hydrothermal fluids provides ideal geological and hydrological environments for the formation of porphyry-related gold systems.

b) Sequence of events

Low sulfidation systems in the southwest Pacific rim exhibit similar paragenetic sequences of alteration and mineralization at all crustal levels, and this is interpreted to reflect the interaction between melts emplaced at high crustal levels and circulating meteoric waters (Fig. 7.1; Leach and Corbett, 1995). The transfer of heat from a melt emplaced at high crustal levels causes heating of waters residing in structures and permeable units. The corresponding change in pressure and temperature conditions produces vertically zoned fluidized breccias, maar volcano/diatreme complexes, and pebble dikes, which utilise pre-existing structures (Section 3.x.d). Such melts also represent the heat sources for the development of convective hydrothermal systems which are dominated by cool dilute meteoric waters. In these hydrothermal systems, fluids circulate to considerable depths along regional and subsidiary structures, intrusion contacts and/or permeable lithologies. These circulating meteoric-dominated waters deposit minerals to form vein systems dominated by quartz and secondary K-feldspar, commonly adularia (Henley and Ellis, 1983). As outlined above, reactive magmatic volatiles are neutralized and reduced at the base of the convecting hydrothermal system in which they become entrained. CO_2 is commonly the dominant magmatic volatile phase (with the obvious exception of water vapour) and is the only major magmatic component which is essentially not modified by secondary processes, although some is converted to methane at low temperatures (Giggenbach, 1987). The deposition of sericite/illite in preference to K-feldspar (Browne, 1991) in progressively later quartz veins is speculated to result from a corresponding increase in volatiles from the crystallizing melt.

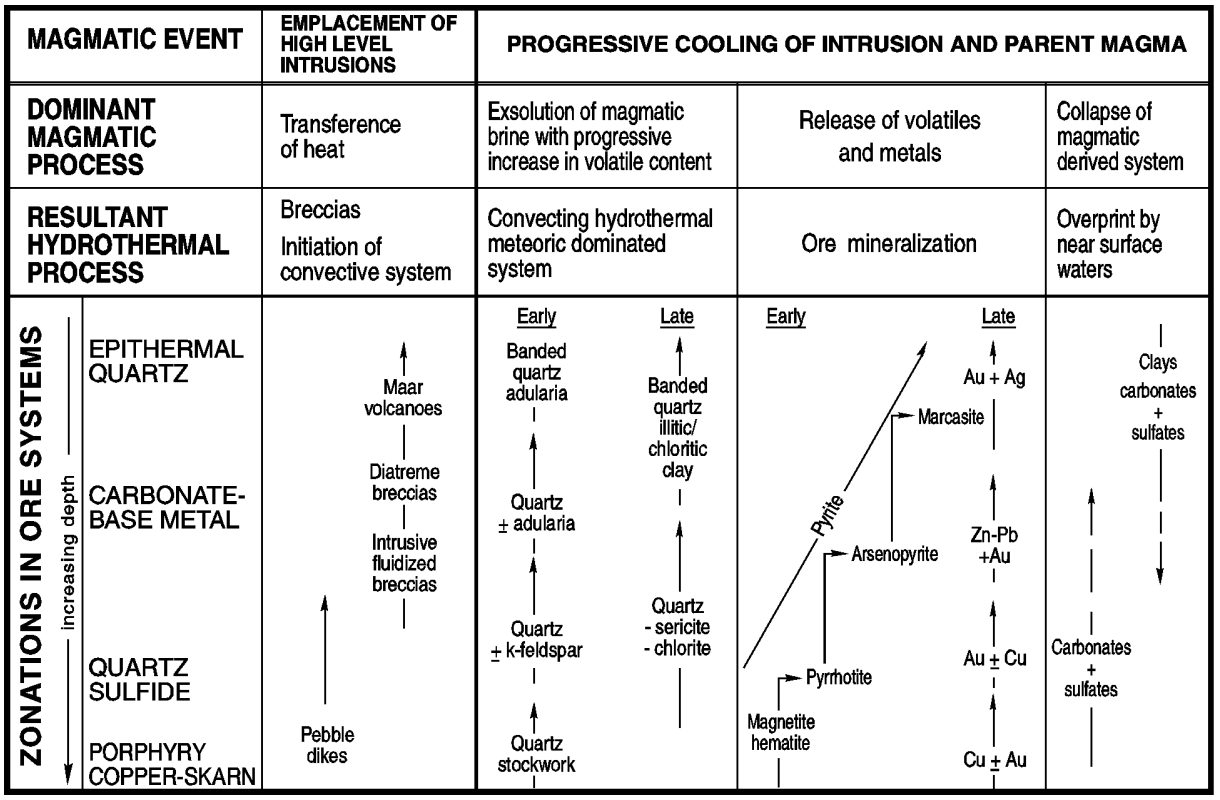

Temporal and spatial zonations in low sulfidation gold systems

FIG. 7.1

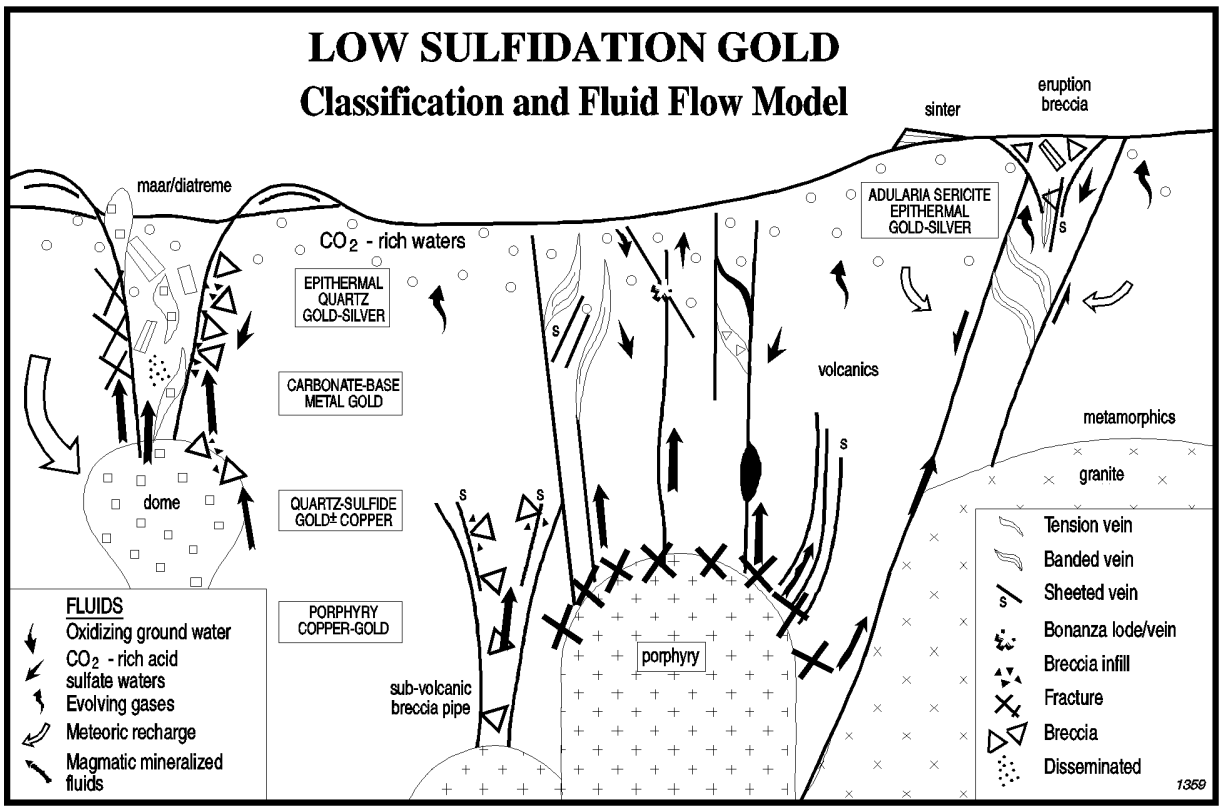

FIG. 7.2

As the intrusion continues to cool, the pressure in the reservoir decreases, resulting in the progressive draw down of near surface CO_2-rich and acid sulfate waters to greater depth. These waters are encountered at depths down to 1.5-2 km into the active hydrothermal system (Reyes, 1990a; Mitchell and Leach, 1991).

Exsolution of most of the volatile phases precedes the late stage segregation of metals from the melt (Cline and Bodnar, 1991). Metal-bearing magmatic fluids are therefore released into structures (and other permeable channelways) late in the paragenetic sequence. These structures are interpreted to contain:
* circulating dilute meteoric waters at all levels in the system,
* dilute, cool, low pH, CO_2-rich and acid sulfate waters up to 1.5-2.0 km depth (but predominantly at <1 km depth),
* relatively oxidized ground waters at shallow epithermal levels.

Petrological studies of low sulfidation systems indicate that mineralization characteristically post-dates the quartz-K-feldspar-sericite/illite vein development (see following examples). During mineralization, iron sulfides are overprinted by base and precious metal minerals, and this is also a common feature of high sulfidation systems (Section 6).

As the hydrothermal system continues to wane, surficial fluids descend to deeper levels, and this results in low temperature clay alteration and carbonate-sulfate deposition which overprint earlier mineral assemblages. At deep porphyry levels, carbonates and sulfates fill open fractures and vughs and may be deposited from magmatic-derived fluids (Zaluski et al., 1994).

c) Types of porphyry-related low sulfidation gold systems

In much of the early geological literature arising from studies in porphyry copper terrains, the term "epithermal" was used to describe all porphyry-related gold deposits formed outside the porphyry environment. During the upsurge of gold exploration in the 1980s, it became apparent that many southwest Pacific gold deposits do not fit neatly into the existing classification of gold systems. The increased database in the 1980s and early 1990's, facilitated the comparison of different deposits, and so the formerly unique Porgera gold deposit (Sillitoe, 1989) has more recently been grouped as part of the carbonate-base metal gold classification (Leach and Corbett, 1993, 1994, 1995; Corbett et al., 1995). Part of the group of gold deposits formerly described as epithermal have now been classed as porphyry-related low sulfidation gold deposits according to the crustal level of formation and relationship to a porphyry source (Leach and Corbett, 1995).

Although telescoping is common and may cause overprinting of alteration zonations (Figs. 7.1, 7.2, 7.3), deposit types are distinguished from deepest to shallow levels as:

<u>Porphyry copper-gold</u> deposits form at deepest levels where magmatic-derived mineralized fluids evolve from a cooling magma and deposit metals within the cooled fractured carapace of porphyry stocks and adjacent competent country rocks, locally termed wall rock-porphyry copper-gold (Section 5).

<u>Quartz-sulfide gold</u> <u>+</u> <u>copper</u> vein/breccia systems occur at shallower levels peripheral to porphyry copper-gold intrusions. In systems with alkalic affinities (e.g., Ladolam, Lihir Island, Papua New Guinea; Carman, 1995) secondary K-feldspar dominates over quartz. Gold mineralization is commonly hosted in massive pyrite/arsenopyrite-chalcopyrite <u>+</u> magnetite/hematite veins, which postdate quartz veins. Lead-zinc are subordinate to copper minerals. It is postulated below that quartz-sulfide vein/breccias are deposited by cooling and dilution during periodical mixing of magmatic-derived fluids with deep circulating meteoric waters, in permeable features (e.g., sheeted fractures, structures, or magmatic hydrothermal breccias; Fig. 7.2).

Carbonate-base metal gold systems form at shallower levels, and/or in later vein sequences than the quartz-sulfide gold ± copper deposits. Gold mineralization is associated with pyrite-sphalerite-galena and carbonate veins, or the matrix to breccias, and only minor copper mineralization is present. It is speculated that these systems form as a result of the mixing of upwelling fluids, which contain a significant magmatic component, with CO_2-rich waters (Leach and Corbett, 1994, 1995).

Epithermal quartz gold-silver systems form at shallow crustal levels or low temperatures, and are locally contemporaneous with, and/or post-date, carbonate-base metal gold deposits. Many of these systems conform to the adularia-sericite epithermal gold-silver deposits described in the geological literature (e.g., Bonham, 1986), for which the term adularia-sericite epithermal gold-silver is used herein (Section 8). The term epithermal quartz gold-silver deposits is applied to those epithermal deposits which demonstrate a more obvious magmatic association for the ore and gangue minerals, than the adularia-sericite systems. Some epithermal systems are transitional between the two styles (e.g., Tolukuma, Papua New Guinea; Cracow, eastern Australia; Section 7.iv.d.3). Both styles of epithermal gold-silver systems are inferred to contain precious metals deposited by the mixing of upwelling mineralized fluids which contain a magmatic component, with oxidizing ground waters (Section 8). Much of the gangue mineralogy comprising quartz, adularia, and quartz pseudomorphing platy carbonate (mainly within adularia-sericite epithermal gold-silver veins), forms in response to the boiling of dominantly meteoric fluids upon periodic, structurally-controlled pressure release, and so may develop the characteristic banded fissure vein ores.

ii) Quartz-sulfide Gold ± Copper Systems

a) Introduction

Quartz-sulfide vein systems occur peripheral to porphyry copper-gold intrusions (Lowell and Guilbert, 1970; Sillitoe and Gappe, 1984) and have locally been mined on a small scale (e.g., veins peripheral to Bingham Canyon, Utah, USA; Babcock et al., 1995). These deposits may form typically bulk low grade gold deposits, in settings generally categorized by pronounced structural control (e.g., Kidston, Ravenswood, eastern Australia), or proximal intrusion source rocks (e.g., Ladolam, Lihir Island, Papua New Guinea). It is speculated that there may also be a genetic link with unseen intrusions (in distal settings) in the formation of some structurally controlled gold deposits in older terrains, such as the Mother Lode deposits (Weir and Kerrick, 1987), some ironstone-hosted gold deposits (e.g., Tennant Creek, Australia; Huston et al., 1993), and in Precambrian quartz-sulfide reefs (e.g., Telfer, Western Australia; Goellnicht et al., 1989; Dimo, 1990). Although Slate Belt-style gold deposits are generally considered to have been derived from a metamorphic fluid (e.g., in eastern Australia, Hill End, Seccombe et al., 1993; and Victoria, Phillips and Hughes, 1995), evidence is emerging for possible magmatic associations (e.g., Sofala-Hill End District, eastern Australia; G. Corbett and T. Leach, unpubl. data: Reefton, New Zealand; Corbett et al., in prep).

Some quartz-sulfide vein systems extend for up to 5 km from the source porphyry such as at Bingham Canyon, Utah, where mining initially focused upon base metal veins and more recently sediment-hosted gold ores (Peters et al., 1966; Sillitoe 1991b; Babcock et al., 1995). Bingham Canyon displays metal zonations from classical porphyry copper-molybdenum, to copper-gold skarns, to lead-zinc-sliver skarns and lead-zinc-silver lodes which overlap the outer skarns, and peripheral sediment hosted gold mineralization (Babcock et al., 1995). Veins peripheral to granitic intrusions in settings such as Cornwall, England were important historical sources of base metals (Edmonds et al., 1975).

In tropical southwest Pacific rim settings quartz-sulfide veins are worked for gold on a small scale by local (commonly illegal) miners (e.g., Philippines; Mitchell and Leach, 1991: Tawere Ridge, Sangihe Island, Indonesia; G. Corbett, unpubl. report: Arakompa, Bilimoia, Papua New Guinea; Corbett et al., 1994b). Here, gold contents tend to be higher than those in the western USA and Chile, although many porphyry-related

quartz-sulfide vein deposits are not of economic importance in terms of the overall gold content (Sillitoe, 1991b). In many Pacific rim tropical settings quartz-sulfide veins are characterized by substantial supergene enrichment, worked by local miners. Drilling of primary ores often fails to substantiate the apparent rich gold contents won by small-scale miners who gouge narrow structures in the supergene weathered environment. Gold is readily liberated from these ores and concentrated by chemical and mechanical processes in steeply dipping structures. We therefore urge caution in the interpretation of high gold grade surface assay data in these systems.

While many quartz-sulfide veins are disappointing exploration targets, in favourable conditions this style of mineralization may form large bulk low grade deposits for instance: Lihir, Papua New Guinea (42 M oz contained Au); in eastern Australia, Kidston (4 M oz Au), Mt Leyshon (>1 M oz Au), Ravenswood-Charters Towers (1-2 M oz Au) and Lake Cowal (2.4 M oz Au). Other deposits (Sillitoe 1991b) include Zhao-Ye, China (approx. 16 M oz Au) and Kori Kollo, Bolivia (5 M oz, Au). The Cadia (10 M oz Au) sheeted vein system, in eastern Australia, (Newcrest Mining Staff, 1996) is transitional between a porphyry copper-gold and quartz-sulfide gold ± copper deposit style.

Of interest, is that analysis of mineral zonations and reconstruction of original fluid plumbing systems may point towards the porphyry source rocks for these systems. Follow up of gold anomalies shedding from peripheral veins led to the identification of the Batu Hijau porphyry copper-gold deposit, Indonesia (R. Burke, pers. commun.; Meldrum et al., 1994), and porphyry targets are apparent from the distribution of peripheral quartz-sulfide vein systems at Bilimoia-Arakompa, Papua New Guinea (below; Corbett et al., 1994b).

b) Structural setting

Quartz-sulfide gold ± copper deposits form in structural settings which tap magmatic source rocks and ore is typically hosted within pre-existing fracture systems which have been dilated during mineralization to form veins, and also as the matrix to breccias. Higher grade ore shoots are common in flexures, jogs and vein intersections. Well developed deposits demonstrate an association with the magmatic source rocks (e.g., the Kidston hydromagmatic breccia pipe, eastern Australia; Ladolam, Lihir Island, Papua New Guinea).

Styles of vein systems which host quartz-sulfide gold ± copper mineralization peripheral to magmatic source rocks are:
* Sheeted vein systems may become prospective by an increase in the density of veins (e.g., Kidston, eastern Australia; Fig. 7.7), or more importantly, in settings where deformation enhances the formation of dilational structural environments within sheeted vein systems (e.g., Cadia, eastern Australia; Figs. 3.11, 3.16). Intersecting sheeted veins at Kidston act as sites of higher fluid flow and hence higher gold grade.
* Dilatant fissure veins (e.g., Ravenswood, eastern Australia; San Cristobal, Chile).
* Tension structures parallel to the direction of compression (Fig. 3.6; e.g., Arakompa, Papua New Guinea; Fig. 7.10).
* Conjugate fractures formed peripheral to porphyry intrusions in orthogonal compression or extension (e.g., Fig. 3.6; Batu Hijau, Indonesia; Meldrum et al., 1994).
* Arc normal structures (e.g., exhumed deep structures host the vein system at Bilimoia, Papua New Guinea; Fig. 7.10).
* Dilational tension vein systems (Lake Cowal, eastern Australia), locally in pull-apart basin fracture arrays (Fig. 3.13).
* Strike-slip movement on conjugate fractures may promote the formation of higher grades in sigmoidal tension veins and flexures (Fig. 3.6; e.g., Batu Hijau, Indonesia; Meldrum et al., 1994).

Breccias which host ore include:
* Fluidized and crackle breccias (Fig. 3.22; e.g., Ladolam, Lihir Island, Papua New Guinea).

* Open space breccias in hydromagmatic breccia pipes (e.g., tourmaline breccia pipes, Chile; Fig. 3.19). At Mt Leyshon, eastern Australia, a tuffisite dyke provides a mechanism for transport of mineralization to the open space breccias (Orr, 1995), while at Kidston and San Cristobal the breccias which are adjacent to sheeted or fissure veins (as the fluid plumbing systems) are best mineralized.

c) Alteration and mineralization

The quartz-sulfide gold ± copper vein/breccia systems have a common paragenetic sequence (Figs. 7.1, 7.2) of deposition summarised as:

1. Early breccias commonly form as precursors to the hydrothermal system in response to the heating of ground waters by the emplacement of a porphyry intrusion, and range from major magmatic hydrothermal breccias (e.g., Kidston, eastern Australia, below), through fault controlled pebble dikes (e.g., Arakompa, Papua New Guinea, below), to fluidized breccias (e.g., Ladolam, Lihir Island, Papua New Guinea, below).

2. Quartz veins typically form medium to coarse grained granular to coxcomb textures associated with pyrite and early K-feldspar and later sericite. In alkalic terrains (e.g., Tabar-Lihir-Tanga-Feni island chain, Papua New Guinea) secondary K-feldspar is the main alteration and vein/breccia gangue mineral. The quartz usually exhibits strained extinction indicative of deposition within a stress regime. Fluid inclusion data (below) indicates that quartz has been deposited from either dilute waters of probable meteoric origin, or in some cases saline to hypersaline brines of possible magmatic origin.

3. The sulfide minerals are interpreted to have been deposited from fluids with a significant magmatic component, and comprise:

i) Early Fe-sulfide and magnetite/hematite are commonly massive and fill fractures and breccia matrix. Pyrite occurs in most instances, and the other iron minerals are zoned in relation to the source intrusion, from early and proximal, to late and distal settings as: magnetite/hematite, through pyrrhotite, to arsenopyrite or arsenean pyrite. The Fe-sulfides commonly contain inclusions of chalcopyrite and base metals (Fig. 7.1).

ii) Chalcopyrite post-dates the Fe-sulfide/oxide minerals (above) and decreases in abundance and significance away from the source intrusion. Bornite is locally encountered in environments transitional to porphyry copper settings. At depth chalcopyrite fills fractures in shattered and brecciated pyrite, whereas at shallow levels minor chalcopyrite overgrows earlier phases, or occurs as inclusions in late auriferous pyrite. The copper minerals are typically accompanied by Bi-Ag-Pb-Te mineralization and locally W-Sn minerals, depending upon the metal content of the source magma.

4. In some cases the sulfide event continues into, or is post-dated by, a late carbonate (or anhydrite e.g., Ladolam, Lihir Island, Papua New Guinea) deposition.

Gold mineralization in quartz-sulfide systems typically occurs in association with sulfide deposition. Refractory gold generally forms distal to the source intrusion, possibly in environments of rapid cooling, probably as sub-microscopic inclusions or within the lattice of pyrite or As-rich pyrite. Non-refractory gold occurs as inclusions in coarser grained pyrite or chalcopyrite formed under deeper conditions of slower cooling in environments more proximal to the source intrusion, commonly with Bi-Ag tellurides. Non-refractory gold in the porphyry-related quartz vein systems typically has a fineness range of 850-950, transitional between the fineness of gold in porphyry copper-gold and carbonate-base metal gold systems (Fig. 4.8).

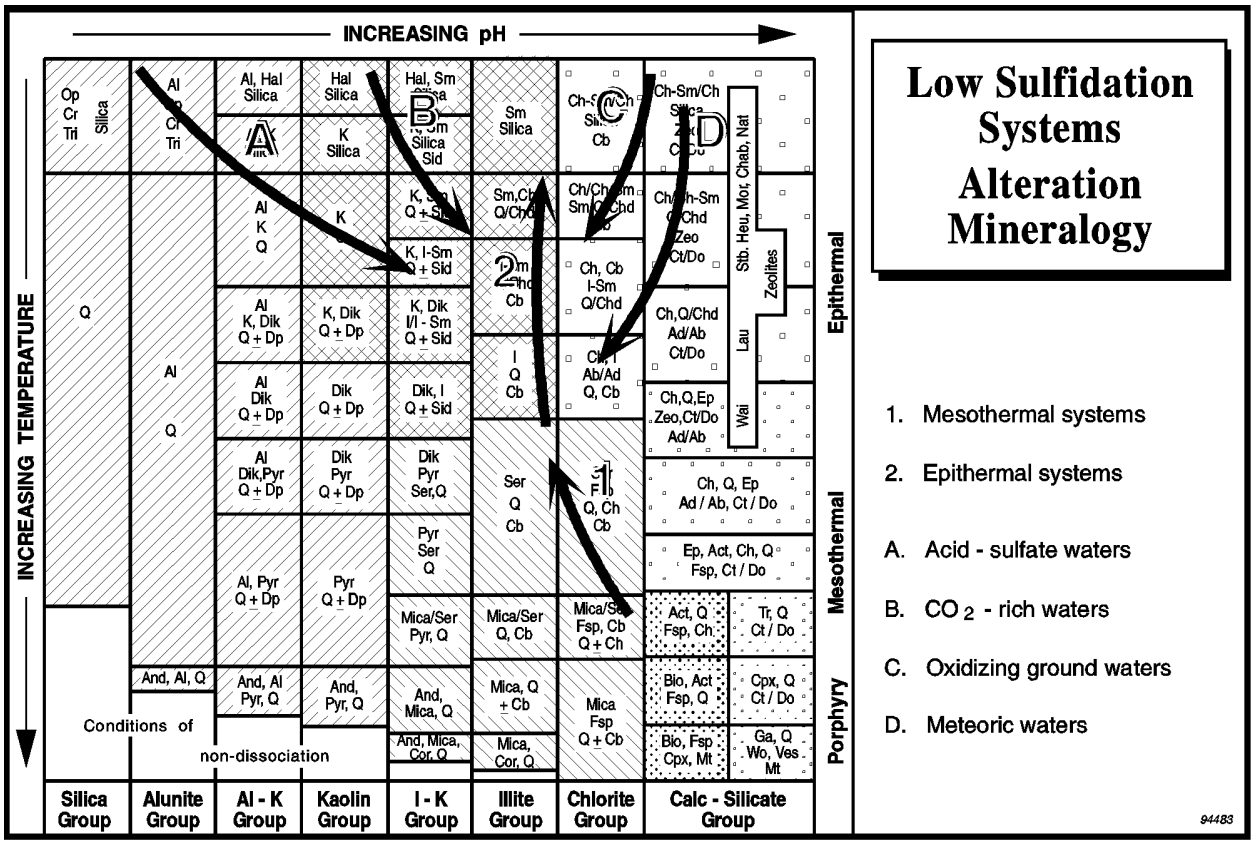
INCREASING pH
INCREASING TEMPERATURE
Low Sulfidation Systems
Alteration Mineralogy
1. Mesothermal systems
2. Epithermal systems
A. Acid - sulfate waters
B. CO 2 - rich waters
C. Oxidizing ground waters
D. Meteoric waters
Epithermal
Mesothermal
Porphyry
Silica Group
Alunite Group
Al - K Group
Kaolin Group
I - K Group
Illite Group
Chlorite Group
Calc - Silicate Group
Conditions of non-dissociation
Zeolites
94483

FIG. 7.3

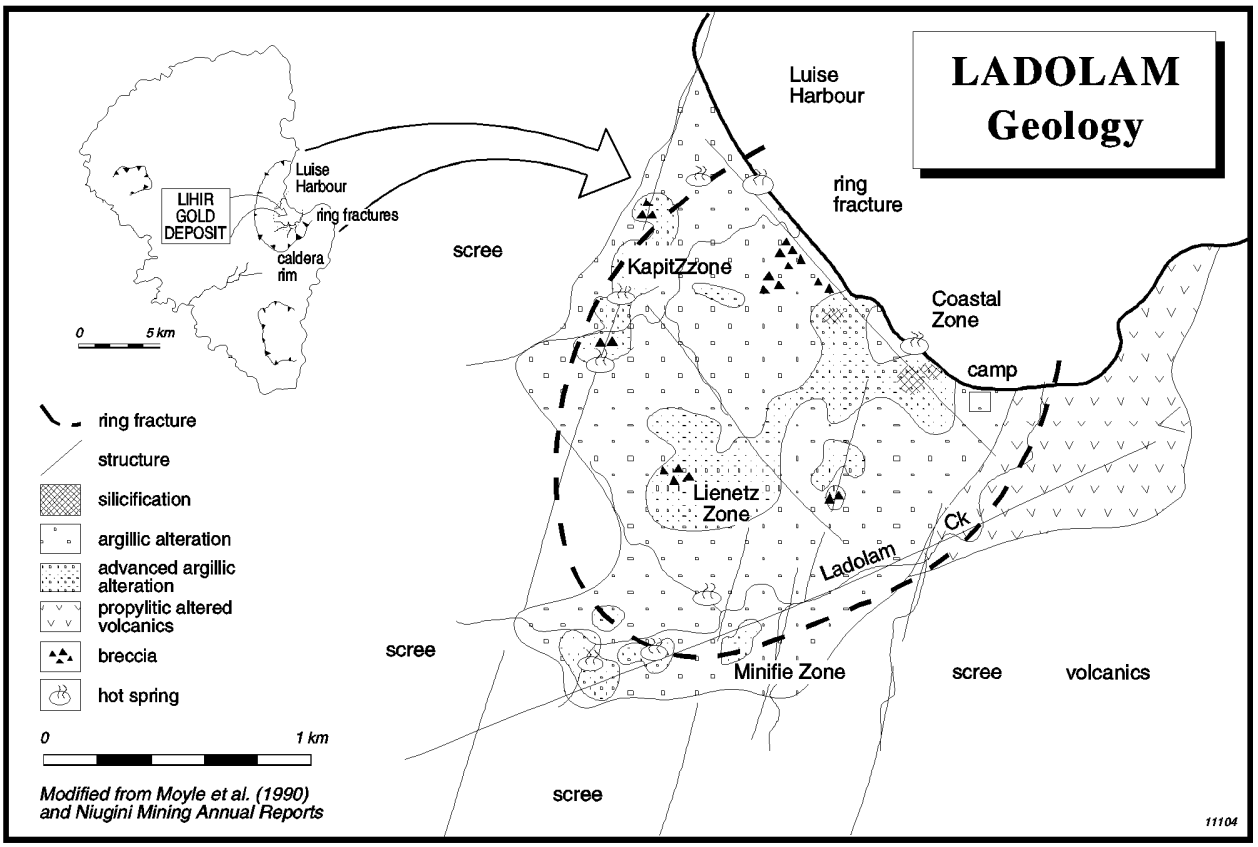
LADOLAM Geology
LIHIR GOLD DEPOSIT
Luise Harbour
ring fractures
caldera rim
0 5 km
Luise Harbour
ring fracture
scree
KapitZone
Coastal Zone
camp
Lienetz Zone
Ck
Ladolam
Minifie Zone
scree
volcanics
ring fracture
structure
silicification
argillic alteration
advanced argillic alteration
propylitic altered volcanics
breccia
hot spring
0 1 km
Modified from Moyle et al. (1990) and Niugini Mining Annual Reports
11104

FIG. 7.4

In the examples outlined below, the authors interpret that mineral deposition in quartz-sulfide gold ± copper systems results from the mixing of hot mineralized magmatic-dominated fluids, evolved from cooling intrusions, with cool, dilute meteoric waters, which circulate to considerable depths along major regional structures (Fig. 7.2).

d) Examples

1. Ladolam gold deposit, Lihir Island, Papua New Guinea

During the Oligocene-Miocene, the southward moving Pacific plate was subducted under the northward moving Australian plate and the New Ireland and New Britain calc-alkaline island arcs formed above a south dipping subduction zone. Collision of the Otong Java Plateau jammed this subduction in the late Miocene, and a new north dipping subduction zone formed south of New Britain in the Pliocene (Fig. 1.2; Section 3.v.c.). Most petrogenetic-tectonic analyses of the region favour models of remelting of oceanic crust to give rise to the shoshonitic volcanism which characterizes the Tabar-Lihir-Feni-Tanga island arc (Solomon, 1990; Solomon and Groves, 1994, McGinnis and Cameron, 1994). North-south trending rifts in the overlying plate, inferred from seismic and gravity anomalies and the alignment of volcanism, host mantle-derived volcanoplutonic rocks which constitute the Tabar-Lihir-Feni-Tanga island chain (Shatwell, 1987; Lindley, 1988; Marlow et al., 1988; McGinnis and Cameron, 1994).

The Ladolam gold deposit, Lihir Island (Fig. 1.2), has a mineable reserve of 14.6 million oz Au, and contained gold of 42.6 million oz (Niugini Mining Annual Report, 1994). The Luise caldera (Fig. 7.4) was targeted in 1982 by the Niugini Mining/Kennecott Joint Venture, which at the time was evaluating the adjacent Tabar Island Group in joint venture with Nord Resources Limited. Prospecting and mapping in 1983 progressed from the identification of mineralized boulders along the beach, to the delineation of soil geochemistry anomalies and drill testing of the Coastal (1983) and Lienetz (1984) zones (Davies and Ballantyne, 1987; Niugini Mining Annual Report, 1984). The Minifie zone was identified in late 1986 from a weak soil anomaly in a hand dug trench in an area of scree on the caldera wall, and drill tested from 1987.

The islands of the Tabar-Lihir-Feni-Tanga arc were built up as Plio-Pleistocene shoshonitic volcanoes (Wallace et al., 1983). The Ladolam gold deposit is hosted in the youngest of several overprinting volcanic edifices which make up Lihir island. Collapse by sideways unroofing probably formed a caldera-like feature, now evident as the Luise Harbour (Moyle et al., 1990; Sillitoe, 1994b; Fig. 7.4). The structure of the Ladolam gold deposit is dominated by NS-NNE structures which reflect the magmatic-hosting rift, ring fractures and possible conjugate fractures. Much of the current thermal activity occurs along the ring fractures and the Minifie mineralization is localized at the intersection of throughgoing NS-NNE structures with the ring fractures (Fig. 7.4).

The Ladolam gold mineralization was described as porphyry gold (Sillitoe, 1989), displaying epithermal gold characteristics (Moyle et al., 1990, 1991), while Carman (1994, 1995) emphasises the porphyry-epithermal telescoping. Subdivision of traditional (porphyry-related) epithermal ore systems (Leach and Corbett, 1995) allows the Ladolam mineralization to be classified here as of the quartz-sulfide gold style while also displaying alkaline porphyry affinities. It must be noted that the shoshonitic host rocks yield an alteration assemblage enriched in K-feldspar (characteristic of this style) and are depleted in quartz.

A sequence of three stages of overprinting alteration and mineralization (Fig. 7.5) is inferred from reviews of the published literature (Davies and Ballantyne, 1987; Moyle et al., 1990, 1991; Plimer et al., 1988; Forth, 1994; Carman, 1995) and personal observations as:

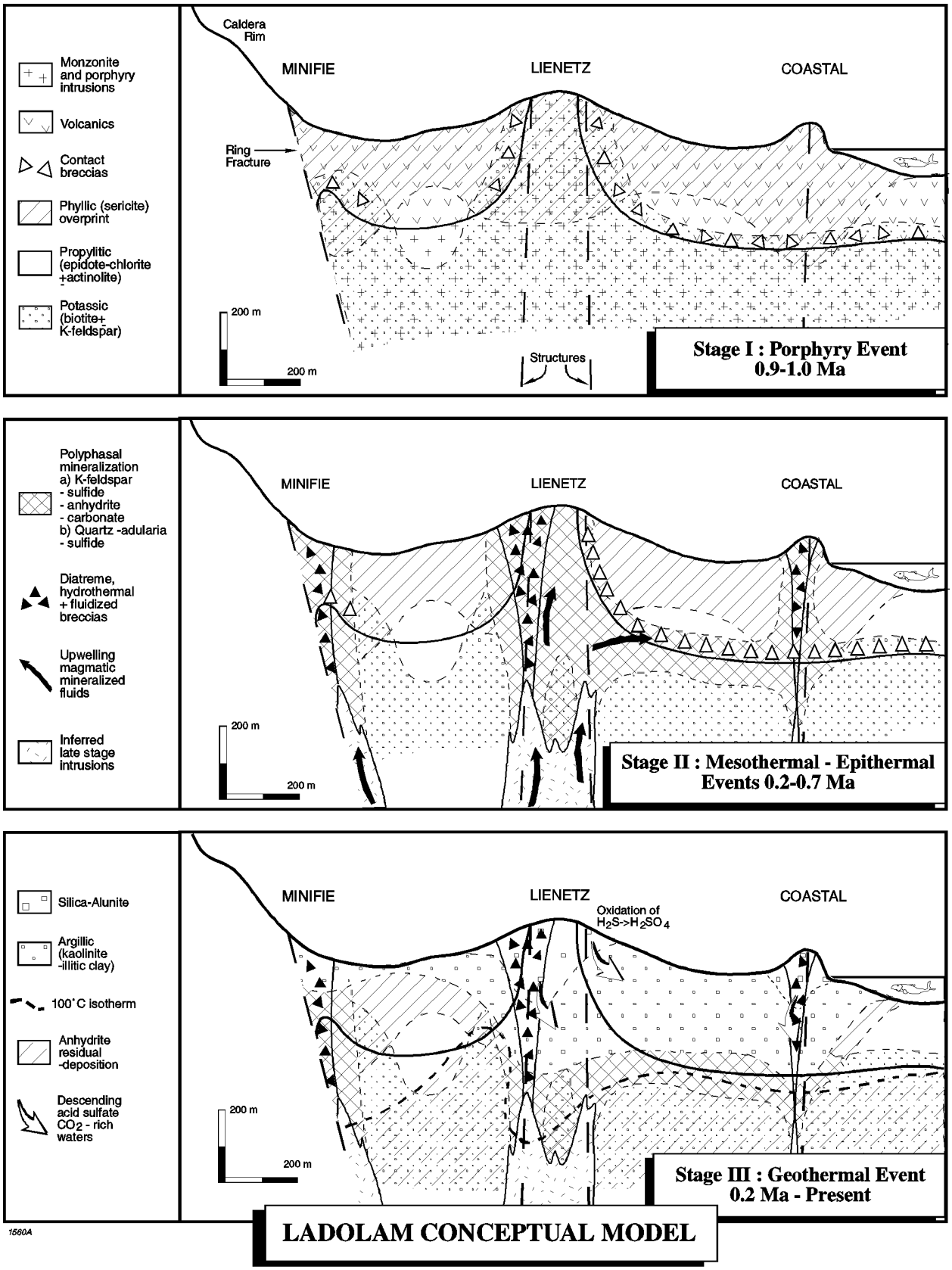
Monzonite and porphyry intrusions
Volcanics
Contact breccias
Phyllic (sericite) overprint
Propylitic (epidote-chlorite ±actinolite)
Potassic (biotite+ K-feldspar)
Caldera Rim
MINIFIE
LIENETZ
COASTAL
Ring Fracture
200 m
200 m
Structures
Stage I : Porphyry Event 0.9-1.0 Ma
Polyphasal mineralization
a) K-feldspar
- sulfide
- anhydrite
- carbonate
b) Quartz -adularia
- sulfide
Diatreme, hydrothermal + fluidized breccias
Upwelling magmatic mineralized fluids
Inferred late stage intrusions
MINIFIE
LIENETZ
COASTAL
200 m
200 m
Stage II : Mesothermal - Epithermal Events 0.2-0.7 Ma
Silica-Alunite
Argillic (kaolinite -illitic clay)
100°C isotherm
Anhydrite residual -deposition
Descending acid sulfate CO_2 - rich waters
MINIFIE
LIENETZ
COASTAL
Oxidation of H_2S->H_2SO_4
200 m
200 m
Stage III : Geothermal Event 0.2 Ma - Present
1560A
LADOLAM CONCEPTUAL MODEL

FIG. 7.5

Stage I Porphyry Emplacement:
The emplacement of a differentiated equigranular biotite monzonite, which grades from microdiorite to syenite in composition, pre- and post-dates andesite to latite porphyry stock and dike development. The intrusions have been emplaced into silica-poor alkali-basaltic (shoshonitic) volcanics, locally forming contact breccias. Alteration related to emplacement of the intrusions is zoned from potassic (biotite-K-feldspar-anhydrite ± magnetite ± apatite) at depth, to propylitic (actinolite-epidote-chlorite-calcite) at shallow levels and peripheral to the intrusions. Biotite alteration has been dated at 0.9-1.0 Ma. Late stage phyllic (sericite-illite) overprint is inferred to be related to the collapse of meteoric waters onto the intrusion and associated breccias, and is possibly associated with very low grade porphyry-style copper mineralization.

Stage II Mesothermal and Epithermal:
Gold mineralization occurs in association with early mesothermal alteration dominated by K-feldspar-anhydrite-sulfide assemblages and is overprinted by later shallow epithermal quartz-adularia vein and wall rock silicification (Carman, 1995). Secondary K-feldspar, as either orthoclase or adularia dated at 0.2-0.7 Ma, provides an indication of the time span of mineralization.

The mesothermal-epithermal activity comprises early brecciation, followed by alteration and mineralization characterized by the deposition of sequential: K-feldspar, then sulfides, followed by anhydrite + carbonate + sulfides ± barite. Anhydrite is reported to occur at depth (Carman, 1994), whereas sulfides + illite are more abundant at shallower levels. Fluid inclusion analyses on anhydrite indicate that deposition occurred from a two phase, moderately saline (5-10 wt % equiv NaCl) brine at temperatures of 210-300°C (Carman, 1995). Halite and other daughter crystals in some liquid-rich inclusions indicate that periodic hypersaline conditions prevailed. Biotite, locally associated with the anhydrite-carbonate veins reflects the high temperature of the porphyry-related veins and was dated at 0.34 Ma. This stage of hydrothermal activity is therefore inferred to be related to intrusions which post-date the biotite monzonite pluton.

Breccias, which appear to be indicative of phreatic and phreatomagmatic (diatreme) eruptions (Section 3.x.d), have acted as permeable host rocks to this stage of hydrothermal activity (Carman, 1995). The latter are typical of high level intrusion environments.

This locally polyphasal sequence of events is similar to that encountered in most southwest Pacific rim porphyry-related low sulfidation quartz-sulfide gold ± copper systems. The host rock composition has influenced the alteration, producing K-feldspar-rich and quartz-poor mineral assemblages. The diatreme breccias have undergone subsequent extensive K-feldspar alteration and associated leaching of plagioclase, sericite and mafics to produce a brittle, vughy, K-feldspar rock. This leaching is especially intense in the breccias, and has formed a subhorizontal vughy zone along the contact breccia at the top of the intrusion between the Lienetz and Coastal zones. This was previously called the 'boiling zone' (Davies and Ballantyne, 1987). The vughy K-feldspar rock is similar in appearance to the vughy residual silica/quartz zone in high sulfidation systems. However, at Lihir the leaching is postulated to be the result of fluid-rock reaction by neutral pH, silica-undersaturated fluids.

The brittle K-feldspar altered volcanics and intrusions have undergone fracturing and associated sulfide deposition in veinlets, fluidized breccias, and sheeted veins, as well as lining or filling leached vughs. The sulfides are dominated by auriferous arsenian pyrite (average 50 ppm Au and 2-4 mole % As; Carman, 1995), minor marcasite and arsenopyrite, and trace chalcopyrite, Fe-poor sphalerite, galena and tennantite. Sulfide mineralization continues into later fracturing and breccia events which are dominated by anhydrite + carbonate deposition. Traces of native gold and gold-silver tellurides are reported to occur as submicroscopic inclusions in pyrite (Moyle et al., 1990), mainly in the sulfide phase, but extending into anhydrite-carbonate deposition. Trace elements associated with gold mineralization (Carman, 1995) include W (<10 to 20 ppm) and Te (10-40 ppm), which suggest a magmatic origin for the ore-bearing fluids.

On the basis of fluid inclusion, isotope and vein/alteration sequences, Plimer et al., (1988) relate gold mineralization to the mixing of upwelling mineralized fluids, with cool meteoric waters. This interpretation is consistent with the models delineated herein. Carman (1995) on the other hand associates refractory gold mineralization in arsenian pyrite with the quenching of upwelling boiling magmatic-derived mineralized fluids by seawater.

A later deposition of epithermal quartz (± calcite-adularia-pyrite and trace base metal sulfides) veins and associated wall rock silicification at the Minifie zone took place under less saline (3-7 wt % NaCl) and slightly cooler (180-270°C) conditions (Carman, 1995). Here, gold-silver mineralization occurs as native gold and argentite in the quartz stockwork veins. This mineralization is interpreted by Carman (1995) to result from quenching, at shallow levels, of boiling mineralized fluids by descending acid sulfate waters.

Stage III Geothermal:
The current geothermal system is postulated to represent the waning of the Stage II epithermal quartz-adularia event. Cristobalite-alunite alteration at shallow levels in previously formed breccia zones at the Lienetz and Coastal zones, grades laterally and at depth through kaolinite-silica-smectite to interlayered illite-smectite alteration. This zoned advanced argillic - argillic alteration overprints earlier mineralogy (Carman, 1994), and is interpreted to result from the draw down of low pH acid sulfate + CO_2-rich waters. These waters probably formed by oxidation and absorption, in ground waters, of gases which evolved from upwelling Stage II fluids. At temperatures below 100°C, the low pH waters could dissolve Stage II anhydrite and carbonate and deposit these phases in hotter environments at depth.

Alunite has been dated at 0.15 Ma, and is also currently forming in the acid sulfate springs at the surface. It is interpreted that waning of the hydrothermal system resulted in a decrease in pressures and the subsequent draw down of the cool acidic fluids. It is speculated that these acid sulfate waters are remobilizing Stage II copper-gold to form luzonite, enargite and locally coarse gold in the Stage 3 event.

The giant Ladolam gold deposit has therefore been formed by the overprinting (or 'telescoping') of a number of hydrothermal events which range from early porphyry to mesothermal and epithermal K-feldspar/quartz-sulfide systems. Similar, but smaller, telescoped hydrothermal K-feldspar/quartz-sulfide gold systems have been recognised on the nearby (Fig. 1.2) Simberi Island (McInnes and Cameron, 1994) and Feni Island (Licence et al., 1987), which display similar host rock compositions to Lihir Island (Wallace et al., 1983).

2. Kidston, eastern Australia

The Kidston gold deposit which contains >4 M oz Au, began production with a resource of 2.7 M oz Au at an average gold grade of 1.58 g/t Au (Baker and Tullemans, 1990), and added 1 M oz at a grade of 1.25 g/t Au within the Eldridge ore zone in early 1995. Kidston gold mineralization is hosted within a breccia pipe related to Permocarboniferous volcanoplutonic activity which cuts Precambrian metamorphic and granodiorite basement rocks. In the region between the Wirra Wirra and Lochaber volcanoplutonic complexes (respectively NW and SW of Kidston), a gravity high reflects outcropping Precambrian rocks which are intruded by quartz-feldspar porphyry and rhyolite dikes, indicative of underlying felsic Permocarboniferous intrusion (Fig. 7.6). The Kidston breccia pipe is inferred to have formed from a magmatic source (Baker and Andrew, 1991) localized at the intersection of a throughgoing structure, the Gilberton Lineament, and the margin of the buried arch of the inferred Permocarboniferous intrusion deduced from regional gravity data (G. Corbett, unpubl. data, 1983; Fig. 7.6). In much the same manner as in porphyry deposits, mineralized fluids may have migrated to the margin of the buried magma source defined by the arch. The Gilberton Lineament is one of many parallel structural

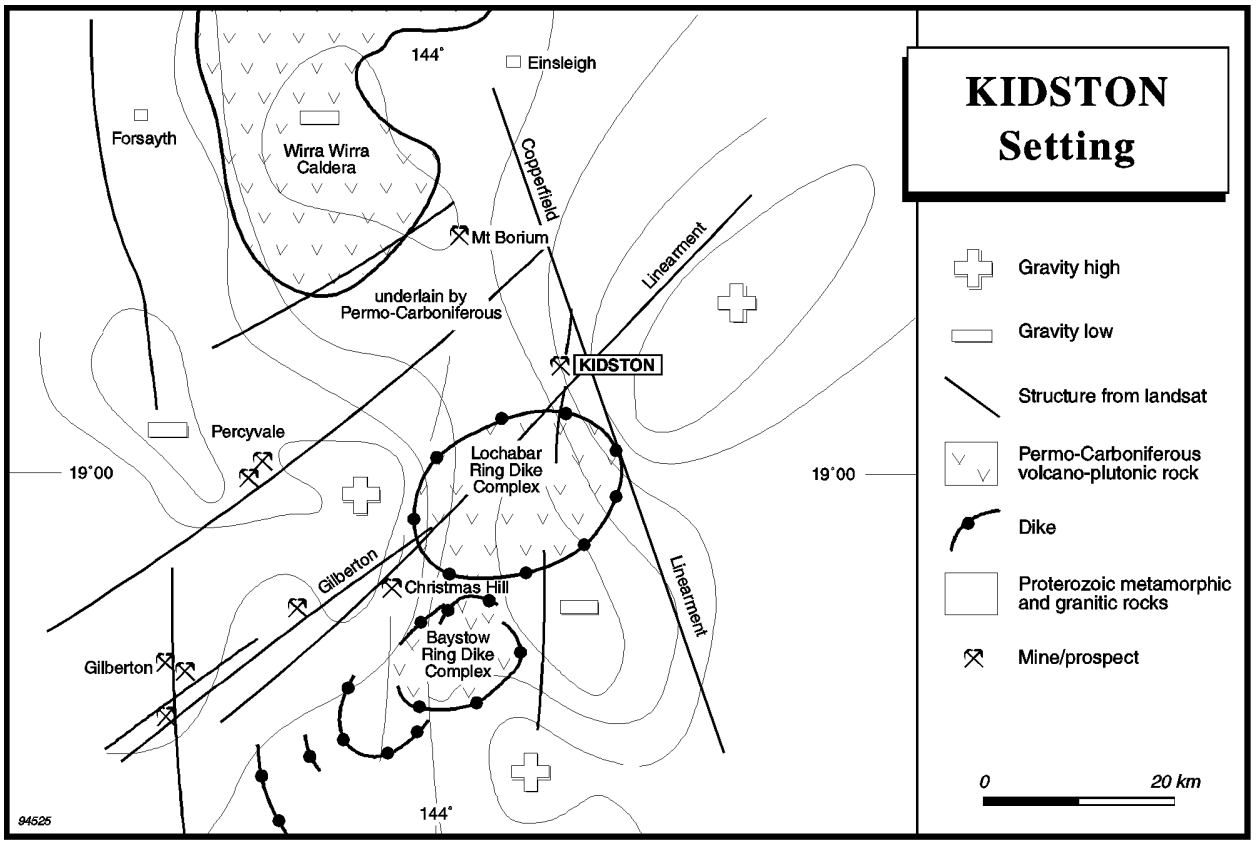
KIDSTON
Setting
Gravity high
Gravity low
Structure from landsat
Permo-Carboniferous volcano-plutonic rock
Dike
Proterozoic metamorphic and granitic rocks
Mine/prospect
0
20 km
144°
Einsleigh
Forsayth
Wirra Wirra Caldera
Copperfield
Mt Borium
Linearment
underlain by Permo-Carboniferous
KIDSTON
Percyvale
19°00
Lochabar Ring Dike Complex
Gilberton
Christmas Hill
Baystow Ring Dike Complex
Linearment
94526

FIG. 7.6

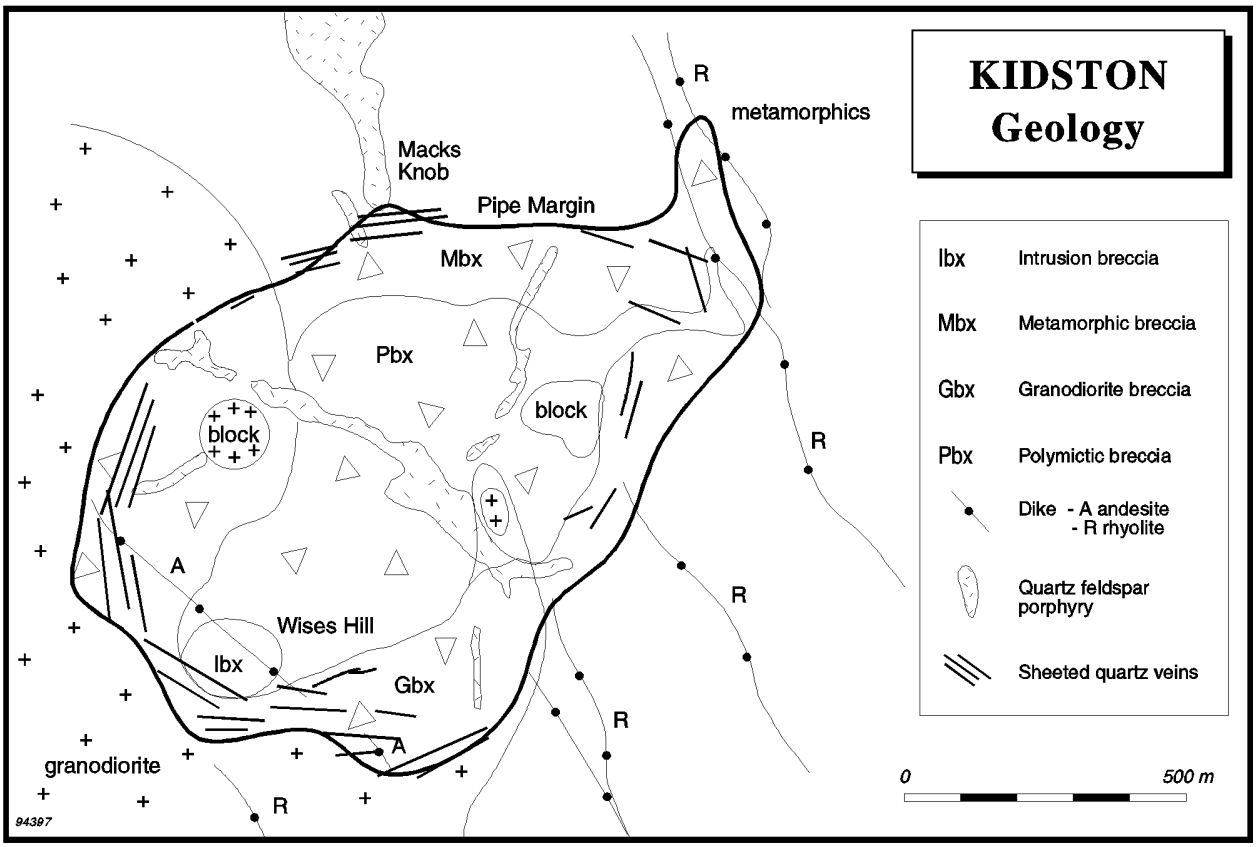
KIDSTON
Geology
Ibx Intrusion breccia
Mbx Metamorphic breccia
Gbx Granodiorite breccia
Pbx Polymictic breccia
Dike - A andesite
- R rhyolite
Quartz feldspar porphyry
Sheeted quartz veins
0
500 m
R
metamorphics
Macks Knob
Pipe Margin
Mbx
Pbx
block
block
A
Wises Hill
Ibx
Gbx
granodiorite
94397

FIG. 7.7

corridors which display protracted histories of movement, including extension which facilitated the emplacement of the Permocarboniferous volcanoplutonism (Fig 7.6; Laing, 1994; G. Corbett, unpubl. data, 1983).

The Kidston breccia pipe is a teardrop shaped body about 1200 x 800 m, elongate in the trend of the Gilberton Lineament. The breccia types (G. Corbett, unpubl. data, 1980) reflect the transition from, intrusion breccias (volcanic breccias in Fig. 7.7) with a high proportion of strongly milled introduced intrusion fragments, to peripheral collapse-style breccias which contain dominantly less milled host rock fragments (metamorphic and granodiorite breccias in Fig. 7.7). The metamorphic foliation in basement fragments becomes progressively reoriented from the regional orientation outside the pipe, as fragments undergo increased milling and rotation towards the centre of the pipe and away from the pipe margins. The contact between metamorphic and granodiorite rocks in the basement continues from outside to within the breccia pipe, as metamorphic and granodiorite breccias, formed by collapse (Fig. 7.7; G. Corbett unpubl. map, 1980). Recent mining has exposed large flat-lying collapse blocks of rebrecciated breccia in the polymictic breccias (Fig. 7.7), transitional between the intrusion and collapse breccias. Baker and Andrew (1991) present a model of overprinting brecciation in which features such as: clasts of quartz-pyrite-magnetite stockwork veins, tourmaline in fragments and breccia matrix, dikes which intrude the breccia, and isotope data, all indicate an intrusion source at depth. These workers describe in situ exfoliation as a mechanism for the development of the rounded intrusive fragments cited above, and suggest that the pipe did not breach the surface. Rhyolite dikes tend to predate pipe formation, and later quartz feldspar porphyry dikes which transect the breccia, predominantly in the central portion of the pipe, may represent an event that tapped a deeper portion of the magma source (Fig. 7.7, Baker and Tullemans, 1990). Sheeted fractures which form kinked polygonal shapes around the pipe margin cross cut the breccia as a final phase of post-brecciation collapse (Fig. 7.7).

Three main stages of alteration, brecciation, vein development and mineralization (Fig. 7.8) have been recognised (Baker, 1987; Baker and Tullemans, 1990; Baker and Andrew, 1991; T. Leach and Graham Corlett, unpubl. report, 1995) as:

Stage I Rhyolite Intrusion:
Emplacement of a high level rhyolite stock was accompanied by quartz stockwork vein development and minor molybdenite-pyrite + arsenopyrite + chalcopyrite mineralization. Tourmaline-sericite + andalusite breccias formed on the margin of the rhyolite stock at Wise's Hill during late stage volatile exsolution. Fluid inclusion data indicates that the fluids were hot (400-500°C) and hypersaline (>40-50 wt % NaCl) during Stage I and hydrothermal activity occurred at depths of approximately 3 km.

Stage II Syn- and Post-Breccia Pipe:
The breccia matrix at Kidston has undergone early potassic alteration to biotite + muscovite + epidote with accompanying pyrite-pyrrhotite mineralization. This was followed by later muscovite-epidote-orthoclase-calcite (propylitic) alteration and pyrite-pyrrhotite + sphalerite mineralization. Minor gold mineralization is associated with epidote in the latter phase of activity. Fluid inclusion data indicate that moderately high temperatures (260-360°C) and salinities (2-10 wt % NaCl) prevailed.

Stage III Quartz-Carbonate Veins:
This is the main gold mineralization event at Kidston, and occurs mostly within sheeted veins around the margins of the breccia pipe (Figs. 7.7, 7.9), and to a lesser extent in the adjacent open space breccias. It is interpreted that the sheeted veins were deposited from fluids derived from the same melt as the post-breccia quartz feldspar dikes.

The sheeted veins (up to 10 cm wide) exploit subparallel fractures, and exhibit a depositional sequence of: quartz + sericite --> sulfides --> carbonates, typical of quartz-sulfide and carbonate-base metal style gold

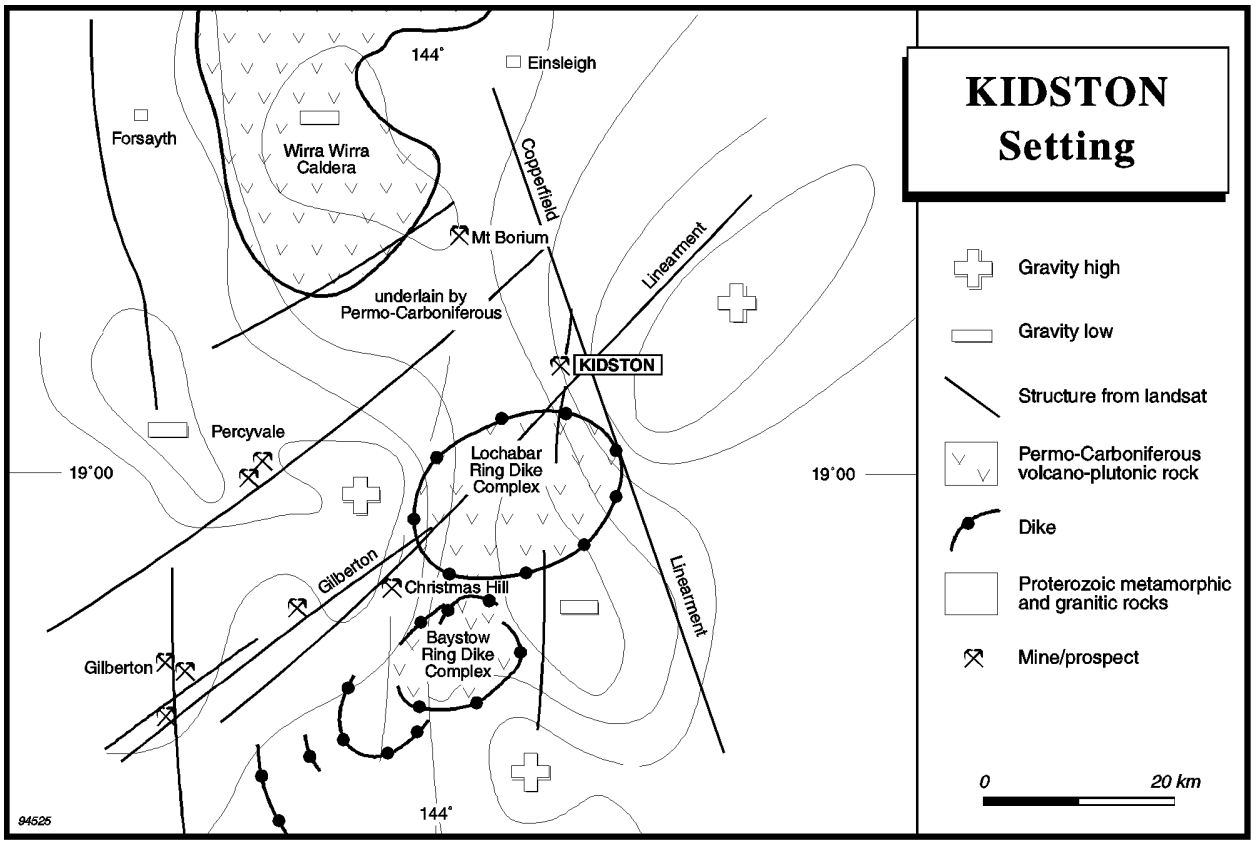
KIDSTON
Setting
Gravity high
Gravity low
Structure from landsat
Permo-Carboniferous volcano-plutonic rock
Dike
Proterozoic metamorphic and granitic rocks
Mine/prospect
0
20 km
144°
Einsleigh
Forsayth
Wirra Wirra Caldera
Copperfield
Mt Borium
Linearment
underlain by Permo-Carboniferous
KIDSTON
Percyvale
19°00
Lochabar Ring Dike Complex
Gilberton
Christmas Hill
Baystow Ring Dike Complex
Linearment
94526

FIG. 7.6

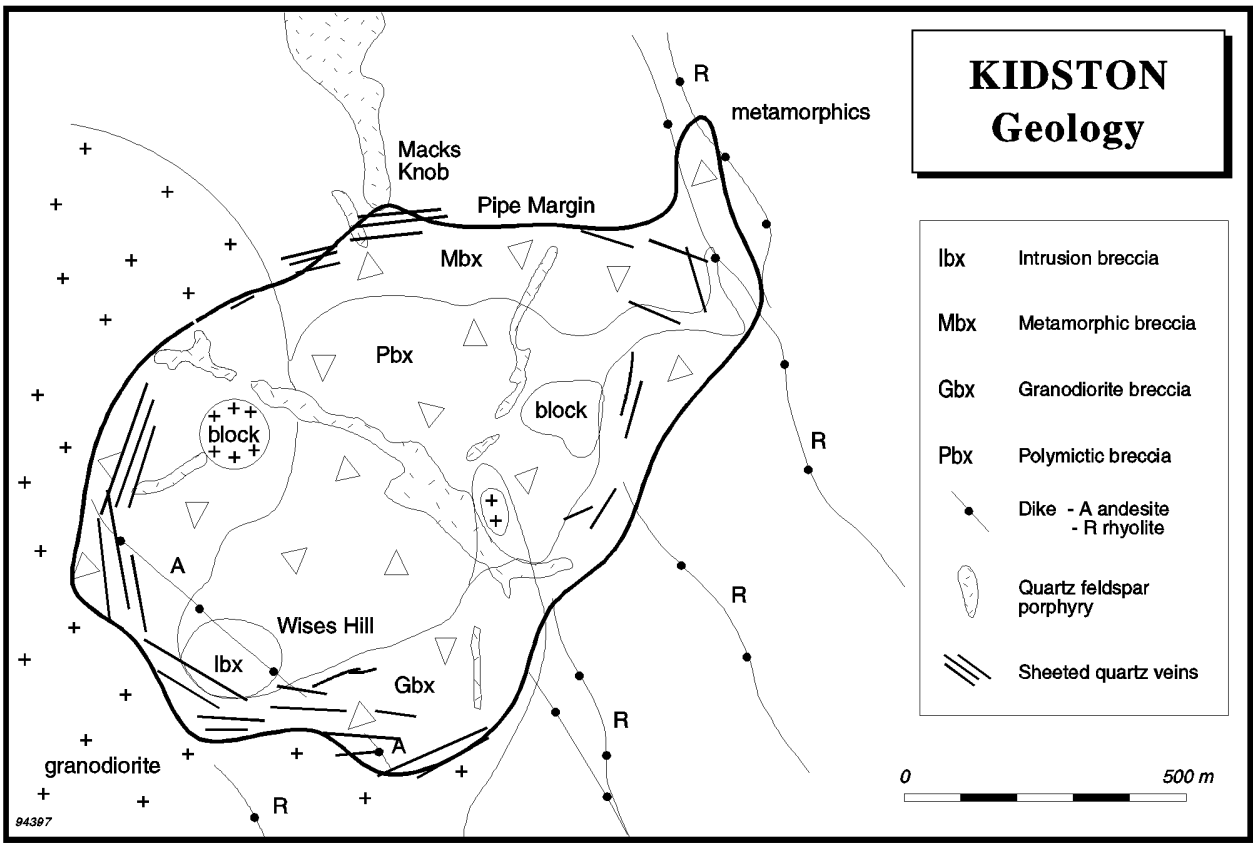
KIDSTON
Geology
Ibx Intrusion breccia
Mbx Metamorphic breccia
Gbx Granodiorite breccia
Pbx Polymictic breccia
Dike - A andesite
- R rhyolite
Quartz feldspar porphyry
Sheeted quartz veins
0
500 m
R
metamorphics
Macks Knob
Pipe Margin
Mbx
Pbx
block
block
A
Wises Hill
Ibx
Gbx
granodiorite
94397

FIG. 7.7

Stage	Stage I	Stage II	Stage III
Event	Rhyolite stocks	Syn- and post-breccia pipe	Sheeted veins (? syn- and post-quartz feldspar porphyry)
Alteration, veins and mineralization	Q - Mo - Py + Apy ± Cpy Stockwork Tourmaline -> andalusite breccia	Early Bio - Py - Po ± Mus ±Ep (potassic) Late Mus + Ep - Ksp Py - Po (±Au ±Sl) Late Ct	Q - Ank / Ct ± Mus / I / Ser Py ± BM ± Apy ± Po ± Mo ± Cpy Main Au mineralization ± Bi Te / S
Conditions from F I data	400 - 450˚ C 40 - 50 wt % NaCl	260 - 360˚ C 2 - 10 wt % NaCl	120 - 300˚ C Early Q: 2 - 10 wt % NaCl Late Cb (+ BM): 0.2 - 0.7 wt % Na Cl

Kidston - Stages of alteration, vein development and mineralization *(data from Baker and Andrew, 1991)*

1230

FIG. 7.8

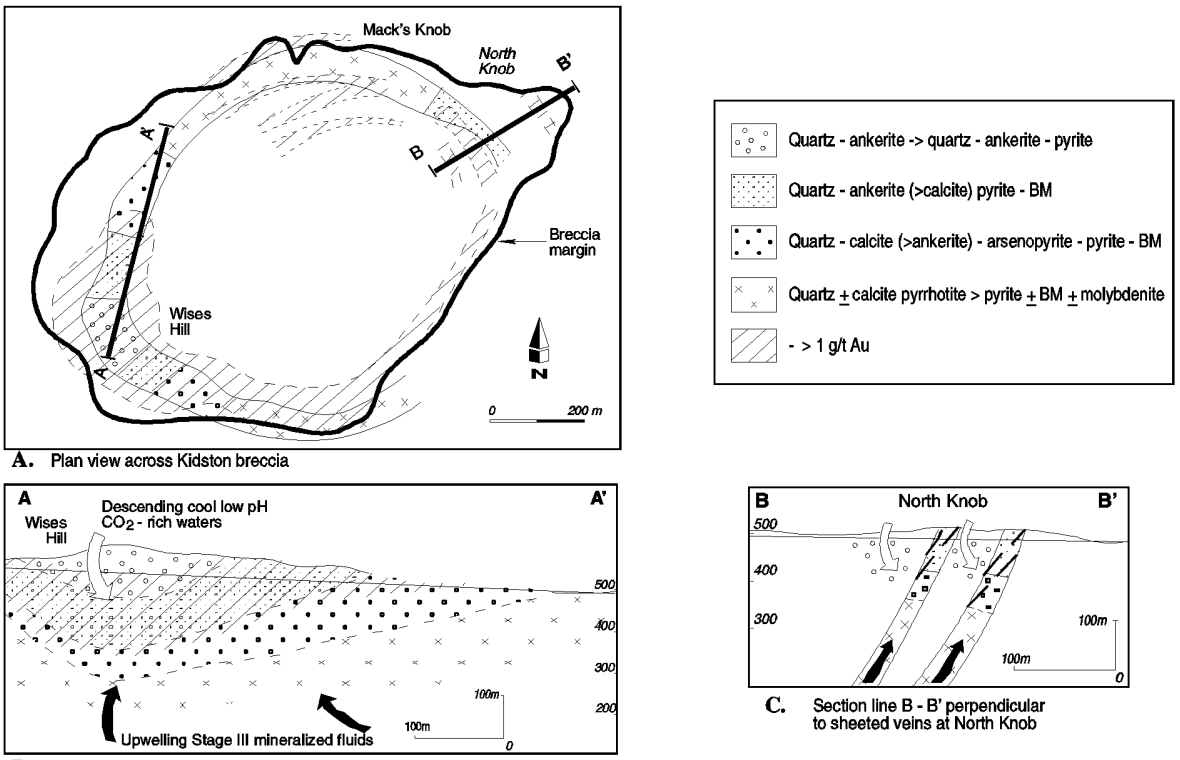

Kidston - Distribution in gangue and ore mineral phases in Stage III sheeted veins *(modified from Baker and Andrew, 1991)*

1231

FIG. 7.9

systems elsewhere in the southwest Pacific. Lateral and vertical zonations are recognised in both gangue and ore phases (Baker, 1987; T. Leach, unpubl. data). Carbonate (mainly ankerite) dominates over quartz at shallow levels, whereas quartz is dominant over carbonate (calcite) at depth and marginal to the ore zones at Wise's Hill and North Knob. The iron phases are zoned pyrite --> arsenopyrite --> pyrrhotite + magnetite with increasing depth and laterally away from the ore zones. Sphalerite and galena are restricted to shallow levels in the ore zones, whereas chalcopyrite persists to depth.

Gold mineralization preferentially occurs in the shallow quartz-ankerite/calcite-pyrite and arsenopyrite zones as inclusions in sphalerite and pyrite, filling fractures and overgrowing pyrite and marcasite, and as intergrowths with Bi- and Ag-tellurides and galena. High fineness gold (906-911) is associated with Bi-minerals in quartz-sulfide veins, moderately high fineness gold with carbonate-base metals (768-891), and low fineness gold (<500) fills late fractures.

Fluid inclusion and mineral isotope data (Baker and Andrew, 1991) indicate that Stage III quartz and carbonate were derived from different fluids. Quartz was deposited over a broad temperature range (120-300°C) from relatively saline (2-10 wt % NaCl) fluids, whereas carbonates were deposited over a similar temperature range but from significantly more dilute (0.2-0.7 wt % NaCl) waters. Isotope data demonstrate that the carbonates were precipitated from fluids containing a significantly higher meteoric component than the quartz. Two-phase fluid inclusions are absent, however this does not necessarily preclude the possibility that some boiling may have locally occurred.

Magmatic-derived mineralized fluids are inferred to have migrated upwards along sheeted fractures in the Wise's Hill and North Knob areas. Cavities formed by later extension host higher grade gold at the intersection of the straight segment sheeted veins (Morrison et al. (1996). Sulfide and gold mineralization in the sheeted veins and adjacent open space breccias is postulated to have taken place in response to the mixing of these upwelling saline, magmatic-derived fluids depositing quartz, with dilute meteoric waters depositing carbonate (Fig. 7.9). The current level of erosion has exposed a system which is transitional in mineralization style from a carbonate-base metal gold at shallow levels, to a quartz-sulfide gold ± copper at deeper levels.

3. Bilimoia District, Papua New Guinea

Gold ± copper-bearing quartz-sulfide veins occur near of Bilimoia village (Fig. 1.2), 15 km north of Kainantu in the Eastern Highlands of Papua New Guinea (Corbett et al., 1994b). Host rocks comprise the Early Mesozoic Bena Bena Formation phyllites which are intruded by syn-tectonic Karmantina Granite Gneiss and Mid Miocene Akuna Granodiorite (Fig. 7.10; Rogerson et al., 1987). Porphyry copper-gold mineralization elsewhere in the region is associated with Late Miocene Elandora Porphyry intrusions (Rogerson and Williamson, 1986a, 1986b). This area lies immediately south of the Markham fault, which represents the suture between the Pacific and Australian plates (Fig. 1.2). Two inferred porphyry centres are localized by the intersection of transfer structures with structures formed parallel to the New Guinea Orogen (Fig. 7.10). Mesothermal veins are hosted within pre-mineral, arc parallel, structures at Bilimoia, and in arc normal structures at Arakompa (Fig. 7.10; Corbett, 1994; Corbett et al., 1994b).

At Bilimoia the slaty cleavage within the Bena Bena Schist basement rocks grades into a crenulation cleavage within the arc parallel structures. As the crenulation cleavage must have formed at depths in the vicinity of 5 km (D. Grey, pers. commun., 1992), these structures represent deep crustal features which have been reactivated and mineralized at higher crustal levels. Mineralization occurs sporadically over strike lengths of up to 2 km along a series of sub parallel structures which vary from slickensided silicified fault faces to puggy shears, and are locally exploited by dikes or milled matrix fluidized breccias (Fig. 7.10).

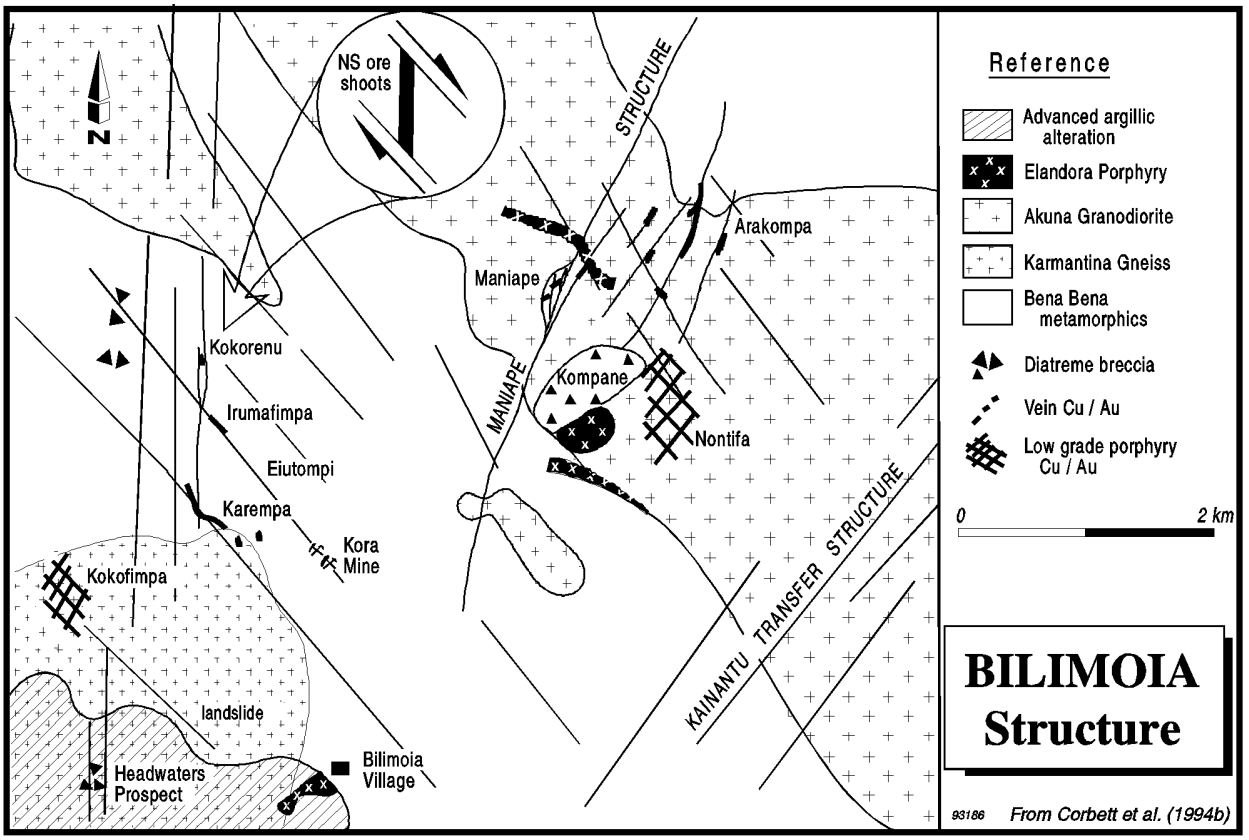

FIG. 7.10

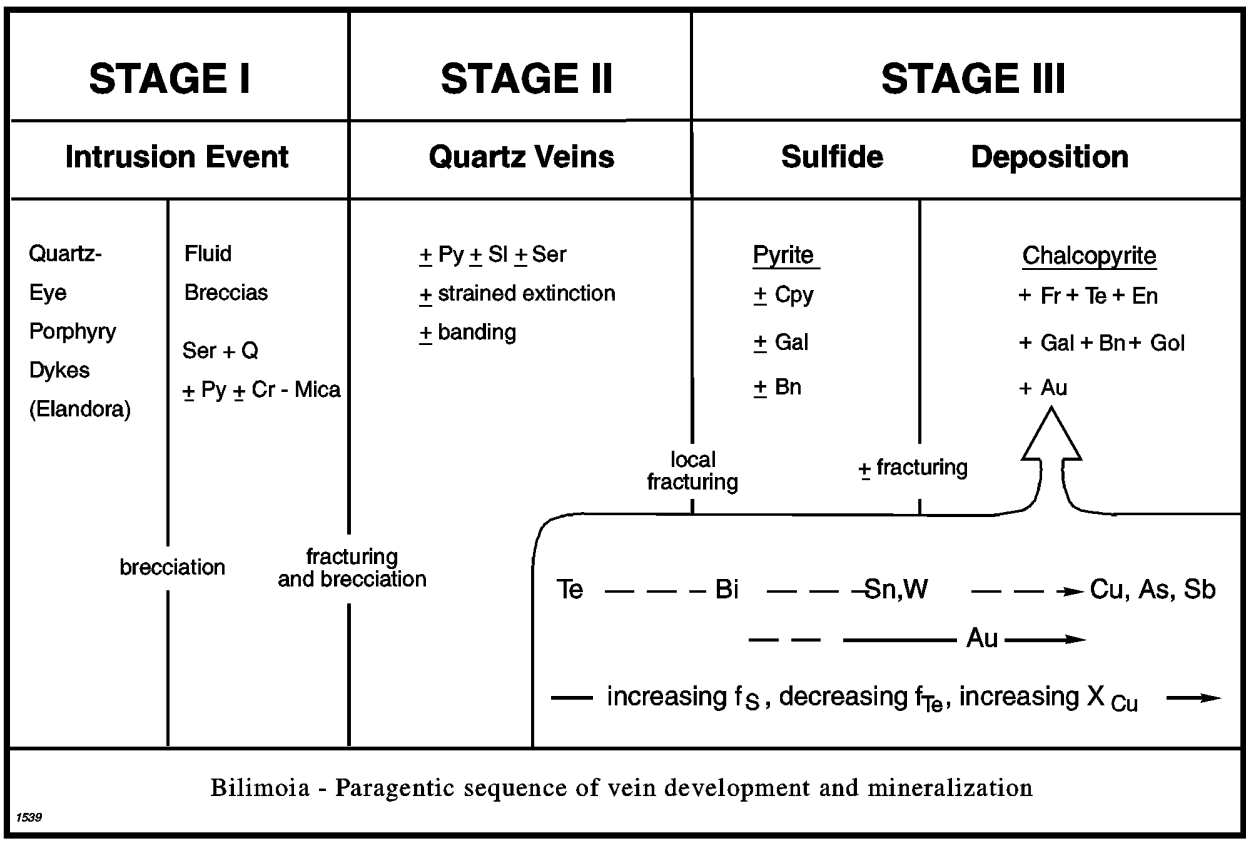

Bilimoia - Paragentic sequence of vein development and mineralization

FIG. 7.11

Mineralized quartz veins are exposed for a vertical extent of over 800 metres on the steep slopes between the Markham Valley and Eastern Highlands. Generally NS trending, higher grade ore shoots occur within or adjacent to the NW trending mineralizing structures, commonly at the intersections of cross structures (Corbett et al., 1994b). The local sigmoidal shapes of the ore shoots and angular relationships with the mineralization trend are consistent with the inference that these mineralized zones formed as tension veins during dextral rotation on the NW trending controlling structures (Corbett, 1994).

The following four stages of vein and breccia development, alteration and mineralization have been identified at Bilimoia (Fig. 7.11; Corbett et al., 1994b):

Stage I Shearing and Brecciation:
An initial stage of shearing and fracturing is locally accompanied by the deposition of fine fluidized breccias composed of quartz-sericite-pyrite. Elsewhere fault controlled milled matrix fluidized breccias which contain fragments of dike correlated with the Elandora Porphyry of Rogerson and Williamson (1986a, 1986b).

Stage II Quartz Veins:
A major event of extensive fracturing and brecciation, formed locally polyphasal crackle breccias or open veins, consisting of clear to milky quartz, grading outwards to crustiform or coxcomb quartz which extends into open cavities. The quartz commonly exhibits strained extinction indicative of deposition within a stress regime and in places is accompanied by minor sericite, pyrite and yellow sphalerite. Wall rock phyllites have locally undergone alteration to the Cr-rich micas, mariposite and fuschite. Fluid inclusion data indicate that the quartz veins were deposited from dilute (>2 wt % NaCl, very locally >3-4 wt % NaCl) waters over a wide temperature range of 210-330°C. There is no consistent zonation in temperatures or salinities over the 800 metre vertical extent of vein development. It is therefore interpreted that quartz deposition took place from dilute meteoric waters circulating within deep crustal structures. In places the quartz is chalcedonic, radiating, or fibrous, indicative of rapid quenching. The local presence of interlayered illite-smectite as a wall rock alteration also implies periodic influx of cool fluids.

Stage III Pyrite + Base Metals:
Quartz vein development is followed by deposition of massive to coarse grained pyrite + fine quartz in cavities and fractures, or in thin fractures cutting the phyllite wall rock. The local intergrowth of pyrite with base metal sulfides (sphalerite, galena, chalcopyrite and tennantite), trace magnetite, and common minute inclusions in pyrite of chalcopyrite, bornite, and hypogene covellite, are all indicative of the development of these veins as a precursor to the main copper-gold mineralization.

Stage IV Copper Mineralization:
Chalcopyrite overgrows pyrite, and in places, together with quartz and sericite, fills fractured and shattered pyrite. Chalcopyrite locally forms intricate intergrowths with bornite. At Karempa (Fig. 7.10), pyrite-chalcopyrite mineralization is accompanied by the deposition of topaz-sericite, diaspore-dickite or sulfates (anhydrite, barite). This is indicative of a periodic influx of moderately low pH, magmatic dominated fluids.

A wide range of W-Sn, Bi-Te-Ag and Cu-As-Sb minerals which accompany chalcopyrite deposition are indicative of the entrainment of late stage fluids with a significant magmatic component, probably derived from emplacement of an Elandora-style silicic felsic porphyry intrusion at depth. The paragenetic sequence of mineralization: tellurides --> Pb, Ag, Bi-sulfides --> Sn, W-sulfides --> Cu, As, Sb-sulfides, is consistent with decreasing fTe2 and increasing fS2 and XCu with time.

The initial deposition of tellurium-rich minerals occurs as: native tellurium which is overgrown by tellurobismuthinite (Bi_2Te_3), followed by lead (altaite - PbTe), and silver (Ag_2Te) tellurides. Later bismuth-rich

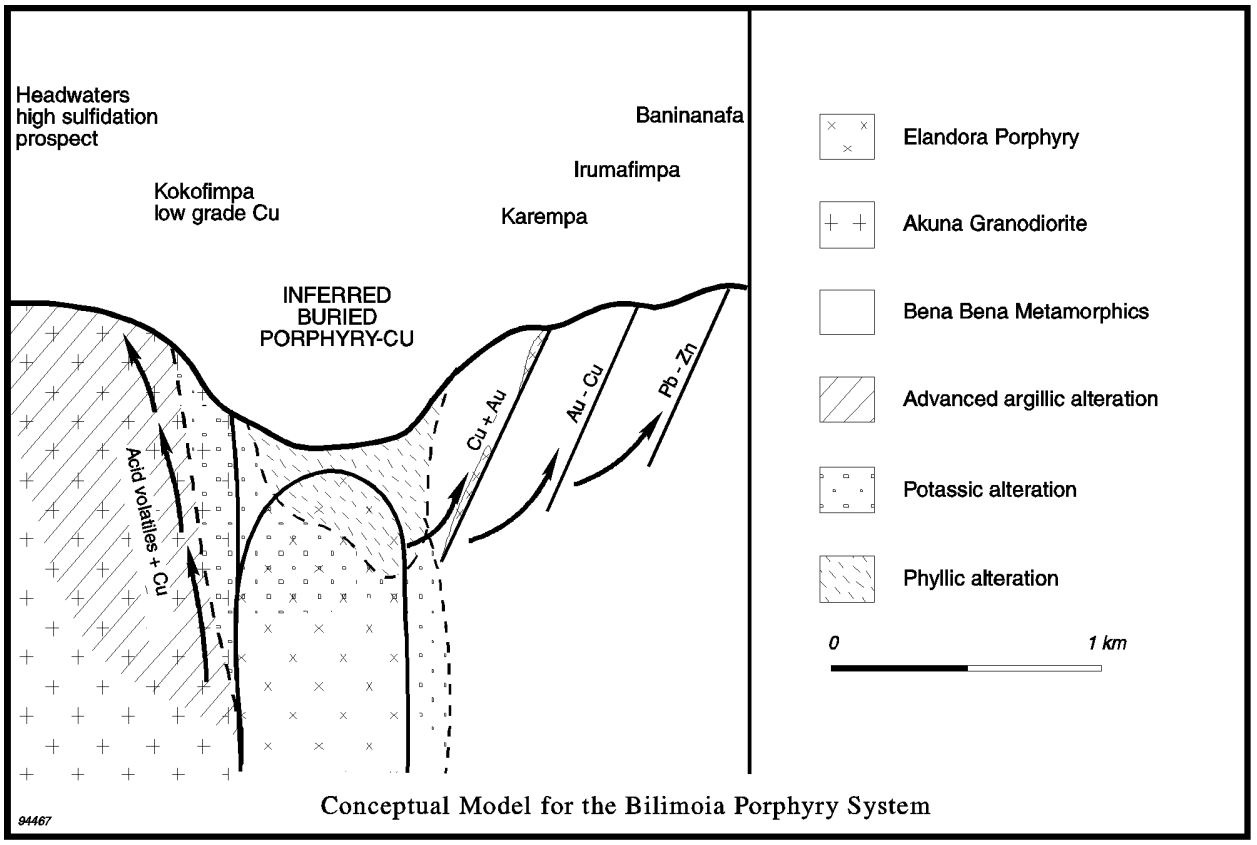

Conceptual Model for the Bilimoia Porphyry System

FIG. 7.12

STAGE I	STAGE II	STAGE III	STAGE IV
Pebble dikes Fluidized and diatreme breccia (Kompane) Early Elandora Porphyry	Quartz veins Coarse, banded, cockscomb strained extinction ± cubic pyrite, local sericite ± epidote, magnetite, carbonate	Pyrite ± quartz Fine-medium grained massive, ± sericite pebble dike event Locally polyphasal ± marcasite inclusions-Cpy, Ga, Sph	Chalcopyrite ± quartz ± sericite Fine grained, locally dilational ± local carbonate ± Bi-Cu-Ag-Pb-Te-S mineralogy ± galena, sphalerite
		Au	
		Fracturing ± brecciation locally depositional	Local fracturing commonly depositional

94473

Arakompa - Paragenetic sequence of vein development and mineralization

FIG. 7.13

phases include tetradymite (Bi_2Te_2S), bismuthinite (Bi_2S_3) and Bi-rich galena. Tin and tungsten minerals appear to post date Bi-Ag-Te mineralization. Ferberite (Fe-wolframite), is relatively common and is overgrown by Sn-Cu minerals such as mawsonite (Sn-rich bornite), and a Sn-As-covellite species. Local Cu-Bi-Te sulfides such as aikinite ($Cu[Pb,Bi]_2S_3$), goldfieldite ($Cu[Te,Sb]S_4$) and Bi-rich enargite are interpreted to be transitional between the early bismuth-telluride, and late copper minerals, characterized by chalcopyrite and minor bornite. The filling of fractures in massive pyrite by native copper, and the formation of covellite and chalcocite, are interpreted to form by supergene alteration of primary chalcopyrite.

The supergene gold, in oxidized quartz veins mined by the local villagers, commonly displays a "mustard" texture, indicative of a primary telluride-rich ore. At depth, hypogene gold occurs as inclusions in chalcopyrite, and also as inclusions in, and overgrowing bismuthinite and hessite incorporated within the chalcopyrite. Near the Kora mine (Fig. 7.10), gold occurs as inclusions in ferberite and in association with pyrite. Primary gold has a fineness of 834-922 (average 858), which is characteristic of quartz-sulfide gold $\pm$ copper systems formed peripheral to porphyry intrusions elsewhere in the southwest Pacific (Fig. 4.8). Gold in the Yar Tree Hill Prospect, 7-8 km along strike southeast of the Bilimoia quartz vein systems, is also present as inclusions in chalcopyrite cutting pyrite, and has a similar fineness (860-940, average 895) to gold at Bilimoia.

It is interpreted that early stage quartz veins and wall rock sericite (fuchsite) alteration were formed from dilute meteoric water-dominated fluids which circulated along the deep crustal Bilimoia structures. The chromium (in fuchsite) may have been derived from the migration of these fluids through ultramafic host rocks at depth (ultramafics crop out to the northwest of the Kainantu region). The emplacement of Elandora Porphyries along these structures has resulted in initial intrusion of fluidized breccias, and shallow level felsic dikes as the precursors to the introduction of mineralizing fluids, which resulted in the deposition of chalcopyrite-pyrite-gold and associated Bi-Te-W-Sn-Ag minerals.

Zonations in styles of alteration, veins and mineralization at Bilimoia suggest that the inferred buried intrusion source for the gold mineralization (Fig. 7.12), may lie in the vicinity of a landslip where phyllic alteration is exposed (Fig. 7.10). Potassic alteration and weak copper mineralization in Akuna granodiorite at nearby Kokofimpa is overprinted by phyllic alteration which extends SE to Bilimoia village (Fig. 7.10). Magmatic volatiles which evolved to the south and west from the buried porphyry resulted in the formation of the shoulder of pervasive advanced argillic (high sulfidation) alteration (Fig. 7.10). This is locally cut by structurally controlled enargite mineralization at the Headwaters Prospect (Fig. 7.10). Mineralized fluids migrated along NS structures and laterally along pre-existing NW-SE structures to form gold mineralization which displays a progressive zonation as: Cu + Au --> Au-Cu --> Pb-Zn, at increasing distances from the inferred porphyry source (Fig. 7.12). Higher gold grade ore-shoots are inferred to have formed at sites of fluid quenching at the intersection of NS structures, along which the magmatic fluids flowed, with the NW host structures. NS trending tension veins formed by dextral strike-slip movement on the NW structures also host mineralization (Corbett et al., 1994b).

At Arakompa, mesothermal quartz veins occur proximal to sub-economic porphyry copper-gold mineralization (Fig. 7.10; Corbett, 1994; Corbett et al., 1994b). Host rocks comprise the mid Miocene basement Akuna Granodiorite, and mineralization may be related to younger Elandora-style porphyry intrusions which crop out in the area (Rogerson and Williamson, 1986a, 1986b). Pre-mineral NNE trending arc normal structures have undergone dilation during subduction-related compression from the NNE, and so correspond to the tensional vein setting discussed in Section 3.iv.a. Intersections with NE trending arc parallel structures represent sites of stockwork vein development. Most mineralization is confined to fault controlled gossanous lodes and adjacent pug zones which display some post mineral movement. Flexures in the controlling faults localize thicker lodes, commonly with elevated gold and copper grades. Both the puggy faults and gossanous lodes are worked by local miners for supergene gold. Pebble dikes recognised in drill core are indicative of the emplacement of a pre-mineral explosive magmatic fluid along the fault structures, and are cut by quartz and sulfide veins. Some contain exotic basement rock fragments carried up from unknown depths.

Four stages of brecciation, vein development, alteration and mineralization are categorised at Arakompa (Figs. 7.13; Corbett et al., 1994b) as:

Stage I Pebble Dikes:
The NNE-trending structures host breccias comprising well milled fragments of phyllic altered Akuna Granodiorite, hornfelsed sediments, and low metamorphic grade phyllites similar to those which crop out at Irumafimpa, and rare early quartz-sericite-pyrite vein clasts.

Stage II Quartz Veins:
Extensive coarse-grained, cockscomb to locally banded quartz deposition, was accompanied by coarse cubic pyrite, sericite, as well as local epidote, magnetite, and carbonate, and cross cuts the pebble dikes. Fluid inclusion data (Fig. 7.14) indicates that the quartz was deposited over a wide temperature range (245-315°C, average 285°C), under local two-phase (boiling) dilute (< 2 wt % NaCl) fluid conditions, similar to quartz veins at Bilimoia.

Stage III Polyphasal Fracturing and Brecciation:
Brecciation of the early quartz veins and pebble dikes was accompanied by deposition of massive fine to coarse grained pyrite, and fine granular quartz. The pyrite commonly contains inclusions of chalcopyrite, bornite, sphalerite, galena and rutile, as a precursor to the Stage 4 mineralization. Limited fluid inclusion data on Stage 3 quartz suggests that the brecciation and quartz-sulfide vein development took place in response to an influx of fluid at a similar temperature (250-290°C), but of significantly higher salinity (4-6.5 wt % NaCl), than the earlier quartz veins (Fig. 7.14).

Stage IV Copper-Gold Mineralization:
Chalcopyrite and minor quartz-sericite overgrow the earlier mineral phases. Local fracturing and brecciation accompanied the copper mineralization. A wide array of Bi-Ag-Pb-Cu + Zn + Sn telluride and sulfide minerals (bismuthinite, cupropavonite, wittichenite and hammarite) was deposited either transitional between Stage III pyrite and Stage IV chalcopyrite, or contemporaneous with the chalcopyrite mineralization (Corbett et al., 1994b). Trace tin phases (stannoidite, kesterite and a Te-canfieldite) are also associated with chalcopyrite deposition.

Gold at Arakompa occurs in the native form, generally as inclusions in Stage III pyrite and Stage IV chalcopyrite, and is commonly associated with Ag-Bi-Cu-Pb-Te + Sn/Zn minerals. Gold displays a high fineness (723-995, average 877), characteristic of quartz-sulfide gold $\pm$ copper systems, transitional between porphyry copper-gold and carbonate-base metal gold systems (Fig. 4.8; Leach and Corbett, 1994, 1995). The higher salinity fluids and the presence of Bi-Te-Sn minerals during Stage III/IV activity are indicative of a significant influx of magmatic-derived fluids during the formation of mineralization at Arakompa.

The increase in copper contents and fluid inclusion temperatures with depth, further suggest that the mineralized fluids have migrated from a porphyry in the vicinity, probably at depth beneath the Arakompa Prospect. These fluids are inferred to have moved upwards, depositing copper and gold into reopened quartz and pyrite-quartz veins at Arakompa, as well as south and west of the Maniape quartz-pyrite veins in a more distal setting (see below). A prominent aeromagnetic high at Arakompa may be related to a magnetite-bearing potassic altered porphyry at depth. Weak copper-gold mineralization is associated with outcropping magnetite-bearing potassic alteration at nearby Nontifa and the peripheral propylitic alteration also contains magnetite (Fig. 7.10).

The Maniape Prospect is discussed as a carbonate-base metal style of gold mineralization in Section 7.iii.i.

4. Hamata, Morobe Goldfield, Papua New Guinea

At Hamata, veins exploit flatly dipping shears within the basement Morobe Granodiorite in the inferred hanging wall of the Upper Watut graben fault (Fig 7.28). The geological setting of the Hamata Prospect is considered more fully in the discussion of the Morobe goldfield (Section 7.iii.i).

Gold mineralization at Hamata occurs within a 50 m thick zone containing two sub-parallel up to 3-4 m wide shear-hosted reefs (Masi and Lower zones, Denwer et al., 1995; Wells and Young, 1991). The host Morobe Granodiorite has undergone intense K-feldspar-sericite alteration within these zones, which overprints high grade propylitic (actinolite-epidote) and local potassic (biotite) alteration. The reefs and smaller veins contain pyrite-hematite-magnetite-quartz alteration.

The paragenetic sequence of vein development and mineralization is summarised from Denwer et al. (1995) as:

Stage I: Early thin veinlets of magnetite, hematite and pyrite exhibit K-feldspar selvages, and are overgrown and cut by K-feldspar-quartz veins. Quartz characteristically contains liquid- and vapour-rich inclusions and halite daughter phases. Fluid inclusion data indicate that the quartz was deposited under relatively hot (270-340°C) and periodic hypersaline (up to 35 wt % NaCl) to moderately saline (3-7 wt % NaCl) conditions, indicative of an environment proximal to a porphyry system.

Stage II: A major stage of massive sulfide-oxide vein development was accompanied by fine grained quartz-sericite deposition. Specular hematite and coarse lath-like magnetite overgrow early pyrite. Chalcopyrite locally seals shattered pyrite, and with sericite-pyrite fills fractures which cut early quartz. Bi-Te (tetradymite) and W (ferberite) mineralization is associated with pyrite-chalcopyrite deposition. Native gold fills fractures and cavities in pyrite, is closely associated with Bi-tellurides, and has a fineness of 816-991 (average 911). The style of gold mineralization at Hamata is therefore very similar to that encountered at Arakompa and Bilimoia.

Stage III: The deposition of local carbonate-base metal sulfide veins in which pyrite, calcite and chalcopyrite are the dominant minerals, is accompanied by minor sphalerite, galena and late stage arsenopyrite. In places hematite and magnetite deposition locally extends into this carbonate-base metal phase of alteration.

Stage IV: Late quartz and/or barite veins contain local arsenopyrite.

The Hamata quartz-sulfide style of gold mineralization occurs at a lower elevation than the other deposits in the Bulolo graben, transitional between the higher level carbonate-base metal gold systems, which are the predominant style of mineralization (below) and an inferred buried porphyry copper-gold source for the alteration and mineralization. The Hamata deposit crops out along the strike of the same structure as the Hidden Valley carbonate-base metal gold deposit, but at several hundred metres lower, in keeping with the overall zonation of these deposit types (Figs. 7.28, 7.29).

v) Exciban, Philippines

Gold mineralization in the Exciban deposits, Camarines Norte district, Philippines, displays features typical of porphyry-related quartz-sulfide gold $\pm$ copper vein systems. The following discussion is taken from James and Fuchs (1990) and Mitchell and Leach (1991).

Mineralization occurs within a set of steeply dipping NNE-trending structures formed at a high angle to the Larap thrust zone. Early quartz veins are hosted in weakly metamorphosed and locally sheared volcanics and arenaceous sediments. The quartz contains abundant halite daughter crystals indicative of hypersaline fluid conditions. Massive sulfide veins are characterized by pyrite and chalcopyrite, the latter commonly as overgrowths and filling fractures and cavities in the pyrite. Native gold occurs as inclusions in pyrite and

chalcopyrite and is generally associated with bismuth telluride minerals (tellurobismuthinite, tetradymite and hedleyite [Bi_7Te_3]).

James and Fuchs (1990) infer a magmatic-dominated source for the veins and mineralization based upon the presence of daughter crystals in fluid inclusions, abundance of telluride minerals and high copper content of the veins. Dacite dikes crop out at the surface and are interpreted to represent high level equivalents of the mineralizing porphyry at depth. These workers attribute the formation of high cobalt levels to the circulation of hydrothermal waters through mafic/ultramafic host rocks at depth.

iii) Carbonate-Base Metal Gold Systems

a) Introduction

Carbonate-base metal gold systems contain appreciable carbonate and base metal, commonly at the expense of quartz, and form at crustal levels which are intermediate between the porphyry and epithermal environments (Figs. 7.1, 7.2; Leach and Corbett, 1993, 1994, 1995). Sillitoe (1989) and Handley and Bradshaw (1986) alluded to the existence of this class of deposit in emphasising the magmatic association and noting an overlap between the epithermal and porphyry environments, especially in relation to the Porgera gold deposit. Henley and Berger (1993) cite the higher temperature mineralogy and deeper level of formation in discussing the difficulty of describing Kelian as an epithermal gold deposit. Similar difficulties in classifying these and other carbonate-base metal gold deposits (e.g., Morobe Goldfield, Woodlark Island, Maniape) within the existing terminology led to the subdivision of the low sulfidation gold deposits used herein (Leach and Corbett, 1993, 1994, 1995). Transitional and overprinting relationships are apparent between the deeper quartz-sulfide gold $\pm$ copper and higher level epithermal quartz gold-silver, and locally adularia-sericite epithermal gold-silver, styles of mineralization.

b) Definition

Carbonate-base metal gold systems develop distal to porphyry intrusions by mixing of magmatic-derived fluids with near surface CO_2-rich waters (Figs. 1.4, 2.4). The form of mineralization varies from fissure to stockwork veins and fill of open space breccias. Milled matrix fluidized breccias which locally form maar volcano/diatreme breccia complexes, are common as pre-mineral phreatomagmatic eruptions which focus fluids degassing from the magmatic source at depth, and also create fracture permeability in the adjacent competent host-rocks. High level porphyry intrusions are common, locally as endogenous domes in association with the maar volcano/diatreme breccia complexes.

Base metal contents typically occur as Zn > Pb > Cu, while carbonates exhibit a wide range of chemistry and spatial zonations with increasing depth from Fe-, to Mn-, Mg-, and Ca-carbonates (Fig. 7.17). Gold mineralization preferentially occurs in association with the Mn/Mg carbonates. There is a progression in time and space (crustal level) from porphyry to epithermal environments. At deeper crustal levels carbonate-base gold mineralization is commonly preceded by quartz-sulfide alteration, and locally porphyry-related quartz stockwork veins. Mineralizing fluids are transitional between dilute circulating meteoric waters, typical of epithermal environments, and high temperature saline porphyry systems.

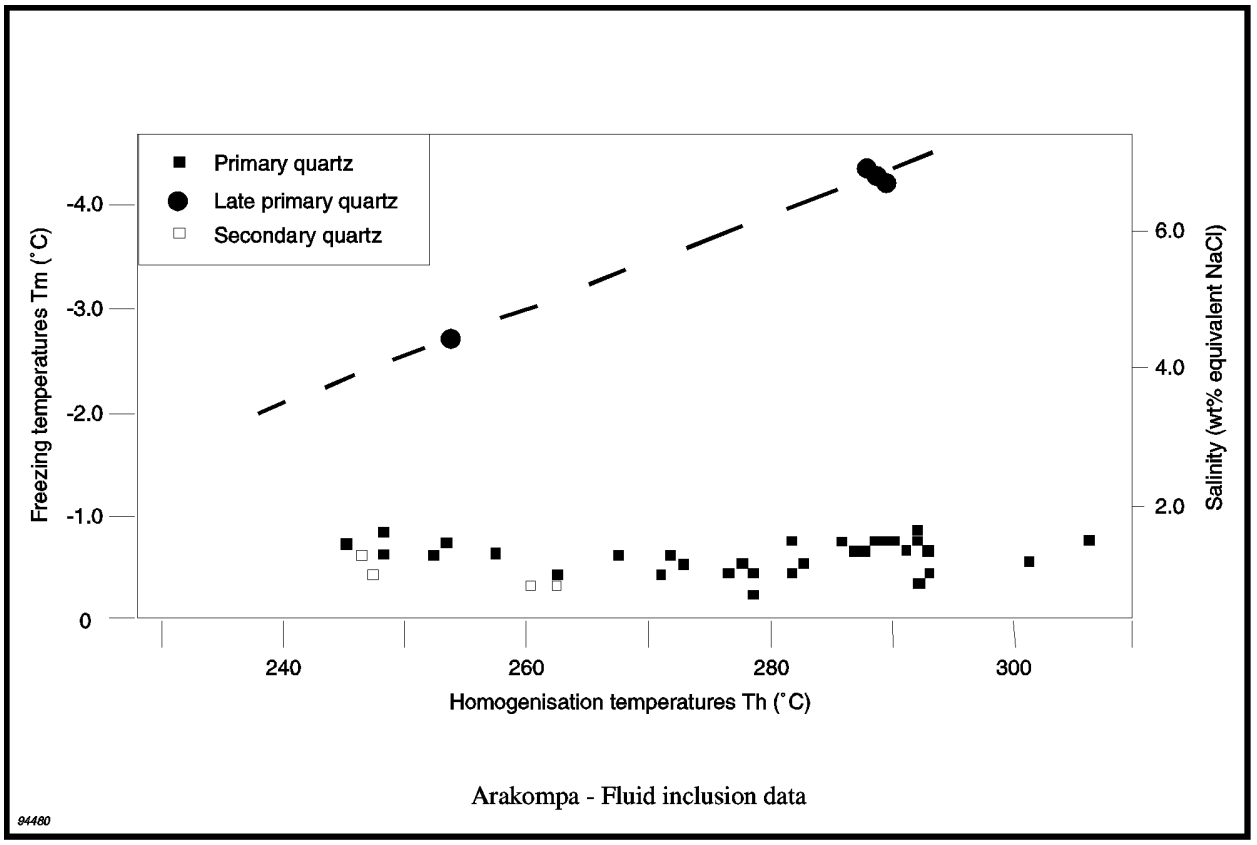

Arakompa - Fluid inclusion data

FIG. 7.14

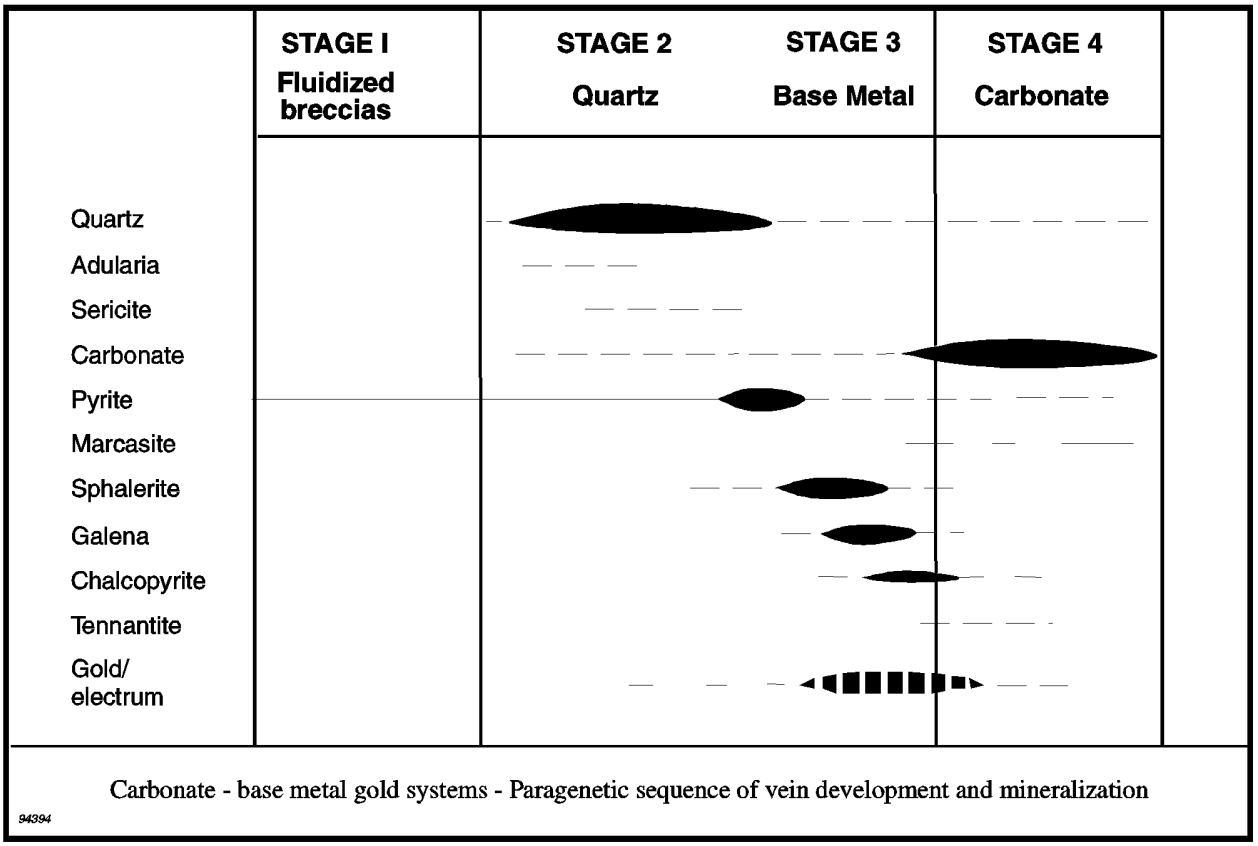

Carbonate - base metal gold systems - Paragenetic sequence of vein development and mineralization

FIG. 7.15

c) Distribution

Some significant southwest Pacific rim carbonate-base metal gold systems are: in Indonesia, Kelian (5.7 M oz Au; van Leeuwen, 1994), Busang (Felderhof et al., 1996), parts of Mt Muro (1 M oz Au; Moyle et al., 1996), and the Cikotok/Cirotan district: in Papua New Guinea, Porgera mineralization types A, B and E (>6 M oz Au), Mt. Kare; the Morobe Goldfield (mostly alluvial production, 3.7 M oz Au; Lowenstein 1982) group of deposits located within the Bulolo graben, including Upper Ridges, Golden Ridges and Golden Peaks at Wau, Edie Creek, Kerimenge (1.8 M oz Au, Hutton et al., 1990), Hidden Valley (2.4 M oz Au, Nelson et al., 1990); Busai and Kulumadau on Woodlark Island (Corbett et al. 1994a), Maniape at Kainantu (Corbett et al., 1994b), the Umuna lode and other prospects on Misima Island: in the Solomon Islands, Gold Ridge: in the Philippines, Acupan (4 M oz Au), Antamok (10 M oz) in the Baguio District and also in eastern Mindanao (Mitchell and Leach, 1991): in eastern Australia, Mt. Terrible (Teale, 1995), and Copper Hill (T. Leach unpubl. data). Some deposits formerly described as adularia-sericite epithermal gold-silver style exhibit affinities with carbonate-base metal systems (e.g., Karangahake, New Zealand), particularly at depth (e.g., Tolukuma, Papua New Guinea). Many other deposits currently termed epithermal display similarities with the carbonate base-metal classification utilised herein (e.g., Montana Tunnels; Sillitoe et al., 1985: Creede District; Foley and Ayuso, 1994).

d) Geological Setting

Carbonate-base metal hydrothermal systems form at crustal levels above the porphyry copper-gold deposits, and so tend to be associated with higher level, possibly differentiated, porphyry intrusions. Partly eroded younger magmatic arcs in competent basement rocks are ideal settings for carbonate-base metal deposits. Magmatic arcs formed under conditions of oblique convergence are conducive to the migration of fluids to settings overlying porphyry environments (e.g. Philippines, Sumatra), whereas fluids might be constrained within the porphyry environment in conditions of orthogonal convergence (Section 3.ix.b; Fig. 3.5). The Bulolo graben (Corbett, 1994), Papua New Guinea (see Fig 7.28) which formed as an intra-arc rift, possibly with associated crustal thinning, represents a locus for the emplacement of high level intrusions and hosts several carbonate-base metal gold occurrences (Kerimenge, Upper Ridges, Edie Creek, Hidden Valley), commonly within basement host rocks. Individual intrusion centres localize carbonate-base metal gold systems at Porgera (Corbett et al., 1995 and references therein), Kulumadau (Corbett et al., 1994a), and Mt Kare (Richards and Ledlie, 1993). The Kelian, Busang and Mt Muro carbonate-base metal gold systems in central Kalimantan, Indonesia (Figs. 1.2, 3.12) are localized by a major crustal structure (Van Leeuwen et al., 1990) which separates rocks of different ages, and delineates the margin of the magmatic arc defined by Carlile and Mitchell (1994).

Many carbonate-base metal gold systems are associated with milled matrix fluidized hydrothermal breccias which locally vent as maar volcano/diatreme breccia phreatomagmatic eruptions (e.g., Kelian; Sillitoe, 1994a: Acupan, Philippines; Domasco and de Guzman, 1977: Kerimenge, Papua New Guinea; Akiro, 1986; Denwer et al., 1995: Wau, Papua New Guinea; Sillitoe et al., 1984), or occur as intrusive dike-like features (e.g. Woodlark Island, Papua New Guinea; Corbett et al., 1994a: Mt Kare, Papua New Guinea; G. Corbett, unpubl. report, 1996).

e) Structure

Carbonate-base metal gold systems are hosted in: fissure veins and breccia zones near diatreme margins (e.g., Kerimenge and Edie Creek, Papua New Guinea; Acupan, Philippines), feeder structures which host higher gold grades and intervening tension gash vein/breccias which host lower grade ore (e.g., Busai, Woodlark Island, Papua New Guinea; Antamok, Philippines), fractured and brecciated intrusion margins (e.g., Kelian, Indonesia; Porgera, Papua New Guinea), dilatancy associated with throughgoing strike-slip structures (e.g., Maniape,

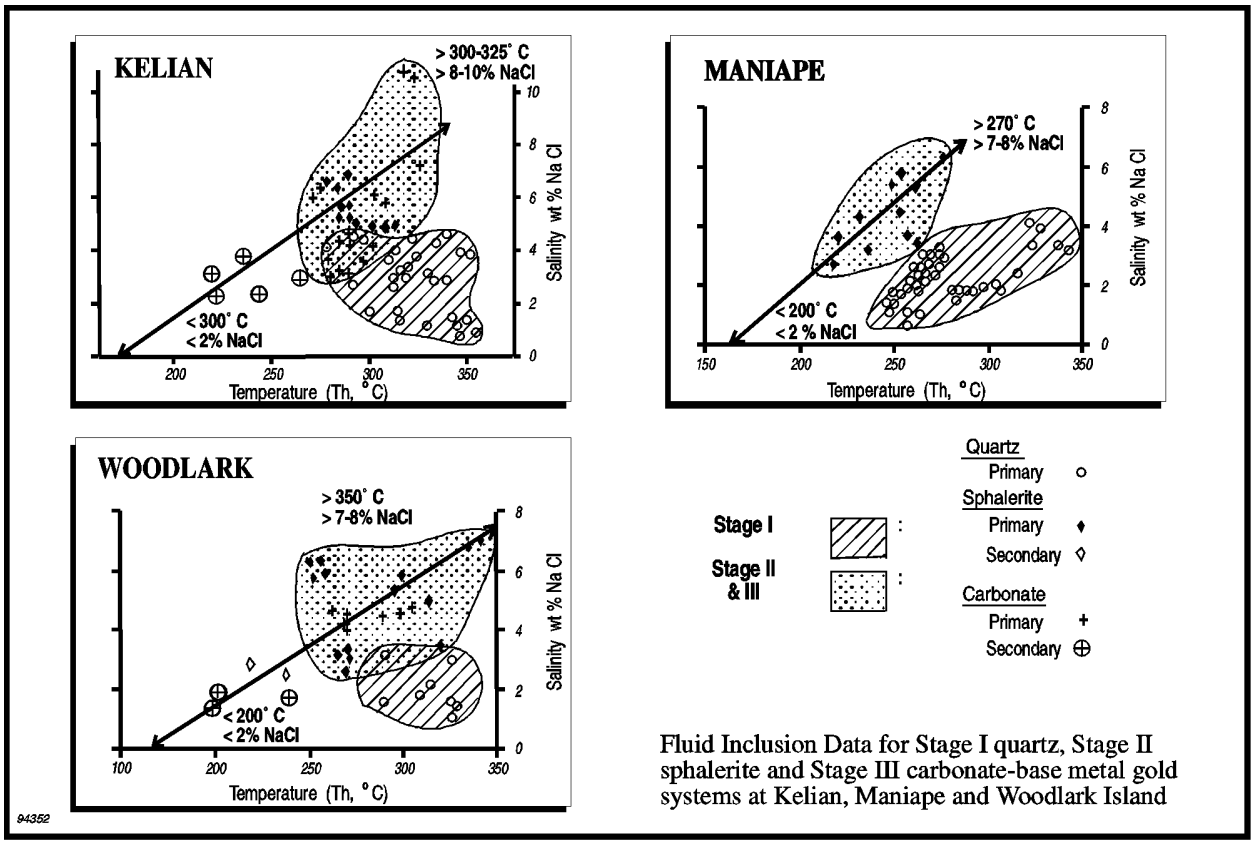

Fluid Inclusion Data for Stage I quartz, Stage II sphalerite and Stage III carbonate-base metal gold systems at Kelian, Maniape and Woodlark Island

FIG. 7.16

Distal to porphyry source or Cool

Vein Type	Carbonate Type	Base Metals	Sphalerite	Fe-Sulfides
quartz>carbonate				pyrite/ marcasite
carbonate>quartz	Fe (siderite)			
	Mn (rhodochrosite)	Zn ≥ Pb > Cu	Zn > Fe	
carbonate	MnMg (kutnahorite)			
	MgCaFe (ankerite)			pyrite
	MgCa (dolomite)			
	CaMg (Mg-calcite)		Fe > Zn	
	Ca (calcite)			pyrite -pyrrhotite (magnetite)
sulfides		Cu > Zn, Pb		

Proximal to porphyry source or Hot

Carbonate-base metal gold systems - Zonations in vein mineralogy and styles of mineralization

94375

FIG. 7.17

Bilimoia District, Papua New Guinea), hanging wall splits (e.g., Kerimenge, Hidden Valley, Upper Ridges in the Wau district Papua New Guinea), or within the matrix to fluidized or diatreme breccias (e.g., Mt Kare, Papua New Guinea: Montana Tunnels, USA; Sillitoe et al., 1985: Bulawan, Philippines; G. Corbett, pers. observation, 1995). Elevated gold grades form by repeated deposition in dilational structures (e.g., Acupan, Philippines; Upper Ridges, Wau, Papua New Guinea), especially if proximal to fluid upflow zones (e.g., GW breccia pipes, Acupan; Domasco and de Guzman, 1977).

Pre-mineral structures and fracturing about the margins of breccia bodies, such as maar volcano/diatreme breccias, control fluid flow. These structural features then represent ideal loci for subsequent hydrothermal fluids and hence mineralization. Thus, an optimum setting for carbonate-base metal gold mineralization might be fracturing near the intersection of major through-going structures and maar volcano/diatreme complexes (e.g., Upper Ridges and Kerimenge, Wau District, Papua New Guinea), or at the contact of veins with diatreme pipe margins (e.g., G.W. breccia pipes at Acupan; Damasco and de Guzman, 1977). Fluidized breccias prepare pre-existing structures which are then exploited by later carbonate-base metal veins (e.g., Busai, Woodlark Island and Mt Kare, Papua New Guinea; Corbett et al., 1994a).

Rock competency is a critical factor in fracture development and hence mineral deposition. At Porgera, intrusion stocks were emplaced into the extremely incompetent Chim Formation shales, and fracture-controlled mineralization occurs within the baked sediments at the intrusion contacts (Corbett et al., 1995 and references therein). Phreatomagmatic (diatreme or milled matrix fluidized) breccias fracture the country rocks and focus mineralizing fluids from the degassing magmatic source. These breccias display alteration characterized by clays which vary with increasing depth from: smectite, to interlayered illite-smectite, to illite and sericite, and show a corresponding increase in rock competency. Carbonate-base metal mineralization associated with diatreme breccias exposed at high crustal levels tends to occur in the fractured country rocks, rather than within the incompetent diatreme (e.g., Kerimenge, Acupan), whereas only at deeper levels do the internal portions of diatreme breccias host mineralization of this style (e.g., Montana Tunnels, USA; Sillitoe et al., 1985: Bulawan, Philippines; G. Corbett, pers. observation, 1995). Similarly, at Kelian, Indonesia, brecciated intrusion margins host mineralization, whereas the incompetent 'muddy breccias' (classified as diatreme breccias by Sillitoe, 1994a) are less well mineralized (van Leeuwen et al., 1990).

f) Alteration and mineralization

A common sequence of overprinting alteration and mineralization recognised for most carbonate-base metal gold systems (Fig. 7.15) is summarised as:

Stage I milled matrix fluidized breccias as diatreme (e.g., Wau, Kelian, Acupan, Kerimenge) or intrusive dike-like bodies (e.g., Busai, Mt Kare), are interpreted to form upon initial intrusion emplacement at depth, coincident with localized propylitic alteration of the host rocks. Such phreatomagmatic breccias provide pre-mineral ground preparation and focus later mineralizing fluids.

Stage II alteration is dominated by quartz, post-dates brecciation, and in some deposits contains either early adularia and/or late sericite/illitic clay. Quartz ranges with decreasing depth from: porphyry-related quartz stockwork veins at deep levels (e.g., Copper Hill, eastern Australia; T. Leach, unpubl. data: Porgera; Richards, 1992), to cockscomb quartz veins at intermediate levels (e.g., Kelian, Morobe Goldfield [Wau District], Woodlark, Maniape), and to crustiform banded quartz-adularia veins at shallow levels (e.g., Tolukuma, Papua New Guinea; Karangahake, New Zealand). Fluid inclusion data indicate that the early quartz in many vein systems was deposited from relatively hot (250-350°C), but dilute (<2-4 wt % NaCl) fluids (Fig. 7.16).

Stage III carbonate-base metal sulfide veins typically overgrow and/or cross cut earlier quartz veins. The base metal sulfides commonly pre-date carbonate and comprise: early pyrite, followed by sphalerite and galena, overgrown by later copper minerals (mainly chalcopyrite followed by tennantite). In most instances, minor base metal sulfide mineralization extends into the carbonate event.

Stage IV carbonates may occur as fine crustiform banded veins, locally alternating with thin quartz-rich carbonate bands. Fluid inclusion data (Fig. 7.16) indicate that the carbonate and sphalerite in many systems were deposited from a significantly saline fluid (> 7-10 wt % NaCl), but at similar or slightly lower temperatures than the earlier quartz. High salinity inclusions in carbonate and sphalerite are interpreted to indicate an influx of fluid with a significant magmatic component during the Stage II-III activity. Figure 7.16 illustrates that the saline mineralized fluids have mixed with cool (<200°C) and dilute (<2 wt % NaCl) waters. These dilution trends project to nil salinity at about 150°C (Fig 7.16), which is a typical temperature of steam-heated CO_2-rich waters in active geothermal systems (Hedenquist, 1990, 1991). The fluid inclusion data support the concept that vein deposition and mineralization in carbonate-base metal gold systems occurs in response to the mixing of saline mineralized fluids with near surface CO_2-rich waters.

Gold mineralization predominantly develops during base metal sulfide deposition and extends into the carbonate vein event. Gold typically occurs in the native state, either as inclusions in pyrite or base metal sulfides, intergrown with carbonate, or filling fractures and vughs in earlier quartz. Some gold mineralization also occurs within late-stage quartz veins, especially where abundant pyrite/arsenopyrite is present (e.g., Kerimenge; Syka and Bloom, 1990: Porgera; Richards, 1992). The average fineness of the gold in carbonate-base metal systems typically lies within the range of 700-850 (Fig. 4.8), intermediate between epithermal quartz gold-silver and quartz-sulfide gold $\pm$ copper systems formed marginal to porphyry intrusions. Silver-rich and telluride minerals are absent from in carbonate-base metal systems compared to their common occurrence in shallower/cooler epithermal quartz gold-silver systems (Section 7.iv).

Late stage hydrothermal activity is either dominated by surficial fluids which result in the deposition of kaolin, interlayered clay, gypsum, and quartz; or by deep fluids which characteristically deposit calcite. Gold mineralization may rarely persist into the initial stages of this late event.

g) Zonations in alteration and mineralization

Carbonate-base metal gold systems display distinctly zoned alteration and mineralization, from regions proximal to an intrusion source or hot conditions, to distal settings where cooler conditions prevail (Fig. 7.17). Carbonate species vary from Fe- and Mn-rich (siderite and rhodochrosite) at shallow levels, or distal to the intrusion source, to Ca- and Mg-rich (calcite, Mg-calcite, dolomite) at depth, or proximal to an inferred intrusion source. The mixed Mn-Mg-Fe-Ca carbonate species (ankerite and kutnahorite) occur between the Fe/Mn and Ca/Mg carbonate end members.

Limited oxygen and carbon isotope analyses on carbonates at Kelian (van Leeuwen et al., 1990), and Porgera (Richards and Kerrich, 1993) indicate that the Ca-rich carbonates display strong magmatic fluid signatures, whereas the Mn-Fe carbonates are more likely to develop from a fluid of surficial origin, and kutnahorite and dolomite formed by a mixing of the two fluid sources. This zonation in carbonate chemistry is interpreted to reflect the descent and heating of cool low pH condensate fluids, and simultaneous mixing of these fluids with upwelling hot magmatic dominated fluids. A similar zonation in carbonate species and modes of formation has been documented for active porphyry-related hydrothermal systems in the Philippines (Leach et al., 1985).

Bulk low grade gold mineralization is usually encountered in the mixed carbonate, kutnahorite/ankerite to rhodochrosite zones, where progressive mixing between descending bicarbonate and upflowing mineralized fluids has taken place, commonly within dilational structural environments. High grade mineralization occurs in

restricted feeder structures where sudden quenching of upwelling fluids occurs close to the inferred magmatic source and in dilational settings of repeated mineralization.

Ores tend to be dominated by sulfides + quartz at depth, and become more carbonate-rich at the expense of these phases at progressively shallower levels. At shallow levels and/or in outflow zones quartz locally dominates over carbonate, (e.g., Karangahake, New Zealand; Tolukuma, Papua New Guinea). This may reflect a transition to adularia-sericite style epithermal vein systems.

Pyrite is the dominant sulfide throughout most systems. However, in some deposits, pyrrhotite becomes more abundant at depth, and in places is intergrown with magnetite (e.g., Kelian, Indonesia). In many systems at shallow levels, marcasite is present, pyrite locally forms colloform bands (melnicovite), and in rare instances is amorphous.

Base metal sulfides (commonly Zn > Pb) dominate over copper minerals in most systems. However, copper contents may increase proximal to inferred magmatic sources, transitional to quartz-sulfide gold $\pm$ copper systems. Sphalerite typically contains chalcopyrite blebs and stringers, and varies from: colourless to yellow (Fe-poor) in cool distal environments, to dark red-brown to opaque (Fe-rich, marmatite) at depth. The increase in Fe-content of sphalerite is correlated with an increase in magmatic component of the mineralizing fluid (Simmons et al., 1988), and/or an increase in temperature (Barton and Skinner, 1979).

h) Fluid flow model

Hot mineralized fluids evolve from cooling shallow level porphyry intrusions and rise along permeable zones such as dilational structures, diatreme or intrusion margins (Fig. 7.2). At depth, these fluids mix with circulating meteoric waters and form gold mineralization within quartz-pyrite/arsenopyrite vein systems, in which copper minerals dominate over lead-zinc sulfides.

Gases, which evolve from these upwelling fluids by boiling and vapour loss, are absorbed by ground water near the surface to form CO_2-rich waters with a minor acid sulfate component (Section 2.iii). Fluid draw down during cooling of porphyry intrusions promotes the downward migration of CO_2-rich waters deep into the hydrothermal system. The CO_2-rich waters are locally entrained in pulses of hot mineralized fluids, and this mixing results in gold mineralization at various crustal levels within carbonate-base metal sulfide vein/breccia systems, depending on available permeability. Features such as diatreme and milled matrix fluidized breccias influence the fluid flow in the many carbonate-base metal gold systems with which they are associated, and should therefore be incorporated into any fluid flow model for these systems.

In carbonate-base metal gold systems an analysis of the alteration zonation, paragenetic sequence, and structure, may be used to trace the flow of both upwelling magmatic dominated mineralized fluids, and descending CO_2-rich waters in order to target: high grade gold zones which result from fluid quenching within feeder structures and settings of repeated mineral deposition, bulk low grade gold mineralization produced by cooling/dilution in progressively cooler environments, and gold-copper mineralization associated with the magmatic (porphyry) source.

Carbonate-base metal gold mineralization passes upward to epithermal quartz gold-silver hydrothermal systems. In near surface outflow zones, repeated boiling and cooling of mineralized fluids results in the formation of commonly colloform banded quartz-adularia veins. In these systems gold mineralization preferentially occurs in thin sulfide-rich bands or breccia zones where hot magmatic fluids have been quenched by cool, oxidizing ground waters (e.g., Tolukuma, Papua New Guinea; Corbett et al. 1994c: Cracow, eastern Australia, G. Corbett and T. Leach, unpubl. data). At depth carbonate-base metal gold deposits grade into

quartz-sulfide gold ± copper systems (e.g., Kidston, eastern Australia). Many ore deposits contain telescoping and overprinting quartz-sulfide gold ± copper, carbonate-base metal gold and epithermal quartz gold-silver styles of mineralization (e.g., Kelian, and Mt Muro, Indonesia; Porgera and Mt Kare, Papua New Guinea).

i) Examples

1. Kelian, Kalimantan, Indonesia

The Kelian mine (5.7 M oz Au), occurs within a linear zone of gold occurrences in Kalimantan, Indonesia (van Leeuwen et al., 1990; Fig. 7.18). The position of this zone at the southern portion of an arcuate belt of structures mapped by Pieters and Supritana (1990), and described as a magmatic arc by Carlile and Mitchell (1994), suggests that this linear zone or structure is a suture or terrain boundary, herein termed the Kalimantan suture. Individual gold deposits are localized at intersections of transfer structures.

The following discussion of Kelian is taken from van Leeuwen et al. (1990), T. Leach (unpubl. reports, 1988-1992), and G. Corbett (unpubl. reports, 1993-1995).

Structure
Kelian occurs within a pull-apart basin, formed as a jog by the dextral rotation on NS structures, during a relaxation in orthogonal convergence to localized extension (Fig. 7.18). The NS structures (e.g., West Prampus fault) and NE structures (Burung fault) acted as basin-bounding structures during the filling of the pull-apart basin with felsic tuffs and epiclastic sediments (Figs. 7.18, 7.19). Local growth faults characterise active sedimentation with basin formation, and rounded quartz pebbles are indicative of a distal sedimentary source. Folded basement carbonaceous shale and sandstone units crop out outside the pull-apart basin (Fig. 7.19). Pre-mineral andesite stocks intrude the tuff/epiclastic sequence and display brecciated and altered contacts. The central andesite forms a lopolith shape while apotheoses of some andesites do not crop out (Figs. 7.19, 7.20). Rhyolite dykes and fluidized muddy breccias which transect the andesite, are indicative of later felsic magmatism with which most of the gold mineralization is associated. The permeable tuff/epiclastic rocks have undergone intense pre-mineral alteration to form competent rocks for later fracture and breccia development.

Continued activation of the structural environment in which the pull-apart basin formed resulted in the development of a series of NE-trending faults and ore-hosting sheeted veins and open space breccias. The sheeted veins are sulfide-rich and at depth are inferred to have acted as feeder structures. Tension vein/breccias formed as high angle dilatant zones between the generally east dipping sheeted fractures, on which slickensides are indicative of normal and strike-slip movement. At high levels the sheeted veins form open space breccias, which are generally filled with sulfides and later carbonate (Fig. 7.19).

Fluidized muddy breccias (van Leeuwen et al., 1990) form part of diatreme/maar volcano complexes (Sillitoe, 1994). The Runcing, Burung and Tepu diatremes form major bodies (Fig. 7.19), while smaller dike-like fluidized injection breccias are common, and overprinting breccia relations are also recognised. Vertical zonations comprise; upper collapse portions of milled carbonaceous shale and lesser introduced fragments such as rhyolite, deeper levels in which the locally derived tuff and lesser andesite fragments predominate over carbonaceous shale, and deepest drill intercepts in which the rhyolite component is well developed. Degrees of rounding vary, with soft yet angular locally derived shale juxtaposed against competent rhyolite which has been milled during more extensive transport. The Runcing diatreme appears to be least eroded and contains features commonly associated with the upper portions of diatremes, (eg. base surge deposits and bedded accretionary

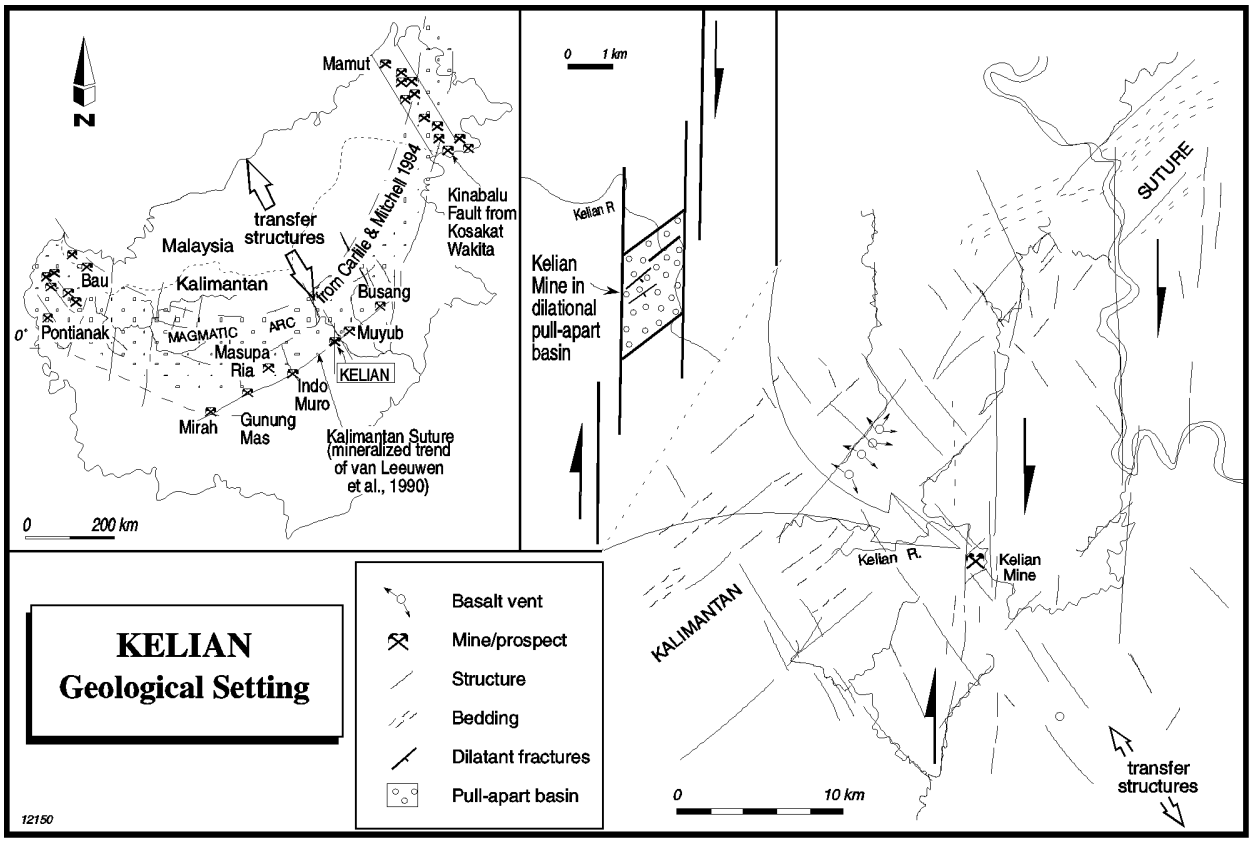

FIG. 7.18

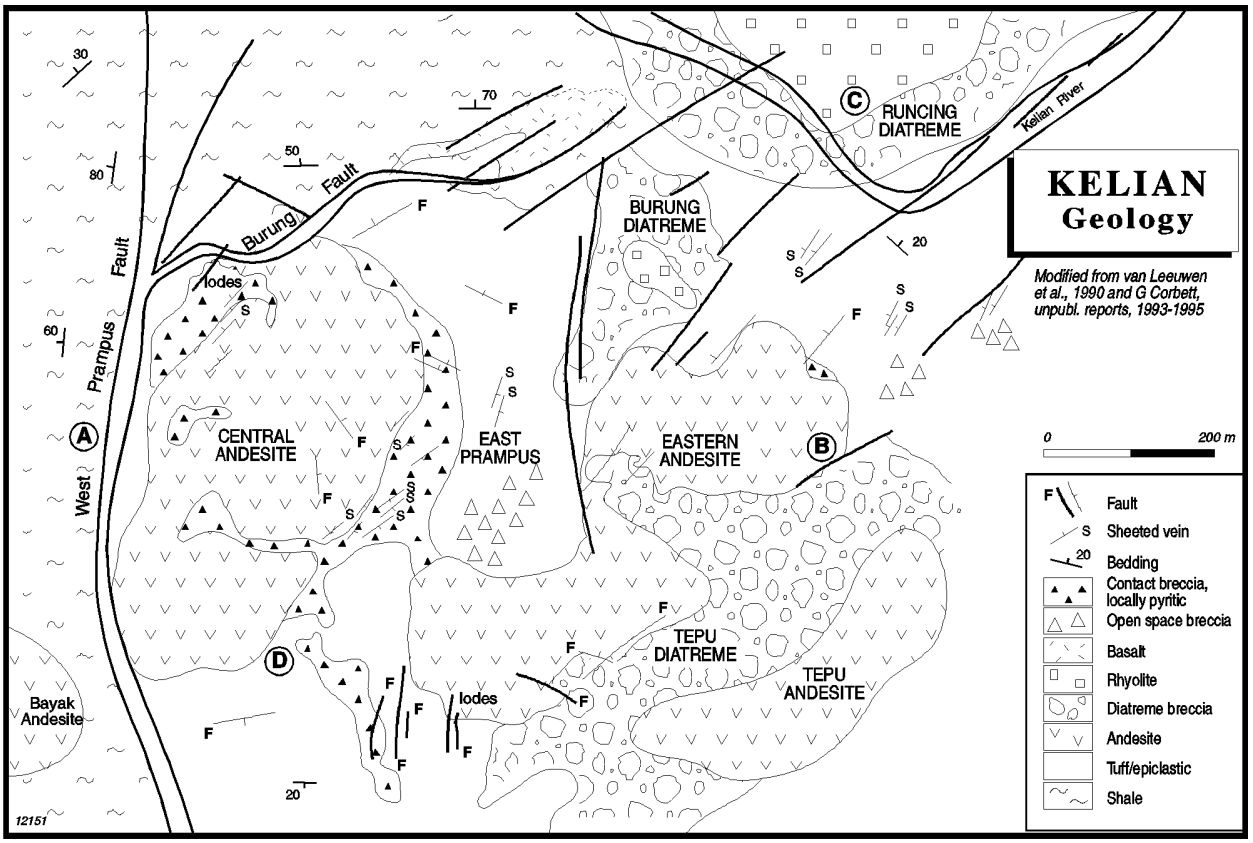

FIG. 7.19

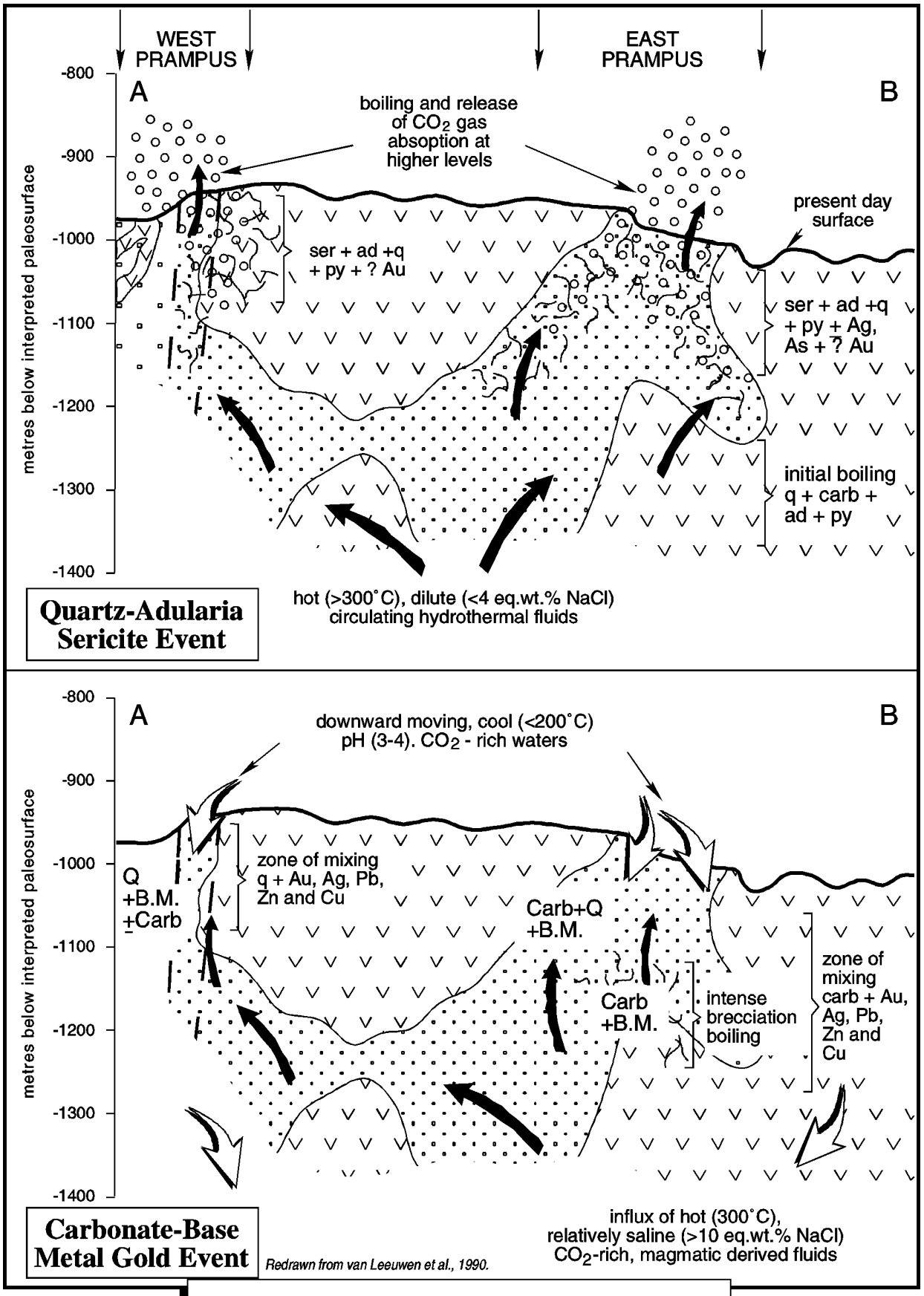

1334

East-West Fluid Flow Vectors and Associated Mineralization at Kelian

FIG. 7.20

apilli), which have probably collapsed to lower levels, given the inferred level of erosion (below). An endogenous dome of rhyolite intrudes this diatreme. While the upper level incompetent muddy breccias, comprised of milled and clay altered carbonaceous shale, do not fracture to host mineralization, deeper levels locally host fracture or breccia fill.

Hydrothermal injection breccias are apparent as a means of introduction of mainly Fe sulfide species, and display decreasing sulfide contents, from fluidized to crackle breccias grading away from feeder structures or the pyrite flooded contact breccias.

Alteration and mineralization

Two main episodes of hydrothermal activity have been recognised at Kelian (Fig. 7.20). The tuff/epiclastic sequence and shattered contacts of andesite intrusions display Stage I quartz-adularia-sericite + calcite and intense phyllic (quartz-sericite + adularia) alteration. Chlorite-carbonate + epidote alteration occurs in the less permeable cores of the andesite intrusions. Adularia is recognised at depth, whereas sericite dominates at shallow levels, and persists in the later alteration. Fluid inclusion analyses on quartz and carbonate suggest that the fluids were periodically boiling at mesothermal (280-350°C) temperatures, and were relatively dilute (< 4 equiv. wt % NaCl) during this stage of hydrothermal activity (Fig. 7.20).

Early fractures and breccias were reactivated during Stage II hydrothermal alteration characterized by deposition of carbonates + quartz and associated base metal and gold mineralization. Localized boiling (indicated by bladed carbonate), and associated brecciation of earlier veins, took place in the vicinity of the blind andesite intrusions and in sheeted fractures in the epiclastic/pyroclastic rocks (Fig. 7.20). The zonation from: carbonate, to carbonate + quartz, and to quartz (locally colloform banded) + carbonate, is indicative of cooling and degassing of the fluid migrating westward and towards shallower levels.

Gold occurs either as inclusions in base metal and iron sulfides, intergrown with mixed element (Mn, Fe, Ca, Mg) carbonates, or filling fractures and cavities in earlier quartz veins and breccias. Gold fineness ranges from 640-950, with an average of 750, typical of carbonate-base metal gold deposits (Fig. 4.8). Fluid inclusion analyses on sphalerites and mixed element carbonates (Fig. 7.16), indicate that this later phase of activity occurred under a similar mesothermal (270-330°C), but more saline (5 to >10 wt % NaCl) environment, than the earlier quartz. The fluid inclusion data indicate that a depth of 500-1000 m below the paleo-water table is exposed by erosion.

Carbonate species are characteristically zoned with depth, and this is best displayed at the northern end of the deposit (Fig. 7.21). Iron (siderite) and manganese (rhodochrosite) carbonates are encountered at shallow levels, whereas magnesium-calcium (dolomite) carbonate persists at depth. Multi-element carbonates (kutnahorite, Mg-Mn-Ca-Fe) are encountered at intermediate depths, where mixing of hot, upwelling Ca-Mg- rich and cool, descending Fe- Mn- rich fluids occurred. This zone of mixing typically delineates the regions of economic gold mineralization. Sphalerite is Fe-poor at shallow levels and in the south, and progressively increases in Fe-content to marmatitic sphalerite at depth and to the northeast.

Hotter conditions at the northern portion of Kelian are apparent in the progression from Fe-Mn carbonates at shallow levels, to Ca-Mg carbonates and pyrrhotite at depth (Fig. 7.21). The local intergrowth of pyrrhotite with magnetite, and change to more Fe-rich sphalerite at depth to the north, are indicative of reducing conditions proximal to an inferred intrusion source. Broad carbonate zonations to the south indicate that progressive mixing and resultant low grade mineralization occurred, whereas telescoped narrow carbonate zones to the north are indicative of rapid quenching of the hot upwelling fluids, and host local high grade gold mineralization. Bent and deformed bladed Mn-rich carbonates in these high grade zones are interpreted to reflect rapid quenching of boiling two phase fluids. Thus at Kelian, alteration styles provide indications of the direction of fluid flow from an inferred magmatic source and assist in the identification of local higher grade zones.

2. Porgera, Papua New Guinea

The Porgera gold mine (contained gold >14 M oz) comprises two mineralized systems: the carbonate-base metal gold deposit mined in the Waruwari open pit, and the epithermal quartz gold-silver mineralization which is extracted mainly from the Zone VII underground mining operation (although locally also present in the open pit; Corbett et al., 1995). Exploration progressed from initial panning of gold downstream by the first Government patrols into the district in 1938, to subsequent alluvial miners, then the evaluation of the bulk low grade potential at Waruwari proceeded during the 1970's, stimulated by the increase in gold price in 1980, and the discovery of the Zone VII high grade in 1983 (Henry, 1988). Production from the underground mine began in 1990 and the open pit in 1992.

The following discussion is mainly taken from Corbett et al., (1995), Fleming et al. (1986), Handley and Henry (1990), Richards (1990), and Richards and Kerrich (1993).

Structure

The Porgera Intrusion Complex (PIC) has been emplaced into locally calcareous shales of the Chim Formation shelf sediments (Davies, 1983) which form part of the uplifted melange of the New Guinea Orogen (Rogerson et al., 1987). Emplacement of the PIC at 6 Ma (Richards and McDougall, 1990), was localized by the intersection of the NNE arc normal Porgera transfer structure (PTS), with WNW arc parallel structures (Figs. 3.4, 7.22; Corbett, 1994; Corbett et al., 1995). One such arc parallel structure to the west of Porgera, evident on the Wabag 1:250,000 geological map (Davies, 1983) and landsat imagery, was mapped by Porgera Joint Venture geologists as a prominent shear (Fig 7.22, Corbett et al., 1995). Transfer structures separate segments of the subducting plate (Fig. 3.3), and are interpreted by Hill (1990) to locally facilitate a dextral rotation of the accretionary prism. Accretionary structures display a change in orientation across the PTS from normal to the transfer structure, and WNW on the western side of the PTS, to NNW to the east (Fig. 7.22). A set of ENE trending structures formed normal to the rotated eastern portion of the accretionary prism are termed accretionary joints (Corbett et al., 1995), and host mineralization (below). The PTS also localizes the Mt Kare intrusion system 15 km SW of Porgera (Corbett 1994; Fig. 7.22).

Gold mineralization is intimately related to the PIC (Richards and Kerrich, 1993), which comprises stocks and dikes of porphyritic hornblende and augite-hornblende diorite, locally containing olivine, and later more calc-alkaline sills and dikes of andesite, and late stage feldspar porphyry (Fig 7.23). The outcropping intrusions are inferred to represent apophyses which radiate from a central feeder, and cap a deeply buried magma evident as a prominent aeromagnetic anomaly (Fig. 7.23, Corbett et al. 1995). A feeder stock in the centre of the PIC, is inferred from the magnetic data, to link the magnetic feature at depth, with the outcropping sill and stock-like intrusions (Fig. 7.23). The Waruwari intrusions do not have a proximal magnetic root and so may have been detached from the original position prior to mineralization. Later cross-cutting feldspar porphyry bodies are inferred to have been derived from the same differentiating intrusion complex as the gold-bearing magmatic fluids. The upper portion of the PIC appears to be tilted to expose the southern edge where sill-like intrusions define scarp-slopes, and north dipping dip-slopes are locally capped by baked sediment (e.g., Peruk, Fig. 7.23; G. Corbett, unpubl. map, 1980).

The structural elements of Porgera (Figs. 7.23, 7.24; Corbett et al., 1995), include:

* NNE trending fractures evident as landsat and air photo lineaments represent the continuation of the deep crustal Porgera transfer structure through the cover of folded and thrusted sediments. Some fractures have

been mapped as shears in the mine area and much of the early carbonate-base metal gold mineralization

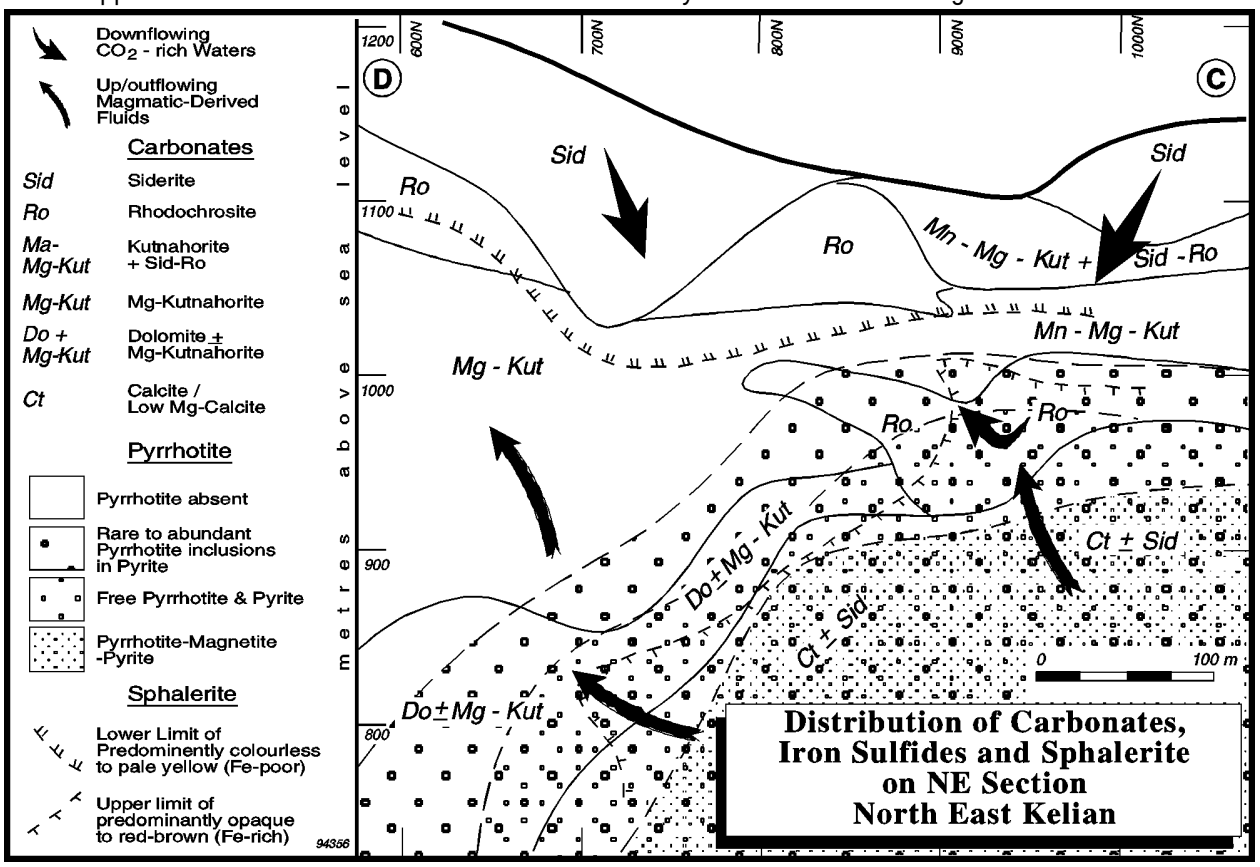

FIG. 7.21

appears to be hosted within NNE fractures which also appear to localize the emplacement of the later stage feldspar porphyry stocks.

* ENE trending accretionary joint structures, which include the Roamane and parallel faults, are inferred to have undergone dilation and some dextral strike slip movement by the regional dextral movement on the Porgera transfer structure (Fig. 7.23; Corbett, 1994). Local extension including dextral and normal fault movement on the Roamane fault provide important ore-hosting dilational environments for the epithermal quartz-roscoelite mineralization discussed in Section 7.iv.d.1. These are well developed as a jog in the Roamane fault and hanging wall splits which extend into the open pit (Fig. 7.24).

A feldspar porphyry emplaced at the intersection of a transfer structure and the Roamane fault, displays an inverted cone shape. The upper portion of the cone extends south to Waruwari Hill, as well as along the Roamane fault and into the hanging wall splits (Figs. 7.23, 7.24). A similar feldspar porphyry at Wangima is localized by a similar intersection and migrated into the ENE accretionary joint mapped (G. Corbett, unpubl. map, 1980) north of the Roamane fault.

Alteration and mineralization

The two styles of alteration, veins and mineralization at Porgera are interpreted by Corbett et al. (1995) to have been deposited from fluids which were sourced from the same melt as the late stage feldspar porphyry intrusions. The Stage I carbonate-base metal alteration, veins and gold mineralization, which are exploited in the open pit, are discussed below. The roscoelite-bearing epithermal quartz gold-silver system is described in a later section (7.iv.d.1).

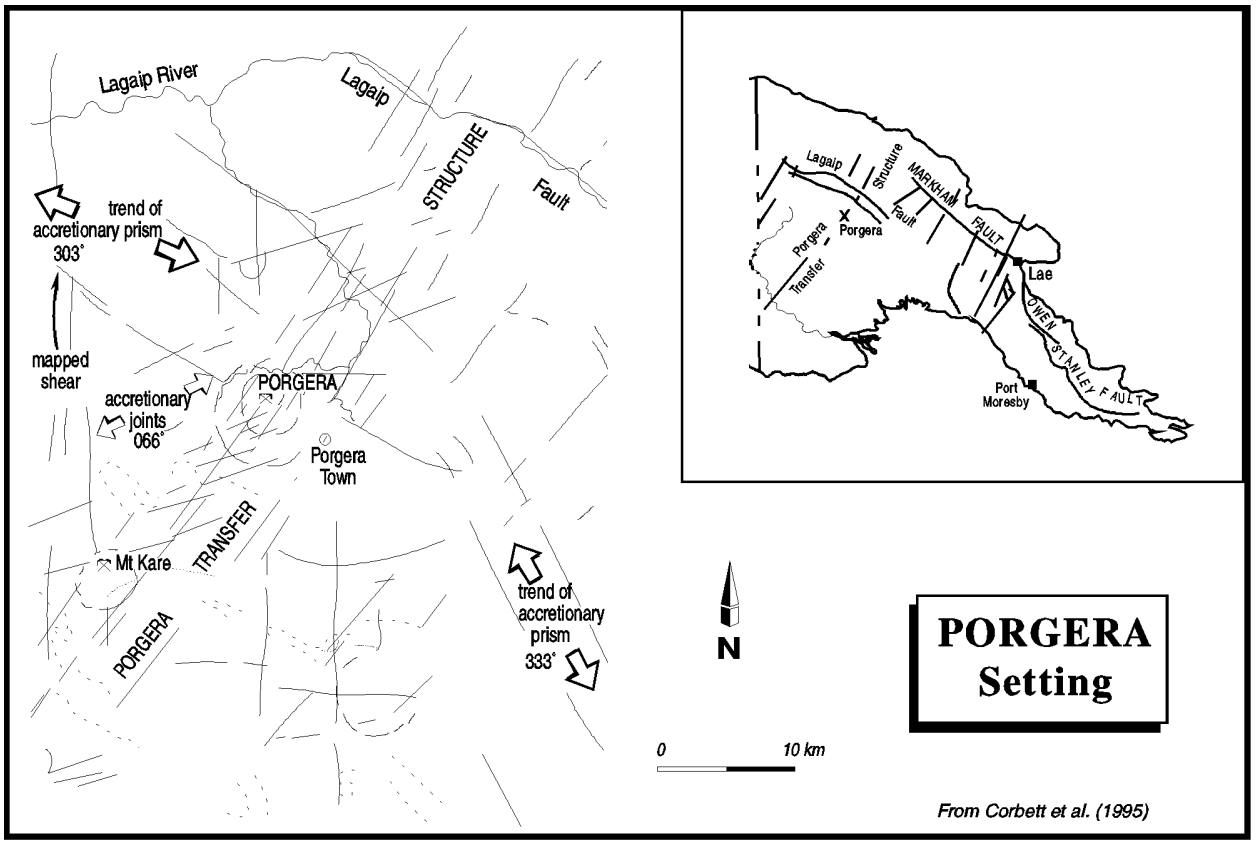

FIG. 7.22

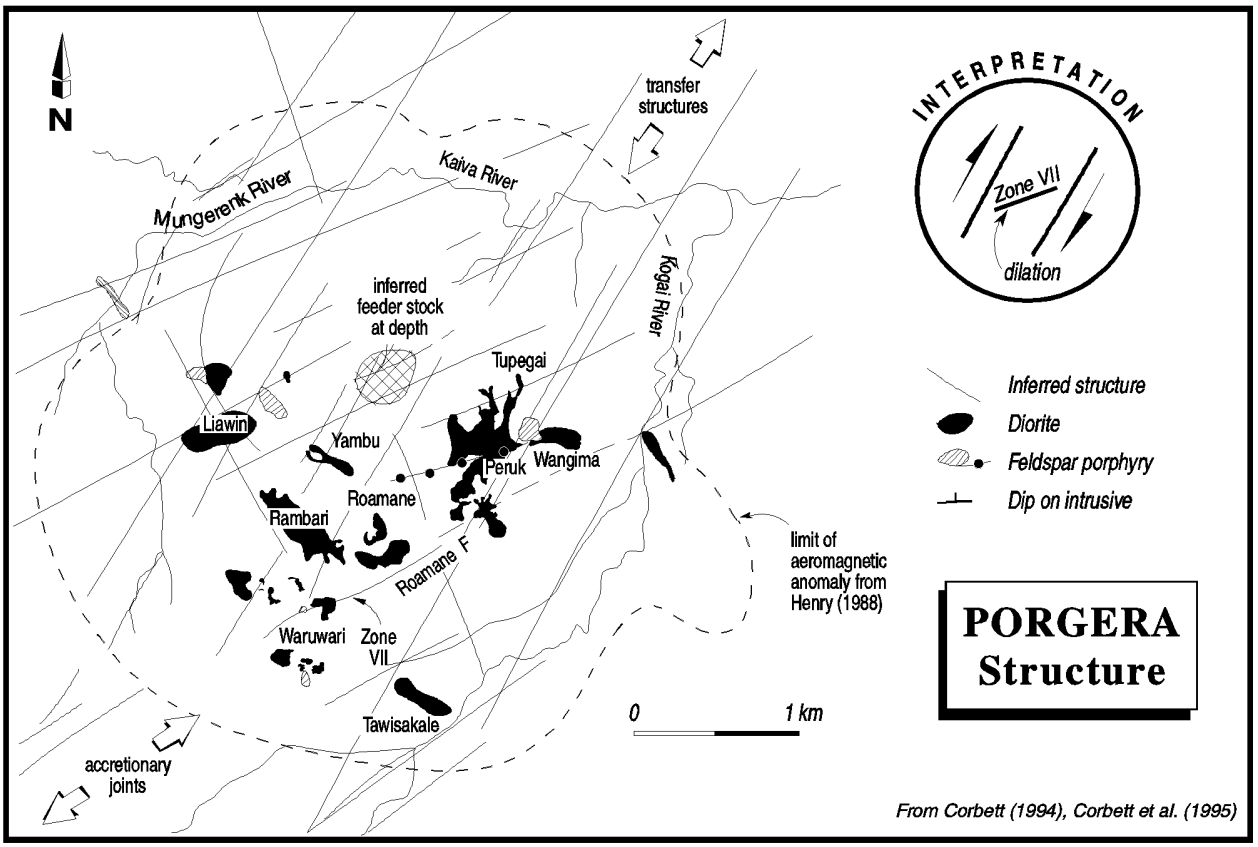

FIG. 7.23

Emplacement of the PIC into incompetent Chim Formation carbonaceous to calcareous sediments resulted in the formation of a zoned brittle contact alteration which extends up to 50-100 m from the intrusions (Figs. 7.24, 7.25). Subsequent fracturing of these brittle altered sediments provided permeability for later hydrothermal fluids, mainly in fractures formed by the PTS. Stage I alteration and mineralization occurred at deep epithermal to mesothermal levels and is characterized by early quartz-sericite alteration, followed by massive sulfide mineralization and late carbonate vein development (Fig. 7.26). Fluid inclusion data (Richards and Kerrich, 1993) reflects cooling from early quartz (average Th approx. 318°C) to later sphalerite (average Th approx. 273°C). These veins equate to the type A and B ores of Fleming et al. (1986). The sequence of sulfide mineralization is described as: pyrite --> sphalerite --> galena --> chalcopyrite/tennantite, and continued into the phase of carbonate deposition. Gold occurs as minute (typically >20-40 micron) inclusions in sulfides, and locally occurs as free gold in carbonate. Gold fineness (average 670, Fig. 4.8) is low for a carbonate-base metal system and decreases progressively during later mineral deposition. This is indicative of cooling during the deposition of Stage I veins, as supported by the above fluid inclusion data (Richards and Kerrich, 1993). Submicroscopic gold is inferred to be associated with localized early pyrite-arsenopyrite mineralization and represents the type C ore of Fleming et al. (1986).

Changes in carbonate and sphalerite composition delineate fluid pathways during Stage I alteration and mineralization. The Fe content of sphalerites, reflected in colour changes from dark red, red-yellow to yellow, declines from north to south (Fig. 7.27). This zonation is interpreted to indicate higher temperatures and a greater magmatic-component (Section 7.iii.g) of Stage I fluids to the north and east of Rambari-Waruwari. This is supported by the occurrence of pyrrhotite in the Jez Lode, northern Rambari (Fig. 7.24). Copper minerals are rare, however significant chalcopyrite + magnetite mineralization at depth and to the north are also indicative of a magmatic source for Stage I fluids in this vicinity.

Carbonates are zoned from: Mn- and Fe-rich (rhodochrosite + siderite, with hypogene hematite) at shallow levels (and locally deep in major structures), through transitional Ca-Mn-Fe-Mg-rich phases (early ankerite, and late dolomite) at intermediate levels, to Ca + Mg-species (calcite and dolomite) at depth and to the north (Fig. 7.27). This zonation in carbonates is interpreted to reflect the descent of cool, oxygenated, possibly bicarbonate fluids down major structures during Stage I activity. Carbon and oxygen isotope data for Stage I carbonates (Richards and Kerrich, 1993) support the model of progressive mixing of magmatic and meteoric waters to produce the observed zonation in carbonate species. Late Stage I calcite and dolomite are in close isotopic equilibrium with host calcareous sediments (Richards and Kerrich, 1993), and are interpreted to have been deposited from surficial bicarbonate waters which have descended, upon waning of Stage I activity, into available open structures.

It is therefore interpreted that Stage I mineralized magmatic fluids have migrated south and west, from the inferred feeder stock (Fig. 7.24), via the NE-trending transfer structures. These fluids are thought to have been cooled and diluted by meteoric waters and to produce the low grade gold mineralization associated with the carbonate-base metal veins and breccia fill. Quenching in cross-cutting structures by cool, oxidizing CO_2-rich waters facilitated the formation of localized higher gold grade. The occurrence of abundant chalcopyrite at depth beneath the East Zone at Roamane, implies that there has also been localized migration of mineralized fluids, from the magmatic source, south along a major NNE-trending structure in that vicinity (Figs. 7.26, 7.27).

The later quartz-roscoelite event of gold mineralization is discussed in Section 7.iv.d.1.i.

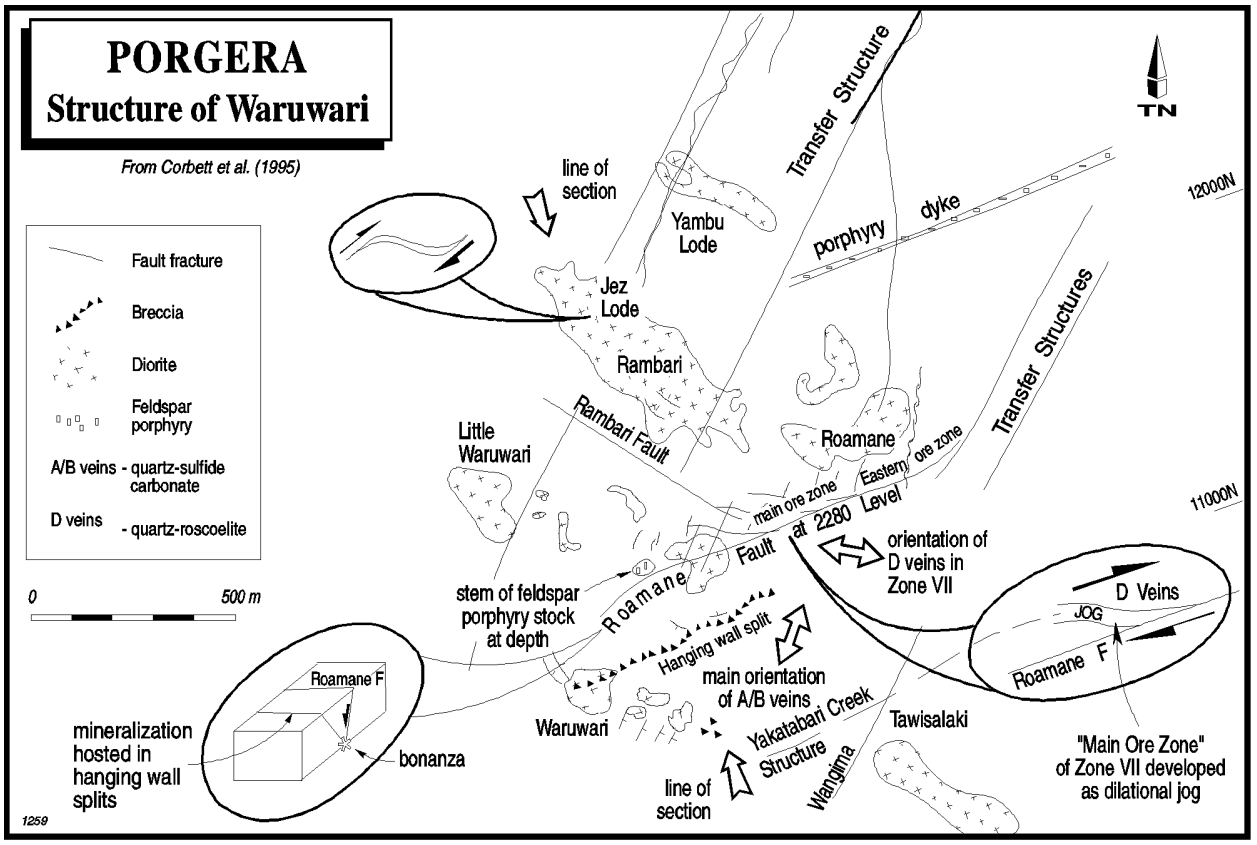

FIG. 7.24

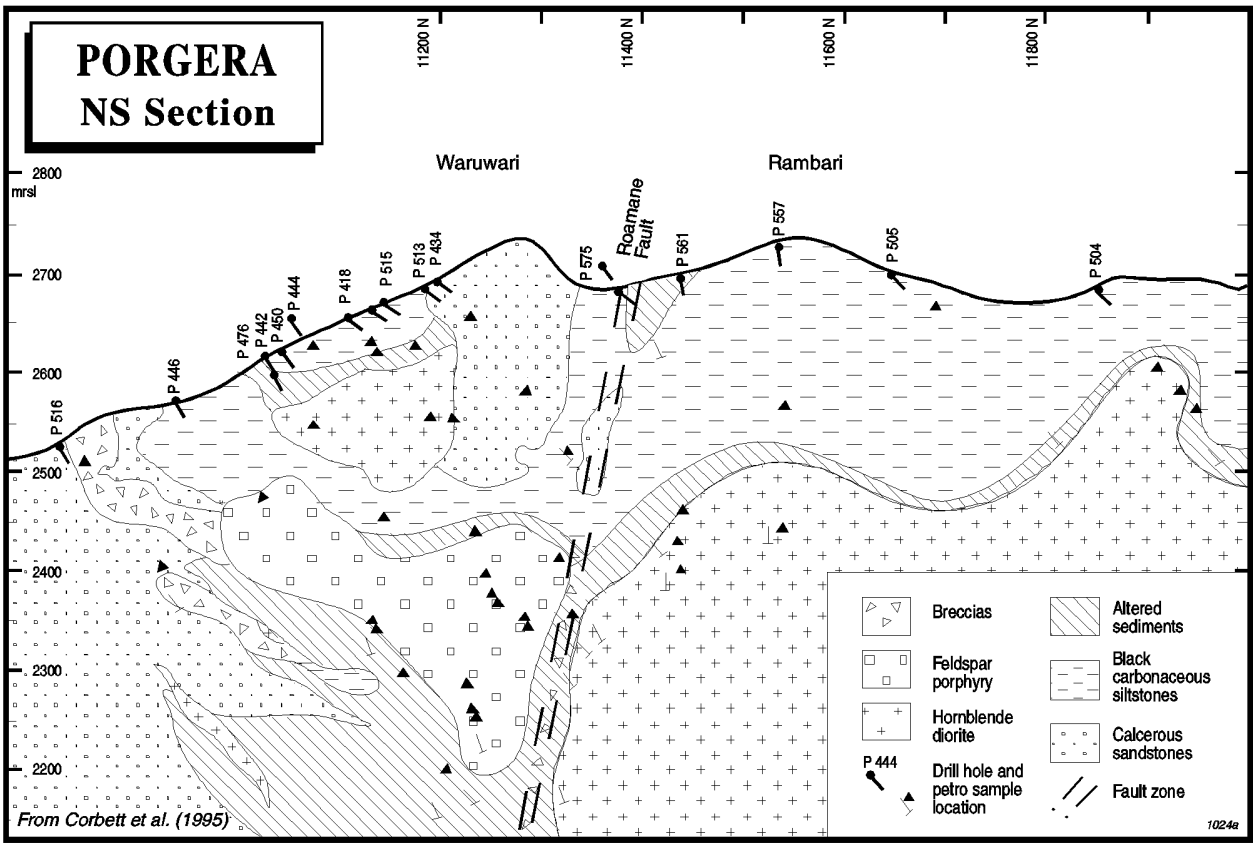

FIG. 7.25

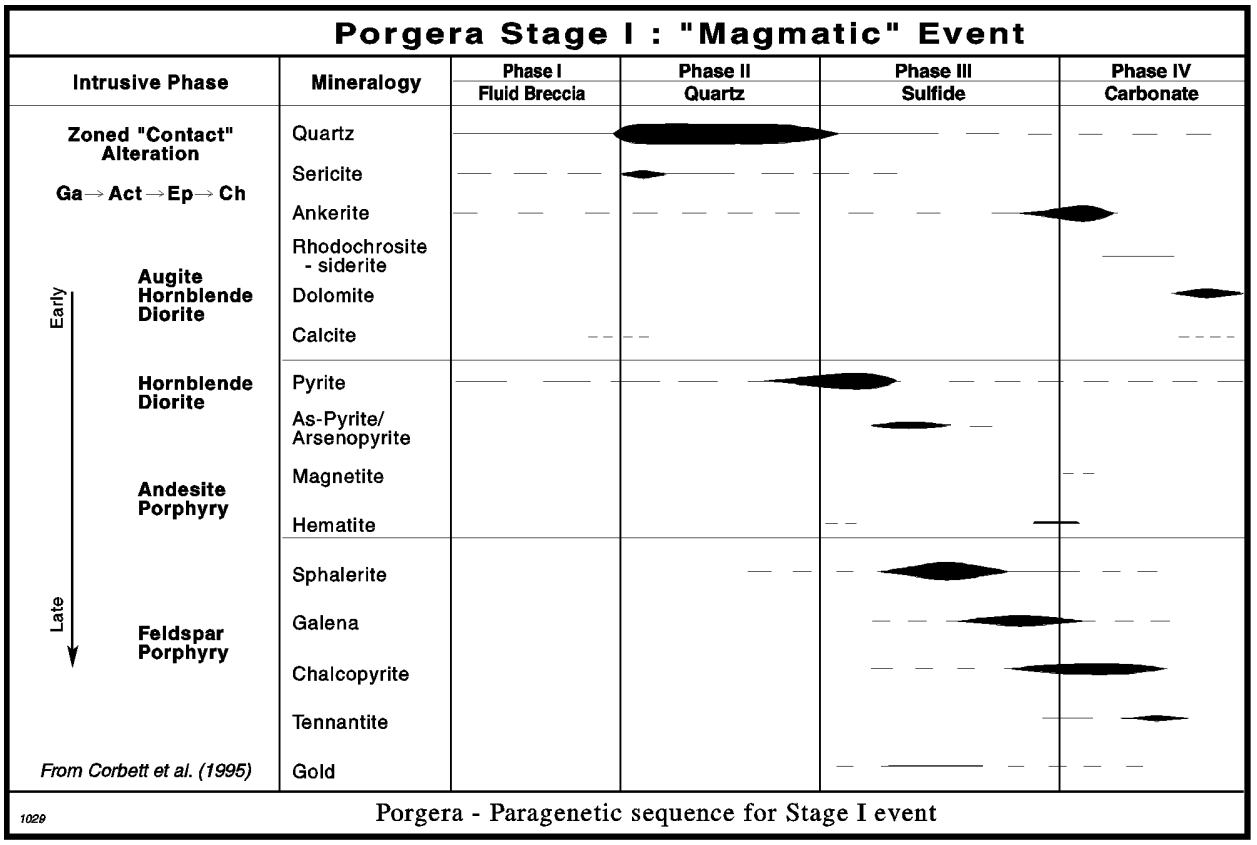

FIG. 7.26

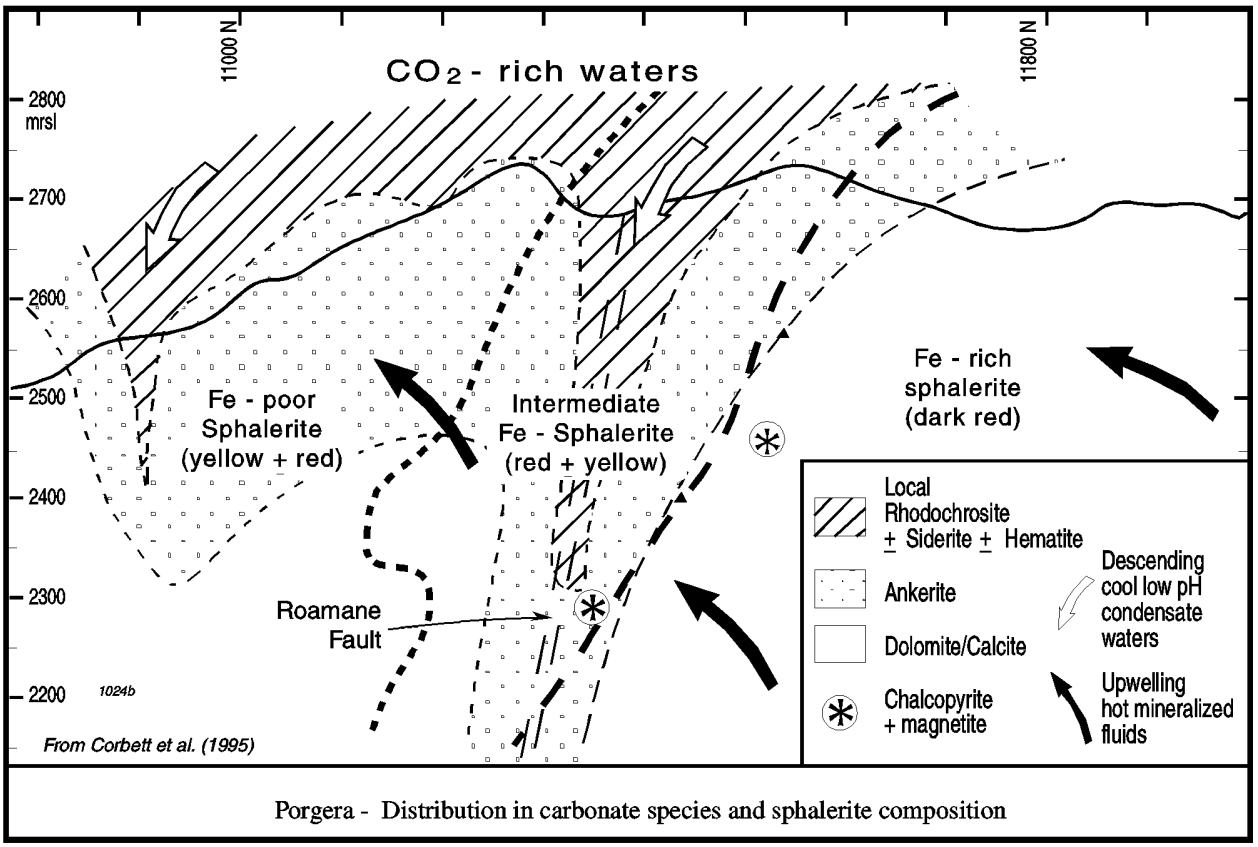

FIG. 7.27

3. Morobe Goldfield, Papua New Guinea

The Morobe Goldfield (Figs. 7.28, 7.29) produced some 3.7 million oz of gold from alluvial and hard rock mining operations between 1926 and 1977 (Lowenstein, 1982), and still contains substantial gold reserves at: Kerimenge (1.8 M oz Au, Hutton et al., 1990), Hidden Valley (2.4 M oz Au, Pascoe, 1991), and Hamata, (1.3 M oz Au, Wells and Young, 1991). Hard rock gold mineralization in the Morobe Goldfield ranges from quartz-sulfide gold ± copper systems at mesothermal levels at Hamata and Kerimenge, to carbonate-base metal gold style systems at mesothermal to epithermal levels at Upper Ridges, Edie Creek, Hidden Valley, and localized epithermal quartz gold-silver mineralization at higher elevations at Kerimenge (Fig. 7.29). The quartz-sulfide gold mineralization at Hamata has been discussed previously (Section 7.ii.d).

Structural setting

The Morobe Goldfield is hosted in the Bulolo graben (Fig. 7.28), an intra-arc rift formed by activation of structures described by Dekker et al. (1990) as Mesozoic basement transfer structures (Corbett, 1994). Basement rocks comprise schist and phyllite of the Cretaceous Kaindi (regionally Owen Stanley) Metamorphics into which the Mid Miocene Morobe Granodiorite has been emplaced (Lowenstein, 1982). Pliocene volcanoplutonism occurred in the Bulolo graben environment of extensional tectonism and crustal thinning as Edie Porphyry flow dome complexes and Bulolo Agglomerate (Dow et al., 1974) extrusive equivalents (Fig. 7.28). Otibanda Formation lacustrine sediments obscure the volcanic and basement rocks in the northern portion of the graben.

Much of the gold mineralization within the Bulolo graben is localized by graben-bounding and intra-graben structures, but occurs in smaller subsidiary structures (Fig. 7.28). Gold mineralization in the hanging wall of the Escarpment fault at Golden Ridges and Upper Ridges, Wau, is described by Sillitoe et al. (1984) as associated with a maar/diatreme complex, although alternative explanations are possible (below). The Ribroaster mine occurs at the intersection of a transfer structure and the Escarpment fault (Fig. 7.28). Corridors of NS fractures appear to localize ore at Edie Creek, Kerimenge and Hidden Valley. The Hamata and Hidden Valley deposits are hosted in competent basement rocks in hanging wall settings to the Upper Watut graben-bounding structure. At Kerimenge, tensional vein/breccias in the hanging wall of the steeply dipping Kerimenge fault, adjacent to the intersection with a maar volcano/diatreme complex, are inferred to have formed by dilation associated with movement on that structure (G. Corbett, unpubl. report, 1985).

Edie Creek

Edie Creek gold mineralization occurs in a 3 km long NW trending corridor of sigmoidal, en echelon lodes (Lowenstein, 1982), formed adjacent to the Nauti diatreme. The lodes display sigmoidal shapes indicative of a formation by deformation of pre-existing NW-trending fractures during sinistral strike-slip movement on the corridor of prominent NS structures, resulting from the extension on the NNW graben structures (Fig. 7.28; Corbett, 1994; Neale et al., in prep). Exposures within Nauti Creek provide a 600 m vertical section through the 5 km long Nauti diatreme. At the more deeply eroded central portion, cobble breccias contain rounded fresh porphyry boulders to several metres across, set in an illite-pyrite altered matrix, and grade towards the southeast at higher elevations, to bedding tuff ring deposits which resemble the Namie Breccia, Wau, described by Sillitoe et al. (1984). Fractured basement rocks exposed by the erosion of Webiak Creek through the tuff ring are worked by small scale miners for gold. The tuff ring partly obscures the Enterprise vein at the NW end of the Edie Creek vein system. Some of the cobble breccias in the western portion of the diatreme could be transitional to conglomerate units.

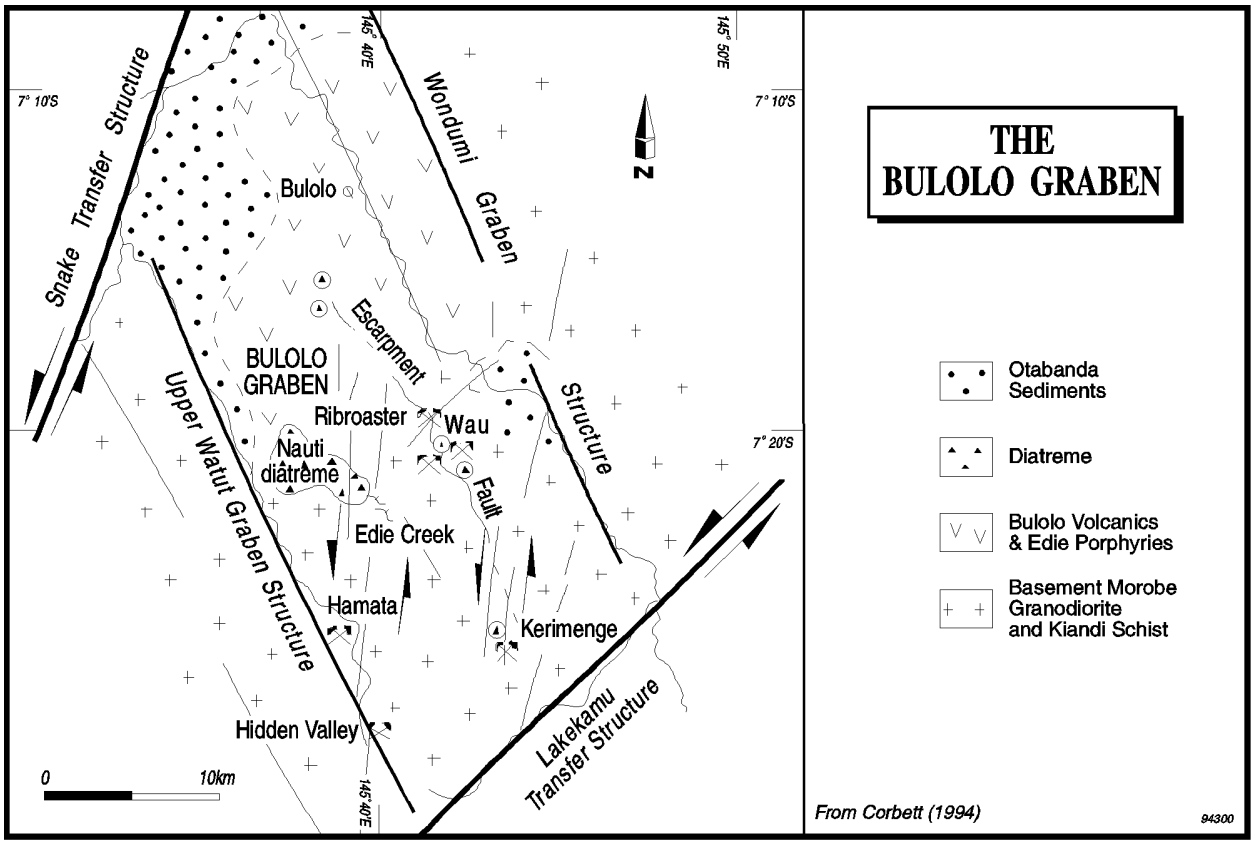

FIG. 7.28

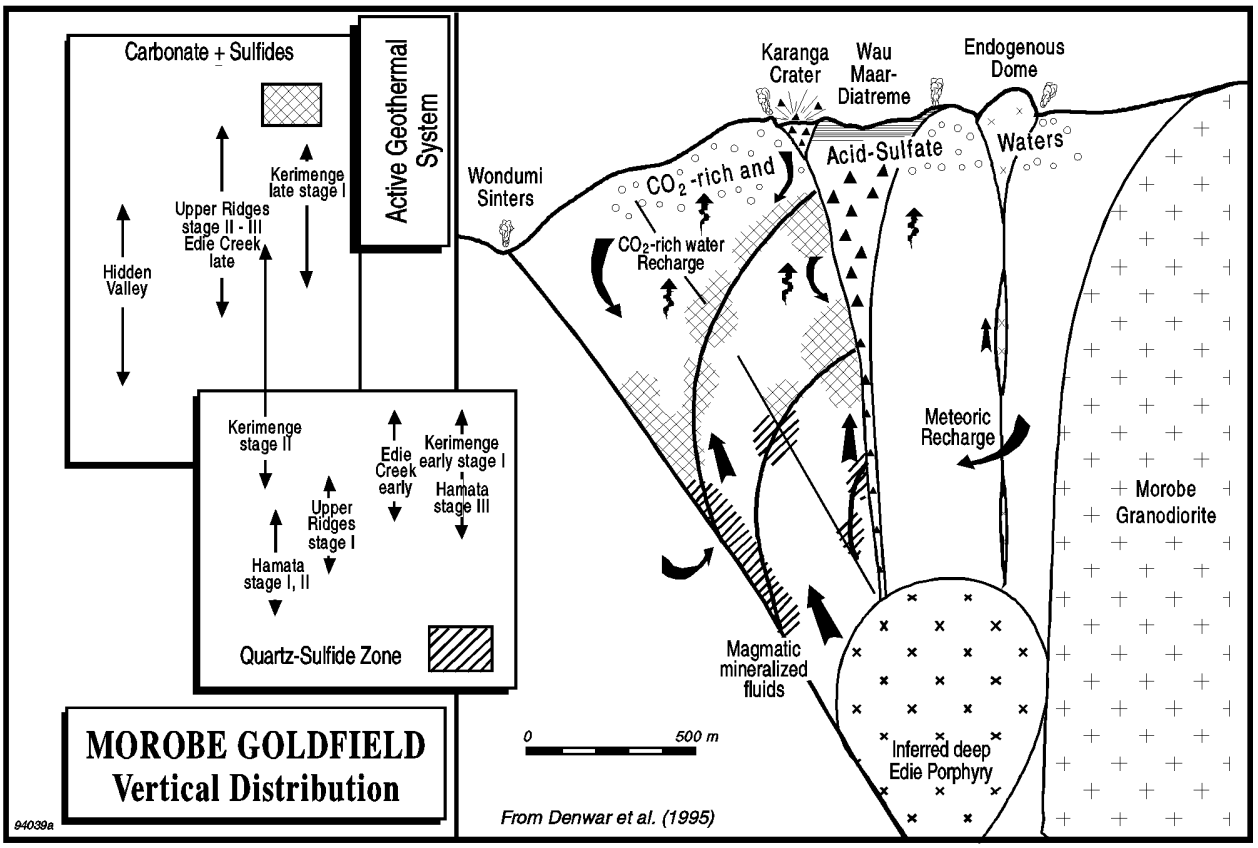

FIG. 7.29

Vertical and horizontal zonation in the vein/lode mineralogy, moving SE away from the diatreme margin, are consistent with the progression from deeper to shallow levels in other carbonate-base metal gold systems. Within the belt of lodes, Lowenstein (1982) records a change in vein types from the NW to SE, moving away from the diatreme margin. At the Enterprise working in the northwest, quartz-pyrite-arsenopyrite occurs at depth, with increased carbonate at higher levels, and a further increase in carbonate in the central portion of the vein system. Carbonate-dominant mineralization occurs at the Day Dawn South mine and further to the SE, distal to the Nauti diatreme margin, at the Midas workings, rich gold grades occur in association with late crystalline quartz within weathered manganese oxide ore (Lowenstein, 1982), and with quartz on fractures at the Nui Pungor's workings (G. Corbett, pers. observation, 1996). Gold and silver show strong positive correlations with manganese (after manganocarbonate) with some of the highest gold grades contained within the crustiform banded Edie Lodes. Lowenstein (1982) recognised a paragenetic sequence at the Karuka mine of: quartz-pyrite --> base metal sulfides --> carbonate + Ag- sulfosalts/sulfides, in banded manganocarbonate veins. This sequence of deposition is characteristic of shallow level carbonate-base metal gold systems. Gold is commonly associated with the base metal sulfides and carbonate. The multiple deformation and mineralization, as seen in the polyphasal banding, is consistent with the sigmoidal shaped lodes having developed as tension gash features.

Wau

Gold mineralization at the Upper Ridges open pit, Wau, is hosted in banded quartz-carbonate-base metal veins which cross-cut Namie Breccia. These rocks are described by Sillitoe et al. (1984) as diatreme tuff ring debris which have slid as allochthonous blocks down the Escarpment fault, and in the case of the Davidsons and Golden Peaks, into the Wau maar volcano/diatreme breccia. Recent mining has created additional exposures which favour a model (Denwer et al., 1995; Fig. 7.30) in which the Namie Breccias are derived from an earlier phreatomagmatic event, possibly emplaced along the Escarpment fault, which also localized the gold mineralization. The younger Wau maar volcano/diatreme breccia displays only minor erosion (below and Sillitoe et al., 1984), whereas the Upper Ridges mineralization formed at considerable depth. The Namie Breccias (and lodes) are termed Davidsons Breccia where cut by later hydrothermal brecciation associated with dacite dike intrusion. Two main stages of alteration and mineralization recognised at Upper Ridges (Denwer et al., 1995; T. Leach, unpubl. reports) are:

Stage I: Quartz-sericite-pyrite alteration and vein development is followed by deposition of massive Fe-rich (marmatitic) sphalerite + galena. Fluid inclusion analyses indicate that the quartz was deposited over a wide temperature range (210-390°C) and from dilute (<1 wt % NaCl) to hypersaline (>25 wt % NaCl) fluids (Syka, 1985; Denwer et al., 1995). The veins display anomalous bismuth-tellurium, and gold occurs as inclusions in pyrite with an average fineness of 613. The presence of coarse sericite wall rock alteration and high fluid inclusion temperatures indicate that these veins formed in the breccias at depths of at least 500-1000 m below the paleosurface. These conditions are comparable to those in which quartz-sulfide auriferous veins at Ribroaster formed (Syka, 1985). Here, ore is localized at a higher elevation than the present position of Upper Ridges, at the intersection of a transfer structure with the Escarpment fault (Figs. 7.28, 7.29).

Stage II: Polyphasal carbonate-base metal-quartz veins grade from: early banded Mn-carbonate, through massive carbonate, to late quartz + carbonate. Minor pyrite, Fe-poor sphalerite, galena and chalcopyrite are intergrown with both carbonate and quartz. Traces of late stage tin-phases (canfieldite and stannite) overgrow the base metal sulfides. Low fineness gold (average 468) occurs as inclusions, with base metal sulfides, in pyrite. Stage II quartz and carbonate were deposited under much cooler conditions (198-220°C) than the early quartz-sulfide veins (Denwer et al., 1995; Syka, 1985).

The Wau maar volcano/diatreme breccia complex crops out as a 1.5 - 2 km wide circular feature rimmed by endogenous dacite domes and filled by epiclastic and pyroclastic material, at an elevation of about 400 m below

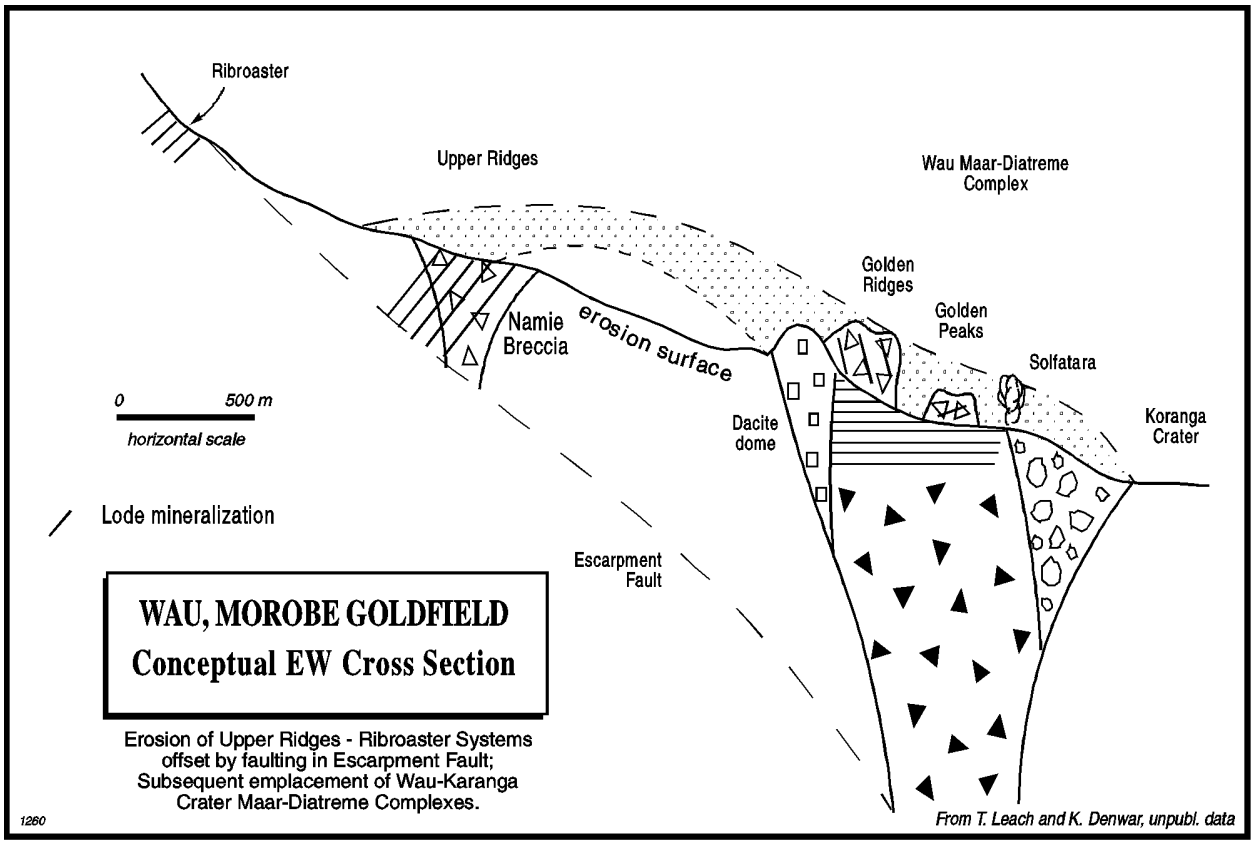

FIG. 7.30

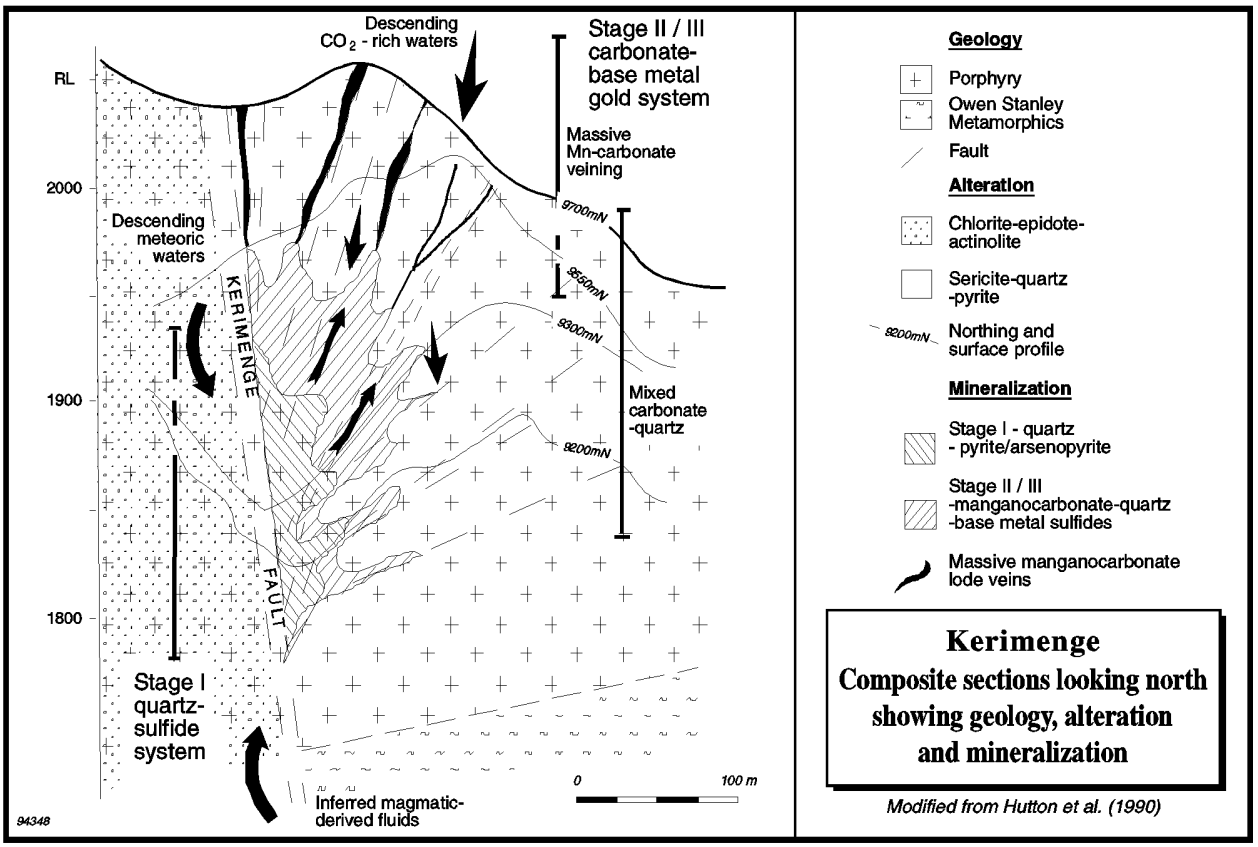

FIG. 7.31

Upper Ridges (Sillitoe et al., 1984). The presence of very low temperature smectite-kaolinite-cristobalite alteration, recent hydrothermal solfataras on the diatreme margins, and a reported historical hydrothermal eruption from Koranga Crater, all suggest that the Wau diatreme-maar complex is very recent. Silica sinters and travertine deposits aligned along the Wondumi graben structure (Fig. 7.28) also appear to be related to current geothermal activity in the Wau region.

It is therefore interpreted that hydrothermal activity at Wau occurred over a protracted period and that alteration and mineralization were focused along the Escarpment fault, and possibly related to emplacement of an Edie Porphyry at depth. Quartz-sulfide gold mineralization formed early and deep in the system, whereas carbonate-base metal style gold mineralization took place later, and possibly at shallower levels. The Escarpment fault may have facilitated emplacement of a young, high level Edie Porphyry, and led to the formation of the Wau maar volcano/diatreme complex and endogenous dacite domes. Ejecta on the margins of the Upper Ridges pit are inferred to have been erupted from the Wau diatreme and cover material derived from an older source (K. Denwer and T. Leach, unpubl. data). Namie-like milled matrix fluidized breccias occur along the Escarpment fault to the north and south of the Wau diatreme, and elsewhere in the region (e.g., Nauti tuff ring; Fig. 7.28). Large allochthonous blocks of quartz-carbonate-sulfide veined Namie Breccia (Golden Peaks and Upper Ridges) have slid into the Wau maar volcano-diatreme, possibly because of recent movements on the Escarpment fault.

Kerimenge

The Kerimenge prospect occurs along the eastern sides of, and within, the NS trending Kerimenge fault close to the intersection with a maar volcano/diatreme breccia (Fig. 7.28, G. Corbett, unpubl. map, 1985; Akiro, 1986). Fracturing at this structural intersection provided an important focus for fluids derived from an inferred porphyry source at depth. Ore-hosting NW trending and SW dipping vein/breccia zones, are inferred to have formed as hanging wall splits, by sinistral and normal movement on the Kerimenge fault (G. Corbett, unpubl. report, 1985; Corbett, 1994; Fig. 7.31). Best gold grades occur at the intersection of the fracture/veins and the controlling Kerimenge fault (Denwer et al., 1995; Hutton et al., 1990; Fig. 7.31).

Two main stages of hydrothermal activity have been recognised at Kerimenge (Fig. 7.31, Syka and Bloom, 1990; Denwer et al., 1995):
Stage I: Quartz-sulfide gold ± copper style low grade, refractory, gold mineralization occurs as:
* Early quartz-sericite-pyrite veins and locally intense silicification overprint zoned porphyry-related biotite/potassic and propylitic alteration.
* Arsenopyrite-pyrite-marcasite-quartz vein/breccias constitute the main event of gold mineralization (resource of 51 Mt at 1.0 g/t gold; Hutton et al., 1990), in which the gold is refractory.
* Late manganocarbonate-illitic clay-arsenopyrite/pyrite + base metal sulfides occur as several metre thick lodes and vein/breccia fill.

The quartz-sulfide veins developed from progressively cooling low temperature (145-240°C) and dilute (<3.3 wt % NaCl) fluids. Pre- or early-Stage I quartz contains daughter phases which indicate that the early fluids were under hypersaline porphyry-related conditions. The Stage I veins and alteration display zonations from deeper levels in the south grading to higher elevations further north as: quartz-sulfide, through quartz-manganocarbonate-illite/sericite at intermediate levels, to manganocarbonate lodes (Fig. 7.31).

Stage II: High grade, non-refractory mineralization co-exists with manganocarbonate veins and breccia fill, and comprises quartz-carbonate-sulfide deposition in dark bands alternating with manganocarbonate, sealing clasts of earlier manganocarbonate vein material in breccia. High fineness (average 837) gold is non-refractory and is associated with hessite, tennantite, chalcopyrite mineralization. Fluid inclusion data (Denwer et al., 1995) indicate that mineral deposition occurred in response to the mixing of cool (160-170°C) CO_2-rich waters related

to manganocarbonate deposition, and hot, but dilute (<2.1 wt % NaCl) upwelling fluids. Gold mineralization at Kerimenge has changed from a refractory quartz-sulfide gold ± copper style system early and at deep levels in the south prospect area, to a non-refractory quartz-carbonate-base metal sulfide deposition at shallow levels in the northern portion of the prospect, preserved from erosion at highest elevations.

Hidden Valley

The Hidden Valley deposit (2.4 M oz Au; Pascoe, 1991) occurs in a stockwork vein zone developed in the hanging wall of the north dipping Hidden Valley fault (Nelson et al., 1990), inferred to represent a continuation of the Upper Watut graben fault extending south from the Hamata deposit (Fig. 7.28). This hanging wall setting is similar to Wau and Kerimenge, and mineralization appears to be elongated along a NS cross structure (Nelson et al., 1990). Nelson (op cit) and co-workers describe the following paragenetic sequence of alteration and mineralization:

1. Quartz-pyrite, with chlorite, epidote.
2. Quartz-hematite-chlorite-pyrite; rare gold with arsenopyrite.
3. Carbonate with
    (a) quartz-adularia
    (b) base metal sulfides-gold-adularia
    (c) kutnahorite-gold-tetrahedrite

Veins containing early quartz-pyrite-arsenopyrite with rare gold are comparable to those in the early quartz-sulfide mineralization at Kerimenge. The sequence of quartz-adularia --> base metal sulfide-gold --> Mn/Mg-carbonate - gold is similar to Stage II/III base metal/carbonate alteration and mineralization recognised in other carbonate-base metal systems (Fig. 7.15).

4. Woodlark Island, Papua New Guinea

Gold was discovered at Woodlark Island, 300 km east to the mainland of Papua New Guinea, in 1895 (Stanley, 1912; Fig. 1.2). Gold production is recorded at 100,000 oz gold from lode, and 83,000 oz from alluvial workings, most of which occurred prior to World War II (McGee, 1978). Although recent coralline limestone deposits obscure much of the geology of Woodlark Island, an analysis of the aeromagnetic data suggests that a central horst block is transected by NW trending cross structures (Fig. 7.32), and may be tilted to the north. Most areas of gold mineralization occur within erosional inliers in the coralline cover (Fig. 7.32; Corbett et al., 1994a). The two main mining centres are at Kulumadau and Busai.

Busai

Between 1902 and 1916 the Murua United mine (known locally as the Busai Pit) produced about 3,500 ounces of gold at a grade of 4.3 g/t Au and with an average fineness of 771-846 (McGee, 1978). The Busai Pit lies at the intersection of a NS structure with a series of NW trending cross structures, which cut a horst block (Figs. 7.32, 7.33). Mineralization occurs in the hanging wall of the arcuate shaped NW-dipping Blue Lode shear. Demagnetisation of primary magnetite in the host Okiduse Volcanics is consistent with outcropping clay alteration (Fig. 7.32).

The bulk of the gold mineralization is hosted in carbonate vein/breccias within shallowly dipping tension gash zones, constrained between the steeply dipping NW structures (Figs. 7.34, 7.35). Carbonate vein/breccias also exploit the structures utilised by the milled matrix fluidized breccias. High grade lodes exploited by the early

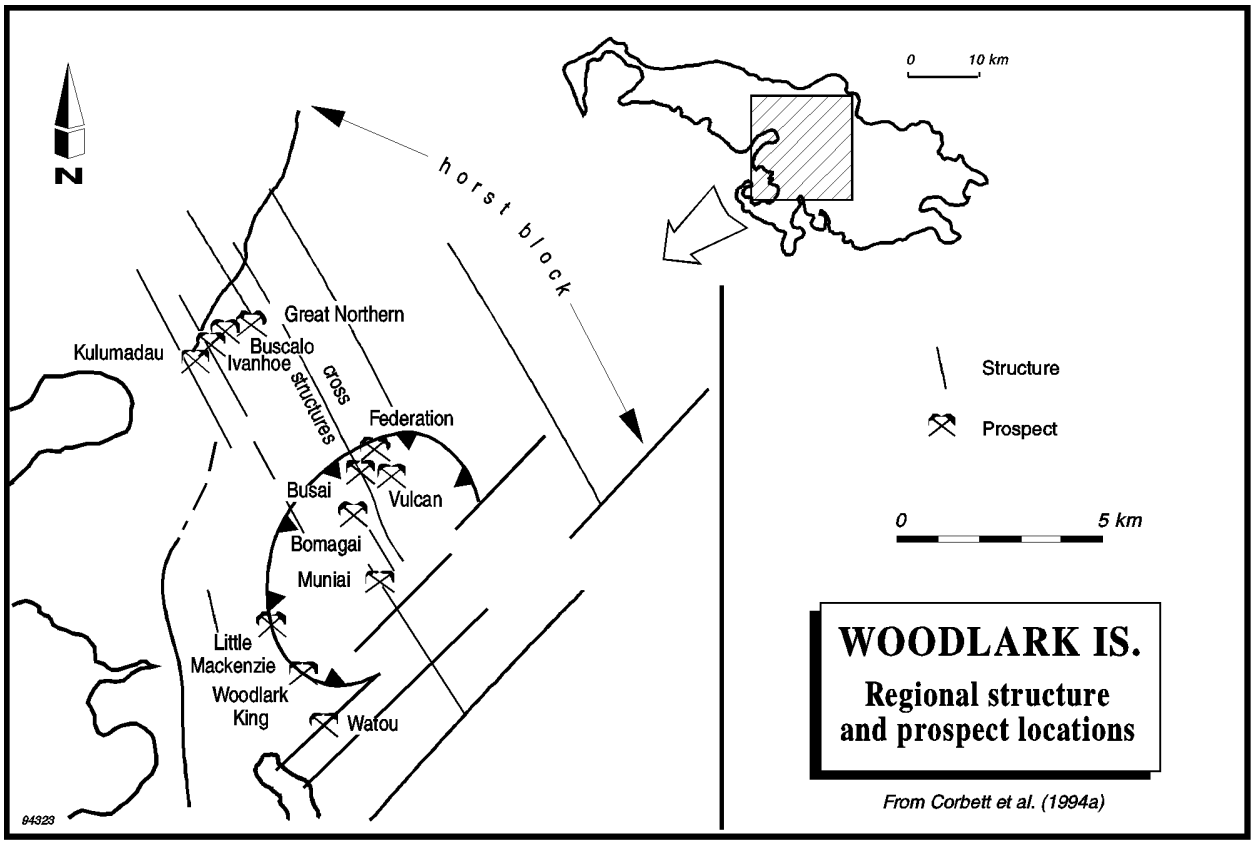

FIG. 7.32

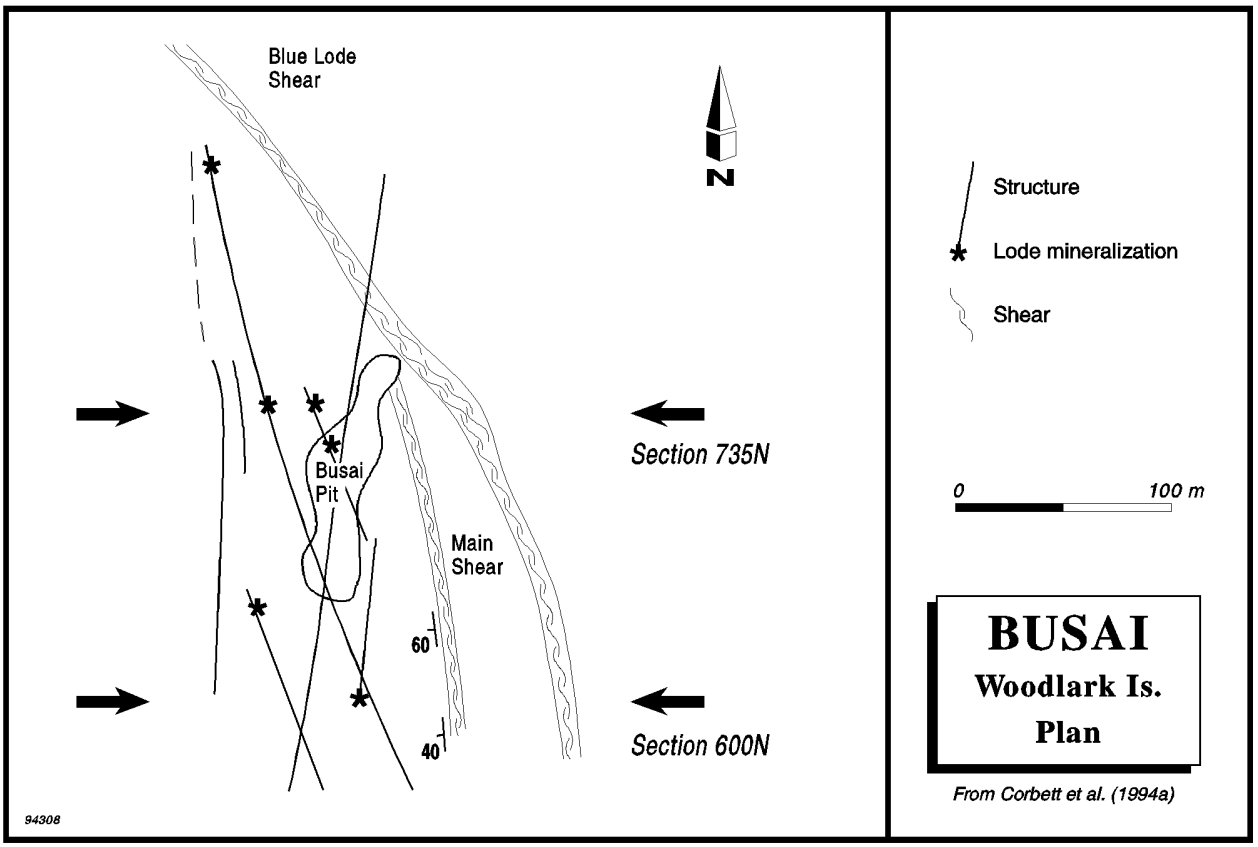

FIG. 7.33

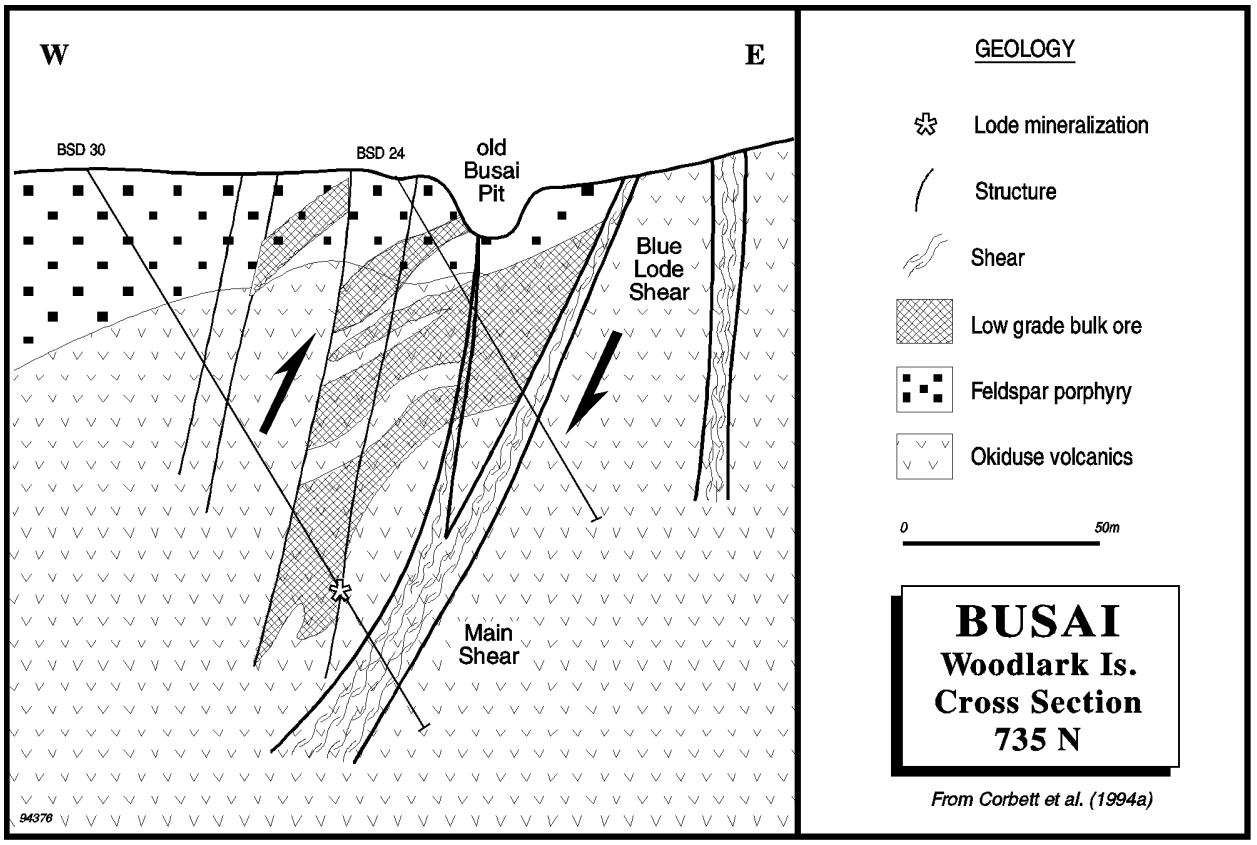

FIG. 7.34

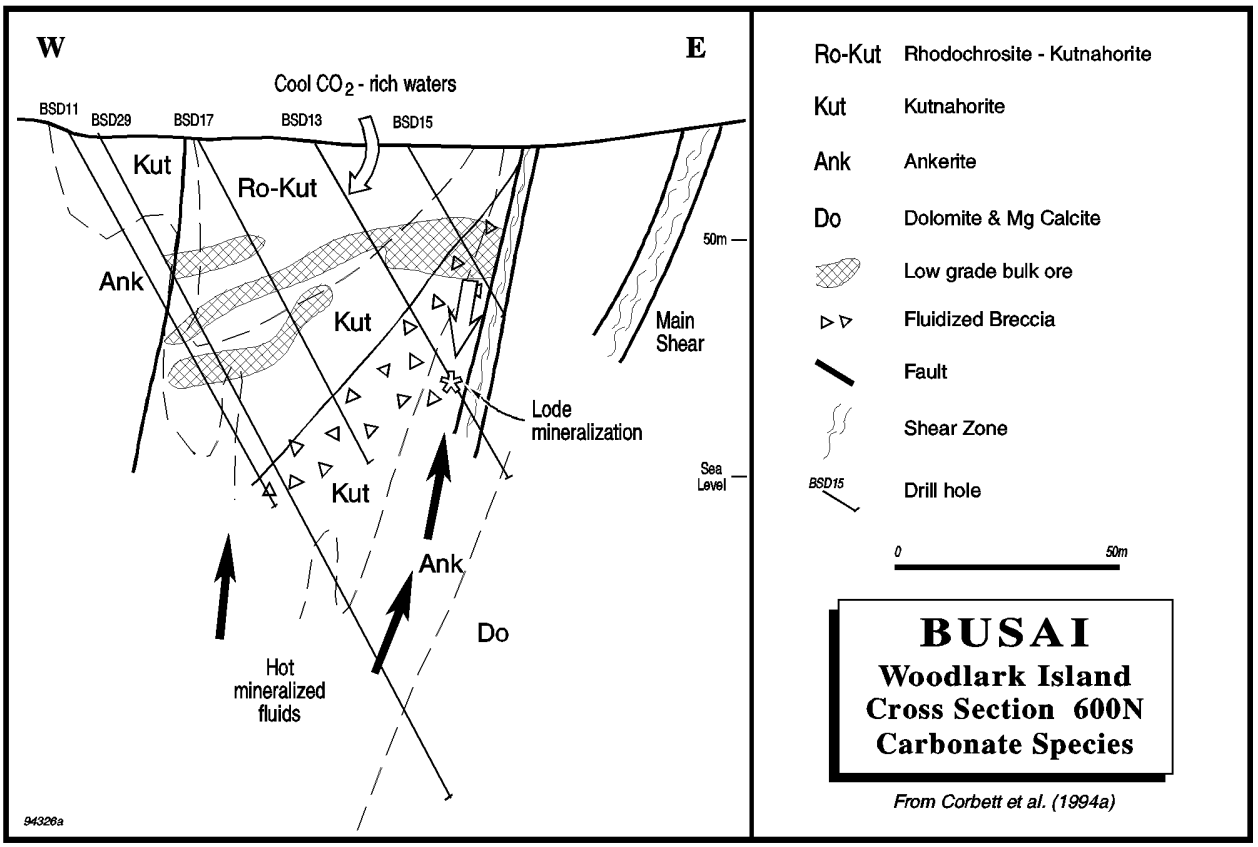

FIG. 7.35

miners and intersected in drilling, are interpreted to represent fissure veins which acted as feeder structures for the shallow dipping tension gash mineralization (Corbett et al., 1994a).

A paragenetic sequence of overprinting structure, alteration and mineralization events has been defined (Corbett et al., 1994b; Fig. 7.36) as:

Stage I: Propylitic alteration of volcanic pile and development of hematitic fracture and breccia fillings, interpreted to be of deuteric origin.

Stage II: Milled matrix fluidized breccias grade upwards from coarse grained, angular fragments at depth, to fine grained 'flinty' chalcedonic silica/pyrite fault fill at shallow levels. These breccias exploit pre-existing structures and provide ground preparation for later mineralization.

Stage III: Banded (polyphasal) quartz-pyrite veins grade from early very fine chalcedonic quartz-pyrite to later coarse grained quartz-pyrite-illitic clay-carbonate, and are equivalent to Stage I quartz described from other carbonate-base metal systems. Local jasperoidal quartz reflects shallow oxidizing environments. Fluid inclusion data indicate that late druzy quartz was deposited from a dilute (<2 wt % NaCl) two phase (boiling) fluid at a temperatures of around 280°C.

Stage IV: Gold mineralization is hosted within carbonate vein/breccias. Fluid inclusion data (Fig. 7.16) and the vertical zonation in carbonate type from Fe/Mn at shallow levels, to mixed Mn/Mg/Fe/Ca at intermediate levels, and to Ca/Mg-carbonate at depth (Fig. 7.35), are interpreted to indicate that mineral deposition resulted from the mixing of hot (>250°C), relatively saline (>6 wt % NaCl) fluids, with cool (<150°C) dilute (<2 wt % NaCl) CO_2-rich fluids. This gradual mixing formed the bulk low grade gold mineralization in shallowly dipping carbonate-filled tensional gash veins. Bonanza gold grades developed in carbonate-quartz breccias within the steeply dipping lodes or feeder structures, and are interpreted to be the product of the quenching of upwelling mineralized fluids by ground waters (Figs. 7.34, 7.35). Rare base metals are overgrown by early quartz and formed prior to, or simultaneous with, carbonate deposition. Gold occurs as electrum mainly intergrown with carbonate, but also as inclusions in sulfides, and displays an average fineness of 830, which is unusually high for carbonate-base metal gold mineralization (Fig. 4.8).

The zonation in the carbonate chemistry from Mn/Mg carbonate at Busai to Mn carbonate at the Federation workings, some 500 m along strike to the north, is consistent with a fluid source to the south (Fig. 7.32).

The Muniai area lies in the centre of a circular feature which may have developed by caldera collapse, defined from the aeromagnetic data (Fig. 7.32). Here, lower temperature propylitic alteration (actinolite-chlorite-albite-epidote-carbonate) is coincident with an aeromagnetic high, possibly indicating that there is magnetite bearing, higher temperature propylitic or potassic alteration at depth. Phyllic overprints low temperature clay alteration at the adjacent Bomagai Prospect (Fig. 7.32). Thus, Busai and the other gold occurrences (e.g., Woodlark King, Little McKenzie, etc.), which form a roughly circular distribution around the margin of the inferred caldera (Fig. 7.32), may have been derived from a central porphyry source.

Kulumadau

Between 1901 and 1950 mining at Kulumadau produced 77,000 ounces of gold at an average grade of 15.9 g/t Au and fineness of 776-859 (McGee, 1978). The Kulumadau mining centre is localized on a major horst-bounding structure, possibly at the intersection of cross structures (Fig. 7.32). Although similar styles of mineralization and overprinting relationships are recognised at Kulumadau and Busai (Corbett et al., 1994a), the intense post-mineral shearing within the Ivanhoe and Kulumadau Lodes at Kulumadau, makes any observations

Phases of Activity	Phase I Propylitic/	Phase II Breccias		Phase III Quartz Veins			Phase IV Base Metals	Phase V Carbonates
		Stage I	Stage II	Stage I	Stage II	Stage III		
Type of Alteration	veins	red matrix breccia	coarse to fine grained fluidized breccia	flinty (dark grey)	flinty (light grey)	fine-course Q veins ± polyphasal ± banding	infilling cavities & fractures	polyphasal late K Ca----Mg-Mn-Fe
Alteration and Mineralization Minerals	Ch-Q-Ch-Cb local Ser/I vesicles colloform Q-Ch	Hm+Q ± Cy	Cy+Py+Q fluid breccia	Q-Py ± Cy local Hm Jasper	Q+Py (light grey)	Q ± Cy+Cb – – Sl – – Fe-rich Fe-poor – –Gal – – –Cpy – –Tn – Au		

Busai - Paragenetic sequence of vein development and brecciation

94477

From Corbett et al. (1994a)

FIG. 7.36

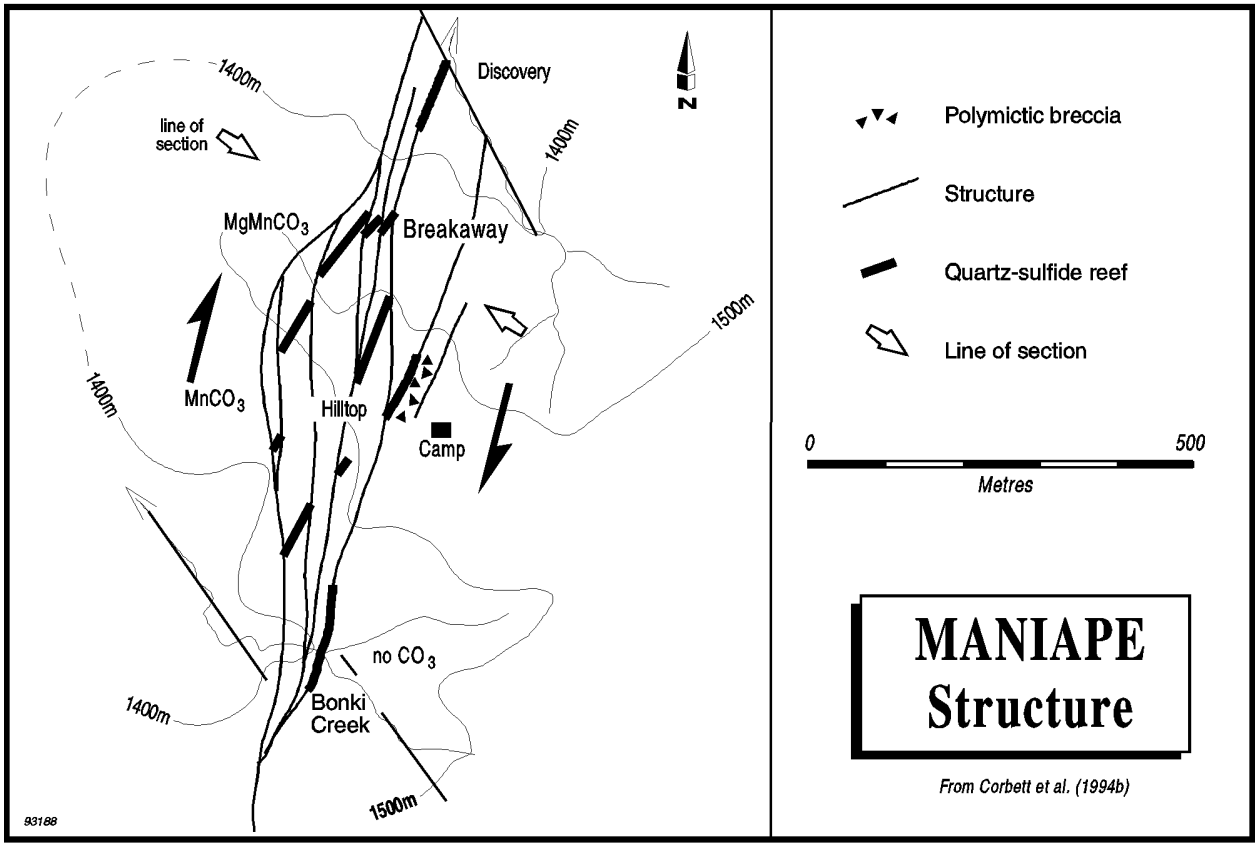

FIG. 7.37

of the spatial relationships difficult. A buried porphyry intrusion is inferred from: the distribution of a set of concentrically zoned aeromagnetic anomalies, high Cu, Pb, Zn geochemistry, vein magnetite overprinted by phyllic alteration, and the relatively high salinity (7-8 wt % NaCl) in fluid inclusion studies. Regional zonation of the mineralization styles within the individual prospects in this area is consistent with the mineralizing fluids having been derived from such a porphyry source (Corbett et al., 1994a).

5. Maniape, Bilimoia District, Papua New Guinea

The Maniape carbonate-base metal gold prospect is located 1.5 km southwest of Arakompa, where an intense magnetic high, and outcropping potassic alteration, are indicative of a porphyry intrusion at depth (Fig. 7.10; Corbett et al., 1994b). The Arakompa and Bilimoia prospects host quartz-sulfide gold ± copper style mineralization discussed in Section 7.ii.d. Dextral strike-slip movement on the 6 km long Maniape fault is interpreted to have created dilatant tension veins, as quartz-sulfide lodes up to several tens of metres long, within an imbricate portion of the fault (Figs. 7.10, 7.37). Mineralization occurs within reactivated competent quartz-sulfide veins and smaller tension fractures formed adjacent to the steeply dipping imbricate faults (Fig. 7.37). Continued post-mineral activation of the Maniape fault system has resulted in extensive shearing and local offsets of mineralization.

A spatial zonation and paragenetic sequence (Fig. 7.39) of structurally controlled alteration and mineralization defined from four drill sections along the Maniape Structure (Corbett et al., 1994b), is summarized as:

Stage I: The lodes formed as locally banded coarse cockscomb quartz to chalcedony, usually intergrown with sericite, carbonate, pyrite and local sphalerite. Quartz veins are accompanied by sericite-quartz-pyrite wall rock alteration which overprints an earlier propylitic alteration. Fluid inclusion data indicate quartz deposition took place at 250-350°C from a relatively dilute (<2-4 wt % NaCl) fluid (Fig. 7.16).

Stage II: Base metal sulfide mineralization post-dates quartz deposition and grades into a major vein episode in which sulfides are intergrown with fine quartz-chlorite-carbonate-illitic clay. Locally, sphalerite is very Fe-poor and is overgrown by galena, followed by chalcopyrite.

Stage III: Carbonate deposition typically occurs within the tension fractures, as late stage colloform banded veins with minor base metal sulfides (predominantly Cu-phases), and within the sulfide veins as alternating bands rich in carbonate and local chlorite. Carbonate is vertically zoned from: Mn-Fe carbonates (rhodochrosite-siderite) at shallow levels, to local Mn-Mg carbonates (kutnahorite and Mg-calcite) at intermediate depths, and to calcite/low Mg-calcite at depth and on the periphery of the system. This is a typical carbonate zonation for carbonate-base metal gold systems. The Mn content of carbonate increases from north to south along the strike of the Maniape Prospect. Fluid inclusion data on sphalerite (Fig. 7.16) indicate that base metal mineralization took place in response to the mixing of a moderately hot (>250-300°C), but relatively highly saline (> 6-7 wt % NaCl) fluid, of probable magmatic derivation, with cool (<200°C), dilute (<2-3 wt % NaCl) waters.

Gold deposition occurs throughout the quartz/clay-base metal sulfide-carbonate vein system, but is predominantly associated with fine quartz-chlorite-illite deposition, described in detail from Bonki Creek, as epithermal quartz gold-silver mineralization (Section 7.iv.2). Gold fineness displays a range of 511-845, with high fineness gold occurring as inclusions in early base metal sulfides and low fineness electrum in the carbonate and quartz-clay veins.

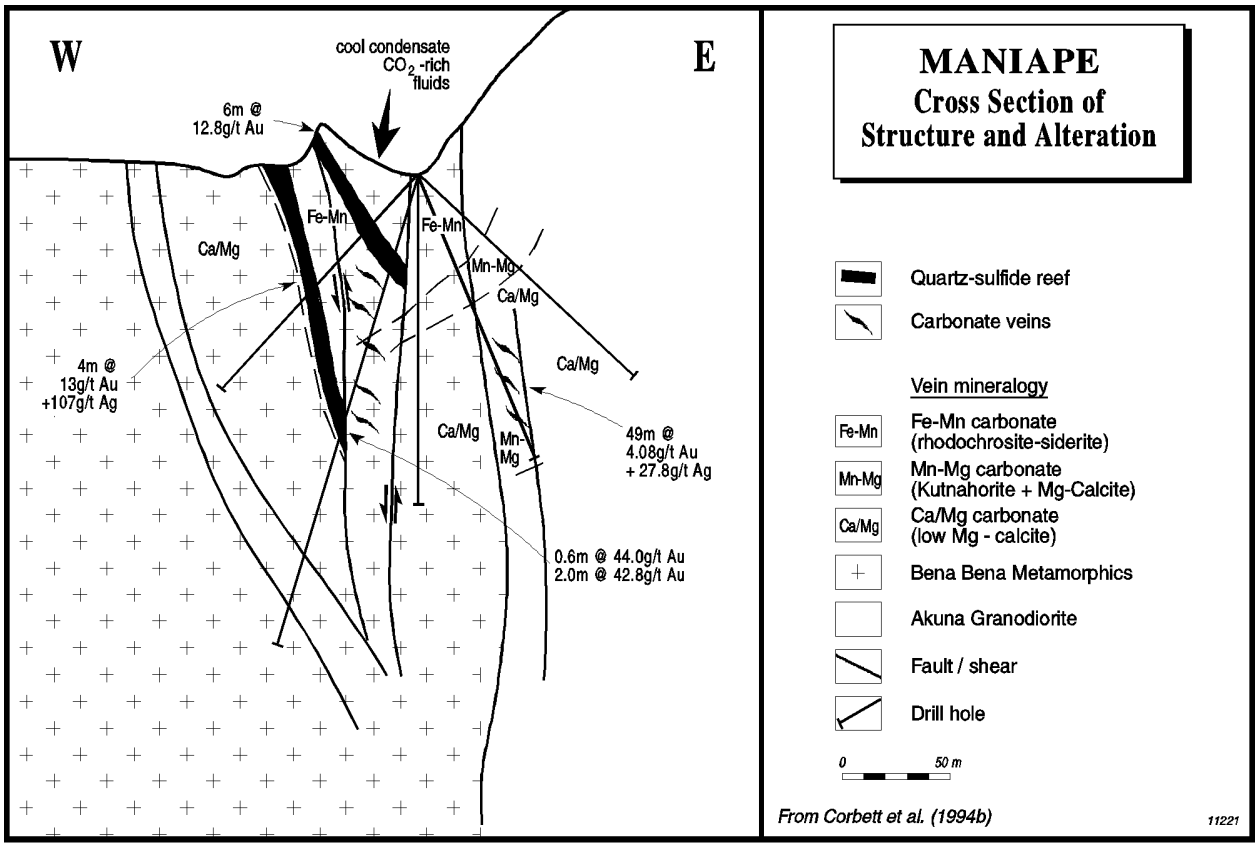

FIG. 7.38

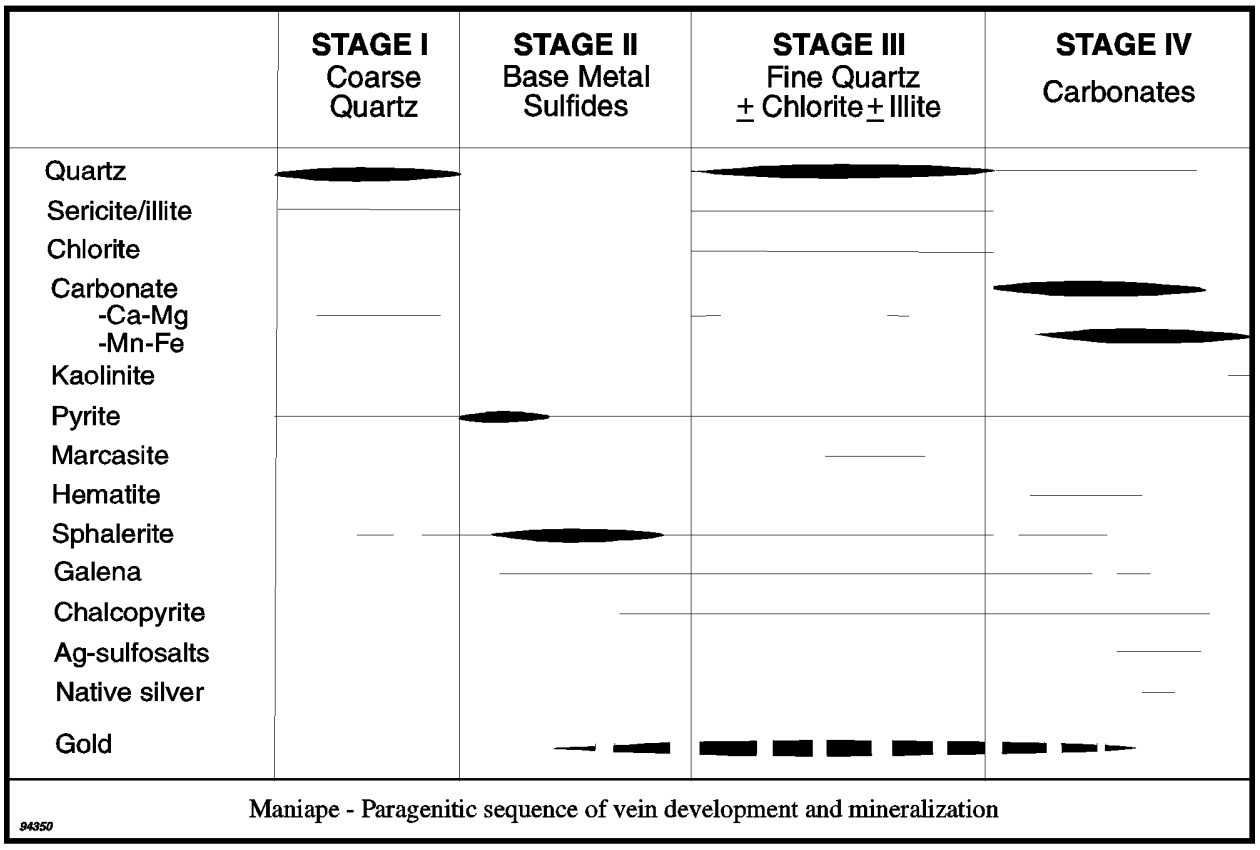

FIG. 7.39

6. Mt Kare, Papua New Guinea

The Mt Kare Prospect, located 16 km SW of Porgera (Fig. 7.22), displays the same early carbonate-base metal gold and late quartz (roscoelite) gold-silver styles of gold mineralization as Porgera. The quartz-roscoelite gold mineralization is discussed below (Section 7.iv.d.1). Local miners are estimated to have extracted 250,000 ounces of gold in 1988 (Welsh, 1990), the first year after discovery of Mt Kare, and up to 1 million ounces of gold by 1991 (Ryan, 1991).

Both the Porgera and Mt Kare intrusion centres lie on the same NE trending Porgera transfer structure (PTS) which, as a deep crustal suture, has allowed mafic intrusions to rise to shallow crustal levels (Corbett, 1994). At Mt Kare, mudstones, calcareous mudstones, sandstone and limestone host rocks are folded by axes oriented in the trend of the PTS and not the NW trend of the accretionary prism. Fault-controlled milled matrix fluidized breccias parallel the trend of the transfer structures and localize mineralization (G. Corbett, unpubl. report, 1996). The structural setting, and similarity of intrusion geochemistry (Richards and Ledlie, 1993) and petrological data (see below), suggest that Porgera and Mt Kare are similar but separate hydrothermal systems, and that Mt Kare in not a thrusted-off portion of Porgera. A baked sediment cap at Peruk suggests that at least part of the Porgera Intrusion Complex is relatively intact. The pronounced aeromagnetic ?deep anomaly at Mt Kare implies that there is a more significant buried intrusion source for the stocks and dikes, than exposed at the surface.

Carbonate-base metal gold mineralization at Mt. Kare occurs at the fractured and brecciated contacts between mafic alkali porphyritic stocks and dikes and the generally baked sediment host rocks (Richards and Ledlie, 1993), as well as within milled matrix fluidized breccias, which are inferred to transport mineralization (Fig. 7.40; G. Corbett, unpubl. report, 1996). The paragenetic sequence of mineral deposition at Mt. Kare (Fig. 7.46; T. Leach, unpubl. reports) is comparable to other carbonate-base metal gold systems (Fig. 7.15), summarised as:

Stage I: Initial quartz-pyrite-sericite/illite-carbonate vein development is accompanied by sericite/illite-quartz-carbonate alteration of the propylitized intrusions and baked sediment host rocks. The pyrite deposited at this stage may be auriferous.

Stage II: Base metal-gold mineralization is associated with pyrite and quartz at shallow levels, grading to carbonate at depth (Fig. 7.40). Early pyrite-galena-sphalerite (red, Fe-rich sphalerite) is progressively overgrown by colourless Fe-poor sphalerite, followed by chalcopyrite, late stage tennantite, and arsenopyrite. The zonation of the carbonate species is similar to other carbonate-base metal gold systems, and although exhibiting a significant overlap grades progressively from higher levels, to deeper in the system as: siderite --> rhodochrosite --> kutnahorite --> dolomite --> calcite (Fig. 7.40). Preliminary fluid inclusion data indicate that kutnahorite was deposited at lower temperatures than earlier sphalerite and late stage calcite, implying that an influx of cool fluids occurred during the carbonate deposition. Gold is present as inclusions in pyrite and sphalerite, and displays a fineness in the range of 720-930, averaging around 820.

Stage III: A late stage illitic-kaolin clay + gypsum-barite overprint at shallow levels is indicative of the descent of cool, moderately low pH condensate fluids during the waning of the hydrothermal system. Calcite-dolomite were deposited at depth.

Although much of the alluvial gold at Mt. Kare was no doubt derived from eroded carbonate-base metal veins, bonanza epithermal quartz silver-gold mineralization has been recognised in late stage quartz-roscoelite (Richards and Ledlie, 1993), discussed in Section 7.iv.d.1. The euhedral nature of much of the alluvial gold is indicative of recrystallization of remobilized supergene gold.

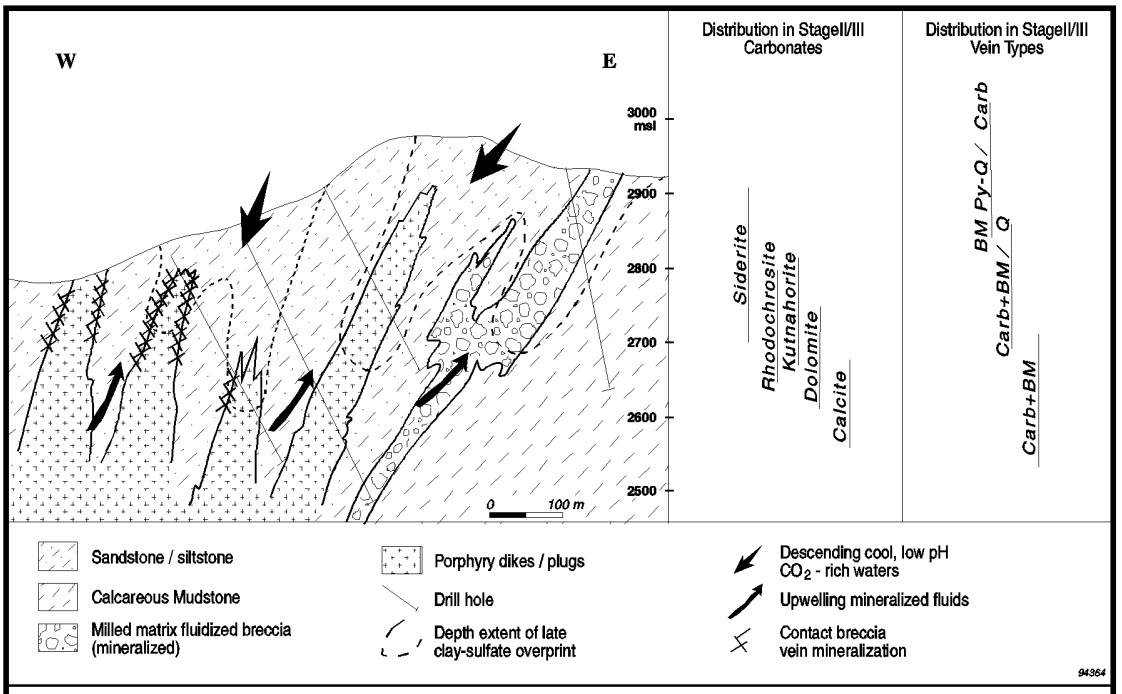

Mt Kare - East-west cross section showing vertical distribution of carbonates and Stage II/III vein types

FIG. 7.40

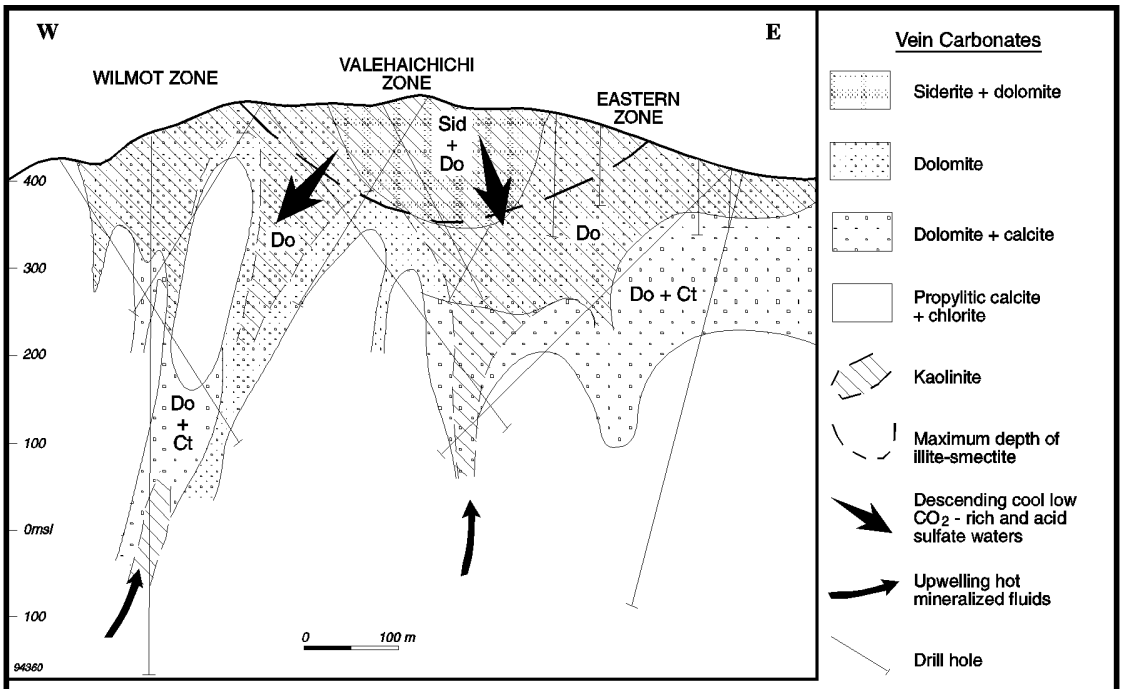

Gold Ridge - Vein carbonate alteration

FIG. 7.41

7. Gold Ridge, Solomon Islands

The Gold Ridge prospect, Solomon Islands, lies on a splay in a regional thoroughgoing structure, which separates differing rock units, and transects Guadalcanal. The 5 x 3.5 km oval shaped rock unit, the Gold Ridge Volcanics, which hosts the prospect, may possibly represent a diatreme breccia. While Hackman (1980) suggests an explosive origin for the rapid facies variations, and notes the pervasive alteration of the matrix, Coleman et al., (1988) describe a "bewildering mixture of chaotic and polymictic conglomerate". The diatreme model (Sillitoe, 1989, Fig. 7) may account for the reported occurrence of carbonized logs and deep sea limestones in the 'conglomerate'.

Gold mineralization at Gold Ridge is hosted in quartz-carbonate-sulfide veins which cut a sequence of volcaniclastic (or possible diatreme) breccias. Veins commonly parallel sedimentary layering, presumably exploiting more competent units. Pervasive alteration is typically low grade propylitic characterized by chlorite-carbonate-quartz-pyrite + albite (Fig. 7.41). Wall rock alteration adjacent to the veins is characterized by illite-carbonate-quartz at depth, and varies to illitic clay-kaolinite-carbonate-quartz + gypsum at near-surficial levels.

The paragenetic sequence of alteration and mineralization (T. Leach, unpubl. report), characteristic of carbonate-base metal gold mineralization, is summarised as:

Stage I: Quartz-pyrite + adularia deposition at 230-390°C, based on fluid inclusion data.

Stage II: Base metal sulfide-carbonate alteration, in which bands of quartz-clay-sulfide locally alternate with carbonate. There is a predominance of carbonate proximal to inferred fluid upflow features, and quartz-sulfides in distal settings. Sulfides exhibit the typical sequence of deposition for carbonate-base metal systems as: early pyrite, followed by sphalerite, galena and late chalcopyrite. Arsenopyrite and marcasite locally overgrow pyrite. Vein carbonates are vertically zoned with increasing depth as: siderite at shallow levels, dolomite at intermediate levels, and calcite at deeper levels (Fig. 7.41). The absence of rhodochrosite-kutnahorite-ankerite at Gold Ridge is interpreted to be a function of the paucity of manganese in the near surface host rocks.

Fluid inclusion data suggest that carbonate, quartz and sphalerite deposition took place over a wide temperature range (197-317°C), indicative of progressively cooling conditions during stage II hydrothermal activity. Gold mineralization appears to be restricted to this stage, and occurs as native gold inclusions in pyrite and sphalerite, intergrown with carbonate, and filling fractures/cavities in Stage I quartz-adularia veins. Bulk low grade mineralization occurs in broad, near surface, siderite-dolomite-illitic clay-kaolinite alteration zones. High grade lode mineralization is encountered at depth in restricted feeder structures.

Stage III: Vertically zoned interlayered clay-illite and kaolinite alteration overprints earlier assemblages and may also form in veins in association with minor gypsum and siderite. This alteration is interpreted to have formed in response to late stage incursion to depth, of low pH, cool, CO_2-rich waters (Figs. 7.2, 7.41). Secondary fluid inclusions in stage III mineralogy are indicative of temperatures in the 130-180°C range for this waning stage of hydrothermal activity.

8. Karangahake, Coromandel Peninsula, New Zealand

Karangahake produced some 1 million oz Au and 3 million oz Ag at an overall average grade of about 15 g/t Au from fissure veins related to Upper Miocene/Pliocene magmatism (Brathwaite and Pirajno, 1993). Carbonate-base metal style gold mineralization, in which ore shoots account for much of the production, occurs over 600 m vertically within andesite-hosted fissure veins, capped by rhyolite-hosted low grade epithermal quartz gold-silver mineralization (Fig. 7.42; Brathwaite, 1989). The Karangahake vein system is localized at the

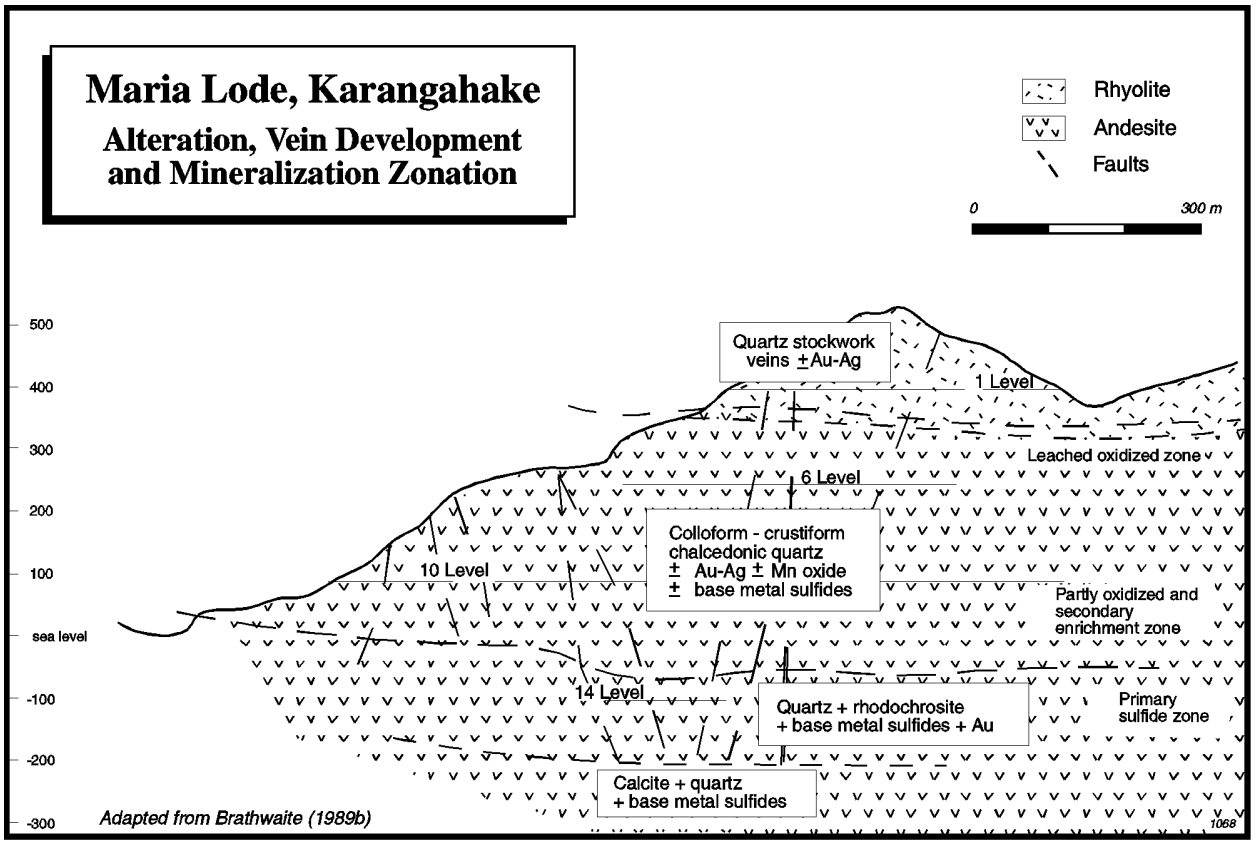

FIG. 7.42

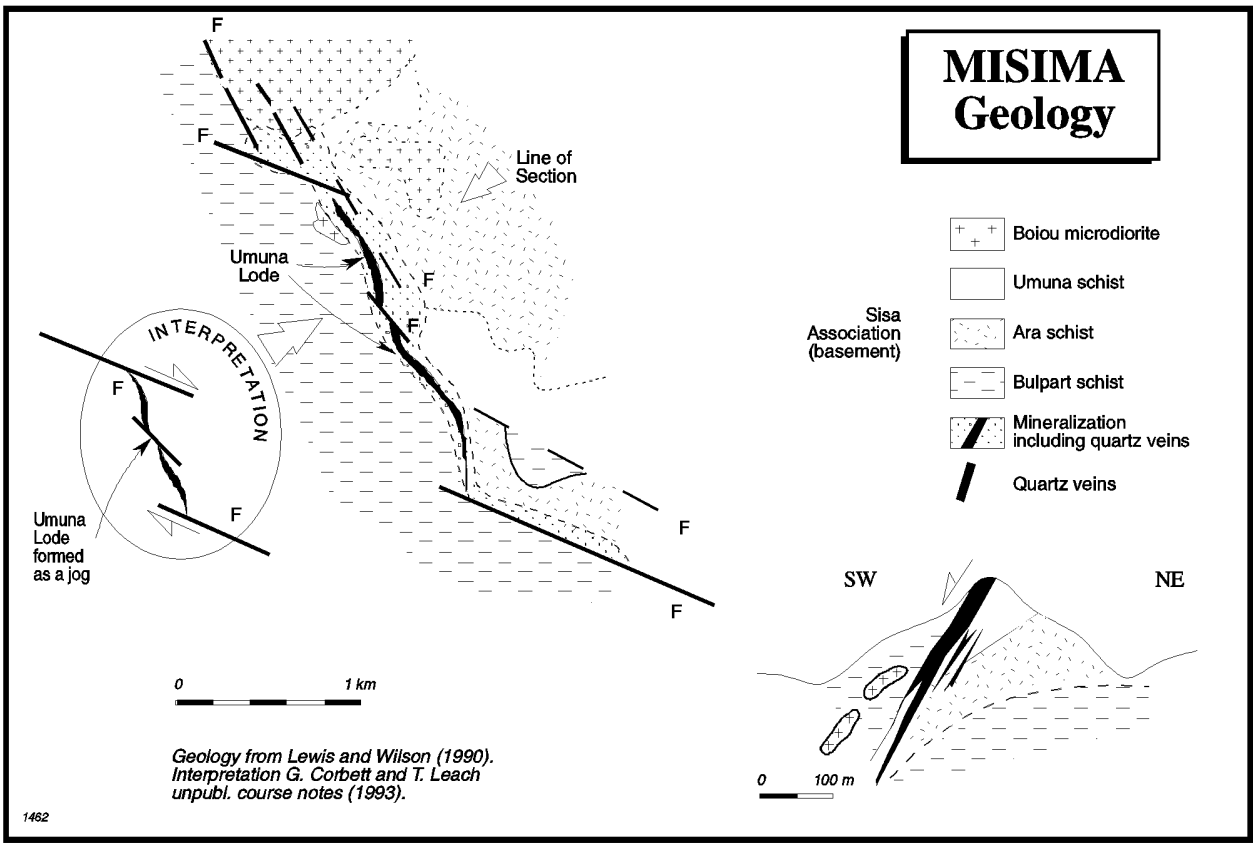

FIG. 7.43

intersection of a bounding structure for the Hauraki graben and a NE trending transfer structure, on which the Golden Cross mine also occurs (Fig. 7.47). Reactivated NS-trending graben structures appear to comprise the main fissure vein hosts such as the Maria Lode.

In the fissure veins at shallow levels, gold mineralization occurs in dark sulfide bands within crustiform banded quartz veins (Brathwaite, 1989), which are comparable to the ginguro ore of the epithermal gold-silver deposits, Japan (Section 8.vi). Low fineness gold (Fig. 4.8) is closely associated with chalcopyrite, argentite, and minor sphalerite and galena, which are intergrown with fine quartz, kaolinite and interlayered clays (T. Leach, unpubl. data). The association of metals with low temperature clay mineral deposition is interpreted to indicate that mineralization resulted from the quenching of metal-bearing fluids by cool surficial waters (Section 8).

At around 300-400 m below the rhyolite-hosted stockwork veins, primary mineralization in the Maria lode grades into banded quartz-rhodochrosite-calcite sulfide vein fill (Fig. 7.42). The sulfide bands are composed of sphalerite, galena, pyrite and chalcopyrite. High grade gold is closely associated with rhodochrosite and chalcopyrite and has a fineness of 535-726 (average 650). At depth, calcite and base metal sulfides become common and the gold grades decline, in a similar manner to most carbonate-base metal systems.

Fluid inclusion analyses on quartz (Brathwaite, 1989) indicate that vein deposition took place at 230-280°C and the presence of rhodochrosite and the low fineness of gold (electrum) are typical of formation at shallow levels in a carbonate-base metal system.

9. Acupan, Baguio District, Luzon, Philippines

The Acupan gold mine, Baguio District, Philippines, is the second largest single gold producer in the Philippines (> 4 M oz Au; Mitchell and Leach, 1991). Cooke and Bloom (1990) and Cooke et al., (1996) describe a diatreme breccia complex (Balatoc Diatreme) which overprints early porphyry copper-gold mineralization and is in turn cut by a banded (polyphasal) fissure vein system. An extensive shoulder of barren high sulfidation alteration caps the ridges several hundred metres above the vein system (UNDP, 1977; Fig. 2.19). The veins parallel a throughgoing regional structure (Figs. 2.18, 2.19) and may be localized at the intersection with a dome inferred by Mitchell and Carlile (1994).

A paragenetic sequence for the carbonate-base metal gold mineralization is described by Cooke and Bloom (1990) and Cooke et al. (1996) as:

Stage I: Early fine grained white-grey chalcedony and later grey quartz-pyrite-sericite ± adularia ± hematite, similar to the 'flinty' quartz at Woodlark Island. Refractory gold, as submicroscopic inclusions in pyrite, forms a significant part of the mineralization.

Stage II: Polyphasal carbonate-quartz overprinting relationships are categorised as: early rhodochrosite-quartz, later quartz-Mn-calcite (± adularia at depth), and late stage calcite-quartz. Post-mineral anhydrite ± calcite ± illite fills cross-cutting fractures and cavities.

Fluid inclusion data (Cooke and Bloom, 1990) illustrate a progressive cooling and dilution during carbonate-quartz deposition. Base metal deposition, predominantly in conjunction with quartz-Mn-carbonate, took place as early sphalerite followed by galena, and later chalcopyrite. Gold mineralization at Acupan occurs in association with Au-Ag tellurides, mainly within the quartz-rhodochrosite-base metal sulfide veins. Gold fineness increases at progressively shallower levels. Cooke et al. (1996) interpret that Te-enrichment during gold mineralization was caused by entrainment of minor amounts of magmatic vapours into a meteoric-dominated hydrothermal system.

10. Umuna Lode, Misima Island, Papua New Guinea

Early mining at Misima produced approximately 0.33 million oz Au from alluvial and hard rock workings from 1888-1943 (Lewis and Wilson, 1990). Although initial exploration in the 1960-1975 period focused on porphyry copper targets, Placer evaluated the bulk low grade gold potential in the early 1980's. Mine production by Placer at the Umuna lode began in 1989, with a published resource of 55.9 Mt at 1.39 g/t Au (2.5 M oz Au) and 21 g/t Ag (Lewis and Wilson, 1990). As of March 1996, Placer have mined 2.2 million oz Au and another 1.27 million oz Au remain (Appleby et al., 1996).

Host rocks comprise low grade (greenschist facies) metamorphic rocks of the Sisa Association, into which are emplaced stocks, dikes and sills of granodiorite, diorite, porphyritic dacite, andesite and latite, collectively labelled the Boiou Microgranodiorite (Williamson and Rogerson, 1983; Lewis and Wilson, 1990). U-Pb analyses of magmatic zircon provide an 8.1 Ma age for these rocks, whereas the 3.72-3.19 Ma K/Ar and Ar/Ar age for hydrothermal sericite indicates that mineralization is much younger (Appleby et al., 1996). These workers genetically relate mineralization to 3.5 Ma alkaline dikes emplaced during detachment faulting.

Gold-silver mineralization on Misima Island is mainly hosted in the Umuna lode and adjacent fractures, developed as part of a 2 km long jog (Umuna fault zone) between two inferred strike-slip structures (Fig. 7.43; G. Corbett, pers. observation, 1991; Appleby et al., 1996). Normal faulting is interpreted for the Umuna fault zone (Adshead and Appleby, 1996), and Appleby et al. (1996) infer that the tensional regime for mineralization occurred around 3.5 Ma in relation to the propagation of the Woodlark spreading axis.

A paragenetic sequence for mineralization at Misima is inferred from previous work (Williamson and Rogerson, 1983; Clarke et al., 1990; Lewis and Wilson, 1990; Appleby et al., 1996; Adshead and Appleby, 1996; N. Adshead, unpubl. report) as:

Stage I Porphyry Copper: Emplacement of the Boiou intrusions was accompanied by local development of zoned calc-silicate and magnetite skarns in the marble units. Copper mineralization associated with chlorite-epidote-calcite-hematite-pyrite-chalcopyrite alteration and veins/veinlets (Adshead and Appleby, 1996) is inferred to have formed as a retrograde phase of the skarn.

Stage II Precious/Base Metal: As outlined above, precious and base metal mineralization at Misima formed within the Umuna lode and adjacent fractures. Lewis and Wilson (1990) noted that the intrusion contacts are commonly brecciated, and these provided permeability which 'spread' mineralization laterally from the fault zone. Gold mineralization is inferred to be much younger than the Boiou intrusions and related to the 3.5 Ma. alkaline (lamprophyre) dikes (above).

The phases of alteration, brecciation, and vein development associated with the precious and base metal mineralization are:

1: Fluidized breccias comprising clasts of Boiou Microgranodiorite and schist are set in a fine grained dark siliceous matrix and may be an immediate precursor to the precious and base metal mineralization. However, the association of these breccias with the emplacement of the Boiou Microgranodiorite cannot be ruled out.

2: Quartz Lodes formed within the Umuna fault zone display banding and open space filling indicative of a strongly dilational character (Williamson and Rogerson, 1983). Massive quartz which pinches and swells preferentially occurs at shallow levels (Lewis and Wilson, 1990).

3: Banded quartz-carbonate veins which transect the massive quartz bodies represent the main phase of mineralization at Misima. Williamson and Rogerson (1983) reported a paragenetic sequence as: quartz + pyrite --> carbonate/quartz --> quartz ± barite --> quartz + pyrite + base metals + Au ± base metals. Wall rock

alteration of plagioclase is characterized by chlorite-muscovite-carbonate-smectite, which grades to chlorite-epidote away from the veins (Adshead and Appleby, 1996). Veins demonstrate the following changes with depth:
* a decrease in the abundance of quartz and increase in abundance of carbonate,
* banded and colloform to coarse crustiform quartz,
* increase in the amount of base metals; barite only occurs at shallow levels,
* Fe-poor to Fe-rich sphalerite,
* stockwork veins of quartz-chalcedony and sheeted and banded quartz-chalcedony ± Mn-Fe-oxide veins at high elevation, through banded quartz-manganese lodes at shallow levels in the open pit, to carbonate-base metal veins at deeper levels.

The manganese is inferred to have been derived from the supergene oxidation of Mn-carbonates similar to other carbonate-base metal systems (e.g., Kerimenge and Woodlark, Papua New Guinea; Karangahake, New Zealand; Antamok and Acupan, Philippines). Polyphasal shearing and brecciation is common within the Umuna fault zone and occurs pre-, syn-, and post-mineralization. Crackle brecciation within the host intrusions, schists, greenstone and quartz lodes is sealed by carbonate-quartz-base metal sulfides ± clay; whereas post-mineral shearing is associated with the development of clay gouges (N. Adshead, unpubl. report, 1996).

The above sequence of events and zonations with increasing depth at Misima is characteristic of southwest Pacific rim carbonate-base metal gold systems, especially those which grade at shallow levels (and/or later events) to epithermal quartz gold-silver style mineralization (e.g., Karangahake). Preliminary fluid inclusion data (Williamson and Rogerson, 1983) indicate that the early quartz was deposited at 261-301°C and from fluids around 4.1 percent weight equivalent NaCl. The sphalerite in the carbonate-base metal event was deposited under cooler (228-244°C, average 238°C) but more saline conditions (5.7-7.9 % wt equiv NaCl). These changes from hot, dilute to cooler but more saline conditions during mineralization suggest that mixing occurred between hot mineralized and cooler meteoric-dominated waters. The abundance of barite at shallow levels is indicative of an influx of sea waters, late in the history of the hydrothermal system.

j) Conclusion

Several southwest Pacific rim carbonate-base metal gold systems demonstrate similarities in setting, mineralogy and paragenesis, and form in environments transitional between the epithermal and porphyry settings (Figs. 7.1, 7.2). Exploration models deduced from an understanding of these deposits indicate:
1. Bonanza gold grades may occur in:
* banded ores formed in dilational structural settings,
* breccias which result from the quenching of magmatic ore fluid with meteoric waters within feeder structures.
2. Hydrothermal systems are localized on major structures, commonly associated with maar volcano/diatreme (phreatomagmatic) breccias, while mineral deposition takes place in adjacent dilatant structures.
3. The zonation in gangue, including carbonates, and sulfide mineralogy, provides indicators which point towards the portions of the system in which better gold grades may occur.
4. Information provided by the alteration and mineralization zonations and structure may also point towards porphyry source rocks for the carbonate-base metal gold mineralization.

iv) Epithermal Quartz Gold-Silver Systems

a) Introduction

There is a group of epithermal gold-silver occurrences which display clear relationships to porphyry sources for the mineralization. Many of the deposits in this group (Porgera Zone VII and Mt Kare, Papua New Guinea; Emperor gold mine, Fiji) could be included within the class of 'alkaline epithermal volcanic hosted precious metal deposits' of Bonham (1988b), or 'alkalic low sulfidation' of Sillitoe (1993b). Some epithermal quartz gold-silver deposits are locally transitional to the classic adularia-sericite epithermal gold-silver deposits (e.g., Tolukuma, Papua New Guinea; Cracow, eastern Australia) which occur as banded fissure veins (Section 8), and also form as distal portions of, or overprinting, carbonate-base metal gold systems (e.g., West Prampus at Kelian, Indonesia; Maniape near Arakompa, Papua New Guinea), as the lowest temperature and highest crustal level member of a continuum of low sulfidation mineralization styles (Leach and Corbett, 1995). These deposits therefore display the most distal relationship to the intrusion source (e.g., Thames, New Zealand) and form in strongly dilational structural settings (Figs. 7.1, 7.2).

Three classes are recognised as those:
1. Associated with intrusions and commonly overprinting carbonate-base metal gold mineralization (e.g., Porgera Zone VII, Mt Kare in Papua New Guinea).
2. Peripheral to intrusions (e.g., Thames, New Zealand; Emperor, Fiji; West Prampus at Kelian, Indonesia; Bonki Creek at Maniape, Bilimoia District, Papua New Guinea).
3. Transitional to adularia-sericite epithermal gold-silver systems (e.g., Tolukuma, Papua New Guinea; Cracow, eastern Australia).

Adularia-sericite epithermal gold-silver deposits have traditionally been interpreted to be related to meteoric waters (Hayba et al., 1985), which circulate to considerable depths and entrain fluids derived from magmatic intrusions (Henley, 1991). Although most of the quartz-sericite-adularia vein material was probably deposited from meteoric fluids, evidence outlined below (and in Section 8) indicates that the gold-silver mineralization was derived from a substantially magmatic fluid.

b) Characteristics

Epithermal quartz gold-silver systems are found in magmatic arc environments, commonly hosted in calc-alkaline volcanic and/or basement metamorphic and sedimentary rocks. While the adularia-sericite epithermal gold-silver deposits are commonly associated with phreatic (eruption) breccias, intrusion-related systems may contain milled matrix fluidized (diatreme) breccias typical of phreatomagmatic eruptions (Section 3.x.d). Epithermal quartz gold-silver systems which are transitional to adularia-sericite epithermal gold-silver systems contain veins of alternating colloform to crustiform bands of coarse grained and fine grained quartz, with varying abundances of adularia, clay and/or carbonate, and quartz pseudomorphing platy carbonate. The clay minerals reflect low temperatures of formation (e.g., smectite, interlayered illite-smectite, kaolin or chloritic clays) and are locally associated with sericite, and carbonate species formed at moderately low fluid pH conditions (Section 7.iii.g). In environments where hydrothermal fluids have had access to mafic intrusions at considerable depths, the vanadium-rich illite, roscoelite, may replace the usual potassium-rich illite/sericite (e.g., Porgera Zone VII and Mt. Kare, Papua New Guinea; Emperor, Fiji).

Sulfide contents are typically low, and iron sulfides dominate over trace base metal sulfides. The common occurrence of marcasite, which reflects moderately oxidizing conditions, and poorly crystalline melnikovite pyrite,

are indicative of deposition at shallow crustal levels. The ore mineralogy is generally silver-rich and low fineness

DISTINCTION between ADULARIA-SERICITE EPITHERMAL and EPITHERMAL-QUARTZ, GOLD-SILVER SYSTEMS		
	Adularia-Sericite-Epithermal Gold-Silver	Epithermal-Quartz Gold-Silver
Setting	Back-arc rift / basin	Magmatic arc
Association	Not obvious intrusion, felsic volcanics commonly present	Intrusions (many alkaline) generally present. Overprinting or subjacent to carbonate-base metal gold mineralization.
Breccias	Eruption (phreatic)	Diatreme or milled matrix fluidized (phreatomagmatic)
Form	Banded fissure veins, sheeted veins and less commonly, stockwork veins	Fissure veins, breccias and ore shoots common
Alteration:		
Vein	Quartz, adularia, quartz pseudomorphing platy carbonate	Quartz, chlorite, illitic clay, local roscoelite
Wall rock	Illite, illite-smectite, kaolinite, chlorite	Illite, illite - smectite, kaolinite, chlorite
Ore minerals	Pyrite >> chalcopyrite > sphalerite, galena Ag-sulfides and sulfosalts	Pyrite marcasite, >> sphalarite, galena,chalcopyrite Ag sulfosalts ± Ag sulfides local hypogene hematite
Metals:		
Primary	Au : Ag high to bonanza grades	Au : Ag bonanza grades common
Accessory	Se > Te	Te
12115		

TABLE 7.1

gold (typically less than 600-700, Fig. 4.8) usually occurs as electrum. The base metal minerals are also silver-rich (e.g., Ag-tetrahedrite [freibergite] and high Ag-galena), and some systems may contain a Ag-rich sphalerite. Silver sulfides and sulfosalts (e.g., argentite, pearsite-polybasite, proustite-pyrargyrite) are also common, as is native silver.

The most striking feature of the ore mineralogy is the common association with tellurium, and in some cases selenium. Whereas Pb- and Bi-telluride minerals dominate in intrusion-related mesothermal quartz-sulfide systems, epithermal quartz gold-silver systems contain Ag-Au-tellurides (e.g., hessite, calaverite, petzite). The presence of telluride minerals has been interpreted (Afifi et al., 1988; Cooke and McPhail, 1996) to be indicative of a magmatic component for the mineralizing fluid.

As described in the following examples, the epithermal quartz gold-silver vein systems are interpreted to develop by mixing of upwelling mineralized fluids with cool ground waters. The quenching of the upwelling fluids results in quartz deposition, with coarse-grained quartz forming under stable conditions, and fine-grained quartz/silica depositing during sudden cooling. Although there is a continuum between epithermal gold-silver and carbonate-base metal gold mineralization (e.g., Karangahake, New Zealand), the scarcity of carbonates is inferred to indicate a predominance of ground water over CO_2-rich waters during ore formation.

Hypogene hematite occurs in many of these systems, and this, in addition to the occurrence of marcasite, is indicative of oxidizing environments. The entrainment of oxidizing ground waters with upwelling mineralized fluids provides an efficient mechanism for the deposition of gold, and may locally form bonanza gold grades (Section 4.vi.a).

c) Structural Setting

Epithermal quartz gold-silver systems form in magmatic arcs, commonly those characterized by oblique subduction and are distinct from the typical back-arc setting of adularia-sericite epithermal gold-silver deposits. Only in well developed dilational ore-hosting environments are epithermal quartz gold-silver systems formed as part of the full continuum of porphyry-related low sulfidation gold deposits. Typical structural settings include: within jogs (e.g., Porgera Zone VII, Papua New Guinea), intersections of cross structures with dilational fractures (e.g., Thames, New Zealand) and fissure veins (e.g., Cracow, eastern Australia), intersections of milled matrix fluidized breccias with throughgoing structures (e.g., Tolukuma, Papua New Guinea), and hanging wall splits (e.g., Porgera Zone VII, Papua New Guinea).

These deposits commonly display structural characteristics typical of both magmatic-related deposits and the classic epithermal adularia-sericite vein systems. Major structures at depth localize porphyry intrusions which set up circulating hydrothermal cells of dominantly meteoric waters. Continued strike-slip activation of these structures in active magmatic arcs may create dilational environments in which banded adularia-sericite epithermal quartz veins form (Sibson, 1987). These same dilational environments assist in the migration of fluids from deeper magmatic source rocks, to shallower levels where epithermal quartz gold-silver systems form, and so there may be a transitional relationship between the two styles of gold deposits. The presence of high level intrusions may promote the development of phreatomagmatic breccias. The recognition of the magmatic association in these deposits may result in the development of differing exploration models (e.g., Tolukuma, Corbett et al., 1994c).

d) Examples

1. ASSOCIATED WITH INTRUSION-RELATED MINERALIZATION

1. Zone VII, Porgera, Papua New Guinea

At Porgera, the Stage II epithermal quartz gold-silver mineralization overprints the earlier Stage I carbonate-base metal gold mineralization described in Section 7.iii.i. While most of the Stage II ore occurs within Zone VII, some also overprints the carbonate-base metal mineralization in the open pit. The following discussion is taken from Corbett et al., (1995), Richards (1992), Richards and Kerrich (1993) and Richards and McDougall (1990).

Porgera Zone VII gold mineralization is hosted within the Roamane fault zone, a south-dipping structure which locally defines the margin of the Porgera Intrusion Complex, and separates the Waruwari and Rambari intrusion systems (Figs. 7.23, 7.24). Corbett (1994) speculated that dextral strike-slip movement on local elements of the Porgera transfer structures may have dilated the Roamane and parallel faults (Fig. 7.23). Normal movement on the Roamane fault has also produced ore-hosting hanging wall and lesser footwall splits. Late stage feldspar porphyry dikes have been emplaced into the intersections of the transfer structures with the Roamane and parallel faults, and migrated along the latter structures to locally intrude hanging wall splits (Figs. 7.23, 7.24, 7.25).

Mapping by Porgera joint venture geologists has shown that at the Main Zone ore of Zone VII comprises EW-trending D vein mineralization (below) formed within a jog resulting from dextral strike-slip movement on the Roamane fault, and overprints the earlier NNE trending A/B vein mineralization (Fig. 7.24). This sense of movement is no doubt imparted by the transfer structures. Bonanza gold grades occur at the intersection of the footwall and hanging wall splits with the Roamane fault. Competent intrusion rocks and contact baked shales underwent brittle fracturing and became important ore hosts, especially where capped by incompetent Chim Formation shales.

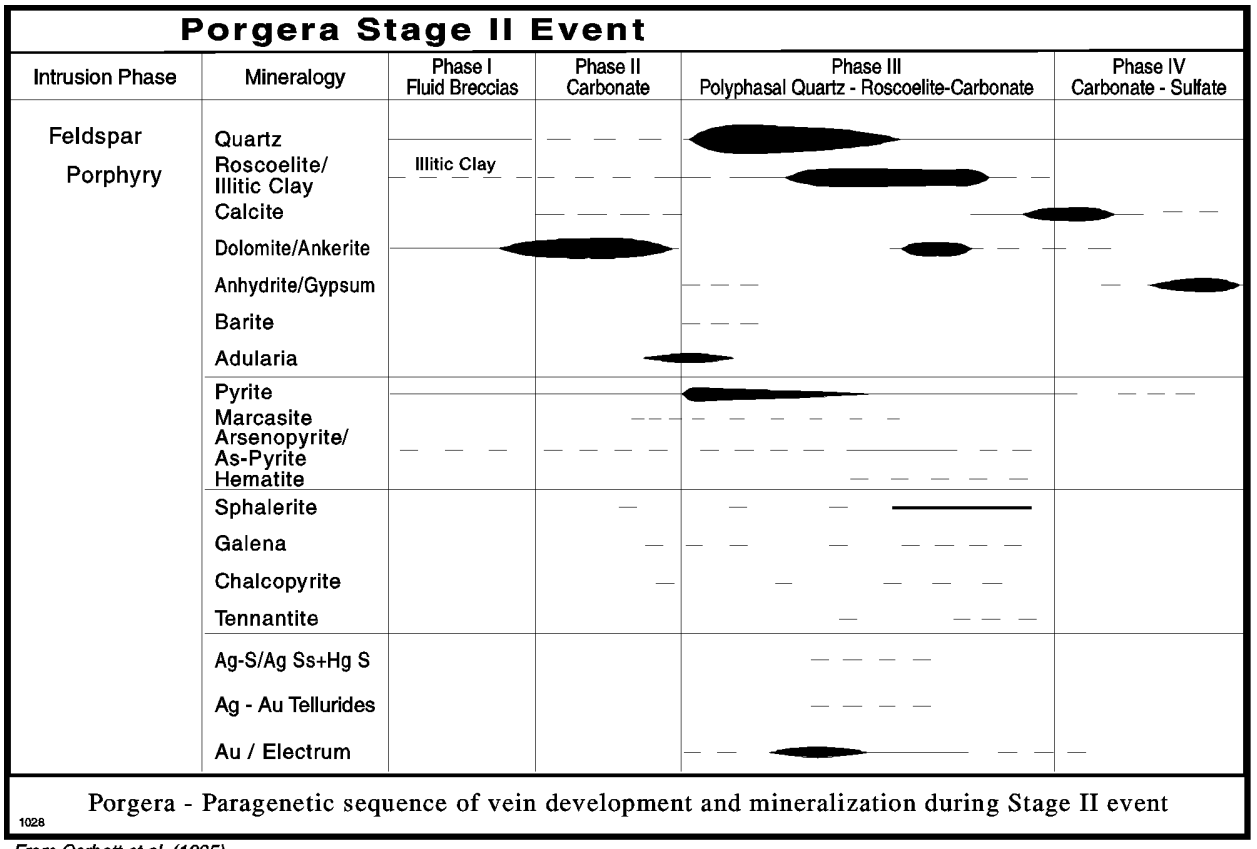

From Corbett et al. (1995)

FIG. 7.44

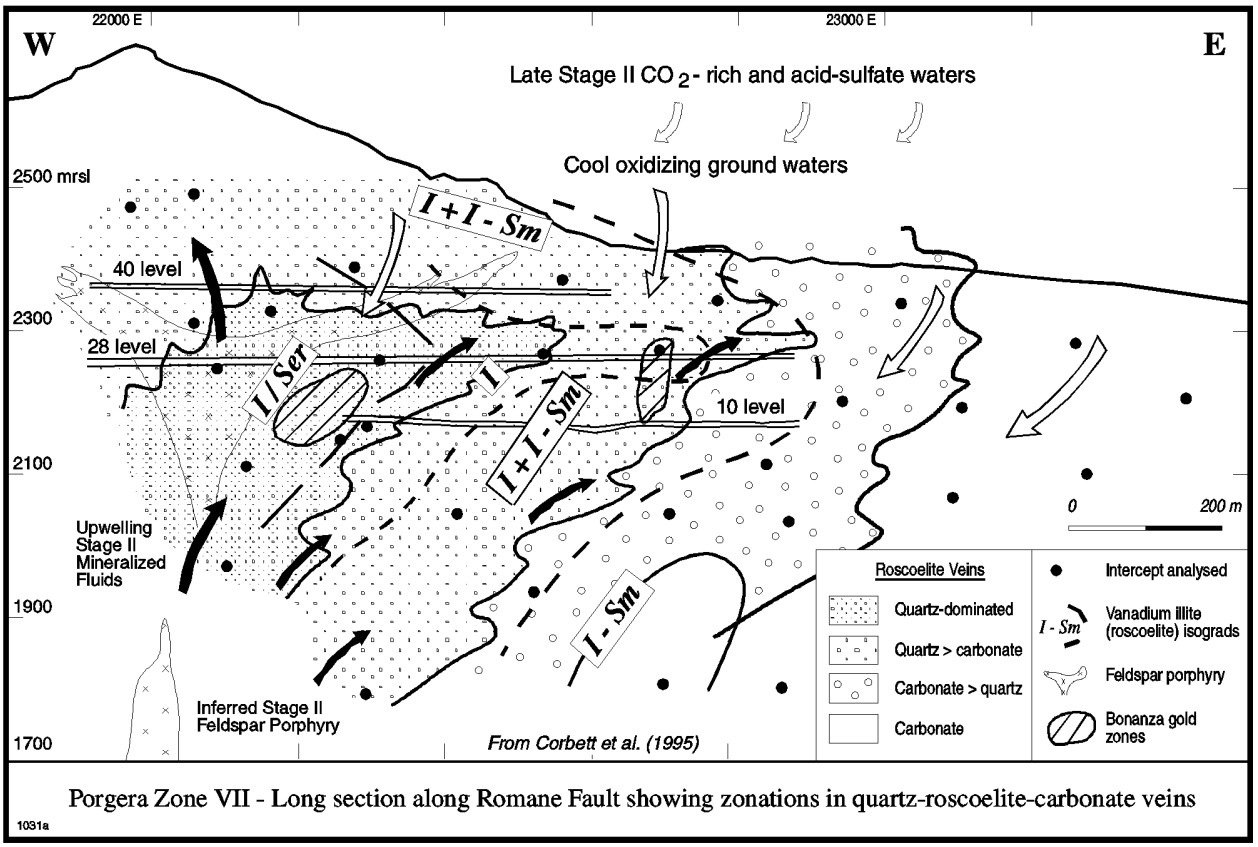

FIG. 7.45

Stage II quartz-roscoelite alteration and mineralization exhibits a paragenetic sequence of: early polyphasal fluidized breccias, followed by massive carbonate deposition, quartz-roscoelite-carbonate vein and vein/breccia development, and final late stage of carbonate and/or sulfate deposition (Fig. 7.44). The stage II quartz-roscoelite-carbonate veins commonly cross-cut and locally brecciate Stage I carbonate-base metal style veins and equate to the Type D ore of Fleming et al. (1986). Petrological evidence indicates that a significant amount of gold mineralization mined in the open pit at Porgera occurs in quartz-roscoelite-carbonate veinlets, which cross cut earlier Stage II quartz-carbonate-base metal veins (type A/B of Fleming et al., 1986).

Very localized feldspar porphyry dikes cut Stage I carbonate-base metal veins, but predate the Stage II quartz-roscoelite gold mineralization. These dikes are inferred to represent apophyses of a very high level late stage intrusion, which is also interpreted as the source of metals for Stage II mineralization. The fluidized breccias probably result from the emplacement of these melts at very shallow crustal levels. Based on carbonate isotope data (Richards and Kerrich, 1993), early massive carbonate, which formed pre-, syn- and commonly post-fluidized breccia emplacement, is interpreted to have been deposited by the heating of late Stage I bicarbonate waters (Figs. 7.44, 7.45).

The main episode of mineralization occurs as a spatially and temporally zoned polyphasal vein and vein/breccia system which contains: quartz, roscoelite (vanadium illite/mica), carbonate, minor sulfides and significant gold mineralization. The crystallinity of roscoelite decreases, and the degree of interlayering with smectite increases along the Roamane fault from depth in the west, to shallow levels further east (Fig. 7.45). The roscoelite-smectite mineralogy is indicative of fluid upflow of >200- 250°C in the vicinity of the pre-Stage I feldspar porphyry and cooling in distal outflow zones to 150-200°C. These temperatures are in agreement with the low temperatures (average 155°C) obtained from fluid inclusion data on late Stage II quartz (Richards and Kerrich, 1993).

The roscoelite-bearing veins grade along the Roamane fault from west towards east and early to later in the paragenetic sequence as: quartz-rich, through mixed quartz-carbonate-bearing, to carbonate-rich (Fig. 7.45). This zonation is interpreted to reflect the dominance of hot upwelling fluids in the west, (which deposited quartz upon cooling), grading easterly and at shallow levels, to zones dominated by cool CO_2-rich waters, which resided in the faults/fractures prior to influx of the mineralized fluids, (and deposited carbonates upon heating).

The quartz-rich roscoelite veins are characterized by coarse gold and associated with Ag-tellurides (mainly hessite), whereas the more carbonate-rich veins are characterized by: fine grained gold associated with silver-sulfosalts and sulfides (freibergite, argentite and polybasite), gold-, silver-, and mercury-tellurides (hessite, petzite, calaverite and coloradorite), and local chalcopyrite and hypogene hematite. The carbonate-rich silver-gold veins equate to Type-E ore of Fleming et al., (1986). Ore mineralogy in the carbonate-rich roscoelite veins is locally mercury-rich, reflecting the removal of mercury from the upwelling fluids by cool ground waters. The gold fineness in Stage II veins averages around 800, and is more comparable to deep epithermal/mesothermal systems than epithermal systems (Fig. 4.8). Gold fineness decreases from an average of 850 in quartz-rich veins, to an average of 741 in carbonate-rich veins, and this increase in silver-content of the gold is interpreted to reflect the cooling trend outlined above. Open fractures and cavities are filled by late stage calcite and local anhydrite, which are commonly overgrown by gypsum. It is interpreted that Stage II saline and metal-bearing mineralized fluids were derived from a melt emplaced at very high levels along the margin of the inferred deep feeder stock to the north of the Roamane fault (Fig. 7.23). Mineralized fluids are postulated to have utilised the same structures as the pre-, and post-Stage I feldspar porphyry intrusions. These fluids then migrated from depth beneath the Main Zone along the dilatant portions of the Roamane fault. Mineralization is inferred to have occurred in response to quenching of the hot fluids (from temperatures of >200-250°C to <150-200°C) by the pre-existing, cool, oxidizing, CO_2-rich waters, which resided in the Roamane fault. Metal-bearing fluids may also have migrated south along NNW structures, and into the Roamane fault at depth below the East Zone (Fig. 7.24).

2. Mt Kare, Papua New Guinea

The carbonate-base metal style gold mineralization at Mt. Kare has been discussed above (Section 7.iii.i). Native gold at Mt Kare is associated with quartz-roscoelite-chlorite vein/breccias within: a NS-trending shear (Richards and Ledlie, 1993), fractured competent locally baked sediments, and porphyritic basic/alkaline intrusions which have undergone intense quartz-illite- interlayered illite-smectite -chlorite-carbonate-pyrite alteration. Anomalous vanadium (indicative of roscoelite) was assayed in an intercept of 32 m @ 308 g/t Au (Carpenter Pacific, press release, March 1997). The paragenetic sequence (Fig. 7.46) of vein formation and mineralization in the quartz-roscoelite vein/breccias is:

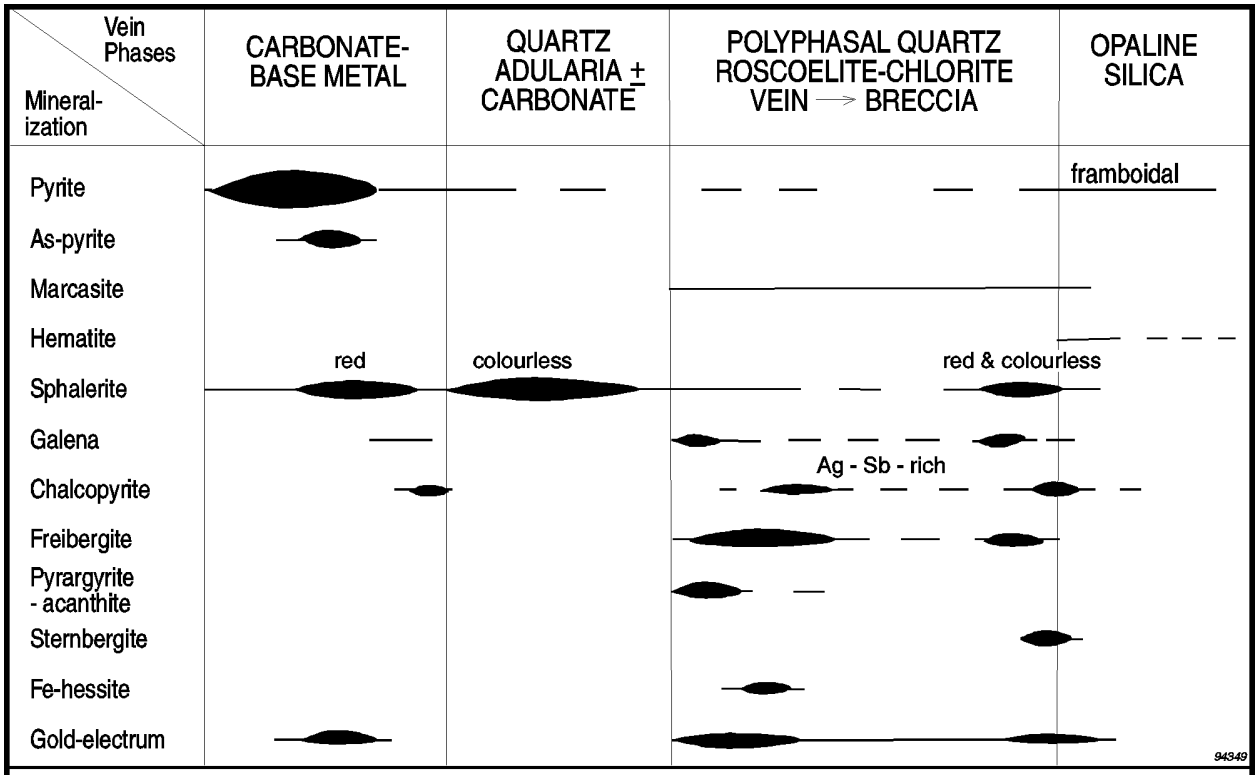

Mt Kare - Paragenetic sequence of vein development and mineralization for the epithermal quartz gold-silver (quartz-roscoelite) event.

FIG. 7.46

Stage I: Carbonate-base metal alteration dominated by: dolomite, pyrite, a dark red (Fe-rich) sphalerite, and lesser galena, As-rich pyrite, and chalcopyrite. High fineness (780-800) gold is intergrown with the dolomite.

Stage II: In places the carbonate is overgrown by banded early colourless sphalerite and later adularia-quartz + carbonate + trace galena.

Stage III: The main phase of mineral deposition comprises: early druzy quartz + roscoelite + chlorite, followed by multiple stage brecciation of earlier veins and fill of the matrix by fine grained quartz/silica + roscoelite-chlorite + carbonate. Abundant native gold occurs throughout the quartz-roscoelite vein/breccia and displays a wide range of fineness (400-870), which decreases during the later stages of deposition. Gold mineralization occurs as electrum deposited with a wide range of Ag-sulfosalts, Ag-sulfides, and tellurides such as freibergite, pyrargarite, acanthite, sternbergite, hessite and stuetzite. The gold is also intergrown with base metal sulfides, mainly colourless sphalerite, galena and an Ag-Sb-rich chalcopyrite. Preliminary fluid inclusion data, in conjunction with

wall rock and vein alteration assemblages, indicate that the coarse quartz-roscoelite was deposited at relatively high temperatures (260-270°C), and brecciation and resealing took place under progressively cooler conditions from around 200-220°C, to as low as 120-140°C. Marcasite in the breccia matrix is indicative of more oxidized conditions during later stage quartz- roscoelite-chlorite deposition.

Stage IV: Late stage fracturing and deposition of colloform banded opaline silica and native gold mineralization occurs in association with specular hematite and framboidal pyrite. The presence of opaline silica is indicative of quenching of the hydrothermal fluids at <100-150°C.

3. Discussion

Similar high gold grade quartz-roscoelite mineralization occurs at both Porgera and Mt Kare in three distinct environments which are also common to other southwest Pacific porphyry-related gold systems (Figs. 7.1, 7.2) as:

1. Refractory gold encapsulated in sulfides occurs in early quartz-sericite/illite-pyrite/arsenopyrite, deposited as a result of the cooling of magmatic fluids by circulating meteoric waters.

2. Later vein/breccias host base metal sulfide-carbonate typically at fractured intrusion margins, and within contact baked sediments. Mineral deposition here results from the mixing of upwelling mineralized fluids with descending CO_2-rich ± sulfate waters. Native gold occurs as inclusions in pyrite/base metal sulfides and is intergrown with carbonate.

3. High grade gold in quartz-roscoelite + chlorite with silver-rich sulfides and tellurides mainly occurs in dilational tension vein/breccias. Mineral deposition results from the quenching of hot mineralized fluids by cool oxidizing ground water. The presence of the vanadium mica/illitic, roscoelite, rather than the more typical potassic-rich illitic clay, is a reflection of the basic/alkaline nature of the host intrusions (Richards and Ledlie, 1993).

Late stage high grade epithermal gold mineralization occurs in association with illite minerals, tellurides, Ag-rich base metal minerals, and local hematite, in other southwest Pacific rim porphyry-related gold deposits in addition to Porgera and Mt Kare (e.g., bonanza grade gold with roscoelite and Au-Ag tellurides at Emperor, Fiji; Ahmad et al., 1987: gold with tellurides, hematite and copper sulfides at Maniape, Kerimenge, Tolukuma, in Papua New Guinea; and Cracow in eastern Australia). Illitic and chloritic clays are common within shallow levels of porphyry-related gold systems (e.g., Maniape, Tolukuma, Cracow), whereas vanadium-mica/illite (roscoelite) is restricted to environments of basic/alkaline intrusions (e.g., Porgera, Mt. Kare, Emperor; Richards and Ledlie, 1993).

2. PERIPHERAL TO INTRUSION-RELATED MINERALIZATION

1. Thames goldfield, New Zealand

The Thames goldfield (1.4 M oz Au; Merchant, 1986) in New Zealand occurs within an epithermal vein system derived from the adjacent Ohio Creek copper-gold porphyry (G. Corbett, unpubl. report, 1989). Gold was mined from quartz-sulfide gold ± copper style reefs within volcanic rocks adjacent to the Ohio Creek Porphyry (e.g., Kaiser Reef) and from bonanza ore shoots in the vicinity of Thames township (Merchant, 1986).

The Ohio Creek copper-gold porphyry has been emplaced into a dilational jog formed by dextral movement, as a result of oblique convergence, on elements of the Hauraki graben fault, which separates the Coromandel

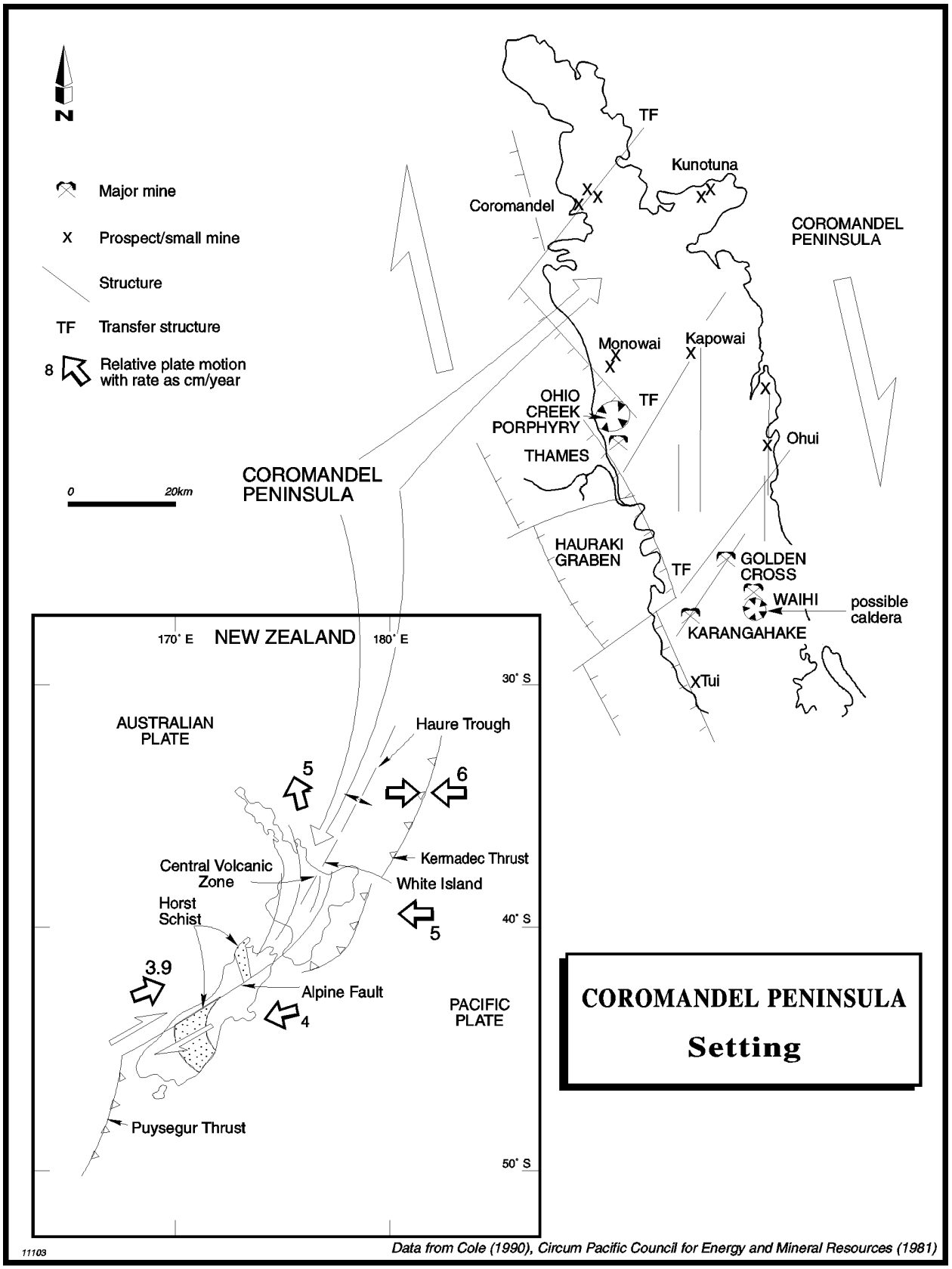
N
Major mine
X Prospect/small mine
Structure
TF Transfer structure
8 Relative plate motion with rate as cm/year
0 20km
TF
Kunotuna
Coromandel
COROMANDEL PENINSULA
Monowai
Kapowai
OHIO CREEK PORPHYRY
TF
THAMES
Ohui
COROMANDEL PENINSULA
HAURAKI GRABEN
TF
GOLDEN CROSS
WAIHI
possible caldera
KARANGAHAKE
Tui
170° E
NEW ZEALAND
180° E
30° S
AUSTRALIAN PLATE
Haure Trough
5
6
Kermadec Thrust
Central Volcanic Zone
White Island
Horst Schist
40° S
5
3.9
Alpine Fault
4
PACIFIC PLATE
Puysegur Thrust
50° S
COROMANDEL PENINSULA
Setting
11103
Data from Cole (1990), Circum Pacific Council for Energy and Mineral Resources (1981)

FIG. 7.47

Peninsula from the Hauraki Gulf (Fig. 7.48, 7.49). This movement has imparted a dilational character to the NE-trending subsidiary faults which host a corridor of slickensided faults and local quartz reefs which extend from the Thames goldfield for 3 km subjacent to Lookout Rocks (Figs. 7.48, 7.49). The Ohio Creek copper-gold porphyry which was investigated by scout drilling in 1978-81 (Merchant, 1986), is partly rimmed by the Lookout Rocks shoulder of barren high sulfidation alteration preserved several hundred metres above creek level (Section 6.ii.b). Detailed mapping defined a zonation in the high sulfidation alteration around feeder structures preserved as breccia zones which are roughly contiguous with the NE-trending quartz reefs (above), and which host the Thames gold mineralization (Figs. 6.7, 7.48; G. Corbett, unpubl. report, 1989).

Merchant (1986) suggests there has been a considerable time gap between the overprinting of early high temperature porphyry copper-gold mineralization by the later lower temperature epithermal gold mineralization at Thames, with which he associates the high sulfidation alteration at Lookout Rocks. However, the presence of andalusite indicates that the Lookout Rocks alteration was derived from a hot fluid venting directly from a porphyry source, and is not of an epithermal acid sulfate origin (T. Leach, unpubl. data., 1989; Section 6.ii.b).

Ore fluids derived during the late degassing of the Ohio Creek Porphyry, or possibly a later andesite intrusion, are inferred (G. Corbett, unpubl. report, 1989; T. Leach, unpubl. data) to have flowed laterally along the NE-trending dilational structures and formed the locally brecciated quartz reefs. Common slickensided faults, and brecciation, attest to the continued activity of the fault controlled quartz veins. Bonanza gold ore at Thames occurs at the intersections to the NE quartz reefs with NS cross structures termed "flinties" by the old miners (Fraser, 1910; Fig. 7.48). Chemical analyses (Fraser, 1910) are consistent with the field identification of the flinties as fault fill chalcedonic quartz and pyrite. Gold deposition took place by cooling and dilution as the ore fluid mixed with ground waters flowing down the cross structures. Chalcedonic quartz is indicative of the rapid cooling and the 670 gold fineness (Fraser, 1910) of epithermal conditions.

2. Emperor gold mine, Fiji

The Emperor gold mine lies on the margin of the 6 km wide Tavua caldera, Viti Levu, Fiji (Fig. 1.2). Eaton and Setterfield (1993) cite a strong spatial and probable genetic relationship between epithermal gold mineralization and porphyry copper-gold intrusions (including subjacent barren high sulfidation alteration), within the Tavua caldera.

The Tavua caldera is one of several porphyry-related gold occurrences which lie along a NE trending extensional Viti Levu Lineament (Hamberger and Isacks, 1988), which was formed parallel to a major offshore transform structure. Epithermal gold mineralization occurs mostly in the competent rocks outside the caldera margin at the intersection with the NE lineament and the WNW-trending Nasivi shear zone. Ore is hosted both in steeply dipping shears and in 20° to 45° dipping faults (termed flatmakes) formed as either: low angle normal faults commonly sub-parallel to lithological contacts (Anderson and Eaton, 1990), during caldera subsidence (Eaton and Setterfield, 1993; Setterfield et al., 1991) or reactivated thrusts (Begg et al., 1997).

The following description of the alteration and mineralization at Emperor has been taken from Ahmad et al. (1987), Anderson and Eaton (1990) and Kwak (1990).

Alteration within the multiple fill basalt-hosted lode structures (flatmakes) occurs as: adularia, sericite, roscoelite, dolomite, ankerite, sulfide and telluride assemblages, and which grade to selvages of ankerite, dolomite, quartz-chlorite, K-feldspar, and peripheral propylitic alteration assemblages of chlorite, tremolite, epidote, ankerite, pyrite and magnetite. Mineralization occurs in thin sulfide-rich bands which alternate with thicker barren quartz bands. Late stage quartz and final calcite fill the lode structures.

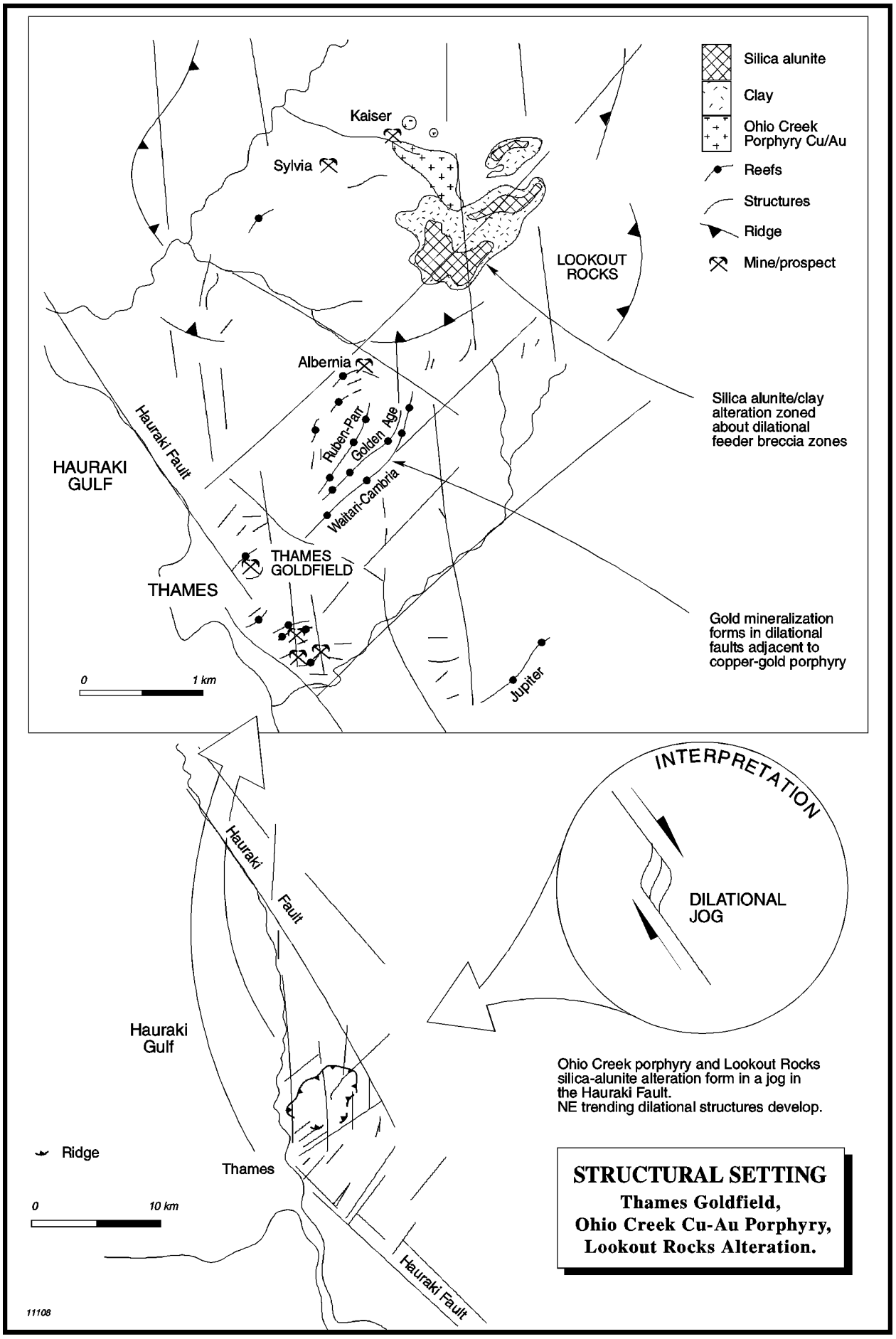
Silica alunite
Clay
Ohio Creek Porphyry Cu/Au
Reefs
Structures
Ridge
Mine/prospect
Kaiser
Sylvia
LOOKOUT ROCKS
Albernia
Ruben-Patt
Golden Age
Waitari-Cambria
Hauraki Fault
HAURAKI GULF
THAMES GOLDFIELD
THAMES
Jupiter
0
1 km
Silica alunite/clay alteration zoned about dilational feeder breccia zones
Gold mineralization forms in dilational faults adjacent to copper-gold porphyry
INTERPRETATION
DILATIONAL JOG
Hauraki Fault
Hauraki Gulf
Ridge
Thames
0
10 km
Hauraki Fault
Ohio Creek porphyry and Lookout Rocks silica-alunite alteration form in a jog in the Hauraki Fault.
NE trending dilational structures develop.
STRUCTURAL SETTING
Thames Goldfield,
Ohio Creek Cu-Au Porphyry,
Lookout Rocks Alteration.
11108

FIG. 7.48

The sulfide bands comprise quartz, dolomite, ankerite, adularia and roscoelite gangue minerals and pyrite, arsenopyrite, marcasite and rare base metal sulfide (low Fe-sphalerite, galena, chalcopyrite and tennantite-tetrahedrite) ore minerals. Various Ag-sulfosalts occur at depth in these bands, whereas Au/Ag-tellurides predominate at shallower levels. Gold occurs as: submicroscopic grains in pyrite and arsenopyrite, in gold/silver-tellurides deposited the early stages of mineralization, and in the native form associated with hessite and petzite in later sulfide bands.

Fluid inclusion analyses on vein quartz are indicative of cooling between the deposition of early (around 300°C), and late veins (200°C), although salinity remained stable at around 5.5-6.2 equivalent weight percent NaCl. Mineralization is inferred from thermodynamics of the various ore phases to have occurred around 200-250°C. Although fluid inclusion analyses indicate that the barren quartz was deposited from a boiling fluid, isotope data suggests that the carbon and sulfur in the mineralized sulfide bands were derived from waters within local sediments, and that the carbon in the late calcite may have had a magmatic origin. Kwak (1990) inferred that Au, Ag, Te, and other metals were derived from a neutral, relatively reduced, bisulfide-rich fluid at temperatures near 300°C, and associated with alkali intrusions. Mineralization is interpreted (Kwak, 1990) to have resulted from the mixing of this magmatic fluid with an acidic, oxidized solution with a significant meteoric component, at around 150°C. The occurrence of tellurides with gold mineralization at Emperor (and elsewhere in the southwest Pacific) is indicative of an influx of volatile-rich magmatic fluids (Cooke and McPhail, 1996).

3. West Prampus, Kelian, Indonesia

The Kelian carbonate-base metal gold deposit has been described in Section 7.iii.i. A model of magmatic fluid flow is apparent from alteration zonations (van Leeuwen et al., 1990). Quartz-sulfide (pyrrhotite-pyrite + magnetite) veins at depth to the northeast of the system, in the vicinity of the Runcing maar volcano/diatreme breccia, progressively grade to the south and higher levels through carbonate-base metal gold mineralization at East Prampus (Figs. 7.19, 7.20, 7.21), and to local gold-bearing epithermal style quartz veins at West Prampus.

Veins dominated by carbonate + base metals occur around a buried andesite in East Prampus, whereas quartz coexists with carbonate-base metal sulfides in veins around the east contact of the central andesite (Fig. 7.19). However in the West Prampus veins, both carbonates and base metal sulfides are subordinate to quartz in veins comprising early chalcedony, colloform to crustiform banded quartz, and minor thin black sulfide bands, characteristic of epithermal quartz gold-silver systems. Fluid inclusion analyses indicate that these epithermal style veins formed at considerably lower temperatures (198-240°C), than the host carbonate-base metal sulfide-bearing quartz veins (290-304°C).

4. Bonki Creek, Maniape, Bilimoia District, Papua New Guinea

The Maniape Prospect has been described previously, as an example of a shallow (or epithermal) crustal level carbonate-base metal gold system (Figs. 7.10, 7.37; Section 7.iii.i; Corbett et al., 1994b). Mn-carbonates are crustiform or colloform banded similar to quartz in gold-silver vein systems. Cool temperatures of deposition (200-260°C) are apparent from the fluid inclusion analyses of carbonates and sphalerite, and these are consistent with the moderate gold fineness (averages range 685-770). In the northern portion of the vein system, quartz-chloritic clay-sulfide deposition, characteristic of intrusion-related epithermal quartz gold-silver systems, alternates with carbonate-base metal bands. Further south at Bonki Creek, quartz-chloritic clay-sulfide deposition occurs to the exclusion of the carbonate-base metal sulfide veins (Fig. 7.37). Sulfide mineralization in the quartz-chloritic clay veins is characterized by Ag-rich minerals such as Ag-sulfosalts (freibergite, acanthite-argentite, pearceite-polybasite), Ag-rich sphalerite (with up to 17% Ag) and native silver. Gold mineralization occurs as low fineness electrum (average 658), and is commonly intergrown with silver minerals and hypogene hematite.

We interpret (Corbett et al., 1994b) that the ore fluid was derived from an intrusion source at depth beneath Arakompa and flowed southward along the Maniape structure (Fig. 7.10, 7.49). This mineralized fluid mixed alternately with CO_2-rich waters, to form carbonate-base metal gold veins, and with oxidizing ground water to form quartz-chloritic clay-sulfide veins, with local high grade gold-silver mineralization. The CO_2-rich waters dominated to the north, in zones more proximal to the fluid source, whereas the cool ground water dominated to the south, in a distal fluid outflow setting.

3. ASSOCIATED WITH ADULARIA-SERICITE EPITHERMAL GOLD-SILVER SYSTEMS

This group of epithermal quartz gold-silver systems represent the most obvious transitions to the adularia-sericite epithermal gold-silver deposits (Section 8). The setting within magmatic arcs and apparent magmatic source for gold mineralization and breccias distinguishes this group of deposits from adularia-sericite epithermal gold-silver deposits which typically form in back-arc environments (Sillitoe, 1993). As with the adularia-sericite deposits, the quartz and adularia are inferred to have been deposited from circulating meteoric waters within a dilational structural environment.

1. Tolukuma, Papua New Guinea

The Tolukuma gold-silver deposit occurs in remote mountainous terrain about 100 km from Port Moresby, Papua New Guinea (Fig. 1.2). It was identified during regional stream sediment prospecting by Newmont Proprietary Limited in 1986, and evaluated by drill testing which established a resource estimated at 654,000 oz Au (Langmead and McLeod, 1990, 1991). Ownership passed to Dome Resources in 1993, and mine development began in 1995 in an operation which will be entirely helicopter supported, without an access road. It is planned to initially exploit a measured resource of 0.44 Mt at 17 g/t Au and 46 g/t Ag, in the central portion of the vein system and exploration of the southern Gulbadi vein is proceeding (Corbett et al., 1994c, Semple et al., 1995).

Structure

Several quartz gold-silver veins occur on the margin of a circular feature (Langmead and McLeod, 1990, 1991) which may have originated by volcanoplutonic collapse. Tolukuma is localized near the intersection of the circular feature and a graben-like contact between basement Cretaceous Owen Stanley Metamorphics and the overlying Pliocene Mt. Davidson Volcanics (Fig. 7.50). Shallow level, dacitic to basaltic andesite, porphyritic plugs and dikes have been emplaced along the faulted contact between the basement phyllite and volcanics, and locally these extend as dikes into the basement rocks. The Tolukuma Hill portion of the vein occurs mostly within volcanic rocks while dacite intrusions and contact breccias host ore at Gulbadi.

Pre-mineral roughly NNW trending graben and NW trending structures were reactivated as the primary ore hosts (Fig. 7.50). Northwest-trending splays to the dipping portions of the graben structures locally host higher grade ore (Fig. 7.50). The dip of the graben varies from steep in the northern segment, to a moderate easterly dip in the Tolukuma Hill area. As a result of the structural re-activation of the graben, the steeply dipping portion extends south to form an ore-hosting NNW trending hanging wall split, above the dipping graben structure (Fig. 7.51).

Northeast-trending faults are evident as pre-, syn- and post- mineralization structures, and these may also be deep basement structures which have localized the emplacement of both the porphyry and milled matrix fluidized breccias (e.g., Tolimi fault). Northeast faults at Gulbadi may have created local high grade zones in dilational jogs, and offset the veins in a manner similar to domino structures (Fig. 7.50, Section 3.iv.b.3). Milled

matrix fluidized breccias are exposed in drill core from the Tolukuma Hill-Tolimi area, but surface exposures are

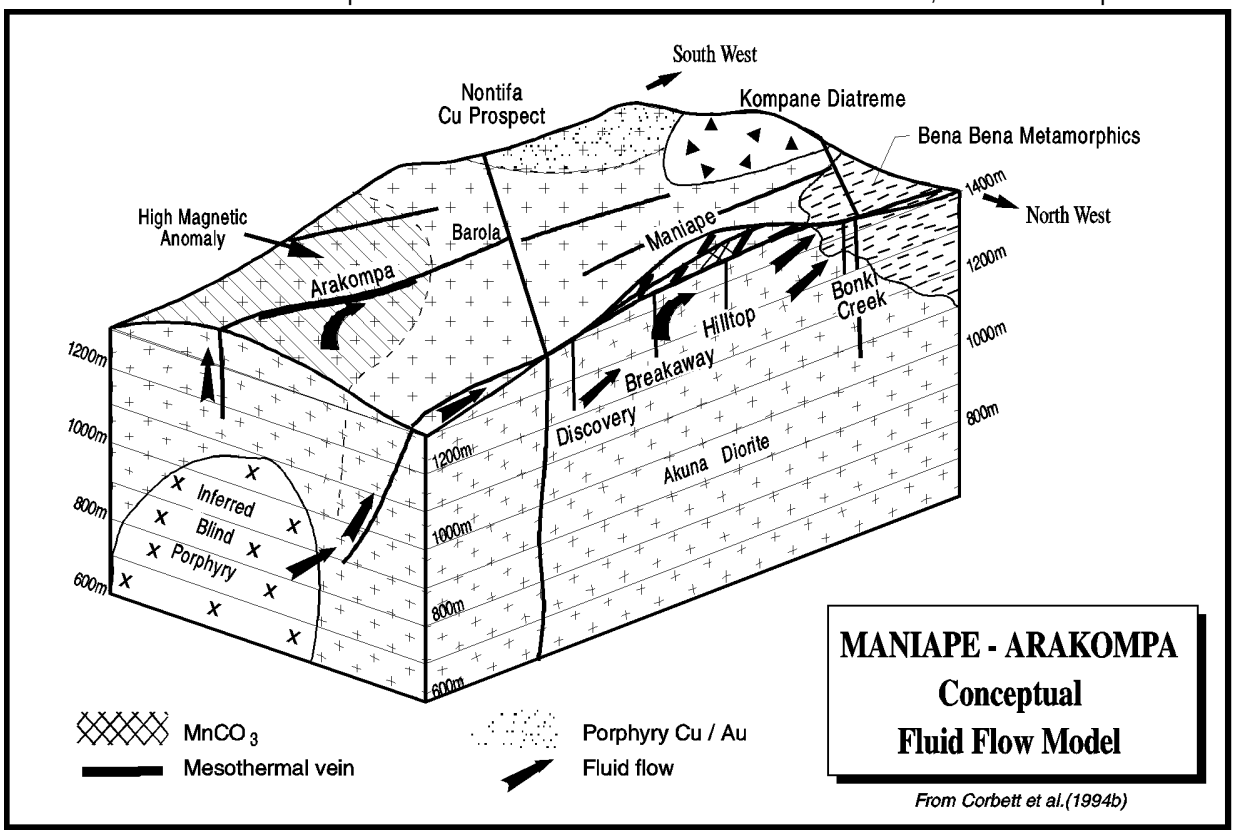

FIG. 7.49

obscured by the shallowly dipping Tolimi fault plane. Breccias comprise variable contents of volcanic (possibly including intrusion) and phyllite fragments within a milled matrix, of mainly phyllite and lesser volcanic material. Volcanic fragments display relict propylitic and later clay alteration and fine disseminated pyrite abounds in the matrix. Many occur as fluidized breccia dikes and locally grade to peripheral crackle breccias. Bedded tuffaceous layers containing accretionary lapilli (tuffisite) are reminiscent of phreatomagmatic breccias typical of diatreme complexes, to which these breccias are genetically linked.

The Tolukuma vein system is mineralized over about 500 m and probably continues as the Gulbadi vein adding an extra 600 m strike length to the south (Fig. 7.50). The Tolukuma vein fills a hanging wall split formed in the Tolukuma Hill area above the dipping graben structure (Fig. 7.51). The 120 vein is a pre-mineralization NW structure which has become dilational during mineralization (Fig. 7.50). High grade ores occur in NW trending splays adjacent to the main veins.

Alteration and mineralization

Four stages of alteration and mineralization are recognised at Tolukuma (Corbett et al., 1994c; Fig. 7.52).

Stage I: Milled matrix fluidized (phreatomagmatic) breccias, and fine grained pyritic, and chloritic breccias are precursors to the mineralization.

Stage II: Early veins comprise colloform to crustiform banded quartz-adularia or fine/coarse quartz, which locally alternates with wide bands of quartz pseudomorphing bladed calcite. Banded quartz + illite is transitional to a Stage III event.

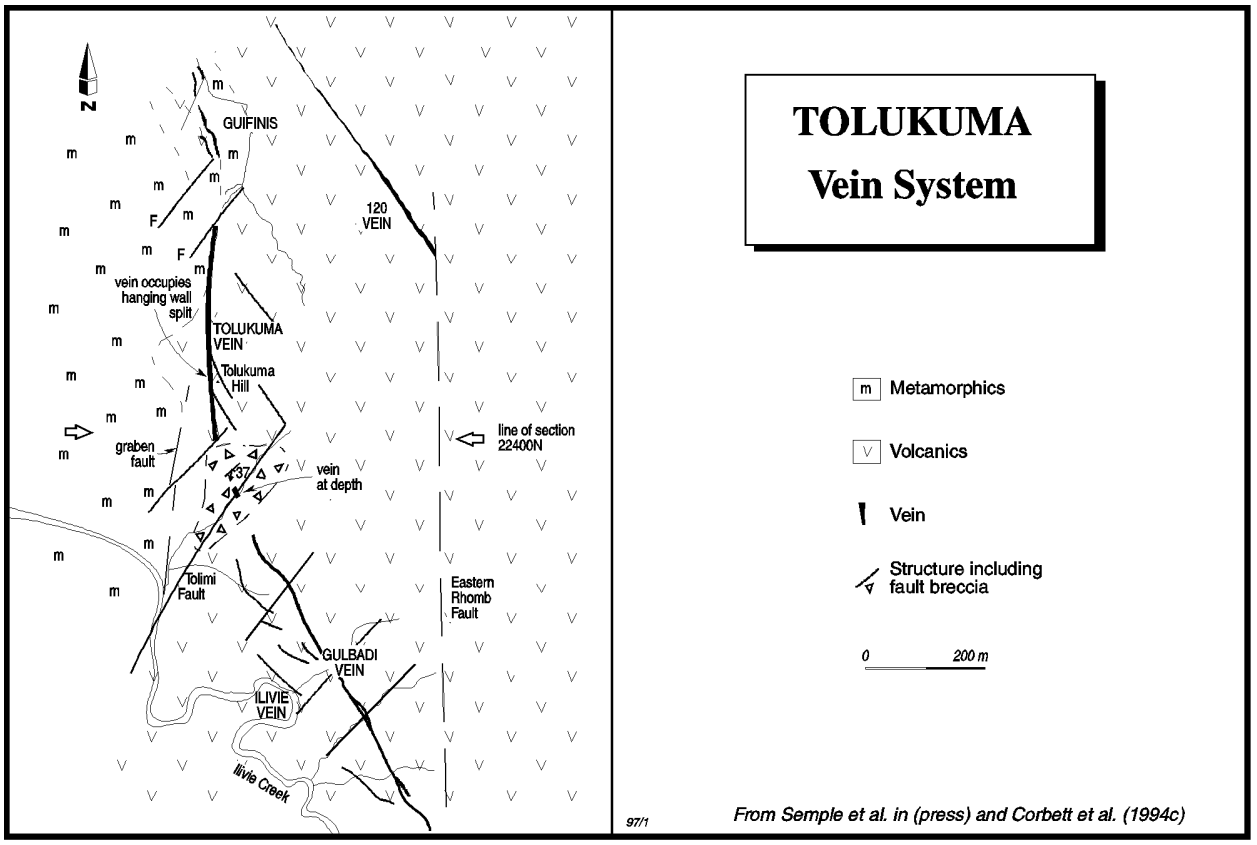

FIG. 7.50

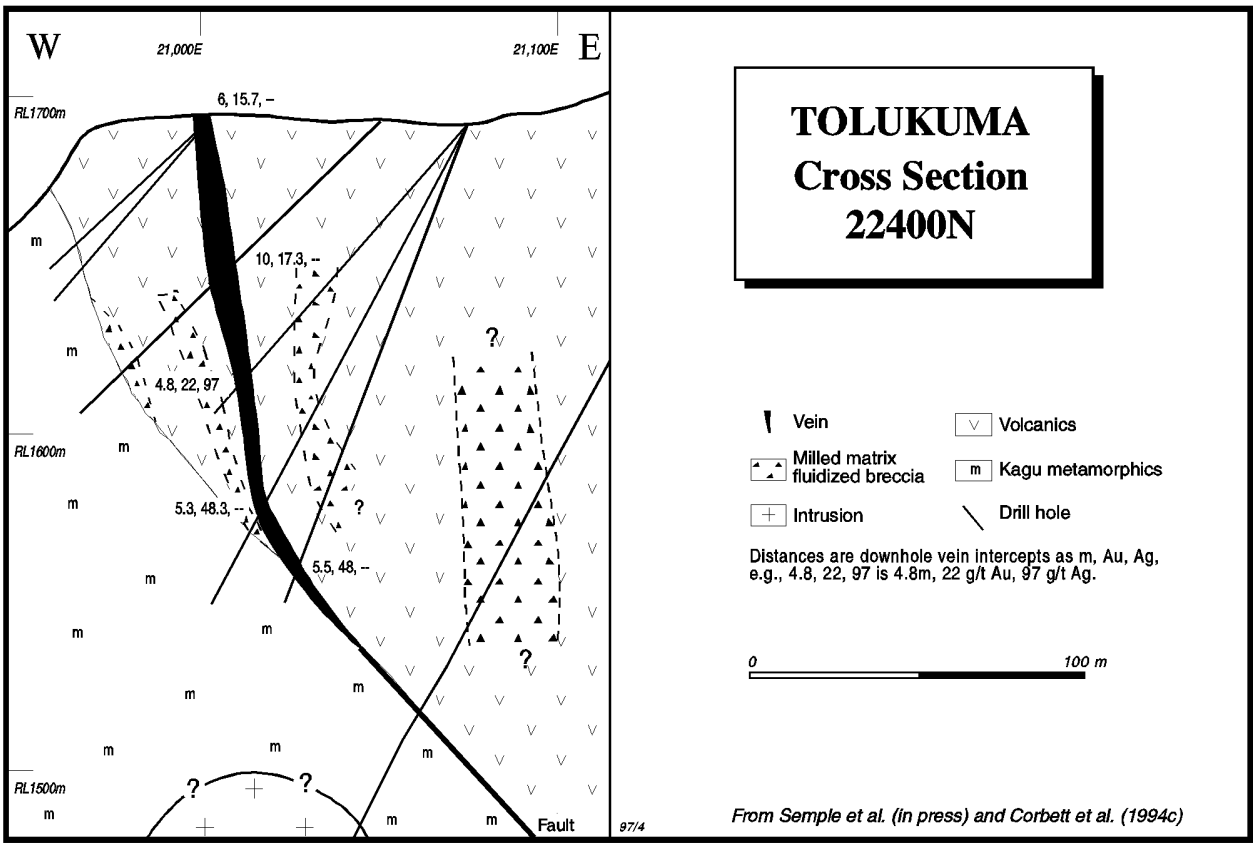

FIG. 7.51

Stage III: Veins of colloform banded fine to coarse quartz which alternates with thin, dark, sulfide bands overprint the Stage II veins. Quartz-clay (chlorite, smectite and kaolin) alteration occurs within fractures, thin breccia zones, and cutting earlier banded veins.

Stage IV: Late- to post-mineral kaolinite-siderite-pyrite/marcasite and chalcedony-quartz occur as crustiform banded veins, and fill cavities. Stibnite is common at lower levels of the 120 vein and in the Gulbadi vein.

The sequence of alteration and mineralization illustrates the progressive evolution of the hydrothermal system. Initial intrusion-style phreatomagmatic breccias (Stage I) preceded early boiling of the hydrothermal system (Stage II), progressive mixing of the hydrothermal fluid with surficial condensate and oxygenated ground waters (Stage III), and collapse of the system with draw down of CO_2-rich waters (Stage IV). Average homogenisation temperatures from fluid inclusions in coarse quartz are 230-240°C. However, filling temperature variations between individual bands in a single vein are indicative of a cyclic sequence of heating and cooling, generally with variations of around 5-15°C, although 55-60°C have been identified. Reversal in homogenisation temperatures were identified in samples at depth in the Gufinis vein to the north, indicative of fluid outflow in that direction. The vein-forming fluids were very dilute, typically around 0-2 wt percent NaCl. Anomalously higher salinity (>2 wt % NaCl) fluids were encountered at shallow levels in veins under Tolukuma Hill (below).

Sulfides, which make up a relatively small proportion (<2-3 %) of the veins, generally occur in thin dark sulfide bands, and locally cross-cut fracture/breccia zones. Pyrite and arsenopyrite dominate within Stage I breccia and Stage II banded veins, whereas marcasite and stibnite are common in the Stage IV veins. Base metal sulfides are mainly confined to Stage III sulfide bands which exhibit a depositional sequence of: pyrite --> sphalerite --> galena --> chalcopyrite --> tennantite. The tennantite, commonly as the Ag-rich mineral freibergite, deposition and other Ag-sulfosalts, Ag-sulfides and native silver, occurred during the Stage III quartz-clay-carbonate vein development, and extended into Stage IV siderite-kaolinite veins. Sulfosalts, including proustite-pyrargarite, polybasite-pearceite and friebergite, are Cu- and Sb-rich in Stage II veins and As-Ag-rich in Stage III bands. Although no separate telluride minerals have been described from Tolukuma, a number of Pb and Cu sulfosalts contain appreciable amounts of tellurium.

Gold occurs almost exclusively as electrum, although some Au-Ag sulfides have been identified. While most electrum is confined within thin Stage III sulfide bands/breccias associated with quartz, clay and/or carbonate, some is locally intergrown with Stage II adularia and fills cavities in quartz after bladed carbonate. The electrum is mostly free, although it locally occurs as inclusions in pyrite, Ag-sulfosalts, chalcopyrite and rarely galena. The fineness of gold at Tolukuma ranges from 597 to 771 (average 686), and Stage II electrum is more Au-rich (average fineness of 730) than Stage III electrum (average fineness of 671).

The Tolukuma gold-silver deposit displays several features typical of the shallow, epithermal levels within an intrusion-related hydrothermal system. The fluidized breccias have tapped the top of the magma source and focused fluids into pre-existing structures in the south Tolukuma Hill - Tolimi region (Figs. 7.50, 7.51, 7.53). The hydrothermal fluids mushroomed to shallow levels within dilational structures at Tolukuma Hill, to produce lateral outflow south along the Gulbadi fault, and north towards Gufinis, and so gold grades do not persist to depth (Fig. 7.53). Initial quartz-adularia-bladed calcite veins formed during a phase of extensive boiling and local mixing with surficial fluids. Subsequent gold mineralization resulted from the mixing, of cool, dilute ground water and local CO_2-rich water, with inferred magmatic fluids. Bonanza gold grades at Tolukuma Hill formed in sulfide bands and breccias, adjacent to the fluid upflow at the margin of the milled matrix fluidized (phreatomagmatic) breccias (Fig. 7.53) and within the hanging wall split (Fig. 7.51), which provided an enhanced medium of fluid flow, and facilitated the rise of high salinity magmatic fluids to an elevated setting.

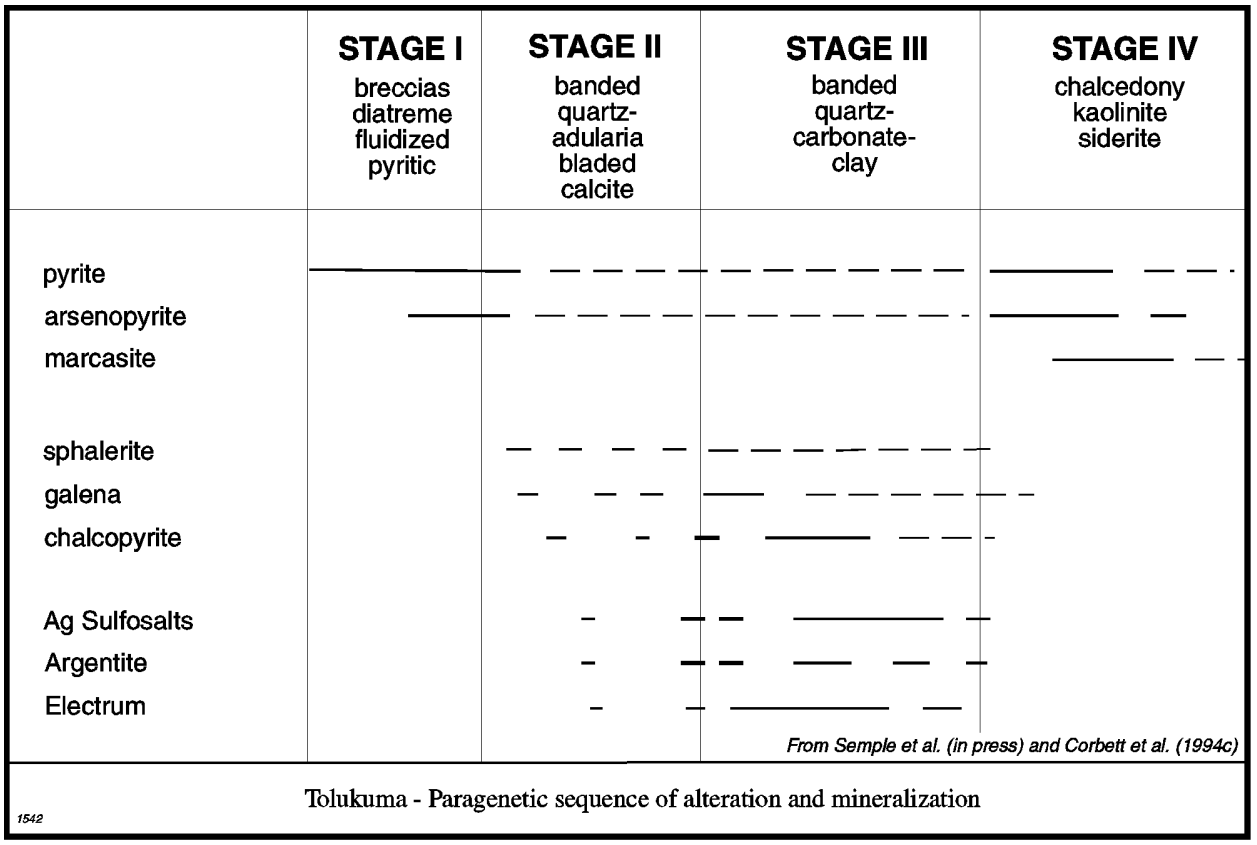

Tolukuma - Paragenetic sequence of alteration and mineralization

FIG. 7.52

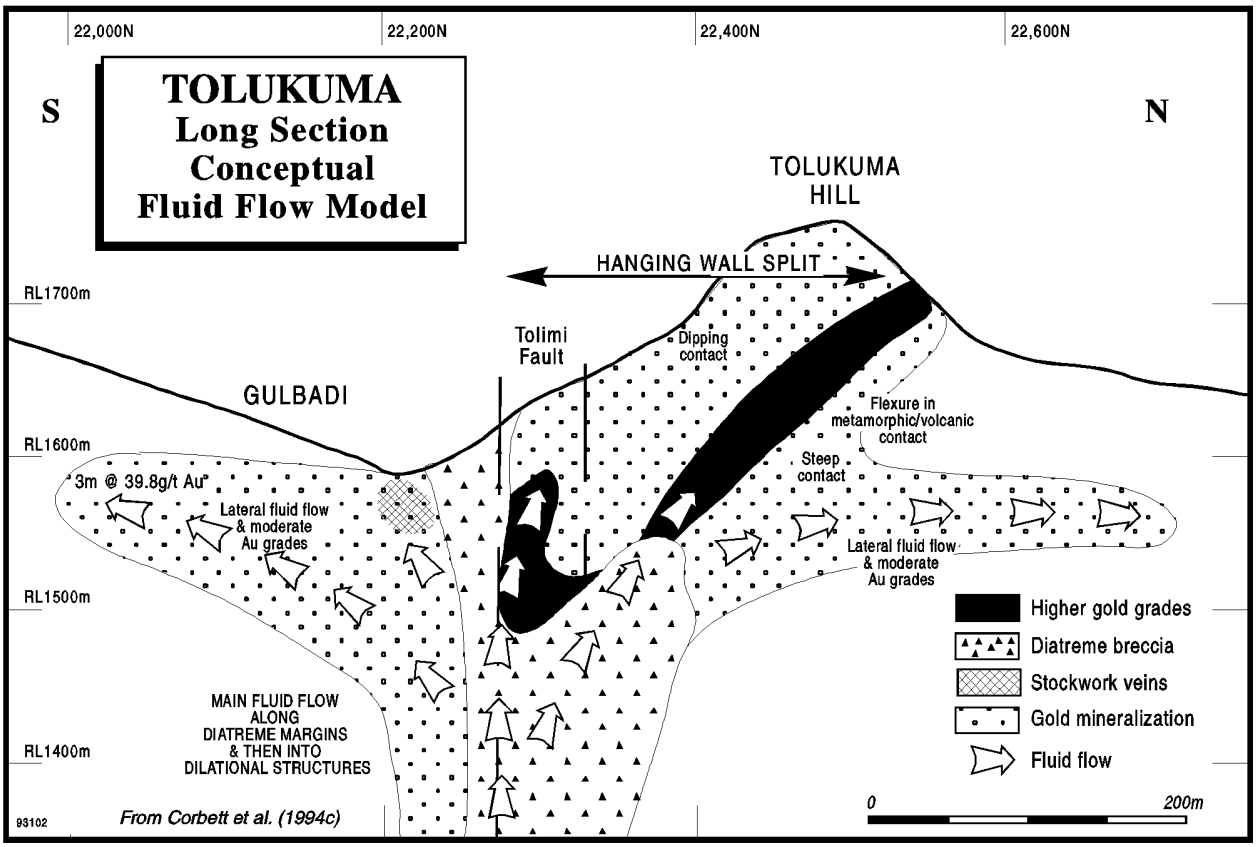

FIG. 7.53

2. Cracow, eastern Australia

The Cracow goldfield is hosted within the Early Permian Camboon Andesite on the eastern margin of the Bowen Basin (Worsley and Golding, 1990; Cracow Mining Venture Staff et al., 1990). Regional geological mapping suggests that an andesitic volcanic centre may lie in the vicinity of the mine (King, 1993). Rhyolite dikes, which intrude the andesite sequence, and a diatreme breccia complex (Sedimentary Holdings, press release, 1995), are indicative of a later and more felsic phase of magmatism. Much of the mineralization was originally obscured by the Jurassic Precipice Sandstone, which still caps the mine area (Fig. 7.54). Open pit and underground operations are concentrated on the Golden Plateau vein system, with minor open pit mining at Golden Mile and the Central Extended region of the White Hope lode (Fig. 7.54). Past production and remaining reserves in the Cracow goldfield are close to 1 million ounces of gold. Although the vein system is essentially quartz-adularia (adularia-sericite epithermal gold-silver) in character, the closer magmatic association places Cracow in the epithermal quartz gold-silver group of deposits.

The Golden Plateau vein system from which most of the Cracow gold production has come, is localized within a roughly EW trending sigmoidal, dilational jog formed by sinistral movement on the constraining major NNW regional structures. These include the faulted contacts between the Back Creek Group and the Camboon Andesite, and the Camboon Andesite and the Torsdale Beds (Fig. 7.54). High grade ore shoots are localized at the intersection of the dilatant EW fissure vein and roughly NS-trending structures, which may have tapped an intrusion at depth. Some also appear to have been active after the mineralizing event. NE transfer structures may have localized a magmatic source in the vicinity of the Cracow goldfield.

Mineralization at Cracow occurs within well banded quartz-adularia veins and breccias. The style of veins varies (Fig. 7.54) from: mainly carbonate-rich in the north and west (e.g., Rose's Pride, Klondike), to banded quartz-adularia (e.g., White Hope, Golden Plateau, Golden Mile), and to quartz-base metal sulfide veins in the southeast (e.g., Dawn, Big Gun). This distribution is interpreted to indicate: shallow levels of erosion to the northwest where fluids were dominated by descending CO_2-rich waters, through to deeper levels of erosion in the southeast, dominated by base metal sulfides deposited from more saline magmatic-derived fluids.

Four stages of vein development and associated mineralization have been recognised in the Cracow goldfield:

I. Quartz-adularia-carbonate veins associated with propylitic alteration.
II. Quartz-chlorite/clay-sulfide veins.
III. Banded (polyphasal) veins of quartz + adularia + calcite + trace sulfides.
IV. Late crustiform quartz + calcite veins.

Stages II and III represent the major events of vein formation, are the only mineralizing events, and are locally contemporaneous.

High grade gold mineralization is associated with the Stage II quartz-chlorite/clay-sulfide event, which occurs (Fig. 7.54) as: rare thin sulfide bands alternating with massive to colloform banded carbonate (e.g., Rose's Pride, Klondike), rare thin dark greenish bands and breccia zones in veins dominated by crustiform to colloform banded quartz-adularia (e.g., Golden Mile, Central Extended/White Hope), low tonnage high gold grade ore shoots and flatmakes (e.g., Golden Plateau), and the matrix to quartz vein/breccias (e.g., Dawn). Sulfides are dominated by pyrite and colourless sphalerite, with minor chalcopyrite and galena. Gold occurs as a high fineness electrum (average 780; Fig. 4.8) and rarely in Au-Ag tellurides (Barber, 1992), which are intergrown with both base metal sulfides and chlorite. Electrum is commonly associated with telluride minerals (mainly hessite, and trace altaite; Worsley and Golding, 1990). Sphalerite from Stage II veins at Central Extended and White Hope was deposited from dilute fluids (< 1-2 wt % NaCl equiv) at moderately high temperatures

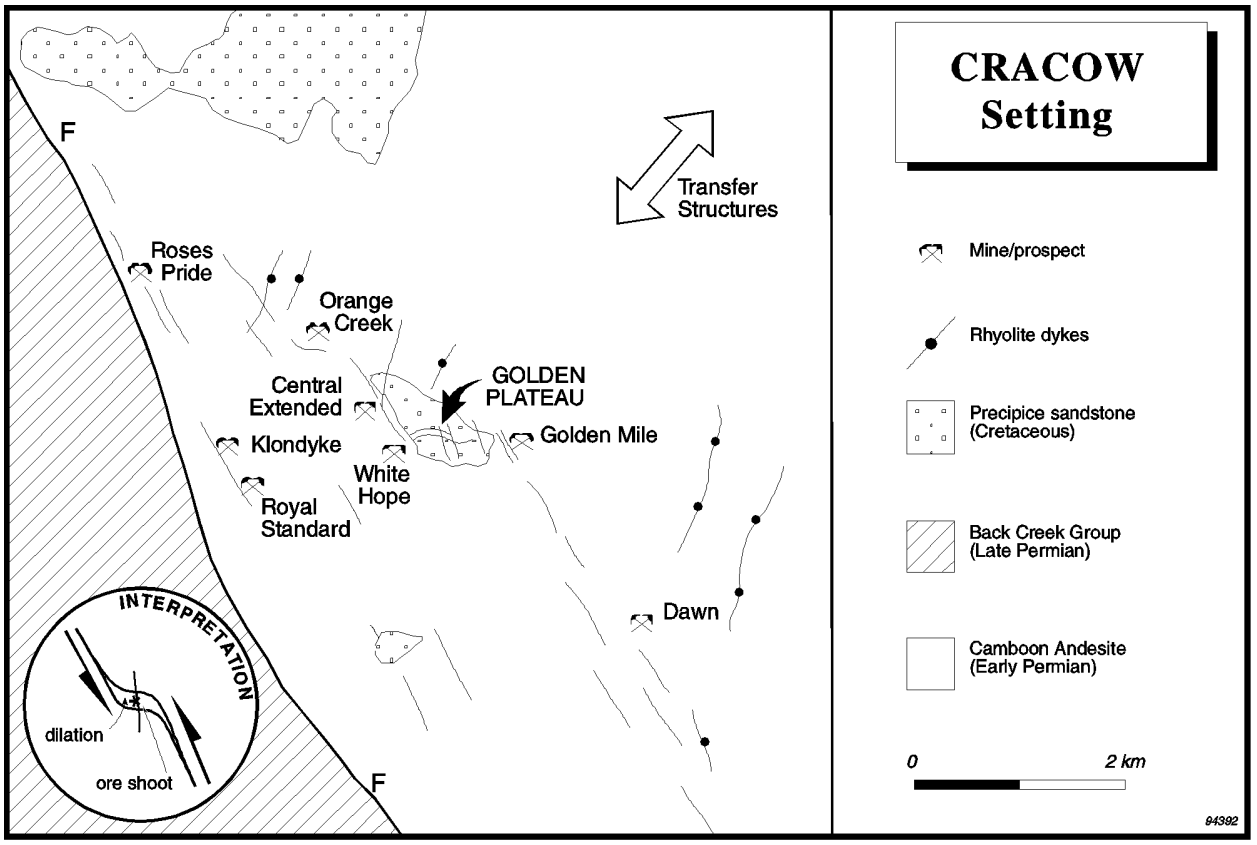

FIG. 7.54

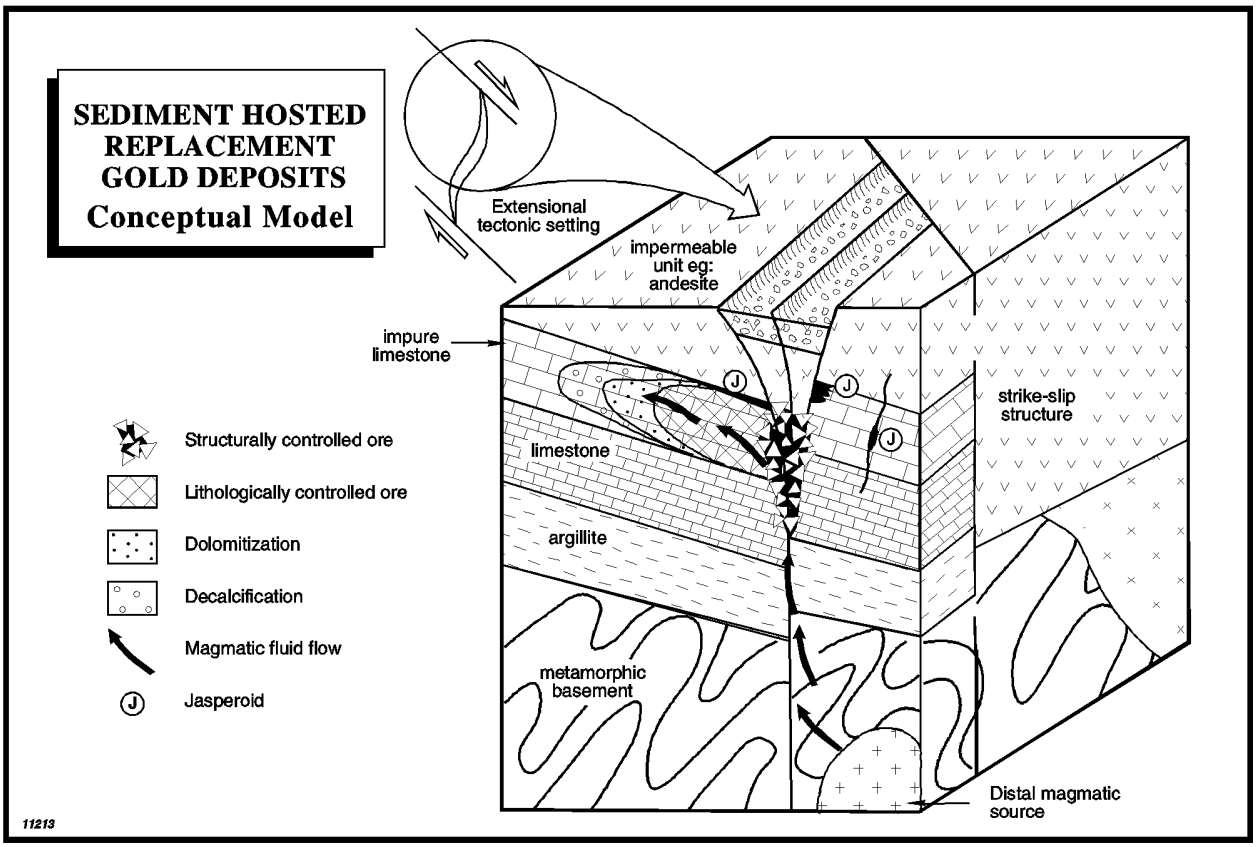

FIG. 7.55

(220-270°C; T. Leach, unpubl. data, 1994).

Stage III quartz-adularia, as crustiform-colloform bands and polyphasal breccia zones incorporating earlier vein clasts, constitutes the bulk of most veins. Adularia is a deep orange colour and dominates in earlier veins. Quartz dominates over adularia in late stage veins, and coarse crystalline, locally amethystine, quartz fills cavities and fractures. The quartz-adularia event contains some of the low grade gold mineralization as electrum intergrown with the gangue minerals (Worsley and Golding, 1990). Fluid inclusion analyses on Stage III quartz from Golden Plateau indicate that deposition occurred under periodic two phase (boiling) conditions, at relatively low temperatures (222-245°C; T. Leach, unpubl. data, 1987) and salinities (<1-2 wt % NaCl; Dong, 1992).

At Golden Plateau the quartz-adularia veins cut andesitic volcanics which have undergone propylitic alteration to an assemblage of quartz-chlorite-carbonate-adularia + epidote + laumontite, and are overprinted by quartz-illitic clay + chlorite + carbonate alteration, adjacent to veins (T. Leach, unpubl. data, 1987). Illitic clays grade from higher temperature illite at depth, through interlayered illite-smectite to smectite + kaolinite at shallow levels.

It is proposed that the quartz-adularia-carbonate veins were deposited from dilute circulating meteoric fluids and associated gold contributes to some low grade gold mineralization. The presence of high grade gold mineralization in chlorite-quartz veins, breccias and bands with tellurides and base metal sulfides suggests that this mineralization is related to a fluid with a significant magmatic component, albeit dilute.

It is postulated that high level felsic stocks at Cracow were emplaced at shallow levels from a magmatic source localized at depth by the intersection of transfer structures and a jog between major regional structures. The eruption of the diatreme breccia helped create the permeability for the later mineralizing fluids. This intrusion initiated the development of a circulating meteoric hydrothermal system, which entrained some magmatic fluids at depth, and deposited auriferous quartz-adularia-carbonate veins upon boiling at shallow levels in dilatant structures. Periodic opening of cross-cutting NS structures focused magmatic fluids from depth, and deposited gold-silver-tellurium and base metals in chlorite-quartz veins upon mixing with entrained ground waters. As a consequence, the ore mined at Cracow contained ore shoots localized at the intersections of the NS cross structures and the EW-trending dilational vein system.

e) Conclusions

Epithermal quartz gold-silver systems represent the end member of the continuum of intrusion-related low sulfidation gold deposit styles, and are locally transitional to the class of adularia-sericite epithermal gold-silver deposits. The epithermal quartz gold-silver deposits are distinguished from the classic epithermal banded quartz-adularia-sericite veins by the more obvious magmatic association.

Veins are dominated by quartz which is intimately associated with either adularia or with illite, smectite and/or kaolin clays and locally with carbonates, particularly siderite. The sulfide content is generally low and marcasite is common. The mineralogy is silver-rich, usually consisting of Ag-sulfosalts, sulfides and native silver. Base metal sulfides are rare and in many cases these contain appreciable silver. Gold generally occurs in low fineness (<700) electrum. Tellurides and telluride-rich sulfides are common in the porphyry-related quartz gold-silver systems, but are conspicuous by their absence in the adularia-sericite epithermal gold-silver systems.

As a continuum of deposit styles, there is a spatial and temporal relationship between epithermal quartz gold-silver and carbonate-base metal gold systems. This is interpreted to represent the variation during the mixing of upwelling intrusion-derived mineralized fluids with either: CO_2-rich ± acid sulfate waters (to produce carbonate-base metal systems), or cool dilute oxidizing ground water (to produce epithermal quartz gold-silver vein systems).

Karangahake in New Zealand, and Misima in Papua New Guinea represent examples of a continuum from carbonate-base metal gold mineralization at depth, to epithermal quartz gold-silver mineralization at progressively shallower crustal levels. Maniape and Kelian represent examples of horizontal zonations from carbonate-base metal gold mineralization formed proximal to an inferred intrusion source, to the quartz gold-silver mineralization in more distal settings. At Mt Kare, the quartz-roscoelite alteration occurs on the margins of the carbonate-base metal gold mineralization. In many systems, the epithermal quartz gold-silver mineralization forms late in the paragenetic sequence (e.g., Maniape), or occurs in late stage breccia zones and veins which cut the carbonate-base metal system (e.g., Zone VII at Porgera). Petrological data at Maniape demonstrates that the two events can be initially contemporaneous, although the epithermal quartz gold-silver mineralization here post-dates much of the carbonate-base metal mineralization.

Some epithermal quartz gold-silver deposits, characterized by banded quartz veins (e.g. Tolukuma and Cracow), are similar to the adularia-sericite epithermal gold-silver systems which occur in New Zealand and Japan (Section 8). However, the epithermal quartz gold-silver systems form within magmatic arc environments and are associated with high level intrusions and fluidized or phreatomagmatic breccias. Telluride-rich phases are common in the epithermal quartz gold-silver systems and gold mineralization is intimately related to illite, chlorite and kaolin clays or with carbonates, in the same manner as the epithermal gold mineralization at Mt. Kare, Porgera and Maniape. On the other hand the adularia-sericite epithermal gold-silver systems form in back-arc basins and are spatially and genetically related to felsic volcanics. These deposits generally lack associations with high level intrusions, typically contain eruption (or phreatic), not phreatomagmatic breccias and the gold mineralization is associated with selenides rather than tellurides (Section 8, Table 7.1).

v) Sediment Hosted Replacement Gold Deposits

a) Characteristics

Sediment hosted replacement gold deposits, also termed Carlin-type gold deposits from where they were first described, have been major gold producers in the western US (98.8 million ounces discovered; Singer, 1995). Most deposits lie along deep crustal fracture systems which define the Carlin and Battle Mountain Trends (Madrid and Roberts, 1990). Significant new discoveries within the Carlin Trend include the Betze-Post and Meikle ore systems (Bettles and Lauha, 1991), with production of 7.1 million ounces and reserves of 28 million ounces of gold at the end of 1994 (Volk et al., 1995). Reviews of this style of gold mineralization by Bagby and Berger (1985), Sawkins (1984), Sillitoe and Bonham (1990), Berger and Bagby (1991), Kuehn and Rose (1995) present geological models for this deposit type. Critical in the development of these models has been the recognition of similar deposit types in other settings (e.g., Bau, Sulawesi; Wolfenden, 1965; Sillitoe and Bonham, 1990: China; Cunningham et al., 1988: Melco and Barney's Canyon deposits, Bingham District, US; Babcock et al., 1992: Mesel, North Sulawesi; Indonesia; Turner et al., 1994; Garwin et al., 1995: and elsewhere in the eastern and western Pacific rim, G. Corbett and T. Leach, unpubl. data; Gemuts et al., 1996: Fig. 1.2).

Aspects of sediment hosted replacement gold deposits discussed more fully in the above reviews include:

* Host rocks, described as silty carbonaceous carbonate, carbonate-bearing shale, dolomite and limestone.
* Structural settings, characterized by extension, including normal faults, common doming, and local caps of impermeable units (Berger and Bagby, 1991). Back-arc settings appear to represent conducive environments.
* Metal association of high fineness gold, and enrichments in As, Hg, Sb, Ba and Tl. Some examples (e.g., Bau, Sillitoe and Bonham, 1990) are enriched in base metals. Many are metallurgically difficult because of arsenic in the ores.
* Magmatic association is commonly represented by felsic dikes which are indicative of the inferred distal relationship of gold mineralization to intrusion source rocks (Sillitoe and Bonham, 1990; Berger and Bagby, 1991).

* Depth of formation which is inferred to be well below epithermal environments (Sillitoe and Bonham, 1990; Kuehen and Rose, 1995).
* Mixing of volatile-rich fluids derived from considerable depth with meteoric fluids is inferred as a mechanism of gold deposition by Kuehen and Rose (1995).

Earlier geological models focused upon the depth of formation and initially described these western US deposits as epithermal, but more recently suggest a deeper level of formation (Sillitoe and Bonham, 1990; Bagby and Berger, 1985). The emphasis on the porphyry association by Sillitoe and Bonham (1990), gives a better framework for the comparison of different examples of sediment hosted replacement gold deposits. Based upon proximity to the magmatic source, these workers present a model in which mineralization is zoned away from porphyry Cu-Mo-Au stocks and propose that many of the deposits formed at depths of 2-3 km.

Sediment-hosted gold deposits are suspected to be derived from low sulfidation magmatic fluids (similar to those for quartz-sulfide gold mineralization) which have come in contact with reactive host rocks. These settings distal to the porphyry source are not conducive to skarn formation. Ore textures are similar to those seen in other Pacific rim systems characterized by leaching of the host rocks by reactive fluids (e.g., alteration in high sulfidation systems) or inferred quartz undersaturated fluids and quenched sulfide deposition (e.g., fluidized breccias at Mesel and Lihir). Extensional tectonism, in particular dilational structures at prospect scale, provide plumbing systems conducive to the transportation of mineralized fluids over considerable distances. We suggest that many deposits feature flow paths in which ore fluids migrated from dilational structures, which localize high grade structurally-controlled ores, and then into reactive lithologies which may host larger volumes of lower gold grade, in lithologically-controlled ores (Fig. 7.55). The relationship between the Post (structurally controlled) and Betze (lithologically controlled) ore systems at Goldstrike, USA (G. Corbett, pers. observations with Barrick geological staff, 1996) and also within Mesel, Indonesia (G.Corbett and T. Leach, unpubl. reports, 1993) and Mercur, USA (G. Corbett, unpubl. report, 1996), provide good examples of these relationships. Analyses of structure and alteration zonation within lithologically controlled ores may point to targets for higher gold grade structurally controlled mineralization.

b) Example

Mesel, North Sulawesi, Indonesia

Recent work on the Mesel gold deposit provides new data on the controls to the formation of sediment hosted gold mineralization in the southwest Pacific (Turner et al., 1994; Garwin et al., 1995; G. Corbett and T. Leach, unpubl. reports). During the exploration by Newmont in the 1980's, traditional stream sediment geochemistry was inhibited by contamination from the extensive workings by pre-World War II Dutch, and recent illegal miners. Reports of silicified outcrops by local villagers resulted in the identification of the discovery outcrop for the Mesel deposit at Hein's Find in 1988 (Turner et al., 1994). Gold production began in 1996 from a resource described by Turner et al. (1994) as 12.25 Mt of 5.21 g/t Au, and more recently by Garwin et al. (1995) as 7.8 Mt at 7.3 g/t Au.

Sediment hosted gold mineralization at Mesel is both structurally and lithologically controlled. Structural controls result from the reactivation of structural elements in response to the varying tectonic framework through geological time, and deformation of the cover by reactivation of basement structures. Lithological control is provided by permeable carbonate rock types and enhanced by alteration dolomitization. Andesite sills act as local impermeable caps to the ore-hosting limestone sequence (Fig. 7.56).

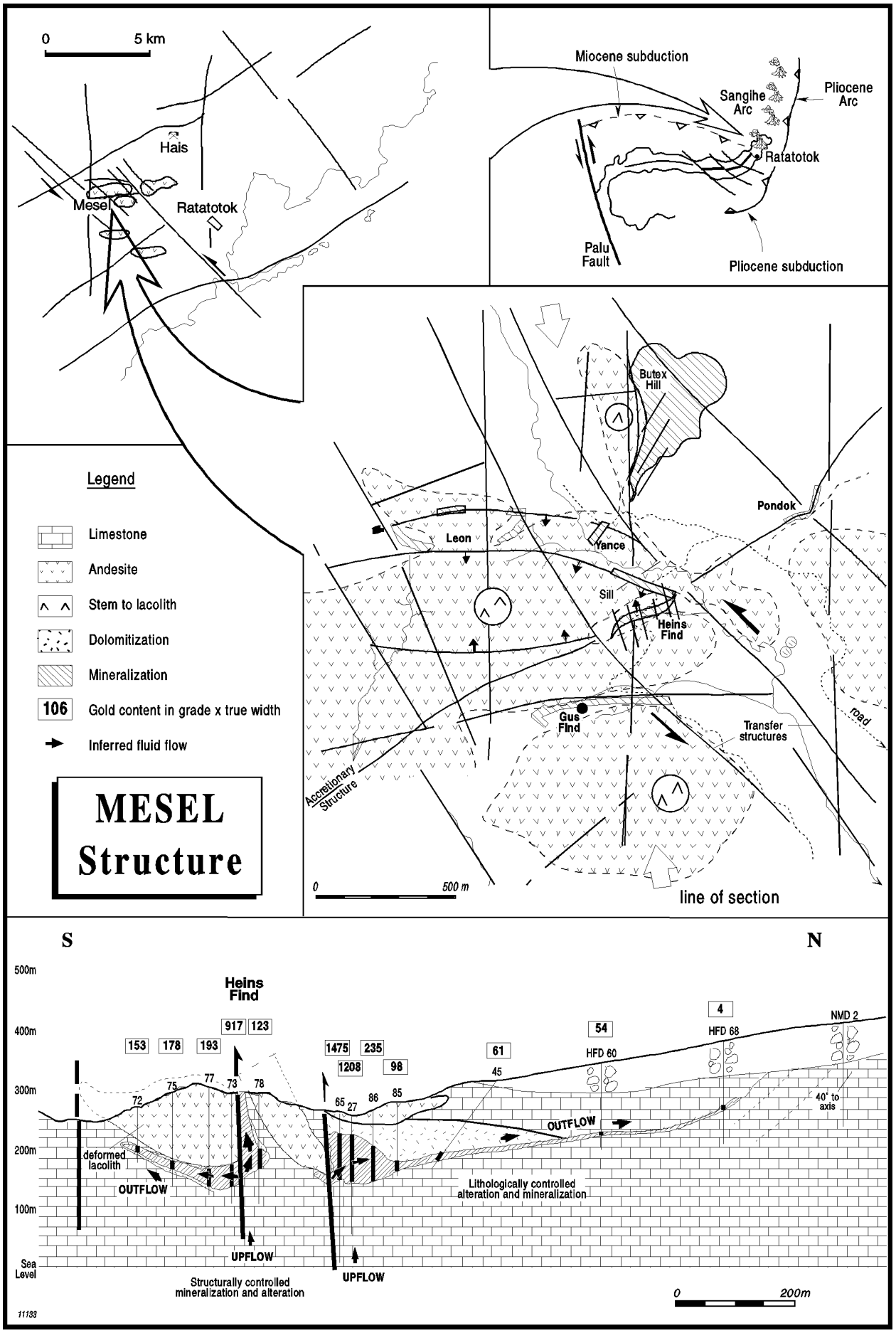
0
5 km
Hais
Mesel
Ratatotok
Miocene subduction
Sangihe Arc
Pliocene Arc
Ratatotok
Palu Fault
Pliocene subduction
Legend
Limestone
Andesite
Stem to lacolith
Dolomitization
Mineralization
106
Gold content in grade x true width
Inferred fluid flow
MESEL Structure
Butex Hill
Pondok
Leon
Yance
Sill
Heins Find
Gus Find
Transfer structures
road
Accretionary Structure
0
500 m
line of section
S
N
500m
400m
300m
200m
100m
Sea Level
Heins Find
153
178
193
917
123
1475
235
1208
98
61
54
4
HFD 60
HFD 68
NMD 2
72
75
77
73
78
65
27
86
85
45
40° to axis
OUTFLOW
deformed lacolith
OUTFLOW
Lithologically controlled alteration and mineralization
UPFLOW
UPFLOW
Structurally controlled mineralization and alteration
0
200m
11133

FIG. 7.56

Structural controls demonstrate a reactivation of existing structures. Miocene extension on EW structures separated by NW transfer faults, provided an environment for carbonate sedimentation overlying the basement volcanic rocks. Later Miocene collision of the Sula Platform caused a rotation of North Sulawesi through 90°, to the present position (Kavalieris et al., 1992; Hamilton, 1979). Compression deformed the cover carbonate sequence and created flexural slip folds with an EW axis. Subsequent andesite intrusion formed EW-trending oval shaped sills capping plug-like feeders, localized on deep basement NS structures (Fig. 7.56). Intrusion along the folded cover sequence has been aided by slip on mudstone units, and the sills are commonly faulted by high angle EW structures.

A change in the stress regime during the Pliocene promoted mineralization within dilational elements of the same structural framework. Fluid upflow for the Mesel mineralization is hosted in EW structures in the cover sequence, which were dilated by sinistral strike-slip movement on the NW-trending basement transfer structures (Fig. 7.56). NNW structures, likened to domino faults (section 3.iv.b.3), localize individual fluid upflow zones at the intersection with dilational faults, and also offset the mineralization during later reactivation (Fig. 7.56).

Alteration and mineralization at Mesel occur within the limestone with local extensions into the overlying andesite. Four main stages of hydrothermal activity are recognised at Mesel (T. Leach, unpubl. reports; Garwin et al., 1995; Figs. 7.57, 7.58):

Stage I: Decalcification and dolomitization occur as the replacement of calcite in the limestone by dolomite adjacent to major faults, in sedimentary breccias, and along the contacts with the overlying andesite. The volume decrease associated with the conversion of calcite to dolomite by the dolomitization process creates secondary porosity. Localized zones of decalcification, without dolomite replacement, occur marginal to the dolomitization. It is speculated that less than neutral pH circulating meteoric waters caused this early alteration.

Stage II: Intense silicification, as a result of the filling of open space and replacement of calcite and dolomite, decreases moving away from areas of inferred fluid upflow, towards outflow settings. Vughy silica rock is speculated to have locally developed through the leaching of carbonates by a less than neutral pH fluid. Alteration in the overlying andesites is zoned from smectite-chlorite at shallow levels, to kaolinite-interlayered clays-gypsum at depth. Kaolinite and illitic clays locally overprint dolomitized limestone, and in places post-date Stage II silicification.

Stage III: The main phase of gold mineralization is associated with quartz-sulfide deposition during polyphasal brecciation of the silicified dolomite and altered limestone. Coarse grained barite was locally deposited with the quartz-sulfide, and in many cases has subsequently been replaced by later quartz. In some cases illite is intergrown with quartz and indicates temperatures of deposition around 200-250°C. Early sulfides comprise simple, coarse pyrite which is intergrown with dolomite during Stage I activity, and with quartz in early Stage III breccias. The pyrite becomes progressively more arsenic-rich during Stage III activity, and here tabular to rhombic arsenical pyrite is intergrown with quartz in breccia matrix, locally grading to arsenopyrite. There is a strong positive correlation between gold grades and arsenical pyrite content. Gold is submicron in size and associated with very fine grained (<10 micron) arsenical pyrite. Gold grades are highest in the polyphasal silicified breccias proximal to feeder (fluid upflow) structures. Gold contents, measured in terms of thickness x grade, decline rapidly from the upflow zone to lithologically controlled outflow zones constrained below the andesite sills (Fig. 7.56). Pyrite which is commonly intergrown with kaolinite in late Stage III and early Stage IV, is fine grained and framboidal, and overgrows earlier pyrite, implying rapid cooling following the main mineralizing event. Stibnite occurs as a late sulfide phase associated with both Stage III quartz veins and Stage IV calcite at shallow levels and in zones peripheral to the ore body.

Stage IV: Post-mineral calcite veins transect earlier alteration and mineralization.

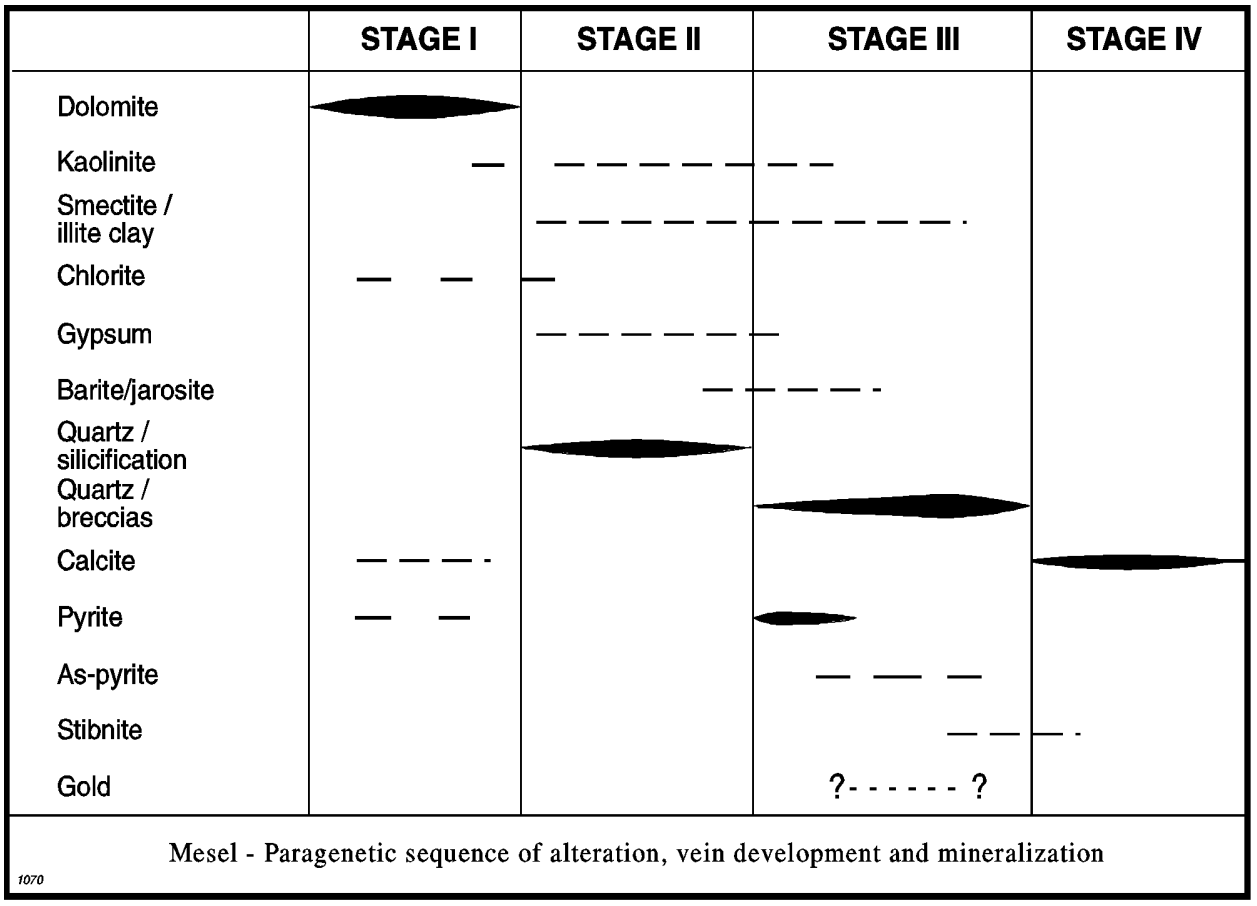

FIG. 7.57

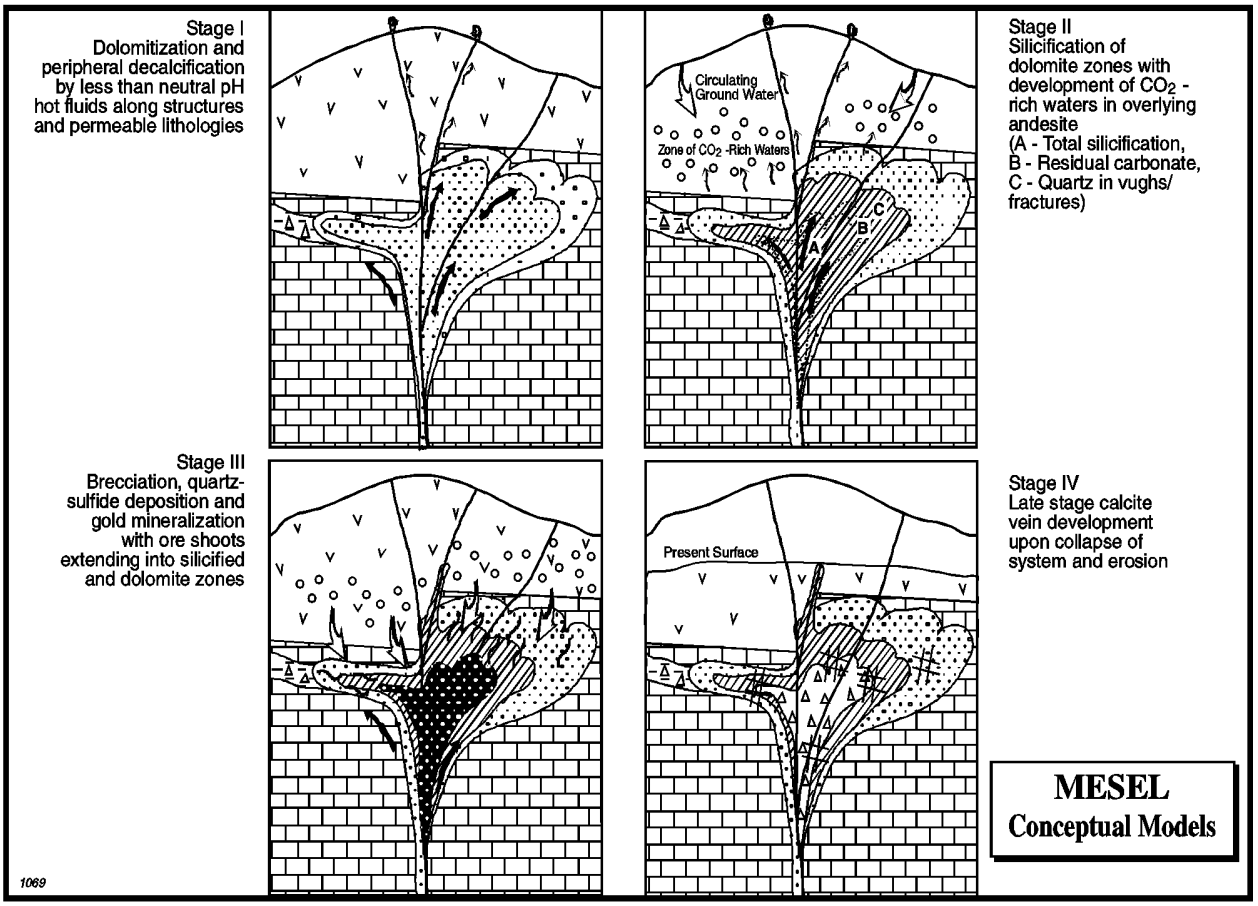

FIG. 7.58

A conceptual fluid flow model for gold mineralization at Mesel suggests that the fluid upflows were localized with dilational EW structures, hosted in reactive calcareous sediments and capped by impermeable andesite aquacludes (Fig. 7.58). The lateral fluid flow was facilitated by permeability in the limestone aquifer beneath the andesite aquaclude. Limestone permeability resulted from decalcification and dolomitization as well as primary porosity in stylolitic fractures and sedimentary breccias. Silicification of dolomitized limestone proximal to the dilational structures created a brittle host rock, which fractured to form breccias containing quartz-pyrite-gold mineralization in the matrix.

It is proposed that dolomitization of the limestone and later silicification of the carbonates was caused by an influx of upwelling hydrothermal fluids of progressively decreased fluid pH, possibly due to an increasing gas content. Romberger (1988) proposed that simple cooling of an upwelling fluid would produce simultaneous dissolution of carbonate and precipitation of silica in Carlin-style sediment hosted replacement gold deposits.

Low pH fluids facilitate the precipitation of arsenic from near neutral hydrothermal fluids (Fournier 1985a). Arehart et al. (1993) illustrate that gold and arsenic are preferentially removed from solution by oxidation under moderately low pH conditions, and result in the co-precipitation of gold with arsenical pyrite or arsenopyrite. It is therefore interpreted that gold-bearing arsenical pyrite mineralization at Mesel developed in response to the mixing of upwelling mineralized fluids with low pH, CO_2-rich waters. The presence of zoned kaolinite-gypsum-smectite-illitic clays at shallow levels at Mesel, and of late kaolinite-pyrite in fractures, supports the model of CO_2-rich waters refluxing back into the hydrothermal system.

8 ADULARIA-SERICITE EPITHERMAL GOLD-SILVER SYSTEMS

i) Classification

Hydrothermal systems have been defined (Lindgren, 1922, 1933; Berger and Eimon, 1983) as epithermal systems if they formed within 1 km of the surface, at temperatures less than 300°C (mainly 150-250°C), and from a fluid of meteoric origin, possibly with some magmatic input (White and Hedenquist, 1990; Simmons, 1995). Epithermal systems are also distinguished from other deposit types by gold to silver ratios (Ferguson, 1929; Hedenquist and Reid, 1985; Morrison et al., 1991), host rock compositions (Lindgren, 1933; Bonham, 1986), and geological settings (White and Hedenquist, 1990). Many workers differentiate two styles of epithermal gold deposits which were initially distinguished as adularia-sericite and acid-sulfate (Hayba et al., 1985; Heald et al., 1987) and more recently as low and high sulfidation systems (Hedenquist, 1987; White and Hedenquist, 1990; Sillitoe, 1993b). The sediment hosted replacement gold deposits (Berger and Henley, 1989) are no longer recognized as necessarily epithermal (Section 7.v.).

In this presentation and in Leach and Corbett (1995), epithermal systems are defined on the basis of their crustal levels (i.e., porphyry, mesothermal, epithermal) and fluid chemistry (low or high sulfidation). As outlined in Section 7, many of the low sulfidation systems in the southwest Pacific described as epithermal quartz gold-silver are categorized on the basis of formation at the highest crustal level in a continuum of magmatic-related deposits from porphyry, through mesothermal to epithermal levels. These are distinguished from the adularia-sericite epithermal gold-silver systems, which lack a discernible relationship to porphyry source rocks and also (Table 7.1):
* Contain economic concentrations of gold and/or silver, and variable concentrations of mercury, arsenic, antimony, lead, zinc and copper.
* Typically occur as fissure veins and less commonly as stockwork vein/breccias and filling open space breccia.
* Occur in back-arc basin settings, rather than magmatic arcs in which the epithermal quartz gold-silver systems predominate.
* Host mineralization in quartz which may exhibit crustiform to banded colloform, locally chalcedonic textures, with quartz pseudomorphs after bladed carbonate.

Oxygen and hydrogen isotope data (Nesbitt, 1996) and geochemical studies on epithermal systems in North and South America (e.g., Field and Fifarek, 1985) indicate that the hydrothermal fluids are almost totally of meteoric origin, although the gold and other metals are interpreted to be derived from magmatic sources (Henley and Hoffman, 1987). Similarly, many quartz vein-hosted epithermal systems in the southwest Pacific, some described in this section, which do not display an obvious magmatic connection, and are therefore distinguished as, adularia-sericite epithermal gold-silver systems. Although the quartz, adularia and sericite veins and wall rock alteration in these systems are deposited from circulating dilute meteoric waters, it is proposed here that the gold-silver mineralization is magmatic in origin. Thus, the epithermal quartz gold-silver and adularia-sericite gold-silver deposits display many similarities, and may also be seen as subsets of the one style (Table. 7.1).

Adularia-sericite epithermal gold-silver systems are subdivided with increasing depth of formation (Fig. 8.1) as systems dominated by:
* sinter and hydrothermal breccias,
* stockwork or sheeted veins,
* fissure veins.

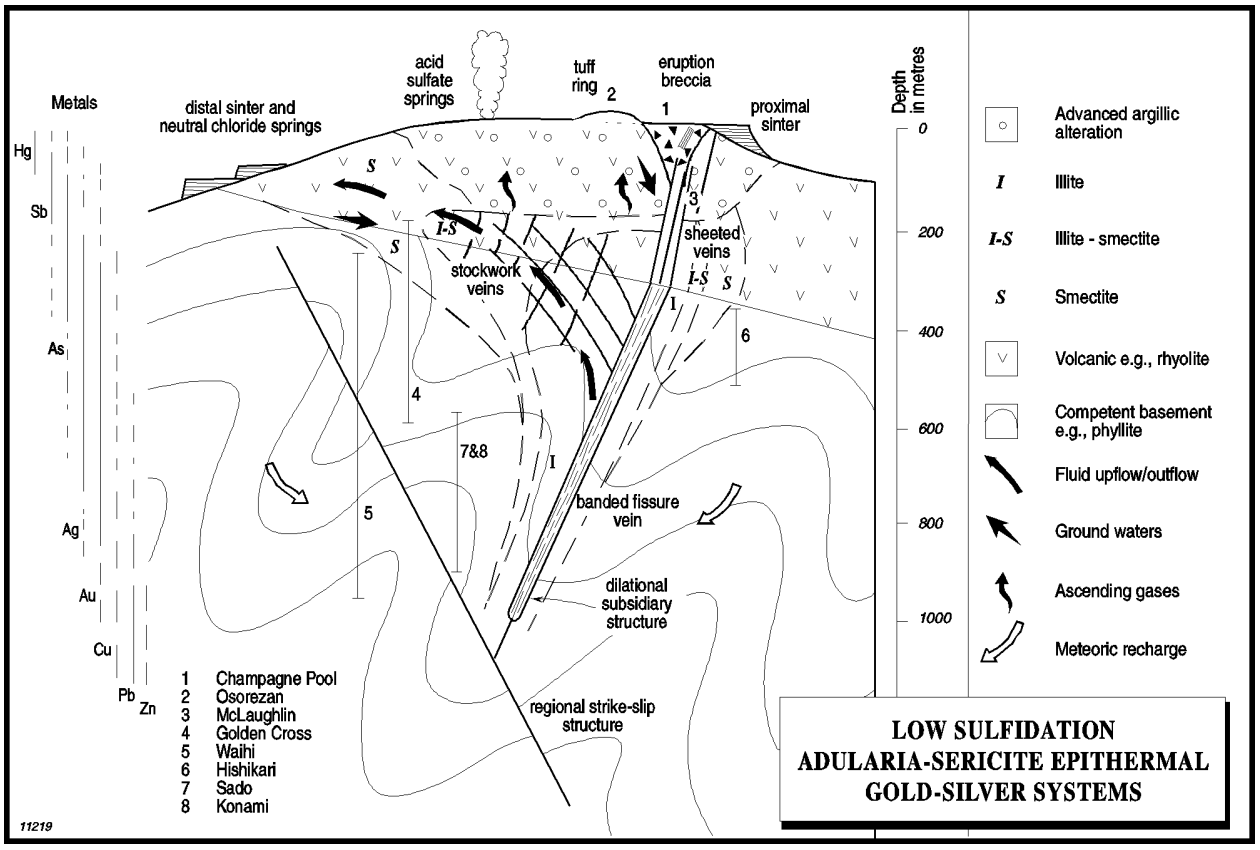

FIG. 8.1

Many adularia-sericite epithermal gold-silver deposits contain differing styles of vein development within one deposit. Golden Cross, New Zealand, extends from fissure veins at depth to overlying stockwork veins, and the McLaughlin, California, from sheeted fissure veins at depth, to surficial eruption breccias and silica sinters, locally cut by stockwork veins (Sherlock et al., 1995).

ii) Examples

Examples of adularia-sericite epithermal gold-silver deposits include: in New Zealand, Waihi (5 M oz Au, 30 M oz Ag; Brathwaite and McKay, 1989), Golden Cross (0.9 M oz Au, 2.6 M oz Ag; Hay, 1989), and in Japan, Hishikari (6.4 M oz Au; Nakayama, 1995), Konomai (2.3 M oz Au, 38 M oz Ag; Austpac Gold et al., 1990), Sado (2.4 M oz Au, 74 M oz Ag; Shikazono et al., 1993), Takatama (0.9 M oz Au, 9 M oz Ag; Seki, 1993), Chitose (0.7 M oz Au, 3.7 M oz Ag; Austpac Gold et al., 1990), and Kushikino (1.7 M oz Au, 16 M oz Ag; Shikazono et al., 1993), although the latter may be transitional to a carbonate-base style of gold deposit. Older rocks in the Drummond Basin, eastern Australia host several adularia-sericite epithermal gold-silver vein and vein/breccia systems: Pajingo (0.73 M oz Au 2.5 M oz Ag; Cornwell and Teddinnik, 1995), the nearby Vera-Nancy (0.78 M oz Au resource, Normandy Limited, press release), Wirralie (0.33 M oz Au, Fellows and Hammond, 1990) and others.

iii) Tectonic Setting

Adularia-sericite epithermal gold-silver deposits typically form within back-arc basins or rifts and are characterized by deep seated felsic intrusions around which are set up circulating hydrothermal systems dominated by meteoric waters (Fig. 2.2). Felsic volcanic and subvolcanic rocks are commonly spatially

associated with mineralization as part of a bimodal suite of volcanic host rocks (Sillitoe, 1992: e.g., Hishikari and Sado in Japan; Ohui, Golden Cross in New Zealand).

Geothermal systems within the active Taupo Volcanic back-arc rift in New Zealand represent analogies to extinct ore-bearing hydrothermal systems, which are inferred to have formed in similar environments (e.g., Coromandel Peninsula, New Zealand; Rubeshibe Belt, Hokkaido and elsewhere in Japan; Drummond Basin, eastern Australia). Basement structures, which controlled the formation of volcanic-hosting rifts in the Miocene Green Tuff Belt of Japan, localize later epithermal gold mineralization. These are best developed in fissure veins within competent basement metamorphic rocks (e.g., Konomai mine and gold occurrences in the Rubeshibe Belt, central Hokkaido; G. Corbett, unpubl. data; Fig. 1.2). In the Coromandel Peninsula of New Zealand, centres of epithermal vein mineralization are localized either by transfer structures which transect the arc at high angles (e.g., Karangahake, Neavesville, Golden Cross, Coromandel, Kapowai; Fig. 7.47), or at the margins of inferred calderas (e.g, Waihi; Fig. 8.7). Karangahake, which as a transitional deposit to a carbonate-base metal gold system, displays a closer relationship to an inferred porphyry source, and is localized at the intersection of a major graben-bounding structure, with a transfer structure (Figs. 7.42, 7.47).

Systems formed in magmatic arc environments may display transitional relationships to intrusion-related styles of gold mineralization (Section 7.iv). Intrusions localized by major structures may set up hydrothermal systems which deposit gangue mineralogy typical of adularia-sericite epithermal fissure veins (quartz, adularia, platy carbonate pseudomorphed by quartz), from circulating meteoric waters. The same dilational environments may also host intrusion-related gold mineralization which becomes more evident as deeper levels in the hydrothermal system are exposed by erosion. The Toka Tindung eruption breccia/fissure vein systems in North Sulawesi, Indonesia (Wake et al., 1996; G. Corbett unpubl. report), occurs in a poorly eroded, localized extensional environment which is classed as an adularia-sericite epithermal gold-silver system. While at Mt Muro, Indonesia (Moyle et al., 1996) some fissure veins contain mineralogy typical of adularia-sericite epithermal gold-silver systems (Simmons and Browne, 1990), the system as a whole displays a lateral zonation indicative of an intrusion source (G. Corbett, unpubl. report, 1996). The Karangahake deposit, which was mined over a vertical interval of 800 m, exhibits a transition from epithermal banded quartz veins at shallow levels to more intrusion-related carbonate-base metal-style alteration and mineralization in the main ore zone at depth (Fig. 7.42). Similarly, Cracow in eastern Australia displays ore mineralogy typical of epithermal quartz-gold mineralization which is superimposed upon an adularia-sericite epithermal gold-silver vein system. At both Karangahake and Cracow most of the gold was mined from ore shoots localized by the intersection of cross structures with the dilational fissure veins which display mineralogies typical of epithermal quartz gold-silver systems.

iv) Structure

Adularia-sericite epithermal gold-silver deposits typically form as fissure veins within dilational structural environments (Section 3.vi.a). In tectonically active terrains major structures may localize intrusions at considerable depth, and by strike-slip movement, produce ore-hosting dilational structural environments within subsidiary fractures. Models of earthquake rupturing have been used to describe mechanisms for fluid transport and repeated mineral deposition (Sibson, 1987) in which boiling or rapid cooling of meteoric waters form banded veins of quartz, adularia, and platy carbonate pseudomorphed by quartz.

In these systems, strike-slip movement on the controlling structures (planes of principal displacement) which are typically barren, produces tension veins as subsidiary structures (Section 3.iv.2,; 3.vi). These are initiated at 45° to the controlling structures and progressive strike-slip movement causes the subsidiary structures to dilate (and host ore) and rotate to orientations close to normal to the controlling strike-slip faults (Fig. 3.9). Great care should be taken to correctly orient drilling to test these vein systems (Fig. 3.10). Flatly dipping veins may develop in settings characterized by pull-apart basin fracture arrays (Fig. 3.13).

Adularia-sericite epithermal gold-silver systems may be vertically zoned (Fig. 3.14) from fissure veins at depth, through overlying stockwork veins which mushroom above the fissure veins, to eruption breccias at highest levels (below). Many fissure veins, particularly those transitional to intrusion-related mineralization styles display spatial relationships to syn-mineral fluidized breccias (e.g., Toka Tindung, Indonesia) and also overprint earlier phreatomagmatic breccias (e.g., Cinola, British Columbia; G. Corbett, pers. observations).

Competent host rocks are necessary for fissure veins to form and host gold mineralization. Permeable volcanic sequences at epithermal levels may undergo alteration to low temperature and incompetent clays; whereas vein systems may be preferentially developed in the more competent intrusions, or intrusion margins, within a subvolcanic rock sequence (e.g., Sado and Chitose, Japan). At Hishikari, Japan, clay alteration of the overlying andesitic tuffs has provided an incompetent cap to the fissure vein mineralization, the main portion of which is confined to about a 100 m vertical extent within the underlying competent Shimanto Group shale (Fig. 6 in Ibaraki and Suzuki, 1993). By contrast, fissure veins hosted in andesites at Waihi were mined vertically over 600 m (Fig. 8.7) and at Golden Cross a fissure vein is capped by a lower gold grade stockwork over a 400 m vertical extent (Fig. 8.5).

v) Fluid Characteristics and Hydrothermal Alteration

As the heated fluid rises within a low sulfidation hydrothermal system, fluid flow is mainly confined to dilatant structures. Two phase (vapour [steam and gas] + liquid) conditions are developed in response to release of gases (mainly CO_2 and minor H_2S), caused by pressure drops as the upwelling fluids reach shallow crustal levels. Hydrothermal fluids are invariably saturated with respect to silica minerals, therefore decreases in temperature upon pressure drops, result in quartz deposition (because quartz solubility is directly related to temperature, Fig. 4.2). Mixing of the hot upwelling fluid with descending cool surficial waters also results in significant deposition of silica minerals, as cristobalite at low temperatures (generally less than 100°C), and quartz at higher temperatures (Leach et al., 1985). Where the hydrothermal fluid discharges at the surface, rapid cooling causes silica super-saturation and deposition of amorphous silica in sinters (Figs. 1.1, 7.3, 8.1).

Silica sinters which form as outflow features, may occur at considerable distances from the upwelling hydrothermal system, and are therefore relatively depleted in precious metals. In certain locations within the upflow zone, gases may become trapped beneath impermeable zones or sealed conduits. When the gas pressure exceeds the lithostatic pressure, the resultant hydrothermal eruptions locally form eruption breccias (Hedenquist and Henley, 1985a). In these settings where hydrothermal fluids may vent directly to the surface, some sinters display anomalous metal contents above the fluid upflow (e.g., Champagne Pool, New Zealand), and are locally brecciated and veined to form ore systems (e.g., McLaughlin, USA). Silica deposition may form a self-sealed cap rock which becomes fractured when the gas pressure exceeds the rock tensile strength and hydrostatic ± lithostatic pressure (Nelson and Giles, 1985; Sillitoe, 1985). Ore formation may be promoted by the repeated activation of this process (Sillitoe, 1985), to form crack-seal breccias (e.g, upper parts of McLaughlin), by the reactivation of structures which facilitate fluid flow in subsidiary fractures.

Quartz is the dominant gangue phase in adularia-sericite gold-silver systems (Hayba et al., 1985). The main controls to quartz deposition are decreases in fluid temperature, and to a much lesser degree, pressure drops and decreases in fluid salinity (Section 4.iv.a). The rate of change in fluid conditions influences the morphology, crystal structure and chemical composition of silica species in general, and quartz in particular. Dong et al. (1995) have documented various quartz textures from selected epithermal systems in Queensland, eastern Australia, and relate these to possible hydrothermal conditions during vein growth.

Where the CO_2 content of the fluid is sufficiently high and release of pressure sudden, rapid boiling may result in the deposition of carbonate (typically calcite) within fluid channelways, generally with a characteristic bladed

habit (Section 4.iv.b). Bladed carbonate is commonly pseudomorphed by quartz because the decrease in temperature upon boiling causes the carbonate to dissolve and quartz to precipitate (Section 4; Simmons and Christenson, 1994).

Rapid boiling and release of CO_2 also results in sudden decrease in P_{CO2} and an increase in fluid pH. In highly permeable channelways, this increase in pH can favour the deposition of potassium feldspar in the characteristic epithermal polymorph, adularia (Browne and Ellis, 1970). Dong and Morrison (1995) suggest that the progressive change in adularia morphology from tabular to rhombic and sub-rhombic, in epithermal systems in Queensland, is indicative of decreasing degrees of Al/Si disordering, which results from increases in the rates at which fluid conditions change during boiling. Adularia is only commonly encountered where there is sufficient potassium in the wall rock (e.g., in rhyolitic volcanic environments such as New Zealand, or shoshonitic volcanics at Vuda, Fiji, and the Lihir-Tabar Islands, Papua New Guinea), and rarely occurs in calc-alkaline terrains such as the Philippines.

At depth in epithermal environments, fluids generally occur at a less than neutral pH (5-6) due to the presence of dissolved gases (Henley et al., 1984). The wall rock immediately adjacent to these structures is typically altered to illitic clays (species being dependent on temperature) ± chlorite. Where permeability is poor and corresponding fluids exhibit neutral pH, wall rock alteration grades outward to propylitic over short distances.

In the near surface environments, rising gases and steam mix with surficial ground waters. The absorption of CO_2 into cool, shallow ground water and hydrothermal aquifers produces a moderately low pH, CO_2-rich water, which reacts with wall rock to form shallow argillic alteration characterized by kaolinite and/or smectite. At higher temperatures this alteration grades to interlayered clays + carbonates ± kaolinite. Carbonate species are zoned in response to a progressive increase in fluid pH as recognised in carbonate-base metal gold deposits (Section 7.iii). Here, siderite forms at low pH, Mn-Mg-carbonates at pH less than neutral, and calcite under near neutral conditions (Fig. 7.17).

The oxidation of H_2S at or near the surface produces acid sulfate fluids which, in response to increased pH due to wall rock reactions, form zoned alteration assemblages of: silica + smectite --> silica + alunite --> silica + alunite -->silica + kaolinite --> silica (opaline silica + kaolinite, cristobalite, tridymite).

Native sulfur may deposit in the silica zone (above) in highly oxidizing environments, such as around gas vents where direct oxidation of H_2S can take place. Gypsum is locally encountered associated with silica-kaolinite where fS_2 is lower. The term <u>acid sulfate</u> is used for these low pH waters formed under surficial environments, whereas <u>high sulfidation</u> is used for alteration formed by hot magmatic-derived fluids (Section 6.i).

Pressure draw downs in the hydrothermal system occur as the heat source for the epithermal system cools and surface waters may penetrate further into the system. During pressure draw down acid sulfate and CO_2-rich waters migrate down permeable structures (Fig. 2.4). These fluids result in overprinting alteration relationships and can also play a significant role in ore deposition.

vi) Mineralization

In epithermal environments, the characteristics of the fluids change significantly over short depth intervals, and this is reflected in the dominant metal contents which grades upwards as: base metals, to precious metals, to surficial mercury. Base metals are transported as chloride complexes (Henley, 1985b), and therefore precipitate at deep levels in response to rapid decreases of temperatures and salinities. In epithermal environments gold is postulated to be transported as a bisulfide complex (Seward, 1982). Under these conditions, gold deposition is controlled by changes in fluid pH, fO_2, and sulfur complexing, brought about either by sudden boiling of the

mineralized fluid, or quenching as a result of mixing with an oxidized, and in places relatively low pH, surficial waters (Brown, 1989; Spycher and Reed, 1989).

Brown (1986) demonstrated that, in the surface pipework of geothermal wells of Broadlands, New Zealand, gold and silver are precipitated in response to rapid boiling which results from substantial pressure drops. In this case it was argued that gold precipitation was promoted by the removal of sulfur from the gold-bisulfide complex during the release of H_2S upon by boiling. The common occurrence of colloform banded quartz with platy carbonate (pseudomorphed by quartz) and adularia (e.g, Waihi, New Zealand), attests to repeated boiling as a mechanism for mineral deposition in veins which also host gold mineralization.

However, in the epithermal gold systems described herein, mixing of hot mineralized fluids with cool, oxidized, and in places low pH surficial waters, is apparent as an important mechanism of gold deposition. Low temperature clays are associated with gold in thin sulfide bands within quartz veins at Cracow (T. Leach, unpubl reports), Golden Cross (Simpson et al., 1995a, 1995b), Waihi (Panther et al., 1995), Tolukuma (Semple et al., 1995), Karangahake (T. Leach, unpubl. reports), and Hishikari (Shikazono and Nagayama, 1993). Hypogene hematite, which is indicative of oxidizing conditions, commonly occurs in association with high grade late stage gold mineralization (White et al., 1995; this study).

In epithermal environments, silver and to a lesser extent copper, can be transported both as bisulfide and chloride complexes (Henley, 1985b), and epithermal systems are therefore typically enriched in these elements. Arsenic and antimony are also probably transported as bisulfide complexes and so display spatial distributions similar to gold and silver (Spycher and Reed, 1989). Acidification is the most effective mechanism for the deposition of arsenic and antimony minerals from solution, with antimony preferentially precipitating at lower temperatures (Spycher and Reed, 1989). Antimony therefore commonly dominates over arsenic at near surface levels. Mercury evolves as a gas during boiling and is deposited upon contact with oxygenated ground water in surficial environments, generally in the form of cinnabar (Spycher and Reed, 1989). Gold is usually present as Ag-rich electrum. Silver is deposited as a variety of sulfide, As-Sb sulfosalts, selenides (rather than as tellurides as in porphyry-related epithermal quartz gold-silver systems), electrum, and as native silver.

vii) Types of Epithermal Gold-Silver Deposits

Three styles of adularia-sericite epithermal gold systems are distinguished on the basis of crustal levels of formation (Fig. 8.1), although it must be emphasised that transitional relationships and telescoping are common. The uppermost sinter and breccias generally do not form economic gold deposits, which are best developed in the fissure vein systems.

a) Sinter and hydrothermal breccia systems

1. Characteristics

Sinter deposits develop from the venting at surface of outflowing hydrothermal fluids, commonly localized by eruption breccias which may overlie fluid upflows within fissure veins (Figs. 3.21, 7.2, 8.1). While some sinters proximal to eruption vents display anomalous geochemistry (e.g., Champagne Pool, New Zealand; below), most are barren of gold but may display anomalous mercury, antimony, and arsenic (e.g., Puhipuhi, New Zealand; below) and many are subjacent to gold-bearing fissure veins (e.g., Toka Tindung, Indonesia; below) or sheeted veins (e.g., McLaughlin, western US; Sherlock et al., 1995; below). Sinter and (hydrothermal) eruption breccia systems (Section 3.x.d.3) are indicative of environments conducive to the identification of buried fissure vein-hosted gold mineralization.

Silica sinter deposits form within surficial fluid outflows in which the cooling waters deposit silica, and alkaline conditions promote biological activity. Walter (1976a, 1976b) and White et al. (1989) illustrate a variety of textures which characterize sinter deposits. Geyserite occurs as microbanded, botryoidal opaline silica deposited in proximity to vents or springs in high energy (splashing) environments (Walter, 1976a; White et al., 1989), commonly as rounded concretions (Nelson and Giles, 1985). Stromatolite algal mats display recognisable textures formed by growth, commonly in settings of fluid flow (White et al., 1989), which may also aid in the identification of sinter deposits. Characteristic features include: plant fragments, readily trapped by the algal mats (Walter, 1976b); vertical columnar stromatolite fabrics formed normal to the trend of bedding (White et al., 1989; Sillitoe 1993b), and surface textures (White et al., 1989). Layering in sinter deposits may vary from well laminated in distal outflows, to botryoidal beds several cm across (and locally brecciated), closer to the vent. Of concern, and as noted by Sillitoe (1993b), is that many pervasively silicified fine grained laminated sediments are often described as 'sinters'. These rocks form by pervasive replacement silicification in subsurface settings, commonly as a single event, and are not indicative of substantial fluid outflows. Large sinter deposits (outflows) may be derived from repeatedly activated fluid conduits which are prospective for gold mineralization in fissure veins. Thus, as the pervasive silicification is not indicative of the same target as a true silica sinter, it important that characteristic features (White et al., 1989 and references therein) are identified to verify the presence of sinters.

At Tarawera, Taupo Volcanic Zone, New Zealand, the famous Pink and White Sinter Terraces which formed during quiescent times, were destroyed in 1886 by a phreatomagmatic eruption, resulting from the contact of a hot magma with cool ground waters (Simmons et al., 1992; Nairn, 1979). Surficial deposits such as these are commonly removed by either erosion or by explosive eruptions, and so are generally only preserved in youthful, poorly eroded, terrains.

2. Examples

Examples of sinter hydrothermal (eruption) breccia systems include: McLaughlin, in the western US (Sherlock et al., 1995); Yamada at Hishikari, Osorezan, Beppu and in the Rubeshibe Belt of Japan; Ohaaki, Champagne Pool (Hedenquist and Henley, 1985), and Puhipuhi (White, 1990) in New Zealand; Toka Tindung, north Sulawesi, Indonesia (Wake et al., 1996) and Anomaly 309 at Twin Hills and elsewhere in the Drummond Basin, eastern Australia (Cunneen and Sillitoe, 1989; White et al., 1989, Ewers et al., 1990b).

1. Champagne Pool in the Waiotapu geothermal field, Taupo Volcanic Zone, New Zealand formed in an eruption breccia pipe, localized by dilational structures within a region of transpressional deformation (Fig. 8.2). Such eruption pipes are common within active geothermal terrains and are interpreted to form by the explosive release of gas pressure which builds up beneath sealed feeder structures (Hedenquist and Henley, 1985a). The Champagne Pool eruption vent which formed some 900 years ago, provides a direct channelway for neutral chloride fluids derived from considerable depth, to vent directly to the surface (Hedenquist and Henley, 1985a). The neutral pH fluid in Champagne Pool occurs at a level above the hydrothermal system which is dominated by acid sulfate waters. The sinter comprises finely banded layers of white amorphous silica, which periodically alternate with very thin bands of an orange-yellow silica precipitate. These precipitates contain up to 80 ppm Au, 170 ppm Ag, 320 ppm Th and 170 ppm Hg (Weissberg, 1969). Periodic mixing of the low pH acid sulfate waters and the metal-bearing neutral chloride fluids is interpreted to have caused the precipitation of the banded auriferous antimony- and arsenic-rich, orange precipitates at the margins of the pool (Hedenquist, 1984). An alternative explanation is that, dissolved CO_2 may cause the waters to maintain a sufficiently low pH to enable precipitation of amorphous arsenic and antimony sulfur compounds, which then absorb Au and Ag from solution (Hedenquist and Henley, 1985a; Simmons et al., 1992).

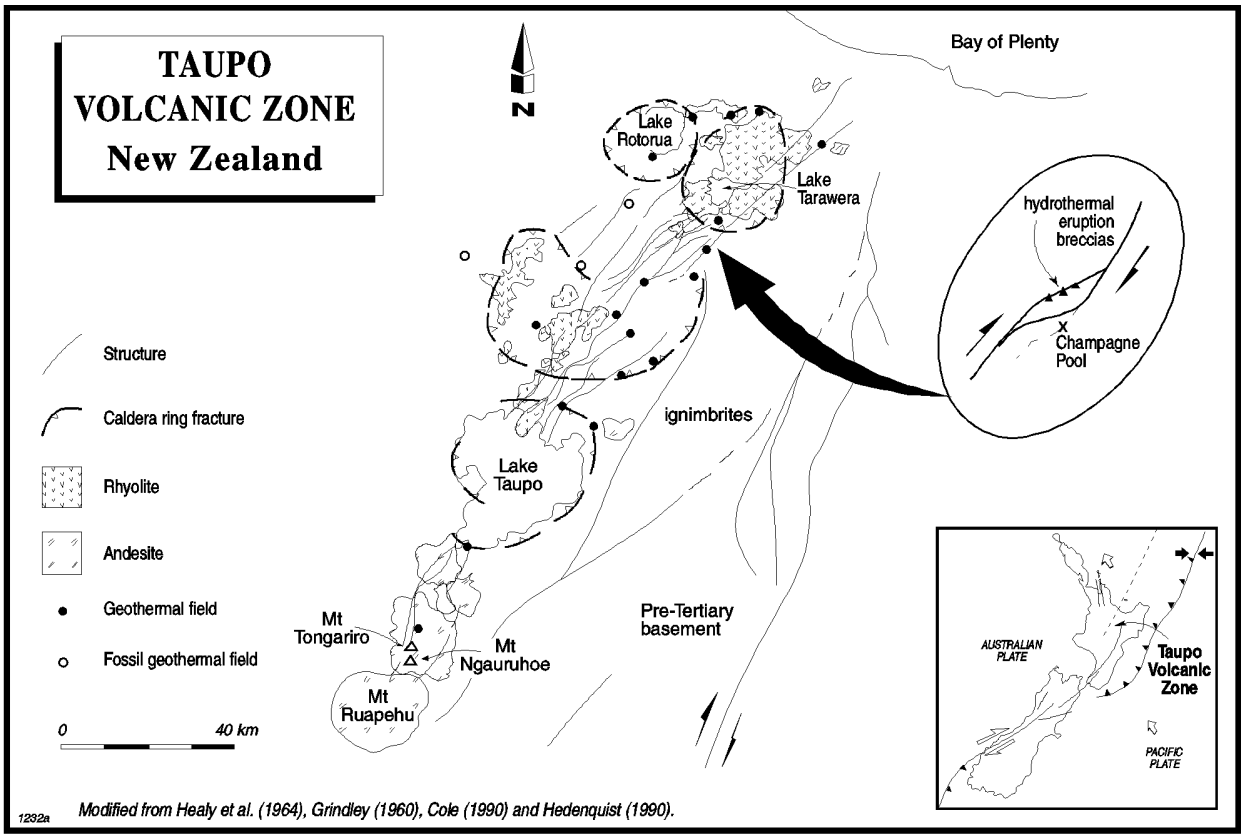
TAUPO
VOLCANIC ZONE
New Zealand
N
Bay of Plenty
Lake Rotorua
Lake Tarawera
hydrothermal eruption breccias
Champagne Pool
Structure
Caldera ring fracture
Rhyolite
Andesite
Geothermal field
Fossil geothermal field
0
40 km
ignimbrites
Lake Taupo
Mt Tongariro
Mt Ngauruhoe
Mt Ruapehu
Pre-Tertiary basement
AUSTRALIAN PLATE
Taupo Volcanic Zone
PACIFIC PLATE
1232a
Modified from Healy et al. (1964), Grindley (1960), Cole (1990) and Hedenquist (1990).

FIG. 8.2

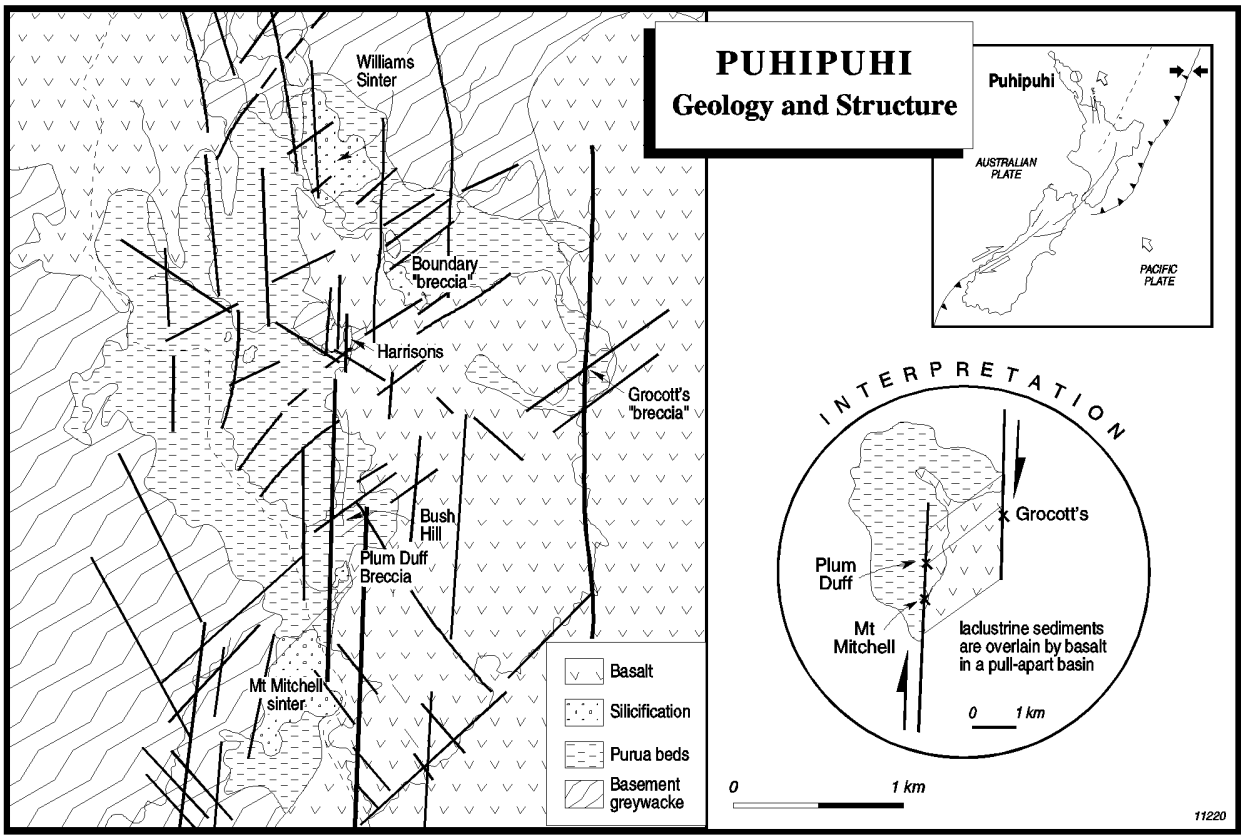
PUHIPUHI
Geology and Structure
Puhipuhi
AUSTRALIAN PLATE
PACIFIC PLATE
Williams Sinter
Boundary "breccia"
Harrisons
Grocott's "breccia"
Bush Hill
Plum Duff Breccia
Mt Mitchell sinter
Basalt
Silicification
Purua beds
Basement greywacke
INTERPRETATION
Grocott's
Plum Duff
Mt Mitchell
lacustrine sediments are overlain by basalt in a pull-apart basin
0
1 km
0
1 km
11220

FIG. 8.3

2. Osorezan is an area of steaming ground on the margin of a summit crater formed at the top of an andesitic volcano on the northern tip of Honshu, Japan, and has long been regarded as a sacred place (Aoki, 1992a, 1992b; Fig. 1.2). Late stage dacite domes and associated tuffs, sinters and eruption breccias occur within an area of acid sulfate alteration. Assays of hot spring precipitates grade to 6510 ppm gold (Aoki, 1993, 1992a, 1992b) and precipitates derived from fluids venting from recent MMAJ drill holes are enriched in arsenic, antimony and mercury (Austpac Gold, unpubl. report). Of interest is that eruption breccias have ejected fragments of mineralization formed at depth. These include; crustiform banded quartz-adularia veins with abundant visible gold, veins which contain galena, sphalerite, chalcopyrite, tetrahedrite, and pyrite, as well as stibnite-chalcedony veins presumably formed at shallow levels (Aoki, 1992a, 1992b). These surficial deposits are therefore interpreted to be derived from a mineralized feeder structure at depth.

3. Puhipuhi, Northland, New Zealand

Eruption breccias (White, 1986) and sinter deposits are aligned along a NS structure inferred to have been active in the formation of a pull-apart basin (G. Corbett and T. Leach, unpubl. report, 1995; Fig. 8.3). Lacustrine sediments extend from the basin to also unconformably overlie the basement greywacke and are in turn overlain by basalt flows. Silver was mined from quartz veins within the basement mostly peripheral to, and about 100 m below, the breccia and some sinter deposits (Brathwaite and Pirajno, 1993). Mercury was produced until 1950 from sinter deposits, eruption breccias and fractured basement, continuing to under the basalt cover (Brathwaite and Pirajno, 1993; G. Brown, 1989; White, 1986). Puhipuhi district has been subject to extensive gold exploration since the early 1980's (Brown, 1989; Brathwaite and Pirajno, 1993).

Eruption breccias at Plumb Duff (Fig. 8.3) are characterised by blocks of bedded sinter cemented by chalcedonic (locally opaline) silica and kaolinite (White, 1986). Similar amorphous silica locally cross-cuts the very well bedded Mt Mitchell sinter which contrasts with the more botryoidal banded nature of the larger blocks of sinter in the Plumb Duff breccia, where White (1986) recognised geyserite. These relationships and the alteration geochemical zonation have been used to target a fluid upflow in the vicinity of Bush Hill, near the Plumb Duff eruption breccia, from which the hydrothermal fluids are inferred to have vented and flowed laterally to form the distal sinters (G. Corbett and T. Leach, unpubl. report, 1995; Grieve et al., in prep). The more peripheral Williams Sinter (Fig. 8.3) contains substantial pervasively silicified sediments.

4. Twin Hills, Drummond basin, northeast Australia

Twin Hills is one of several Late Devonian to Early Carboniferous epithermal gold occurrences within the northern Drummond Basin of eastern Australia (Perkins et al., 1995; Fig. 1.2). At the 309 anomaly within the Twin Hills prospect, bedded geochemically barren sinter deposits which host plant fragments (Plutonic Resources, unpubl. data.) and geyserite, crop out on the flanks of a low hill from where poor exposures yielded anomalous gold in rock chips. Sinters close to the low hill display rounded several cm wide botryoidal beds, whereas those further away are more flatly bedded, suggesting that fluid flowed from a source near the hill. Diamond drill testing of the low hill identified a large body of silicified and pyritic clastic rocks, interpreted (G. Corbett, unpubl. report, 1996) to represent eruption breccias. Fragments of host volcaniclastic rocks are generally angular and locally derived, although some rounded rebrecciated examples are present. The lack of sedimentary structures discounts an origin as a conglomerate and no juvenile intrusion fragments, typical of a diatreme breccia, were recognised within the strongly matrix supported breccias. Syn-eruption alteration constitutes intense silica-pyrite flooding, best developed in the breccia matrix, and clay-pyrite alteration continues for several cm across steeply dipping contacts into the enclosing volcaniclastic sediments. Gold mineralization typically occurs as electrum within banded quartz-chalcedony sheeted veins which transect the eruption breccia. These are well developed in the vicinity of the rebrecciated breccias (G. Pietsch, pers. commun, 1996). The sinters are interpreted to have formed as hydrothermal fluid outflows from the eruption breccia vent which localized vein mineralization.

5. Toka Tindung north Sulawesi, Indonesia

At Toka Tindung, the Pleistocene Ako fissure vein and adjacent Western stockwork/fissure vein systems (Wake et al., 1996) are currently under evaluation (0.47 M oz Au; Aurora Gold, press release, January 1997). The veins lie subjacent to an eruption breccia which contains fragments of volcanics, lacustrine sediments, carbonized wood, and sinter in a matrix of strongly silica-pyrite altered sand to mud sized material (Wake et al., 1996; G. Corbett, unpubl. report, 1996). Larger sinter blocks occur towards the centre of eruption breccia. Although partly obscured by the tuff apron to the eruption breccia and young ash deposits, the vein system has been traced for about 500 m laterally and for 150 m below the apron. Fluidized breccia dikes exploit pre-existing structures which also host mineralized banded fissure veins close to the eruption breccia. Recent drilling targeted (G. Corbett, unpubl. report, 1996) to test veins close to the eruption breccia (and obscured by the tuff apron), several hundred metres from the discovery outcrop, has yielded high gold grades (A. Moyle, written commun., 1996). Thus, hydrothermal fluids are inferred to vent as sinters (disrupted by later eruptions) and have been channelled at depth into dilational structures to form fissure veins, which display higher gold grades closer to inferred fluid upflow centres.

b) Stockwork quartz vein gold-silver deposits

1. Characteristics

Stockwork veins predominate at depths of 100-400 m below the paleosurface, and are transitional between overlying sinter/breccia deposits, formed at near surficial levels, and deeper fissure veins (Fig. 8.1). Although the term stockwork is generally taken by many geoscientists to represent a random set of veins, many stockworks occur as steeply dipping sheeted veins (e.g., McLaughlin, western US), and so are transitional to fissure veins.

In the upper levels of fissures where confining pressures no longer exceed lithostatic pressures, fluids may mushroom laterally out from the fissures to form stockwork fractures, typically in hanging wall settings above dipping fissure veins (Fig. 8.1). In the Golden Cross and Karangahake mines, New Zealand, mineable fissure veins are capped by lower grade stockwork deposits.

Alteration within the stockwork veins is characterized by interlayered clays, which are locally capped and/or overprinted by kaolin - gypsum + alunite assemblages in response to draw down of surficial acid sulfate and CO_2-rich waters.

2. Examples

Examples of stockwork quartz vein gold deposits in the southwest Pacific include the upper portions of Karangahake, and Golden Cross, New Zealand, and Misima, Papua New Guinea. The transition between stockwork and deeper fissure veins at Golden Cross is discussed below, and McLaughlin, western US, hosts an example of a transition between sheeted (stockwork) veins and subjacent sinter/hydrothermal breccias

1. The McLaughlin gold mine in California USA, occurs outside the southwest Pacific, but contains well documented sinter and hydrothermal eruption breccias which overlie ore-grade sheeted quartz veins (Lehrman, 1986; Tosdal et al., 1993; Sherlock 1993; Sherlock et al., 1995). McLaughlin was discovered in 1978 by exploration which targeted former mercury mines within sinter deposits, and began production with initial reserves of 2.9 M oz Au at a grade of 4.7 g/t Au (Lehrman, 1986). The ore body is described by Lehrman (1986) as hosted in multistage chalcedony quartz vein stockwork, pervasive silica flooding, and breccia formed below the extensive sinter sheet. More recent work following mine development demonstrates that the quartz veins are sheeted and these veins constitute much of the recent ore (Tosdal et al., 1993, Sherlock et al., 1995). Although

previously mined for mercury, the sinter sheet is typically barren of gold (<10 ppb), except where it has undergone hydrothermal brecciation or is cut by sheeted quartz veins (Sherlock, 1993). McLaughlin lies in a region of transpressional tectonism in which strike-slip movement on major structures has facilitated the formation of the sheeted vein systems (Tosdal et al., 1993). Mineralized veins formed in subsidiary structures (Section 3.iv), occur at high angles to the structural grain, and are overlain by the sinter/eruption breccia deposits (Sherlock et al., 1995). Thus there appears to be a clear relationship between the higher gold grade sheeted veins in the fluid upflow, and lower grade mineralization in sinter/breccia deposits formed as outflows.

c) Fissure vein gold-silver deposits

1. Characteristics

Fissure veins or reefs develop within dilational structural environments controlled by major crustal structures in competent host rocks (Fig. 8.1; Sections 3.iv and vi). These deposits typically form at 300-400 m below the surface (200 m at Golden Cross; Fig. 8.5), but may locally extend to much deeper crustal levels (e.g., 800 m at Waihi; Fig. 8.7). The seismic pumping model of Sibson (1987) provides a mechanism for the formation of banded veins by repeated mineral deposition in volcanically active terrains characterized by strike-slip structures (Section 3.iv.b). Here, rapid boiling of rising meteoric-dominated fluids within the fissure forms the characteristic gangue mineral assemblage of crustiform banded quartz, adularia and platy calcite pseudomorphed by quartz. Metal deposition may be promoted by the quenching or sudden mixing of mineralizing fluids as they ascend into structures which are saturated with cool, commonly low pH, and in some cases oxidized, surficial fluids. Bonanza gold grades develop within dilational structures which promote high rates of fluid flow and rapid quenching. Most of the gold-silver mineralization is deposited in sulfide bands associated with fine quartz and low temperature clays.

Fissure vein deposits develop zoned alteration assemblages which at depth, grade laterally over short distances, from illite or sericite near the feeder structures, to peripheral alteration dominated by carbonate-chlorite ± epidote assemblages. At shallower levels hydrothermal fluids are no longer confined to the feeder structures and mushroom out into extensive two phase zones (Fig. 2.3) to form broad areas of low temperature illitic clay alteration. Careful analyses of the zonations in clay alteration and modelling of the dilational structural environment may point towards high grade fissure vein systems at depth (e.g., Golden Cross, below).

2. Examples

1. Golden Cross, New Zealand

At Golden Cross, gold mineralization occurs in a low grade stockwork resource of 2.3 Mt at 2.8 g/t Au and 13 g/t Ag which overlies the Empire fissure vein containing 3 Mt at 7.2 g/t Au and 17 g/t Ag (Hay, 1989).

Golden Cross forms part of the Hauraki Goldfield (production 9.7 M oz Au) in which Coromandel Group island arc andesitic volcanics deposited from the early Miocene, and are overlain by Late Miocene to younger Whitianga Group rhyolitic volcanics (Skinner, 1986; Simmons et al., 1992), with which adularia-sericite epithermal gold deposits are associated (Brathwaite and Pirajno, 1993). New Zealand occurs at a plate margin in a regime of oblique collision, thereby imparting a dextral strike slip component of movement to major NS structures in the Coromandel Peninsula (Fig. 7.47).

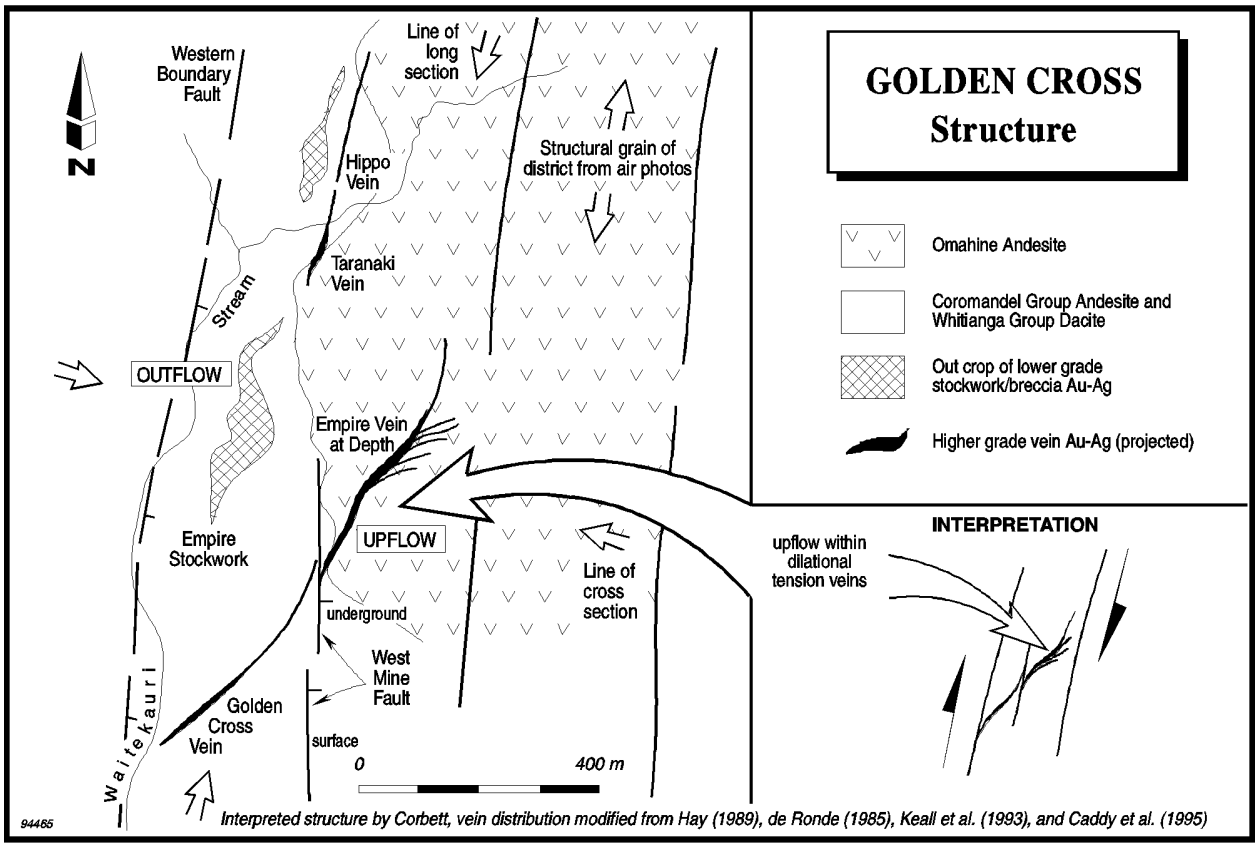
GOLDEN CROSS
Structure
Omahine Andesite
Coromandel Group Andesite and Whitianga Group Dacite
Out crop of lower grade stockwork/breccia Au-Ag
Higher grade vein Au-Ag (projected)
N
Western Boundary Fault
Line of long section
Hippo Vein
Structural grain of district from air photos
Taranaki Vein
Stream
OUTFLOW
Empire Vein at Depth
Empire Stockwork
UPFLOW
Line of cross section
underground
West Mine Fault
Golden Cross Vein
surface
0
400 m
Waitekauri
INTERPRETATION
upflow within dilational tension veins
94465
Interpreted structure by Corbett, vein distribution modified from Hay (1989), de Ronde (1985), Keall et al. (1993), and Caddy et al. (1995)

FIG. 8.4

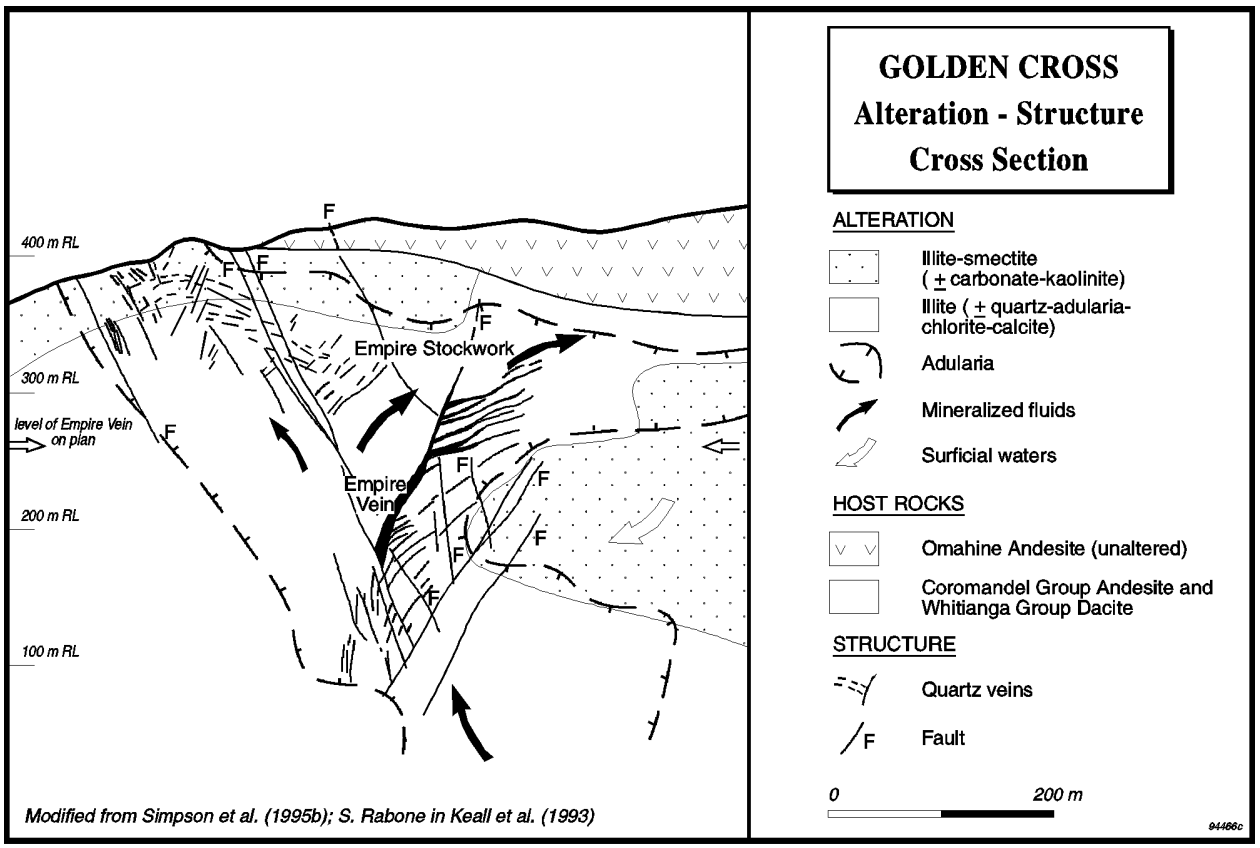
GOLDEN CROSS
Alteration - Structure
Cross Section
400 m RL
300 m RL
level of Empire Vein on plan
200 m RL
100 m RL
Empire Stockwork
Empire Vein
F
ALTERATION
Illite-smectite (± carbonate-kaolinite)
Illite (± quartz-adularia-chlorite-calcite)
Adularia
Mineralized fluids
Surficial waters
HOST ROCKS
Omahine Andesite (unaltered)
Coromandel Group Andesite and Whitianga Group Dacite
STRUCTURE
Quartz veins
Fault
0
200 m
Modified from Simpson et al. (1995b); S. Rabone in Keall et al. (1993)
94466c

FIG. 8.5

Early miners exploited the Hippo, Taranaki and Golden Cross veins. The Golden Cross ore deposit comprises the steeply dipping Empire fissure vein and an overlying Empire stockwork which mushrooms as a broad zone of argillic alteration, silicification, and quartz veins formed at shallow levels (Figs. 8.4, 8.5; Hay, 1989; Keall et al., 1993). Although exploration initially focused upon the stockwork, the periphery of which was exposed in an adit and road cuttings (Fig 8.4), a vertical drill hole (number 27 in the programme), remained in silicification and eventually intersected the underlying fissure vein from 210-238 m (Hay, 1989).

An office-based early interpretation (G. Corbett, unpubl. data, 1989) utilised the dextral oblique (compression from NE) convergence, and suggested that NS-trending air photo linears, evident as drainage patterns, defined NS structures, and fissure veins formed as en echelon tension veins, constrained between these structures (Figs. 7.47, 8.4). Omahine Andesite, then interpreted from fracture-controlled clay alteration as a pre-mineral cap, is regarded by more recent workers (Caddy et al., 1995; Keall et al., 1993) as post-mineral. Caddy et al. (1995) provide a structural model for ore formation in which the Empire fissure vein and associated footwall splays formed during NE compression, and the stockwork veins developed during a later reversal of compression (Fig. 8.5). The NS faults display syn- and post-mineralization activation in this model.

Simpson et al. (1995b) recognized two stages of alteration at Golden Cross (Fig. 8.5). Illite alteration associated with quartz-adularia-chlorite-calcite-pyrite envelops the Empire vein and stockwork vein systems, and is interpreted to have been derived from upwelling alkali chloride waters. The distribution of adularia reflects a confined upflow at depth and a broad mushrooming at shallow levels, as the hydrothermal fluids outflow within the stockwork fracture system (Fig. 8.5). Later alteration is characterized by interlayered illite-smectite alteration associated with carbonate-kaolinite at shallow levels, and marginal to the veins (within a permeable pyroclastic unit) to the veins, and is interpreted to have been derived from descending, cooler CO_2-rich steam-heated waters (Fig. 8.5; Simpson et al., 1985b).

The distribution of clay mineralogy in the stockwork vein system above and parallel to the Empire vein illustrates how alteration mapping can be used to identify zones of hot fluid upflow as the possible sites of ore grade feeder zones in epithermal environments (Fig. 8.6; T. Leach, unpubl. data). High temperature illite is confined at depth to the region immediately adjacent to the quartz reef, whereas the distribution of interlayered clays reflects a mushrooming of the fluid at shallow levels within the quartz stockwork vein system. The presence of low temperature interlayered clays at significant depth to the north and south of the alteration zone suggests that there has been a recharge of cool waters there.

The characteristics of the Empire Reef are described by Simpson, et al. (1995a). The reef is a colloform banded quartz vein system composed of coarse quartz $\pm$ adularia bands alternating with thin bands of fine quartz $\pm$ clays (mainly kaolinite), and rare carbonate bands. Clasts of early fluidized breccias are incorporated in banded veins, and late stage banded veins cut earlier banded quartz veins. Thin dark auriferous sulfide bands are composed of very fine quartz $\pm$ kaolinite, pyrite, silver ($\pm$ selenide) sulfosalts and sulfide (e.g., pyrargyrite and argentite), and trace chalcopyrite. Gold occurs as electrum either intergrown with the silver minerals or with fine quartz. Kaolinite and carbonate also fill vughs in earlier bands, locally with associated gold mineralization (Simpson, et al 1995a; T. Leach, pers. observations).

Two stages of hydrothermal activity have taken place at Golden Cross (de Ronde and Blattner, 1988; Simpson, et al., 1995a, 1995b):
I. An early stage of upwelling high temperature dilute fluids deposited the bulk of the quartz-adularia veins and zoned quartz-adularia-chlorite-illite-calcite-pyrite alteration envelops the Empire vein.
II. A late stage influx of cool descending bicarbonate-sulfate fluids deposited kaolinite-carbonate in the veins associated with gold mineralization, and carbonate + low temperature clay minerals (kaolinite, smectite, interlayered illite-smectite) at shallow levels and at depth around the margins of the Empire vein.

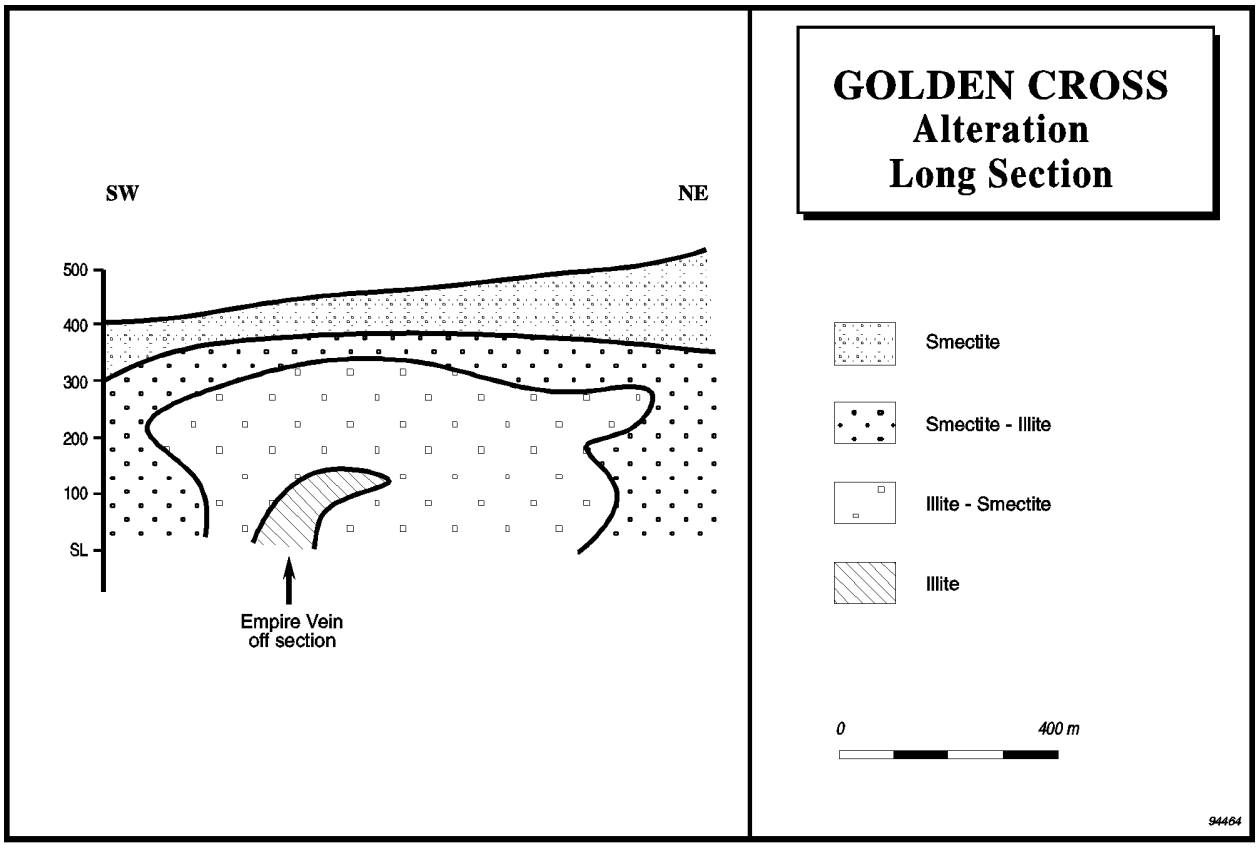
GOLDEN CROSS
Alteration
Long Section
SW
NE
500
400
300
200
100
SL
Empire Vein
off section
Smectite
Smectite - Illite
Illite - Smectite
Illite
0
400 m
94464

FIG. 8.6

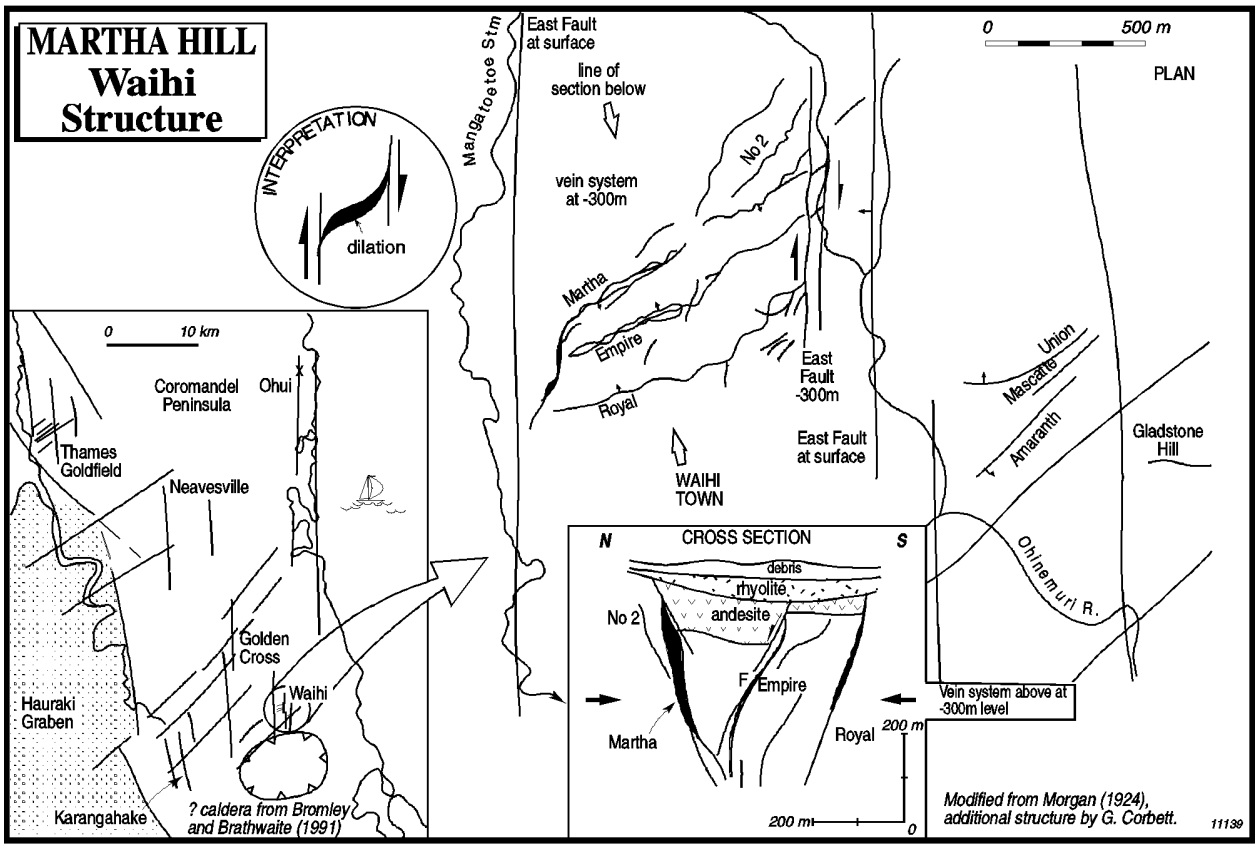
MARTHA HILL
Waihi
Structure
INTERPRETATION
dilation
Mangatoetoe Stm
East Fault
at surface
line of
section below
vein system
at -300m
No 2
Martha
Empire
Royal
East
Fault
-300m
East Fault
at surface
WAIHI
TOWN
0
500 m
PLAN
Union
Mascatte
Amaranth
Gladstone
Hill
Ohinemuri R.
0
10 km
Coromandel
Peninsula
Ohui
Thames
Goldfield
Neavesville
Golden
Cross
Waihi
Hauraki
Graben
Karangahake
? caldera from Bromley
and Brathwaite (1991)
N
CROSS SECTION
S
debris
rhyolite
andesite
No 2
F
Empire
Martha
Royal
200 m
200 m
0
Vein system above at
-300m level
Modified from Morgan (1924),
additional structure by G. Corbett.
11139

FIG. 8.7

It is interpreted herein that the two stages were periodically contemporaneous, and mixing of the hot, upwelling fluids and the cool, low pH, CO_2-rich waters was an important mechanism for gold-silver deposition.

2. Martha Hill, Waihi, New Zealand

At the Martha Hill mine, Waihi, a quartz vein lode system was mined underground to a depth of 600 m and for a strike of 1600 m, from 1883 to 1952, and produced an estimated 5.2 million ounces gold and 30.3 million ounces silver. The mine was reopened in 1988 to mine lower grade stockwork veins in an open-pit resource of 8 Mt of 2.9 g/t Au and 28 g/t Ag (Brathwaite and McKay 1989, Simmons et al., 1992).

The Waihi vein systems developed at 6.58-7.24 Ma., within Miocene andesites adjacent to an inferred caldera margin (Fig. 8.7; Bromley and Brathwaite, 1991; Brathwaite and McKay, 1989), and is partly obscured by Quaternary ash units. Mineralization is hosted within a series of subparallel steep to moderately dipping fissure veins and intervening stockwork veins (Fig. 8.7; Morgan, 1924; Wellman, 1954; Brathwaite and McKay, 1989). The largest vein, the Martha Lode, was traced for a strike of 1600 m, varied to widths of up to 30 m, and mined to depths exceeding 450 m (Brathwaite and McKay, 1989). The smaller Empire vein joins the Martha lode and, like the Royal vein, dips more shallowly and towards the Martha lode (Fig. 8.7).

The veins trend roughly ENE and are constrained between NS-trending faults partly identified on mine data (Morgan, 1924), and also inferred from the drainage pattern on the air photos (G. Corbett, unpubl. data; Fig. 8.7). Early mining recognised a dextral offset to the veins by the eastern set of bounding faults (Morgan, 1924; Fig. 8.7). The Martha lode and associated veins formed as en echelon fissure veins within a dilational jog between the NS-trending strike-slip structures (Sibson, 1987), during oblique plate convergence (Figs. 7.46, 8.7). This jog developed as a pull-apart basin, which from changes in thickness of the pre-mineral andesite and post-mineral debris, displayed a protracted history of activity (Fig. 8.7), consistent with the tectonic setting (Fig. 7.47). The main veins form the bounding faults for the pull-apart basin.

Mineralization occurs in veins which change from thin crustiform to colloform banded chalcedony and fine quartz at shallow levels, to crustiform banding of coarser quartz and thin sulfide-rich bands at deeper levels (Brathwaite and McKay, 1989). Quartz-adularia-illite alteration envelops the veins, and grades laterally away from the veins to calcite-chlorite alteration. Late stage chlorite and illite-smectite overprint the other alteration assemblages, especially in fault/shear zones (Brathwaite and McKay, 1989; Jennings et al., 1990).

Gold-silver mineralization formed late in the depositional sequence as electrum and acanthite, mainly in thin sphalerite-galena-chalcopyrite bands, within crustiform banded quartz (Brathwaite and McKay, 1989; Panther et al., 1995). Mamilliary or ripple-like features in these crustiform bands are coated by kaolinite (Panther et al., 1995), and suggest that mineral deposition occurred from a colloidal solution (Saunders, 1990), under relatively low pH conditions. Fluid inclusion analyses on late stage clear and amethystine quartz (Brathwaite and McKay, 1989) identified depositional temperatures which cluster around 220-270°C, and very dilute salinities (<2-4 wt % equiv NaCl). The local presence of 3-20 percent sulfide (pyrite, sphalerite, galena and chalcopyrite) within the veins, along with reported elevated molybdenum contents at depth (Simmons et al., 1992), suggest that a significant component of magmatic fluid may have been present during the mineralization at Waihi.

iii) Hishikari, Kyushu, Japan

The Hishikari mine in Japan illustrates the importance of rock competency and fluid quenching in the formation of bonanza ore grades. Although some earlier mining is evident, the Hishikari vein system was discovered in 1980 during exploration by the Metal Mining Agency of Japan which began in 1975 (Nakayama, 1995; Izawa et al., 1990; Sillitoe, 1995c; and references therein). Production began in 1989 with reserves of 1.4 Mt at 70 g/t Au

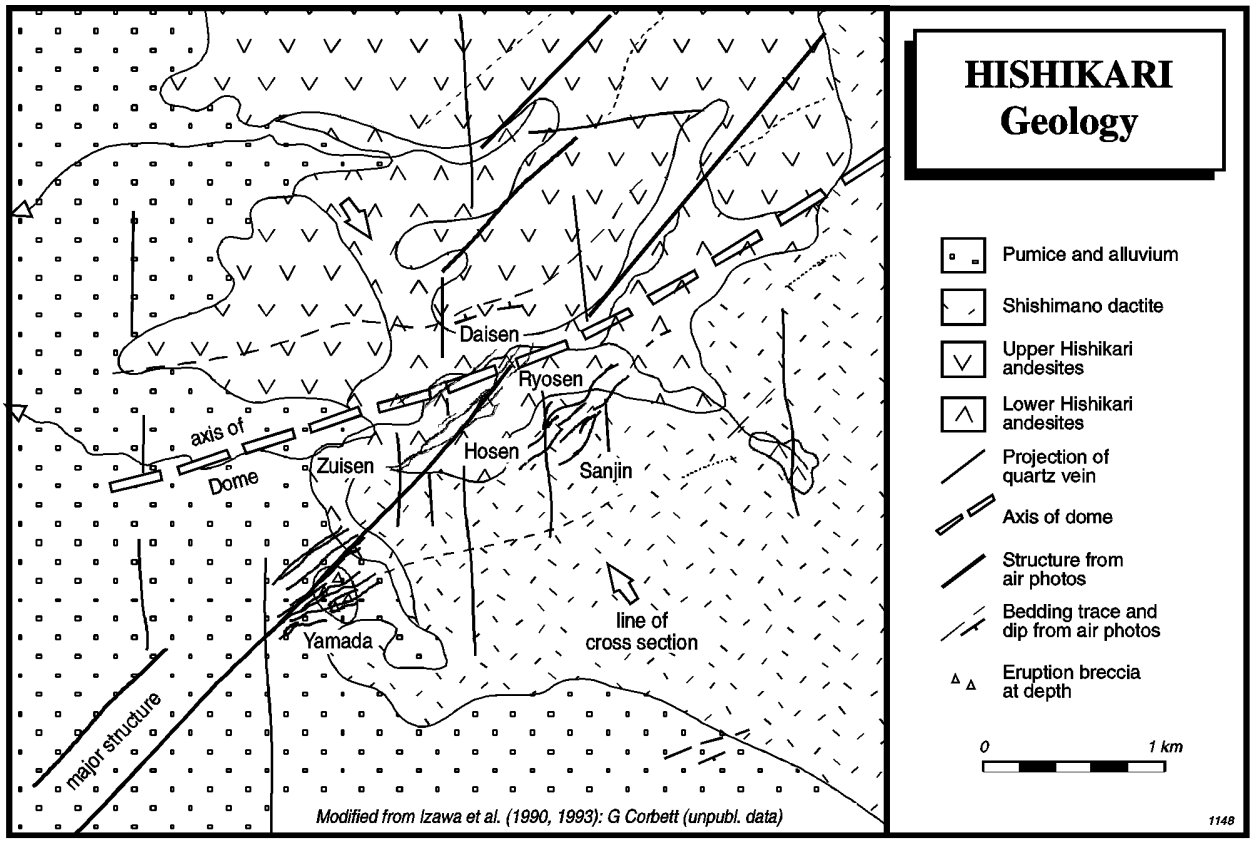
HISHIKARI
Geology
Pumice and alluvium
Shishimano dactite
Upper Hishikari andesites
Lower Hishikari andesites
Projection of quartz vein
Axis of dome
Structure from air photos
Bedding trace and dip from air photos
Eruption breccia at depth
0
1 km
Daisen
Ryosen
Hosen
Zuisen
Sanjin
Yamada
axis of Dome
major structure
line of cross section
Modified from Izawa et al. (1990, 1993): G Corbett (unpubl. data)
1148

FIG. 8.8

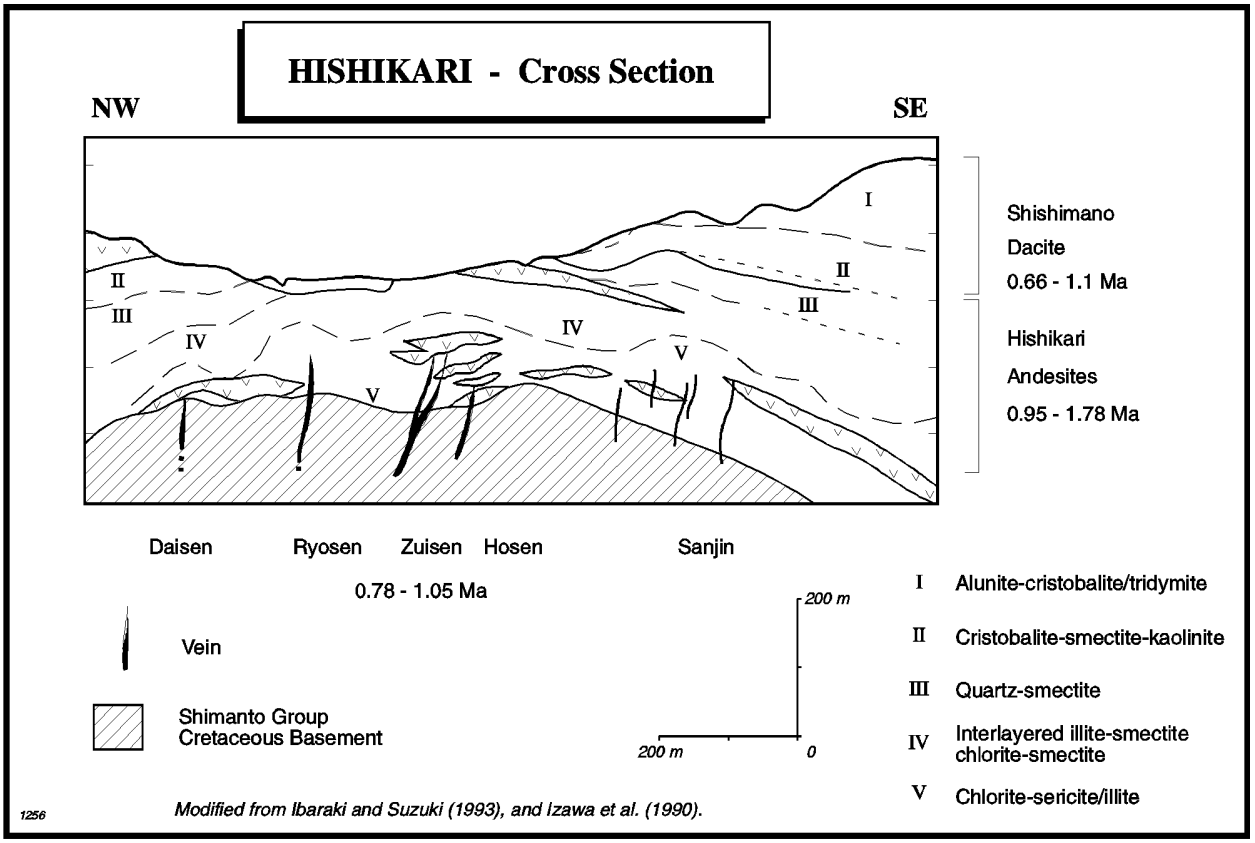
HISHIKARI - Cross Section
NW
SE
I
II
III
IV
V
Shishimano
Dacite
0.66 - 1.1 Ma
Hishikari
Andesites
0.95 - 1.78 Ma
Daisen
Ryosen
Zuisen
Hosen
Sanjin
0.78 - 1.05 Ma
Vein
Shimanto Group
Cretaceous Basement
200 m
200 m
0
I Alunite-cristobalite/tridymite
II Cristobalite-smectite-kaolinite
III Quartz-smectite
IV Interlayered illite-smectite chlorite-smectite
V Chlorite-sericite/illite
1256
Modified from Ibaraki and Suzuki (1993), and Izawa et al. (1990).

FIG. 8.9

(3.2 M oz Au) at Honko, the main Hishikari vein system comprising the Diasen, Ryosen, Zuisen, and Hosen veins (Fig. 8.8), and an additional 2 Mt at 20-25 g/t Au at Yamada (Izawa et al., 1990). Further exploration of these veins, and the addition of the Sanjin ore zone (Fig. 8.8), brought the production and reserves to 3.2 Mt at 63 g/t Au at Honko-Sankin and 2 Mt at Yamada, or a total of 8.3 million oz gold (Ueno, 1993 in Sillitoe 1995c).

A steeply dipping set of fissure veins are aligned along the intersection of a major throughgoing structure evident on the remote sensing imagery (G. Corbett, unpubl. data, 1987) with the crest of a dome (Fig. 8.8). Host rocks comprise a basement Shimanto Group shale which does not crop out in the mine area, overlying Hishikari andesite lava and breccias, a cap of Shishimano dacitic pyroclastics (Izawa et al., 1990). The dome in the basement Shimanto Group shales in this area is apparent as a gravity high (Izawa et al., 1990). The initial formation of the vein system resulted in clay alteration of the permeable tuff breccias. During continued activation of the ore-hosting structural environment, the clay altered andesites deformed in a plastic manner and only the brittle basement shales dilated to host the fissure veins. Thus, much of the gold deposition took place in the 100 metre vertical interval at the top of the competent basement shale (Fig. 8.9). Bonanza gold grades occur at the upper contact of banded veins with the volcanic breccias. This contrasts with the Martha Mine, Waihi, New Zealand (above), where the vein system has been mined over a vertical extent of some 600 metres, but at a lower gold grade.

The Shimanto Group Shales are unaltered except for thin chlorite-illite selvages immediately adjacent to the veins. However, the more permeable overlying andesitic tuffs have undergone intense alteration which exhibits a vertical zonation typical of adularia-sericite epithermal gold-silver systems. Chlorite-illite alteration proximal to the veins grades at progressively shallower levels to zones of: interlayered illite-smectite and chlorite-smectite, quartz-smectite, cristobalite-smectite-kaolinite and sporadic alunite-cristobalite /tridymite (Izawa et al., 1990; Fig 8.9). This alteration zonation reflects a transition from: near neutral, relatively hot conditions associated with quartz-adularia veins at depth, to cool surficial conditions associated with acid sulfate and CO_2-rich waters (Section 2.iii).

The occurrence of smectite-kaolinite-cristobalite alteration in the andesites, cool homogenization temperatures of fluid inclusions in quartz (<200°C in andesites at 100 m level, Izawa et al., 1990), and lacustrine sediments filling an eruption breccia crater immediately overlying the Yamada veins (Izawa et al., 1993), all indicate that the Hishikari vein system was formed at very shallow epithermal levels in the hydrothermal system (less than 50 m erosion). The age of mineralization at 0.84-1.01 Ma (from adularia), is consistent with the age of the Hishikari Andesites and Shishimano Dacite (Izawa et al., 1990; Ibaraki and Suzuki, 1993; Fig. 8.9).

The colloform banded fissure veins at Hishikari grade from: alternating quartz and adularia near the wall rock, to alternating quartz and clay (mainly smectite, minor kaolinite, illite and chlorite) in the central portions of the veins (Nagayama, 1993), and contain local gypsum, carbonates (calcite and Mn-Fe-Ca carbonate) and zeolites (laumontite and wairakite, Izawa et al., 1990). Coarse bands are composed of blocky adularia and flaky quartz, the latter either pseudomorphs bladed carbonate, or was deposited directly from a boiling fluid.

Gold occurs as electrum (average fineness 700), commonly associated with chalcopyrite, naumannite (Ag-selenide) and other Ag-minerals, or as isolated grains with quartz (Izawa et al., 1990). High silver grade black sulfide bands (ginguro ore) are composed of Cu-Ag sulfosalts, sulfide, tellurides and selenides, and commonly occur in thin bands between early adularia-quartz and later smectite-quartz bands (Izawa et al., 1990; Shikazono and Nagayama, 1993). Gold-silver mineralization is sparse in the coarse quartz and adularia bands, but abundant in thin bands of very fine grained quartz-clay (smectite or kaolinite), quartz, or quartz-adularia (Izawa et al., 1990). On the basis of the clay mineralogy and fluid inclusion data (Izawa et al., 1990), it appears that the fine sulfide bands (and the bulk of the gold) were deposited at significantly lower temperatures ($\leq$ 200-210°C) and periodically lower fluid pH, than the quartz-adularia veins (T_h averages 240°C in adularia; Izawa et al., 1990). Mineralization is interpreted (Izawa et al., 1990), to result from the mixing of rapidly upwelling and

boiling, hot mineralized fluids with cool ground waters. Oxygen isotope analyses (Matsuhisa and Aoki, 1994) demonstrate that up to 30 percent more magmatic fluid was associated with formation of sulfide-rich bands, than the unmineralized or low grade bands. This is indicative of a magmatic source for the metals and consistent with the age relationships described above.

It is evident that two distinct hydrothermal processes have taken place at Hishikari:
I. An initial phase of alteration was dominated by deposition of quartz-adularia veins under relatively hot (approximately 240°C; Izawa, et al., 1990) two phase conditions, and hosted in the Shimanto Group shales. Minor gold mineralization may have been associated with this event. Steam heated CO_2-rich and local acid sulfate waters at shallow levels formed zoned clay alteration in the overlying andesite.
II. A later, and locally contemporaneous, alteration deposited fine quartz, clays, and associated sulfides, selenides and high to bonanza grade gold mineralization. These veins are interpreted to have formed in response to the quenching of upwelling, boiling, metal-bearing magmatic fluid by surficial acidic waters (Izawa et al., 1990; Shikazono and Nagayama, 1993).

The presence of vertically zoned carbonates at Hishikari, possibly associated with descending CO_2-rich waters, illustrates a minor carbonate-base metal component to ore development. Typical carbonate-base metal gold systems have been recorded elsewhere in Japan (Akiba, 1957; in Nagayama 1993).

9 CONCLUSION

i) Introduction

An understanding of the possible processes involved in the formation of, and the distinction between different styles of Pacific rim gold-copper systems, can provide a sound geological foundation in mineral exploration. Such an understanding can help distinguish projects which warrant further consideration from those which should be abandoned. The development of new ideas can also facilitate re-evaluation of areas explored using earlier, possibly inappropriate models.

The processes, models and methods described in this short course were developed by geologists actively undertaking exploration for, and the development of, gold-copper deposits in the southwest Pacific region. As such, the models have been applied in actual field settings and are continuously being modified as new field data emerges.

The models presented here have been used successfully during all stages of mineral exploration from: project generation, grassroots reconnaissance exploration, target delineation, various drilling stages including project evaluation and development, and to the expansion of known resources. In addition, accurate resource estimates are dependent on reliable geological models (Lewis, 1992).

ii) Gold-Copper Exploration Models During Project Generation

Sections 2 and 3 demonstrated how active porphyry-related geothermal systems and many significant ore bodies are localized by major crustal arc parallel or arc normal structures. However, the flow of hydrothermal fluids in active systems and the fossil ore bodies is controlled by dilational subsidiary structures, commonly formed adjacent to major structures: typically as tension veins, as splays, hanging wall splits, flexures, or dilational jogs. While competent host rocks are required as hosts for fracture/breccia-controlled mineralization, many dilatant vein systems are capped by pull-apart basins, filled with clastic sediments. Successful project generation can utilise this understanding to delineate fertile exploration ground (e.g., the giant porphyry copper deposit in Chile, La Escondida, was discovered by following the trace of the Domeyko fault; Lowell, 1991b).

Similarly, transfer structures in Papua New Guinea represent deep crustal fractures which have facilitated dextral rotation of the mainland during oblique convergence, but are partly obscured by deformed younger sediments. These major structures localize intrusion centres, and by movement, develop ore hosting dilational environments in subsidiary structures (e.g., Porgera Zone VII, Papua New Guinea). While transfer structures localize the Porgera, Wafi and Yandera porphyry centres, the Frieda River Porphyry and associated Nena high sulfidation gold-copper mineralization are localized by accretionary structures, typically at splays or intersections of transfer structures. The Nena mineralization is hosted within a dilational ore environment created by inferred movement on the major arc parallel structures. The Bulolo graben, which hosts the Morobe goldfield, Papua New Guinea, developed during intra-arc rifting aided by movement on transfer structures. Crustal thinning initiated magmatism with which diatreme breccias and fracture controlled gold mineralization are associated.

Thus, the recognition of favourable structural settings within magmatic arcs from remote sensing and aeromagnetic imagery may define more promising areas for follow-up reconnaissance exploration. Different volcanic and tectonic settings host varying styles of gold and copper mineralization, in part dependent upon crustal level.

iii) Gold-Copper Exploration Models in Reconnaissance Prospecting

The recognition of the styles of hydrothermal alteration present in stream float during first pass reconnaissance prospecting, can aid in the rapid identification of the type of gold-copper mineralization in the district. Different gold-copper resources should be prospected by the most appropriate methods.

Porphyry copper targets can quickly be identified from alteration styles and from the types of quartz veins present. An exploration programme initially targeting auriferous quartz-sulfide veins led to the eventual discovery of the Batu Hijau porphyry copper deposit, Indonesia (Meldrum et al., 1994). The identification of residual or vughy silica boulders which are commonly barren, because of supergene leaching, can lead to the discovery of significant high sulfidation systems. The stream geochemical signature is weak only short distances downstream from the Miwah high sulfidation system in Sumatra, however silicified boulders occurred 45 km downstream from the source outcrop (Williamson and Fleming, 1995). The Wafi River high sulfidation system in Papua New Guinea, was discovered from mineralized silicified float boulders, although the stream geochemical signature was short and very weak.

At Tolukuma, in Papua New Guinea, the identification of banded epithermal quartz float, similar to vein systems in New Zealand and Japan, downstream from the present mine during the follow up of BLEG stream anomalies, hastened discovery of the vein system (Langmead and McLeod, 1990).

iv) Gold-Copper Exploration Models in Project Development

The processes and concepts presented in this manual are best utilised on the prospect-scale where they can provide a framework to develop exploration strategies on larger data bases. The integration of structure and alteration/mineralization with geophysics, geochemistry, and geological mapping can assist in prioritising the more promising prospects.

This manual presents the structural and petrological methods or tools which the authors use during mineral exploration. Detailed structural mapping on surface and in drill holes can be used to identify the optimum sites for maximum fluid permeability. The development of alteration zonations and changes in styles of mineralization are aimed at defining fluid flow directions within the most favourable host rocks or structures. The development of paragenetic sequences of alteration, vein development and ore phases may identify the causes of mineralization, and specifically the settings of high grade mineralization. The integration of structure, alteration and mineralization may facilitate the development of fluid flow models which point to targets displaying the greatest potential for mineralization, in particular high grade zones. These models provide an indication of the direction of the source intrusion, which may also be mineralized.

It is important to map the structure of vein systems and ensure that drilling is correctly oriented. Mineralization commonly occurs in dilational subsidiary fractures formed at high angles to the more major controlling structures. Drilling oriented normal the major structures could intersect mineralized veins at very low angles to the core axis. Resources drill tested in this manner may be downgraded.

Although porphyry copper systems all share similar features, each one is unique. This manual provides a conceptual framework in which to understand the processes which take place during the development of a porphyry copper system. The inference that porphyry gold-copper systems are derived from larger unseen magma sources at depth, by fluid flow along sheeted fracture/vein systems, may aid in the identification of higher grade mineralization. These concepts may help to unravel the overprinting alteration, vein development and mineralization events, and thereby target potential ore zones through the meaningful mapping of alteration and mineralization zonations. An understanding of the structural setting of mesothermal vein systems, in conjunction with delineation of zonations in the styles of gangue phases and ore minerals in these veins, can provide vectors which point to potentially ore grade porphyry sources.

The recognition of zonations in alteration assemblages and ore mineralogy, is of paramount importance in the successful definition of high sulfidation systems. These data, in conjunction with the identification of favourable structural zones of maximum brecciation, can lead to targeting zones of high grade mineralization (e.g., Mt. Kasi, Fiji), or areas of similar mineralization to those already known (e.g., Malaria Zone at Wafi). The recognition of

mineralized clasts within breccias may provide exploration strategies (e.g., diatreme breccias at Lepanto, Philippines; Sillitoe, 1995c) and the analysis of alteration zonation and structure provide fluid flow vectors to target mineralized porphyry intrusions (e.g., Wafi, Papua New Guinea; Erceg et al., 1991).

Porphyry-related low sulfidation gold systems exhibit both vertical and horizontal zonations, away from the intrusion source. Carbonate-base metal gold systems are commonly associated with diatreme or other fluidized breccias. In these systems, the recognition of zonations in gangue phases and ore mineralization within a favourable structural framework can provide exploration targets. Mineralization is encountered in zones of mixed carbonates, whereas high grade zones may be located either in upflow zones where optimum mixing occurs (e.g., Kelian, Indonesia), or in near surface zones where mixing with oxidized ground waters can produce bonanza quartz gold-silver mineralization (e.g., Porgera). Significant zones of mixing, between upwelling mineralized fluids and ground waters previously drawn down as an intrusion cools, occur within dilational structures.

Epithermal gold-silver deposits are localized within dilational ore hosting structural environments. Repeated seismic pumping funnels mineralized fluids through these structures (Sibson, 1987), where mixing with cool, oxidized ground waters may form bonanza grade deposits. It is therefore necessary in epithermal gold-silver systems to define zones of dilation within competent host rocks. These commonly form at high angles to the weakly mineralized controlling major structures. An understanding of these relationships is important in planning drill testing. At near surface levels the bonanza quartz reefs may be buried beneath large stockwork systems within argillically altered host rocks. Alteration zonations within this argillic blanket can be used to provide vectors to the blind feeder zone (e.g., Golden Cross).

v) Flexible models

It is necessary to evolve exploration models by continual field testing and so the models delineated herein must not be applied rigidly. It is important to focus upon the processes involved rather than the actual models presented in this short course. These models are continuing to evolve as they are tested by application to field examples, and therefore are intended to be used as only a framework upon which to develop suitable prospect-specific exploration models. Obtain an appropriate overall model for the project, then mould it to fit the data specific to that unique environment.

GOOD LUCK & GOOD HUNTING

10 ACKNOWLEDGMENTS

The geological models presented herein evolved as we presented our ideas to our peers at short courses, and in our consulting work, but have only been synthesised during the writing of this manual. We thank those peers. The concept of this short course came from our associations with Ian Plimer (Melbourne University) and Dave

Semple (when at Highlands Gold) and only continued following positive reactions from our fellow geoscientists, in particular Max Baker, Pat Browne, Mike Smith, John Thompson, Theo van Leeuwen and Neil Phillips. We thank Alan Coope who suggested the idea of publication to the SEG, Gary Sidder followed through, Patricia Sheahan and Ray Coveney shepherded it through the editorial process and Neil Phillips, John Thompson and Jeff Hedenquist acted as reviewers. Ray Merchant, David Hilyard, Tony Crawford, Pat Browne, Max Baker, Jorge Skarmeta, Paul Lennox, and Bill Laing provided many useful comments to the text. Many clients and geologists have provided continuing encouragement, especially Tony Williamson, Tony Bainbridge, Kim Denwer, Mark Arundell, Gavin Thomas, Ron Stewart, Mike Erceg, David Heberlein, Colin Burge, Mark Hartley, and Trevor Neale. In addition Greg acknowledges the inspiration and technical assistance of Richard Sillitoe, Max Baker and Jorge Skarmeta, and Terry appreciates the support of his colleagues Antony Coote, Graeme Corlett, and Michele Hawke. Geoimage assisted Greg with remote sensing imagery for research purposes.

The following companies are thanked for permission to publish work: Alkane Exploration N.L., Austpac Gold N.L., Aurora Gold Ltd, Atapa Minerals, Barrick Gold Corporation, Carpenters Pacific Resources, Chase Minerals (Philippines) Corporation, Climax Arimco Mining Corporation, CRA Exploration, Coeur Gold N.Z, Cyprus Gold Australia, Delta Gold N.L., Dome Resources N.L., Gympie Eldorado Gold Mines, Highlands Gold Limited, International Pursuit Corporation, Kelian Equatorial Mining, Macraes Mining Co. Ltd., Misima Mines Pty., Misty Mountain Gold, P.T. Newmont Indonesia, Newcrest Mining, Niugini Mining Limited, North Exploration Limited, Pacific Islands Gold, Placer Pacific, Porgera Joint Venture, P.T. Rio Tinto Indonesia, RGC Exploration, Werrie Gold N.L..

Denese Oates provided Greg with encouragement, painstakingly composited and proof read manuals, set out references, with the assistance of Sue Ho, and drafted figures with the assistance of Zanna Oates, Kerry Oates and Andy Lidgard. Susan Pond's constant support and legitimate herbs kept Terry on track.

11 REFERENCES CITED

Adshead, N.D and Appleby, K., 1996, The Umuna Au-Ag deposit, Misima Island, Papua New Guinea: Spatial but not genetically associated with porphyry *in* Porphyry related copper and gold deposits of the Asia Pacific Region, Cairns, Australia, 12-13 August 1996, proceedings: Adelaide, Australian Mineral Foundation, p. 14.1-14.10.

Ahmad, M., Solomon, M., and Walshe, J.L., 1987, Mineralogical and geochemical studies of the Emperor gold telluride deposit, Fiji: ECONOMIC GEOLOGY, v. 82, p. 345-370.

Afifi, A.M., Kelly, W.C., and Essene, E.J., 1988, Phase relations among tellurides, sulfides and oxides: II Application to telluride-bearing ore deposits: ECONOMIC GEOLOGY, v. 83, p. 395-404.

Akiro, K., 1986, The geology and mineralization of the Kerimenge Gold Prospect, Wau District, Morobe Province, *in* Papua New Guinea mineral development symposium, 1986, Madang: Parkville, The Australasian Institute of Mining and Metallurgy, p. 59-62.

Allen, J.M., Artmont, G.J., and Palmer, K., 1995, Application of alluvial gold mineralogy to exploration of the Central Ranges, Iran Jaya, Indonesia, *in* Pacific Rim Congress 95, 19-22 November 1995, Auckland, New Zealand, proceedings: Carlton South, The Australasian Institute of Mining and Metallurgy, p. 7-12.

Allibone, A.H., 1993, Paragenetic relations and the origin of advanced argillic alteration in shear hosted hydrothermal systems of the central Lachlan fold belt, Australia: Unpublished Ph.D. thesis, Townsville, James Cook University at North Queensland, 300 p.

Allibone, A.H., Cordery, G.R., Morrison, G.W., Jaireth, S., and Lindhorst, J.W., 1995, Synchronous advanced argillic alteration in a shear zone-hosted magmatic hydrothermal Au-Ag deposit at Temora (Gidginbung) Mine, New South Wales, Australia: ECONOMIC GEOLOGY, v. 90, p. 1570-1603.

Anderson, W.B., and Eaton, P.C., 1990, Gold mineralization at the Emperor Mine, Vatukola, Fiji, *in* Hedenquist, J.W., White, N.C., and Siddeley, G., eds., Epithermal gold mineralization of the Circum Pacific: Journal of Geochemical Exploration, v. 35, p. 267-296.

Aoki, M., 1992, Active gold mineralization in an evolving magmatic hydrothermal system at Osorezan, Northern Honshu *in* Epithermal gold in Asia and the Pacific, mineral concentrations and hydrocarbon accumulation in the ESCAP Region, 6, Proceedings of workshop on epithermal gold mineralisation, 9-18 May 1989, Tsukuba, Japan: Bangkok, United Nations Economic and Social Commission Asia and Pacific, p. 28-33.

Aoki, M., 1992, Magmatic fluid discharging to the surface form the Osorezan geothermal system, north Honshu, Japan: Japan Geological Survey Report 279, p. 16-21.

Aoki, M., 1993, The Osorezan-type gold deposit *in* Shikazono, N., Naito, K., and Izawa, E., 1993, Editors preface, eds., High grade epithermal mineralization - the Hishikari deposit: The Society of Resource Geology, Resource Geology Special Issue, v. 14, Editors Preface, p. iii-x.

Appleby, K, Circosta, G., Fanning, M and Logan, K., 1996, New model for controls on gold-silver mineralization on Misima Island: Mining Engineering, v. 48, p. 33-36.

Arehart, G.B., Chryssoulis, S.L., and Kesler, S.E., 1993, Gold and arsenic in iron sulfides from sediment-hosted disseminated gold deposits: ECONOMIC GEOLOGY, v. 88, p. 171-185.

Arevalo, E.M., 1986, Opaque minerals in some Tongonan geothermal wells, *in* 8th New Zealand geothermal workshop, 5-7 November 1986, Auckland, New Zealand, proceedings: Auckland, University of Auckland Geothermal Institute, p. 97-103.

Arribas, A. Jr., 1995, Characteristics of high-sulfidation epithermal deposits, and their relation to magmatic fluid, *in* Thompson, J.F.H., ed., Magmas, fluids and ore deposits: Mineralogical Association of Canada Short Course Handbook, v. 23, p. 419-454.

Arribas, A. Jr., Hedenquist, J.W., Itaya, T., Okada, T., Conception, R.A., and Garcia, J.S. Jr., 1995, Contemporaneous formation of adjacent porphyry and epithermal Cu-Au deposits over 300 ka in northern Luzon, Philippines: Geology, v. 23, p. 337-340.

Asami, N., and Britten, R.M., 1980, The porphyry copper deposits at the Frieda River Prospect, Papua New Guinea: Mining Geology Special Issue, v. 8, p. 117-139.

Austpac Gold N. L., Resources Project Department, Nissho, I., and Corbett, G.J., 1990, Epithermal gold deposits of Japan, *in* Pacific Rim Congress 90, 6-12 May 1990, Gold Coast, Queensland, proceedings: Parkville, The Australasian Institute of Mining and Metallurgy, p. 641-644.

Babcock, R.C. Jr., Black, J.E., and Ballantyne, G.H., 1992, Summary of the geology of the Bingham Canyon District, Utah: 1992 Porphyry Copper Short Course, Spokane, Washington, Course Notes, Northwest Mining Association.

Babcock, R.C. Jr., Ballantyne, G.H., and Phillips, C.H., 1995, Summary of the Bingham Canyon District, Utah, *in* Pierce, F.W., and Bolm, J.G., eds., Porphyry copper deposits of the American Cordillera: Arizona Geological Society Digest, v. 20, p. 316-335.

Bagby, W.C., and Berger, B.R., 1985, Geologic characteristics of sediment-hosted, disseminated precious-metal deposits in the western United States, *in* Berger, B.R., and Bethke, P.M., eds., Geology and geochemistry of epithermal systems: Reviews in Economic Geology, v. 2, p. 169-202.

Bainbridge, A.L., Corbett, G.J., and Leach, T.M., 1993, The Nena high sulfidation epithermal Cu/Au system, Frieda River Copper, Papua New Guinea: The application of new ideas, *in* Second national meeting, Specialist Group in Economic Geology, Armidale, New South Wales, abstracts: Geological Society of Australia Abstracts, v. 34, p. 3-4.

Bainbridge, A.L., Corbett, G.J., and Leach, T.M., 1994, The Nena high sulfidation system, Frieda River Copper, Papua New Guinea, *in* Rogerson, R., ed., Geology, exploration and mining conference, June 1994, Lae, Papua New Guinea, proceedings: Parkville, The Australasian Institute of Mining and Metallurgy, p. 131-137.

Baker, E.M., 1987, Geologic, petrographic and fluid inclusion study of breccia hosted gold mineralization at Kidston, north Queensland: Unpublished Ph.D. thesis, Townsville, James Cook University of North Queensland, 409 p.

Baker, E.M., 1992, The Manakayan diatreme complex and its relationship to copper-gold mineralization, Northern Luzon, Philippines, *in* MINexpo, 17 October 1992, Las Vegas: Washington, American Mining Congress, p. 69-74.

Baker, E.M., and Andrew, A.S., 1991, Geologic, fluid inclusion, and stable isotope studies of the gold-bearing breccia pipe at Kidston, Queensland, Australia: ECONOMIC GEOLOGY, v. 86, p. 810-830.

Baker, E.M., and Tullemans, F.J., 1990, Kidston gold deposit, *in* Hughes, F.E., ed., Geology of the mineral deposits of Australia and Papua New Guinea: Australasian Institute of Mining and Metallurgy Monograph 14, p. 1461-1465.

Baker, E.M., Kirwin, D.J., and Taylor, R.G., 1986, Hydrothermal breccia pipes: Economic Geology Research Unit, James Cook University, EGRU Contribution, v. 12, p. 45.

Baldwin, J.T., Swain, H.D., and Dow, A.S., 1978, Geology and grade distribution of the Panguna porphyry deposit, Bougainville, Papua New Guinea: ECONOMIC GEOLOGY, v. 73, p. 690-702.

Barber, S.J., 1992, The geology and gold mineralization of the Warrego-Golden Mile Mine, Cracow, central Queensland: Unpublished B.Sc. (Honours) thesis, Townsville, James Cook University of North Queensland.

Barnes, H.L., 1979, Solubilities of ore minerals, *in* Barnes, H.L., ed., Geochemistry of hydrothermal ore deposits, 2nd edition: New York, John Wiley & Sons, p. 404-460.

Barnett, P.R., Delfin, F., and Española, O.S., 1985, Geothermal exploration in the southern Philippines, *in* 1985 international symposium on geothermal energy, 26-30 August 1985, Kilua-Kona, Hawaii, proceedings: Transactions of Geothermal Resources Council, Hawaii, v. 9, p. 389-394.

Barton, P.B., and Skinner, B.J., 1979, Sulfide mineral stabilities, *in* Barnes, H.L., ed., Geochemistry of hydrothermal ore deposits, 2nd edition: New York, John Wiley & Sons, p. 278-403.

Beane, R.E., 1983, The magmatic-meteoric transition: Geothermal Resources Council Special Report, v. 13, p. 145-253.

Beane, R.E., and Titley, S.R., 1981, Porphyry copper deposits. Part II Hydrothermal, alteration and mineralisation: ECONOMIC GEOLOGY, 75th Anniversary Volume, p. 235-269.

Begg, G.C., Loucks, R.R., Gray, D., Foster, D.A., Kent, A.J., and Cooke, D.R., 1997, Magmas, fluids and tectonics: The Emperor story: Geological Society of Australia, Abstracts No 44, pp. 9.

Bening, L.G., and Seward, T.M., 1994, The solubility of gold as $AuHS^0$ in high temperature hydrosulphide solutions: European Journal of Mineralogy, v. 6, p. 24.

Berger, B.R., and Bagby, W.C., 1991, The geology and origin of Carlin-type gold deposits, *in* Foster, R.P., ed., Gold metallogeny and exploration: Glasgow, Blackie, p. 210-248.

Berger, B.R., and Eimon, P.L., 1983, Conceptual models of epithermal precious metal deposits, *in* Shanks, W.C. III, ed., Cameron volume on unconventional mineral deposits: New York, American Institute of Mining, Metallurgy and Petroleum Engineering, and Society of Mining Engineers, p. 191-205.

Berger, B.R., and Henley, R.W., 1989, Advances in the understanding of epithermal gold-silver deposits with special reference to the western United States: ECONOMIC GEOLOGY MONOGRAPH 6, p. 405-423.

Bettles, K.H., and Lauha, E.A. 1991, Gold deposits of the Goldstrike mine, Carlin Trend, Nevada, *in* World Gold '91, Cairns, Australia, 21-26 April 1991, proceedings: Parkville, The Australasian Institute of Mining and Metallurgy and Society of Mining Engineers, p. 252-257.

Biddle, K.T., and Christie-Blick, N., 1985, Glossary - strike-slip deformation, basin formation, and sedimentation, *in* Ethington, R.L., ed., Strike-slip deformation, basin formation and sedimentation: Society of Economic Paleontologists and Mineralogists Special Publication, v. 37, p. 375-383.

Binns, R.A., Scott, S.D., Bogdanov, Y.A., Lisitzin, A.P., Gordeev, V.V., Finlayson, E.J., Boyd, T., Dorret, L.E., Wheeler, G.E., and Muravyev, K.G., 1993, Hydrothermal oxide and gold-rich sulfate deposits of Franklin Seamount, Western Woodlark Basin, Papua New Guinea: ECONOMIC GEOLOGY, v. 88, p. 2122-2153.

Binns, R.A., Parr, J.M, Scott, S.D., Gemmell, J.B., and Herzig, P.M., 1995, PACMANUS: An active seafloor hydrothermal field on siliceous volcanic rocks in the eastern Manus Basin, Papua New Guinea, *in* Pacific Rim Congress 95, 19-22 November 1995, Auckland, New Zealand, proceedings: Carlton South, The Australasian Institute of Mining and Metallurgy, p. 49-54.

Blès, J-L., and Feuga, B., 1986, The fracture of rocks: New York, Elsevier, 131 p. (French original “La fracturation des roches”, translated by Wanklyn, J.).

Blount, C.W., and Dickson, F.W., 1969, Solubility of anhydrite ($CaSO_4$) in NaCl-H_2O from 100°C to 450C and 1 to 1000 bars: Geochimica et Cosmochimica Acta, v. 33, p. 227-245.

Bogie, I., and Lawless, J.V., 1986, The relationship between volcanic centres and active hydrothermal systems of the Bicol Peninsula, Luzon, Philippines, *in* 8th New Zealand geothermal workshop, 5-7 November 1986, Auckland, New Zealand, proceedings: Auckland, University of Auckland Geothermal Institute, p. 123-128.

Bogie, I., and Lawless, J.V., 1987, Controls on the hydrology of large volcanically-hosted geothermal systems: Implications for exploration for epithermal mineral deposits, *in* Pacific Rim Congress 87, 26-29 August 1987, Gold Coast, Queensland, proceedings: Parkville, The Australasian Institute of Mining and Metallurgy, p. 57-60.

Bogie, I., Lawless, J.V., and Pornuevo, J.B., 1987, Kaipohan: An apparently non-thermal manifestation of hydrothermal systems in the Philippines: Journal of Volcanology and Geothermal Research, v. 31, p. 281-292.

Bodnar, R.J., 1995, Fluid inclusion evidence for a magmatic source for metals in porphyry copper deposits, *in* Thompson, J.F.H., ed., Magmas, fluids and ore deposits: Mineralogical Association of Canada Short Course Handbook, v. 23, p. 139-152.

Bonham, H.F., 1986, Models for volcanic hosted epithermal precious metal deposits: A review, *in* Proceedings of symposium 5: Volcanism, hydrothermal systems and related mineralisation, February 1986, Auckland: Auckland, International Volcanological Congress, p.13-18.

Bonham, H.F., 1988a, Bulk mineable gold deposits of the western United States: ECONOMIC GEOLOGY MONOGRAPH 6, p. 193-207.

Bonham, H.F., Jr., 1988b, Models for volcanic-hosted epithermal precious metal deposits, *in* Schafer, R.W., Cooper, J.J., and Vikre, P.G., eds., Bulk mineable precious metal deposits of the western United States, symposium proceedings, 6-8 April 1987, Reno, Nevada: Reno, Geological Society of Nevada, p. 259-271.

Boric, R.P., Diaz, F.F., and Maksaev, V.J., 1990, Geología y yacimientos metaliferos de la region de Antofagasta: Instituto de Investigaciones Geológicas, Chile, Boletin, v. 40, 246 p. (in Spanish).

Brathwaite, R.L., 1989, Geology and exploration of the Karangahake gold-silver deposit, *in* Kear, D., ed., Mineral deposits of New Zealand: Australasian Institute of Mining and Metallurgy Monograph 13, p. 73-78.

Brathwaite, R.L., and McKay, D.F., 1989, Geology and exploration of the Martha Hill gold-silver deposit, Waihi, *in* Kear, D., ed., Mineral deposits of New Zealand: Australasian Institute of Mining and Metallurgy Monograph 13, p. 83-88.

Brathwaite, R.L., and Pirajno, F., 1993, Metallogenic map of New Zealand: New Zealand Institute of Geological and Nuclear Sciences Monograph 3, 215 p.

Brathwaite, R.L., Christie, A.B., and Skinner, D.N.B., 1989, The Hauraki Goldfield - regional setting, mineralisation and recent exploration, *in* Kear, D., ed., Mineral deposits of New Zealand: Australasian Institute of Mining and Metallurgy Monograph 13, p. 45-56.

Brimwall, C.H., and Ghiorso, M.S., 1983, Origin and ore-forming consequences of the advanced argillic alteration process in hypogene environments by magmatic gas contamination of meteoric fluids: ECONOMIC GEOLOGY, v. 78, p. 73-90.

Britten, R.M., 1981, The geology of the Frieda River Copper prospect, Papua New Guinea: Unpublished Ph.D. thesis, Canberra, The Australian National University, 395 p.

Brooker, M., and Jaireth, S., 1995, Mount rawdon, Southeast Queensland, Australia - A diatreme-hosted gold-silver deposit, ECONOMIC GEOLOGY, V. 90, P. 1799-1817.

Bromley, C.J., and Brathwaite, R.L., 1991, Waihi basin structures in light of recent geophysical surveys, *in* Proceedings of the 25th annual conference, New Zealand branch, Auckland, The Australasian Institute of Mining and Metallurgy, p. 225-238.

Brown, G.A., 1989, Mineral potential of Northland, *in* Kear, D., ed., Mineral deposits of New Zealand: Australasian Institute of Mining and Metallurgy Monograph 13, p. 33-37.

Brown, K.L., 1986, Gold deposition from geothermal discharges in New Zealand: ECONOMIC GEOLOGY, v. 81, p. 979-983.

Brown, K.L., 1989, Kinetics of gold precipitation from experimental hydrothermal sulphide solutions: ECONOMIC GEOLOGY MONOGRAPH 6, p. 320-327.

Browne, P.R.L., 1978, Hydrothermal alteration in active geothermal fields: Annual Reviews in Earth and Planetary Sciences, v. 6, p. 229-250.

Browne, P.R.L., 1991, Hydrothermal alteration and geothermal systems: Unpublished Geothermal Diploma Course Notes, Auckland, Auckland University, 98 p.

Browne, P.R.L. and Ellis, A.J., 1970, The Ohaaki-Broadlands geothermal area, New Zealand: Mineralogy and related geochemistry: American Journal of Science, v. 269, p. 97-131.

Burnham, C.W., 1979, Magmas and hydrothermal fluids, *in* Barnes, H.L., ed., Geochemistry of hydrothermal ore deposits, 2nd edition: New York, John Wiley & Sons, p. 71-136.

Burnham, C.W., 1985, Energy release in subvolcanic environments: Implications for breccia formation: ECONOMIC GEOLOGY, v. 80, p. 1515-1522.

Burton, C.K., 1983, Observations on the geology of the porphyry copper sub-province of Southern Negros, Philippines: Geological Society of Malaysia, Bulletin 16 p. 215-239.

Caddy, S.W., McOnie, A.W., and Rutherford, P.G., 1995, Volcanic stratigraphy, structure and controls to mineralization, Golden Cross Mine, New Zealand, *in* Pacific Rim Congress 95, 19-22 November 1995, Auckland, New Zealand, proceedings: Carlton South, The Australasian Institute of Mining and Metallurgy, p. 93-98.

Candela, P.A., and Piccoli, P.M., 1995, Model ore-metal portioning from melts into vapour/brine mixtures, *in* Thompson, J.F.H., ed., Magmas, fluids and ore deposits: Mineralogical Association of Canada Short Course Handbook, v. 23, p. 101.

Carlile, J.C., and Kirkegaard, A.G., 1985, Porphyry copper-gold deposits of the Tombulilato District, North Sulawesi, Indonesia: An extension of the Philippine porphyry copper-gold province, *in* Asia Mining '85, 11-14 February 1985, Manila: London, Institute of Mining and Metallurgy, p. 351-363.

Carlile, J.C., and Mitchell, A.H.G., 1994, Magmatic arcs and associated gold and copper mineralization in Indonesia: Journal of Geochemical Exploration, v. 50, p. 91-142.

Carlile, J.C., Digdowirogo, S., and Darius, K., 1990, Geological setting, characteristics and regional exploration for gold in the volcanic arcs of North Sulawesi: Journal of Geochemical Exploration, v. 35, p. 105-140.

Carman, G.D., 1994, Genesis of the Ladolam gold deposit, Lihir Island, Papua New Guinea: Unpublished Ph.D. thesis, Melbourne, Monash University, unpublished.

Carman, G.D., 1995, The Lihir Island gold deposit, Papua New Guinea: The dynamic role of magmatic-hydrothermal processes in its formation, *in* Clark, A.h. Ed., Giant Ore Deposits II: Controls on the scale of orogenic magmatic-hydrothermal mineralization, Second Giant Ore deposits Workshop, April 25-27, 1995, Kingston, Ontario, proceedings, (second, corrected printing) p. 732-753.

Carter, R.M., and Norris, R.J., 1976, Cainozoic history of southern new Zealand: an accord between geological observations and plate tectonic predictions: Earth and Planetary Sciences Letters, v. 31, p. 85-94.

Cas, R.A.F., and Wright, J.V., 1987, Volcanic successions modern and ancient: London, Allen and Unwin, 528 p.

Cathles, L.M., 1977, An analysis of the cooling of intrusives by ground-water convection which includes boiling: ECONOMIC GEOLOGY, v. 72, p. 804-826.

Chivas, A.R., 1978, Porphyry copper mineralization at the Koloula Igneous Complex, Guadalcanal, Solomon Islands: ECONOMIC GEOLOGY, v. 73, p. 645-677.

Christie, A.B., and Brathwaite, R.L., 1986, Epithermal gold-silver and porphyry copper deposits of the Hauraki Goldfield - a review, *in* Henley, R.W., Hedenquist, J.W., and Roberts, P.J., eds., Guide to the active epithermal (geothermal) systems and precious metal deposits of New Zealand: Monograph Series in Mineral Deposits, Berlin, Gebruder Borntraeger, v. 26, p. 129-145.

Circum-Pacific Council for Energy and Mineral Resources, 1981, Plate Tectonic map of the Circum Pacific Region: Tulsa, American Association of Petroleum Geologists.

Clarke, D.S., Lewis, R.W. and Waldron, H.M., 1990, Geology and trace-element geochemistry of the Umuna gold-silver deposit, Misima Island, Papua New Guinea: Journal of Geochemical Exploration, v. 36, p. 201-223.

Cline, J.S., and Bodnar, R.J., 1991, Can economic porphyry copper mineralization be generated by a typical calc-alkaline melt?: Journal of Geophysical Research, v. 96, p. 8113-8126.

Cline, J.S., and Bodner, R.J., 1994, Direct evolution of brine from a crystallizing melt at the Questa, New Mexico, molybdenum deposit: ECONOMIC GEOLOGY, v. 89, p. 1780-1802.

Cline, J.S., and Vanko, D., 1995, Magmatically generated saline brines related to molybdenum at Questa, New Mexico, U.S.A., *in* Thompson, J.F.H., ed., Magmas, fluids and ore deposits: Mineralogical Association of Canada Short Course Handbook, v. 23, p. 153-174.

Cole, J.W., 1984, Taupo-Rotorua depression: An ensialic marginal basin of North Island, New Zealand, *in* Kokelaar, B.P., and Howells, M.F., eds., Marginal basin geology: volcanic and associated sedimentary and tectonic processes in modern and ancient marginal basins: Special Publication of the Geological Society of London, v. 16, p. 109-120.

Cole, J.W., 1990, Structural control and origin of volcanism in the Taupo Volcanic Zone, New Zealand: Bulletin Volcanology, v. 52, p. 445-259.

Coleman, P.J., Haig, D.W., and Wilkins, N.A., 1988, Puzzling occurrence of a deep sea ooze in a modern island arc terrain in the Solomon Islands: Search, v. 19, p. 90-91.

Colley, H., and Flint, D.J., 1995, Metallic mineral deposits of Fiji: Mineral Resources Department of Fiji, Memoir 4, 196 p.

Comsti, M.E.C., Villones, R.I., De Jesus, C.V., Natividad, A.R., Rollan, L.A., and Duroy, A.C., 1990, Mineralization at the Kelly gold mine, Baguio district, Philippines: Fluid-inclusions and wall-rock alteration: Journal of Geochemical Exploration, v. 35, p 341-362.

Concepsion, R.A., and Cinco, J.C., Jr., 1989, Geology of Lepanto Far Southeast gold-rich porphyry copper deposit, Mankayan, Benguet, Philippines: 28th International Geological Congress, Washington D.C., Abstracts, v. 1, p. 319-320.

Corbett, G.J., 1994, Regional structural control of selected Cu/Au occurrences in Papua New Guinea, *in* Rogerson, R., ed., Geology, exploration and mining conference, June 1994, Lae, Papua New Guinea, proceedings: Parkville, The Australasian Institute of Mining and Metallurgy, p. 57-70.

Corbett, G.J., and Hayward, S.B., 1994, The Maragorik high sulfidation Cu/Au system - an update, *in* Rogerson, R., ed., Geology, exploration and mining conference, June 1994, Lae, Papua New Guinea, proceedings: Parkville, The Australasian Institute of Mining and Metallurgy, p. 125-129.

Corbett, G.J., and Taylor, G., 1994, The Mt Kasi high sulfidation system, Fiji, *in* Rogerson, R., ed., Geology, exploration and mining conference, June 1994, Lae, Papua New Guinea, proceedings: Parkville, The Australasian Institute of Mining and Metallurgy, p. 147-153.

Corbett, G.J., First, D.M., and Hayward, S.B., 1991, The Maragorik prospect, East New Britain, Papua New Guinea, *in* Rogerson, R., ed., Proceedings of the PNG geology, exploration and mining conference, 1991, Rabaul: Parkville, The Australasian Institute of Mining and Metallurgy, p. 112-116.

Corbett, G.J., Leach, T.M., Shatwell, D.O., and Hayward, S., 1994a, Gold mineralization on Woodlark Island, Papua New Guinea, *in* Rogerson, R., ed., Geology, exploration and mining conference, June 1994, Lae, Papua New Guinea, proceedings: Parkville, The Australasian Institute of Mining and Metallurgy, p. 92-100.

Corbett, G.J., Leach, T.M., Thirnbeck, M., Mori, W., Sione, T., Harry, K., Digan, K., and Petrie P., 1994b, The geology of porphyry-related mesothermal vein gold mineralization north of Kainantu, Papua New Guinea, *in* Rogerson, R., ed., Geology, exploration and mining conference, June 1994, Lae, Papua New Guinea, proceedings: Parkville, The Australasian Institute of Mining and Metallurgy, p. 113-124.

Corbett, G.J., Semple, D., and Leach, T.M., 1994c, The Tolukuma Au/Ag vein system, Papua New Guinea, *in* Rogerson, R., ed., Geology, exploration and mining conference, June 1994, Lae, Papua New Guinea, proceedings: Parkville, The Australasian Institute of Mining and Metallurgy, p. 230-238.

Corbett, G.J., Leach, T.M., Stewart, R., and Fulton, B., 1995, The Porgera gold deposit: Structure, alteration and mineralisation, *in* Pacific Rim Congress 95, 19-22 November 1995, Auckland, New Zealand, proceedings: Carlton South, The Australasian Institute of Mining and Metallurgy, p. 151-156.

Cooke, D.R., and Bloom, M.S., 1990, Epithermal and subjacent porphyry mineralization, Acupan, Baguio district, Philippines: A fluid inclusion and paragenetic study, *in* Hedenquist, J.W., White, N.C., and Siddeley, G., eds., Epithermal gold mineralization of the circum Pacific: Journal of Geochemical Exploration, v. 35, p. 297-340.

Cooke, D.R., Bloom, M.S., and Cartwright, I., 1993, The Acupan South porphyry copper-gold prospect, Baguio district, Philippines: Relationship to epithermal mineralization, *in* Second national meeting, Specialist Group in Economic Geology, Armidale, New South Wales, abstracts: Geological Society of Australia Abstracts, v. 34, p. 16-17.

Cooke, D.R. and McPhail, D.C., 1996, Telluride mineralization in low sulfidation epithermal veins - contribution of magmatic volatiles: Geological Society of Australia, Abstracts, no. 41, p. 96.

Cooke, D.R., McPhail, D.C., and Bloom, M.S., 1996, Epithermal Gold Mineralization, Acupan, Baguio District, Philippines: Geology, Mineralization, Alteration and the Thermochemical Environment of Ore Deposition: ECONOMIC GEOLOGY, v. 91, p. 243-272.

Cornwell, J., and Treddinnik, I., 1995, Geology and geochemistry and mining of the Pajingo epithermal vein system, *in* Mineral Deposits of Northeast Queensland: Geology and Geochemistry, EGRU, James Cook University, Townsville, Australia, Contribution 52, p. 54-68.

Cox, S.F., 1994, Deformational controls on the dynamics of fluid migration and ore genesis in metamorphic environments, *in* 12th Australian Geological Convention, Perth, 26-30 September 1994, Abstracts: Geological Society of Australia Abstracts, v. 37, p. 74.

Cox, D.P., and Singer, D.A., 1988, Distribution of gold in porphyry copper deposits: U.S. Geological Survey Open File Report 88-46, 22p.

Cox, S.C., and Craw, D, 1995, Structural permeability in the Southern Alps hydrothermal system, New Zealand, *in* Pacific Rim Congress 95, 19-22 November 1995, Auckland, New Zealand, proceedings: Carlton South, The Australasian Institute of Mining and Metallurgy, p. 157-162.

Cox, S.F., Sun, S-S, Etheridge, M.A., Wall, V.J., and Potter, T.F., 1995, Structural and geochemical controls on the development of turbidite-hosted gold quartz vein deposits, Wattle Gully mine, central Victoria, Australia: ECONOMIC GEOLOGY, V. 90, P. 1722-1746.

CRA P.N.G. Limited, 1994, The Wafi Prospect: Unpublished poster display, Geology, exploration and mining conference, June 1994, Lae, Papua New Guinea, The Australasian Institute of Mining and Metallurgy.

Cracow Mining Venture Staff, Worsley, M.R., and Golding, S.D., 1990, Golden Plateau gold deposits, *in* Hughes, F.E., ed., Geology of the mineral deposits of Australia and Papua New Guinea: Australasian Institute of Mining and Metallurgy Monograph 14, p. 1509-1514.

Creelman, R.A., Lipton, I.T., and Stagg, R.N., 1990, Browns Creek Gold Deposit, *in* Hughes, F.E., Ed., Geology of the mineral deposits of Australia and Papua New Guinea: Australasian Institute of Mining and Metallurgy Monograph 14, p. 1399-1401.

Crerar, D.A., and Barnes, H.L., 1976, Ore solution chemistry, V: Solubilities of chalcopyrite and chalcocite assemblages in hydrothermal solutions at 200°C to 300°C: Economic Geology, v. 71, p. 772-794.

Crowell, J.C., 1962, Displacement along the San Andreas Fault, California: Geological Society of America Special Paper, v. 71, p. 1-59.

Crowell, J.C., 1974, Origin of late Cenozoic basins in southern California, *in* W.R. Dickinson, ed., Tectonics and sedimentation: Society of Economic Paleontologists and Mineralogists Special Paper 22, p. 190-204.

Cunneen, R., 1996, Recent developments in the geology of the Gympie goldfield, *in* Mesozoic geology of eastern Australia, 23-26 September 1996, Brisbane, Geological Society of Australia, Extn. Abs. 43, p. 162-166.

Cunneen, R., and Sillitoe, R.H., 1989, Palaeozoic hot spring sinter in the Drummond Basin, Queensland, Australia: ECONOMIC GEOLOGY, v. 84, p. 135-142.

Cunningham, C.G., Ashley, R.P., Chou, I-M., Huang, Z., Wan, C., and Li, W., 1988, Newly discovered sedimentary-rock hosted disseminated gold deposits in the People's Republic of China: ECONOMIC GEOLOGY, v. 83, p. 1462-1467.

Damasco, F.V., and de Guzman, M.T., 1977, The G.W. gold orebodies in the Acupan mine of the Benguet Corporation: 6th Symposium on Mineral Resources Development, Baguio City, Philippines, proceedings 6 p.

Davidson, J., and Mpodozis, C., 1991, Regional geologic setting of epithermal gold deposits, Chile: ECONOMIC GEOLOGY, v. 86, p. 1174- 1186.

Davies, H., 1983. Wabag, Papua New Guinea 1:250,000 geological series: Port Moresby, Department of Mineral Resources, Geological Survey of Papua New Guinea.

Davies, H.L., 1991, Tectonic setting of some mineral deposits in the Papua New Guinea region, *in* Rogerson, R., ed., Proceedings of the PNG geology, exploration and mining conference, 1991, Rabaul: Parkville, The Australian Institute of Mining and Metallurgy, p. 49-57.

Davies, R.M., and Ballantyne, G.H., 1987, Geology of the Ladolam gold deposit, Lihir Island, Papua New Guinea, *in* Pacific Rim Congress 87, 26-29 August 1987, Gold Coast, Queensland, proceedings: Parkville, The Australasian Institute of Mining and Metallurgy, p. 943-949.

Degeling, P.R., Corbett, G.J., Leach, T.M., 1995, The Peak Hill high sulfidation gold deposit, N.S.W., *in* Pacific Rim Congress 95, 19-22 November 1995, Auckland, New Zealand, proceedings: Carlton South, The Australasian Institute of Mining and Metallurgy, p. 175-180.

Dekker, F., Balkwill, H., Slater, A., Herner, R., and Kampschuur, W., 1990, A structural interpretation of the onshore eastern Papuan fold belt, based on remote sensing and fieldwork, *in* Carman, G.J., and Carman, Z., eds., Petroleum exploration in Papua New Guinea: Proceedings of the first petroleum convention, 12-14 February 1990, Port Moresby: Port Moresby, Brown Prior Anderson, p. 319-336.

Denwer, K.P., Leach, T.M., and Mowat, B.A., 1995, Mineralization of the Morobe Goldfield, Morobe Province, Papua New Guinea, *in* Pacific Rim Congress 95, 19-22 November 1995, Auckland, New Zealand, proceedings: Carlton South, The Australasian Institute of Mining and Metallurgy, p. 181-186.

de Ronde, C.E.J., 1985, Studies on a fossil hydrothermal system at Golden Cross, Waihi, New Zealand: Unpublished M.Sc. thesis, Auckland, University of Auckland, 168 p.

de Ronde, C.E.J., 1889, Fluid chemistry and isotope characteristics of sea floor hydrothermal systems and associated VMS deposits: Potential for magmatic contributions, *in* Thompson, J.F.H., ed., Magmas, fluids and ore deposits: Mineralogical Association of Canada Short Course Handbook, v. 23, p. 479-509.

de Ronde, C.E.J., and Blattner, P., 1988, Hydrothermal alteration, stable isotopes and fluid inclusions of the Golden Cross epithermal gold silver deposit, Waihi, New Zealand: ECONOMIC GEOLOGY, v. 83, p. 895-917.

Dilles, J.H., and Einaudi, M.T., 1992, Wall-rock alteration and hydrothermal flow paths about the Ann-Mason porphyry copper deposit - Nevada: A 6 km vertical reconstruction: ECONOMIC GEOLOGY, v. 87, p. 1963-2001.

Dimo, G., 1990, Telfer gold deposits, *in* Hughes, F.E., ed., Geology of the mineral deposits of Australia and Papua New Guinea: Australasian Institute of Mining and Metallurgy Monograph 14, p. 643-651.

Dong, G., 1992, Preliminary study on paragenesis and fluid inclusion analyses from the outside prospects at Cracow, *in* Report to A.M.I.R.A. Project 247: Melbourne, Australian Minerals Industries Research Association, p. 104-112.

Dong, G., and Morrison, G.W., 1995, Adularia in epithermal veins, Queensland: morphology, structural state and origin: Mineral Deposita, v. 30, p. 11-19.

Dong, G., Morrison, G.W., and Jaireth, S., 1995, Quartz textures in epithermal veins, Queensland - classification, origin and implication: ECONOMIC GEOLOGY, v. 90, p. 1841-1856.

Donnelly-Nolan, J.M., Burns, M.G., Goff, F.E., Peters, E.K., and Thompson, J.M., 1993, The Geysers-Clear Lake area, California: Thermal water, mineralization, volcanism, and geothermal potential: ECONOMIC GEOLOGY, v. 88, p. 301-316.

Dow, D.B., Smit, J.A.J., and Page, R.W., 1974, Wau, Papua New Guinea, 1:250,000 geological series, sheet SB-55-14 - explanatory notes: Canberra, Bureau of Mineral Resources, Geology and Geophysics

Dunoyer de Segonzac, G., 1968, The birth and development of the concept of diagenesis: Earth Science Reviews, v. 4, p. 153-201.

Durney, D.W., and Ramsay, J.G., 1973, Incremental strains measured by syntectonic crystal growths, *in* De Jong, K.A., and Scholten, R., eds., Gravity and tectonics: New York, Wiley, p. 67-96.

Eastoe, C.J., 1978, A fluid inclusion study of the Panguna porphyry copper deposit, Bouganville, Papua New Guinea: ECONOMIC GEOLOGY, v. 73, p. 721-728.

Eastoe, C.J., 1979, The formation of the Panguna porphyry copper deposit, Bougainville, Papua New Guinea, with an appendix on the Frieda porphyry copper deposit, New Guinea: Unpublished Ph.D. thesis, Hobart, University of Tasmania, 255 p.

Eastoe, C.J., 1983, Sulfur isotope data and the nature of the hydrothermal systems at the Panguna and Frieda Porphyry copper deposit, Papua New Guinea: ECONOMIC GEOLOGY, v. 78, p. 201-213.

Eaton, P.C., and Setterfield, T.N., 1993, The relationship between epithermal and porphyry hydrological systems within the Tavua Caldera, Fiji: ECONOMIC GEOLOGY, v. 88, p. 1053-1083.

Edmonds, E.A., McKeown, M.C., and Williams, M., 1975, British regional geology, South-West England, 4th edition: London, National Environment Council, British Geological Survey, 136 p.

Egert, E, and Kasaneva, S., 1995, The San Cristobal Gold District, Antofagasta, Chile, *in* Pacific Rim Congress 95, 19-22 November 1995, Auckland, New Zealand, proceedings: Carlton South, The Australasian Institute of Mining and Metallurgy, p. 197-202.

Einaudi, M.T., 1982a, Descriptions of skarns associated with porphyry copper plutons, southwestern North America, *in* Titley, S.R., ed., Advances in geology of porphyry copper deposits, southwestern North America: Tuscon, University of Arizona Press, p. 139-183.

Einaudi, M.T., 1982b, General features and origin of skarns associated with porphyry copper plutons, southwestern North America, *in* Titley, S.R., ed., Advances in geology of porphyry copper deposits, southwestern North America: Tuscon, University of Arizona Press, p. 185-209.

Einaudi, M.T., Meinert, L.D., and Newberg, R.J., 1981, Skarn deposits: ECONOMIC GEOLOGY, 75th Anniversary Volume, p. 317-392.

Elders, W.A., Hoagland, J.R., McDowell, S.D., and Cobo, J.M., 1979, Hydrothermal mineral zones in the geothermal reservoir of Cerro Prieto: Geothermics, v. 8, p. 201-209.

Ellis, A.J., 1959, The solubility of calcite in carbon dioxide solutions: American Journal of Science, v. 257. p. 354-365.

Ellis, A.J., 1963, The solubility of calcite in sodium chloride solutions at high temperatures: American Journal of Science, v. 261, p. 259-267.

Ellis, A.J., and Mahon, W.A., 1977, Chemistry and geothermal systems: New York, Academic Press, 392 p.

Erceg, M.M., Craighead, G.A., Halfpenny, R., and Lewis, P.J., 1991, The exploration history, geology and metallurgy of a high sulfidation epithermal gold deposit at Wafi River, Papua New Guinea, *in* Rogerson, R., ed., Proceedings of the PNG geology, exploration and mining conference, 1991, Rabaul: Parkville, The Australasian Institute of Mining and Metallurgy, p. 58-65.

Etheridge, M.A., 1983, Differential stress magnitudes during regional deformation and metamorphism: upper bound imposed by tensil fracturing: Geology, v. 11 p. 231-234.

Etheridge, M.A., Symonds, P.A., and Powell, T.C., 1988, Application of the detachment model for continental extension to hydrocarbon exploration in extensional basins: The APEA Journal, 1988, p. 167-187.

Ewers, G.R., Tolfey, C.E., and Erceg, M.M., 1990, Red Dome gold deposit, *in* Hughes, F.E., ed., Geology of the mineral deposits of Australia and Papua New Guinea: Australasian Institute of Mining and Metallurgy Monograph 14, p. 1455-1460.

Ewers, G.R., Wood, D.G., Tedder, I.J., White, N.C., and Hoffman, C.F, 1990, Epithermal gold prospects in the Conway area, north Drummond Basin, Queensland, *in* Pacific Rim Congress 90, 6-12 May 1990, Gold Coast, Queensland, proceedings: Parkville, The Australasian Institute of Mining and Metallurgy, p. 357-362.

Felderhof, J.B., de Guzman, M.T., Puspos, C.M., and Nassey, J.M., 1995, Mineralization in a maar diatreme-dome complex: Busang Gold Deposit, East Kalimantan, Indonesia: Unpublished paper, Prospectors and Developers Conference, Toronto, March. 1995, 9 p.

Fellows, M.L., and Hammond, J.M., 1990, Wirralie Gold Deposit, *in* Hughes, F.E., ed., Geology of the mineral deposits of Australia and Papua New Guinea: Australasian Institute of Mining and Metallurgy Monograph 14, p. 1489-1492.

Ferguson, H.G., 1929, The mining districts of Nevada: ECONOMIC GEOLOGY, v. 24, p. 131-141.

Field, C.W., and Fifarek, R.H., 1985, Light stable-isotope systematics in the epithermal environment, *in* Berger, B.R., and Bethke, P.M., eds., Geology and geochemistry of epithermal systems: Reviews in Economic Geology, v. 2, p. 99-128.

Fleming, A.W., Handley, G.A., Williams, K.L., Hills, A.L., and Corbett, G.J., 1986, The Porgera gold deposit, Papua New Guinea: ECONOMIC GEOLOGY, v. 81, p. 660-680.

Foley, N.K., and Ayuso, R.A., 1994, Lead isotope compositions as guides to early gold mineralization: The North Amethyst Vein System, Creede District, Colorado: ECONOMIC GEOLOGY, v. 89. p. 1842-1859.

Ford, J.H., 1978, A chemical study of alteration at the Panguna porphyry copper deposit, Bouganville, Papua New Guinea: ECONOMIC GEOLOGY, v. 73, p. 703-720.

Ford, J.H., and Green, D.C., 1977, An oxygen and hydrogen isotope study of the Panguna porphyry copper deposit, Bouganville: Journal of the Geological Society of Australia, v. 24, p. 63-80.

Forth, J., 1994, Dewatering and the geothermal control for the proposed mine, Lihir Island, Papua New Guinea, *in* Rogerson, R., ed., Geology, exploration and mining conference, June 1994, Lae, Papua New Guinea, proceedings: Parkville, The Australasian Institute of Mining and Metallurgy, p. 212-218.

Fournier, R.O., 1985a, The behaviour of silica in hydrothermal solutions, *in* Berger, B.R., and Bethke, P.M., eds., Geology and geochemistry of epithermal systems: Reviews in Economic Geology, v. 2, p. 45-62.

Fournier, R.O., 1985b, Carbonate transport and deposition in the epithermal environment, *in* Berger, B.R., and Bethke, P.M., eds., Geology and geochemistry of epithermal systems: Reviews in Economic Geology, v. 2, p. 63-72.

Fraser, C., 1910, The geology of the Thames subdivision, Hauraki, Auckland: New Zealand Geological Survey Bulletin, v. 10, p. 136.

Garcia, J.S., 1991, Geology and mineralization characteristics of the Mankayan mineral district, Benguet, Philippines, *in* Matsuhisa, Y., Aoki, M., and Hedenquist, J.W., eds., High temperature acid fluids and associated alteration and mineralization: Geological Survey of Japan Report, v. 277, p. 21-30.

Garcia, J.S., and Bongolan, M.B., 1989, Developments in enargite ore search at Lepanto, Mankayan, Benguet, Philippines *in* Symposium on mineral resources development, November 1987, Manila, Philippines, proceedings: Manila, Philippine Mine Safety Association, p. 1-21.

Garrett, S., 1996, The geology and mineralization of the Dinkidi porphyry related Au-Cu deposit, *in* Porphyry related copper and gold deposits of the Asia Pacific Region, Cairns, Australia, 12-13 August 1996, proceedings: Adelaide, Australian Mineral Foundation, p. 6.1-6.15.

Garwin, S.L., Hendri, D., and Lauricella, P.F., 1995, The geology of the Mesel sediment-hosted gold deposit, North Sulawesi, Indonesia, *in* Pacific Rim Congress 95, 19-22 November 1995, Auckland, New Zealand, proceedings: Carlton South, The Australasian Institute of Mining and Metallurgy, p. 221-226.

Gemmel, J.B., Simmons, S.F., and Zantop, H., 1988, The Santo Nino silver-lead-zinc vein, Fresnillo district, Zacatecas, Mexico: ECONOMIC GEOLOGY, v. 83, p. 1597-1618.

Gemuts, I., Little, M.L., and Giudici, J., 1996, Precious and base metal deposits in Argentina: SEG Newsletter No. 25, p. 1-14.

Giggenbach, W.F., 1987, Redox processes governing the chemistry of fumarolic gas discharges from White Is., New Zealand: Applied Geochemistry, v. 2, p. 143-161.

Giggenbach, W.F., 1991, Redox processes accompanying the deposition of minerals in volcanic magmatic-hydrothermal systems, *in* Matsuhisa, Y., Aoki, M., and Hedenquist, J.W., eds., High temperature acid fluids and associated alteration and mineralization: Geological Survey of Japan Report, v. 277, p. 91-96.

Giggenbach, W.F., 1992, Magma degassing and mineral deposition in hydrothermal systems along convergent plate boundaries: ECONOMIC GEOLOGY, v. 87, p. 1927-1944.

Glen, R.A., 1987, Copper and gold deposits in deformed turbidites at Cobar, Australia: Their structural control and hydrothermal origin: ECONOMIC GEOLOGY, v. 82, p. 124-140.

Goellnicht, N.M., Groves, D.I., McNaughton, N.J., and Dimo, G., 1989, An epigenetic origin for the Telfer gold deposit, Western Australia: ECONOMIC GEOLOGY MONOGRAPH 6, p. 151-167.

Grieve, P., Corbett, G., and Leach, T, in prep, A conceptual model for gold-silver mineralization at Puhipuhi, Northland, New Zealand: Proceedings, 1997 New Zealand Minerals and Mining Conference.

Grindley, G.W., 1960, Sheet 8 Taupo, Geological Map of New Zealand: Wellington, New Zealand, Department of Scientific and Industrial Research.

Grauch, V.J.S., Jachens, R.C., and Blakely, R.J., 1995, Evidence for a basement feature related to the Cortez disseminated gold deposits and implications for regional exploration in Nevada: ECONOMIC GEOLOGY, v. 90, p. 203-207.

Gunnlaugsson, E., and Arnorsson, S., 1982, The chemistry of iron in geothermal systems in Iceland: Journal of Volcanology and Geothermal Research, v. 14, p. 281-299.

Gustafson, L.B., 1978, Some major factors of porphyry copper genesis: ECONOMIC GEOLOGY, v. 73, p. 602-607.

Gustafson, L.B., and Hunt, J.P., 1975, The porphyry copper deposit at El Salvador, Chile: ECONOMIC GEOLOGY, v. 70, p. 857- 912.

Hackman, B.D., 1980, The geology of Guadalcanal, Solomon Islands: Institute of Geological Sciences, Natural Environment Research Council, London, Overseas Memoirs, v. 6, 115 p.

Hall, R.J., Britten, R.M., and Henry, D.D., 1990, Frieda River copper-gold deposits, *in* Hughes, F.E., ed., Geology of mineral deposits of Australia and Papua New Guinea: Australasian Institute of Mining and Metallurgy Monograph 14, p. 1709-1715.

Hamburger, M.W., and Isacks, B.L., 1988, Diffuse back-arc deformation in the southwestern Pacific: Nature, v. 332, p. 599-604.

Hamilton, W.B., 1979, Tectonics of the Indonesian region: U.S. Geological Survey Professional Paper, v. 1078, 345 p.

Handley, G.A., and Bradshaw, P.M.D., 1986, The Porgera gold deposit, Papua New Guinea, *in* Macdonald, A.J., ed., Proceedings of Gold '86, an international symposium on the geology of gold deposits: Toronto, Gold '86, p. 416-424.

Handley, G.A., and Henry, D.D., 1990, Porgera gold deposit, *in* Hughes, F.E., ed., Geology of mineral deposits of Australia and Papua New Guinea: Australasian Institute of Mining and Metallurgy Monograph 14, p. 1717-1724.

Hanmer, S., and Passchier, C., 1991, Shear-sense indicators: A review: Geological Survey of Canada Paper, v. 90-17, 72 p.

Harper, R.J., and Arevalo, E.M., 1982, A geoscientific evaluation of the Baslay-Dauin Prospect, Negros Oriental, Philippines, *in* 4th Pacific geothermal conference, incorporating 4th New Zealand geothermal workshop, 1982, Auckland, New Zealand, proceedings: Auckland, University of Auckland Geothermal Institute, p. 235-240.

Harvey, C.C., and Browne, P.R.L., 1991, Mixed layered clay geothermometry in the Wairakei geothermal field, New Zealand: Clay and Clay Minerals, v. 39, p. 614-621.

Harvey, C.C., Leach, T.M., and MacDonald, W.J., 1983, Integrated geoscientific exploration at Meager Creek, British Colombia, *in* Proceedings of the 7th Annual EPRI Geothermal Conference and Workshop. San Diego, June 1993, p. 78-83.

Hay, K.R., 1989, Exploration case history of the Golden Cross gold prospect, Waihi, New Zealand, *in* Kear, D., ed., Mineral deposits of New Zealand: Australasian Institute of Mining and Metallurgy Monograph 13, p. 67-72.

Hayba, D.O., Bethke, P.M., Heald, P., and Foley, N.K., 1985, Geologic, mineralogic and geochemical characteristics of volcanic-hosted epithermal precious-metal deposits, *in* Berger, B.R., and Bethke, P.M., eds., Geology and geochemistry of epithermal systems: Reviews in Economic Geology, v. 2, p. 129-162.

Heald, P., Foley, N.K., and Hayba, D.O., 1987, Comparative anatomy of volcanic hosted epithermal deposits: acid-sulfate and adularia-sericite types: ECONOMIC GEOLOGY, v. 82, p. 1-26.

Healy, J., Schofield, J.C., Thompson, B.N., 1964, Sheet 5 Rotorua, Geological Map of New Zealand: Wellington, New Zealand, Department of Scientific and Industrial Research.

Hedenquist, J.W., 1984, Studies on active gold mineralization in the Waiotapu Geothermal System, New Zealand, AusIMM Regional Conference on Gold - Mining, Metallurgy and Geology, Kalgoorlie, Oct 1984, proceedings: Carlton South, The Australasian Institute of Mining and Metallurgy.

Hedenquist, J.W., 1986, Geothermal systems of the Taupo Volcanic Zone, New Zealand: Their characteristics and relation to volcanism and mineralisation, *in* Smith, I.M., ed., Late Cenozoic volcanism in New Zealand: Royal Society of New Zealand Bulletin, v. 23, p. 134- 138.

Hedenquist, J.W., 1987, Mineralization associated with volcanic related hydrothermal systems in the Circum Pacific Basin, *in* Horn, M.K., ed., Transactions of the 4th circum Pacific energy and mineral resources conference, 17-22 August 1987, Singapore: Tulsa, American Association of Petroleum Geologists, p. 513-523.

Hedenquist, J.W., 1990, The thermal and geochemical structure of the Broadlands-Ohaaki Geothermal System, New Zealand: Geothermics, v. 19, p. 151-185.

Hedenquist, J.W., 1991, Boiling and dilution in the shallow portion of the Waiotapu geothermal system, New Zealand: Geochimica et Cosmochimica Acta, v. 55, p. 2753-2765.

Hedenquist, J.W., and Henley, R.W., 1985a, Hydrothermal eruptions in the Waiotapu geothermal system, New Zealand: Their origin, associated breccias, and relation to precious metal mineralization: ECONOMIC GEOLOGY, v. 80, p. 1640-1668.

Hedenquist, J.W., and Henley, R.W., 1985b, Effect of CO_2 on freezing point depression measurements of fluid inclusions - evidence from active systems and implications for epithermal ore deposition: ECONOMIC GEOLOGY, v. 80, p. 1379-1406.

Hedenquist, J.W., and Lowenstern, J.B., 1994, The role of magmas in the formation of hydrothermal ore deposits: Nature, v. 370, p. 519-526.

Hedenquist, J.W., and Reid, F., 1985, Epithermal gold: Sydney, Earth Resources Foundation, University of Sydney, p. 311.

Hedenquist, J.W., Matsuhisa, Y., Izawa, E., Marumo, K., Aoki, and Sasaki, K., 1988, Epithermal gold mineralisation of acid-leached rocks in the Nansatsu district of southern Kyushu, Japan, *in* Bicentennial Gold 88, extended abstracts, oral programme: Geological Society of Australia Abstracts, v. 22, p. 183-190.

Hedenquist, J.W., Simmons, S.F., Giggenbach, W.F., and Eldridge, C.S., 1993, White Island, New Zealand, volcanic-hydrothermal system represents the geochemical environment of high-sulfidation Cu and Au ore deposition: Geology, v. 21, p. 731-734.

Hedenquist, J.W., Matsuhisa, Y., Izawa, E., White, N.C., Giggenbach, W.F., and Oaki, M., 1994, Geology, geochemistry, and origin of high sulfidation Cu-Au mineralization in the Nansatsu District, Japan: ECONOMIC GEOLOGY, v. 89, p. 1-30.

Heidrick, T.L., and Titley, S.R., 1982, Fracture and dike patterns in Laramide Plutons and their structural and tectonic implications, *in* Titley, S.R., ed., Advances in geology of porphyry copper deposits, southwestern North America: Tuscon, University of Arizona Press, p. 73-92.

Heidrick, T.L., and Rehrig, W.A., 1972, A dynamic model for fracturing and diking Laramide stocks and porphyry copper deposits of Arizona: Geological Society of America, Abstracts, v. 3, p. 387.

Heinrich, C.A., Ryan, C.G., Mernagh, T.P., and Eadington, P.J., 1992, Segregation of ore metals between magmatic brines and vapour: A fluid inclusion study using PIYE microanalysis: ECONOMIC GEOLOGY, v. 87, p. 1566-1583.

Heithersay, P.S., 1991, The shoshonite-associated Endeavour 26 North porphyry Cu-Au deposit, Goonumbla, New South Wales: Unpublished Ph.D. thesis, Canberra, The Australian National University, 187 p.

Heithersay, P.S., and Walshe, J.L., 1995, Endeavour 26 North: A porphyry copper-gold deposit in the Late Ordovician, shoshonitic Goonumbla Volcanic Complex, New South Wales, Australia: ECONOMIC GEOLOGY, v. 90, p. 1506-1532.

Heithersay, P.S., O'Neill, W.J., van der Helder, P., Moore, C.R., and Harbon, P.G., 1990, Goonumbla porphyry copper district - Endeavour 26 North, Endeavour 22 and Endeavour 27 copper-gold deposits, *in* Hughes, F.E., ed., Geology of the mineral deposits of Australia and Papua New Guinea: Australasian Institute of Mining and Metallurgy Monograph 14, p. 1385-1398.

Hemley, J.J., and Hunt, J.P., 1992, Hydrothermal ore-forming processes in the light of studies in rock-buffered systems: II Some general geological applications: ECONOMIC GEOLOGY, v. 87, p. 23-43.

Hemley, J.J., Montoya, J.W., Marinenko, J.W., and Luce, R.W., 1980, Equilibria in the systems Al_2O_3-SiO_2-H_2O and some general implications for alteration/mineralization processes: ECONOMIC GEOLOGY, v. 75, p. 210-228.

Hemley, J.J., Cygan, G.L., Fein, J.B., Robinson, G.R., and D'Angelo, W.M., 1992, Hydrothermal ore-forming processes in the light of studies in rock-buffered systems, I: Iron-copper-zinc-lead sulphide solubility relations: ECONOMIC GEOLOGY, v. 87, p. 1- 22.

Henley, R.W., 1973, Solubility of gold in hydrothermal chloride solutions: Chemical Geology, v. 11, p. 73-87.

Henley, R.W., 1985a, The geothermal framework for epithermal deposits, *in* Berger, B.R., and Bethke, P.M., eds., Geology and geochemistry of epithermal systems: Reviews in Economic Geology, v. 2, p. 1-24.

Henley, R.W., 1985b, Ore transport and deposition in epithermal environments, *in* Herbert, H.K., and Ho, S.E., eds., Stable isotopes and fluid processes in mineralization: Geology Department and University Extension, The University of Western Australia, Publication, v. 23, p. 51-69.

Henley, R.W., 1991, Epithermal gold deposits in volcanic terranes, *in* Foster, R.P., ed., Gold metallogeny and exploration: Glasgow, Blackie, p. 133-164.

Henley, R.W., and Berger, B.R., 1993, What is an exploration model anyway? - An analysis of the cognitive development and use of models in mineral exploration, *in* Kirkham, R.V., Sinclair, W.D., Thorpe, R.I., and Duke, J.M., eds., Mineral exploration modelling: Geological Association of Canada Special Paper, v. 40, p. 41-50.

Henley, R.W., and Brown, K.L., 1985, A practical guide to the thermodynamics of geothermal fluids and hydrothermal ore deposits, *in* Berger, B.R., and Bethke, P.M., eds., Geology and geochemistry of epithermal systems: Reviews in Economic Geology, v. 2, p. 25-44.

Henley, R.W., and Ellis, A.J., 1983, Geothermal systems ancient and modern: a geothermal review: Earth Sciences Review, v. 19, p. 1-50.

Henley, R.W., and Hedenquist, J.W., 1986, Introduction to the geochemistry of active and fossil geothermal systems, *in* Henley, R.W., Hedenquist, J.W., and Roberts, P.J., eds., Guide to the active epithermal (geothermal) systems and precious metal deposits of New Zealand: Monograph Series in Mineral Deposits, Berlin, Gebruder Borntraeger, v. 26, p. 1-22.

Henley, R.W, and Hoffman, C.F., 1987, Gold: Sources to resources, *in* Pacific Rim Congress 87, 26-29 August 1987, Gold Coast, Queensland, proceedings: Parkville, The Australasian Institute of Mining and Metallurgy, p. 159-168.

Henley, R.W., and McNabb, A., 1978, Magmatic vapour plumes and ground water interaction in porphyry copper emplacement: ECONOMIC GEOLOGY, v. 73, p. 1-19.

Henley, R.W., Truesdall, A.H., and Barton, P.B. Jr., eds., 1984, Fluid mineral equilibria in hydrothermal systems: Reviews in Economic Geology, v. 1, 267 p.

Henry, D.D., 1988, Porgera - the first fifty years, *in* Bicentennial Gold 88, extended abstracts, oral programme: Geological Society of Australia Abstracts, v. 22, p. 144-149.

Hewitt, W.V., Leckie, J.F., Lorraway, R., Moule, K., Rush, P.M., Seegers, H.J., and Torr, G.L., 1980, Ok Tedi Project - geology of principal ore deposits: BHP Technical Bulletin, v. 24, no. 1, p. 3- 10.

Hezig, P.M., Hannington, M.D., Fouquet, Y., von Stackelberg, U., and Petersen, D., 1993, Gold-rich polymetallic sulfides from the Lau Back Arc and implications for the geochemistry of gold in sea-floor hydrothermal systems of the southwest Pacific: ECONOMIC GEOLOGY, v. 88, p. 2182-2209.

Hill, K.C., 1990, Structural styles and hydrocarbons in the Papuan Fold Belt, a review, *in* Carman, G.J., and Carman, Z., eds., Petroleum exploration in Papua New Guinea: Proceedings of the first petroleum convention, 12-14 February 1990, Port Moresby: Port Moresby, Brown Prior Anderson, p. 301-310.

Hobbs, B.E., Means, W.P., and Williams, P.F., 1976, An outline of structural geology: New York, Wiley International Edition, 571 p.

Hodgson, C.J., 1993, Mesothermal lode-gold deposits, *in* Kirkham, R.V., Sinclair, W.D., Thorpe, R.I., and Duke, J.M., eds., Mineral exploration modelling: Geological Association of Canada Special Paper, v. 40, p. 635-678.

Holland, H.D., and Malinin, S.D., 1979, The solubility and occurrence of non-ore minerals, *in* Barnes, H.L., ed., Geochemistry of hydrothermal ore deposits, 2nd edition: New York, John Wiley & Sons, p. 461-501.

Holtzberger, I.R., Bainbridge, T., Hitchmann, S., and Wilkes, M., 1996, The Frieda River-Nena copper and gold deposits: Discovery and assessment: A case history, *in* Porphyry related copper and gold deposits of the Asia Pacific Region, Cairns, Australia, 12-13 August 1996, proceedings: Adelaide, Australian Mineral Foundation, p. 11.1-11.12

Huston, D.L., Bolger, C., and Cozens, G., 1993, A comparison of mineral deposits at the Geko and White Devil Deposits: Implications for ore genesis in the Tennant Creek district, Northern Territory, Australia: ECONOMIC GEOLOGY, v. 88, p. 1198-1225.

Hutton, M.J., Akiro, A.K., Cannard, C.J., and Syka, M.C., 1990, Kerimenge gold prospect, *in* Hughes, F.E., ed., Geology of the mineral deposits of Australia and Papua New Guinea: Australasian Institute of Mining and Metallurgy Monograph 14, p. 1769-1772.

Ibaraki, K., and Suzuki, R., 1993, Gold-silver quartz-adularia veins of the Main, Yamada and Sanjin deposits, Hishikari gold mine; a comparative study of their geology and ore deposits, *in* Shikazono, N., Naito, K., and Izawa, E., eds., High grade

epithermal mineralization - the Hishikari deposit: The Society of Resource Geology, Resource Geology Special Issue, v. 14, p. 1-12.

Irianto, B., and Clark, G.H., 1995, The Batu Hijau porphyry copper gold deposit, Sumbawa Island, Indonesia, *in* Pacific Rim Congress 95, 19-22 November 1995, Auckland, New Zealand, proceedings: Carlton South, The Australasian Institute of Mining and Metallurgy, p. 299-304.

Irvine, R.J., and Smith, M.J., 1990, Geophysical exploration for epithermal gold deposits, *in* Hedenquist, J.W., White, N.C., and Siddeley, G., eds., Epithermal gold mineralization of the circum Pacific: Journal of Geochemical Exploration, v. 35, p. 375-412.

Isaacs, M.J., Herzer, R.H., Brook, F.J., and Hayward, B.W., 1994, Undated Cretaceous and Cenozoic sedimentary basins of Northland, New Zealand: New Zealand Institute of Geological and Nuclear Sciences Monograph 8, ?? p.

Izawa, E., and Cunningham, C.G., 1989, Hydrothermal breccia pipes and gold mineralization in the Iwashita ore body, Iwato Deposit, Kyushu, Japan: ECONOMIC GEOLOGY, v. 84, p. 715-724.

Izawa, E., Urashima, Y., Ibaraki, K., Suzuki, R., Yokoyama, T., Kawasaki, K., Koga, A., and Taguchi, S., 1990, The Hishikari gold deposit: High grade epithermal veins in Quaternary volcanics of southern Kyushu, Japan, *in* Hedenquist, J.W., White, N.C., and Siddeley, G., eds., Epithermal gold mineralization of the circum Pacific: Journal of Geochemical Exploration, v. 35, p. 1-56.

Izawa, E., Naito, K., Ibaraki, K., and Suzuki, R., 1993, Mudstones in a hydrothermal eruption crater above the gold-bearing vein system of the Yamada deposit at Hishikari, Japan, *in* Shikazono, N., Naito, K., and Izawa, E., eds., High grade epithermal mineralization - the Hishikari deposit: The Society of Resource Geology, Resource Geology Special Issue, v. 14, p. 85-92.

James, L.P., and Fuchs, W.A., 1990, Exploration of the Exciban gold-copper-tellurium vein system, Camarines Norte, Philippines, *in* Hedenquist, J.W., White, N.C., and Siddeley, G., eds., Epithermal gold mineralization of the circum Pacific: Journal of Geochemical Exploration, v. 35, p. 363-386.

Jannas, R.R., Beane, R.E., Ahler, B.A., and Brosnahan, D.R., 1990, Gold and copper mineralization at the El Indio deposit, Chile, *in* Hedenquist, J.W., White, N.C., and Siddeley, G., eds., Epithermal gold mineralization of the circum Pacific: Journal of Geochemical Exploration, v. 35, p. 197-232.

Jennings, K., Browne, P.R.L., Clarke, D.S., and Brathwaite, R.L. 1990, Aspects of hydrothermal alteration at the Waihi epithermal Au-Ag deposit, New Zealand: 12th New Zealand Geothermal Workshop Proceedings, p. 237-242.

Johnson, R.W., 1987, Delayed partial melting of subduction-modified magma sources in western Melanesia: New results from the Late Cainozoic, *in* Pacific Rim Congress 87, 26-29 August 1987, Gold Coast, Queensland, proceedings: Parkville, The Australasian Institute of Mining and Metallurgy, p. 211-219.

Kavalieris, I., 1994, The Grasberg superporphyry: Ore Deposit Studies and Exploration Models, Short Course Notes, Hobart, CODES, University of Tasmania, p. 3.1-3.49.

Kavalieris, I., Turvey, D.J., and Heesterman, L.J.L., 1987, The geology and mineralization of the Mangani Mine, Sumatra, Indonesia, *in* Pacific Rim Congress 87, 26-29 August 1987, Gold Coast, Queensland, proceedings: Parkville, The Australasian Institute of Mining and Metallurgy, p. 221-225.

Kavalieris, I., van Leeuwen, T.M., and Wilson, M., 1992, Geological setting and styles of mineralization, north arm of Sulawesi, Indonesia: Journal of Southeast Asian Earth Sciences, v. 7, p. 113-129.

Keall, P.C., Cook, W.C., Mathews, S.J., and Purvis, A.H., 1993, The geology of the Golden Cross orebody, Complex veining and evolving mining responses: Proceedings of the 27th Annual Conference 1993, New Zealand Branch of the Australasian Institute of Mining and Metallurgy, p. 143-160.

Kearney, P., and Vine, F., Global Tectonics, Oxford, Blackwell Science, 333 p.

King, S., 1993, The stratigraphy and volcanology of the Camboon Volcanics, Cracow, South East Queensland: Unpublished B.Sc. (Honours) thesis, Melbourne University.

Koide, H., and Bhatacharji, S., 1975, Formation of fractures around magmatic intrusions and their role in ore localization: ECONOMIC GEOLOGY, v. 70, p. 781-799.

Kosaka, H., and Wakita, K., 1978, Some geologic features of the Mamut porphyry copper deposit, Sabah, Malaysia: ECONOMIC GEOLOGY, v. 73, p. 618-627.

Kristmannsdotter, H., 1984, Types of clay minerals in hydrothermally altered basaltic rocks: Reykjanes, Iceland: Jokull, v. 26, p. 30-39.

Krupp, R.E., and Seward, T.M., 1987, The Rotokawa geothermal system, New Zealand: An active epithermal gold depositing environment: ECONOMIC GEOLOGY, v. 82, p. 1109-1139.

Kuehn, C.A., and Rose, A.W., 1995, Carlin gold deposits Nevada: Origin in a deep zone of mixing between normally pressured and overpressured fluids: ECONOMIC GEOLOGY, v. 90, p. 17-36.

Kwak, T.A.P., 1990, Vein genesis, geochemical and flow controls on ore mineralization at the Emperor Gold Mine, Vatukoula, Fiji, *in* Hedenquist, J.W., White, N.C. and Siddley, G., eds., Epithermal gold mineralization of the Circum-Pacific: Geology, geochemistry, origin and exploration, II: Journal of Geochemical Exploration, v. 36, p. 297-337.

Laing, W.P., 1994, Palaeozoic structural framework and regional plumbing system of northeastern Queensland, *in* Henderson, R.A., and Davis, B.K., eds., New developments in geology and metallogeny: Northern Tasman Orogenic Zone, extended conference abstracts: Economic Geology Research Unit, James Cook University, EGRU Contribution, v. 50, p. 125-131.

Lang, J.R., Stanley, C.R., and Thompson, J.F.H., 1995, Porphyry copper-gold deposits related to alkalic igneous rocks in the Triassic-Jurassic arc terrains of British Columbia, *in* Pierce, F.W., and Bolm, J.G., eds., Porphyry copper deposits of the American Cordillera: Arizona Geological Society Digest, v. 20, p. 216-236.

Langmead, R., and McLeod, R.L., 1990, Tolukuma gold deposit, *in* Hughes, F.E., ed., Geology of the mineral deposits of Australia and Papua New Guinea: Australasian Institute of Mining and Metallurgy Monograph 14, p. 1777-1781.

Langmead, R.P., and McLeod, R.L., 1991, Characteristics of the Tolukuma Au-Ag deposit, *in* Rogerson, R., ed., Proceedings of the PNG geology, exploration and mining conference, 1991, Rabaul: Parkville, The Australasian Institute of Mining and Metallurgy, p. 77-81.

Large, R.R., 1994, Hydrothermal transport and deposition of copper and gold, *in* CODES Short Course Manual 2: Hobart, University of Tasmania, p. 337-350.

Lawless, J.V., and Gonzalez, R.C., 1982, Geothermal geology and review of exploration, Biliran Is., *in* 4th Pacific geothermal conference, incorporating 4th New Zealand geothermal workshop, 1982, Auckland, New Zealand, proceedings: Auckland, University of Auckland Geothermal Institute, p. 161-166.

Lawless, J.V., Bromley, C.J., Leach, T.M., Licup, A.C., Cope, D.M., and Recio, C.M., 1983, Bacon-Manito Geothermal Field: A geoscientific exploration model, *in* 5th New Zealand geothermal workshop, 1983, Auckland, New Zealand, proceedings: Auckland, University of Auckland Geothermal Institute, p. 97-102.

Lawrence, L.J., 1984, Surface and near surface gold at Vuda, Fiji, in Gold - mining, metallurgy and geology, regional conference, 9-11 October 1984, proceedings: Perth and Kalgoorlie Branches, The Australasian Institute of Mining and Metallurgy, p. 385-396.

Lawrie, K.C, Mernagh, T.P., and Ellis, P., 1997, Host rock control on localization of the Gidginbung epithermal high sulfidation gold deposit, Geological Society of Australia, Abstracts No. 44, p. 45.

le Cloarec, M.E., Allard, P., Ardouin, B., Giggenbach, W.F., and Sheppard, D.S., 1992, Radioactive isotopes and trace elements in gaseous emissions from White Is., New Zealand: Earth and Planetary Sciences Letters, v. 108, p. 19-28.

Leach, T.M., and Bogie, I., 1982, Overprinting of hydrothermal regimes in the Palimpinon geothermal field, southern Negros, Philippines, *in* 4th Pacific geothermal conference, incorporating 4th New Zealand geothermal workshop, 1982, Auckland, New Zealand, proceedings: Auckland, University of Auckland Geothermal Institute, p. 179-183.

Leach, T.M., and Corbett, G.J., 1993, Porphyry-related carbonate base metal gold systems: The transition between the epithermal and porphyry environments, *in* Second national meeting, Specialist Group in Economic Geology, Armidale, New South Wales, abstracts: Geological Society of Australia Abstracts, v. 34, p. 39-40.

Leach, T.M., and Corbett, G.J., 1994, Porphyry-related carbonate base metal gold systems: Characteristics, *in* Rogerson, R., ed., Geology, exploration and mining conference, June 1994, Lae, Papua New Guinea, proceedings: Parkville, The Australasian Institute of Mining and Metallurgy, p. 84-91.

Leach, T.M., and Corbett, G.J., 1995, Characteristics of low sulfidation gold-copper systems in the southwest Pacific, *in* Pacific Rim Congress 95, 19-22 November 1995, Auckland, New Zealand, proceedings: Carlton South, The Australasian Institute of Mining and Metallurgy, p. 327-332.

Leach, T.M., and Erceg, M.M., 1990, The Wafi River high sulphur epithermal gold deposit, Papua New Guinea, *in* Pacific Rim Congress 90, 6-12 May 1990, Gold Coast, Queensland, proceedings: Parkville, The Australasian Institute of Mining and Metallurgy, p. 451-456.

Leach, T.M., and Muchemi, G.G., 1987, Geology and hydrothermal alteration of the north and west exploration wells in the Olkaria geothermal field, Kenya, *in* 9th New Zealand geothermal workshop, 1987, Auckland, New Zealand, proceedings: Auckland, University of Auckland Geothermal Institute, p. 187-192.

Leach, T.M., and Weigel, D.A., 1984, An evaluation of reflected light microscopy for Philippine geothermal prospecting, *in* 6th PNOC-EDC Workshop, 1984, Manila, proceedings: Manila, PNOC-EDC Geothermal Division.

Leach, T.M., Wood, C.P., and Reyes, A.G., 1983, Geology and hydrothermal alteration of the Tongonan geothermal field, Leyte, Republic of the Philippines, *in* 4th international symposium on water-rock interaction, 29 August - 3 September 1983, Misasa, Japan, extended abstracts: publisher not known, p. 275-278.

Leach, T.M., Umali, D.U., and del Rosario, R.C., 1985, Epithermal mineral zonation in an active island arc: The Bacon-Manito geothermal system, Philippines, *in* 7th New Zealand geothermal workshop, 6-8 November 1985, Auckland, New Zealand, proceedings: Auckland, University of Auckland Geothermal Institute, p. 109-114.

Lehrman, N.J., 1986, The McLaughlin Mine, Napa and Yolo Counties, California, *in* Tingley, J.V., and Bonham, H.F. Jr., eds., Precious metal mineralization in hot springs systems, Nevada-California: Nevada Bureau of Mines and Geology Report, v. 41, p. 85-89.

Lewis, R.W., 1992, Issues and challenges in mineral resource evaluation, *in* Resource evaluation symposium, 15 October 1992, Sydney, New South Wales, abstracts: Sydney, S.M.E.D.G. and A.I.G.

Lewis, R.W., and Wilson, G.I., 1990, Misima gold deposit, *in* Hughes, F.E., ed., Geology of the mineral deposits of Australia and Papua New Guinea: Australasian Institute of Mining and Metallurgy Monograph 14, p. 1741-1745.

Licence, P.S., Terrill, J.E., and Fergusson, L.J., 1987, Epithermal gold mineralization, Ambite Island, P.N.G., *in* Pacific Rim Congress 87, 26-29 August 1987, Gold Coast, Queensland, proceedings: Parkville, The Australasian Institute of Mining and Metallurgy, p. 273-278.

Lindgren, W., 1922, A suggestion for the terminology of certain mineral deposits, ECONOMIC GEOLOGY, v. 17, p. 292-294.

Lindgren, W., 1933, Mineral deposits: New York, McGraw-Hill, 930 p.

Lindley, I.D., 1986, Wild Dog telluride occurrence, East New Britain, *in* Papua New Guinea mineral development symposium, 1986, Madang, Papua New Guinea, proceedings: Parkville, The Australasian Institute of Mining and Metallurgy, p. 71.

Lindley, I.D., 1987, The discovery and exploration of the Wild Dog gold-silver deposit, East New Britain, PNG, *in* Pacific Rim Congress 87, 26-29 August 1987, Gold Coast, Queensland, proceedings: Parkville, The Australasian Institute of Mining and Metallurgy, p. 283-286.

Lindley, I.D., 1988, Early Cainozoic stratigraphy and structure of the Gazelle Peninsula, East New Britain: An example of extensional tectonics in the New Britain arc-trench complex: Australian Journal of Earth Sciences, v. 35, p. 231-244.

Lindley, I.D., 1990, Wild Dog gold deposit, *in* Hughes, F.E., ed., Geology of the mineral deposits of Australia and Papua New Guinea: Australasian Institute of Mining and Metallurgy Monograph 14, p. 1789-1792.

Logan, J.M., Friedman, M., Higgs, N., Dengo, C., and Shimamoto, T., 1979, Experimental studies of simulated gouge and their application to studies of natural fault zones: U.S. Geological Survey Open File Report 79-1239, p. 305-343.

Lowder, G.G., and Dow, J.A.S., 1978, Geology and exploration of porphyry copper deposits in North Sulawesi, Indonesia: ECONOMIC GEOLOGY, v. 73, p. 628-644.

Lowell, D.J., 1991a, How Kalamazoo was found, *in* Hollister, V., ed., Case histories of mineral discoveries, volume 3, Porphyry copper, molybdenum, and gold deposits, volcanogenic deposits and deposits in layered rock: Colorado, Society of Mining, Metallurgy and Exploration, p. 33.

Lowell, D.J., 1991b, The discovery of the La Escondida orebody: ECONOMIC GEOLOGY MONOGRAPH 8, p. 286-288.

Lowell, D.J., and Guilbert, J.D., 1970, Lateral and vertical alteration-mineralization zoning in porphyry ore deposits: ECONOMIC GEOLOGY, v. 65, p. 373-408.

Lowell, J.D., 1985, Structural styles in petroleum exploration: Tulsa, OGCI Publications, 477 p.

Lowenstein, J.B., 1994, Dissolved volatile concentrations in an ore-forming magma: Geology, v. 22, p. 893-896.

Lowenstein, P.L., 1982, Economic geology of the Morobe Goldfield: Geological Survey of Papua New Guinea Memoir, v. 9, 244 p.

MacDonald, G.D., and Arnold, L.C., 1994, Geological and geochemical zoning of the Grasberg igneous complex, Irian Jaya, Indonesia, *in* van Leeuwen, T.M., Hedenquist, J.W., James, L.P., and Dow, J.A.S., eds., Mineral deposits of Indonesia - discoveries of the past 25 years: Journal of Geochemical Exploration, v. 50, p. 143-178.

Madrid, R.J., and Roberts, R.J., 1990, Origins of gold belts in north-central Nevada *in* The Geology and Ore Deposits of the Great Basin, Field Trip 15 Guide Book, Geological Society of Nevada, Reno, Nevada, p. 927-939.

Malihan, T.D., 1987, The gold-rich Dizon porphyry copper mine in the western central Luzon Island, Philippines; its geology and tectonic setting, *in* Pacific Rim Congress 87, 26-29 August 1987, Gold Coast, Queensland, proceedings: Parkville, The Australasian Institute of Mining and Metallurgy, p. 303-307.

Mancano,D.P., and Campbell, A.R., 1995, Microthermometery of enargite-hosted fluid inclusions from the Lepanto, high sulfidation Cu-Au deposit: Geochimica et Cosmochimica Acta, v. 59, p. 3909-3916.

Marlow, M.S., Exon, N.F., Ryan, H.F., and Dadisman, S.V., 1988, Offshore structure and stratigraphy of New Ireland Basin in northern Papua New Guinea, *in* Geology and offshore resources of Pacific island arcs - New Ireland and Manus region, Papua New Guinea: Circum-Pacific Council for Energy and Mineral Resources, Earth Sciences Series, v. 9, p. 137-155.

Mason, D.R., and McDonald, J.A., 1978, Intrusive rocks and porphyry copper occurrences of the Papua New Guinea-Solomon Islands region: A reconnaissance study: ECONOMIC GEOLOGY, v. 73, p. 857-877.

Mathias, G.K., Simmons, S.F., and Fleming, J., 1995, High sulfidation alteration at the Island Copper porphyry copper deposit, Vancouver Island, Canada, *in* Pacific Rim Congress 95, 19-22 November 1995, Auckland, New Zealand, proceedings: Carlton South, The Australasian Institute of Mining and Metallurgy, p. 365- 370.

Matsuhihsa, Y. and Aoki, M., 1994, Temperature and oxygen isotope variations during formation of the Hishikari epithermal gold-silver veins, southern Kyushu, Japan: ECONOMIC GEOLOGY, v. 89, p. 1608-1613.

Matsuhisa, Y., Hedenquist, J.W., and Aoki, A., 1990, High temperature acid fluids and associated alteration and mineralization, *in* Third symposium on deep-crust fluids, 15-16 October 1990, Tsukuba, Japan, extended abstracts: Tsukuba, Geological Survey of Japan, p. 45-50.

Mawer, C.K., 1992, Kinematic indicators in shear zones, *in* Bartholomew, M.J.D., Hyndman, W., Mogk, D.W., and Mason, R., eds., Basement tectonics 8: Characterization and comparison of ancient and Mesozoic continental margins: Dordrecht, Kluwer Academic Publishers, p. 67-81.

McCallum, M.E., 1985, Experimental evidence for fluidization processes in breccia pipe formation: ECONOMIC GEOLOGY, v. 80, p. 1523-1543.

McClay, K., 1987, The mapping of geological structures: Milton Keynes, Geological Society of London Handbook Series, Open University Press, 161 p.

McGee, W.A., 1978, Gold production from Woodlark Island: Geological Survey of Papua New Guinea Report 78/17, 25 p.

McGinnis, B.I.A., and Cameron, E.M., 1994, Carbonated, alkaline hybridized melts from a sub-arc environment: mantle wedge samples from the Tabar-Lihir-Tanga-Feni arc, Papua New Guinea: Earth and Planetary Science Letters, v. 122, p. 125-141.

McKinstry, H.E., 1948, Mining geology: New York, Prentice-Hall, 680 p.

McMillan, W.J., and Panteleyev, A., 1980, Ore deposit models; 1, porphyry copper deposits: Geoscience Canada, v. 7, p. 52-63.

McPhie, J., Doyle, M., and Allen, R., 1993, Volcanic textures: A guide to the interpretation of textures in volcanic rocks: Hobart, Centre for Ore Deposit and Exploration Studies, University of Tasmania, 198 p.

Meinert, L.D., 1989, Gold skarn deposits - geology and exploration: ECONOMIC GEOLOGY MONOGRAPH 6, p. 537-552.

Meinert, L.D., 1992, Skarns and skarn deposits. Geoscience Canada, v. 19, p. 145-162.

Meldrum, S.J., Aquino, R.S., Gonzales, R.I., Burke, R.J., Suyadi, A., Irianto, B., and Clarke, D., 1994, The Batu Hijau porphyry copper-gold deposit, Sumbawa Island, Indonesia: Journal of Geochemical Exploration, v. 50, p. 203-220.

Merchant, R.J., 1986, Mineralization in the Thames district - Coromandel, *in* Henley, R.W., Hedenquist, J.W., and Roberts, P.J., eds., Guide to the active epithermal (geothermal) systems and precious metal deposits of New Zealand: Monograph Series in Mineral Deposits, Berlin, Gebruder Borntraeger, v. 26, p. 147-163.

Mertig, H.J., Rubin, J.N., and Kyle, J.R., 1994, Skarn Cu-Au ore bodies of the Gunung Bijih (Ertsberg) district, Irian Jaya, Indonesia: Journal of Geochemical Exploration, v. 50, p. 179-202.

Meyer, C., and Hemley, J.J., 1967, Wall rock alteration, *in* Barnes, H.L., ed., Geochemistry of hydrothermal ore deposits: New York, Holt, Rinehart, and Winston, p. 166-235.

Mitchell, A.H.G., and Carlile, J.C., 1994, Mineralization, antiforms and crustal extension in andesitic arcs: Geological Magazine, v. 131, p. 231-242.

Mitchell, A.H.G., and Garson, M.S., 1981, Mineral deposits and global tectonic settings: London, Academic Press, 421 p.

Mitchell, A.H.G., and Leach, T.M., 1991, Epithermal gold in the Philippines; island arc metallogenesis, geothermal systems and geology: London, Academic Press, 457 p.

Morgan, P.G., 1924, The geology and mines of the Waihi District Hauraki Goldfield: New Zealand Geological Survey Bulletin, v. 26, 218 p.

Morrison, G.W., 1988, Palaeozoic gold deposits of northeast Queensland, *in* Bicentennial Gold 88, extended abstracts, oral programme: Geological Society of Australia Abstracts, v. 22, p. 91-101.

Morrison, G.W., Rose, W.J., and Jaireth, S., 1991, Geological and geochemical controls on the silver content (fineness) of gold in gold-silver deposits: Ore Geology Reviews, v. 6, p. 333-364.

Morrison, G., Seed, M., Bobis, R., and Tullemans, F., 1996, The Kidston gold deposit: A piston-cylinder model for gold mineralisation in a porphyry Mo system: Geological Society of Australia Abstracts, v. 41, p. 303.

Moyle, A.J., Doyle, B.J., Hoogvliet, H., and Ware, A.R., 1990, The Ladolam gold deposit, Lihir Island, Papua New Guinea, *in* Hughes, F.E., ed., Geology of the mineral deposits of Australia and Papua New Guinea: Australasian Institute of Mining and Metallurgy Monograph 14, p.1793-1805.

Moyle, A.J., Doyle, B.J., Hoogvliet, H., and Ware, A.R., 1991. The geology and mineralization of the Ladolam gold deposit, Lihir Island, Papua New Guinea, *in* Rogerson, R., ed., Proceedings of the PNG geology, exploration and mining conference, 1991, Rabaul: Parkville, The Australasian Institute of Mining and Metallurgy, p. 101-111.

Moyle, A.J., Bishoff, K., Alexander, K.R., and Hoogvliet H., 1996, Mt Muro gold deposit, Indonesia, *in* Porphyry related copper and gold deposits of the Asia Pacific Region, Cairns, Australia, 12-13 August 1996, proceedings: Adelaide, Australian Mineral Foundation, p. 7.1-7.9.

Müller, D., and Groves, D.I., 1993, Direct and indirect associations between potassic igneous rocks, shoshonites and gold-copper deposits: Ore Geology Reviews, v. 8, p. 383-406.

Müller, D., and Groves, D.I., 1995, Potassic igneous rocks and associated gold-copper mineralization: Springer-Verlag Lecture Notes in Earth Sciences, v. 56, 210 p.

Muntean, J.L., Kesler, S.E., Russell, N., and Polanco, J., 1990, Evolution of the Monte Negro acid-sulfate Au-Ag deposit, Pueblo Viejo, Dominican Republic: Important factors in grade development: ECONOMIC GEOLOGY, v. 85, p. 1738-1758.

Murray, C.G., 1990, Tasman Fold Belt in Queensland, *in* Hughes, F.E., ed., Geology of the mineral deposits of Australia and Papua New Guinea: Australasian Institute of Mining and Metallurgy Monograph 14, p. 1431-1450.

Mutschler, F.E., and Mooney, T.C., Precious-metal deposits related to alkalic igneous rocks: Provisional classification, grade-tonnage data and exploration frontiers *in* Kirkham, R.V., Sinclair, W.D., Thorpe, R.I., and Duke, J.M., eds., Mineral exploration modelling: Geological Association of Canada Special Paper, v. 40, p. 479-520.

Nagayama, T., 1993, Precipitation sequence of veins at the Hishikari deposits, Kyushu. Japan, *in* Shikazono, N., Naito, K., and Izawa, E., eds., High grade epithermal mineralization - the Hishikari deposit: The Society of Resource Geology, Resource Geology Special Issue, v. 14, p. 13-27.

Nairn, I.A., 1979, Rotomahana-Waimangu eruption, 1886: base surge and basaltic magma: New Zealand Journal of Geology and Geophysics, v. 22, p. 363-378.

Nakayama, K., 1995, Case history of the discovery of the Hishikari gold deposit, Japan, *in* Pacific Rim Congress 95, 19-22 November 1995, Auckland, New Zealand, proceedings: Carlton South, The Australasian Institute of Mining and Metallurgy, p. 429-434.

Nash, J.T., 1976, Fluid inclusion petrology - data from porphyry copper deposits and applications to exploration: U.S. Geological Survey Professional Paper, v. 907-D, p. 16.

Nelson, C.E., and Giles, D.L., 1985, Hydrothermal eruption mechanisms and hot spring gold deposits: ECONOMIC GEOLOGY, v. 80, p. 1633-1639.

Nelson, R.W., Bartram, J.A., and Christie, M.H., 1990, Hidden Valley gold-silver deposit, *in* Hughes, F.E., ed., Geology of the mineral deposits of Australia and Papua New Guinea: Australasian Institute of Mining and Metallurgy Monograph 14, p. 1763-1767.

Nesbitt, B.E., 1996, Applications of oxygen and hydrogen isotopes to exploration for hydrothermal mineralization: SEG Newsletter, October 1996, p. 1, 8-12.

Newcrest Mining Staff, 1996, The Cadia 'wallrock-porphyry'-style gold-copper deposit, NSW, *in* Porphyry related copper and gold deposits of the Asia Pacific Region, Cairns, Australia, 12-13 August 1996, proceedings: Adelaide, Australian Mineral Foundation, p. 16.1-16.10.

North Limited, 1995, Lake Cowal gold project: Minfo New South Wales Mining and Exploration Quarterly, Department of Mineral Resources, v. 48, p. 34-38.

Norton, D., and Knight, J.E., 1977, Transport phenomena in hydrothermal systems - cooling plutons: American Journal of Science, v. 277, p. 937- 981.

O'Driscoll, E.S.T., 1986, Observations of the lineament-ore relation: Philosophical Transactions of the Royal Society of London, Section A, v. 317, p. 195-218.

Orr, T.H., 1995, The Mt Leyshon Gold Mine: Geology and mineralization, *in* Beams, S., ed., Mineral Deposits of Northeast Queensland, Australia, Economic Geology Research Unit, James Cook University, EGRU Contribution, 52, p 116-136.

Oviedo, L., Fuster, N., Tschischow, N., Ribba, L., Zuccone, A., Grez, E., and Aguliar, A., 1991, General geology of the La Coipa precious metal deposit: ECONOMIC GEOLOGY, v. 86, p. 1287-1300.

Pascoe, G.J., 1991, Hidden Valley gold project development summary, 1987-1991, *in* Rogerson, R., ed., Proceedings of the PNG geology, exploration and mining conference, 1991, Rabaul: Parkville, The Australasian Institute of Mining and Metallurgy, p. 69-76.

Panther, C.A., Mauk, J.L. and Arehart, G.B., 1995, A petrographic and oxygen isotope study of banded epithermal veins from the Martha Hill Au-Ag Mine, Waihi, New Zealand, *in* Pacific Rim Congress 95, 19-22 November 1995, Auckland, New Zealand, proceedings: Carlton South, The Australasian Institute of Mining and Metallurgy, p. 447-452.

Park, R.G., 1988, Geological structures and moving plates: Glasgow, Blackie, 337 p.

Paull, P.L., Hodkinson, I.P., Morrison, G.W., and Teale, G.S., 1990, Mount Leyshon gold deposit, *in* Hughes, F.E., ed., Geology of the mineral deposits of Australia and Papua New Guinea: Australasian Institute of Mining and Metallurgy Monograph 14, p. 1471-1481.

Pennington J., and Kavalieris, I., 1997, New advances in the understanding of the Grasberg copper-gold porphyry system, Iran Jaya, Indonesia, *in* Pacific Treasure Trove - Copper-Gold Deposits of the Pacific Rim, Prospectors and Developers Association of Canada, Toronto, p. 79-97.

Perkins, C., Walshe, J.L., and Morrison, G., 1995, Metallogenic episodes of the Tasman Fold Belt System, eastern Australia: ECONOMIC GEOLOGY, v. 90, p. 1443-1466.

Peters, W.C., James, A.J., and Field, C.W., 1966, Geology of the Bingham Canyon porphyry copper deposit, Utah, *in* Titley, S.R., and Hicks, C.L., eds., Geology of the porphyry copper deposits in southwestern North America: Tuscon, University of Arizona Press, p. 165-175.

Petit, J.P., 1987, Criteria for the sense of movement on fault surfaces in brittle rocks: Journal of Structural Geology, v. 9, p. 597-608.

Phillips, G.N., and Hughes, M.J., 1995, Victorian gold: A sleeping giant: SEG Newsletter, v. 21, p. 1, 9-13.

Phillips, W.J., 1973, Mechanical effects of retrograde boiling and its probable importance in the formation of some porphyry ore deposits: Transactions of the Institute of Mining and Metallurgy, v. 82, p. B90-98.

Phillips, W.J., 1974, The dynamic emplacement of cone sheets: Tectonophysics, v. 24, p. 69-84.

Phillips, W.J., 1986, Hydraulic fracturing effects in the formation of mineral deposits: Transactions of the Institute of Mining and Metallurgy, Section B, v. 95, p. 17-24.

Pieters, P.E., and Supriatna, S., 1990, Geological map of West Central and East Kalimantan, 1:1,000,000 scale: Bandung, Indonesia, Geological Research and Development Centre.

Pirajno, F., 1992, Hydrothermal mineral deposits principles and fundamental concepts for the exploration geologist: Berlin, Springer-Verlag, 709 p.

Plimer, I.R., Andrew, A.S., Jenkins, R., and Lottermoser, B.G., 1988, The geology and geochemistry of the Lihir gold deposit, Papua New Guinea, *in* Bicentennial Gold 88, extended abstracts, oral programme: Geological Society of Australia Abstracts, v. 22, p. 139-143.

PNOC-EDC Geothermal, 1982, Report on Daklan geothermal exploration: Unpublished internal report, Manila, PNOC-EDC Geothermal Division, 34 p. (with permission).

PNOC-EDC Geothermal, 1983, Bacon-Manito Geothermal Project: First stage development: Unpublished KRTA internal report, Manila, PNOC-EDC Geothermal Division, 58 p. (with permission).

PNOC-EDC Geothermal, 1985a, Review of surface prospecting and exploration drilling, North Davao geothermal prospect: Unpublished internal report, Manila, PNOC-EDC Geothermal Division, 54 p. (with permission).

PNOC-EDC Geothermal, 1985b, Geology and petrology of Acupan Well AC1D: Unpublished internal report, Manila, PNOC-EDC Geothermal Division, 56 p. (with permission).

Porter, I.W., and Ripley, E., 1985, Petrologic and stable isotope study of the gold-bearing breccia pipe at the Golden Sunlight deposit, Montana: ECONOMIC GEOLOGY, v. 80, p 1689-1706.

Porter, R.R.G., 1990, Pajingo gold deposits, *in* Hughes, F.E., ed., Geology of the mineral deposits of Australia and Papua New Guinea: Australasian Institute of Mining and Metallurgy Monograph 14, p. 1483-1487.

Price, N.J., 1966, Fault and joint development in brittle and semi-brittle rock: New York, Pergamon Press, 176 p.

Price, N.J., and Cosgrove, J.W., 1990, Analysis of geological structures: Cambridge, Cambridge University Press, 502 p.

Pudjowalujo, H., 1990, Cenozoic tectonics of North Sumatra with particular reference to the Sumatran fault system, *in* Pacific Rim Congress 90, 6-12 May 1990, Gold Coast, Queensland, proceedings: Parkville, The Australasian Institute of Mining and Metallurgy, p. 209-215.

Ramsay, J.G., 1967. Folding and fracturing of rocks: New York, McGraw-Hill Book Company, 568 p.

Ramsay, J.G., and Huber, M.I., 1987, Techniques of modern structural geology, volume 2, folds and fractures: London, Academic Press, 700 p.

Ramsden, A.R., McAndrew, J., Cousens, D.R., Kinealy, K.M., and Hansen, G., 1985, Free gold in porphyry copper mineralization and its genetic and metallurgical significance: CSIRO Division of Mineralogy and Geochemistry Research Review, 1985, p. 43-44.

Reyes, A.G., 1985, A comparison of acid and neutral pH hydrothermal alteration in the Bacon-Manito, Philippines: Unpublished M.Sc. thesis, Auckland, Auckland University, p. 258.

Reyes, A.G., 1990a, Petrology of Philippines geothermal systems and the application of alteration mineralogy to their assessment: Journal of Volcanology and Geothermal Research, v. 43, p. 279-309.

Reyes, A.G., 1990b, Mineralogy, distribution and origin of acid alteration in Philippine geothermal systems, *in* Third symposium on deep-crust fluids, 15-16 October 1990, Tsukuba, Japan, extended abstracts: Tsukuba, Geological Survey of Japan, p. 51-58.

Reyes, A.G., 1995, Geothermal systems in New Zealand and the Philippines - why are they so different, *in* Pacific Rim Congress 95, 19-22 November 1995, Auckland, New Zealand, proceedings: Carlton South, The Australasian Institute of Mining and Metallurgy, p. 485-490.

Reyes, A.G., Giggenbach, W.F., Saleros, J.D.M., Salonga, N.D., and Vergara, M.C., 1993, Petrology and geochemistry of Alto Peak, a vapour-cored hydrothermal system, Lyete Province, Philippines, *in* Sussman, D., Ruaya, J.R., Reyes, A.G., and Hedenquist, J.W., eds., Geothermal systems of the Philippines: Geothermics, v. 22, p. 479-519.

Reyes, A.G., and Tolentino, B.S., 1982, The distribution of alteration in Philippine geothermal areas, *in* ASEAN conference on petroleum, October 1981, Manila, Philippines, proceedings.

Reynolds, T.J., and Beane, R.E., 1985, Evolution of hydrothermal fluid characteristics at the Santa Rita, New Mexico, porphyry copper deposit: ECONOMIC GEOLOGY, v. 80, p. 1328-1347.

Richards, J.P., 1990, Petrology and geochemistry of alkalic intrusives at the Porgera gold deposit, Papua New Guinea: Journal of Geochemical Exploration, v. 35, p. 141-199.

Richards, J.P., 1992, Magmatic-epithermal transitions in alkalic systems: Porgera gold deposit, Papua New Guinea: Geology, v. 20, p. 547-550.

Richards, J.P., 1995, Alkalic-type epithermal gold deposits - a review, *in* Thompson, J.F.H., ed., Magmas, fluids, and ore deposits: Mineralogical Association of Canada Short Course Handbook, v. 23, p. 367-400.

Richards, J.P., and Kerrich, R., 1993, The Porgera gold mine, Papua New Guinea: Magmatic hydrothermal to epithermal evolution of an alkalic-type precious metal deposit: ECONOMIC GEOLOGY, v. 88, p. 1017-1052.

Richards, J.P., and Ledlie, I., 1993, Alkalic intrusive rocks associated with the Mt Kare gold deposit, Papua New Guinea: Comparison with the Porgera Intrusive Complex: ECONOMIC GEOLOGY, v. 88, p. 755-788.

Richards, J.P., and McDougall, I., 1990, Geochronology of the Porgera gold deposit, Papua New Guinea: Resolving the effects of excess argon on K-Ar and $^{40}Ar/^{39}Ar$ age estimates for magmatism and mineralization: Geochimica Cosmochimica Acta, v. 54, p. 1397-1415.

Riedel, W., 1929, Zur Mechanik geologischer Brucherscheinungen: Zentralblatt für Mineralogie, Geologie und Palaeontologie, v. 1929 B, p. 354-368 (in German).

Robinson, B.W., Villasenor, L.B., and Clemante, V.C., 1987, Preliminary stable isotope investigations of acid fluids in geothermal systems in the Philippines, *in* 9th New Zealand geothermal workshop, 1987, Auckland, New Zealand, proceedings: Auckland, University of Auckland Geothermal Institute, p. 71-71.

Rock, N.M.S., 1991, Lamprophyres: Glasgow, Blackie Academic Press, 285 p.

Rock, N.M.S., Groves, D.I., Perring, C.S., and Golding, S.D., 1989, Gold, lamprophyres and porphyries: What does their association mean?: ECONOMIC GEOLOGY MONOGRAPH 6, p. 609-626.

Roedder, E., 1984, Fluid inclusions: Reviews in Mineralogy, v. 12, 644 p.

Rogerson, R., and Williamson, A., 1986a, Age, petrology and mineralization associated with two Neogene intrusive types in the eastern highlands of Papua New Guinea: Geological Survey of Papua New Guinea Report 85/2, 20p.

Rogerson, R., and Williamson, A., 1986b, Age, petrology and mineralization associated with two Neogene intrusive types in the eastern highlands of Papua New Guinea, *in* Teh, G.H., and Paramanthan, S., eds., Fifth regional congress on geology, mineral and energy resources of Southeast Asia, 9-13 April 1984, proceedings: Bulletin of the Geological Society of Malaysia, v. 20, p. 487-502.

Rogerson, R., Hilyard, D., Francis, G., and Finlayson, E., 1987, The foreland thrust belt of Papua New Guinea, *in* Pacific Rim Congress 87, 26-29 August 1987, Gold Coast, Queensland, proceedings: Parkville, The Australasian Institute of Mining and Metallurgy, p. 579-583.

Romberger, S.B., 1988, Disseminated gold deposits, *in* Roberts, E.G., and Sheahan, P.A., eds., Ore deposit models: Waterloo, Geological Association of Canada, p. 21-30.

Rose, A.W., and Bart, D.M., 1979, Hydrothermal alteration, *in* Barnes, H.L., ed., Geochemistry of hydrothermal ore deposits, 2nd edition: New York, John Wiley & Sons, p. 173-227.

Ruaya, J.R., Ramos, M.N., and Gonfianti, R., 1992, Assessments of magmatic components of fluids at Mt. Pinatubo volcanic-geothermal systems, Philippines, from chemical and isotopic data: Geological Survey of Japan Report, v. 279, p. 141-151.

Rubin, J.N., 1993, Precious metal distribution, Gunung Bijah (Ertsberg) District, Indonesia: Geological Society of America, Abstracts with Program, v. 25, p. A275-276.

Rush, P.M., and Seegers, H.J., 1990, Ok Tedi copper-gold deposit, *in* Hughes, F.E., ed., Geology of the mineral deposits of Australia and Papua New Guinea: Australasian Institute of Mining and Metallurgy Monograph 14, p. 1747-1754.

Ryan, D., 1993, CRAE's exploration programmes in the Temora and Cobar goldfields, *in* New South Wales the state of exploration, Proceedings, Sydney, New South Wales Department of Mineral Resources, p. 25-27.

Ryan, P., 1991, Black bonanza: A landslide of gold: Melbourne, Hyland House Publishing, 140 p.

Rye, R.O., 1993, The evolution of magmatic fluids in the epithermal environment: The stable isotope perspective: ECONOMIC GEOLOGY, v. 88, p. 733-753.

Rye, R.O., Bethke, J.W., and Wasserman, M.D., 1992, The stable isotope geochemistry of acid sulfate alteration: ECONOMIC GEOLOGY, v. 87, p. 225-262.

Saunders, J.A., 1990, Colloidal transport of gold and silica in epithermal precious metal systems: Evidence from the Sleeper Deposit, Humbolt County, Nevada: Geology, v. 18, p. 757-760.

Saunders, J.A., 1994, Silica and gold textures in bonanza ores of the Sleeper deposit, Humboldt County, Nevada: Evidence for colloids and implications for epithermal ore-forming processes: ECONOMIC GEOLOGY, v. 89, p. 628-638.

Sawkins, F.J., 1984, Metal deposits in relation to plate tectonics: New York, Springer-Verlag, 325 p.

Sawkins, F.J., O'Neil, J.R., and Thompson, J.M., 1979, Fluid inclusion and geochemical studies of gold vein deposits, Baguio District, Philippines: ECONOMIC GEOLOGY, v. 74, p. 1420-1434.

Scheibner, E., 1985, Suspect terrains in the Tasman Fold Belt, *in* Howell, D.G., ed., Tectonostratigraphic terrains in the Circum-Pacific region: Circum-Pacific Council for Energy and Mineral Resources, American Association of Petroleum Geologists, Earth Science Series, v. 1, p. 493-514.

Schoen, R., White, D.E., and Hemley, J.J., 1973, Argillization by descending acid at Steamboat Springs, Nevada: Clay and Clay Minerals, v. 22, p. 1-22.

Scott, K.M., 1978, Geochemical aspects of alteration-mineralisation at Copper Hill, New South Wales, Australia: ECONOMIC GEOLOGY, v. 73, p. 966-976.

Seastress, J.R., 1982, Subsurface geology of Nasuji-Sogongon sector, Southern Negros Geothermal Field, Philippines, *in* 4th Pacific geothermal conference, incorporating 4th New Zealand geothermal workshop, 1982, Auckland, New Zealand, proceedings: Auckland, University of Auckland Geothermal Institute, p. 173-178.

Seccombe, P.K., and Barnes, H.L., 1990, Experimental mobility of sulfides along hydrothermal gradients: ECONOMIC GEOLOGY, v. 85, p. 1099-1113.

Seccombe, P.K., Lu, J., Andrew, A.S., Gulson, B.L., and Mizon, K.J., 1993, Nature and evolution of metamorphic fluids associated with turbidite-hosted gold deposits: Hill End goldfield, NSF, Australia: Mineralogical Magazine, v. 57, p. 423-436.

Segall, P., and Pollard, D.D., 1980, Mechanics of discontinuous faults: Journal of Geophysical Research, v. 85, p. 4337-4350.

Seki, Y., 1993, Geologic setting of the Takatama gold deposit, Japan: An example of caldera-related epithermal gold mineralization, *in* Shikazono, N., Naito, K., and Izawa, E., eds., High grade epithermal mineralization - the Hishikari deposit: The Society of Resource Geology, Resource Geology Special Issue, v. 14, p. 123-136.

Semple, D.G., Corbett, G.J., and Leach, T.M., 1995, The Tolukuma gold-silver vein system, Papua New Guinea, *in* Pacific Rim Congress 95, 19-22 November 1995, Auckland, New Zealand, proceedings: Carlton South, The Australasian Institute of Mining and Metallurgy, p. 509-514.

Semple, D.G., Corbett, G.J., and Leach, T.M., in press, The Tolukuma gold-silver veins deposit, Papua New Guinea, *in* Geology of the mineral deposits of Australia and Papua New Guinea: Australasian Institute of Mining and Metallurgy Monograph 22.

Setterfield, T.N., Eaton, P.C., Rose, W.J., and Sparkes, R.S.J., 1991, The Tavua caldera, Fiji: A complex shoshonitic caldera formed faulting and downsagging: Journal of the Geological Society (London), v. 148, p. 115-127.

Seward, T.M., 1973, Thio complexes of gold in hydrothermal ore solutions: Geochimica et Cosmochimica Acta, v. 37. p. 379-399.

Seward, T.M., 1976, The stability of chloride in complexes of silver in hydrothermal solutions up to 350°C: Geochimica et Cosmochimica Acta, v. 40. p. 1329-1341.

Seward, T.M., 1982, The transport of gold in hydrothermal systems *in* Gold '82 Rotterdam, A.A. Bolkema, p. 165-181.

Seward, T.M., 1984, The transport and deposition of gold in hydrothermal systems, *in* Foster, R.P., ed., Gold '82: The geology, geochemistry and genesis of gold deposits: Rotterdam, A.A. Balkema, p. 165-181.

Seward, T.M., and Sheppard, D.S., 1986, Waimangu geothermal field, *in* Henley, R.W., Hedenquist, J.W., and Roberts, P.J., eds., Guide to the active epithermal (geothermal) systems and precious metal deposits of New Zealand: Monograph Series in Mineral Deposits, Berlin, Gebruder Borntraeger, v. 26, p. 81-92.

Sewell, D.M., and Wheatley, C.J.V., 1994, Integrated exploration success for gold at Wetar, Indonesia, *in* van Leeuwen, T.M., ed., Mineral deposits of Indonesia: Journal Geochemical Exploration, v. 50, p. 337-350.

Shatwell, D., 1987, Epithermal gold mineralization and Late Cenozoic magmatism in the Melanesian outer arc, *in* Pacific Rim Congress 87, 26-29 August 1987, Gold Coast, Queensland, proceedings: Parkville, The Australasian Institute of Mining and Metallurgy, p. 393-398.

Sheppard, D.S., and Lyon, G.L., 1984, Geothermal fluid chemistry of the Orakeikorako Field, New Zealand: Journal of Volcanology and Geothermal Research, v. 22, p. 329-349.

Sheppard, S.M.F., Nielson, R.L., and Taylor, H.P. Jr., 1971, Hydrogen and oxygen isotope ratios in minerals from porphyry copper deposits: ECONOMIC GEOLOGY, v. 66, p. 515-542.

Sherlock, R.L., 1993, The genesis of the McLaughlin Mine sheeted vein complex, fluid inclusion and stable isotope evidence, *in* Rytuba, J.J., ed., Active geothermal systems and gold-mercury deposits in the Sonoma-Clear Lake volcanic fields, California: Society of Economic Geologists Guide Book Series, v. 16, p. 330-349.

Sherlock, R.L., Tosdal, R.M., Lehrman, N.J., Graney, J.R., Losh, S., Jowett, E.C., and Kesler, S.E., 1995, Origin of the McLaughlin mine sheeted vein complex: Metal zoning, fluid inclusion, and isotopic evidence: ECONOMIC GEOLOGY, v. 90, p. 2156-2181.

Shikazono, N., and Nagayama, T., 1993, Origin and depositional mechanism of the Hishikari gold-quartz-adularia mineralization, *in* Shikazono, N., Naito, K., and Izawa, E., eds., High grade epithermal mineralization - the Hishikari deposit: The Society of Resource Geology, Resource Geology Special Issue, v. 14, p. 47-56.

Shinohara, H., and Kazahaya, K., 1995, Degassing processes related to magma chamber crystallisation, *in* Thompson, J.F.H., ed., Magmas, fluids and ore deposits: Mineralogical Association of Canada Short Course Handbook, v. 23, p. 101-128.

Sibson, R.H., 1986, Earthquakes and lineament infrastructure: Philosophical Transactions of the Royal Society of London, Section A, v. 317, p. 63-79.

Sibson, R.H., 1987, Earthquake rupturing as a mineralizing agent in hydrothermal systems: Geology, v. 15, p. 701-704.

Sibson, R.H., 1989, Earthquake faulting as a structural process: Journal of Structural Geology, v. 11, p.1-14.

Sibson, R.H., 1991, Fluid flow in seismogenic crust, *in* Structural geology in mining and exploration, extended abstracts: Geology Department (Key Centre) & University Extension, The University of Western Australia, Publication, v. 25, p. 38-42.

Sibson, R.H., 1992, Earthquake faulting, induced fluid flow, and fault-hosted gold mineralization, *in* Bartholomew, M.J., Hyndman, D.W., Mogok, D.W., and Mason, R., eds., Basement tectonics 8: Characterization and comparison of ancient and Mesozoic continental margins: Dordrecht, Kluwer Academic Publishers, p. 603-614.

Sibson, R.H., 1993, Load-strengthening versus load-weakening faulting: Journal of Structural Geology, v. 15, p. 123-128.

Sibson, R.H., 1995, Structural permeability and fluid flow in fault-fracture meshes, *in* Pacific Rim Congress 95, 19-22 November 1995, Auckland, New Zealand, proceedings: Carlton South, The Australasian Institute of Mining and Metallurgy, p. 521-526.

Sillitoe, R.H., 1979, Some thoughts on gold-rich porphyry copper deposits: Mineral Deposits, v. 14, p. 161-174.

Sillitoe, R.H., 1983, Enargite-bearing massive sulfide deposits in porphyry copper systems: ECONOMIC GEOLOGY, v. 78, p. 348-352.

Sillitoe, R.H., 1985, Ore breccias in volcanoplutonic arcs: ECONOMIC GEOLOGY, v. 80, p. 1467-1514.

Sillitoe, R.H., 1987, Copper, gold and subduction: a trans-Pacific perspective, *in* Pacific Rim Congress 87, 26-29 August 1987, Gold Coast, Queensland, proceedings: Parkville, The Australasian Institute of Mining and Metallurgy, p. 399-403.

Sillitoe, R.H., 1989, Gold deposits in western Pacific arcs: The magmatic connection: ECONOMIC GEOLOGY MONOGRAPH 6, p. 274-291.

Sillitoe, R.H., 1991a, Gold metallogeny of Chile - an introduction: ECONOMIC GEOLOGY, v. 86, p. 1187-1205.

Sillitoe, R.H., 1991b, Intrusion related gold deposits, *in* Foster, R.P., ed., Gold metallogeny and exploration: Glasgow, Blackie, p. 165-203.

Sillitoe, R.H., 1992, Geotectonic setting of western Pacific gold deposits, *in* Bartholomew, M.J., Hyndman, D.W., Mogok, D.W., and Mason, R., eds., Basement tectonics 8: Characterization and comparison of ancient and Mesozoic continental margins: Dordrecht, Kluwer Academic Publishers, p. 665-678.

Sillitoe, R.H., 1993a, Gold-rich porphyry copper deposits: Geological model and exploration implications, *in* Kirkham, R.V., Sinclair, W.D., Thorpe, R.I., and Duke, J.M., eds., Mineral exploration modelling: Geological Association of Canada Special Paper, v. 40, p. 465-478.

Sillitoe, R.H., 1993b, Epithermal models: Genetic types, geometric controls and shallow features, *in* Kirkham, R.V., Sinclair, W.D., Thorpe, R.I., and Duke, J.M., eds., Mineral exploration modelling: Geological Association of Canada Special Paper, v. 40, p. 403-417.

Sillitoe, R.H., 1994a, Indonesian mineral deposits - introductory comments, comparisons and speculations, *in* van Leeuwen, T.M., Hedenquist, J.W., James, L.P., and Dow., J.A.S., eds., Mineral deposits of Indonesia - discoveries of the past 25 years: Journal of Geochemical Exploration, v. 50, p. 1-12.

Sillitoe, R.H., 1994b, Erosion and collapse of volcanoes; Causes of telescoping in intrusion-centred ore deposits: Geology, v. 22, p. 945-948.

Sillitoe, R.H., 1995a, The influence of magmatic-hydrothermal models on exploration strategies for volcanic-plutonic arcs, *in* Thompson, J.F.H., ed., Magmas, fluids and ore deposits: Mineralogical Association of Canada Short Course Handbook, v. 23, p. 511-525.

Sillitoe, R.H., 1995b, Exploration of porphyry copper lithocaps, *in* Pacific Rim Congress 95, 19-22 November 1995, Auckland, New Zealand, proceedings: Carlton South, The Australasian Institute of Mining and Metallurgy, p. 527-532.

Sillitoe, R.H., 1995c, Exploration and discovery of base- and precious-metal deposits in the circum-Pacific region during the last 25 years: Tokyo, Japan, Metal Mining Agency of Japan. 127 p.

Sillitoe, R.H., 1996, Characteristics and controls of the largest porphyry copper-gold and epithermal gold deposits in the circum-Pacific region: Geological Society of Australia, Abstracts, No. 41, p. 394.

Sillitoe, R.H., and Angeles, C.A. Jr., 1985, Geological characteristics and evolution of a gold-rich porphyry copper deposit at Guinaoang, Luzon, Philippines, *in* Asian Mining '85: London, Institute Mining and Metallurgy, p. 15-26.

Sillitoe, R.H., and Bonham, H.F., 1984, Volcanic landforms and ore deposits: ECONOMIC GEOLOGY, v. 79, p. 1286-1298.

Sillitoe, R.H., and Bonham, H.F., 1990, Sediment-hosted gold deposits: Distal products of magmatic-hydrothermal systems: Geology, v. 18, p. 157-161.

Sillitoe, R.H., and Gappe, I.M. Jr, 1984, Philippine porphyry copper deposits: Geologic settings and characteristics: United Nations Economic and Social Commission for Asia and the Pacific, Bangkok, CCOP Technical Publication, v. 14, 89 p.

Sillitoe, R.H., and Sawkins, F.J., 1971, Geologic, mineralogic, and fluid inclusion studies relating to the origin of copper-bearing tourmaline breccia pipes, Chile: ECONOMIC GEOLOGY, v. 66, p. 1028-1041.

Sillitoe, R.H., Baker, E.M., and Brooks, W.A., 1984, Gold deposits and hydrothermal eruption breccias associated with a maar volcano at Wau, Papua New Guinea: ECONOMIC GEOLOGY, v. 79, p. 638-655.

Sillitoe, R.H., Grauberger, G.L., and Elliott, J.S., 1985, A diatreme hosted gold deposit at Montana Tunnels, Montana: ECONOMIC GEOLOGY, v. 80, p. 1707-1721.

Sillitoe, R.H., Hannington, M.D., and Thompson, F.F.H, 1996, High sulfidation deposits in the volcanogenic massive environment: ECONOMIC GEOLOGY, v. 91, p. 204-212.

Sillitoe, R.H., Marquardt, J.C., Ramirez, F., Becerra, H., and Gomez, M., 1994, Geology of MM: A concealed porphyry copper deposit in the Chuquicamata district, northern Chile: 7th Congreso Geologico Chileno, 1994, Conception, Chile, 1994, proceedings, v. 2, p. 1619.

Simmons, S.F., 1995, Magmatic contributions to low sulfidation epithermal deposits, *in* Thompson, J.F.H., ed., Magmas, fluids and ore deposits: Mineralogical Association of Canada Short Course Handbook, v. 23, p. 455-478.

Simmons, S.F., and Browne, P.R.L., 1990a, A three dimensional model of the distribution of hydrothermal alteration within the Broadlands-Ohaaki Geothermal Field, *in* 12th New Zealand geothermal workshop, 1990, Auckland, New Zealand, proceedings: Auckland, University of Auckland Geothermal Institute, p. 25-30.

Simmons, S.F., and Browne, P.R.L., 1990b, Mineralogic, geochemical and fluid-inclusion studies of epithermal gold-bearing veins at the Mt Muro Prospect, Central Kalimantan (Borneo), Indonesia: Journal of Geochemical Exploration, v. 35, p. 63-103.

Simmons, S.F., and Christensen, B.W., 1994, Origins of calcite in the Broadlands-Ohaaki geothermal system, New Zealand: American Journal of Science, v. 294, p. 361-400.

Simmons, S.F., Gemmel, J.B., and Sawkins, F.J., 1988, The Santo Nino silver-lead-zinc vein, Fresnillo, Mexico. Part II. Physical and chemical nature of ore-forming solutions: ECONOMIC GEOLOGY v. 83, p. 1619-1641.

Simmons, S.F., Brown, P.R.L., and Brathwaite, R.L., 1992, Active and extinct hydrothermal systems of the North Island, New Zealand: Society of Economic Geologists Guide Book Series, v. 15, 121 p.

Simpson, C.R.J., Mauk, J.L., Arehart, G.B., and Mathews, S.J., 1995a, The formation of banded epithermal quartz veins at the Golden Cross Mine, Waihi, *in* Pacific Rim Congress 95, 19-22 November 1995, Auckland, New Zealand, proceedings: Carlton South, The Australasian Institute of Mining and Metallurgy, p. 545-550.

Simpson, M.P., Simmons, S.F., Mauk, J.L., and McOnie, A., 1995b, The distribution of hydrothermal minerals at the Golden Cross epithermal Au-Ag deposit, New Zealand, *in* Pacific Rim Congress 95, 19-22 November 1995, Auckland, New Zealand, proceedings: Carlton South, The Australasian Institute of Mining and Metallurgy, p. 551-556.

Singer, D.A., 1993, World class base and precious metal deposits - a quantative analysis: ECONOMIC GEOLOGY, v.90, p. 88-104.

Skinner, D.N.B., 1986, Neogene volcanism of the Hauraki Volcanic Region, *in* Smith,I.E.M., ed., Late Cenozoic Volcanism in New Zealand: Royal Society of New Zealand Bulletin, 23, p. 21-47.

Smith, I.E., Okada, T., Itaya, T., and Black, P.M., 1993, Age relationships and tectonic implications of late Cenozoic basaltic volcanism in Northland, New Zealand: NZ Journal Geology and Geophysics, v. 36, p. 385-393.

Solomon, M., 1990, Subduction, arc reversal, and the origin of porphyry copper-gold deposits in island arcs: Geology, v. 18, p. 630-633.

Solomon, M., and Groves, D.I., 1994, The geology and origin of Australia's mineral deposits: Oxford Monographs on Geology and Geophysics, v. 24, 951 p.

Spencer, R.A., Tyne, E.D.,Daggar, D.H., and McIntyre, J.I., 1992, Aeromagnetic map of New South Wales: NSW Department of Mineral Resources and Australian Geological Survey Organisation.

Spycher, N.F., and Reed, M.H., 1989, Evolution of a Broadlands-type epithermal ore fluid along alternative P-T paths: Implications for the transport and deposition of base, precious and volatile metals: ECONOMIC GEOLOGY, v. 84, p. 328-359.

Stanley, E.R., 1912, Report on the geology of Woodlark Island: Port Moresby, Government Printer, 19 p.

Steiner, A., 1977, The Wairakei geothermal area, North Island, New Zealand: New Zealand Geological Survey Bulletin, v. 90, p. 136.

Steven, T.A., and Ratte, J.E., 1960, Geology and ore deposits of the Summitville district, San Juan Mountains, Colorado: U.S. Geological Survey Professional Paper, v. 487, 90 p.

Stoffregen, R., 1987, Genesis of acid-sulfate alteration and Au-Cu-Ag mineralisation at Summitville, Colorado: ECONOMIC GEOLOGY, v. 82, p. 1575-1591.

Stuart-Alexander, D.E., Shoemaker, E.M., and Moore, H.J., 1972, Geologic map of the Mule Ear diatreme, San Juan County, Utah: U.S. Geological Survey, Miscellaneous Investigations Series, Map 1-674.

Stuart-Smith, P.G., 1991, The Gilmore Fault Zone - the deformational history of a possible terrain boundary within the Lachlan fold belt, New South Wales: BMR Journal of Australian Geology and Geophysics, v. 12, p. 35-50.

Supple, D.W., Warren, A.Y.E., Watkind, J.J., Chapman, J., Tenison-Woods, K., and Barron., L., 1986, A reconnaissance study of the geology and gold deposits of the West-Wylong-Temora-Adelong district: New South Wales Geological Survey Quarterly Notes 64, p. 1-23.

Sverjensky, D.A., Hemley, J.J., and D'Angelo, W.M., 1991, Thermodynamic assessment of hydrothermal alkali feldspar-mica- aluminosilicate equilibria: Geochimica et Cosmochimica Acta, v. 55, p. 989-1004.

Swanson, M.T., 1988, Pseudotachylite-bearing strike slip duplex structures in the Fort Foster Brittle zone, Maine: Journal of Structural Geology, v. 10, p. 813-828.

Syka, M.C., 1985, Paragenetic, fluid inclusions, geochemical and stable isotope studies in epithermal vein mineralization in the Wau District, Papua New Guinea: Unpublished B.Sc. (Honours) thesis, Melbourne, Monash University.

Syka, M.M., and Bloom, M.S., 1990, The geology and paragenesis of epithermal gold mineralization at the Kerimenge prospect, Papua New Guinea, *in* Pacific Rim Congress 90, 6-12 May 1990, Gold Coast, Queensland, proceedings: Parkville, The Australasian Institute of Mining and Metallurgy, p. 293-299.

Taylor, B., 1979, Bismark Sea: Evolution of a back-arc basin: Geology, v. 7 p. 171-174.

Taylor, G., 1987, Breccia formation and its relation to gold mineralization at Mount Kasi, Fiji, *in* Pacific Rim Congress 87, 26-29 August 1987, Gold Coast, Queensland, proceedings: Parkville, The Australasian Institute of Mining and Metallurgy, p. 597-601.

Taylor, R.G., and Pollard, P.J., 1993, Mineralized breccia systems; methods of recognition and interpretation: Economic Geology Research Unit, James Cook University, EGRU Contribution, v. 46, 31 p.

Tatsumi, Y., and Eggins, S., 1995, Oxford, Blackwell Science, 211 p.

Tchalenko, J.S., 1970, Similarities between shear zones of different magnitudes: Geological Society of America Bulletin, v. 81, p. 1625-1640.

Tchalenko, J.S., and Ambraseys, N.N., 1970, Structural analysis of the Dasht-Bayaz (Iran): Earthquake fractures: Geological Society of America Bulletin, v. 81, p.41-60.

Teale, G.S., 1995, Epithermal gold mineralization at Mt Terrible N.S.W., and its implications for the Currabubula to Boggabri Volcanic Corridor, *in* State of exploration conference, Sydney, New South Wales, proceedings: Sydney, N.S.W. Department of Mineral Resources.

Thompson, J.F.H., Abidin, H.Z., Both, R.A., Martosuroyo, S., Rafferty, W.J., and Thompson, A.J.B., 1994, Alteration and epithermal mineralization in the Maspua Ria volcanic centre, Central Kalimantan, Indonesia: Journal of Geochemical Exploration, v. 50, p. 429-456.

Thompson, J.F.H., Lessman, J., and Thompson, A.J.B., 1986, The Temora gold-silver deposit: A newly recognised style of high sulfur mineralization in the Lower Palaeozoic of Australia: ECONOMIC GEOLOGY, v. 81, p. 732-738.

Thompson, T.B., Tripple, A.D., and Dwelley, P.C., 1985, Mineralized veins and breccias of the Cripple Creek district, Colorado: ECONOMIC GEOLOGY, v. 80, p. 1669-1688.

Titley, S.R., 1978, Copper, molybdenum and gold contents of some porphyry copper systems of the southwestern and western Pacific: ECONOMIC GEOLOGY, v. 73, p. 977-981.

Titley, S.R., 1990, Evolution and style of fracture permebility in intrusion-centred hydrothermal systems, *in* The Role of Fluids in Crustal Processes, Studies in Geophysics, Washington, National Academy Press, p. 50-63.

Titley, S.R., 1993, Characteristics of porphyry copper occurrence in the American Southwest, *in* Kirkham, R.V., Sinclair, W.D., Thorpe, R.I., and Duke, J.M., eds., Mineral exploration modelling: Geological Association of Canada Special Paper, v. 40, p. 433-464.

Titley, S.R., and Heidrick, T.L., 1978, Intrusion and fracture styles of some mineralized porphyry systems in the southwestern Pacific and their relationship to plate interactions: ECONOMIC GEOLOGY, v. 73, p. 891-903.

Titley, S.R., Fleming, A.W., and Neale, T.I., 1978, Tectonic evolution of the porphyry copper system at Yandera, PNG: ECONOMIC GEOLOGY, v. 73, p. 810-828.

Tosdal, R.M., Enderlin, D.A., Nelson, G.C., and Lehrman, N.J., 1993, Overview of the McLaughlin precious metal deposit, Napa and Yolo Counties, Northern California, *in* Rytuba, J.J., ed., Active geothermal systems and gold-mercury deposits in the Sonoma-Clear Lake volcanic fields, California: Society of Economic Geologists Guide Book Series, v. 16, p. 312-329.

Turner, S., 1986, Fluid inclusion, alteration and ore mineral studies of an epithermal vein system: Mount Kasi, Vanua Lava, Fiji, *in* Proceedings of symposium 5: Volcanism, hydrothermal systems and related mineralisation, February 1986, Auckland: Auckland, International Volcanological Congress, p. 87-94.

Turner, S.J., Flindell, P.A., Hendri, D., Hardjana, I., Lauricella, P.F., Lindsay, R.P., Marpaung, B., and White, G.P., 1994, Sediment-hosted gold mineralization in the Ratatotok district, North Sulawesi, Indonesia, *in* van Leeuwen, T.M., Hedenquist, J.W., James, L.P., and Dow, J.A.S., eds., Mineral deposits of Indonesia - discoveries of the past 25 years: Journal of Geochemical Exploration, v. 50, p. 317-336.

United Nations Development Project, 1977, Geology and mineralization in the Baguio area, northern Luzon: New York, United Nations Development Programme, Technical Report DP/UN/PHI-85-001/5, 82 p.

Urashima, Y., Saito, M., and Sato, E., 1981, The Iwato gold ore deposits, Kagoshima Prefecture, Japan: Society of Mining Geologists of Japan Special Issue, v. 10, p. 1-14 (in Japanese with English abstracts).

van Leeuwen, T.M., 1994, 25 years of mineral exploration and discovery in Indonesia, *in* van Leeuwen, T.M., Hedenquist, J.W., James, L.P., and Dow, J.A.S., eds., Mineral deposits of Indonesia - discoveries of the past 25 years: Journal of Geochemical Exploration, v. 50, p. 13-90.

van Leeuwen, T.M., Leach, T.M., Hawke, A.A., and Hawke, M.M., 1990, The Kelian disseminated gold deposit, East Kalimantan, Indonesia, *in* Hedenquist, J.W., White, N.C., and Siddeley, N., eds., Epithermal gold mineralization of the Circum Pacific: Journal of Geochemical Exploration, v. 35, p. 1-61.

Vennemann, T.W., Muntean, J.L., Kesler, S.E., O'Neil, J.R., Valley, J.W., and Russell, N., 1993, Stable isotope evidence for magmatic fluids in the Pueblo Viejo epithermal acid sulfate Au-Ag deposit, Dominican Republic: ECONOMIC GEOLOGY, v. 88, p. 55-71.

Vila, T., Sillitoe, R.H., Betzhold. J., and Viteri, R., 1991, The porphyry gold deposit at Marte, Northern Chile: ECONOMIC GEOLOGY, v. 86, p. 1271-1286.

Volk, J.A, Lauha, E., Leonardson, R.W., and Rahn, J.A., 1995, Structural geology of the Betze-Post and Meikle deposits, Elko and Eureka Counties, Nevada *in* Structural geology of the Carlin trend, Geology and Ore Deposits of the American Cordillera, Symposium field trip guidebook: Reno, Geological Society of Nevada, 16 p.

Wake, B.A., Silvio, N.M, Lattore, A.Q., Iswahyudi, A.S., and Purwanto, A., 1996, Geology of the Toka Tindung epithermal gold deposit, North Sulawesi, Indonesia, *in* Porphyry related copper and gold deposits of the Asia Pacific Region, Cairns, Australia, 12-13 August 1996, proceedings: Adelaide, Australian Mineral Foundation, p. 9.1-9.8.

Wallace, D.A., Johnson, R.W., Chappell, B.W., Arculus, R., Perfit, M.R., and Crick, I.H., 1983, Cainozoic volcanism of the Tabar, Lihir, Tanga and Feni Islands, Papua New Guinea; geology whole-rock analyses, and rock forming mineral compositions: Bureau of Mineral Resources, Geology and Geophysics Report, v. 243, B.M.R. Microfilm MF 197.

Walshe, J.L., Heithersay, P.S., and Morrison, G.W., 1995, Toward an understanding of the metallogeny of the Tasman fold belt system: ECONOMIC GEOLOGY, v. 90, p. 1382-1401.

Walter, M.R., 1976a, Geyserites of Yellowstone National Park: An example of abiogenic "stromatolites", *in* Stromatolites, Developments in Sedimentology 20, Amsterdam, Elsevier Scientific Publishing Company, p. 88-112.

Walter, M.R., 1976b, Hot-spring sediments in Yellowstone National Park, *in* Stromatolites, Developments in Sedimentology 20, Amsterdam, Elsevier Scientific Publishing Company, p.489-498.

Ward, C.W., 1980, Exploration of the Okoy geothermal field, Negros, Philippines, *in* 2nd New Zealand geothermal workshop, 3-5 November 1980, Auckland, New Zealand, proceedings: Auckland, University of Auckland Geothermal Institute, p. 105-108.

Watmuff, G., 1978, Geology and alteration-mineralization zoning in the central portion of the Yandera porphyry copper prospect, Papua New Guinea: ECONOMIC GEOLOGY, v. 73, p. 829-856.

Weir, R.H., and Kerrick, D.M., 1987, Mineralogic, fluid inclusion and stable isotope studies of several gold mines in the Mother Lode, Tuolumne and Mariposa Counties, California: ECONOMIC GEOLOGY, v. 82, p. 328-344.

Weissberg, B.G., 1969, Gold-silver ore-grade precipitates from New Zealand thermal waters: ECONOMIC GEOLOGY, v. 64, p. 95-108.

Weissberg, B.G., Brown, P.R.L., and Seward, T.M., 1979, Ore metals in active geothermal systems, *in* Barnes, H.L., ed., Geochemistry of hydrothermal ore deposits, 2nd edition: New York, John Wiley & Sons, p. 738-780.

Wellman, H.W., 1954, Stress formation controlling lode formation and faulting at Waihi Mine and notes on the stress pattern in the northwestern part of the North Island of New Zealand: New Zealand Journal of Science and Technology, v. 36B, p. 201-206.

Wells, K., and Young, D.J., 1991, Geology and exploration of the Hamata deposit, *in* Rogerson, R., ed., Proceedings of the PNG geology, exploration and mining conference, 1991, Rabaul: Parkville, The Australasian Institute of Mining and Metallurgy, p. 66-68.

Welsh, T.C., 1990, The mineral industry in Papua New Guinea, *in* Hughes, F.E., ed., Geology of the mineral deposits of Australia and Papua New Guinea: Australasian Institute of Mining and Metallurgy Monograph 14, p. 1681-1688.

Wesnousky, S.G., 1988, Seismological and structural evolution of strike-slip faults: Nature, v. 335, p. 340-342.

White, D.E., 1981, Active geothermal systems and hydrothermal ore deposits: ECONOMIC GEOLOGY, 75th Anniversary Volume, p. 392-423.

White, G., 1986, Puhipuhi mercury deposit, *in* Henley, R.W., Hedenquist, J.W., and Roberts, P.J., eds., Guide to the active epithermal (geothermal) systems and precious metal deposits of New Zealand: Monograph Series in Mineral Deposits, Berlin, Gebruder Borntraeger, v. 26, p. 193-198.

White, N.C., 1991, High sulfidation epithermal gold deposits: characteristics and a model for their origin, *in* Matsuhisa, Y., Aoki, M., and Hedenquist, J.W., eds., High temperature acid fluids and associated alteration and mineralization: Geological Survey of Japan Report, v. 277, p. 9-20.

White, N.C., and Hedenquist, J.W., 1990, Epithermal environments and styles of mineralization: variations and their causes, and guidelines for exploration: Journal of Geochemical Exploration, v. 35, p. 445-474.

White, N.C, and Hedenquist, J.W., 1995, Epithermal gold deposits: Styles, characteristics and exploration: SEG Newsletter, v. 23, p. 1, 9-13.

White, N.C., Wood, D.G, and Lee, M.C., 1989, Epithermal sinters of Palaeozoic age in north Queensland, Australia: Geology, v. 17, p. 718-722.

White, N.C., Leake, M.J., McCaughey, S.N., and Parris, B.W., 1995, Epithermal gold deposits of the southwest Pacific: Journal of Geochemical Exploration, v. 54, p. 87-136.

Wiebenga, W.A., 1973, Crustal structure of the New Britain - New Ireland region, *in* Coleman, P.J., ed., The Western Pacific: Island arcs, marginal seas, geochemistry: Nedlands, University of Western Australia Press, p. 163-177.

Wilkins, C., 1997, Structural control of the Browns Creek gold-copper skarn deposit, Blaney, NSW: Geological Society of Australia, Abstracts No. 44, p. 73.

Wilcox, R.E., Harding, T.P., and Seely, D.R., 1973, Wrench tectonics: American Association of Petroleum Geologists Bulletin, v. 57, p. 74-96.

Willis, G.F., and Tosdal, R.M., 1992, Formation of gold veins and breccias during dextral strike slip faulting in the Mesquite mining district, south-eastern California: ECONOMIC GEOLOGY, v. 87, p. 2002-2022.

Williamson, A., and Fleming, G.J., 1995, Miwah prospect high sulfidation Au-Cu mineralisation, northern Sumatra, Indonesia, *in* Pacific Rim Congress 95, 19-22 November 1995, Auckland, New Zealand, proceedings: Carlton South, The Australasian Institute of Mining and Metallurgy, p. 637-642.

Williamson, A and Rogerson, R., 1983, Geology and mineralization of Misima Island: Geological Survey of Papua New Guinea Report 83/12, 124 p.

Wilson, T.J., 1965, A new class of faults and their bearing on continental drift: Nature, v. 4995, July 24, 1965, p. 343-347.

Windh, J., 1995, Saddle reef and related gold mineralization, Hill End gold field Australia: Evolution of an auriferous vein system during progressive deformation: ECONOMIC GEOLOGY, v. 90, p. 1764-1775.

Wolfe, J.A., Manuzon, M.S., and Divis, A.F., 1978, The Taysan porphyry copper deposit, Southern Luzon Island, Philippines: ECONOMIC GEOLOGY, v. 73, p. 608-618.

Wolfe, R., 1994, Geology, paragenesis and alteration geochemistry of E48: Unpublished B.Sc. (Honours) thesis, Hobart, University of Tasmania, 106 p.

Wolfeden, E.B., 1965, Bau mining district, West Sarawak, Malaysia, Part 1: Bau: Geological Survey of Malaysia, Borneo Region Bulletin, v. 7, 147 p.

Woodcock, N.H., and Fisher, M., 1986, Strike-slip duplexes: Journal of Structural Geology, v. 8, p. 725-730.

Wormald, P.J., Orr, T.O.H., and Hodkinson, I.P., 1991, The Mount Leyshon gold mine (NE Queensland), and intrusive breccia and igneous complex, *in* World Gold '91, Cairns, 21-26 April 1991, proceedings: Parkville, The Australasian Institute of Mining and Metallurgy and Society of Mining Engineers, p. 223-232.

Worsley, M.R., and Golding, S.D., 1990, Golden Plateau gold deposits, *in* Hughes, F.E., ed., Geology of the mineral deposits of Australia and Papua New Guinea: Australasian Institute of Mining and Metallurgy Monograph 14, p. 1709-1514.

Wyborn, D., 1992, The tectonic significance of Ordovician magmatism in the eastern Lachlan fold belt: Tectonophysics, v. 214, p. 177-192.

Yanez, G., Mpodozis, C., and Tomlinson, A.J., 1994, Eocene dextral oblique convergence and sinistral shear along the Domeyko Fault System: A thin viscous sheet approach with asthenospheric drag at the base of the crust: 7th Congreso Geologico Chileno, 1994, Conception, Chile, 1994, Proceedings, Actas, p. 1478-1482.

Yoshioka, T., 1996, Evolution of fault geometry and development of strike-slip basins: Comparative studies on the transform zones of Turkey and Japan: The Island Arc, 5, p 405-419.

Zaide, M.C., 1984, Interpretation of rock-dating results in the south-east Negros Geothermal Field: Unpublished internal report, Manila, PNOC-EDC Geothermal Division, 21 p. (with permission).

Zaluski, G., Nesbitt, B., and Muehlenbarks, 1994 Hydrothermal alteration and stable isotope systematics of the Babine Porphyry Cu Deposits, British Columbia: Implications for fluid evolution in porphyry systems: ECONOMIC GEOLOGY, v. 89, p. 1518-1542.

Zhang, X., and Sanderson, D.J., 1996, Numerical modelling of the effects of fault slip on fluid flow around extensional faults: Journal of Structural Geology, v. 18, p. 109-118.

APPENDIX 1

MINERAL ABBREVIATIONS:

Ab-albite; Act-actinolite; Ad-adularia; Ah-anhydrite; Al-alunite; And-andalusite; Ank-ankerite; Apy-arsenopyrite; Au-native gold; Ba-barite; Bio-biotite; BM-base metal (sulphides); Bn-bornite; Chab-chabazite; Cb-carbonate; Ch-chlorite; Ch-Sm - interlayered chlorite-smectite; Chd-chalcedony; Cor-corundum; Cpx-clinopyroxene; Cpy-chalcopyrite; Cr-cristobalite; Ct-calcite; Cy-illitic clay; Do-dolomite; Dik-dickite; Dp-diaspore; El-electrum; En-enargite; Ep-epidote; Fr-ferberite; Fsp-feldspar; Ga-garnet; GalGn-galena; Gol-goldfieldite; Hal-halloysite; Heu-heulandite; Hm-hematite; I-illite; I-Sm - interlayered illite-smectite; K-kaolinite; Kut-kutnahorite; Lau-laumontite;

Mo-molybdenite; Mt-magnetite; Mor-mordenite; Mus-muscovite; Nat-natrolite; Op-opaline silica; Po-pyrrhotite; Py-pyrite; Pyr-pyrophyllite; Q-quartz; S-sulphide/sulfur; Ser-sericite; Sid-siderite; Sl-sphalerite; Sm-smectite; Ss-sulfosalt; Stb-stilbite; Te-telluride/native tellurium; Tn-tennantite; Tr-tremolite; Tri-tridymite; Tt-tetrahedrite; Ves-vesuvianite; Wai-wairakite; Wo-wollastonite; Zeo-zeolite.